Volume Change Consideration in Determining Appropriate Unsaturated Soil Properties for Geotechnical Applications

by

Elham Bani Hashem

A Dissertation Presented in Partial Fulfillment
of the Requirements for the Degree
Doctor of Philosophy

Approved April 2013 by the
Graduate Supervisory Committee:

Sandra Houston, Chair
Edward Kavazanjian
Claudia Zapata

ARIZONA STATE UNIVERSITY

May 2013

ABSTRACT

Unsaturated soil mechanics is becoming a part of geotechnical engineering practice, particularly in applications to moisture sensitive soils such as expansive and collapsible soils and in geoenvironmental applications. The soil water characteristic curve, which describes the amount of water in a soil versus soil suction, is perhaps the most important soil property function for application of unsaturated soil mechanics. The soil water characteristic curve has been used extensively for estimating unsaturated soil properties, and a number of fitting equations for development of soil water characteristic curves from laboratory data have been proposed by researchers. Although not always mentioned, the underlying assumption of soil water characteristic curve fitting equations is that the soil is sufficiently stiff so that there is no change in total volume of the soil while measuring the soil water characteristic curve in the laboratory, and researchers rarely take volume change of soils into account when generating or using the soil water characteristic curve. Further, there has been little attention to the applied net normal stress during laboratory soil water characteristic curve measurement, and often zero to only token net normal stress is applied. The applied net normal stress also affects the volume change of the specimen during soil suction change. When a soil changes volume in response to suction change, failure to consider the volume change of the soil leads to errors in the estimated air-entry value and the slope of the soil water characteristic curve between the air-entry value and the residual moisture state. Inaccuracies in the soil water characteristic curve may lead to inaccuracies in estimated soil property functions such as

unsaturated hydraulic conductivity. A number of researchers have recently recognized the importance of considering soil volume change in soil water characteristic curves.

The study of correct methods of soil water characteristic curve measurement and determination considering soil volume change, and impacts on the unsaturated hydraulic conductivity function was of the primary focus of this study. Emphasis was placed upon study of the effect of volume change consideration on soil water characteristic curves, for expansive clays and other high volume change soils. The research involved extensive literature review and laboratory soil water characteristic curve testing on expansive soils. The effect of the initial state of the specimen (i.e. slurry versus compacted) on soil water characteristic curves, with regard to volume change effects, and effect of net normal stress on volume change for determination of these curves, was studied for expansive clays. Hysteresis effects were included in laboratory measurements of soil water characteristic curves as both wetting and drying paths were used.

Impacts of soil water characteristic curve volume change considerations on fluid flow computations and associated suction-change induced soil deformations were studied through numerical simulations.

The study includes both coupled and uncoupled flow and stress-deformation analyses, demonstrating that the impact of volume change consideration on the soil water characteristic curve and the estimated unsaturated hydraulic conductivity function can be quite substantial for high volume change soils.

DEDICATION

To my wonderful husband

ACKNOWLEDGMENTS

First and foremost I offer my sincerest gratitude to my committee chair, Dr. Sandra L. Houston on her supervision and guidance during my study and research. Her perpetual energy and enthusiasm in research had motivated me greatly. In addition, she was always accessible and willing to help me with my research. As a result, research life became smooth and rewarding for me. She is an excellent teacher and mentor and I shall always be indebted to her.

I gratefully acknowledge Dr. Claudia Zapata for her advice and crucial contribution, which made her a backbone of this dissertation. Many thanks to Dr. William N. Houston, Dr. Delwyn G. Fredlund, and Dr. Edward Kavazanjian for their guidance and for making the valuable inputs, I am much indebted to them for their advice and comments.

I am grateful to Dr. Sam Abbaszadeh for his wonderful support, help, and guidance through this research, particularly with regard to the numerical modeling and laboratory testing procedures.

I would also like to thank the laboratory manager, Mr. Peter Goguen for his help throughout my laboratory testing program. Many thanks to Dr. Marcelo Sanchez and Ajay Shastri of Texas A&M University for their help with numerical modeling using CODE-BRIGHT.

This dissertation was partially funded by National Science Foundation (NSF) under grant number 1031238.The opinions, conclusions, and interpretations expressed in this dissertation are those of the authors, and not necessarily of NSF.

TABLE OF CONTENTS

Page

CHAPTER Page

CHAPTER Page

CHAPTER Page

APPENDIX Page

LIST OF TABLES

Table Page

Table Page

Table Page

LIST OF FIGURES

Figure Page

Figure Page

Figure Page

Figure Page

Figure Page

Figure Page

Figure Page

Figure Page

Figure Page

Figure Page

Figure Page

Figure Page

Figure Page

Chapter 1

INTRODUCTION

1.1. Background

Unsaturated soil mechanics has gradually become a part of geotechnical engineering practice, particularly in the areas of expansive and collapsible soils and geoenvironmental engineering. The Soil Water Characteristic Curve (SWCC) which is often referred to as the soil water retention curve is one of the main parameters which has been developed and used by researchers for many years in the study of unsaturated soils. The SWCC has been used in the estimation of unsaturated soil property functions, in general, and has been used for decades for estimation of the unsaturated hydraulic conductivity function (Fredlund et al. 2000, van Genuchten and Mualem, 1980).

The SWCC defines the amount of water in a soil for different values of soil suction. The amount of water in the soil is commonly defined in one of several ways. Three common variables used to define the amount of water in the soil are: gravimetric water content, w, volumetric water content, θ, and degree of saturation, S. SWCC's in terms of all three measures of soil water content are used to obtain information such as the air-entry value and residual suction, and when the soil does not undergo volume change (e.g., sands), should yield similar values (Fredlund, 2006).

The SWCC can be used to estimate the unsaturated hydraulic conductivity of a soil. The drying SWCC is generally measured in the laboratory and therefore, the hydraulic conductivity function is typically determined based on the drying curve.

However, the hydraulic conductivity function for the wetting curve can be estimated based on measured or estimated hysteresis loops (Pham et al, 2003).

SWCC's have been established in agriculture-related disciplines for many years. A number of devices have been developed for applying a wide range of soil suction values (Fredlund, 2006). Typical pressure plate apparatuses and their range of suction application are: Tempe cells (100 kPa) (Reginato and van Bavel 1962); volumetric pressure plate (200 kPa); and large pressure plate (500 and 1,500 kPa) (Fredlund and Rahardjo 1993). ASTM standard (ASTM 2003 Standard D-6836-02) provides a detailed description for the determination of the soil water characteristic curves using several testing procedures.

One of the most common devices that has been used for determining SWCC's in geotechnical engineering is the oedometer-type pressure plate device, such as developed and manufactured by GCTS, SWC-150. This device is shown in Figure 1.1 (GCTS, 2004). This apparatus was used in this study to determine SWCC's of expansive clays. This system was used for suctions smaller than 1500kPa, as the maximum capacity of high air-entry value (HAEV) ceramic stones for this device is 1,500kPa matric suction. For matric suction values higher than 1,500kPa, filter paper testing was performed. SWCC tests that were carried out as a part of this study will be described in later sections.

Figure 1.1. Oedometer pressure plate device, SWC-150 (GCTS, 2004)

One of the major uses of the SWCC is for estimating properties of unsaturated soils such as unsaturated hydraulic conductivity function. For example, the SWCC and saturated hydraulic conductivity of soils are used to estimate the unsaturated soil hydraulic conductivity function. One of the uses of the unsaturated hydraulic conductivity function is in the estimation of the rate and extent of fluid flow through a soil profile (e.g. rate of changes in suction) which can in turn be used to estimate amount of suction-change induced deformation of expansive soils upon wetting. Therefore, correct measurement of the SWCC would appear to be essential to determination of unsaturated hydraulic conductivity functions.

1.2. Problem Statement

Even though the soil water characteristic curve has been measured and used by numerous researchers throughout the years, the effect of volume change of high volume change soils (e.g. oil sands tailings, expansive soils, and collapsible soils) has rarely been considered when determining the SWCC's that are used in estimation of soil properties. This may lead to inaccuracies in the SWCC's, including the air-entry value. It has been the common practice to estimate some of the major unsaturated soil property functions (e.g., unsaturated hydraulic conductivity function, shear strength) by using the SWCC, further demonstrating the importance of accurate determination of the SWCC.

In recent years, the importance of considering the volume change of soils during suction change has been recognized by a number of researchers, including Salager et al. (2010), Pe´ron et al. (2007), Nuth and Laloui (2011), Stange and Horn (2005), Mbonimpa et al. (2006), Perez-Garcia, et al. (2008), and Fredlund and Houston, (2013). Through literature study it was found that the effect of net normal stress which is applied to the soil specimen during the SWCC test has also been under-studied. Only very few researchers have conducted studies for finding the impact of net normal stress on SWCC's (both drying and wetting cycles of SWCC) which in this research was found to be important, particularly with regard to effect of net normal stress on volume change of the soil during SWCC testing on expansive clays. Furthermore, the effect of initial state of the soil specimen including initial moisture content on SWCC has not been studied by a lot of researchers. It is known that the initial condition of the soil (slurry versus

compacted at or near optimum moisture content) can have a significant effect on the SWCC of the soil, particularly with regard to soil volume change (Fredlund, 2002).

Correction of SWCC's for soil volume change during the test may have a considerable impact on air-entry value and shape of the SWCC, depending on the amount of volume change that occurs in response to changes in soil matric suction. This, in turn, may have a significant impact on unsaturated soil properties derived from the SWCC's (e.g. soil hydraulic properties such as unsaturated hydraulic conductivity function). No studies on numerical modeling of the effect of correction of the SWCC for soil volume change on hydraulic properties of the soils (and its impact on amount of wetting-induced deformation of expansive soils was found in the literature, and this represents another important area of study that is addressed in this research.

1.3. Research Objectives and Scope of Work

An extensive literature review was conducted regarding the methods of SWCC determination and the models available to best-fit the SWCC data obtained from laboratory experiments. This literature search SWCC's included the study of typical air-entry values and hysteresis. Emphasis was placed upon the SWCC's of clays. Use of soil water characteristic curves in constitutive relations for unsaturated soils such as unsaturated hydraulic conductivity functions was also studied through a literature search. Some of the commonly-used equations for estimating unsaturated hydraulic conductivity functions of soils based on the SWCC were studied. This part of the literature search included studying the methodologies used for developing the equations for estimating

unsaturated hydraulic conductivity functions as well as the applications of the proposed equations.

The importance of correcting the SWCC's (including SWCC's in terms of volumetric water content and degree of saturation) for soil volume change that occurs during the SWCC test was studied through literature search and laboratory experiments. Additional literature search and laboratory experiments were carried out to assess the effect of net normal stress on the shape of SWCC with regard to the soil volume change. Drying and wetting SWCC experiments were conducted with various net normal stresses to find the effect of net normal stress on volume change of expansive clays during SWCC test. Moreover, the importance of initial condition of the specimen (slurry versus compacted specimen) was evaluated through literature search and laboratory experiments. The entire laboratory testing in this research was performed on expansive soils, as an example of relatively high volume-change materials of interest in geotechnical engineering applications.

In this research, the SWCC's of three highly expansive soils were measured. The soils tested in this study have been collected from areas in Anthem, Arizona, San Antonio, Texas, and Denver, Colorado. For simplicity these soils will be referred to as Anthem, San Antonio, and Colorado through this dissertation. Properties of the soils tested as well as the test procedure and results are presented in this report. Volume change of these soils during suction change was measured and taken into account for establishing the SWCC's. It was found that volume change consideration plays a major

role in the shape of the SWCC particularly regarding the air-entry value (AEV) determination.

In addition to the SWCC tests conducted on compacted specimens, slurry specimens of Anthem, Colorado, and San Antonio soils were also tested and the resulting SWCC's were compared against the SWCC's obtained from the compacted specimens of the same soils. It was found that the initial state of the specimen has a significant effect on the shape of the SWCC, particularly due to high volume change of slurry specimens during the test.

As the next part of this study, complete determination of the SWCC's for three soils of Anthem, Colorado, and San Antonio were carried out which included both drying and wetting paths. During this set of tests, effect of net normal stress and hysteresis on the SWCC of expansive soils was studied. The net normal stress values applied to the soil specimens were varied form only a seating load (7 kPa) to around 54% of the swell pressure of the soil samples. Suction measurement and control methods used in the laboratory testing included axis translation and filter paper methods.

The last part of this study included numerical modeling of one-dimensional fluid flow through an expansive soil profile and the deformations due to changes in suction under constant net normal stress. In this study, the rate of changes in suction through the soil was evaluated using three computer programs SVFLUX, VADOSE/W, and CODE-BRIGHT. In this numerical modeling study, the effect of correcting SWCC for soil volume change on hydraulic properties of the unsaturated soils and on results of the fluid flow modeling (rate of advancement of wetted front and degree of saturation within the

profile) was assessed. Furthermore, effect of volume change correction of SWCC on amount of deformation caused by changes in soil suction was evaluated.

1.4. Report Organization

This report is organized in the following manner. After the introduction which covers the research objectives and scope of work, Chapter 2 presents an extensive literature review on the methods used for measuring and generating SWCC's. Also air-entry value of clays and hysteresis present in SWCC's that were studied through literature search are presented. Furthermore, impact of net normal stress (i.e. stress state) and initial state of the specimen (slurry versus compacted) on SWCC is summarized. An extensive literature review was carried out regarding state of practice for correcting SWCC's for soil volume change that occurs during SWCC test. Equations developed by researchers to best-fit SWCC data was also studied and presented. Also use of the SWCC in constitutive relations for unsaturated soils, particularly unsaturated hydraulic properties was studied. An extensive literature review was conducted on most common models used for unsaturated hydraulic conductivity of soils. Three of the most common models (which are used in most of the available computer codes for modeling of fluid flow through soils) were studied and are presented in more detail in Chapter 2 (i.e. literature review chapter).

Chapter 3 covers the laboratory testing program that was carried out as a part of this study. This chapter presents the test methods and procedures, laboratory equipment, and basic properties of the soils used in the study. Results of the testing program and necessary comparisons and analyses of the results are also illustrated in this chapter.

Chapter 4 includes the numerical modeling conducted of the expansive soils tested in laboratory as a part of this study. In this chapter the computer programs and models and equations utilized are described along with the data used regarding geometry of the model, boundary conditions, materials properties and analysis type. This chapter covers numerical modeling for one-dimensional fluid flow through the soil as well as coupled flow-deformation modeling. The results of each modeling effort, as well as the analysis and synthesis of the results, are presented in chapter 4.

Chapter 5 includes the numerical modeling conducted for oil sands tailings. Oil sands tailings exhibit extreme volume change upon change in suction. The properties of this material were obtained from literature. Numerical modeling was done on oil sands tailings to establish trends for results and the models, material properties and analyses of results for this set of numerical modeling is presented Chapter 5.

Chapter 6 summarizes the main findings, contributions, and conclusions of this research. Chapter 6 also presents recommendations for future research work. References and several supporting Appendices are also included at the end of this research.

Chapter 2

LITERATURE REVIEW

2.1. Introduction

The soil water characteristic curve (SWCC) is a measure of amount of water in soils at different suctions. Among the different methods for applying suction to the soil specimens as a part of SWCC tests, the axis translation method has been utilized most widely, since in this method suction is easily controlled.

The axis-translation technique allows the pore-water pressure, u_w, in an unsaturated soil to be measured (or controlled) using a ceramic disk with very small pores (i.e. high air-entry disk- HAED) (Powers et al., 2007). A HAED acts as a semi-permeable membrane that separates air and water. The separation of water and air phases can be achieved only up to the air-entry value of the disk, which is the matric suction beyond which free air passes through the disk.

The SWCC can be used to estimate unsaturated soil property functions such as unsaturated hydraulic conductivity. Therefore, the accuracy of the unsaturated soil property functions depends on the accuracy of the SWCC. Several factors such as soil structure, initial water content, void ratio, and compaction method can have significant effects on the SWCC. Among these factors, stress history and initial water content has been reported to have the greatest effect on the soil structure, which in turn plays a significant role on the shape of the SWCC (Zhou et al. 2005).The air-entry value of the soil and the rate of desaturation is reportedly affected by the initial density and amount of disturbance to the soil (Fredlund and Houston, 2009). A distinctive point on SWCC is the

air-entry value. The air-entry value (AEV) corresponds to the value of matric suction at which the largest voids within the soil specimen begin to drain freely.

The amount of water in the soil versus suction can be represented by SWCC using three terms of gravimetric water content, volumetric water content, and degree of saturation. The SWCC in terms of gravimetric water content can be most easily measured in laboratory as it only include measurement of mass of water and mass of dry soil. The degree of saturation and volumetric water content require a measurement of the volume of the soil specimen in addition to measurement of the water content. Measurement of volume change of unsaturated soils has been carried out by a number of researchers and is reportedly quite demanding and requires more time and experimental care (Mbonimpa et al. 2006).

2.2. Soil Water Characteristic Curve Determination

Figure 2.1 presented by Fredlund and Houston (2009) shows a typical SWCC. There are four key parameters on any soil-water characteristic curve (Pham et al. 2003). These are the water content at zero soil suction (i.e. water content of the soil at saturation), the air-entry value, the slope of the curve (particularly between the air-entry and residual points) and the residual water content. Three zones of desaturation can be seen within the curve. The key features on the SWCC are the air-entry value and the residual value for suction and water content.

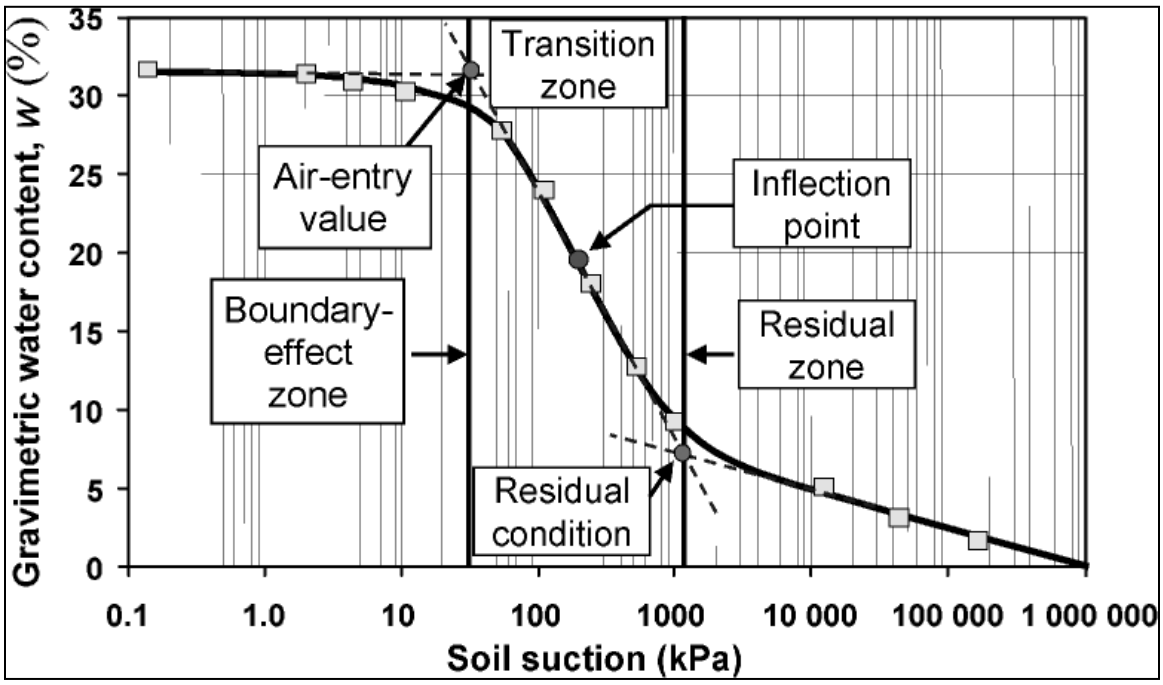

Figure 2.1. Zones of desaturation defined by the desorption branch of the soil-water characteristic curve (Fredlund and Houston, 2009)

Soil-water characteristic curves generated for soils with different historical stress states are presented in Figure 2.2. The initially slurried soil represents the maximum volume change condition (Fredlund, 2002).

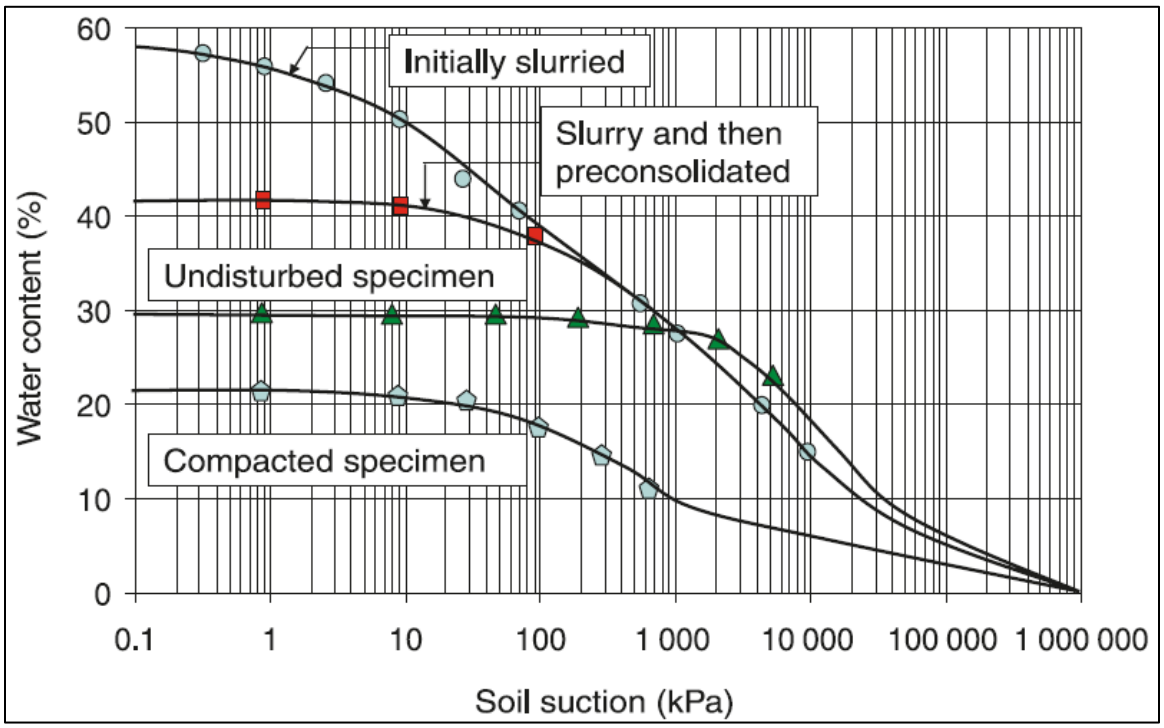

Figure 2.2. Illustration of the influence of initial state on the soil-water characteristic curve (modified from Fredlund 2002).

SWCC's for slurry specimens of Regina clay (Fredlund 1964), Jossigny loam (Fleureau et al. 1995), and kaolinite (Fleureau et al. 2004) are shown in Figures 2.3 and 2.4 along with best-fitting curves. Very high water release of these slurry specimens even at relatively small values of suction can be seen in this figure.

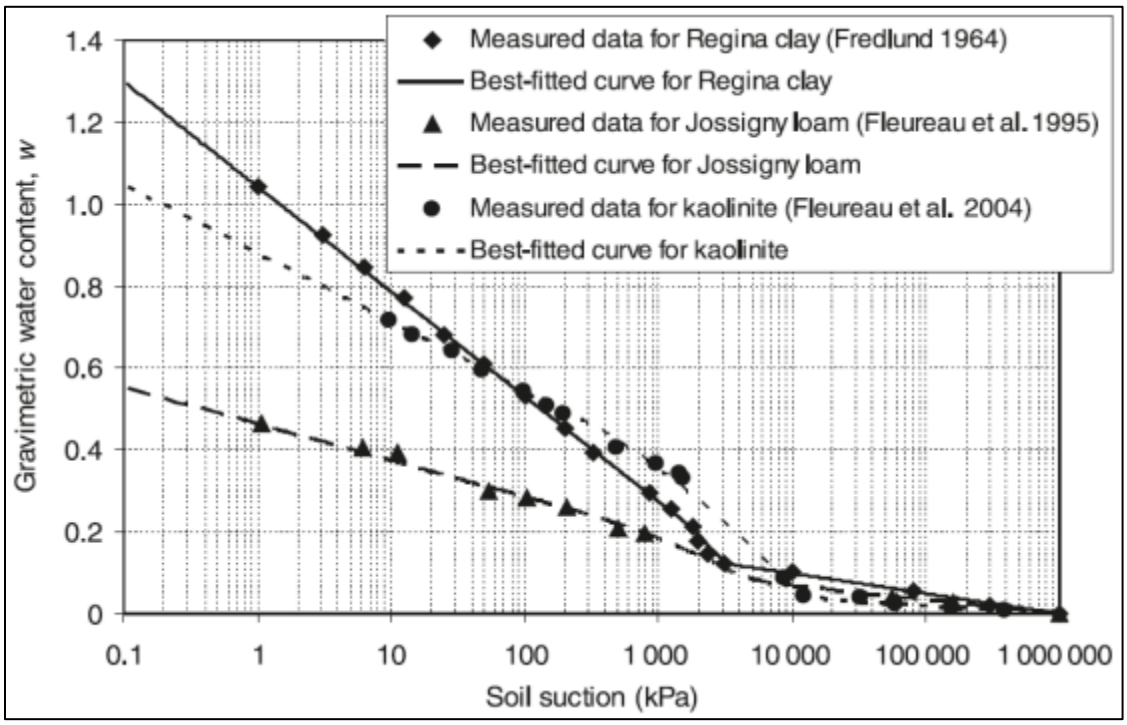

Figure 2.3. Best-fitting curves along with the measured data points for the three soils collected from the literature research (Pham and Fredlund, 2008)

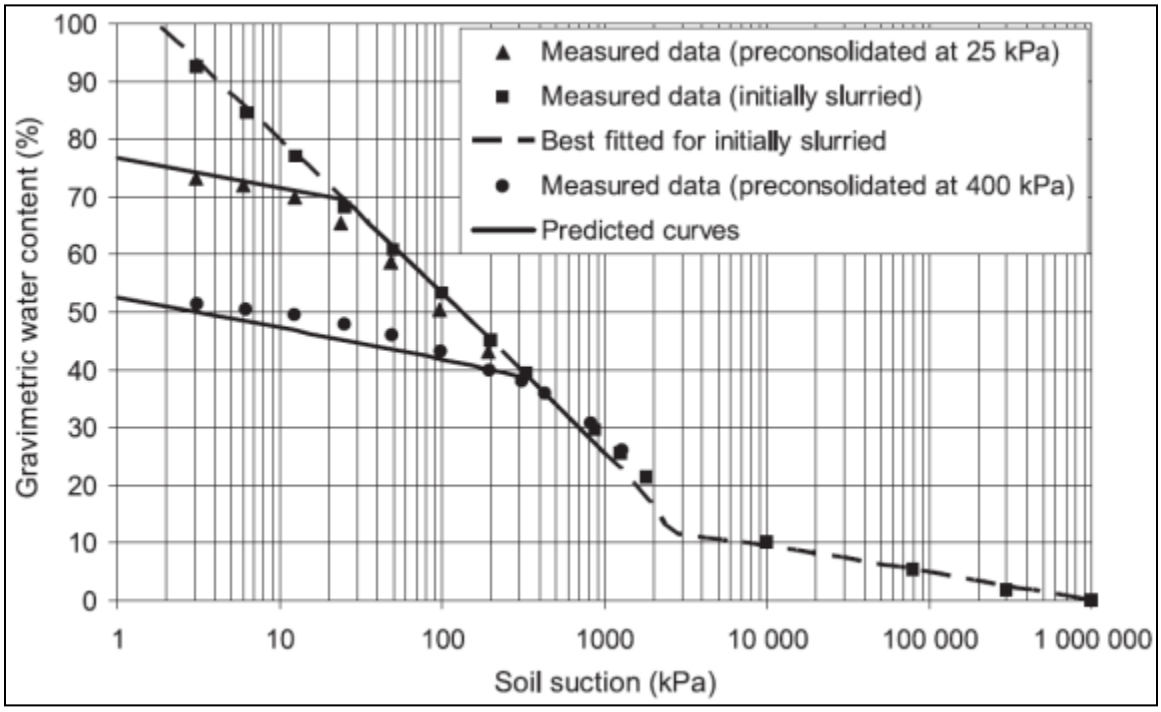

Figure 2.4. Measured data points (Fredlund 1964), best fit, and predicted SWCC's for Regina clay

2.3. Air-Entry Value (AEV) of Clays

As explained previously, air-entry value of a soil is defined as the matric suction at which desaturation of the largest pores within the soil begins. The air-entry value of a specific soil is related to the radius of the largest pore (i.e. if the largest pore is relatively small, the air-entry value will be relatively large). Numerous researchers have found that the saturation water content and air-entry value generally increases with the plasticity of the soil (Fredlund and Xing, 1994). Fredlund (2011, 2013) reported that air-entry of soils is generally quite close to their plastic limit. Consequently, the author concluded that there is an approximate correlation between the plastic limit of a soil and its air-entry value. Upon further drying, another point is reached where the soil dries without any further volume change. This can be referred to as the true "shrinkage limit" of the soil and the gravimetric water content appears to approximately correlate with residual soil conditions. Some other authors, however, reported different degrees of saturation (less than 100%) for soils at plastic limit. Ito and Azam (2010), for example, conducted laboratory experiments on expansive soils and reported degrees of saturation at plastic limit of about 80% and 60% at the shrinkage limit.

Li et al. (2009) reported that dry density has a great effect on air-entry value and storage water coefficient of SWCC. Therefore, it can be concluded that AEV for the compacted and slurry specimens can be significantly different. The researchers concluded that AEV of soil samples of lower initial water content is lower and water in soil sample of lower initial water content is excreted easily when AEV is low. They also found that the AEV of soil decreases gradually with consolidation pressure value increasing.

According to James et al. (1997), it is possible that when soil dry density is smaller, the pore space of soil internal structure is relatively larger and its connectivity is very well. So the excretion rate of water in soil sample is relatively fast during the process of inlet air and dehydration. The water is dehydrated under lower value of matrix suction (i.e. relatively smaller AEV). However, the pore of higher dry density soil sample is smaller and much micro pore exists in soil. The pore water in the micro pore is excreted difficultly (i.e. high AEV).

According to Harrington and Horseman (2003), for soils with 60% or more particles smaller than 80 μm, the AEV can be predicted using the following linear relationship:

$$AEV = 32.4\ w_L - 466.7\ (kPa) \quad (2.1)$$

Tinjum et al. (1997) studied the SWCC's from pressure plate tests of four compacted clay barrier soils prepared at different compaction water contents and compaction efforts. Their results also showed that more plastic soils tended to have higher air-entry values when compacted at a wet of optimum water content or with higher compaction effort.

According to Bilsel (2004), the higher the porosity, the lower the air-entry value expected and the faster the desaturation period. The AEV is directly proportional to the plasticity index and inversely proportional to the amount of coarse fraction.

Figure 2.5 shows the trend of AEV with change in plasticity index (PI) and coarse fraction of the soil tested by Bilsel (2004).

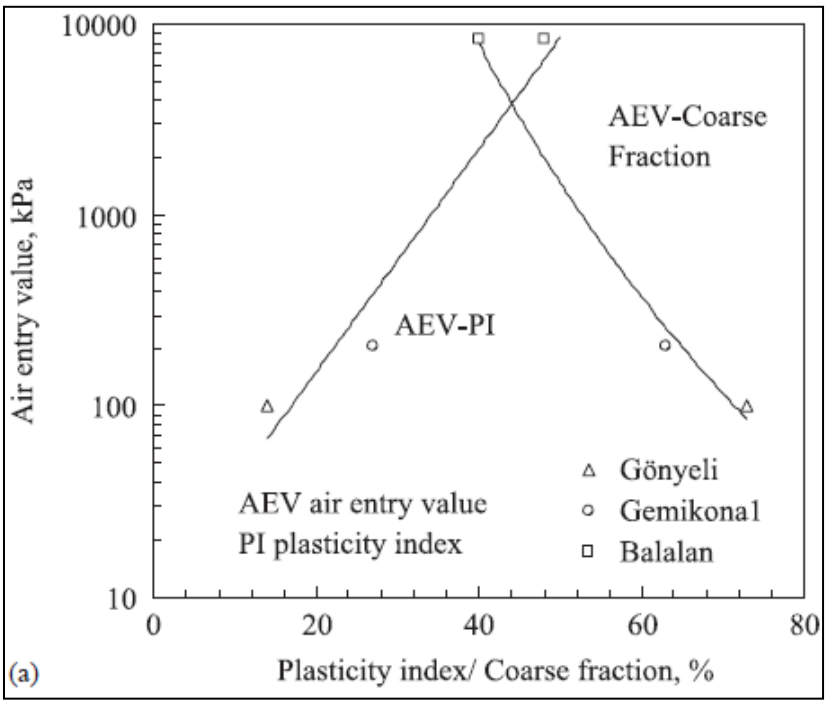

Figure 2.5. Relationships between the air-entry value and plasticity index and percentage of coarse fraction, Bilsel (2004)

2.4. Hysteresis in Soil Water Characteristic Curves

The hysteresis loop that is observed between the wetting and drying paths of a SWCC indicates that the soil water characteristic curve is not a unique function. The non-uniform pore size distribution in a soil may result in hysteresis in the soil water characteristic curve. Figure 2.6 shows that at a given soil suction, the water content of the drying curve is higher than that of the wetting curve (i.e. the drying curve lies above the wetting curve). Furthermore, the end point of the wetting curve differs from the starting point of the drying curve because of air entrapment in the soil. The above reasons are considered to be the main causes for hysteresis in the soil water characteristic curve (Fredlund and Rahardjo, 1994). Depending on the in-situ stress state of a soil, there are

generally a number of intermediate drying or wetting scanning curves which lie in between the main drying and wetting curves.

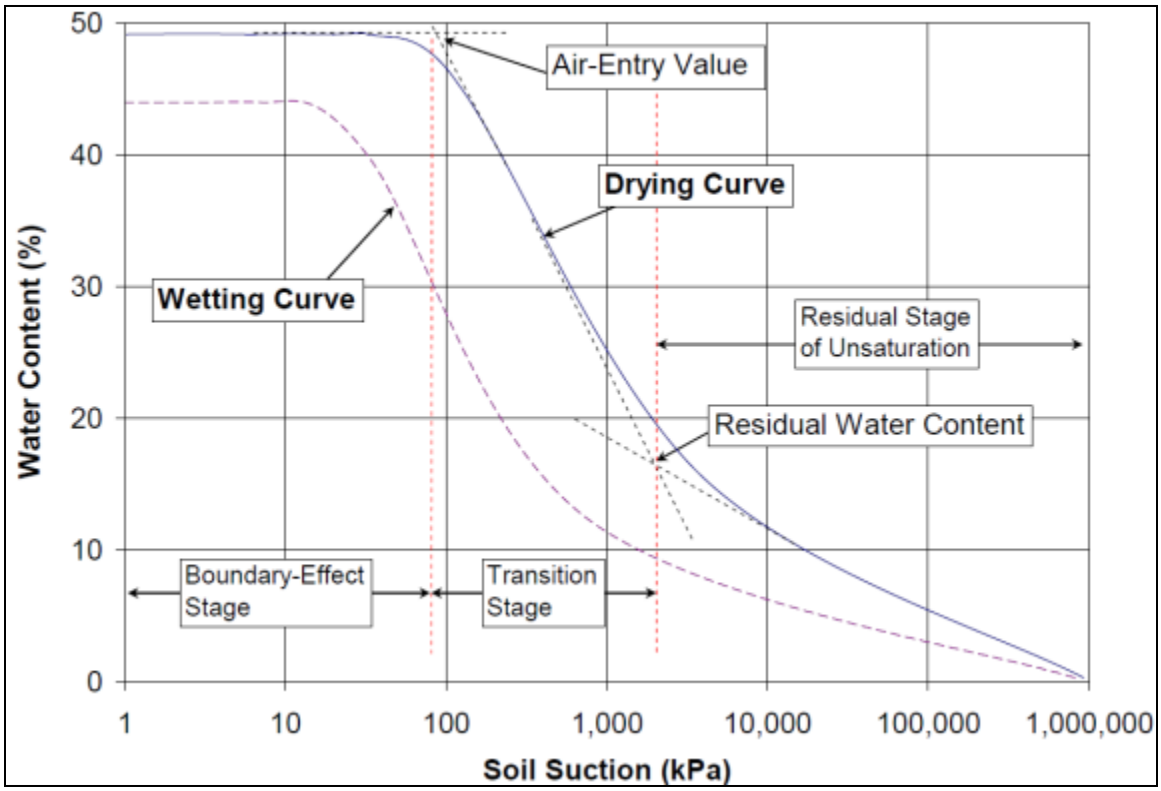

Figure 2.6. Definition of Variables Associated with the Soil Water Characteristic Curve along with wetting and drying curves (modified after Fredlund, 2000 and Chao, 2007)

Fredlund and Houston (2009) illustrated hysteresis in SWCC's and its effect on hydraulic conductivity function estimated from SWCC. This is shown in Figure 2.7.

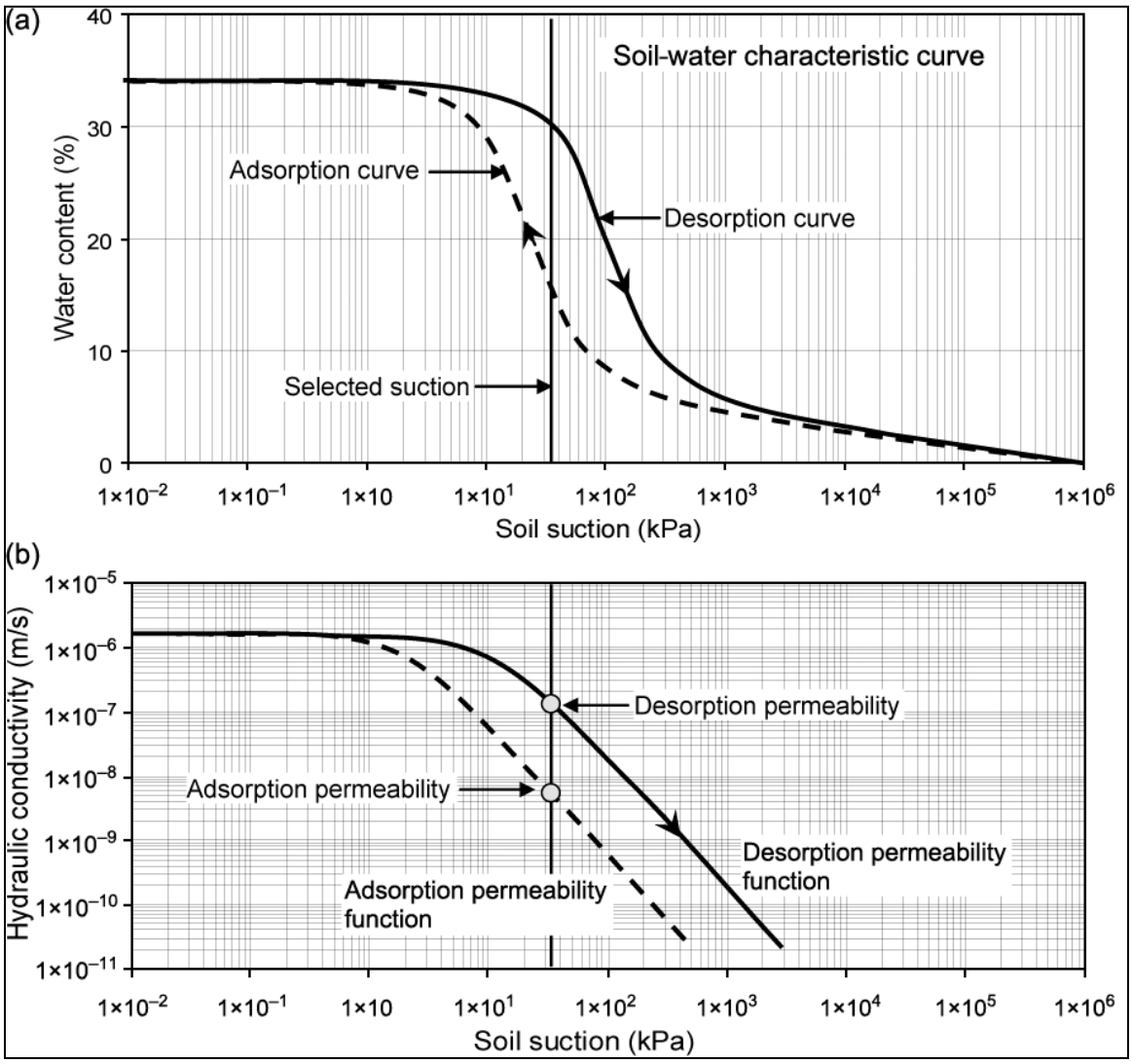

Figure 2.7. Hysteresis in the unsaturated hydraulic conductivity function associated with the drying and wetting soil-water characteristic curve (SWCC) branches. (*a*) Desorption and adsorption SWCC's showing hysteresis; (*b*) effect of SWCC hysteresis on the unsaturated hydraulic conductivity function (Fredlund and Houston, 2009)

Figures 2.8 and 2.9 presented by Pham et al. (2003) illustrate the different curves (e.g. initial drying, wetting, and boundary drying).

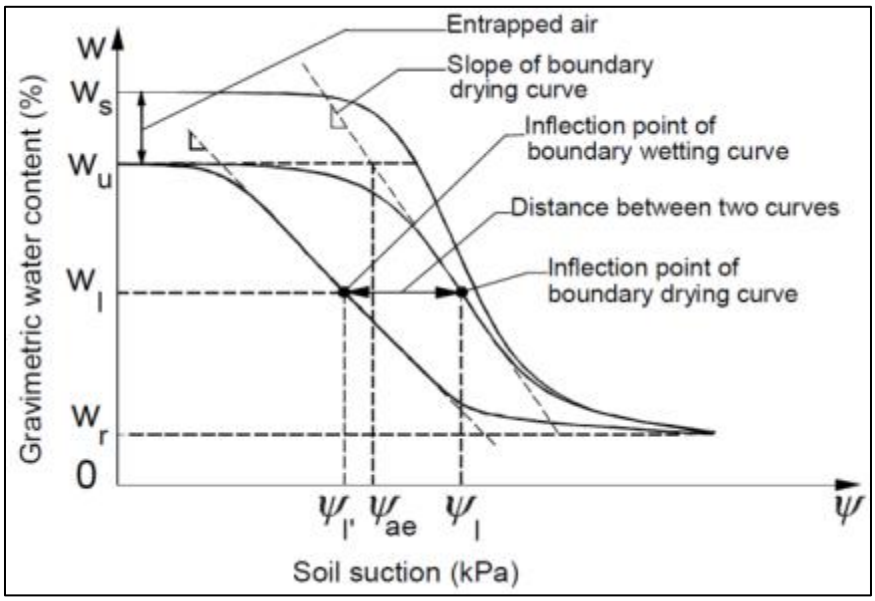

Figure 2.8. Schematic illustration of the slope and distance between the two boundary hysteretic soil-water characteristic curves (Pham et al., 2003)

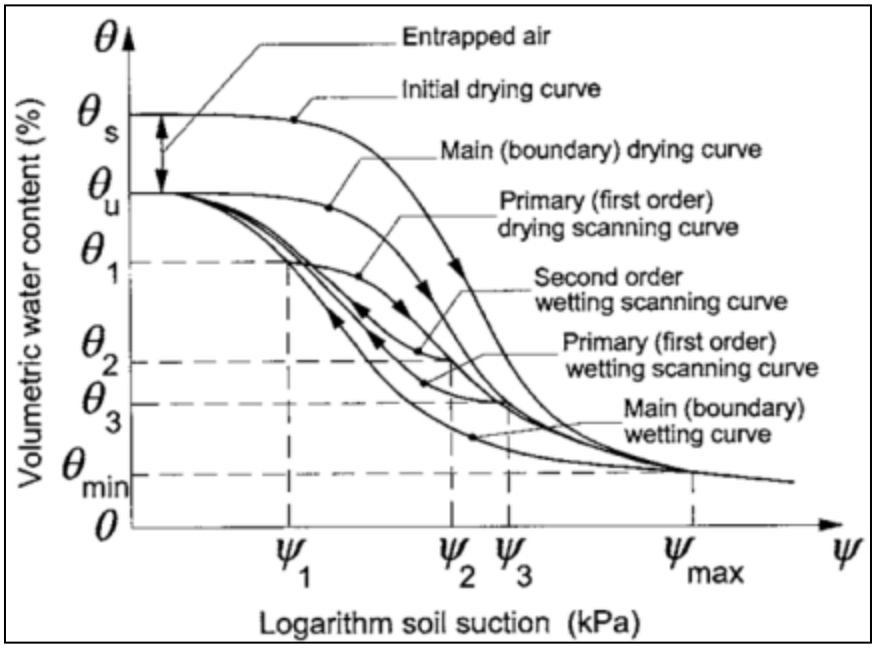

Figure 2.9. Bounding and scanning curves that comprise the drying and wetting behavior of an unsaturated soil (Pham et al. 2003)

Pham (2001) suggested using the estimation values shown in Table 2.1 as an approximation of the lateral shift between the drying and wetting curves when measured data showing the actual shift is not available.

Table 2.1. Suggested shifts of the inflection point between the drying and wetting curves for various soils (Pham 2001)

Soil type	Range of typical shifts (% of a log cycle)	Average shift (% of a log cycle)
Sand	15–35	25
Silt and loam	35–60	50
Clay	—	Up to 100

Pham et al., (2003) reported that the residual water content obtained from the initial drying curve and the boundary wetting curve are essentially the same. Rogowski (1971) reported that the water content at zero soil suction on the initial drying curve is the water content at saturation, while the water content at zero soil suction on the boundary hysteresis curve is approximately equal to 90% of that at saturation.

Pham et al., (2003) used equations and statistical analysis to estimate the distance between the two boundary hysteresis curves. The soil data for this study was obtained from laboratory tests on two soils from Saskatchewan as well as a database of 32 soils obtained from the literature. Following developing an equation the authors compared the measured and estimated drying curves some of which are shown in Figures 2.10 and 2.11.

In the study by Pham et al., (2003) the difference between the hysteresis loops at the inflection points of the two curves was assumed to be the primary indicator of the magnitude of hysteresis. The authors observed that the drying bounding curve and the wetting bounding curves tended to be approximately parallel. Moreover, the authors

reported that for sands, the distance between the main drying and wetting curves was in the range of 0.15 and 0.35 of a log cycle. They also found that the spacing between the main drying and wetting curves for more well-graded loam soils varied between 0.35 and 0.60 of a log cycle.

Several other researchers have measured and evaluated the hysteresis in SWCC's for different soils (e.g. Mualem 1976, Gillham et al., 1976, Topp, 1971, Fleureau et al. 1995, Romero et al. 1999, Feng & Fredlund 1999, Pham 2002, Fleureau et al. 2004, Lins and Schanz 2004, Yang et al. 2004, Fredlund et al. 2011). Figures 2.12 through 2.16 illustrate come of the hysteresis in SWCC measured by different researchers throughout the years, particularly for silty and clayey soils. It can be seen that for all of the cases, the wetting SWCC lies below the drying SWCC. Moreover, generally the end point of the wetting curve is smaller than the starting point of the drying SWCC. This is because some air becomes entrapped in the soil after it is wetted from a stress state in excess of residual suction. Furthermore, the slope of the drying curve is approximately parallel to that of the wetting curve.

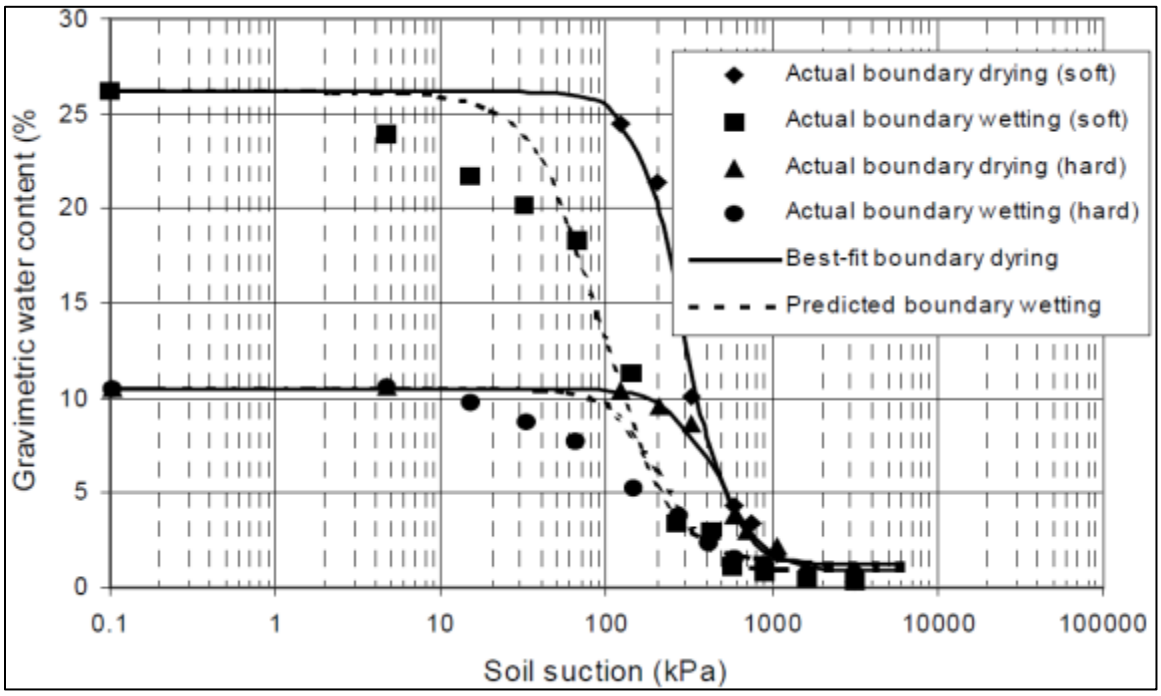

Figure 2.10. Boundary drying and wetting curves for the soft and hard chalks (Pham et al., 2003)

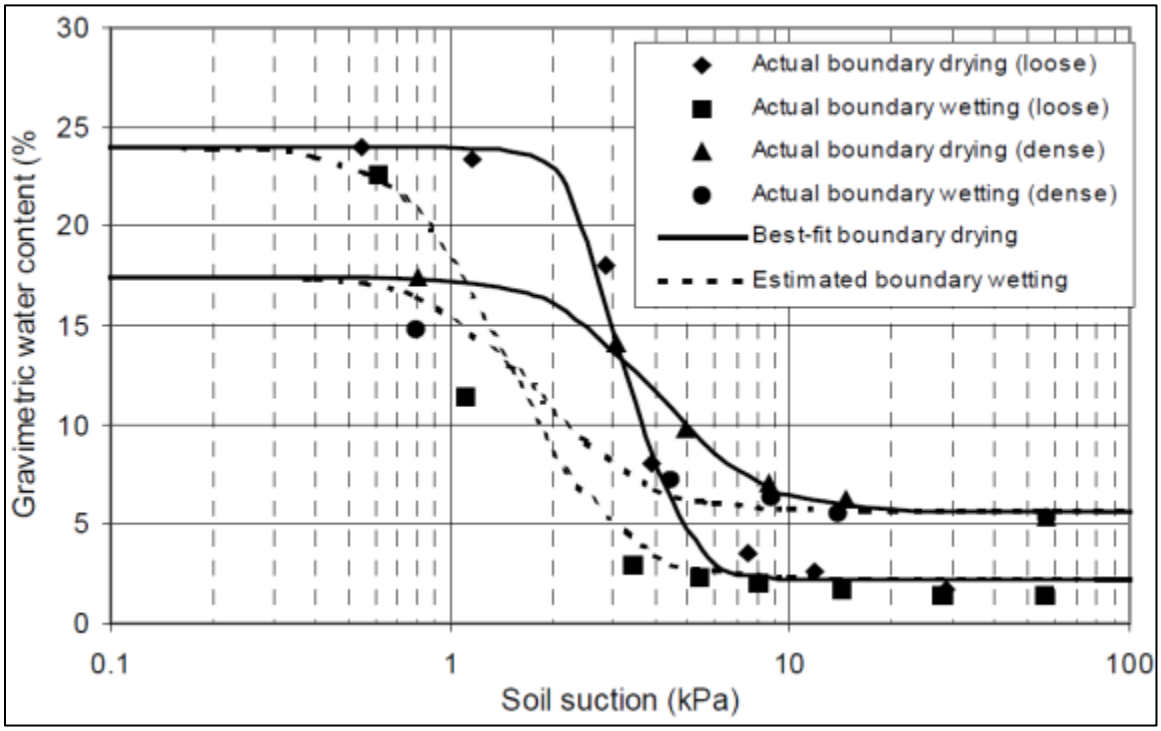

Figure 2.11. Boundary drying and wetting curves for the loose and dense silty sands (Pham et al., 2003)

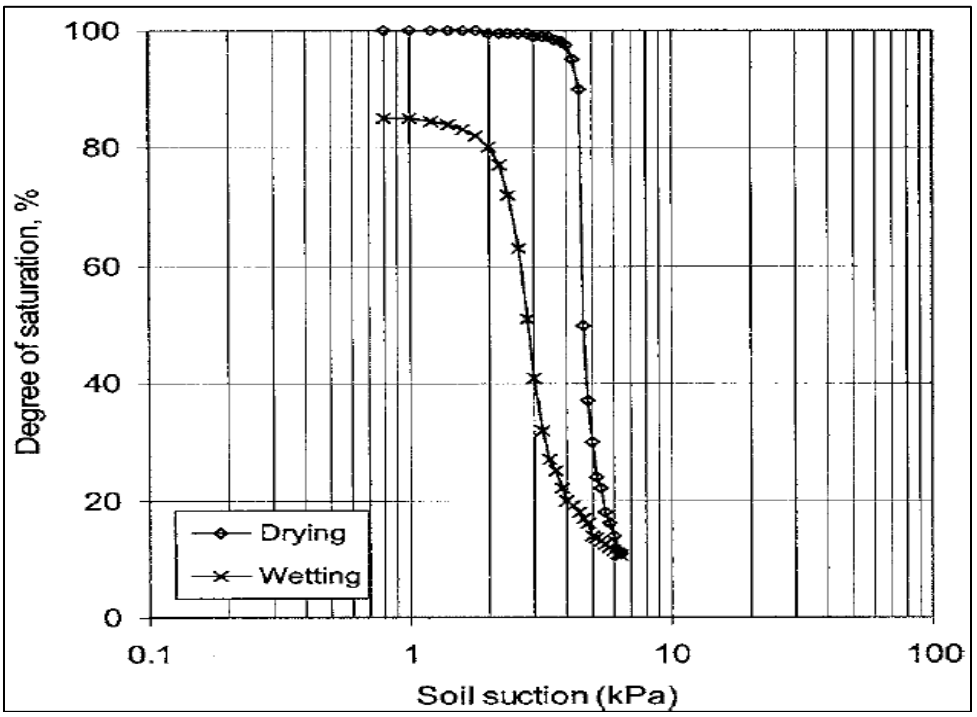

Figure 2.12. The SWCC for the glass beads showing hysteresis during drying and wetting cycles (Mualem 1976)

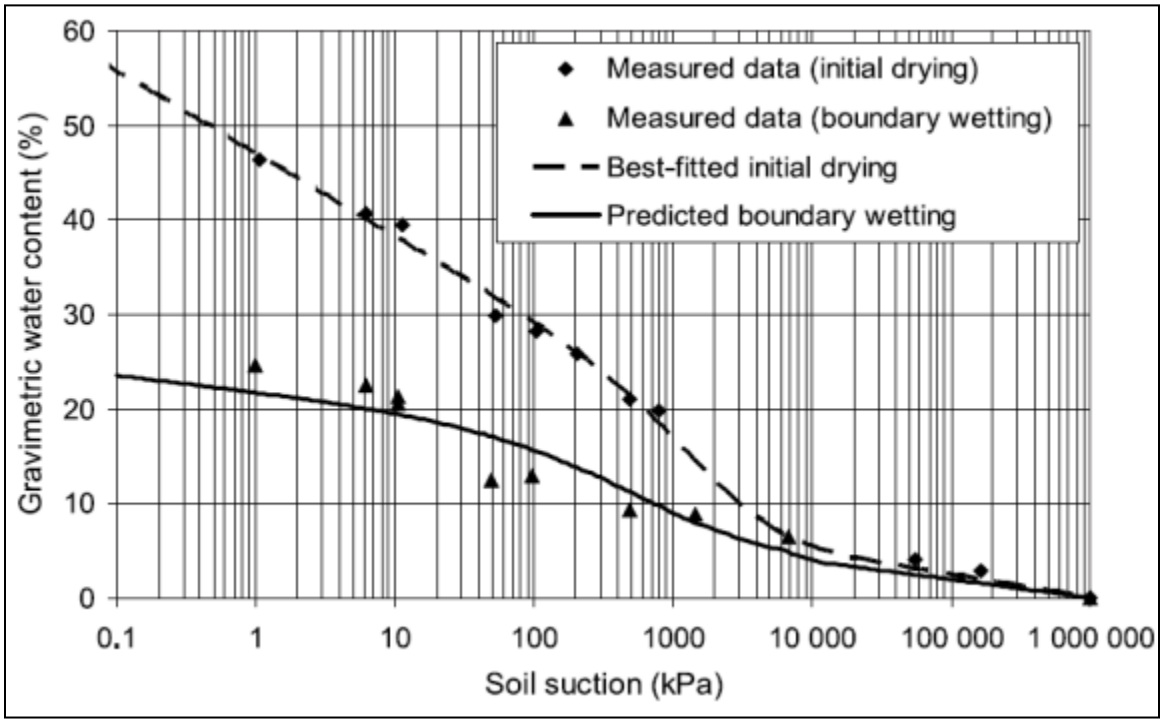

Figure 2.13. Measured data points (Fleureau et al. 1995), best-fitted initial drying, and predicted boundary wetting SWCC's for Jossigny silt

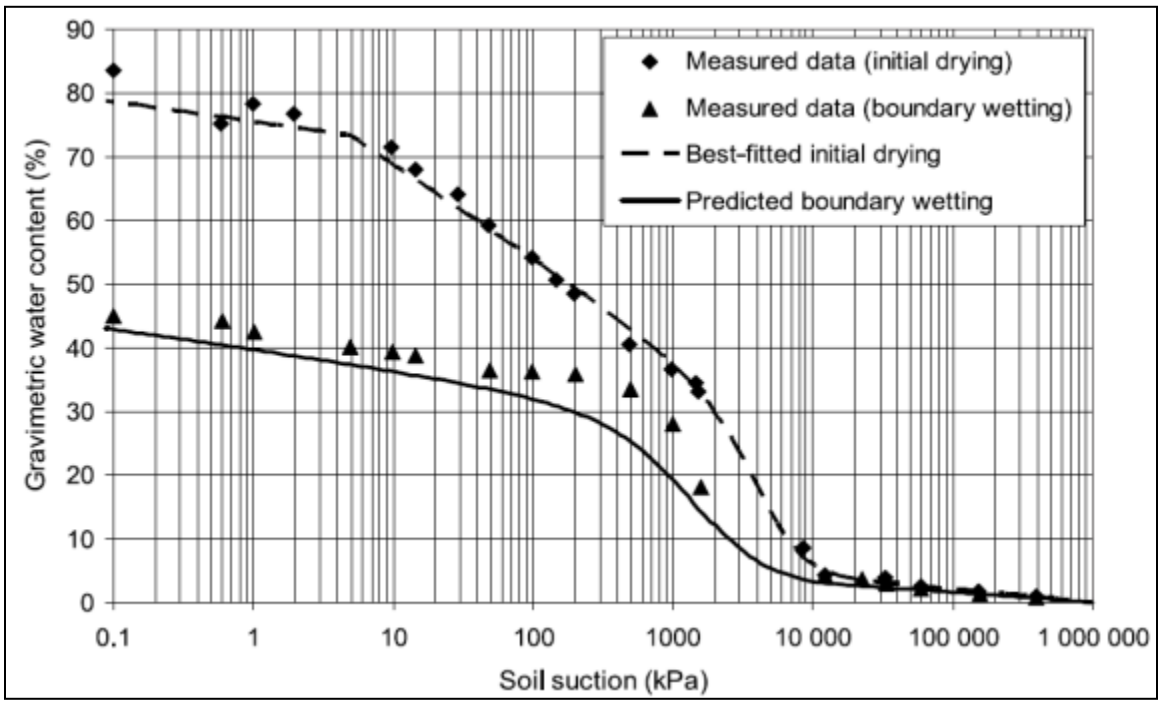

Figure 2.14. Measured data points (Fleureau et al. 2004), best-fitted initial drying, and predicted boundary wetting SWCC's for kaolinite.

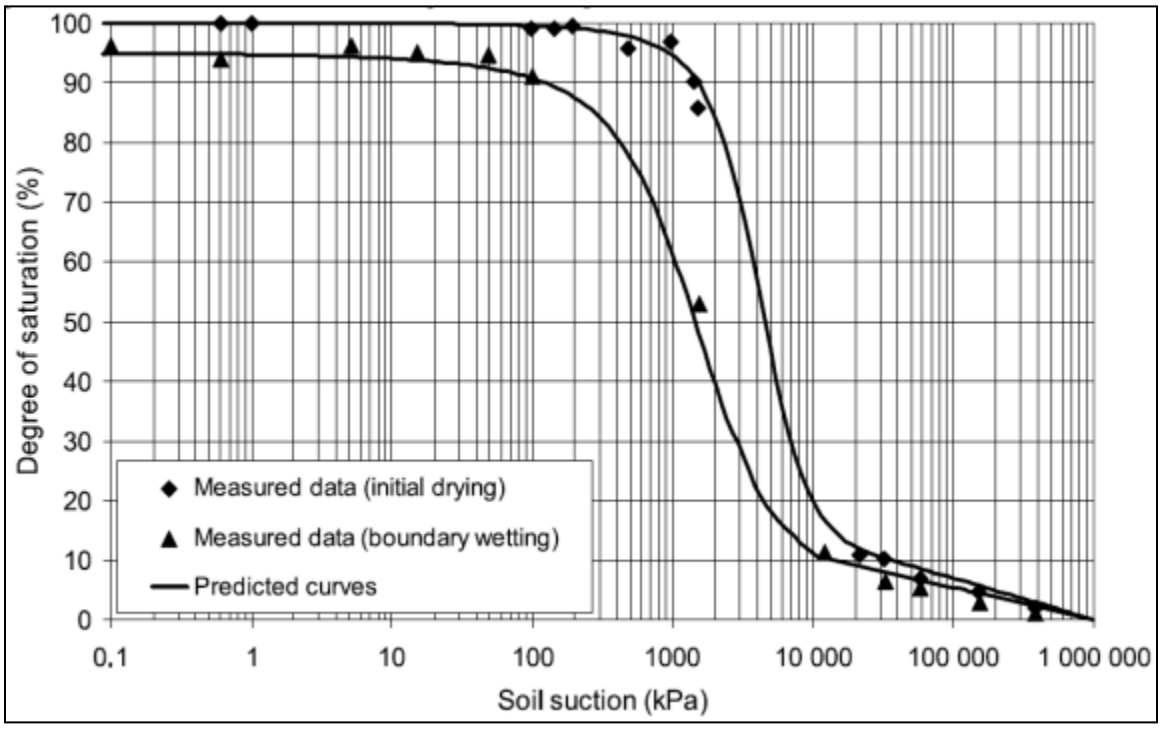

Figure 2.15. Measured data points (Fleureau et al. 2004) and predicted degree of saturation SWCC's for kaolinite

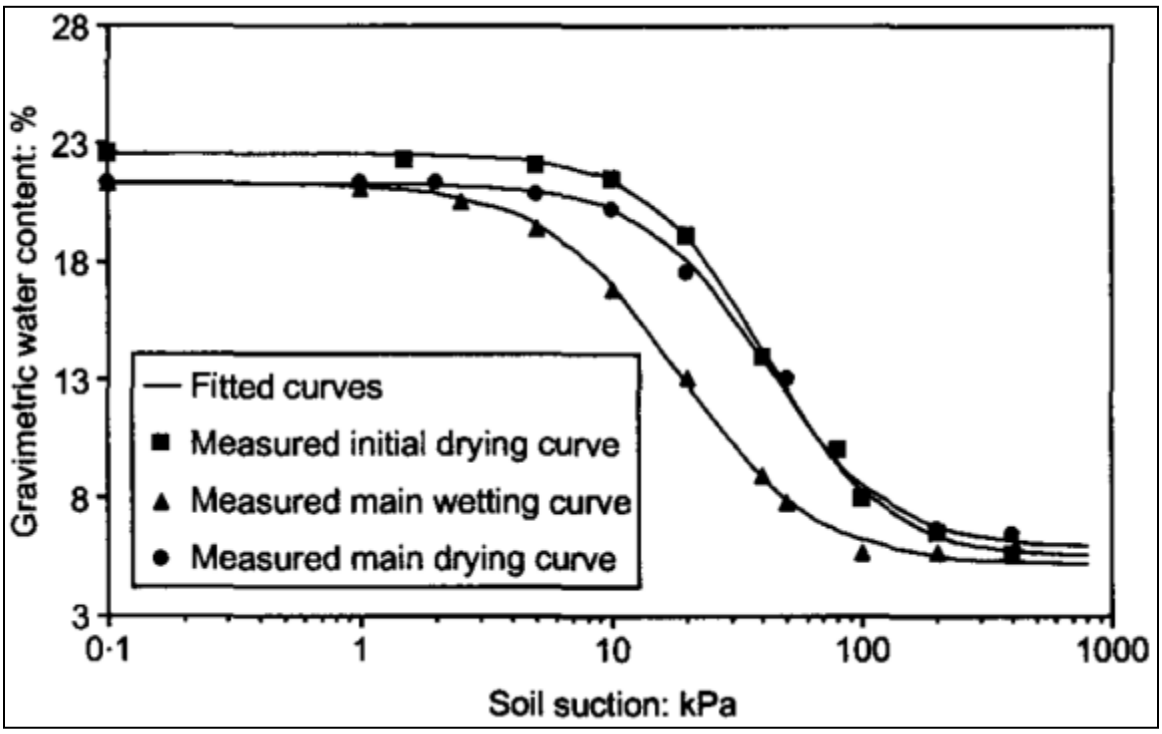

Figure 2.16. Hysteretic SWCC for Processed silt (Pham et al., 2003). The continuous lines are best fit using Feng & Fredlund (1999)

2.5. Impacts of Stress State on Soil Water Characteristic Curves

SWCC has possibly been used more than any other individual soil property to describe the behavior of the unsaturated soil. There are numerous correlations in the literature that use SWCC to estimate the fundamental soil properties such as shear strength and hydraulic properties. The main reason that SWCC has become so popular in the unsaturated soil mechanics is that the technology of its determination has been studied extensively and improved during the past two decades so conducting an SWCC test is relatively inexpensive nowadays. The accuracy of the determination of the SWCC depends on various factors such as: sample preparation technique; initial moisture content of the sample at which it is compacted to the SWCC ring, the water change volume measurement technique; and stress state such as normal stress applied to the specimen

during the course of the test. The focus of this part is on the later factor which is the influence of the stress state on the SWCC.

In the field, due to its depositional history, soil normally experiences a certain stress, which is recognized to have some influence on SWCC (Fredlund and Rahardjo, 1993). Only a few studies have been carried out to investigate the effect of stress state on the SWCC. Vanapalli et al. (1999) postulated that the initial molding water content and stress history have the most influence on the soil water characteristic. Vanapalli et al. evaluated the influences of stress history by loading and unloading specimens in a conventional oedometer type device. The suction-water content relationship ranging from 0 to 1,000,000 kPa was determined using a pressure plate apparatus and vacuum desiccators. The authors used a sandy clay till obtained from Indian Head, Saskatchewan, Canada for the testing program. The properties of this soil are shown in Table 2.2.

Table 2.2. Summary of the soil properties used in Vanapalli et al. (1999) study

Soil Type	Sand %	Silt %	Clay %	ω_L %	ω_P %	USCS Classification
Indian Head Till	28	42	30	35.5	16.8	CL

Since a conventional pressure plate apparatus did not allow specimens to be loaded externally during testing, the authors decided to use specimens that had a stress history which means that the specimens had a known equivalent pressure. Figure 2.17 illustrates the procedure used to induce a predetermined equivalent pressure. After placing a specimen in oedometer, it was saturated and loaded to 200 kPa (Point A in Figure 2.17). Then it was allowed to swell under a small nominal pressure of 3.5 kPa (point B in Figure 2.17). Although the specimen has experienced the maximum pressure

of 200 kPa, after swelling under the nominal 3.5 kPa pressure it had a void ration corresponding to 100 kPa on the initial compression curve. Thus, the equivalent pressure for this specimen is equal to 100 kPa.

SWCC's were developed for sample prepared dry of optimum and subjected to a range of equivalent pressures (25, 35, 80 and 200 kPa). Figure 2.18 shows the results for all of the SWCC's and it can be clearly seen that the air-entry value of the samples tend to increase as the equivalent pressure increases. Beyond the AEV, samples subjected to higher equivalent pressures exhibited higher degree of saturation at a given suction. Vanapalli et al. attributed this effect to the macrostructure of the soil. The authors believe that the macrostructure governs the SWCC behavior for specimens compacted with initial water contents dry of optimum, particularly at low suction values. However, for specimens compacted at the optimum or wet of optimum, the SWCC was not significantly influenced by the stress state for the tested range (i.e. 0-200 kPa).

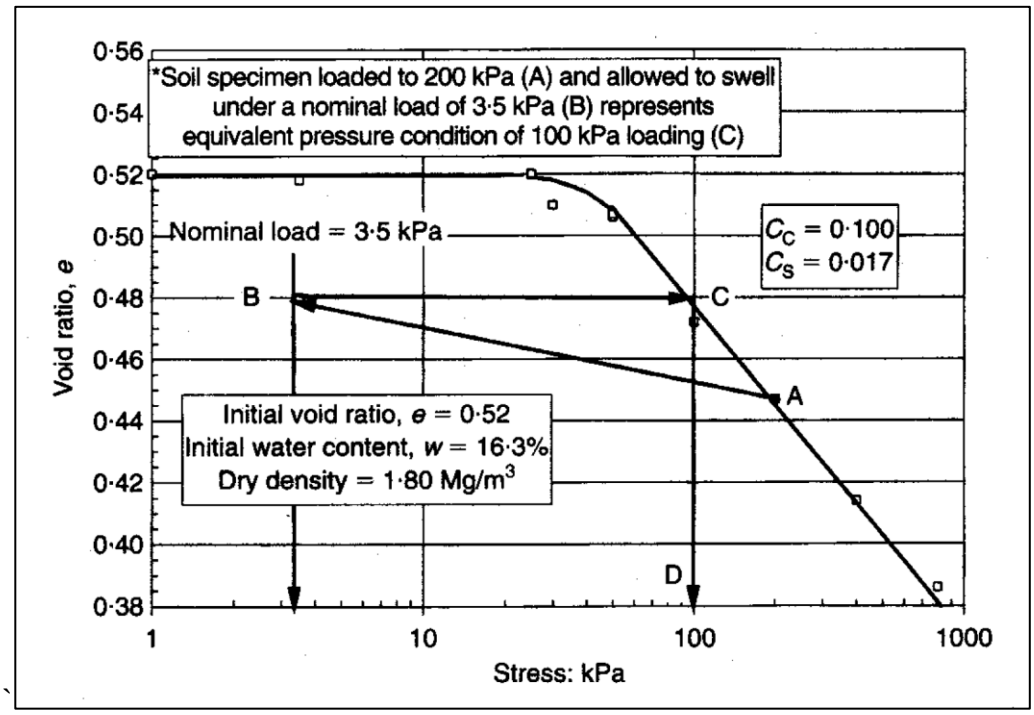

Figure 2.17. Illustration of the equivalent pressure concept (Vanapalli et al. (1999))

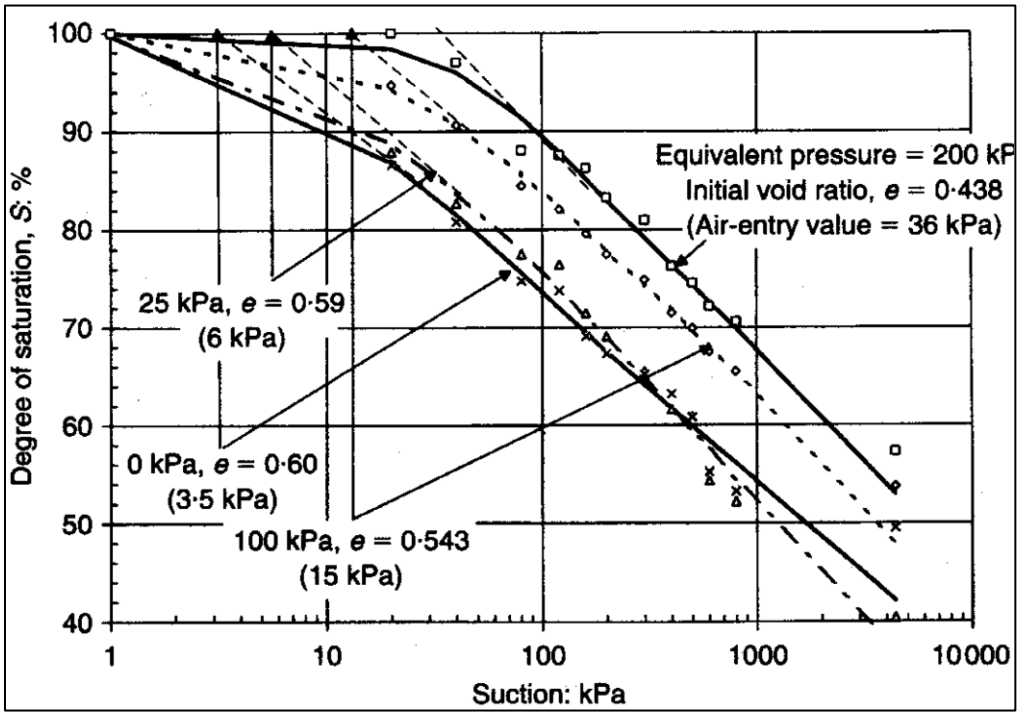

Figure 2.18. The effect of the equivalent pressure on the SWCC for specimens compacted dry of optimum (Vanapalli et al. (1999))

Vanapalli et al. (1999) showed that the SWCC is not significantly affected by either the initial moisture content or the stress state at higher suctions (i.e. > 20,000 kPa). This is shown in Figure 2.19.

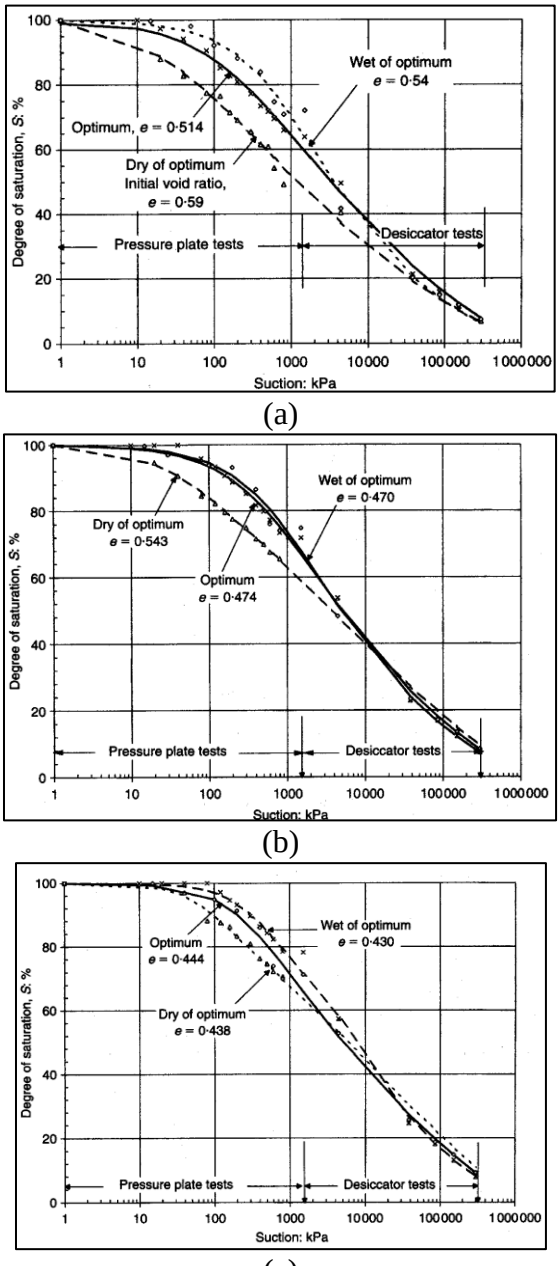

Figure 2.19. The effect of the equivalent pressure on the SWCC at high suction values (Vanapalli et al. (1999))

Ng and Pang (2000) studied the influence of the stress state on the SWCC of an "undisturbed" or natural, completely decomposed volcanic soil. They used a modified volumetric pressure plate extractor capable of controlling the one-dimensional total net normal stress and axial deformation.

The soil used in this study was obtained from an undisturbed 200 × 200 × 200 mm^3 block sample excavated from a slope in Shatin, Hong Kong. Table 2.3 summarizes some index properties of the soil.

Table 2.3. Index properties of the decomposed volcanic soil (Ng and Pang, 2000)

Specific gravity (Mg/m3)	2.62
Maximum dry density (kg/m3)	1,603
Optimum moisture content (%)	22
Initial moisture content (%)	30
Gravel content (%)	4.9
Sand content (%)	20.1
Silt content (%)	36.6
Clay content (%)	37.1
Coefficient of curvature Cc	1.057
Coefficient on uniformity Cu	319.9
Liquid limit (%)	55.4
Plastic limit (%)	33.4
Plasticity index (%)	22

Three undisturbed samples were directly cut from the block into oedometer ring and then submerged in de-aired water inside a desiccator subjected to a small vacuum for about 24 hours for saturation. One of the samples was placed in the conventional volumetric pressure plate extractor to determine the SWCC with zero normal stress and the other two with 40 and 80 kPa of vertically applied net normal stresses under K_o conditions. Free drainage from top and bottom was allowed for the first 24 hours after

applying the pressures for pre-consolidation purposes. Then the samples were subjected to suction for SWCC determination. The SWCC results are shown in Figure 2.20.

The results from Ng and Pang study indicated that under zero suction, soil samples loaded to a higher net normal stress exhibit a lower initial volumetric water content. There is a tendency to change the volumetric water content at a slower rate as values of suction increases for the soil loaded to a higher stress. Furthermore, there is a general and consistent trend for a soil specimen to possess a larger air-entry value when it is subjected to a higher stress. This is probably attributed to the presence of smaller interconnected pores in the soil specimen under higher applied load.

In general, stress history of the applied normal stress does not seem to affect the shape of the SWCC significantly; however, the AEV increases and the rate of degree of saturation change decreases with increasing the net normal stress.

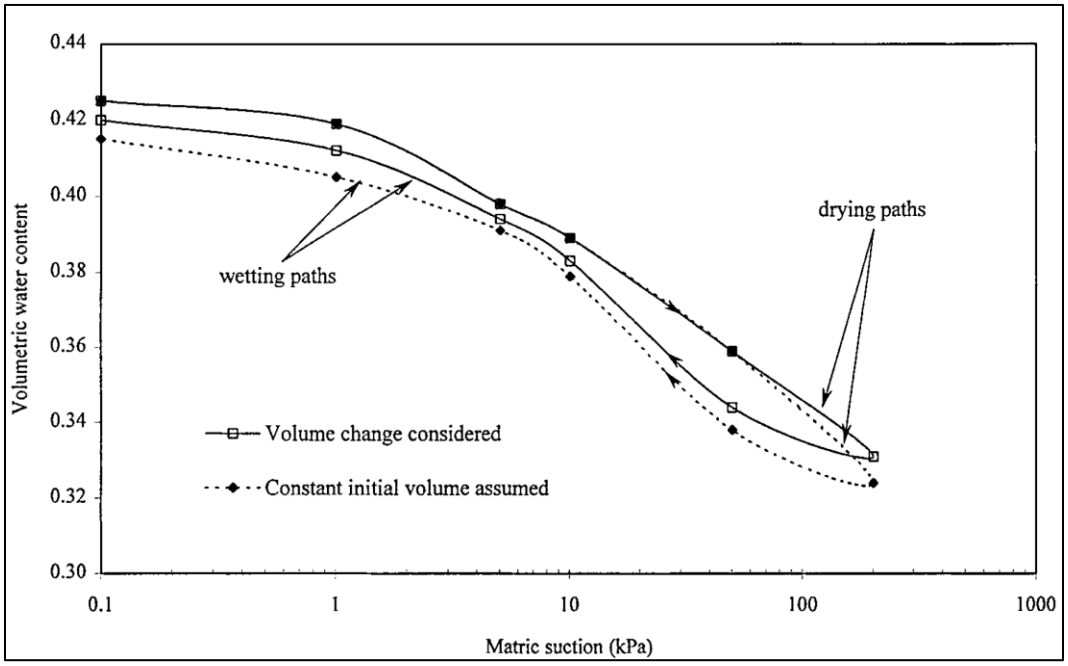

Figure 2.20. The effect of the net normal stress on the SWCC (Ng and Pang (2000))

2.6. Correcting Soil Water Characteristic Curves for Soil Volume Change

Suction induced volume change in expansive soils occurs due to changes in the water content of the soil which affects the stress equilibrium of the soil. Consequently, when determining the SWCC of an expansive soil, it is important to consider the volume change that occurs as the suction (and hence the water content of the soil) changes during the test (Chao et al., 2008). This reportedly is not the common practice and the SWCC is usually measured assuming no volume change of the soil specimen. This assumption may not be correct for expansive soils. When determining the SWCC of an expansive soil, it is important to consider the volume change that occurs as the suction changes during the test (Chao et al. 2008).

Soil water characteristic curve fitting equations have been generated by a number of researchers (e.g., Gardner 1956; Brooks and Corey 1964; van Genuchten 1980; Fredlund and Xing 1994). Although not always mentioned, the underlying assumption of most SWCC fitting equations is that the soil is sufficiently stiff so that there is no change in void ratio of the soil (i.e. soil volume change) during the test (Mbonimpa et al., 2006, Chiu and Ng, 2012). Nonetheless, some of these equations have been extended for use in case of high volume change materials. Pham and Fredlund (2008) proposed two SWCC equations for best-fitting the SWCC for a wide range of soils types including high volume change clays. A number of researchers have attempted to predict the SWCC's of expansive soils (Chertkov 2004; Mbonimpa et al. 2006). Gallipoli et al. (2002, 2003) have proposed an expression for the degree of saturation based on the well-known van Genuchten (1980) model, where the shape parameter which is related to the air-entry

value, is expressed as a function of void ratio. The van Genuchten (1980) model has also been used by Stange and Horn (2005) who proposed an expression for volumetric water content by accounting for the dependence of the saturated and residual volumetric water contents and the shape parameters on void ratio *e*.

Mbonimpa et al. (2006) extended modified Kovács model which predicts the soil water characteristic curve using basic properties for incompressible soils to clayey soils showing suction induced volume change. The authors performed this by introducing the shrinkage curve in the formulation. The authors used previously measured data points for soil water characteristic curve and shrinkage curve from SOILVISION (SoilVision Systems Ltd., 1999), Fleureau et al. (1993, 2002), and Biarez et al. (1987) for validating their model.

A soil volume measurement method that has been used by some researchers is measuring the displaced volume of a fluid when the soil sample is dipped in it. Salager et al. (2010) recommended the use of Kerdane as this fluid was found to generate reasonable results. The principle of the method was first described by Head (1980), and the use of Kerdane has been described among others by Zerhouni (1991) and Abou-Bekr et al. (2005). In this method of volume measurement, the specimen gets destroyed. The authors mentioned that due to destructiveness of this technique, it is not appropriate for testing natural soils, where variability among specimens may become a major issue.

According to Salager et al. (2010), the water characteristic behavior of a soil is better represented by a surface instead of the usual curve. The researchers determined the surface based on measurement of void ratio, suction, and water content along the drying

path. Salager et al. (2010) established an experimental program in which suction was applied to the previously saturated samples in a pressure-plate apparatus. At equilibrium, the water content and void ratio of the samples were measured. The method used by the authors for volume measurement was based on the general method using fluid displacement described, for instance. The fluid used for volume change measurement was Kerdane. Kerdane is light hydro-treated petroleum distillate with density of about 800 kg/m^3 essentially designed for heating and used as fuel in mobile heating devices such as domestic oil stoves.

Ng and Pang (2000) reported the issues related to volume change when determining the SWCC of a sandy silt and clay mixture using a modified pressure plate extractor. The authors proposed to verify the no volume change assumption throughout the drying-wetting processes. They concluded that the conventional assumption of no volume change in the pressure plate tests would lead to inaccurate estimation of the soil properties.

Stange and Horn (2005) conducted laboratory experiments on sandy and silty soil samples collected at three sites in Germany in order to determine the SWCC. They measured the gravimetric water contents and the volumes of the samples after each equilibration, which were used to calculate volumetric water contents. The actual soil volume was determined using vernier caliper measurements. The authors found the importance of considering the volume change during the tests.

Chao et al. (2008) conducted experiments on Claystone samples of the Denver and Pierre Shale Formations obtained near Denver, Colorado using the SWC-150 device

and the filter paper method. The authors studied the effect of the volume changes on the SWCC of expansive soils. The authors used calipers to measure the height and diameter of the sample in order to determine the volume. Measurements of the weight and volume of the sample at equilibrium were recorded throughout the experiment. The authors reported importance of measuring the volume change during the test and correcting the SWCC for the volume change.

Pham and Fredlund (2008) developed two equations for SWCC based on the laboratory tests starting from a slurry condition and continuing to completely dry conditions, during which the sample exhibited high volume changes. Both of the proposed SWCC equations define the soil suction versus gravimetric water content over the entire range of possible soil suctions.

Fredlund and Houston (2013) reported that not correcting SWCC's for soil volume change that occurs during the SWCC test (particularly soils with high volume change potential), can lead to unrealistic results namely the estimated air-entry value of the soils. The authors described the procedure with which the SWCC obtained from laboratory results can be corrected for volume change with the use of a shrinkage curve. The authors suggested two approaches for correcting SWCC's for the volume change, the first one being to use laboratory devices capable of volume change measurement. The next method is to generate shrinkage curves which define the relationship between gravimetric water content and void ratio of the soil tested. For developing the shrinkage curve the authors suggested using digital micrometers for soil volume measurement. Fredlund and Houston (2013) demonstrated the importance of considering the soil

volume change (as soil suction changes) by developing SWCC's for oil sands tailings and Regina clay with and without volume change consideration and compared the results (i.e. with particular focus on air-entry value of the soils).

These SWCC's are shown in Figures 2.21 and 2.22. The authors recommended using volume corrected SWCC in terms of degree of saturation for the estimation of the true air-entry value of the soil.

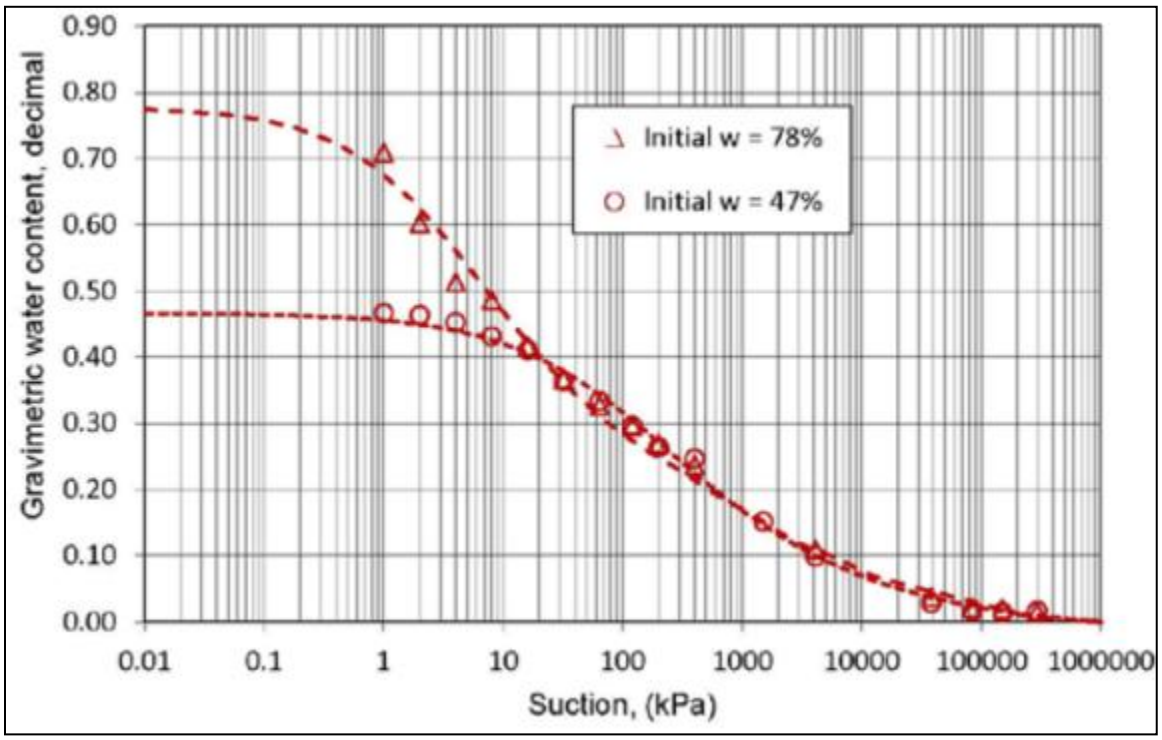

a)

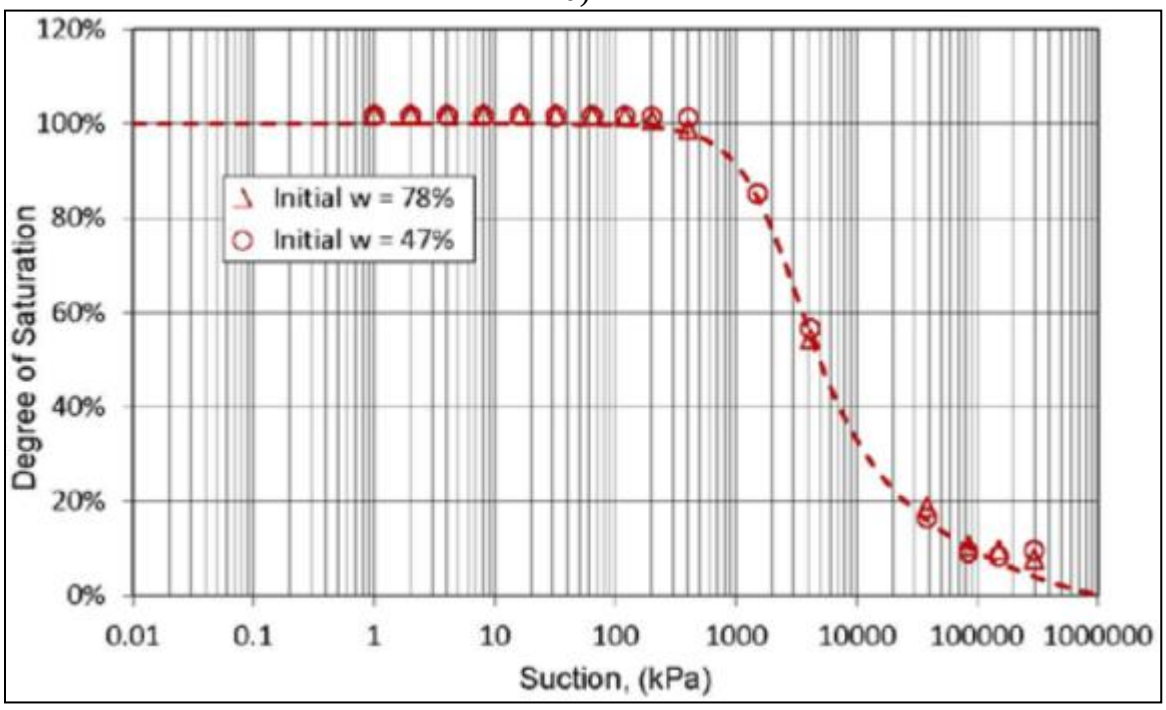

b)

Figure 2.21. a) Gravimetric water content SWCC's measured on the Oil Sands tailings with two initial moisture contents of 78% and 47%, b) SWCC's plotted as the degree as

saturation versus suction for the Oil Sands tailings considering volume change of the soil (After Fredlund and Houston, 2013)

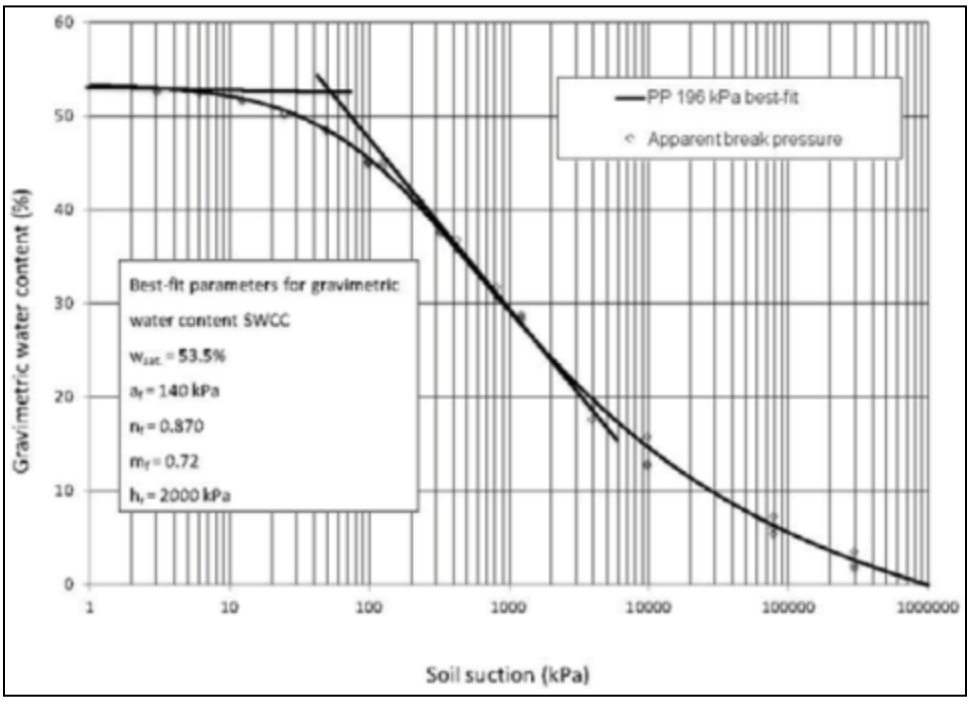

a)

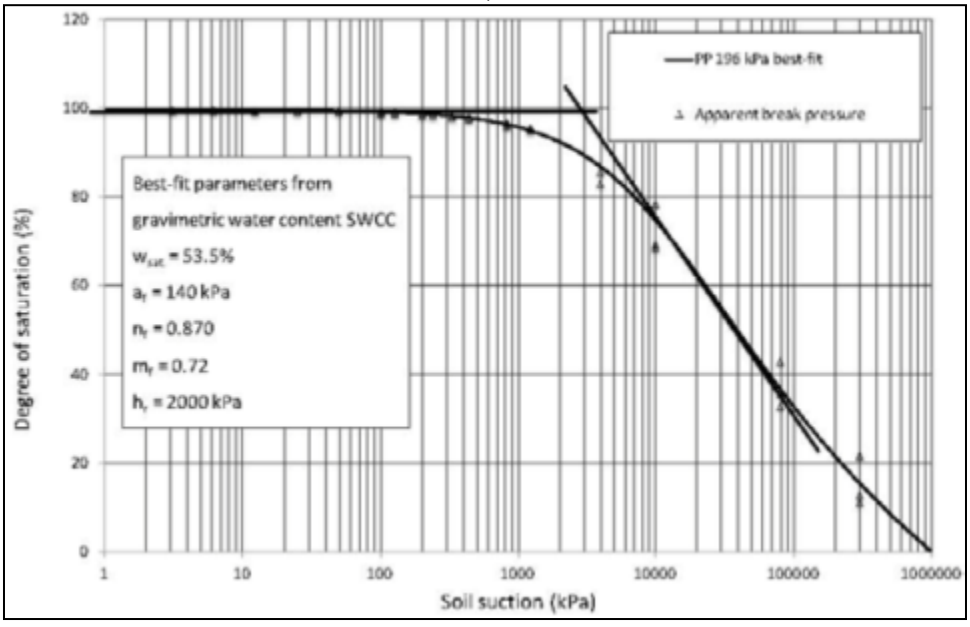

b)

Figure 2.22. a) Gravimetric water content SWCC's on Regina clay preconsolidated to 196 kPa, b) SWCC's plotted as the degree as saturation versus suction for the Regina clay

preconsolidated to 196 kPa considering volume change of the soil (After Fredlund and Houston, 2013)

Ng and Pang (2000) studied the effect of volume changes on the SWCC during a wetting and drying cycle using a modified volumetric pressure plate extractor in which the total normal stress can be controlled one-dimensionally and the axial deformation can be measured. The authors, like many others, recognized the importance of volume change measurement and consideration in generating SWCC's.

Chiu and Ng (2012) conducted a laboratory study in which they used a modified triaxial apparatus and a one-dimensional stress controllable pressure plate apparatus to measure the SWCC. The modified apparatus used in their study is a double-cell triaxial system where an open-ended, bottle-shaped inner cell is installed inside a conventional triaxial cell together with a differential pressure transducer to measure the total volume change of a specimen (schematic shown in Figure 2.23). The authors used the volume measurements throughout the test for generating volume corrected SWCC in terms of degree of saturation. Throughout the drying and wetting tests, the vertical displacement, volume change, and water volume change of the specimens were continuously monitored. The authors found it important to account for volume change when determining SWCC. The authors recommended use of degree of saturation SWCC.

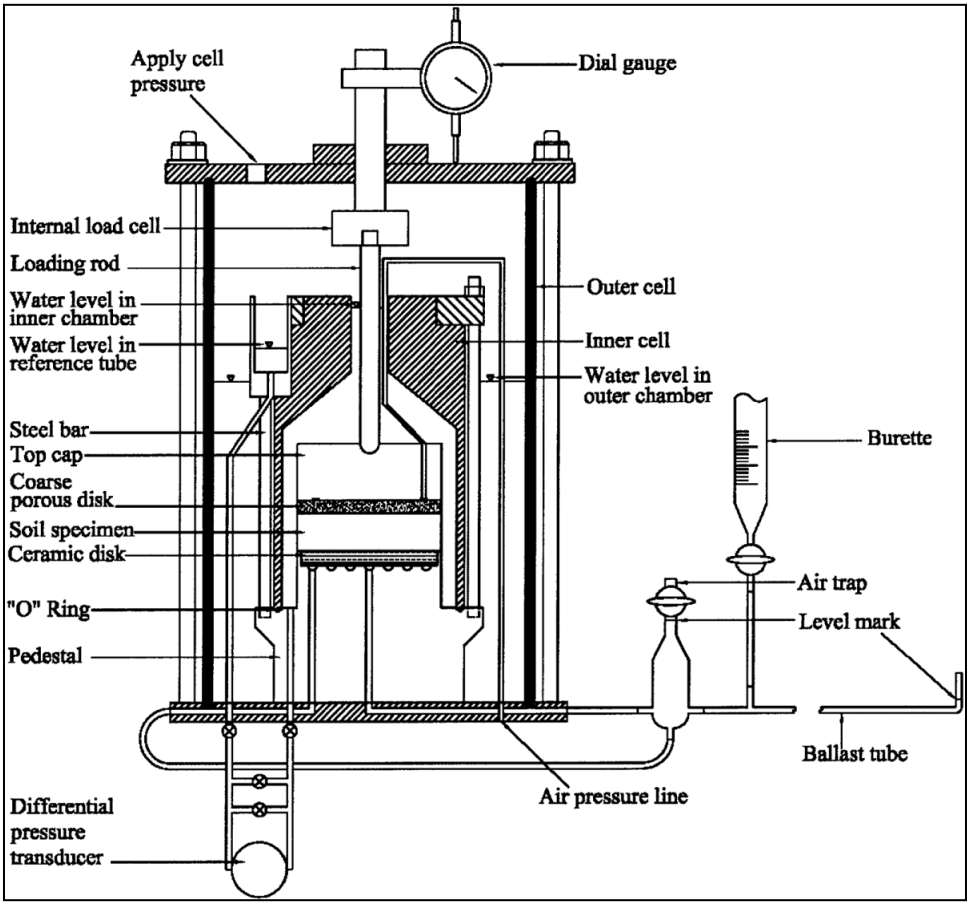

Figure 2.23. Schematic layout of modified triaxial stress path apparatus (After Ng et al., 2012)

Vazquez and Durand (2011) determined the SWCC of high plasticity clay by running the test, while measuring the dimensions of the sample throughout the test using a caliper. Like many other researchers, the authors found the importance of volume change consideration for obtaining the true SWCC.

Liu et al. (2011, 2012) reported that the volume change measurement is essential for obtaining the true degree of saturation at different suction values throughout the SWCC test. The authors measured the vertical (axial) volume change measurement method in which a vertical load is applied to the sample to ensure the contact between the

sample and the confining ring. This method, obviously assumes that the full contact of soil and ring is maintained throughout the test, therefore, considerable volume measurement errors may occur for the cases in which the full contact of soil and confining ring is not maintained throughout the test. The authors developed a modified SWCC device which can measure and record volume changes during the test. Liu et al. (2011, 2012) also evaluated the effect of volume change on the SWCC. They found the volume change of the soil to be an important factor in the soil SWCC. The authors reported the case in which the initial volumetric water content of the soil was 0.1. For this case, a volume change of 3% occurred during the test, and not considering it led to 0.3% error in the volumetric water content determination. The authors reported that the errors become larger with larger initial water content values of the soil.

Cui et al. (2006) conducted SWCC tests and developed curves for Romainville clay from the basin of Paris. Two suction control methods were used: 1) the osmotic method for low suction range (1-6.1 MPa) and 2) the vapor equilibrium technique for high suction range (6.1- 216 MPa). The authors followed both wetting and drying curves and at each suction soil samples were weighed and the volume of samples was determined by using a mercury immersion system. For the volume measurement of the soil, the soil samples were first weighed in air, then immersed in mercury and weighed again. The obtained weights allowed the volume to be determined.

Qi and Michel (2011) developed an apparatus for continues measurement of the SWCC and shrink/swell properties of soil during wetting/drying cycles. During the test with this apparatus, sample height, weight and pressure head were recorded every minute

during drying and wetting cycles using a linear variable differential transducer (LVDT), a balance, and a ceramic cup inserted at the center of the sample and connected to a pressure transmitter.

Huang et al. (1998) proposed a model to fit SWCC data for highly compressible materials. However, their model did not allow representation of some features that are relevant for highly compressible materials, such as nonlinear variation of the void ratio for suctions lower than the air-entry value, partial desaturation that occurs in the vicinity of the air-entry value, and variation of the void ratio for suctions higher than the air-entry value (Parent et al., 2007).

Price and Schlotzhauer (1999) reported that accounting for suction induced volumetric changes plays a significant role in the accuracy of the SWCC. Cabral et al. (2004) described a testing apparatus, based on the axis translation technique that allows measurement of volumetric changes continuously during determination of the SWCC in highly compressible materials.

Parent et al. (2007) conducted a test in which water content, matric suction, and volumetric deformation data of the material tested were obtained using an experimental technique that allowed determination of the SWCC's of highly compressible materials (such as highly plastic clays). Additionally, Parent et al. (2007) reported that volumetric changes occurred during desaturation (i.e. shrinkage) can significantly influence the shape of the SWCC. The authors mentioned that specifically, the volumetric changes affect the calculated volumetric water content or degree of saturation. They found that volumetric water contents are underestimated if volume changes are not accounted for,

which leads to inaccuracies in the SWCC's, thus inaccurately predicted unsaturated hydraulic conductivity functions that are based on SWCC's. The authors also developed a new model for describing the suction induced consolidation curve (void ratio function) and SWCC for soils with high volume change potential. The authors recommended that in the case of soils with high volume change potential, the air-entry value should be determined on a degree of saturation versus suction relationship, rather than on the volumetric water content versus suction curve, because the volumetric water content of a compressible specimen can start to decrease while the material remains saturated, which might be misleading when trying to determine air-entry value on such a curve.

Nuth and Laloui (2008) recommended using degree of saturation SWCC as opposed to gravimetric moisture content. The authors reported that when the soil undergoes volume change during a suction increase, only the degree of saturation variable clearly defines the air-entry value for the soil (as opposed to gravimetric and volumetric water content).

Parent et al. (2007) presented a set of plots comparing the SWCC's with and without volume change consideration. Based on the data, the authors found that volumetric water contents are underestimated if volume changes are not considered, particularly at high matric suction values. They concluded that the degree of saturation is significantly higher when accounting for volume changes.

Li et al. (2007) obtained the SWCC of Maryland expansive clay by laboratory testing. The authors reported the SWCC's in terms of gravimetric water content and degree of saturation. The authors found that the true air-entry value and other unsaturated

soil properties for an expansive soil can only be obtained from the SWCC in terms of degree of saturation in which volume change of the soil throughout the test is considered. The authors used dial gauges to measure the soil volume change during the test.

2.7. Equations to Best-Fit Soil Water Characteristic Curves Data

Numerous equations have been proposed to best-fit SWCC data. Several of these equations are sigmoidal in character and provide a continuous function over the entire soil suction range. These equations have two or more fitting soil parameters. The equations with more fitting parameters are more likely to closely fit the SWCC data obtained from laboratory (Fredlund and Houston, 2009). The saturated volumetric water content, θ_s, which is present in numerous SWCC fit equations, is determined by considering porosity of the soil whereas the residual volumetric water content, θ_r, is not always determined in the laboratory (Chao, 2007).

Gardner equation (1958) is as follows:

$$\theta_d = \frac{1}{1+\alpha_g \psi^{n}{}_g} \tag{2.2}$$

Where θ_d =w/w_s= dimensionless water content, ψ : any soil suction, α_g is a soil parameter which is a function of the air-entry value of the soil and n_g is a soil parameter which is a function of the rate of water extraction from the soil at the suctions beyond the air-entry value.

Brooks and Corey (1964) equation has the following form:

$$\theta_n = 1 \text{ or } \theta(\psi) = \theta_s \text{ for } \psi \le \psi_{aev} \tag{2.3}$$

$$\theta_n = \left(\frac{\psi}{\psi_{aev}}\right)^{-\lambda_{bc}} \text{ or } \theta(\psi) = \theta_s \left(\frac{\psi}{a}\right)^{-n} \text{ for } \psi > \psi_{aev} \quad (2.4)$$

Where $\theta_n=(w-w_r) / (w_s-w_r)$= normalized water content, θ_s : volumetric water content at saturation, $\theta(\psi)$: volumetric water content corresponding to any soil suction, ψ_{aev} = air-entry value of the soil, ψ : any soil suction, and λ_{bc} = pore size distribution index.

Brutsaert (1967) equation is as follows:

$$\theta_n = \frac{1}{1+\left(\frac{\psi}{\alpha_b}\right)^{nb}} \text{ or } \theta(\psi) = \frac{\theta_s}{1+\left(\frac{\psi}{\alpha}\right)^{n}} \quad (2.5)$$

Where a_b is a soil parameter which is primarily a function of the air-entry value of the soil and n_b is a soil parameter which is primarily a function of the rate of water extraction from the soil at the suction beyond the air-entry value. A modification of Boltzman equation established by McKee and Bumb (1984) is as below:

$$\theta(\psi) = \theta_s \text{ for } \psi \le \psi_{aev} \quad (2.6)$$

$$\theta(\psi) = \theta_s \exp\left(\frac{a-\psi}{n}\right), \text{ for } \psi > \psi_{aev} \quad (2.7)$$

In Laliberte (1969) equation which has the following form:

$$\theta_n = \frac{1}{2} erfc\left[a_1 - \frac{b_1}{c_1 + \left(\frac{\psi}{\psi_{aev}}\right)}\right] \quad (2.8)$$

The parameters a_l, b_l, and c_l are assumed to be unique functions of the pore-size distribution index.

The equation by Farrel and Larson (1972) is as follows:

$$w = w_s - \frac{1}{\alpha_f} \ln \frac{\psi}{\psi_{aev}} \tag{2.9}$$

Where w_s is the saturation gravimetric water content. The equation proposed by Campbell (1974) is presented as:

$$w = w_s \left(\frac{\psi}{\psi_{aev}} \right)^{-1/b_c} \quad \text{for } \psi \geq \psi_{aev} \tag{2.10}$$

$$w = w_s \text{ for } \psi < \psi_{aev} \tag{2.11}$$

The van Genuchten (1980) equation appears to be the most commonly used continuous function for a SWCC. However, according to Fredlund and Houston (2009) its accuracy is somewhat questionable outside the range between the air-entry value and residual suction. This equation has the following form:

$$\theta_n = \frac{1}{\left[1 + \left(\frac{\psi}{\psi_{aev}} \right)^n \right]^m} \text{ or } \theta(\psi) = \frac{\theta_s}{\left[1 + (a\psi)^n \right]^m} \tag{2.12}$$

Van Genuchten – Mualem (van Genuchten 1980) equation has the following form:

$$\theta_n = \frac{1}{\left[1 + \left(\frac{\psi}{\psi_{aev}} \right)^n \right]^m}, \; m = 1 - \frac{1}{n} \tag{2.13}$$

While van Genuchten – Burdine (van Genuchten 1980) equation shows a small difference compared to van Genuchten – Mualem and has the following form:

$$\theta_n = \frac{1}{\left[1+\left(\frac{\psi}{\psi_{aev}}\right)^n\right]^m},\ m = 1-\frac{2}{n} \tag{2.14}$$

In Van Genuchten (1980) equation, *a* is a soil parameter which is primarily a function of air-entry value of the soil; *n* is a soil parameter which is primarily a function of the rate of water extraction from the soil beyond the air-entry value; and *m* is a soil parameter which is primarily a function of the residual water content.

McKee and Bumb (1987) equation is as below:

$$\theta_n = \frac{1}{1+\exp\left(\frac{\psi - a_m}{n_m}\right)} \tag{2.15}$$

In Fredlund and Xing (1994) equation which is one of the most commonly used SWCC fit equations is as below:

$$w(\psi) = C(\psi)\frac{w_s}{\left\{\ln\left[e+\left(\frac{\psi}{a_f}\right)^{n_f}\right]\right\}^{m_f}} \tag{2.16}$$

$$C(\psi) = 1-\frac{\ln\left(1+\frac{\psi}{\psi_r}\right)}{\ln\left[1+\left(\frac{1{,}000{,}000}{\psi_r}\right)\right]} \tag{2.17}$$

Where a_f is a soil parameter which is primarily a function of the air-entry value of the soil; n_f is a soil parameter which is primarily a function of the rate of water extraction from the soil, once the air-entry value has been exceeded; m_f is a soil

parameter which is primarily a function of residual water content; and $C(\psi)$ is a correction factor which is primarily a function of the suction at which residual water content occurs. SWCC equation proposed by Fredlund and Xing (1994) uses a factor that always directs the equation to a soil suction of 1,000,000 kPa at zero water content. This equation can also be written as:

$$w(\psi) = C(\psi) \frac{w_s}{\left\{ \ln\left[e + \left(\frac{(u_a - u_w)}{(u_a - u_w)_{aev}} \right)^n \right] \right\}^m} \tag{2.18}$$

$$C(\psi) = \frac{-\ln\left(1 + \left(\frac{\psi}{\psi_r}\right)\right)}{\ln\left(1 + \left(\frac{10^6}{\psi_r}\right)\right)} + 1 \tag{2.19}$$

where $w(\psi)$ = water content at any soil suction; $C(\psi)$ = correction factor directing all SWCC curves to 1,000,000kPa at zero water content; ψ_r = residual suction; $(u_a - u_w)_{aev}$ = soil parameter indicating the inflection point that bears a relationship to the air-entry value; *n*= soil parameter related to the rate of desaturation; and *m*= soil parameter related to the curvature near residual conditions.

Feng and Fredlund (1999) equation is as below:

$$w(\psi) = \frac{ab + c\psi^d}{b + \psi^d} \text{ or } \theta(\psi) = \frac{\theta_s b + c\psi^d}{b + \psi^d} \tag{2.20}$$

Tani equation (Tani 1982) has the following form:

$$\theta(\psi) = \theta_s \left(1 + \frac{a - \psi}{a - n}\right) \exp\left(-\frac{a - \psi}{a - n}\right) \tag{2.21}$$

Fermi equation (McKee and Bumb 1987) is as below:

$$\theta(\psi) = \frac{\theta_s}{1+\exp\left[(\psi - a)/n\right]} \tag{2.22}$$

Pereira and Fredlund (2000) equation has the following form:

$$\theta(\psi) = \theta_r + \frac{\theta_s - \theta_r}{\left[1 + (\psi / c)^b\right]^a} \tag{2.23}$$

Fredlund and Pham (Pham 2005) equation is as below:

$$w(\psi) = \left\{\left[w_s - \frac{C_c}{G_c}\log(\psi) - w_r\right]\frac{a}{\psi^b + a} + w_r\right\} \times \left\{1 - \frac{\ln\left(1 + \frac{\psi}{\psi_r}\right)}{\ln\left(1 + \frac{10^6}{\psi_r}\right)}\right\} \tag{2.24}$$

Mualem (1976) equation is:

$$\theta = \theta_r + \frac{\theta_s - \theta_r}{\left[1 + a\psi^b\right]^c} \tag{2.25}$$

Williams, et al. (1983) equation has the following form:

$$\ln\psi = a + b\ln\theta \tag{2.26}$$

2.8. Use of Soil Water Characteristic Curves in Constitutive Relations for Unsaturated Soils

Various empirical models and equations have been proposed for the estimation of some of unsaturated soil property functions (e.g., unsaturated hydraulic conductivity, shear strength, volume change). In each case, the estimation procedure involves the use of the saturated soil properties in conjunction with the SWCC. This fact further demonstrates the importance of SWCC in unsaturated soil mechanics. One of the major

used of SWCC is for estimation of unsaturated hydraulic conductivity functions of soils. Some of the most common equations proposed by researchers use hydraulic conductivity of the soil at full-saturation condition along with its SWCC in order to estimate the unsaturated hydraulic conductivity function. The use of such equations has proven to be of practical significance due to the fact that measurement of unsaturated hydraulic conductivity of soils is a time-consuming and expensive procedure.

2.9. Models of Unsaturated Hydraulic Conductivity

The hydraulic conductivity of a saturated soil is typically considered to be constant (McCartney et al. 2007). However, the hydraulic conductivity may change drastically as the soil becomes unsaturated (i.e. suctions beyond the air-entry value).

The relationship between hydraulic conductivity and matric suction is usually referred to as the k_{unsat}-function and represents the change in the hydraulic conductivity of the soil versus matric suction. Since volumetric moisture content (or degree of saturation) of the soil is related to its matric suction (by SWCC), in some literature k_{unsat}-function curve may also be plotted as hydraulic conductivity versus volumetric moisture content (or degree of saturation). In a saturated soil, all the pore spaces between the solid particles are filled with water. Once the air-entry value is k_{unsat}-function exceeded air enters the largest pores and the air-filled pores become non conductive. This phenomenon increases the tortuosity of the flow path. As a result, the ability of the soil to transport water (i.e. the hydraulic conductivity of the soil) decreases (GEO-SLOPE International Ltd., 2012).

Figure 2.24 reported form McCartney et al. (2007) illustrates experimental data points measured by various researchers. It can be seen that at high volumetric moisture content values, coarse-grained soils have higher hydraulic conductivity, while fine-grained soils have lower hydraulic conductivity. The rate of decrease in hydraulic conductivity of coarse-grained soils with decreasing moisture content is steeper than that of fine-grained soils (McCartney et al. 2007).

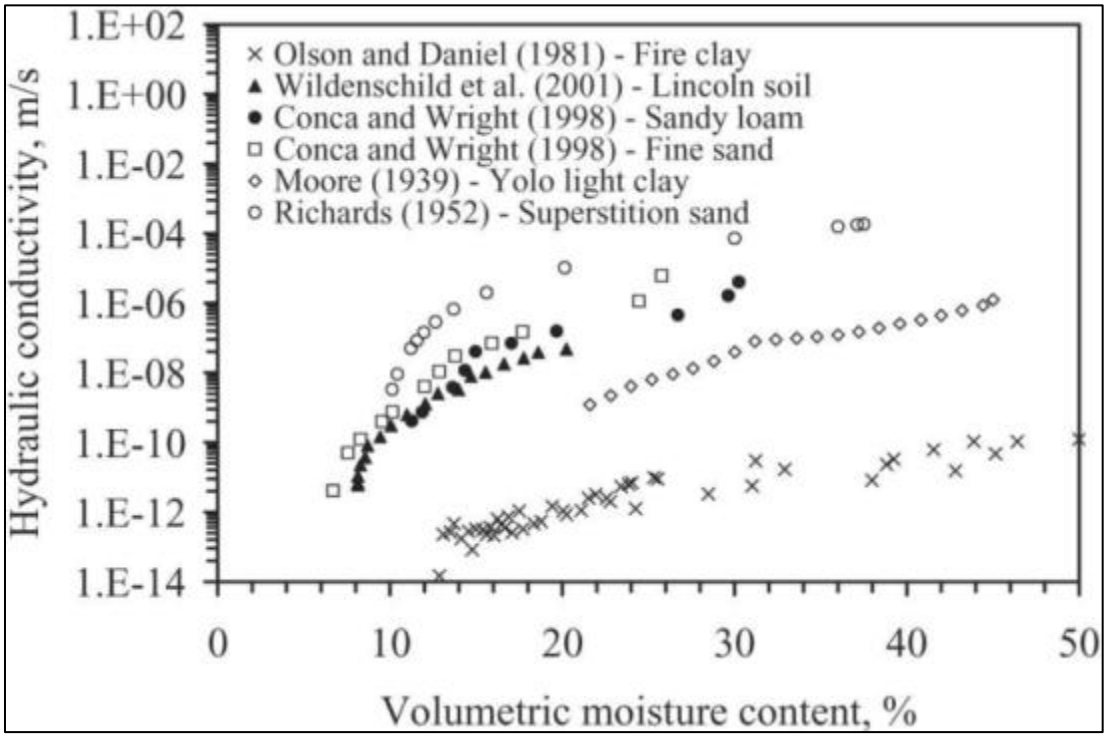

Figure 2.24. Experimental k_{unsat} for different soils (McCartney et al. 2007)

Fredlund et al., (2004) described that there are two main approaches to obtain the unsaturated hydraulic conductivity function of soils, namely empirical equations, and statistical models. When using empirical equations some measured unsaturated hydraulic conductivity data are required. For use of statistical equations, however, only the

saturated hydraulic conductivity and the soil-water characteristic curve are required (Fredlund et al., 2004).

Fredlund et al., (2004) reported a list of the most commonly used empirical equations for determining the unsaturated hydraulic conductivity function as follows. These equations generate unsaturated hydraulic conductivity function as a function of volumetric water content.

- Equation by Averjanov (1950): $k_r = \Theta^n$, where $\Theta = \frac{\theta - \theta_r}{\theta_s - \theta_r}$ and n= 3.5 (2.27)
- Equation by Campbell (1973): $k = k_s \left(\frac{\theta}{\theta_s} \right)^n$ (2.28)
- Equation by Davidson et al. (1969): $k = k_s \exp\left[\alpha(\theta - \theta_s)\right]$ (2.29)

Fredlund et al., (2004) also reported a list of the most commonly used empirical equations for determining the unsaturated hydraulic conductivity function which generate unsaturated hydraulic conductivity function as a function of soil matric suction:

- Equation by Brooks and Corey 1964:
  - $k = k_s$ for $\psi \le \psi_{aev}$ (2.30)
  - $k_r = (\psi / \psi_{aev})^{-n}$ for $\psi \ge \psi_{aev}$ (2.31)
- Equation by Gardner (1958):
  - $k_r = \exp(-\alpha\psi)$ (2.32)
  - $k = k_s / (\alpha\psi^n + 1)$ (2.33)
- Equation by Richards (1931): $k = \alpha\psi + b$
- Equation by Rijtema (1965):

- $k = k_s$ for $\psi \le \psi_{aev}$ (2.34)
- $k_r = \exp\left(-\alpha\left(\psi - \psi_{aev}\right)\right)$ for $\psi_{aev} \le \psi \le \psi_l$ (2.35)
- $k = k_l\left(\frac{\psi}{\psi_l}\right)^{-n}$ for $\psi \ge \psi_l$, where ψ_l is the residual soil suction and k_l is the coefficient of unsaturated hydraulic conductivity at $\psi = \psi_l$

- Equation by Wind (1955): $k = \alpha\psi^{-n}$ (2.36)

A list of most commonly used statistical equations for estimating the unsaturated hydraulic conductivity function of soils is as follows (Fredlund et al., 2004):

- Burdine (1953): $k_r(\theta) = \frac{k(\theta)}{k_s} = \Theta^2 \frac{\int_{\theta_r}^{\theta} \frac{d\theta}{\psi^2(\theta)}}{\int_{\theta_r}^{\theta_s} \frac{d\theta}{\psi^2(\theta)}}$ (2.37)
- Kunze et al. (1968): $k(\theta)_i = \frac{k_s}{k_{sc}} . \frac{T_s^2 \rho_w g}{2\mu_w} . \frac{\theta_s^p}{n^2} . \sum_{j=i}^{m} \left[(2j + 1 - 2i)\psi_i^{-2}\right]$ (2.38)
- Mualem (1976): $k_r(\theta) = \Theta^{0.5}\left(\frac{\int_{\theta_r}^{\theta} \frac{d\theta}{\psi(\theta)}}{\int_{\theta_r}^{\theta_s} \frac{d\theta}{\psi(\theta)}}\right)^2$ (2.39)

There are numerous functions available for predicting the unsaturated hydraulic conductivity. Most accurate models may depend on soil type (Jacquemin, 2011). Some of the most commonly used equations for determining the k_{unsat}-function are presented in this section.

The model by Richards (1931) is as follows:

$$k = a + b\psi \tag{2.40}$$

Where *k*= unsaturated hydraulic conductivity coefficient, and ψ =soil suction.

The equation by Wind(1955) is as follows:

$$k = a\psi^{-b} \tag{2.41}$$

Gardner (1956) measured k_{unsat} values using the outflow data from pressure plate or hanging column approaches. Gardner (1958) proposed the following equation:

$$k = a\theta^{b} \text{ or } k = k_s e^{-a\psi} \tag{2.42}$$

Another form of Gardner equation (1958) is as follows:

$$k_w = \frac{k_s}{1 + a\left(\frac{(u_a - u_w)}{\rho_w g}\right)^n} \tag{2.43}$$

Where:

a= function breaking point constant

n= slope function constant

ρ_w = density of water

Brooks and Corey (1964) proposed the following equation based on the equation by Burdine (1953):

$$k_r(\psi) = (\alpha\psi)^{-2-3\lambda} \tag{2.44}$$

Brooks and Corey (1964) equation is also illustrated as follows:

$$k_w = k_s, \text{ for } (u_a - u_w) \le (u_s - u_w)_b \tag{2.45}$$

$$k_w = k_s\left[\frac{(u_s - u_w)_b}{(u_a - u_w)}\right]^n, \text{ for } (u_a - u_w) > (u_s - u_w)_b \tag{2.46}$$

Where:

k_w = unsaturated hydraulic conductivity

k_s = saturated hydraulic conductivity

$(u_s - u_w)_b$ = air entry value of the soil

$(u_a - u_w)$= soil matric suction

n= empirical constant

Arbhabhirama and Kridakorn (1968) proposed the following equation:

$$k_w = \frac{k_s}{\left[\frac{(u_a - u_w)}{(u_a - u_w)_b}\right]^{n'} + 1} \tag{2.47}$$

Where n′= Empirical constant.

The model proposed by Kunze et al. (1968) is based on the SWCC of the soil. This model has been reported to be fairly accurate in predicting unsaturated conductivity values over a wide suction range (Fredlund et al. 1994). The equation proposed by Kunze et al (1968) is as follows:

$$k(\theta_i) = \frac{k_s}{k_{sc}} \frac{T_s^2 \rho_w g}{2\mu_w} \frac{\theta_s^p}{N^2} \sum_{j=i}^{m} \left[(2j+1-2j)\psi_j^{-2}\right] = A_d \sum_{j=i}^{m} \left[(2j+1-2j)\psi_j^{-2}\right] \tag{2.48}$$

$i = 1,2,...,m$

$$A_d = \frac{k_s}{k_{sc}} \frac{T_s^2 \rho_w g}{2\mu w} \frac{\theta_s^p}{N^2} \tag{2.49}$$

$$k_{sc} = \sum_{j=i}^{m} \left[(2j-1)\psi_j^{-2}\right] \tag{2.50}$$

Where:

$k(\theta_i)$: Predicted hydraulic conductivity for a given volumetric water content (m/s).

i: Interval number which increases as the volumetric water content decreases.

m: Total number of intervals between the saturated vol. water content and the lowest volumetric water content.

k_s: Measured saturated hydraulic conductivity (m/s).

k_{sc}: Saturated hydraulic conductivity or scaling factor (m/s).

A_d: Adjusting constant.

T_s: Surface tension of water (kN/m).

ρ_w: Water density (kg/m^3).

g: Gravitational acceleration (m/s^2).

μ_w: Absolute viscosity of water (N s/m^2).

θ_s: Volumetric water content at S=1.0.

p: Pore size factor = 2 (Green and Corey, 1971)

N: Total number of intervals computed between the saturated volumetric water content and the lowest water content.

ψ_j: Matric suction corresponding to the jth interval (kPa)

Davidson et al.(1969) proposed the equation:

$$k = k_s \exp\left[b(\theta - \theta_s)\right] \tag{2.51}$$

Campbell (1973) equation is as follows:

$$k = k_s\left(\frac{\theta}{\theta_s}\right)^{2b+3} \quad \text{, where:} \quad b = \frac{\Delta\log(\psi)}{\Delta\log(\theta)} \tag{2.52}$$

Campbell (1974) proposed the following equation based on the equation by Childs and Collis-George (1950):

$$k_r = \left(\frac{\psi}{\psi_{aev}}\right)^{-2(2/b)} \tag{2.53}$$

Van Genuchten (1980) proposed an equation for the soil-water characteristic curve. By substituting his equation into the statistical models that were developed for estimating the unsaturated hydraulic conductivity function proposed by Burdine (1953) and Mualem (1976), van Genuchten (1980) derived an equation for estimating the unsaturated hydraulic conductivity function. Van Genuchten (1980) proposed the following equation based on the equation by Burdine (1953):

$$k_r(\psi) = \frac{1-(\alpha\psi)^{n-2}\left[1+(\alpha\psi)^n\right]^{-m}}{\left[1+(\alpha\psi)^n\right]^{2n}} \tag{2.54}$$

Where: $m = 1 - \frac{2}{n}$

Van Genuchten (1980) proposed the following equation based on the equation by Mualem (1976):

$$k_r(\psi) = \frac{\left\{1-(\alpha\psi)^{n-1}\left[1+(\alpha\psi)^n\right]^{-m}\right\}^2}{\left[1+(\alpha\psi)^n\right]^{0.5}} \tag{2.55}$$

Where: $m = 1 - \frac{2}{n}$

Fredlund and Xing (1994) proposed the following equation based on Childs and Collis-George (1950):

$$k_r = \frac{\int_{\ln(\psi)}^{b} \frac{\theta(e^y) - \theta(\psi)}{e^y} \theta'(e^y) dy}{\int_{\ln(\psi)}^{b} \frac{\theta(e^y) - \theta_s}{e^y} \theta'(e^y) dy} \quad (2.56)$$

Where θ = volumetric water content, $k_r = k/k_s$ = relative hydraulic conductivity, θ_s = saturated volumetric water content.

Leong and Rahardjo (1997) proposed the following equation:

$$k_w = k_s \left[\ln\left(e + \left(\frac{\psi}{a} \right)^n \right) \right]^{-pm} \quad (2.57)$$

Where:

m: Air entry value of the soil.

ψ : Soil matric suction.

a, n, and p= Empirical constant.

The equations presented by Broods and Corey (1964), Gardner (1958), and van Genuchten et al. (1980), are some of the equations that use semi-empirical fits to model the unsaturated hydraulic conductivity function. All of these functions include empirical constants that are usually determined based on soil properties such as the air-entry value and the slope of the curve (Jacquemin, 2011).

Huang et al. (1997) proposed an equation which uses empirical constants and requires input for void ratio or stress state. Huang et al. (1997) model is described below:

$$k_w = k_{so} 10^{b(e-e_o)}, \text{ for } \psi \leq \psi_{aev} \quad (2.58)$$

$$k_w = k_{so} 10^{b(e-e_o)} \left[\frac{\psi_{aevo} 10^{a(e-e_o)}}{\psi} \right]^{2\lambda+2}, \text{ for } \psi > \psi_{aev} \quad (2.59)$$

Where:

k_{so}: Saturated hydraulic conductivity at e_o

e: Void ratio of soil.

e_o: Initial void ratio.

ψ_{aev}: Suction corresponding to the air-entry value.

ψ_{aevo}: Air-entry value at a void ratio at e_o.

a, and b: Empirical constants

λ: Pore size distribution index, where: $n = 2\lambda + 2$

n: Porosity

In the next section three of the most commonly used equations for estimating the unsaturated hydraulic conductivity function of soils are described in more detail. The purpose of this in-depth literature review was to study the basis upon which these equations have been developed and validated and also to find the applications for each model (i.e. is the model applied best for coarse or fine-grained materials). The description of these three models includes the methods which the researchers utilized for developing the models as well as the validation of the models by comparing the estimated values against measured values of unsaturated hydraulic conductivity. The three models that are described are the model by Green and Corey (1971), Fredlund et al. (2004), and van Genuchten (1980).

2.9.1. Model Proposed by Green and Corey (1971)

Green and Corey (1971) proposed an equation for predicting unsaturated hydraulic conductivity versus water content of soils. The Green and Corey (1971) equation has been modified from the Marshall (1958) and Millington and Quirk (1959) equations. The researchers reported that the equation adequately predicted the experimentally measured values and provided satisfactory conductivity data for many applications. Green and Corey (1971) equation is shown below:

$$k(\theta)_i = \frac{k_s}{k_{sc}} . \frac{30T^2}{\mu g \eta} . \frac{\zeta^p}{n^2} . \sum_{j=i}^{m} \left[(2j + 1 - 2i) h_i^{-2} \right] \quad (2.60)$$

Where:

$k(\theta)_i$ = the calculated conductivity for a specified water content or negative pore-water pressure (cm/min),

$\frac{k_s}{k_{sc}}$ = the matching factor (measured saturated conductivity / calculated saturated conductivity),

i= the last water content class on the wet end (e.g. i=1 identifies the pore class corresponding to the lowest water content, and i = m identifies the pore class corresponding to the saturated water content),

h_i = the negative pore-water pressure head for a given class of water-filled pores (cm of water),

n= the total number of pore classes between i and m,

θ = volumetric water content (cm3/cm3),

T= surface tension of water (Dyn/cm),

ζ = the water-saturated porosity,

η = the viscosity of water (g/cm /s^{-1}),

g= the gravitational constant

μ = the density of water (g/cm^3), and

p= a parameter that accounts for the interaction of pore classes

The following are some suggested values of 'p' given by various authors: Marshall (1958): 2.0; Millington and Quirk (1961): 1.3; and Kunze et al. (1968): 1.0.

The shape of the conductivity function is controlled by the term (GeoStudio, 2012): $\sum_{j=i}^{m}\left[(2j+1-2i)h_i^{-2}\right]$ (2.61)

The term: $\frac{30T^2}{\mu g \eta}.\frac{\zeta^p}{n^2}$ is a constant for a particular function and can be taken to be 1.0 when determining the shape of the hydraulic conductivity function (GeoStudio, 2012). Green and Corey (1971) then compared some experimentally measured data on a Guelph loam previously reported by Elrick and Bowman (1964) against hydraulic conductivity values calculated by their proposed model, for which the authors reported reliable predictions of the experimentally measured values.

Green and Corey (1971) also compared available measured hydraulic conductivity data on glass beads from Topp and Miller (1966) against calculated values. The authors matched the calculated curves at the saturated conductivity point and reported adequate representation of the data.

Green and Corey (1971) also validated their model by comparing the calculated values against previously measured hydraulic conductivity data by the following researchers:

- Topp (1969) experiment on desorption and adsorption cases on Rubicon sandy loam
- Green et al. (1964) experiment on an Iowas loess soil, Ida silt loam
- Nielsen et al. (1964) experiment on Panoche clay loam obtained from different depths

It should be mentioned that for all comparisons, the calculated and experimental data were matched at θ_s. All the curves were plotted in terms of hydraulic conductivity versus volumetric moisture content (θ).

In case of Rubicon sandy loam, all of the computed curves for the adsorption case were plotted beneath the measured hydraulic conductivities. Computed curves for desorption case were within the envelope formed by the experimental values except at the lower water contents. The agreement between measured and calculated data for Ida silt loam was not as well as one for Guelph loam and glass beads.

Regarding comparing measured data provided by Nielsen et al. (1964) on Panoche clay loam with calculated values using Green and Corey (1971) equation, some of the plots showed good agreement while some other plots showed serious deviation of calculated data from measured data. It should be noticed that unlike other comparisons, the calculated and measured conductivities were matched at $\theta_s = 0.35$ cm^3/cm^3 because the saturated conductivity was not available.

2.9.2. Model Proposed by Fredlund et al. (2004)

Fredlund et al. (2004) proposed a model for estimating the unsaturated hydraulic conductivity function which is an integration form of the suction versus water content relationship. The authors also best fit the proposed equation to data obtained from the literature where both the soil-water characteristic curve and the values of unsaturated hydraulic conductivity were measured. The authors reported the fit between the measured and estimated values to be excellent.

Fredlund et al. (2004) used equation by Kunze et al. (1968) and SWCC fitting equation by Fredlund and Xing (1994) for the prediction of the unsaturated hydraulic conductivity function of soils. Throughout the process, the authors assumed that the volume change of the soil structure is negligible. The authors proposed the following equation:

$$k_r(\psi) = \Theta(\psi) \frac{\int_{\ln(\psi)}^{b} \frac{\theta(e^y) - \theta(\psi)}{e^y} \theta'(e^y) dy}{\int_{\ln(\psi_{aev})}^{b} \frac{\theta(e^y) - \theta_s}{e^y} \theta'(e^y) dy} \quad (2.62)$$

Where:

b = ln(1,000,000), and

y is a dummy variable of integration representing the logarithm of suction.

Fredlund et al. (2004) compared between measured and predicted unsaturated hydraulic conductivity values using their equation for five soils (shown in Table 2.4). The plots showing this comparison are shown in Figures 2.25 through 2.29. The authors reported that predicted and measured data show good agreement except for the data from Yolo

light clay (measured data from Moore 1939). Fredlund et al. (2004) reported that it would appear that there may have been errors involved in the measured unsaturated hydraulic conductivity data for the suctions greater than 4 kPa. The authors also stated that the prediction of unsaturated hydraulic conductivity for clayey soils is generally less accurate than that of sandy soils. The proposed model by Fredlund et al. (2004) was found to be most satisfactory for sandy soils, whereas agreement with experimental data is often unsatisfactory for fine-grained soils.

Table 2.4. Soil properties and SWCC fitting parameters (Fredlund and Xing, 1994) for the example soils (Fredlund et al. 2004)

Soil type	θ_s	k_s x 10^{-6} (m/s)	a	n	m	C_r
Touchet silt loam (GE3)	0.43	—	8.34	9.90	0.44	30.0
Columbia sandy loam	0.458	—	6.01	11.86	0.36	30.0
Yolo light clay	0.375	0.123	2.70	2.05	0.36	100.0
Guelph loam						
drying	0.52	3.917	5.61	2.24	0.40	300.0
wetting	0.43	—	3.12	4.86	0.23	100.0
Superstition sand	—	18.3	2.77	11.20	0.45	300.0

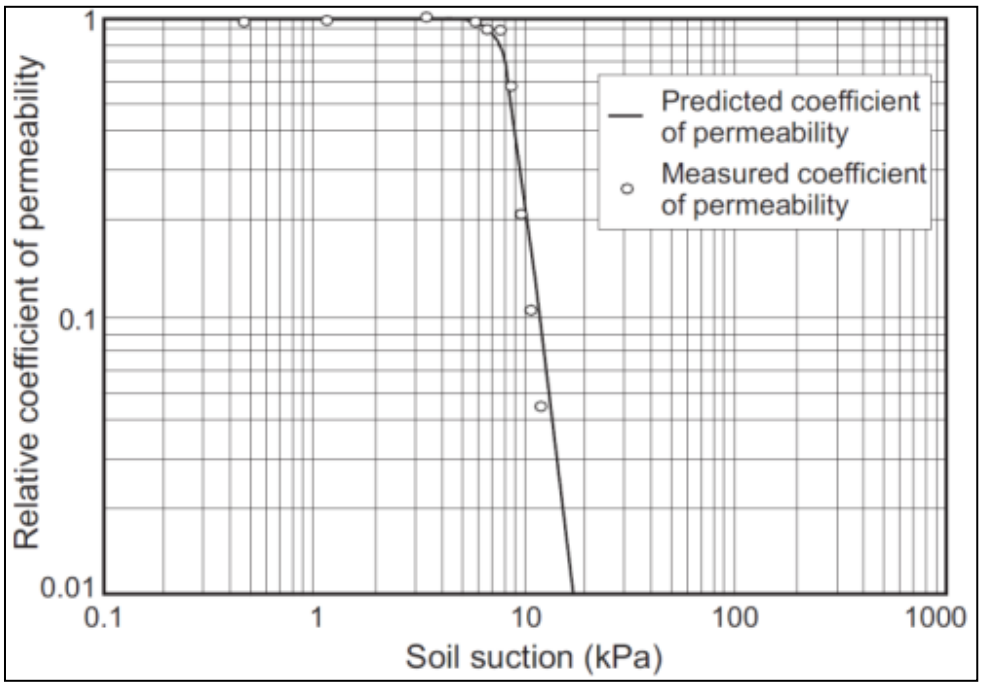

Figure 2.25. Comparison of the predicted relative unsaturated hydraulic conductivity using equation by (Fredlund et al. 2004) with the measured data for Touchet silt loam (GE3) (measured data from Brooks and Corey 1964)

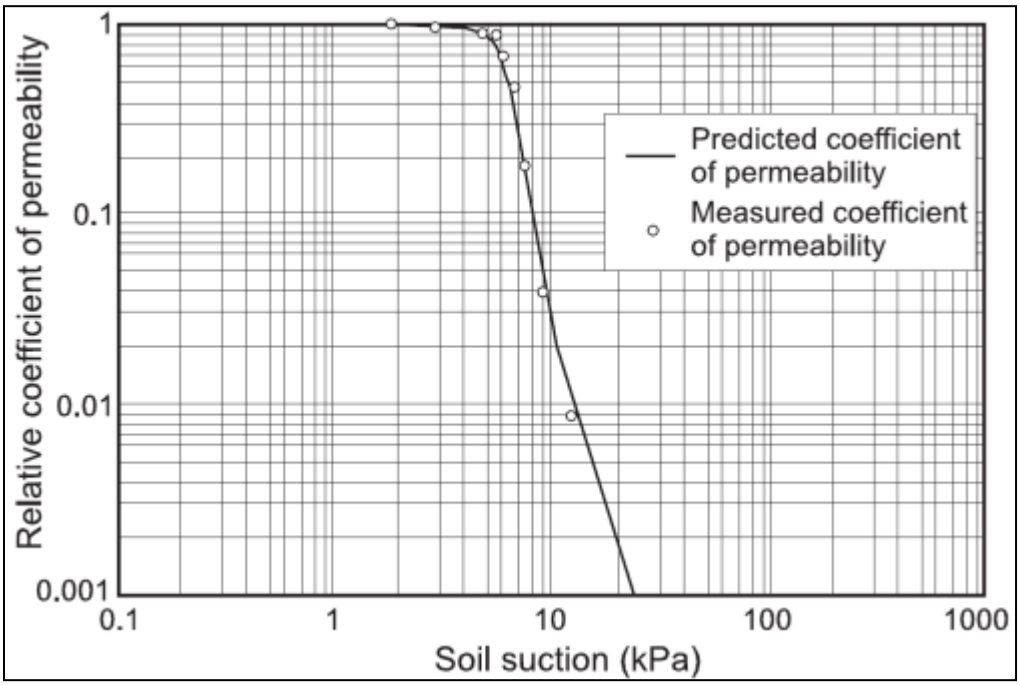

Figure 2.26. Comparison of the predicted relative unsaturated hydraulic conductivity using equation by (Fredlund et al. 2004) with the measured data for Columbia sandy loam (measured data from Brooks and Corey 1964)

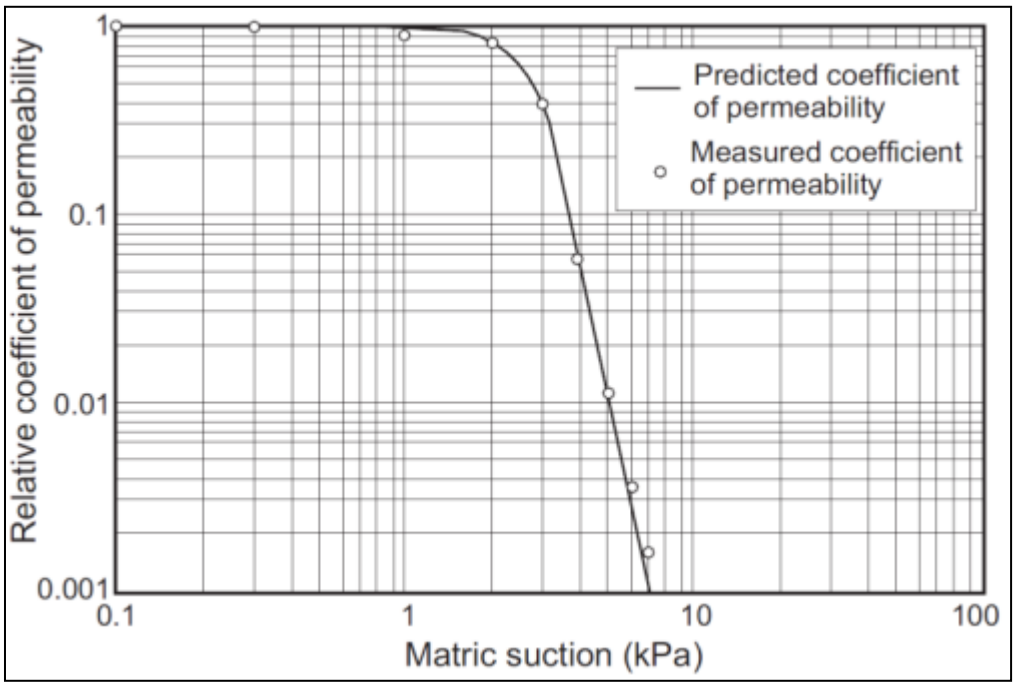

Figure 2.27. Comparison of the predicted relative unsaturated hydraulic conductivity using equation by (Fredlund et al. 2004) with the measured data for Superstition sand (measured data from Richards 1952)

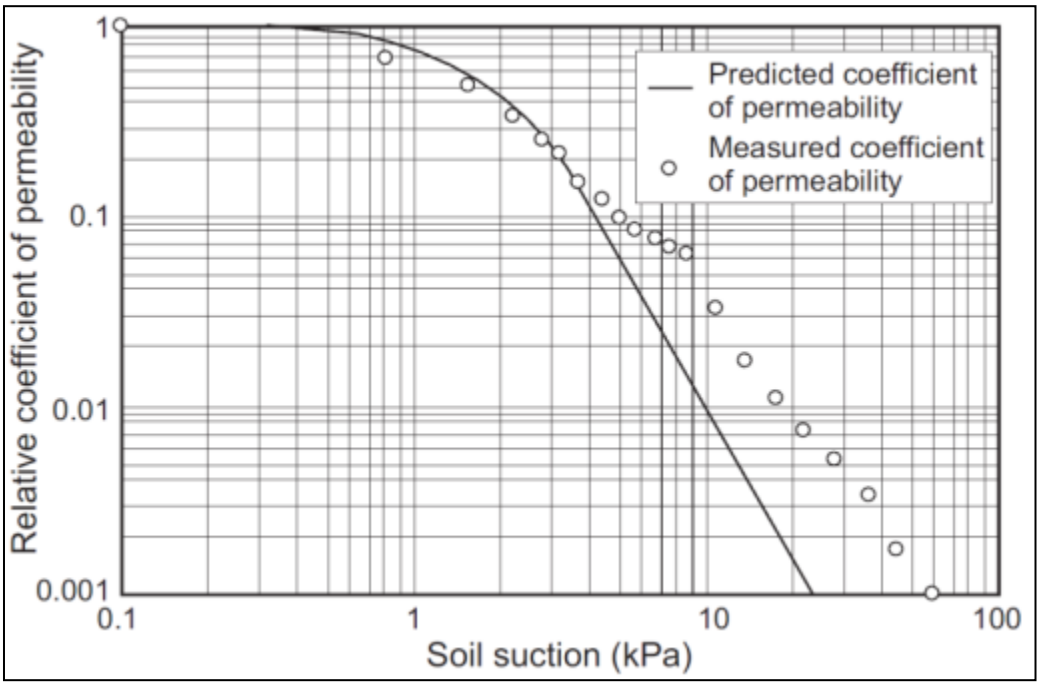

Figure 2.28. Comparison of the predicted relative unsaturated hydraulic conductivity using equation by (Fredlund et al. 2004) with the measured data for Yolo light clay (measured data from Moore 1939)

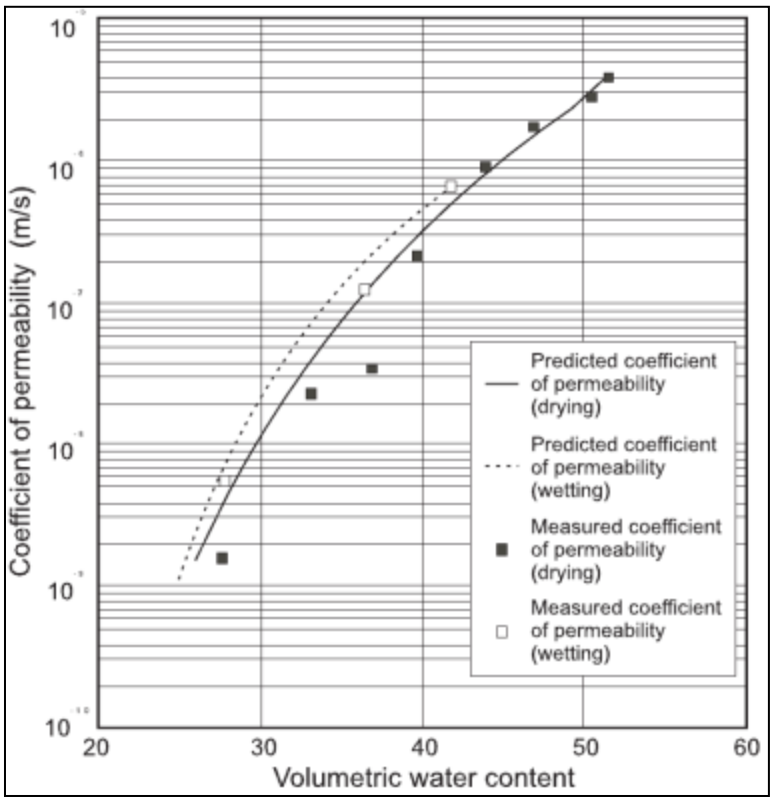

Figure 2.29. Comparison of the predicted relative unsaturated hydraulic conductivity using equation by (Fredlund et al. 2004) with the measured data for Guelph loam (measured data from Elrick and Bowman 1964)

2.9.3. Model Proposed by van Genuchten (1980)

Van Genuchten (1980) proposed equations for finding relative hydraulic conductivity. These equations were obtained by substituting the van Genuchten (1980) SWCC model into the Mualem (1976) or Burdine (1953) form of equation of unsaturated hydraulic conductivity function. Van Genuchten reported that preliminary tests indicated that the Burdine-based equation was in lesser agreement with experimental data than the Mualem-based expression. Van Genuchten compared the results obtained with the closed-form equation based on the Mualem theory against measured data for a few soils.

The following equation was developed by Mualem (1976) for predicting the relative hydraulic conductivity (k_r) from SWCC:

$$k_r = \Theta^{1/2}\left[\frac{\int_0^{\Theta}\frac{1}{h(x)}dx}{\int_0^{1}\frac{1}{h(x)}dx}\right]^2 \tag{2.63}$$

Where h is the pressure head, given here as a function of the dimensionless water content:

$$\Theta = \frac{\theta - \theta_r}{\theta_s - \theta_r} \tag{2.64}$$

Where s and r indicate saturated and residual values of SWCC in terms of θ. Van Genuchten stated that in order to solve the equation presented above an expression relating the dimensionless water content to the pressure head is needed. For this purpose, the author suggested using equation below:

$$\Theta = \left[\frac{1}{1+(ah)^n}\right]^m \tag{2.65}$$

Where a, n, and m are parameters to be defined. The relative hydraulic conductivity as a function of water content is expressed as:

$$k_r(\Theta) = \Theta^{1/2}\left[1-\left(1-\Theta^{1/m}\right)^m\right]^2 \tag{2.66}$$

Where $m = 1 - \frac{1}{n}$

Van Genuchten (1980) reported that the relative hydraulic conductivity function can also be expressed in terms of pressure head by the following expression:

$$k_r(h) = \frac{\left\{1 - (ah)^{n-1}\left[1 + (ah)^n\right]^{-m}\right\}^2}{\left[1 + (ah)^n\right]^{m/2}} \tag{2.67}$$

Where $m = 1 - \frac{1}{n}$

Van Genuchten (1980) also conducted a brief comparison of his model to the one developed by Brooks and Corey (1964). Brooks and Corey (1964) used the Burdine theory to predict the relative hydraulic conductivity function. The authors derived the following expressions:

$$k_r(\Theta) = \Theta^{3+2\lambda} \tag{2.68}$$

$$k_r(h) = (ah)^{-2-3\lambda} \tag{2.69}$$

Van Genuchten described that through parameter substitution, similar equations can be derived for the Mualem (1976) theory:

$$k_r(\Theta) = \Theta^{5/2+2/\lambda} \tag{2.70}$$

$$k_r(h) = (ah)^{-2-5\lambda/2} \tag{2.71}$$

Van Genuchten reported that the SWCC are almost identical for sufficiently low values of θ between the two sets of models. However, the authors reported large deviations between the two models when θ approaches saturation. This is shown in Figure 2.30.

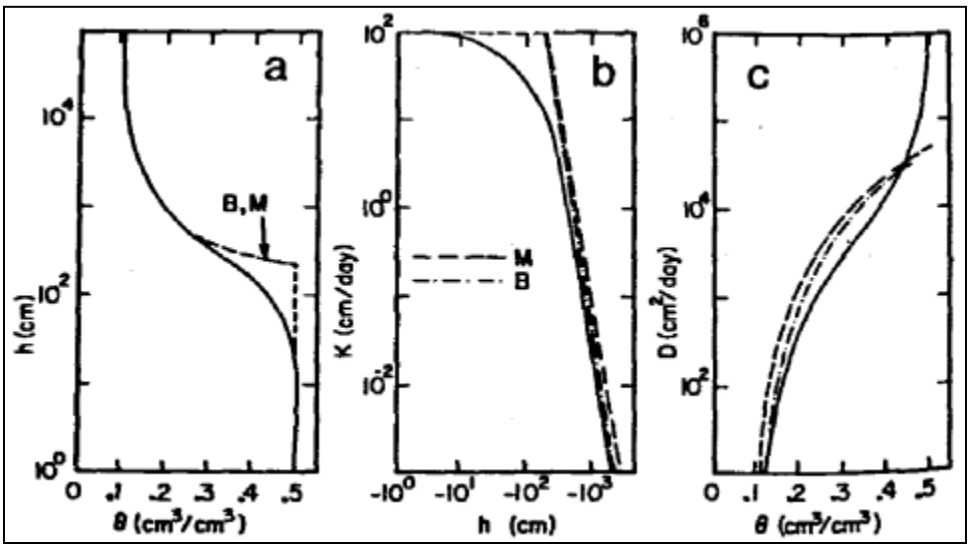

Figure 2.30. Comparison of the hydraulic conductivity function by van Genuchten (solid lines) with curves obtained by applying wither Mualem theory (M; dashed line) or the Burdine theory (B; dashed-dotted line) to the Brooks and Corey model of the SWCC (van Genuchten, 1980)

Van Genuchten (1980) also validated his model against experimental data. Figures 2.31 through 2.35 show this comparison for different soil types. There is general good agreement between measured and calculated values of soil hydraulic properties, except for Beit Nova clay for which can Genuchten equation does not agree with measured data.

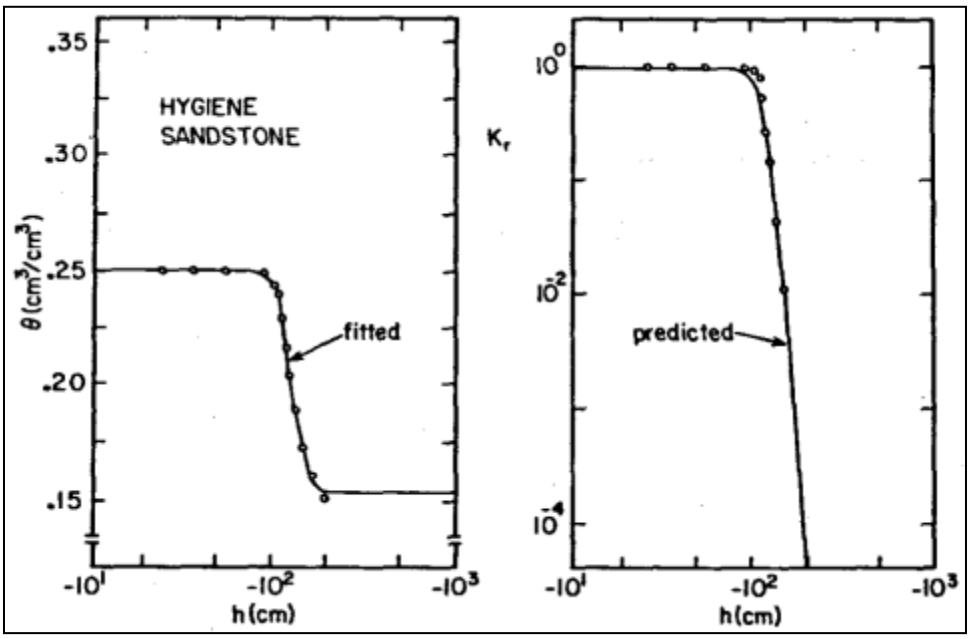

Figure 2.31. Measured (circles) and calculated curves using van Genuchten equation (solid lines) of the soil hydraulic properties of Hygiene Sandstone (van Genuchten, 1980)

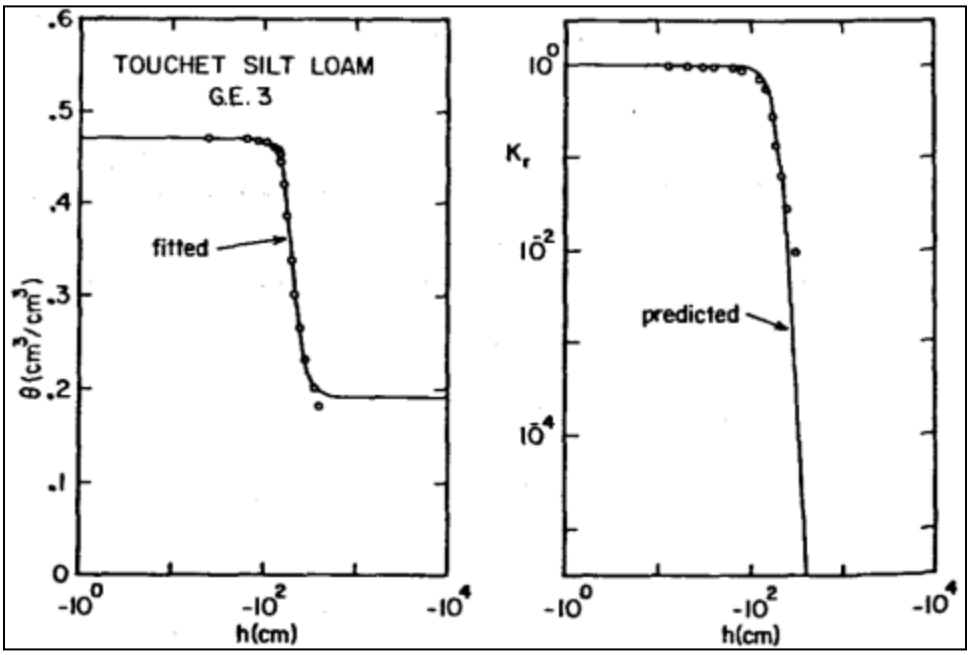

Figure 2.32. Measured (circles) and calculated curves using van Genuchten equation (solid lines) of the soil hydraulic properties of Touchet sit loam G.E.3 (van Genuchten, 1980)

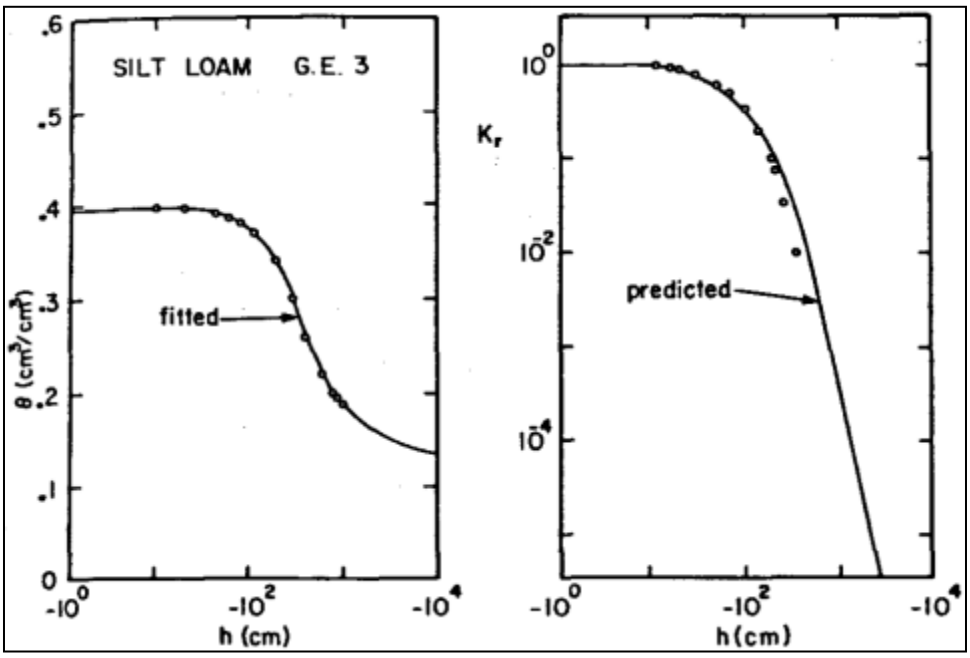

Figure 2.33. Measured (circles) and calculated curves using van Genuchten equation (solid lines) of the soil hydraulic properties of sit loam G.E.3 (van Genuchten, 1980)

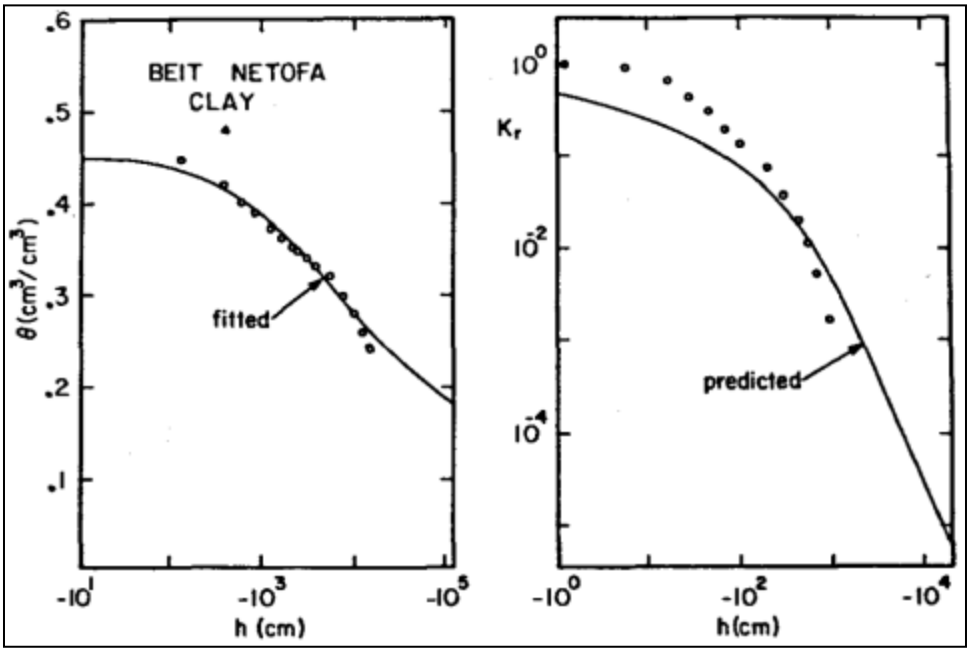

Figure 2.34. Measured (circles) and calculated curves using van Genuchten equation (solid lines) of the soil hydraulic properties of Beit Netofa Clay (van Genuchten, 1980)

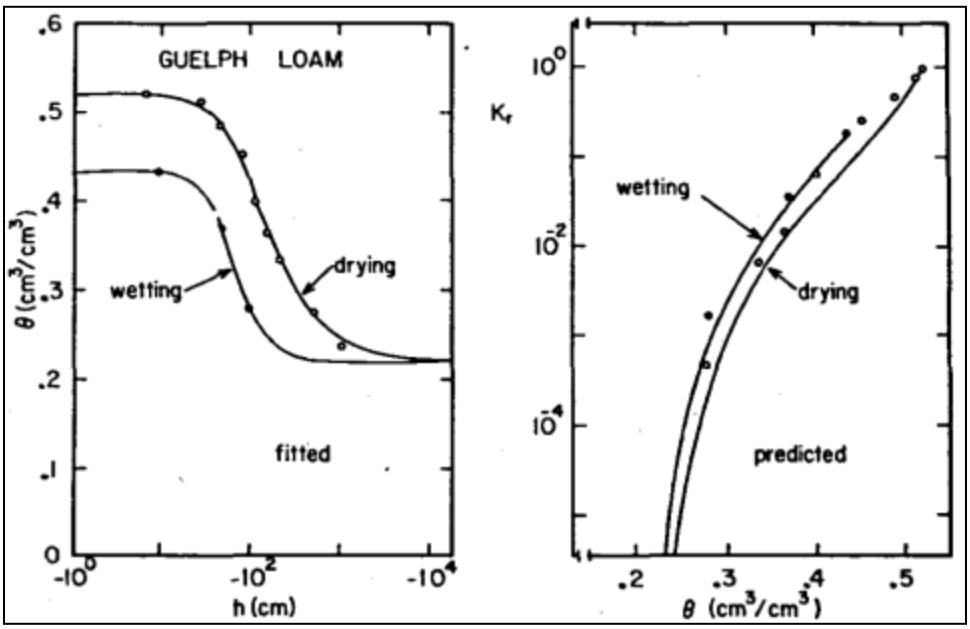

Figure 2.35. Measured (circles) and calculated curves using van Genuchten equation (solid lines) of the soil hydraulic properties of Guelph loam (van Genuchten, 1980)

2.10. Current State of Knowledge

The SWCC can be used to estimate unsaturated soil property functions such as unsaturated hydraulic conductivity. Therefore, the accuracy of the unsaturated soil property functions depends on the accuracy of the SWCC. Several factors such as soil structure, initial water content, void ratio, and compaction method can have significant effects on the SWCC. Among these factors, stress history and initial water content has been reported to have the greatest effect on the soil structure, which in turn plays a significant role on the shape of the SWCC (Zhou et al. 2005).The air-entry value of the soil and the rate of desaturation is reportedly affected by the initial density and amount of disturbance to the soil (Fredlund and Houston, 2009).

Even though the soil water characteristic curve has been measured and used by numerous researchers throughout the years, the effect of volume change of high volume

change soils (e.g. oil sands tailings, and expansive soils) has rarely been considered when determining the SWCC's. This may lead to inaccurate SWCC's including the air-entry value. Furthermore, it has been the common practice to estimate some of the major unsaturated soil property functions (e.g., unsaturated hydraulic conductivity function, shear strength) by using SWCC, which is a further support for recognizing the importance of establishing true SWCC of high volume change soils. In recent years, importance of considering the volume change of soils during suction change has been recognized by a number of researchers; namely Salager et al. (2010), Pe´ron et al. (2007), Nuth and Laloui (2011), Stange and Horn (2005), Mbonimpa et al. (2006), Perez-Garcia, et al. (2008), and Fredlund and Houston, (2013).

Through literature study it was found that effect of net normal stress which is applied to the soil specimen during the SWCC test, has also been under-studied. Only very few researchers have conducted studies for finding the impact of net normal stress on SWCC's (both drying and wetting cycles of SWCC) which in this research was found to be important, particularly with regard to effect of net normal stress on volume change of the soil during SWCC test on expansive clays. Furthermore, the effect of initial state of the soil specimen including initial moisture content on SWCC has not been studied by a lot of researchers. It is known that the initial condition of the soil (slurry versus compacted at or near optimum moisture content) can have a significant effect on the SWCC of the soil, particularly with regard to soil volume change (Fredlund, 2002).

Correction of SWCC's for soil volume change during the test may have a considerable impact on air-entry value and shape of the SWCC. This, in turn, may have a

significant impact on unsaturated soil properties derived from the SWCC's (e.g. soil hydraulic properties such as unsaturated hydraulic conductivity function). No studies on numerical modeling of the effect of correction of SWCC for soil volume change on hydraulic properties of the soils (e.g. advancement of wetted front) and its impact on amount of suction-change induced deformation of expansive soils was found in the literature.

An extensive literature review was conducted regarding the methods of SWCC determination and the models available to best-fit the SWCC data obtained from laboratory experiments. During this literature search SWCC's including typical air-entry values and hysteresis were studied. Emphasis was placed upon the SWCC's of clays because expansive clays were used as an example of high volume change soils for purposes of this study on the effect of volume change on unsaturated soil properties and flow-deformation. Use of soil water characteristic curves in constitutive relations for unsaturated soils such as unsaturated hydraulic conductivity functions was also studied through literature search. Some of the equations most commonly used to estimate unsaturated hydraulic conductivity functions of soils based on the SWCC were studied. This part of literature search included studying the methodologies used for developing the equations for estimating unsaturated hydraulic conductivity functions as well as the applications of the proposed equations. There are two main approaches to obtain the unsaturated hydraulic conductivity function of soils, namely empirical equations, and statistical models. When using empirical equations some measured unsaturated hydraulic conductivity data are required. For use of statistical equations, however, only the

saturated hydraulic conductivity and the soil-water characteristic curve are required. It was found that the most common equations used for estimating unsaturated hydraulic conductivity functions of soils were developed for silts and sands. Undisturbed and compacted specimens of silts and sands were used for developing or validating these equations. Volume change of soils was not considered when developing these equations and these equations work best for silts and sands and may not accurately estimate unsaturated hydraulic conductivity functions of clays.

The importance of correcting SWCC's (including SWCC's in terms of volumetric water content and degree of saturation) for soil volume change that occurs during the SWCC test was studied through literature search. Additional literature search was carried out to assess the effect of net normal stress on the shape of SWCC with regard to the soil volume change throughout the test. Drying and wetting SWCC were studied through literature search. Moreover, the importance of initial condition of the specimen (slurry versus compacted specimen) was evaluated through literature search.

The literature review showed that slurry specimens undergo significant volume change during SWCC test. Therefore, for a certain clayey soil the SWCC of the slurry specimen may be different from that of the compacted specimen, not only because of difference in soil structure but also due to large differences in volume change behavior.

The typical air-entry values of clays were studied through literature search. As explained previously, air-entry value of a soil is defined as the matric suction at which desaturation of the largest pores within the soil begins. The air-entry value of a specific soil is related to the radius of the largest pore (i.e. if the largest pore is relatively small,

the air-entry value will be relatively large). Numerous researchers have found that the saturation water content and air-entry value generally increases with the plasticity of the soil (Fredlund and Xing, 1994). Fredlund (2011, 2013) reported that air-entry of soils is generally quite close to their plastic limit. Consequently, the author concluded that there is an approximate correlation between the plastic limit of a soil and its air-entry value. Some other authors, however, reported different degrees of saturation (considerably less than 100%) for soils at plastic limit (Ito and Azam, 2010, Li et al., 2009).

The hysteresis loop present between the wetting and drying paths of a SWCC was also studied through literature search. Numerous researchers have measured SWCC's including drying and wetting paths and presented the hysteresis associated with the curves. It was found that at a given soil suction, the water content of the drying curve is higher than that of the wetting curve (i.e. the drying curve lies above the wetting curve). Furthermore, the end point of the wetting curve differs from the starting point of the drying curve because of air entrapment in the soil. It was found from the literature search that the wetting SWCC lies below the drying SWCC. Moreover, generally the end point of the wetting curve is smaller than the starting point of the drying SWCC. This is because some air becomes entrapped in the soil after it is wetted from a stress state in excess of residual suction. Furthermore, the slope of the drying curve is approximately parallel to that of the wetting curve.

The impact of net normal stress applied to the specimen during the SWCC test was studied through literature search. Very limited data was found regarding effect of net normal stress on the shape of the SWCC's. It was found that in general, stress history of

the applied normal stress does not seem to affect the shape of the SWCC significantly; however, the AEV increases and the rate of degree of saturation change decreases with increasing the net normal stress.

During the literature review, particular focus was placed upon studying whether in common practice SWCC's are corrected for soil volume change. This was studied particularly for the soils with high volume change potential. Suction induced volume change in expansive soils occurs due to changes in the water content of the soil which affects the stress equilibrium of the soil. Consequently, when determining the SWCC of an expansive soil, it is important to consider the volume change that occurs as the suction (and hence the water content of the soil) changes during the test (Chao et al., 2008). This reportedly is not the common practice and the SWCC is usually measured assuming no volume change of the soil specimen. This assumption is not correct for expansive soils. When determining the SWCC of an expansive soil, it is important to consider the volume change that occurs as the suction changes during the test (Chao et al. 2008). Soil water characteristic curve fitting equations have been generated by a number of researchers (e.g., Gardner 1956; Brooks and Corey 1964; van Genuchten 1980; Fredlund and Xing 1994). Although not always mentioned, the underlying assumption of most SWCC fitting equations is that the soil is sufficiently stiff so that there is no change in void ratio of the soil (i.e. soil volume change) during the test (Mbonimpa et al., 2006, Chiu and Ng, 2012). Nonetheless, some of these equations have been extended for use in case of high volume change materials. Pham and Fredlund (2008) proposed two SWCC equations for best-fitting the SWCC for a wide range of soils types including high volume change clays. A

number of researchers have attempted to predict the SWCC's of expansive soils (Chertkov 2004; Mbonimpa et al. 2006). It was found that in recent years a number of researchers have recognized the importance of considering soil volume change when establishing SWCC's. A number of researchers have conducted SWCC tests during which the volume and mass of the specimen has been recorded and the volume change of the specimen has been incorporated when generating the SWCC's. At the same time, the measured data found on comparing volume change corrected and uncorrected SWCC's was very limited and the researchers either reported the SWCC that is corrected for volume change or the SWCC uncorrected for volume change.

A number of researchers recommended using degree of saturation SWCC as opposed to gravimetric moisture content. The authors reported that when the soil undergoes volume change during a suction increase, only the degree of saturation variable clearly defines the air-entry value for the soil (as opposed to gravimetric and volumetric water content).

Equations to best-fit soil water characteristic curves data were also studied through literature search. Numerous equations have been proposed to best-fit SWCC data. Several of these equations are sigmoidal in character and provide a continuous function over the entire soil suction range. These equations have two or more fitting soil parameters. The equations with more fitting parameters are more likely to closely fit the SWCC data obtained from laboratory (Fredlund and Houston, 2009).

Various empirical models and equations have been proposed for the estimation of some of unsaturated soil property functions (e.g., unsaturated hydraulic conductivity,

shear strength, volume change). In each case, the estimation procedure involves the use of the saturated soil properties in conjunction with the SWCC. This fact further demonstrates the importance of SWCC in unsaturated soil mechanics. One of the major used of SWCC is for estimation of unsaturated hydraulic conductivity functions of soils. Some of the most common equations proposed by researchers use hydraulic conductivity of the soil at full-saturation condition along with its SWCC in order to estimate the unsaturated hydraulic conductivity function. The use of such equations has proven to be of practical significance due to the fact that measurement of unsaturated hydraulic conductivity of soils is a time-consuming and expensive procedure. Numerous available equation for estimating unsaturated hydraulic conductivity functions of soils were studied. Three of the most commonly used equations for estimating the unsaturated hydraulic conductivity function of soils were also described in more detail. The purpose of this in-depth literature review was to study the basis upon which these equations have been developed and validated and also to find the applications for each model (i.e. is the model applied best for coarse or fine-grained materials). The description of these three models includes the methods which the researchers utilized for developing the models as well as the validation of the models by comparing the estimated values against measured values of unsaturated hydraulic conductivity. The three models that are described are the model by Green and Corey (1971), Fredlund et al. (2004), and van Genuchten (1980). It was found that the underlying assumption for generating these equations have been that the authors assumed that the volume change of the soil structure is negligible.

Chapter 3

LABORATORY TESTING

3.1. Introduction

The Soil Water Characteristic Curve (SWCC) describes the relationship between either gravimetric water content, w, volumetric water content, θ , or degree of saturation, S, and matric soil suction, $(u_a - u_w)$, of the soil. The matric suction can be determined by either a direct or indirect method. A direct measurement of matric suction is commonly obtained with the axis translation technique. A common axis translation measurement device is the pressure plate apparatus. An oedometer-type pressure plate device is one common device used in geotechnical engineering to directly measure matric suction of samples using the axis translation technique (Perera, et al., 2004).

In this study, a 1-D oedometer-type pressure plate device (i.e. SWC-150 device) and the filter paper method were utilized to obtain the soil water characteristic curves for expansive soils. The SWC-150 device is an oedometer-type pressure plate device that was designed and manufactured by Geotechnical Consulting and Testing Systems, Inc. (GCTS, 2004) and is an unsaturated soil testing apparatus with flexibility for controlling the matric suction while applying various net normal stress values. The SWC-150 stainless steel SWCC apparatus allows use of a single soil specimen to obtain the entire SWCC, up to the matric suction value of 1500 kPa (i.e., 15 bars), with any number of equilibrium data points. This device can be used for determining SWCC of disturbed and compacted (i.e. remolded specimens), initially slurried, or undisturbed specimens,

starting with either dry or wet conditions. Figure 3.1 provides a sketch of the device and illustrates the various parts within the system.

The device consists of a pressure cell assembly, a pressure panel, and a pneumatic loading frame. In the SWCC cell, a pressure compensator is incorporated into the loading ram to compensate for the upward thrust on the piston due to the pressure inside the SWCC cell. The pressure cell assembly is made of stainless steel and includes the necessary plumbing and valves for flushing of diffused air to prevent a volume error caused by the air that may get trapped in the base of the system.

Several different high-air-entry-value (HAEV) ceramic stones rated at 100, 300, 500, and 1500 kPa can be interchanged. The High Air Entry Disk (HAED) that is used in SWC-150 device is designed so that it allows water to infiltrate through the disk but it does not allow air to pass through the disk up to an air pressure corresponding to the bubbling pressure of the stone (Abbaszadeh, 2011). Typical high air entry ceramic stones capacities are 1, 3, 5, and 15 bars (1bar= 100kPa). By knowing the maximum suction that will be applied to the specimen, an appropriate ceramic stone is selected for use. It is very important not to exceed the capacity of the stone during testing. It is also possible to change the stones in the middle of a test; however it can only be achieved once the specimen is equilibrated at the previously applied suction, and care should be taken to prevent any water loss from the sample (Abbaszadeh, 2011).

Air pressure provided by central hydraulic pressure systems or air cylinders can be used to supply the inlet pressure to the pressure regulator while holding the pore water pressure to zero (by venting the water to the atmosphere). When the ceramic stone is

saturated and the sample is in good contact with the stone, it can be assumed that the pore water pressure is equal to the atmospheric pressure because the water compartment is vented to atmosphere. Thus, the matric suction of the soil would be equal to the value of the applied air pressure inside the cell.

The mounted high air entry value ceramic stone rests on a grooved surface of the cell base which is shown in Figures 3.2 and 3.3. The grooved channel is connected to the two volumetric tubes that are used to measure changes in water content of sample. The volume indicator tubes are graduated to read the amount of water released from the specimen (during drying SWCC test) or absorbed into the specimen (during wetting SWCC test) during tests. When water level does not move for a few days under a constant suction, it can be assumed that the soil sample has reached equilibrium.

It is important to cover the top of the volumetric tubes to prevent water evaporation from the tubes. Placement of rubber stoppers which fit the water tubes and a thin film of oil on top of the water column have been shown to minimize evaporation of water. In case of using rubber stoppers existence of small holes in the rubber stoppers allow air to move into or out of the water tubes as the level of water changes during tests. During wetting test level of water lowers in the water tubes as the water is absorbed into the specimen during which existence of small holes in rubber stoppers allows air to enter the tubes and replace the water that is absorbed by the specimen. During drying test level of water increases in the water tubes as the water is released from the specimen. Existence of small holes in rubber stoppers allows air to escape from the tubes and prevents increase in pressure of the air inside the tubes. The purpose of grooved channel

is to keep the ceramic stone saturated and to facilitate in flushing of diffused air (Padilla et al, 2006).

This device also allows for application of vertical load to the sample. This is done by placing loads on the rod at the top of the device (shown in Figure 3.1). The load can be applied with dead weights or by placing the SWC-150 in a load frame. LVDT's (Linear Variable Differential Transformer) or regular dial gauges can be installed to the loading ram part of the device, in order to measure the axial deformation of the specimen. A porous stone with a diameter slightly less than inner diameter of the ring that holds the specimen is placed on top of the soil. Upon assembling of the cell, the loading rod or loading plate becomes in contact with the porous stone and hence ensures uniform application of load to the sample.

For assembling the cell, first the wall(s) of the cell will be placed on the O-ring at the base of the cell and then the top plate is placed on the walls. The top and bottom plates are secured by tightening the four 4.5-inch long socket-head cap screws which seals the cell.

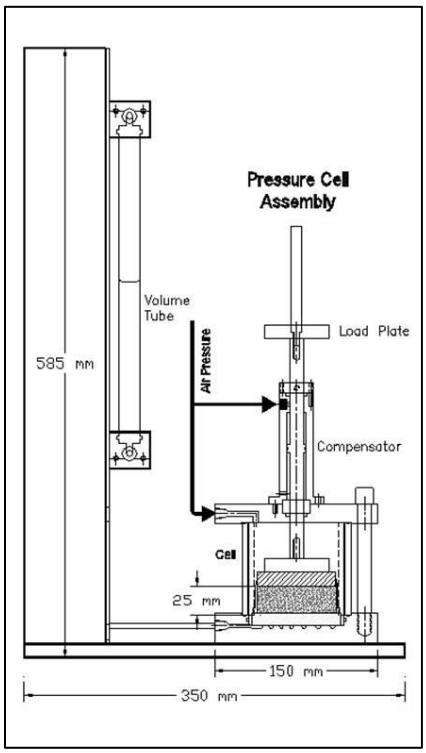

Figure 3.1. SWC-150 Cell with pneumatic loading frame (GCTS, 2004)

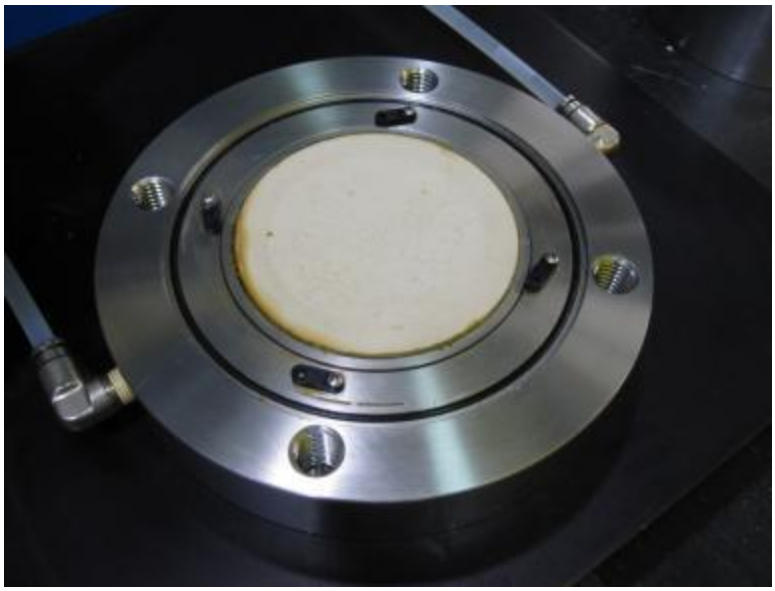

Figure 3.2. GCTS SWC-150 cell bottom plate (base) with mounted high air entry ceramic disk

Figure 3.3. SWC-150 cell bottom plate (base) with grooved channel (Abbaszadeh, 2011)

The SWC-150 device was used to measure data points of SWCC for suctions less than 1500kPa. For measurement of water content versus suction for larger suction values the filter paper test was used. The filter paper method for measuring soil suction was developed in the agricultural soil science discipline, and has been used routinely by the Water Resources Division of the U.S. Geological Survey for many years (McQueen and Miller, 1968). Attempts have been made to use the filter paper method for engineering applications (McKeen and Nielson, 1978; McKeen, 1981 and 1985; McKeen and Hamberg, 1981; Ching and Fredlund, 1984; Houston, et al., 1994; Bulut, et al., 2001; Leong, et al., 2002; Bulut and Wray, 2005; Oliverira and Fernando, 2006). An advantage of the filter paper method is the wide range of values of soil suction over which it can be used and its simplicity whereas a disadvantage for the use of this method is the degree of accuracy required for weighing the filter paper and associated sensitivity to operator error.

The principle of the filter paper method is that the suction of a filter paper will come to equilibrium with that of the soil sample. The relative humidity inside the container which holds the soil and filter paper will be controlled by the soil suction. Equilibrium can be reached by either liquid or vapor moisture exchange between the filter paper and the soil specimen. By using the filter paper method it is possible to measure either the total or the matric suction of a soil (ASTM D5298-94). When the filter paper is placed in contact with the water in the soil, the soil suction measured at equilibrium will be the matric suction of the soil, because the salt content of the water in the filter paper will be the same as that of the soil water (Chao, 2007).

In this method, a specimen of the soil along with a calibrated filter paper is placed in a closed container. Filter paper tests for measuring soil suction must be conducted with great care in order to minimize error and obtain accurate results. It has been found to be critical that the specimens for filter paper test should be placed and kept in a temperature-controlled environment (Jacquemin, 2011). The soil sample and the filter paper are allowed to equilibrate for a period of time at a constant temperature.

3.2. Laboratory Tests Performed

As a part of this study, Soil Water Characteristic Curves (SWCC) of three clays, Anthem, Colorado, and San Antonio, were determined. The tested soils have different clay mineralogies and variable degrees of swell potentials. Points on the SWCC in the low range of suction (below 1,500kPa) were obtained using the SWC-150. For suction values greater than 1,500 kPa, points on the SWCC were determined using the filter paper test.

During this study, the effect of the initial state of the sample including its initial moisture content on the SWCC was studied. For this purpose, slurry specimens and compacted specimens (prepared at 95% of maximum standard dry density compacted at optimum moisture content) were prepared and tested and the results were compared against each other.

Also the effect of volume change of expansive clays on their SWCC was studied. It was found that volume change that occurs during suction change under applied load can be significant, and affects the SWCC, including key features of the SWCC such as the AEV. The impacts of volume change on AEV have been previously discussed by Fredlund and Houston (2013). Taking the soil volume change into account, therefore, may lead to more accurate estimation of soil properties such as shear strength and hydraulic conductivity when these unsaturated soil properties are estimated using saturated property measurements plus the SWCC (Fredlund et al. 2003).

As another part of this study, the effect of net normal stress upon the SWCC of the samples was evaluated. For this purpose, SWCC's of soil specimens prepared at the same initial density and moisture content (95% of maximum standard dry density and optimum moisture content) were measured under different net normal stress values. The values of applied net normal stresses were: 7kPa, ~25%, and ~50% of the swell pressure of the soil. Furthermore, SWCC's including drying and wetting curves for different net normal stress values were measured and analyzed. In the following sections, basic properties of the test soils used in this study are presented.

3.3. Soils Used in the Laboratory Testing Program

Three clays were tested as a part of this study. These soils were collected from Arizona, Colorado, and Texas and are referred to as Anthem, Colorado, and San Antonio soils in this study. Basic properties of these soils were determined at Arizona State University by a research team and the data are shown in Table 3.1 and Figures 3.4 through 3.6. Natural moisture content, for shallow deposit field conditions, were 6% for Anthem and Colorado, and 5% for San Antonio. ASTM Standards used are:

- ASTM D6913 - 04(2009) Particle-Size Distribution) Using Sieve Analysis
- ASTM D422 - 63(2007) Particle-Size Distribution) Using Hydrometer Test
- ASTM D698 - 12– Standard test Methods for Laboratory Compaction Characteristics of Soils Using Standard Efforts
- ASTM D854 - 10– Standard Test Methods for Specific Gravity of Soil Solids by Water Pycnometer
- ASTM D4318 - 10– Standard Test Methods for Liquid Limit, Plastic Limit, and Plasticity Index of Soil

Table 3.1. Basic Properties of the Soils Investigated in this Study

Soil	Anthem	Colorado	San Antonio
USCS Classification	CL	CH	CH
%Sand (4.36mm - 0.074mm)	11	1	1
%Silt (0.074mm - 0.002mm)	57	50	35
%Clay < 0.002mm	32	49	54
Liquid Limit (LL)	48%	65%	66%
Plastic Limit (PL)	21%	23%	24%
Plasticity Index (PI)	27%	42%	42%
Shrinkage Limit (SL)	15%	11%	12%
Maximum Dry Density (gr/cm^3)	1.715	1.65	1.609
Maximum Dry Unit Weight (lb/ft^3)	107	103	100.4
Optimum Moisture Content (%)	18%	19%	22%
Specific Gravity	2.723	2.778	2.795

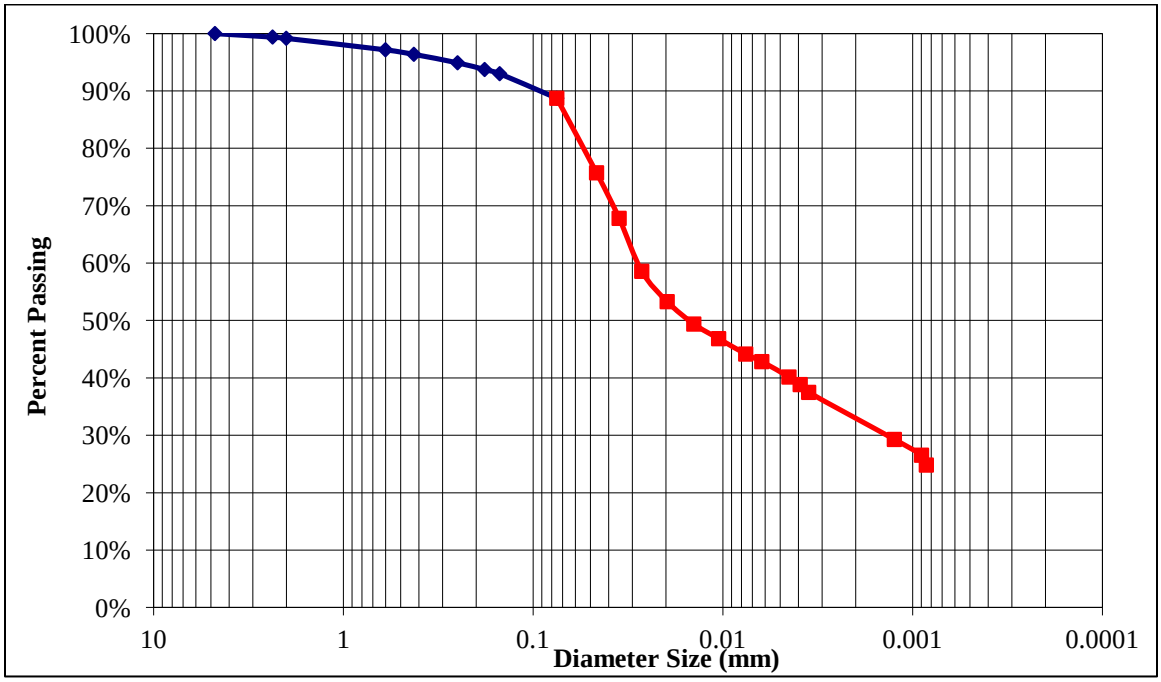

Figure 3.4. Particle Size Distribution for Anthem Soil

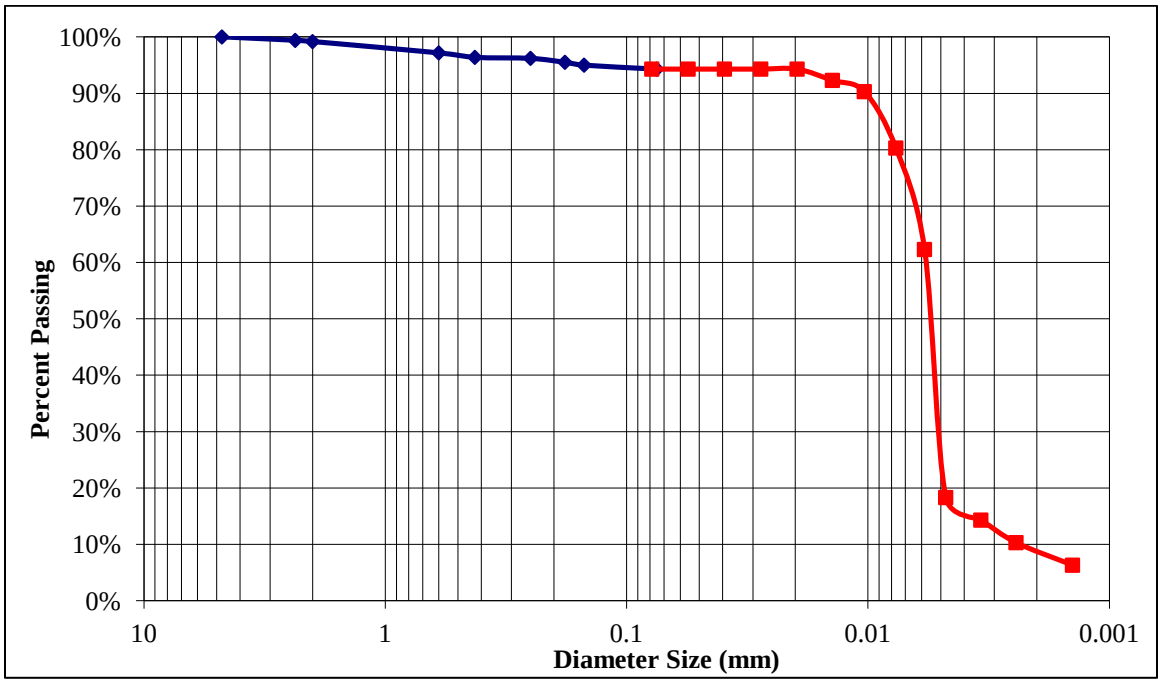

Figure 3.5. Particle Size Distribution for Colorado Soil

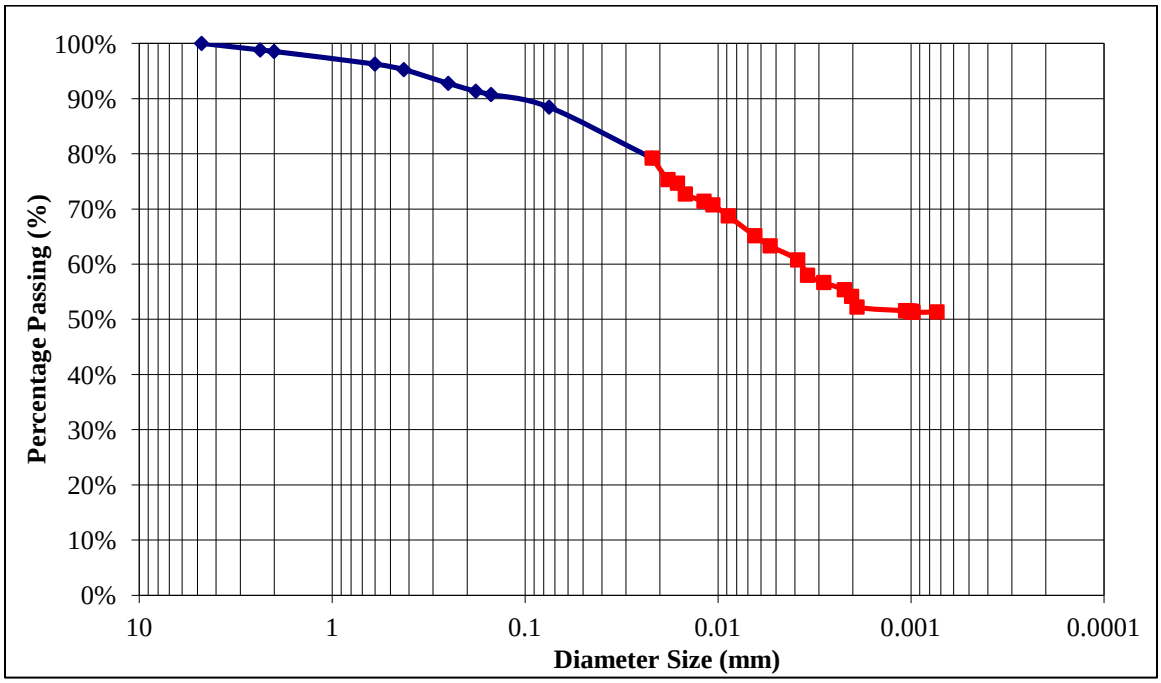

Figure 3.6. Particle Size Distribution for San Antonio Soil

3.4. Soil Water Characteristic Tests

3.4.1 SWCC Determination Using 1-D Oedometer Pressure Plate Cells

Table 3.2 shows the list of SWCC tests conducted as a part of this study. A total of 21 SWCC tests were performed. Compacted specimens of Anthem, Colorado, and San Antonio soils were prepared by compacting the soil at 95% standard maximum dry density and at optimum moisture content. Due to high plasticity of soils in this study, existence of clods was noticed upon wetting of the soil. As an attempt to break the clods using mortar and pestle, the soils were pulverized and passed through US No. 100 sieve. However, it was noticed that clods would re-appear when water was added to the soil to reach the optimum moisture content. The required quantity of distilled water was added to the soils using a spray bottle to reach the water content to optimum. Afterwards, the soil was sealed in plastic bags and left for at least 15 days for equilibrium. The longer duration required for equilibrium was due to fine-grained particles of the soil and its high plasticity. After equilibrium was reached, the soil was compacted in three layers into standard SWCC brass rings at 95% maximum dry density.

Table 3.2. List of SWCC Tests Conducted as a Part of this Study

Test No.	Soil	Specimen Type	Test Type	Net Normal Stress	SWCC Path
1	Anthem	Compacted	Original	7 kPa (Seating Load)	Drying
2	Colorado	Compacted	Original	7 kPa (Seating Load)	Drying
3	San Antonio	Compacted	Original	7 kPa (Seating Load)	Drying
4	Anthem	Compacted	Replicate	7 kPa (Seating Load)	Drying
5	Colorado	Compacted	Replicate	7 kPa (Seating Load)	Drying
6	San Antonio	Compacted	Replicate	7 kPa (Seating Load)	Drying
7	Anthem	Slurry	Original	3 kPa (Token Load)	Drying
8	Colorado	Slurry	Original	3 kPa (Token Load)	Drying
9	San Antonio	Slurry	Original	3 kPa (Token Load)	Drying
10	Anthem	Slurry	Replicate	3 kPa (Token Load)	Drying
11	Colorado	Slurry	Replicate	3 kPa (Token Load)	Drying
12	San Antonio	Slurry	Replicate	3 kPa (Token Load)	Drying
13	Anthem	Compacted	Original	7 kPa (Seating Load)	Drying and Wetting
14	Anthem	Compacted	Original	23% Swell Pressure	Drying and Wetting
15	Anthem	Compacted	Original	46% Swell Pressure	Drying and Wetting
16	Colorado	Compacted	Original	7 kPa (Seating Load)	Drying and Wetting
17	Colorado	Compacted	Original	21% Swell Pressure	Drying and Wetting
18	Colorado	Compacted	Original	42% Swell Pressure	Drying and Wetting
19	San Antonio	Compacted	Original	7 kPa (Seating Load)	Drying and Wetting
20	San Antonio	Compacted	Original	27% Swell Pressure	Drying and Wetting
21	San Antonio	Compacted	Original	54% Swell Pressure	Drying and Wetting

The amount of soil (at optimum moisture content) needed for preparing a specimen at 95% maximum dry density was found by first measuring the dimensions of the brass ring. For example, for preparing a sample of San Antonio soil, the dimensions of the ring were measured to be height: 2.543cm, and Diameter: 6.075cm. The volume of the ring was calculated to be 73.71cm^3. As mentioned previously, for San Antonio, $\rho_{d,\ max}$= 1.609 gr/cm^3, and therefore, 95% of $\rho_{d,\ max}$= 1.529 gr/cm^3. At optimum moisture content (22%), the moist density is: ρ_{moist}= 1.529*1.22= 1.865 gr/cm^3. The mass of water required to achieve 22% moisture content for the San Antonio soil was added to the soil to be compacted into the ring. For the previously mentioned ring dimensions this can be

calculated to be: Mass of 22% moist soil needed for ring 1: 1.865 (gr/cm^3)*73.71 (cm^3) = 137.47 gr.

Specimens were compacted into brass rings with height of ~2.5 cm and diameter of ~6.4 cm in three layers. Each layer was prepared with soil weighing one third of the total targeted weight of the soil specimen for the ring. Top surfaces of the two bottom compacted layers were scarified using a sharp-edged tool to establish good contact between the soil layers. The height of each layer was kept to one third of the ring height. A steel rod with diameter of about 18 mm was used for compaction to achieve a dry density of 95% standard maximum dry unit weight of soil.

At least two replicates of each test were run on specimens prepared from the same soil. The purpose of running replicate tests was to achieve higher reliability in test results and to better know measurement scatter through generating more data points. After preparation, compacted specimens were soaked in water to reach saturation (or close to saturation) condition. Due to the fact that the soils tested were all expansive clays, in order to minimize swell during specimen soaking, some seating load was applied to the specimens. The amount of net normal stress applied was around 15kPa. The specimens were soaked for a few days (6 to 10 days). Saturated specimens were then taken out of water and the excess water was mopped from exterior of the ring using a paper towel and the mass of saturated soil plus ring was recorded. After measuring the saturated mass of the specimen, the specimen was ready to start the test.

For the low range of suction (lower than 1500kPa) the test was carried out in the SWC-150 oedometer-pressure plate cells (GCTS, 2004). This apparatus, as mentioned

previously, uses axis translation method to control matric suction. Air pressure provided by central hydraulic pressure system (for air pressures up to 700kPa) or air cylinders (for air pressures up to 1500kPa) was used to supply the inlet pressure to the pressure regulator while holding the pore water pressure to zero. By this method matric suction values of up to 1500kPa were achieved.

At the beginning and throughout the test, the water in the tubes (which was distilled and de-aired water) was flushed using a flushing device to expel any trapped air in the groove at the bottom of the cell (underneath the high air entry stone). While flushing, care was taken not to introduce more air into the grooves located in the bottom plate and also not to spill any water from the top of the tubes. When no more air bubbles were observed during flushing, the device was assumed to be ready to use and the test was started by applying the desired net normal stress and cell pressure (i.e. suction).

The tests in this study were generally started at matric suction of 10kPa to 25kPa. The saturated specimens were set in the device (at the center of the HAEV ceramic stone) and the device was assembled and the net normal stress and suction were applied to the specimen. Net normal stress was applied by putting weights on the loading ram which is located at the top of the cell. The specimens were allowed to equilibrate at each suction value, which due to high plasticity and low permeability of the soils took about one month (for each suction point). During this time water levels in the tubes were monitored and if no change in water level was noticed for 5 to 7 days, it was assumed that the sample has reached equilibrium. At this point, the air pressure was released and the SWCC device was dismantled (in drying SWCC paths) and the specimen was weighed

and any deformation (axial and radial) was measured by use of electronic calipers. For the cases in which SWCC device was not dismantled (e.g. at low suctions during wetting cycles when the only volume change was axial due to large net normal stress values which minimized the radial shrinkage of the soil), the volume change of the soil specimen was measured by use of dial gauges installed at the top of the device, and the amount of water released from the specimen (or absorbed into the specimen) was measured by monitoring the levels of water in the tubes.

For the cases with low suction (200kPa or less, and depending on the applied net normal stress) when the full contact between the soil and ring was maintained, the cell was not disassembled. This was due to the fact that there was no radial shrinkage of the specimen and it was assumed that the volume change of the sample was only in the vertical direction. For these cases only the water level change was monitored for water content determination (i.e. no direct measurement of the mass of the specimen was made after equilibration) and vertical deformation of the soil was measured using dial gauges. It should be mentioned that under high values of suction (greater than 200kPa) particularly for the tests with smaller net normal stresses, it was noticed that the soil tended to pull away slightly from the ring (i.e. radial shrinkage due to drying) and therefore, volume change of the soil was both radial and vertical. For these cases the cells were dismantled after equilibration and the radial and axial deformations were determined by calipers.

At the end of the last pressure increment, the pressure was released and the apparatus was disassembled. Following measurement of the weight and dimensions of

specimen, the specimen was kept in the oven for drying for at least 24 hours at 110 ºC and its dry weight was recorded. The obtained data was used to determine volumetric water content, degree of saturation, and gravimetric water content of the soil specimens for different suction values.

The gravimetric water content was found by determining the mass of water and solids by over drying the soil. By definition, gravimetric water content is the ratio of the mass of water to the dry mass of soil:

$$w = \frac{M_w}{M_s} \tag{3.1}$$

Where w is the gravimetric water content, M_w is the mass of water present in the soil, and M_s is the mass of solids. Degree of saturation is the ratio of volume of water to the volume of voids:

$$S = \frac{V_w}{V_v} \tag{3.2}$$

Where S is the degree of saturation, V_w is the volume of water, and V_v is the volume of voids. Degree of saturation can also be calculated by using the following equations:

$$S = \frac{wG_s}{\frac{G_s\gamma_w}{\gamma_d} - 1} \tag{3.3}$$

Where G_s is the specific gravity of the soil, w is the water content, γ_w is the unit weight of water, and γ_d is the dry unit weight of the soil. As mentioned previously, specific gravities of the Anthem, Colorado, and San Antonio soils and are listed in Table

3.1. The dry density of the specimens was also calculated for each suction tested by measuring the volume and mass of the specimen. This data was used for each suction tested to find the degree of saturation of the specimen.

In order to evaluate importance of volume change measurement in determining SWCC's, the degree of saturation of the soils were once calculated based on the initial volume of the specimen (i.e. the volume of the specimen at the time of starting the SWCC test). The values of degrees of saturation of the specimens were also calculated based on the instantaneous volume of the specimen, which is the true volume of specimen at the time of equilibrium at each suction. For determining the instantaneous volume of the specimen the amount of radial and/or axial deformation was taken into account. The SWCC's that were generated based on the instantaneous volume of the specimen are referred to as volume corrected SWCC's and the SWCC's that were generated based on the initial volume of the specimen (i.e. volume change of the specimen throughout the test was not considered in determining the SWCC) are referred to as volume uncorrected SWCC's.

Volumetric water content is defined as the ratio of volume of water to the total volume of the specimen:

$$\theta = \frac{V_w}{V_T} = \frac{V_w}{V_s + V_v} \tag{3.4}$$

Where θ is the volumetric water content, V_w is the volume of water, V_s is the volume of solids, V_v is the volume of voids, and V_T is the total volume of the specimen. The equations for volumetric water content can also be written as:

$$\theta = \frac{w\gamma_d}{\gamma_w} \tag{3.5}$$

Values of water content and γ_d were known for the specimen equilibrated at certain suction values. Similar to calculating degree of saturation, volumetric water content for each suction was calculated once based on the initial volume of the specimen (i.e. ignoring volume change of the specimen throughout the test) and once based on the instantaneous volume of the specimen which was determined by measuring radial and axial deformations of the specimen by using calipers. The SWCC in terms of volumetric water content that was generated based on the initial volume of the specimen is referred to as volume uncorrected SWCC and the one generated based on the instantaneous volume of the specimen is referred to as volume corrected SWCC. The results of the SWCC tests are presented later in this chapter.

The slurry specimens were made by first measuring the mass of the ring. The ring was then set on top of the High Air Entry Disk (HAED) of SWCC device. HAED was kept saturated prior to starting of the test. Pulverized soil at natural moisture content was then added to the ring with a small compaction effort until the ring was filled with soil. The mass of soil added to the ring was determined by weighing the soil container before and after putting soil in the ring. When the ring was filled with soil water was added very slowly allowing the water to penetrate into the soil and fill the ring uniformly. The mass of added water was also measured by knowing the mass of water container before and after putting water in the ring. By knowing the dimensions of the ring and mass of soil, the soil moisture content, and mass of water, the dry and wet density of soil in the ring

was calculated and used for determining volumetric water content and degree of saturation values for each suction.

Similar to SWCC tests for compacted specimens, slurry specimens were allowed to equilibrate at each suction value. Also a token load (≈7kPa) was applied to the specimens. The purpose of the token load is that it helps provide a positive contact between the soil specimen and the ceramic stone for efficient water migration to and from the soil specimen. Due to high volume change of slurry specimens, upon equilibration at each suction, the SWCC cell was dismantled and the soil specimen was weighed and its volume change (axial and radial deformation) was measured by calipers when there was sample shrinkage. At the end of each test, the samples were weighed and volume changes were measured and recorded and the samples were dried in an oven with temperature of 110^0C for 16 to 20 hours in order to calculate the final water content of the soil. The obtained data was used to compute the required parameters such as volumetric water content, and degree of saturation. Appendix A includes some of the images of the compacted and slurry specimens equilibrated at different suction values tested in this study. The images illustrate volume change of soils throughout the tests.

3.4.2 SWCC Determination Using Filter Paper Test

The SWCC data points for larger suction range (greater than 1,500kPa) were measured by filter paper. For the filter paper test in this study, Whatman's No. 42 filter paper was used. The filter paper tests were conducted in accordance to the article titled "Laboratory Filter Paper Suction Measurements" (Houston, Houston and Wagner, 1994).

A filter paper in contact with the soil specimens allows water in the liquid phase and solutes to exchange freely and therefore, measures matric suction (Rahardjo and Leong, 2006). A total of two filter papers were used in each of the filter paper tests. The soil was compacted at 95% maximum dry density and the filter papers were placed in between the layer of the soil to ensure close contact between soil and filter paper. At least one month was allowed for matric suction equilibrium.

In the filter paper tests for this study, whenever handling the filter papers, latex gloves were worn to avoid contamination of the filter papers to dust or any residue. The filter papers were cut into small pieces. The small pieces of filter paper were then wrapped inside clean filter papers to avoid direct contact between the soil and the small piece of filter paper. Filter paper was then placed in between compacted layers of soil (compacted at 95% maximum dry density and at different moisture contents) in glass jars. The surface of soil where the filter paper was placed was scarified to ensure good contact between the soil and the filter paper.

The filter papers within the soil was allowed time to equilibrate to the soil moisture content for the duration of about one month and then the filter papers were taken out and weighed and the moisture content was determined by oven drying. When the filter paper was to be removed and weighed, the soil around the filter paper was first removed. For this portion of the test also, latex gloves were used to avoid contamination of filter papers. The filter paper was carefully removed from the soil and immediately placed in a plastic bag with previously measured mass. The bag containing the filter paper was weighed and then the piece of filter paper was dried in an oven at a

temperature of 110^0C for 24 hours. The dry mass of filter paper was then determined and the moisture content of the filter paper was calculated. All of the weights (expect specimen weight) were measured using a scale with 10^{-4} grams accuracy.

The filter paper water content was then related to the soil matric suction. The moisture content of the soil taken out of the jar was also determined. In order to increase the accuracy of test results, two or three measurements of water contents and suction were taken from each jar (at various locations within the jar). The relationship between the filter paper water content and the soil matric suction is specific to the type of filter paper used. Since Whatman's No. 42 filter paper was used, the following relationship was used (Chandler and Gutierrez, 1986):

$$\psi(pF) = 5.850 - 0.0622 w_{filterpaper} \tag{3.6}$$

$$\psi(kPa) = \gamma_w \times 10^{\psi(pF)} \tag{3.7}$$

Where:

$\psi(pF)$: Soil matric suction in pF

$\psi(kPa)$: Soil matric suction in kPa

$w_{filterpaper}$: Filter paper water content

γ_w: Unit weight of water

With the wet and dry mass of filter papers, the correlation above can be used to determine the matric suction of the soil within which the filter paper has been placed previously. The results of filter paper test are presented in the following sections.

3.5. Results of SWCC Tests

A total of 21 SWCC experiments were conducted as a part of this study. The SWCC results for Anthem, Colorado, and San Antonio slurry and compacted specimens are presented in this section.

The van Genuchten (1980) fit for SWCC was used to best-fit the data points obtained from the laboratory results. The reason for using van Genuchten (1980) fit for SWCC over other common equations (e.g. Fredlund and Xing, 1994) was that the van Genuchten (1980) fit was used for the numerical modeling which was conducted as another task in this study. Three computer programs were used for the numerical modeling (SVFLUX, VADOSE/W, and CODE-BRIGHT). The only SWCC fit equation that these three programs have in common is the van Genuchten (1980) fit. For this reason, and in order to be consistent throughout the SWCC fitting process, van Genuchten (1980) was used to best-fit SWCC's to the data obtained from laboratory experiments.

Van Genuchten (1980) has the following form:

$$\theta = \theta_r + \frac{\theta_s - \theta_r}{\left[1 + \left(\frac{\psi}{a}\right)^n\right]^m} \tag{3.8}$$

Where:

θ = the volumetric water content,

θ_s = the saturated volumetric water content,

θ_r = the residual water content

ψ = the negative pore-water pressure (i.e. matric suction), and

a, n, m = curve fitting parameters

"a" has units of pressure and corresponds to the air-entry value of the SWCC (i.e. larger "a" indicates larger AEV's). "a" has also been defined as the pivot point about which the "n" parameter changes the slope of the function (Geo-Slope, 2012). "n" corresponds to the slope of the curve, i.e. larger values of "n" indicate larger slope of the curve in the region between the air-entry value and the residual suction. "m" is related to "n" with the expression: $m = \frac{n-1}{n}$

The parameter m affects the sharpness of the sloping portion of the curve as it enters the lower plateau (Geo-Slope, 2012). The same form of van Genuchten equation can be applied to the SWCC's in terms of gravimetric water content and degree of saturation. Van Genuchten (1980) equation for SWCC in terms of degree of saturation (S) is as below:

$$S = S_r + \frac{S_s - S_r}{\left[1 + \left(\frac{\psi}{a}\right)^n\right]^m} \tag{3.9}$$

Throughout the following sections, SWCC data points obtained from laboratory tests are presented along with the best-fit curve using van Genuchten equation. The values of van Genuchten equation parameters (a, n, and m) are also presented for each SWCC in order to make the necessary comparisons.

3.5.1. SWCC of Compacted Specimens

Compacted specimens of Anthem, Colorado, and San Antonio soils were prepared and tested under net normal stress of 7kPa (seating load). The purpose of this set of testing was to find the impact of soil volume change on the shape of the SWCC's, with particular focus on the air-entry values and slope in the transition zone.

The SWCC plots show that the compacted specimens never achieved complete saturation even upon complete submergence (due to the presence of occluded air-bubbles). On other words, 100% saturation was not obtained when soaking the specimens under water (with load on the top of specimens). It should also be mentioned that at the end of wetting tests, 100% saturation was not obtained due to presence of occluded air-bubbles.

Two replicate specimens of each soil, which were prepared at the same density and water content, were tested in order to find the reproducibility and reliability of results. The results that are shown in Figures 3.7 through 3.15 suggest good reproducibility of tests.

Table 3.3 contains the list of van Genuchten SWCC fit parameters for the SWCC tests conducted on compacted specimens of Anthem, Colorado, and San Antonio soils. The applied net normal stress in this series of tests was 7kPa (i.e. seating load). A seating load was used to ensure good contact between the specimen and the high air-entry stone throughout the test. As shown in the Table 3.3, for a certain soil, values of "a" are larger for the SWCC's in terms of volumetric water content and degree of saturation compared to the "a" for SWCC's in terms of gravimetric water content. The is due to the fact that

the SWCC's in terms of volumetric water content and degree of saturation are corrected for soil volume change that occurred throughout the test. The soils tested in this study are expansive soils which shrink upon drying (i.e. increase in suction). This leads to decrease in volume of the specimen which is in fact decrease in the volume of voids as the soil particles are assumed to stiff enough so that no volume change of the soil particles occurs during the change in suction. As described in earlier sections of this chapter volumetric water content and degree of saturation of soils are defined by the following equations:

$$\theta = \frac{V_w}{V_T} = \frac{V_w}{V_s + V_v} \tag{3.10}$$

$$S = \frac{V_w}{V_v} \tag{3.11}$$

It can be found from these equations that for a certain amount of water, a decrease in volume of voids will lead to larger values of volumetric water content and degree of saturation. Therefore, at a certain suction, SWCC that has been corrected for soil volume change generally shows larger values of volumetric water content and degree of saturation. At the same time, the soil volume change cannot be incorporated in the SWCC in terms of gravimetric water content. This leads to larger AEV's of the SWCC's that are in terms of volumetric water content and degree of saturation compared to the SWCC in terms of gravimetric water content. Values of “a” parameter shown in Table 3.3 support this theory. It can be seen that the "a" parameter, which corresponds to the air-entry value of the SWCC, is larger for volumetric water content and degree of saturation (S) SWCC's compared to gravimetric water content (w) SWCC's for all three soils tested. As an example, for Anthem soil the value of "a" parameter for SWCC in terms of gravimetric

water content is 40, while the values of “a" for SWCC's in terms of volumetric water content and degree of saturation are 50 and 60, respectively. The same increase in values of "a" is observed for Colorado and San Antonio soils.

Table 3.3 also shows values of "n" parameter for SWCC's in terms of gravimetric water content, volumetric water content, and degree of saturation for different soils. It can be seen that in general, for a certain soil, value of "n" is larger for SWCC's in terms of volumetric water content and degree of saturation compared to the SWCC in terms of gravimetric water content. This means that for a certain soil, the slope of SWCC in terms of gravimetric water content(in the range between the air-entry and residual values) is smaller than this slope in SWCC's in terms of volumetric water content and degree of saturation.

Table 3.3. Values of van Genuchten fitting parameters for SWCC's in terms of gravimetric water content (w), volumetric waster content (θ), and degree of saturation (S) for compacted specimens tests under net normal stress of 7kPa (seating load)

Soil	Specimen Type	"a" Parameter			"n" Parameter			SWCC	Description
		w	θ	S	w	θ	S		
Anthem	Compacted	40	50	60	1.170	1.175	1.170	Corrected	Average of two replicates for each soil
Colorado	Compacted	80	120	210	1.200	1.210	1.245	Corrected	
San Antonio	Compacted	40	60	105	1.170	1.175	1.200	Corrected	

Table 3.4 presents van Genuchten fitting parameters and air-entry values for compacted specimens of Anthem, Colorado, and San Antonio soil tested under net normal stress of 7kPa. In this table, values of "a" and "n" can be compared for the cases of volume corrected SWCC against volume uncorrected SWCC that were developed in terms of volumetric water content and degree of saturation. As previously mentioned,

volume corrected SWCC's were developed by using the instantaneous volume of the specimen while in volume uncorrected SWCC's initial volume of the specimen was utilized and the soil volume change throughout the test was ignored. Data in Table 3.4 demonstrate the difference in the van Genuchten fitting parameters, particularly the "a" parameter between the volume corrected and uncorrected SWCC. For example, it can be seen from Table 3.4 that "a" increases from 90 for the volume uncorrected SWCC of Colorado soil in terms of volumetric water content to 130 for the volume corrected SWCC. Also "a" increases from 40 for the volume uncorrected SWCC of San Antonio soil in terms of degree of saturation to 100 for the volume corrected SWCC. Table 3.4 also shows larger AEV for corrected SWCC's compared to uncorrected SWCC's. It can also be seen that generally AEV is larger for SWCC in terms of degree of saturation compared to the SWCC in terms of volumetric water content.

The "n" parameter for volume corrected and volume uncorrected SWCC's are also shown in Table 3.4. It can be seen that for a certain soil, "n" parameter is generally larger for the volume corrected SWCC (i.e. larger slopes of the curve in the range of air-entry and residual suctions) compared to the volume uncorrected SWCC. This seems to be the case for both SWCC's in terms of volumetric water content and degree of saturation.

Table 3.4. Values of van Genuchten fitting parameters and air-entry value (AEV) for SWCC's in terms of volumetric waster content (θ), and degree of saturation (S), and air-entry values for compacted specimens tests for volume corrected and uncorrected SWCC's tested under net normal stress of 7kPa (seating load)

Soil	Specimen Type	"a" Parameter		"n" Parameter		AEV		SWCC
		θ	S	θ	S	θ	S	
Anthem	Compacted	25	25	1.150	1.155	11	15	Uncorrected
Anthem	Compacted	35	60	1.155	1.170	20	50	Corrected
Colorado	Compacted	90	80	1.225	1.210	50	60	Uncorrected
Colorado	Compacted	130	150	1.225	1.220	80	90	Corrected
San Antonio	Compacted	35	40	1.170	1.180	20	30	Uncorrected
San Antonio	Compacted	55	100	1.175	1.220	50	70	Corrected

Based on the equations for volumetric water content and degree of saturation (i.e. $\theta = \frac{V_w}{V_T} = \frac{V_w}{V_s + V_v}$ and $S = \frac{V_w}{V_v}$) and the SWCC's in terms of gravimetric water content, volumetric water content and degree of saturation obtained from this study, it was found that the SWCC in terms of degree of saturation best predicts the unsaturated soil properties. SWCC in terms of degree of saturation better captures the volume change of the soil that occurs during the SWCC test. This agrees with findings of other researchers (e.g. Li et al., 2007, Parent et al., 2007, Chiu and Ng, 2012, Fredlund and Houston, 2013) who recommended using degree of saturation SWCC's versus gravimetric or volumetric moisture content SWCC's. From Tables 3.3 and 3.4 it can be seen that for volume corrected SWCC's of any given soil, the value of "a" (and also AEV) is larger for the SWCC in terms of degree of saturation compared to these values for SWCC in terms of gravimetric water content and volumetric water content . This suggests that the air-entry values of the volume corrected SWCC's in terms of degree of saturation are generally

larger compared to air-entry values in SWCC's in terms of gravimetric water content and volumetric water content . The soils tested in this study are expansive clays (USCS classification of CL and CH) and the air-entry values obtained from SWCC's in terms of degree of saturation best describe the properties of these expansive clays.

The SWCC's generated for compacted specimens of Anthem, Colorado, and San Antonio soils which were tested under the net normal stress of 7kPa (i.e. seating load) are presented in Figures 3.7 through 3.21. The methodology that was used for finding AEV was SWCC's are shown in Figures 3.22, 3.23, and 3.24. In this method, tangent lines are drawn to the segment of the SWCC which shows suctions smaller than AEV. Another tangent is drawn to the curve in the transition zone (the zone between the AEV and residual). The point at which these two tangents cross is known as the air-entry value. Results of filter paper test are also shown in these figures. It was concluded that correcting SWCC's for soil volume change that occurs in the course of experiment plays a significant role in the shape of SWCC, particularly regarding the air-entry value. This agrees with findings by Fredlund and Houston (2013). In summary, for all the compacted specimens of the three soils, the shape of SWCC's in which gravimetric water content is plotted versus the soil suction is significantly different from the shape of SWCC's in which degree of saturation is plotted versus soil suction. The reason is that in the gravimetric moisture content plots, the volume change of the soil during suction variation is not considered. Whereas, for the SWCC's showing the volumetric water content or degree of saturation, the volume change of the soil has been taken into account. Because the soils in this study are all expansive soils, when the suction is increased and the soil

starts to desaturate, the volume of soil decreases, otherwise known as shrinkage. This can also be seen in the images of the soil samples which are provided in Appendix A. When calculating degree of saturation of the soil with its instantaneous volume (which is smaller than the initial soil volume at the beginning of the test), the degree of saturation is higher than the case in which the degree of saturation has been calculated based on the initial volume of the specimen.

Another major finding from this SWCC lab test is that due to existence of clods in soils with high plasticity during the compaction process, the air entry value of these soils turns out to be smaller than initially expected. The relatively low air entry values observed are believed to be the result of existence of clods creating air entry values more consistent with coarser-grained materials.

In order to evaluate the effects of clods on SWCC of these clays, with particular focus on the air entry value, SWCC tests were performed on slurry specimens. In slurry specimens, the pulverized soil was entirely saturated with water and therefore clods did not appear within the specimen. The results of SWCC tests on slurry specimens are presented in the next section of this chapter.

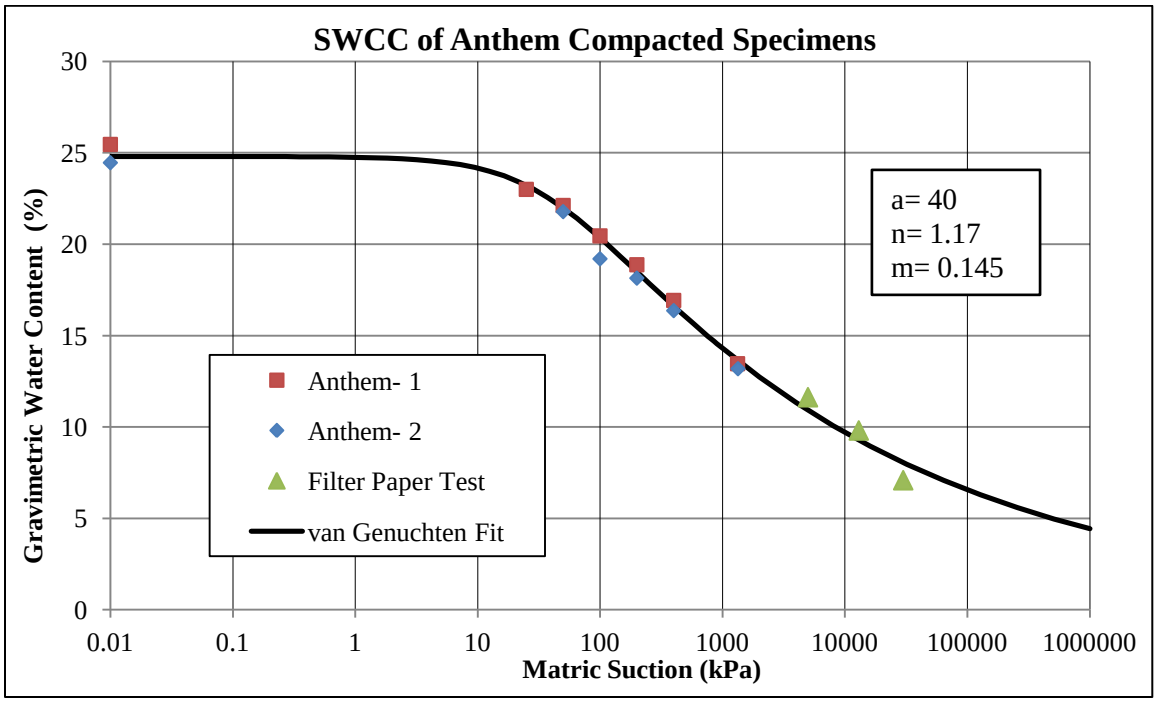

Figure 3.7. Gravimetric Water Content versus Soil Suction for Compacted Specimens of Anthem including Filter Paper Test Results

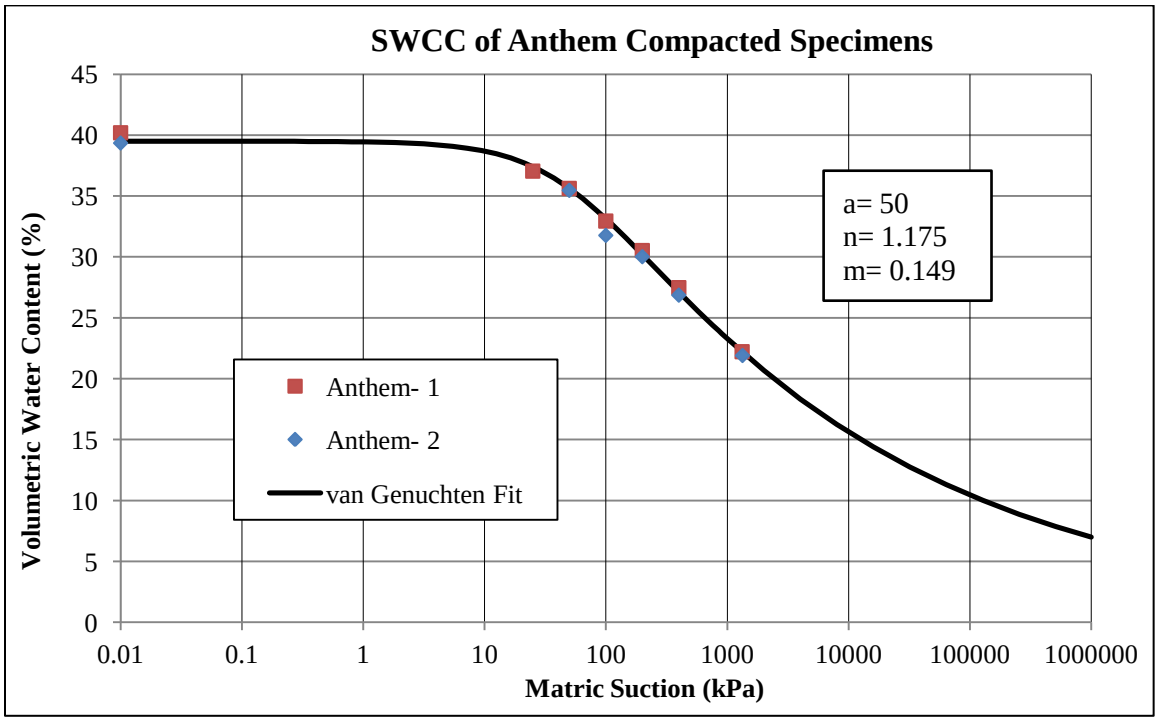

Figure 3.8. Volumetric Water Content versus Soil Suction for Compacted Specimens of Anthem, SWCC's are corrected for soil volume change

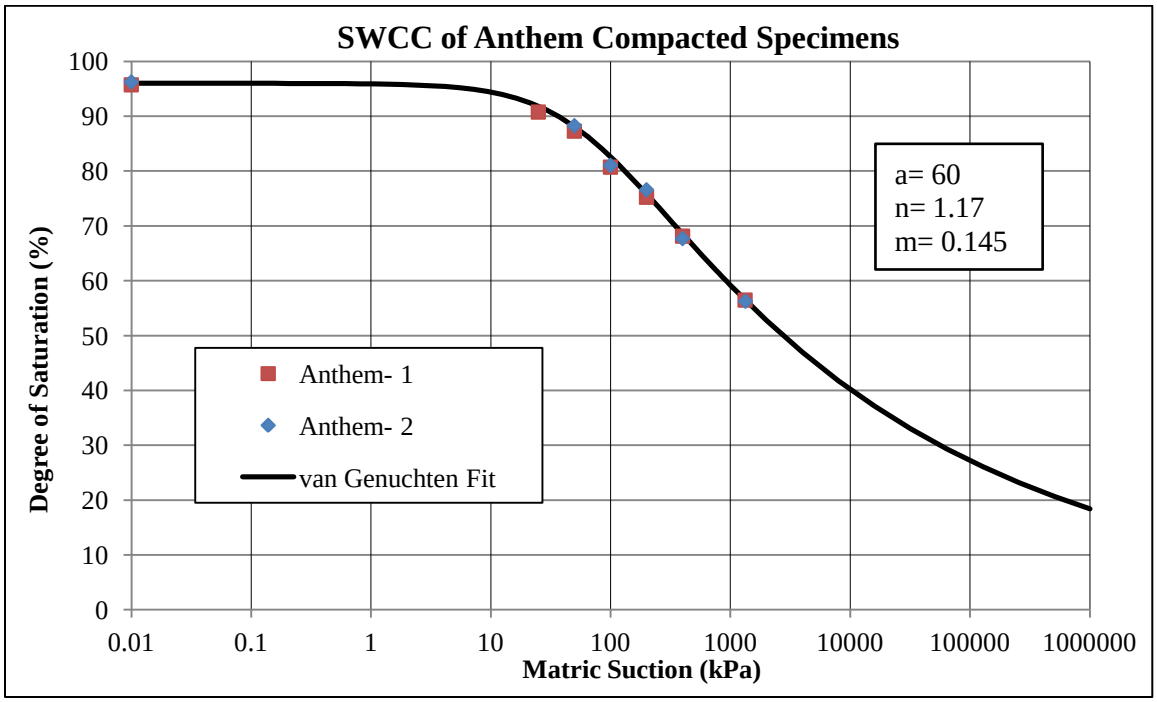

Figure 3.9. Degree of Saturation versus Soil Suction for Compacted Specimens of Anthem, SWCC's are corrected for soil volume change

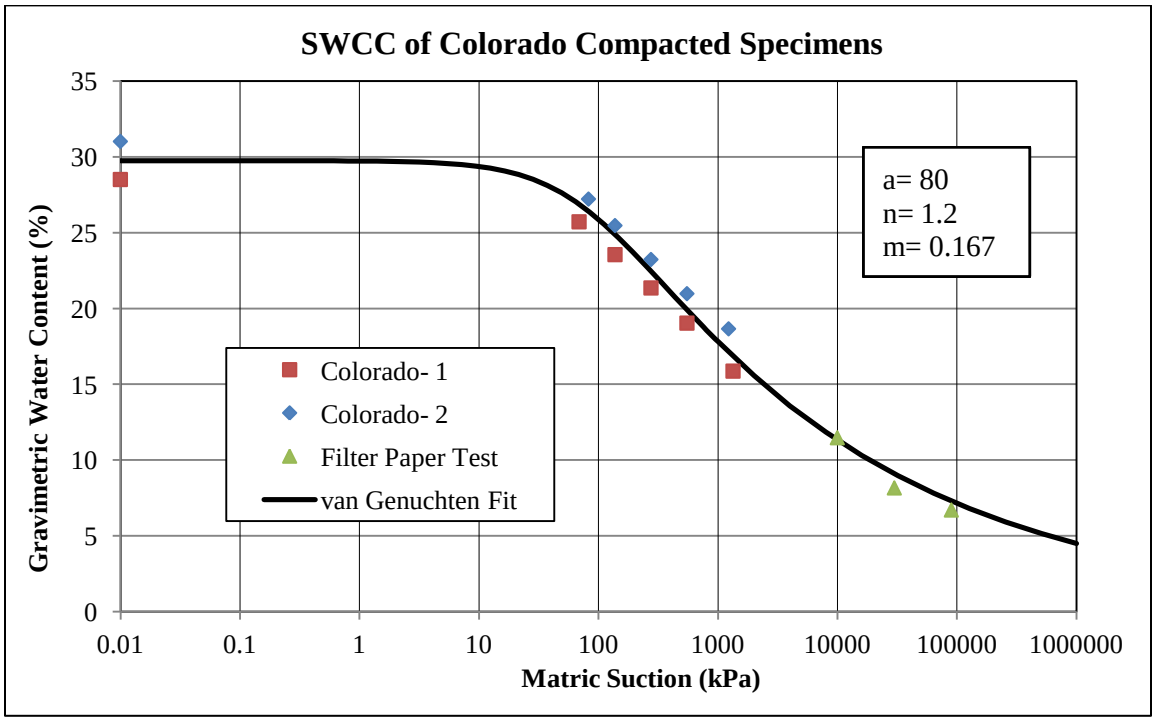

Figure 3.10. Gravimetric Water Content versus Soil Suction for Compacted Specimens of Colorado including Filter Paper Test Results

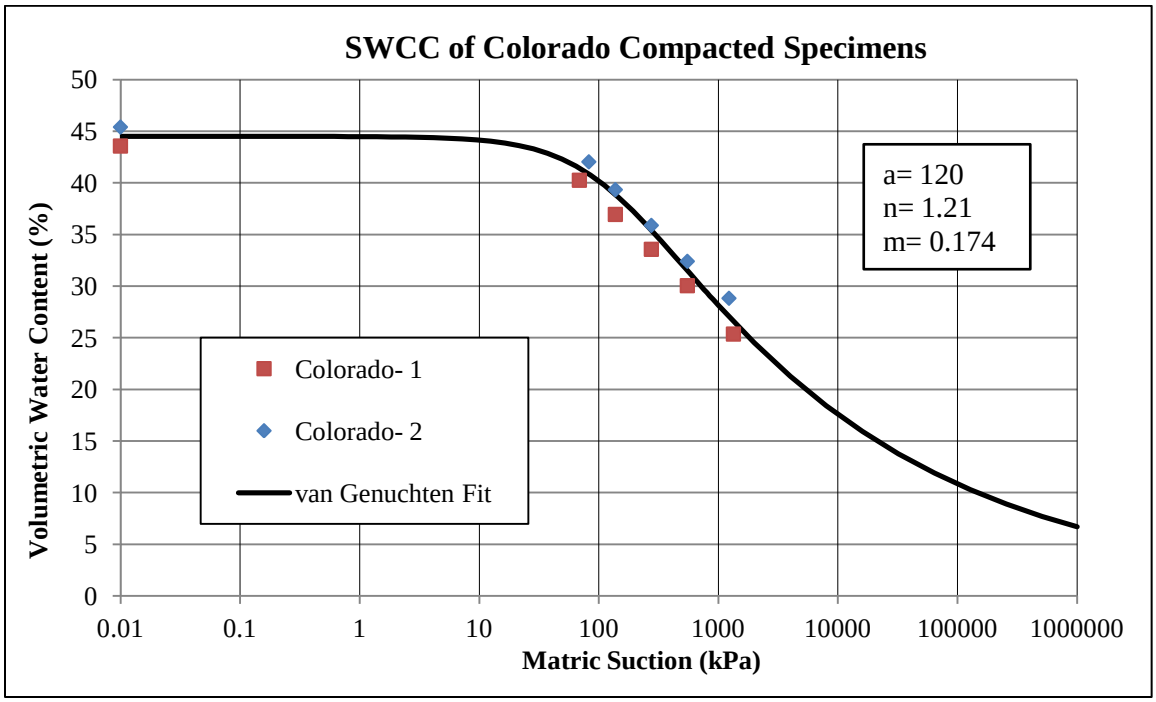

Figure 3.11. Volumetric Water Content versus Soil Suction for Compacted Specimens of Colorado, SWCC's are corrected for soil volume change

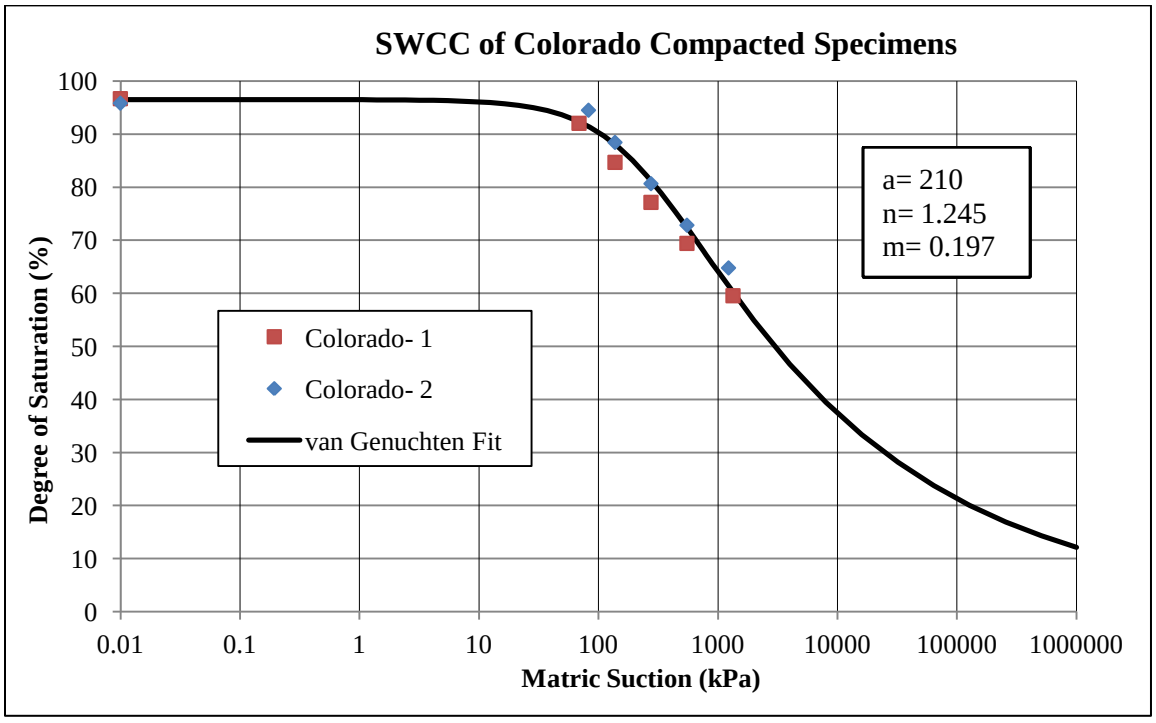

Figure 3.12. Degree of Saturation versus Soil Suction for Compacted Specimens of Colorado, SWCC's are corrected for soil volume change

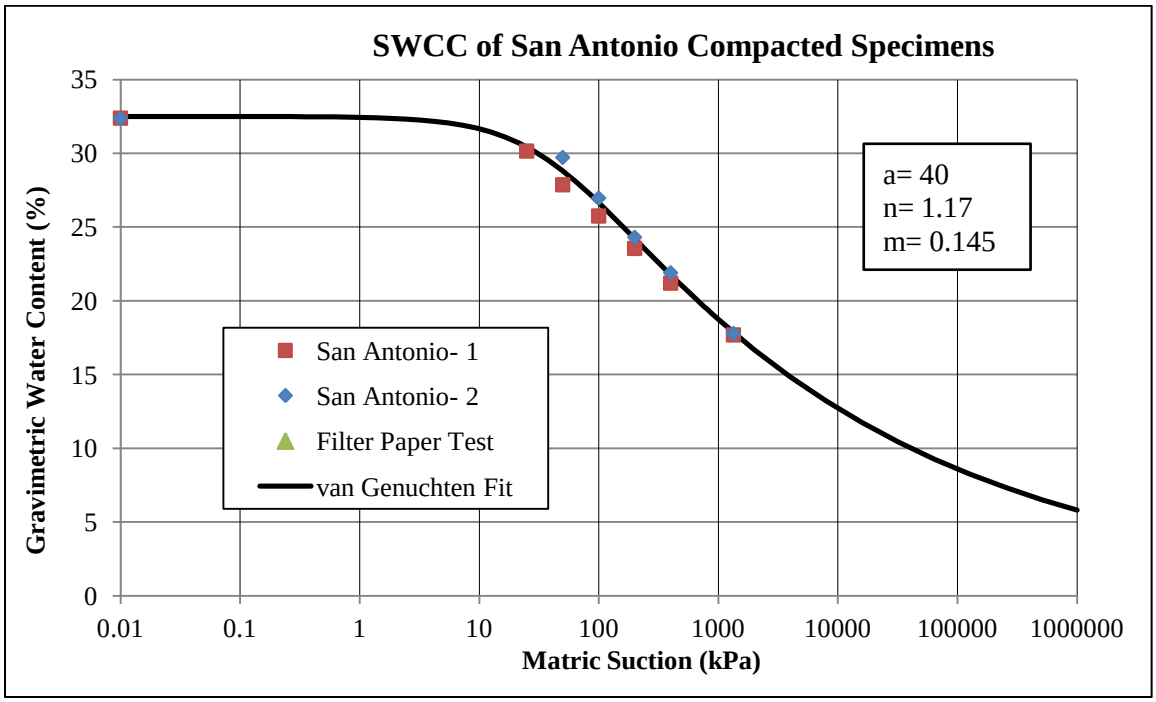

Figure 3.13. Gravimetric Water Content versus Soil Suction for Compacted Specimens of San Antonio including Filter Paper Test Results

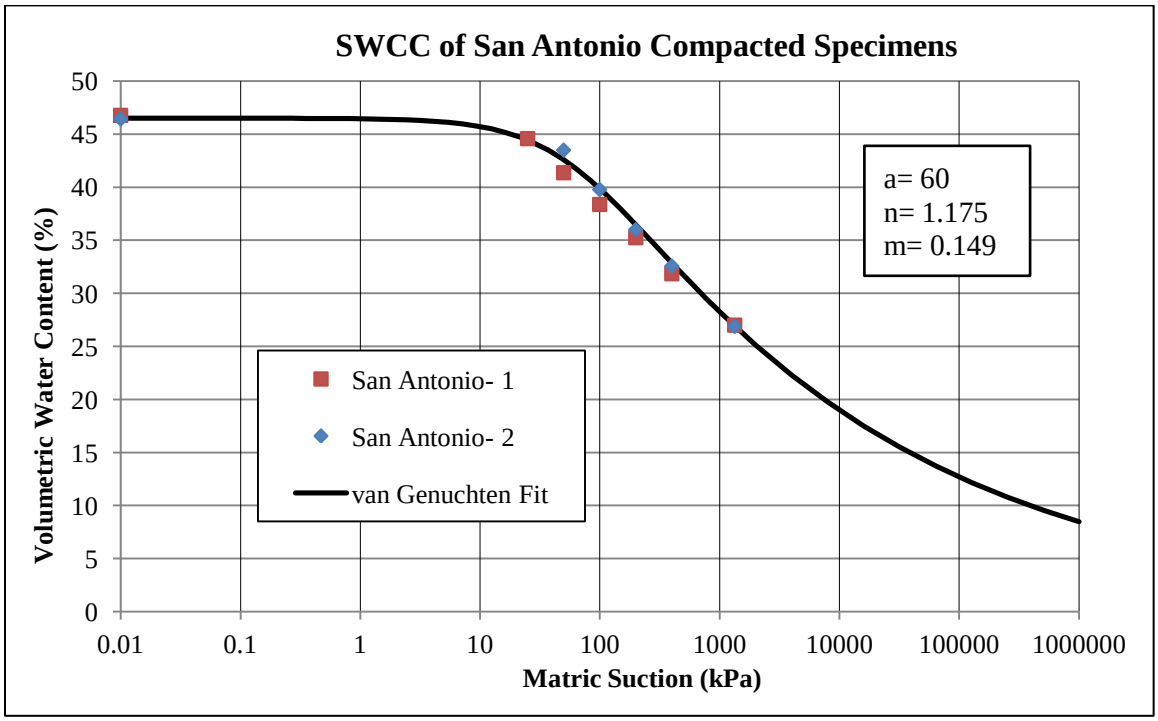

Figure 3.14. Volumetric Water Content versus Soil Suction for Compacted Specimens of San Antonio, SWCC's are corrected for soil volume change

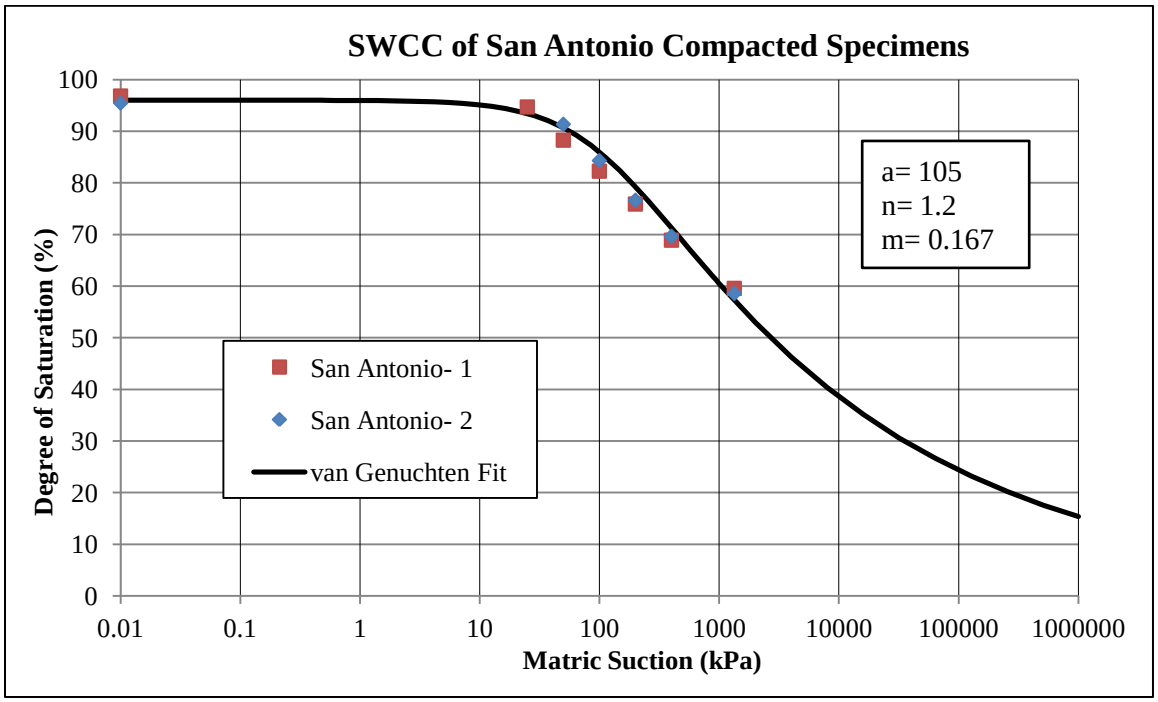

Figure 3.15. Degree of Saturation versus Soil Suction for Compacted Specimens of San Antonio, SWCC's are corrected for soil volume change

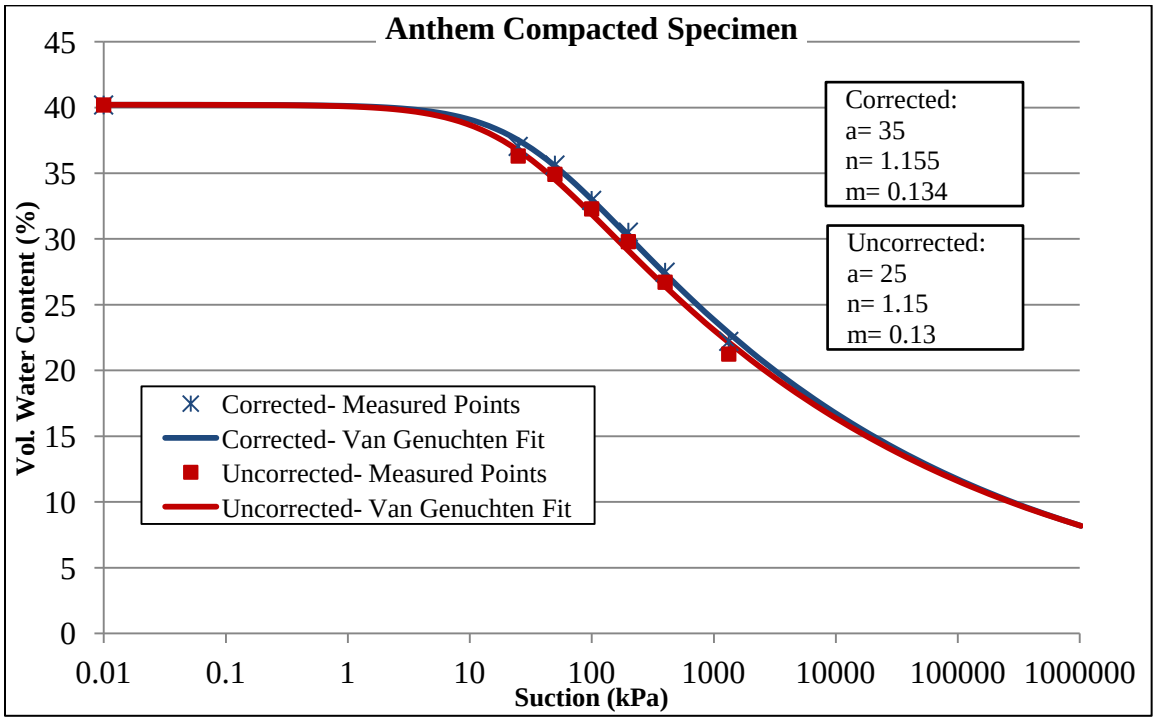

Figure 3.16. Corrected and Uncorrected SWCC for Soil Volume Change in Terms of Volumetric Water Content versus Soil Suction for Compacted Specimen of Anthem

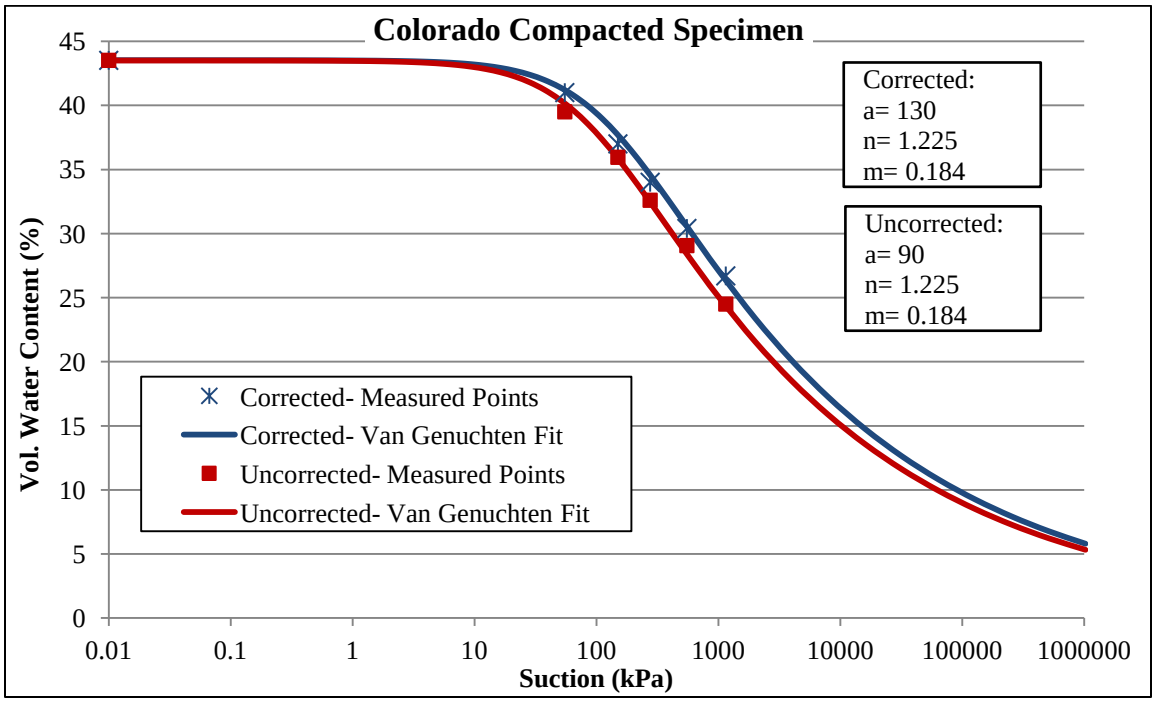

Figure 3.17. Corrected and Uncorrected SWCC for Soil Volume Change in Terms of Volumetric Water Content versus Soil Suction for Compacted Specimen of Colorado

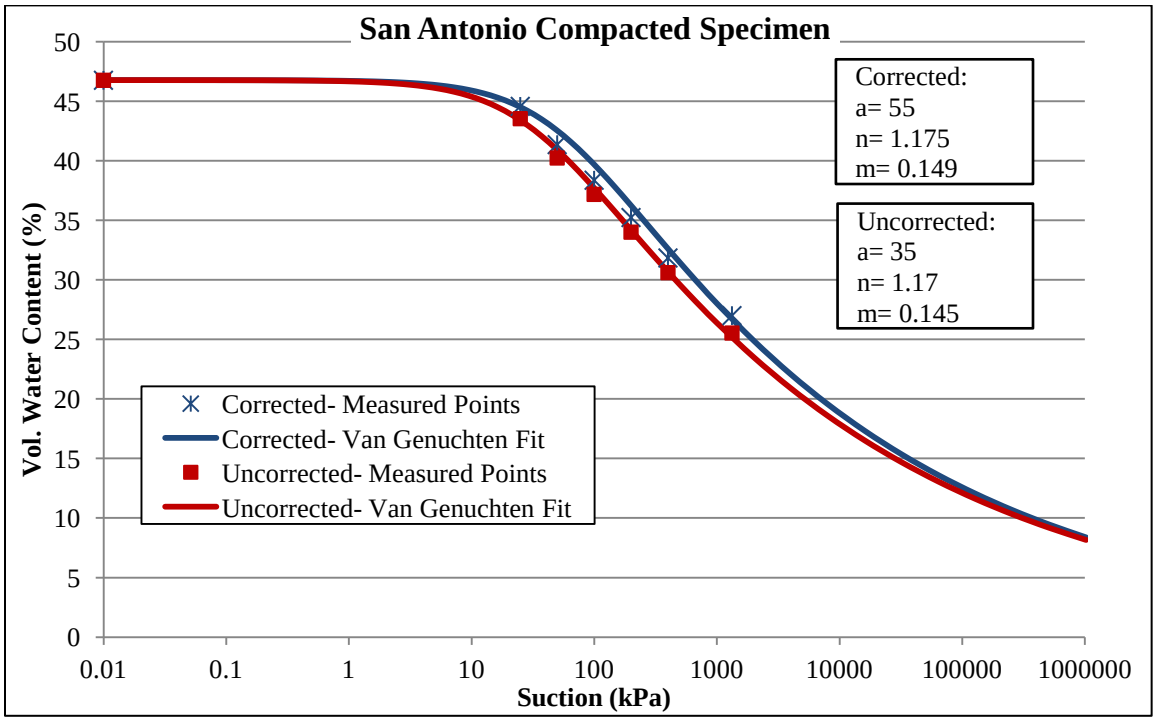

Figure 3.18. Corrected and Uncorrected SWCC for Soil Volume Change in Terms of Volumetric Water Content versus Soil Suction for Compacted Specimen of San Antonio

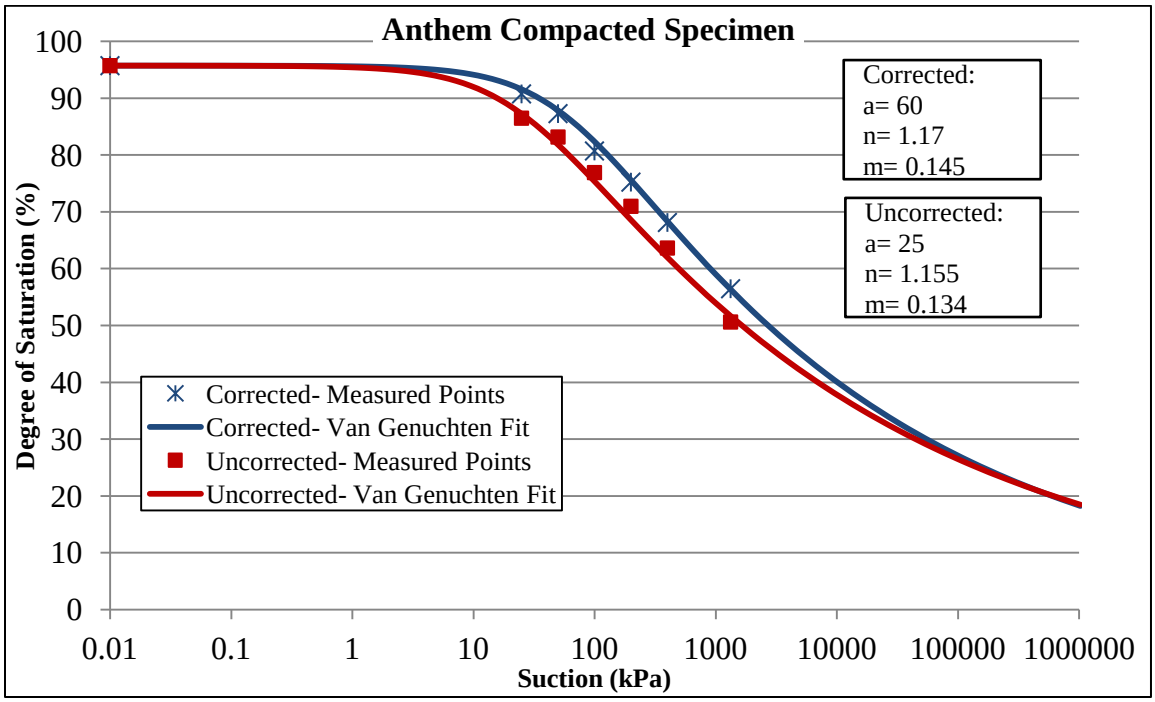

Figure 3.19. Corrected and Uncorrected SWCC for Soil Volume Change in Terms of Degree of Saturation versus Soil Suction for Compacted Specimen of Anthem

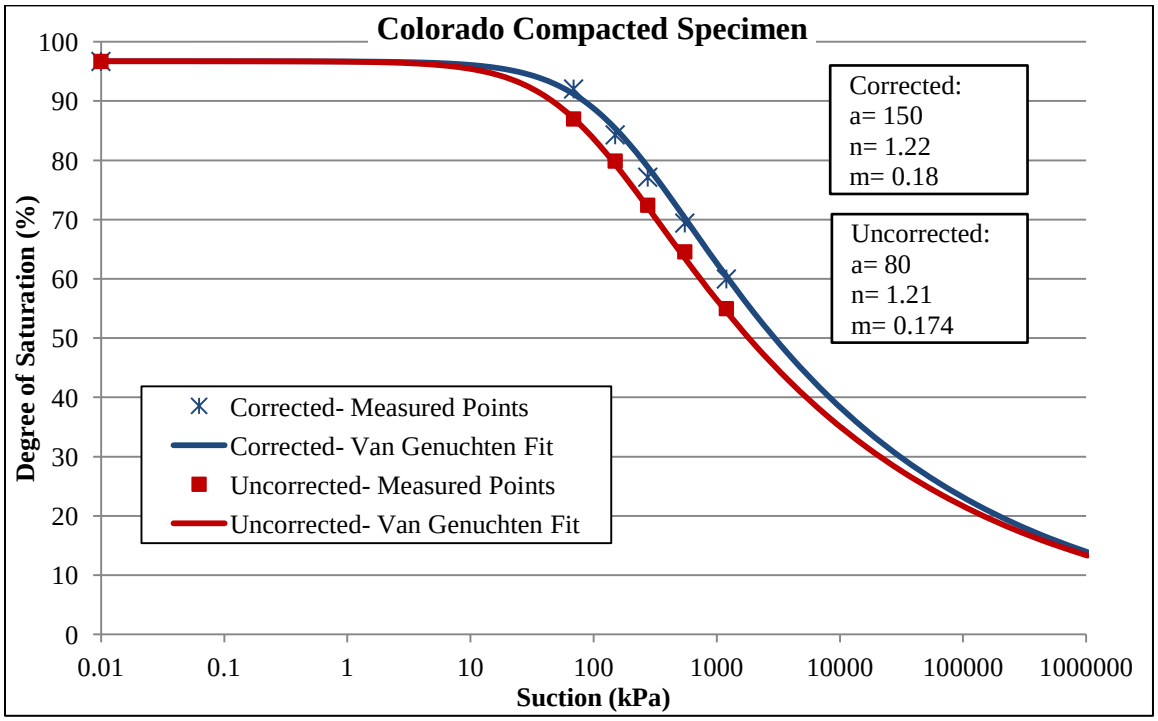

Figure 3.20. Corrected and Uncorrected SWCC for Soil Volume Change in Terms of Degree of Saturation versus Soil Suction for Compacted Specimen of Colorado

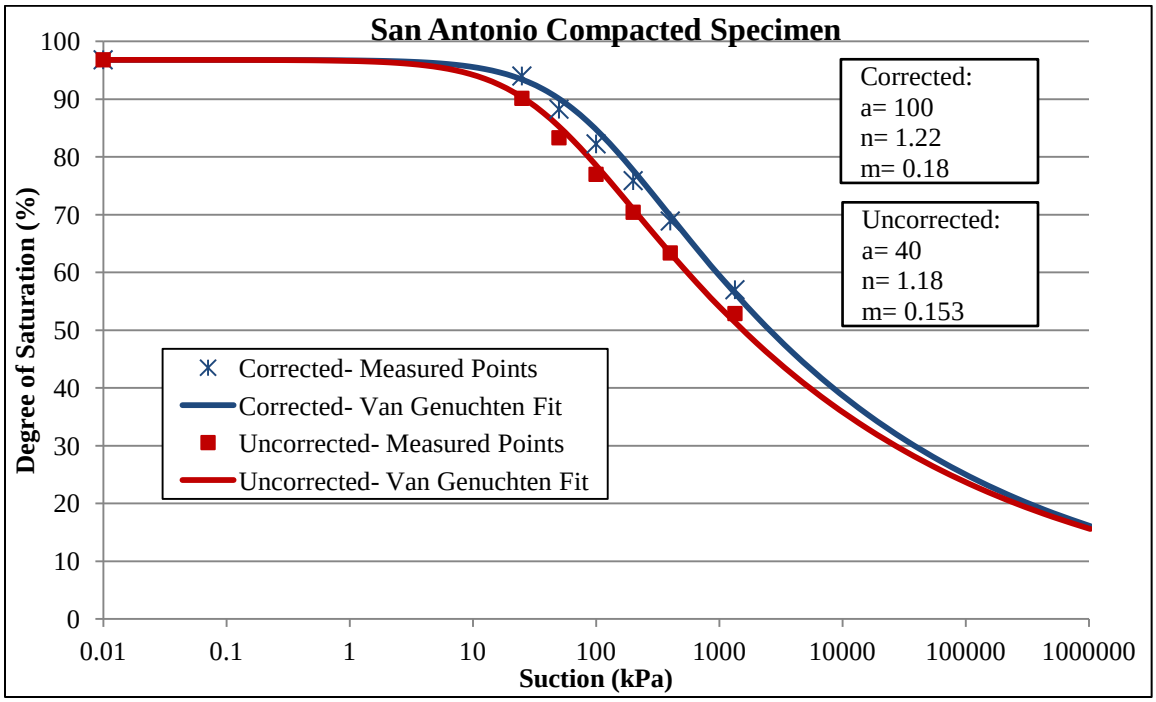

Figure 3.21. Corrected and Uncorrected SWCC for Soil Volume Change in Terms of Degree of Saturation versus Soil Suction for Compacted Specimen of San Antonio

Figures 3.22 through 3.24 show the method used to find the air-entry value of SWCC in terms of gravimetric water content, volumetric water content, and degree of saturation. These figures illustrate that for SWCC's in terms of volumetric water content and degree of saturation, the air-entry value is larger for volume corrected SWCC compared to volume uncorrected SWCC. It can also be seen from these figures that air-entry value found from SWCC in terms of degree of saturation are generally larger than that found from SWCC's in terms of gravimetric water content and volumetric water content.

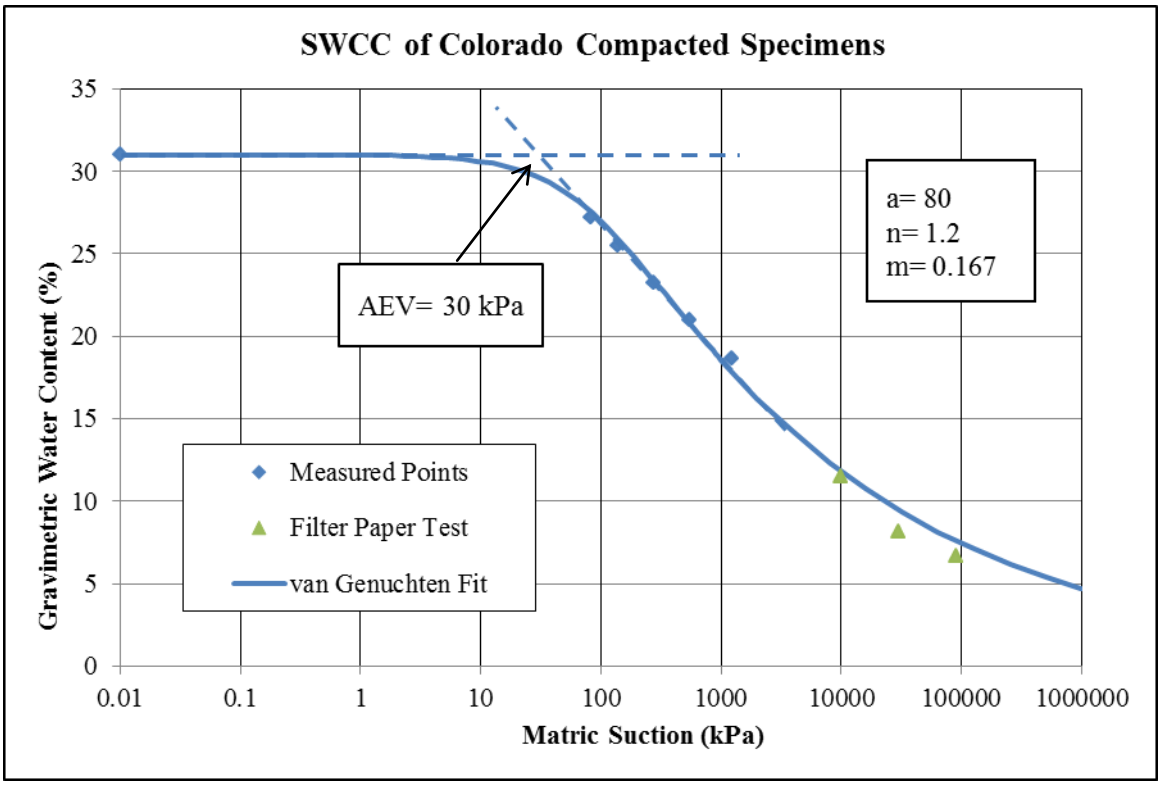

Figure 3.22. SWCC in terms of gravimetric water content for compacted specimen of Colorado showing the method used for obtaining the AEV

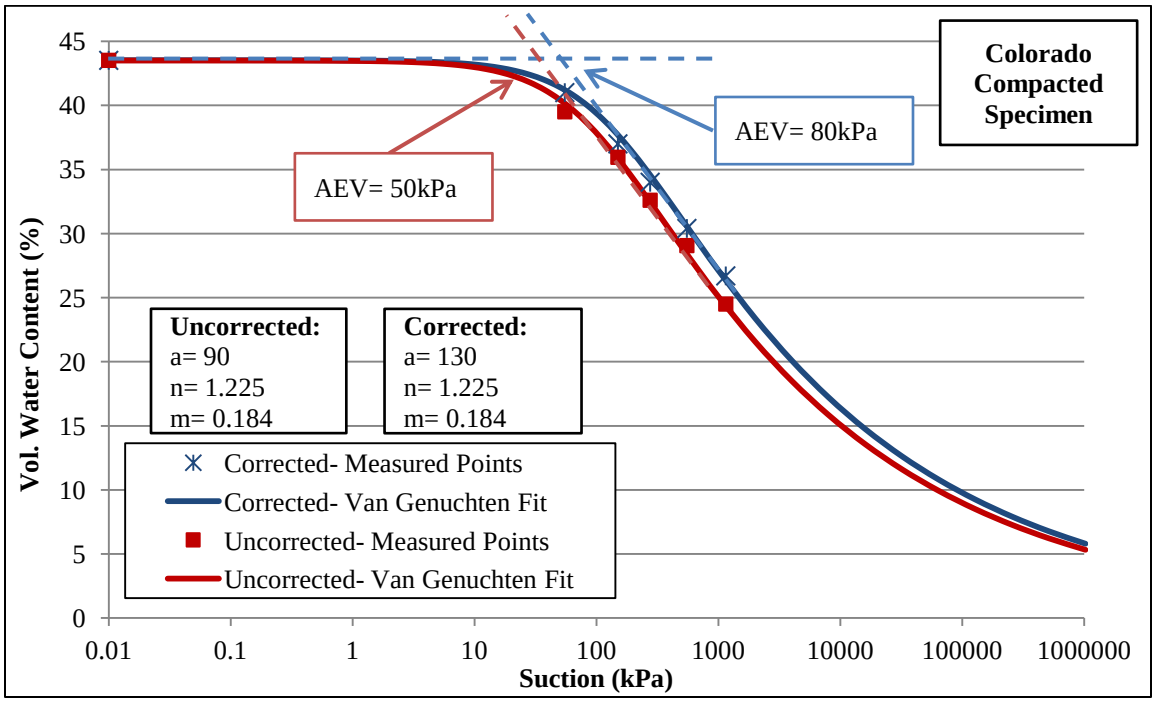

Figure 3.23. SWCC in terms of volumetric water content for compacted specimen of Colorado showing the method used for obtaining the AEV

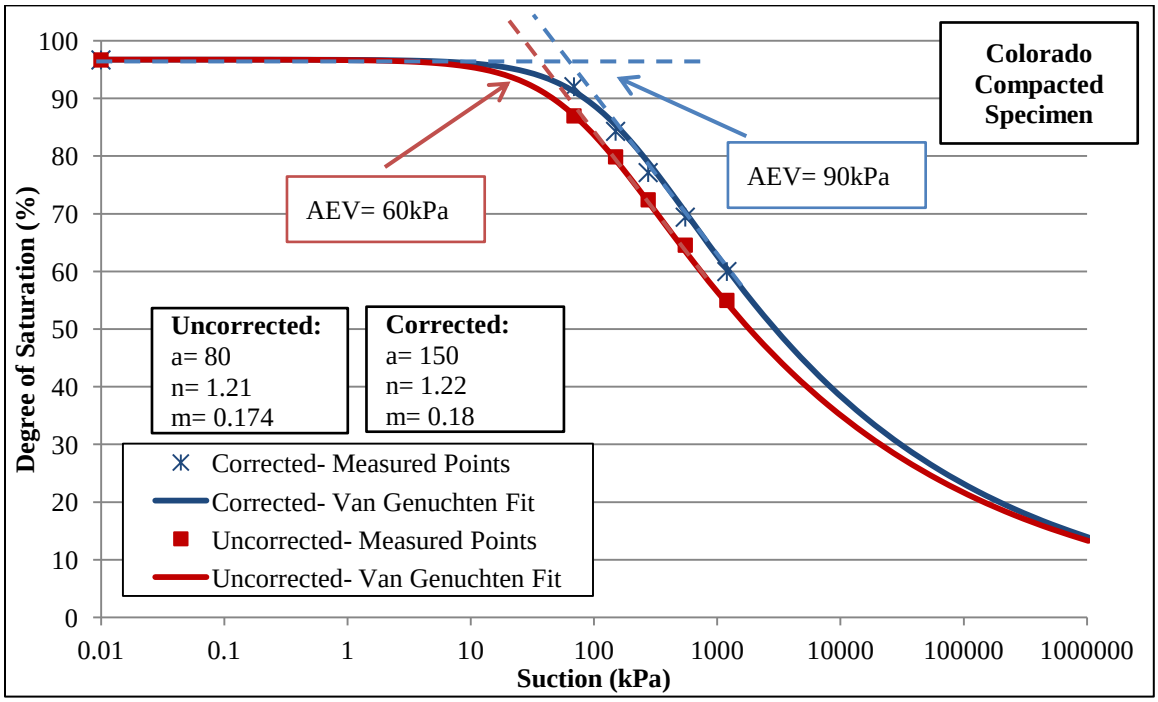

Figure 3.24. SWCC in terms of degree of saturation for compacted specimen of Colorado showing the method used for obtaining the AEV

3.5.2. SWCC of Slurry Specimens

The slurry specimens were prepared by mixing certain amount of soil and water to make sure that the specimen had reached 100% saturation. Drying SWCC test was then conducted on saturated specimens (of three soil types of Anthem, Colorado, and San Antonio). Moisture content and volume change of the specimens were measured during the test and SWCC's were established for these slurry specimens. SWCC's in terms of volumetric moisture content and degree of saturation were corrected for soil volume change during the test. These SWCC's are shown in Figures 3.25 through 3.33.

It should be mentioned that performing SWCC on slurry specimens in the 1-D device is rather challenging due to very high and often non-uniform volume change of these specimens, which often present challenges regarding measuring the volume change if the specimen during changes in matric suction. It is recommended that image processing software be utilized for measurement of volume change of slurry specimens.

The difficulty in volume change measurement of slurry specimens was pronounced for low net normal stresses. It was found that applying net normal stresses to the slurry specimens (even small net normal stresses in the order of 3- 7kPa) leads to more uniform shrinkage of the specimens. Uniform volume changes are generally easier to measure. Therefore, in all of the SWCC tests on slurry specimens a token load of 3kPa was used. Another advantage of using a token load is to ensure a good contact between the specimen and the high air-entry disc of the SWCC device throughout the test.

As for compacted specimens, it was found that for slurry specimens too, correcting SWCC's for soil volume change plays a significant role in shape of the SWCC

and particularly on the air-entry value. This was found by comparing SWCC's in terms of gravimetric moisture content versus SWCC's in terms of degree of saturation and volumetric moisture content. SWCC's in terms of gravimetric moisture content are not corrected for soil volume change (as they are generated based on masses of water and dry soil), while SWCC's in terms of degree of saturation and volumetric moisture content were corrected for volume change. Large differences were found between shapes of SWCC's corrected and uncorrected for volume change that were established for slurry specimens. Since the volume change of slurry specimens are significantly larger than the volume change of compacted specimens, the difference between the volume corrected and uncorrected SWCC's were found to be significantly larger for slurry specimens compared to compacted specimens. This is shown in Figures 3.27, 3.30, and 3.33 which present SWCC's in terms of degree of saturation established for slurry specimens.

It was found that SWCC's corrected for volume change (particularly SWCC in terms of degree of saturation) are the better indicator of true air entry value of soils which undergo significant volume change during suction variation (such as slurry specimens).

Table 3.5 presents values of "a" and "n" parameters of the van Genuchten fit for establishing SWCC's of slurry specimens in terms of gravimetric water content, volumetric water content, and degree of saturation.

Table 3.5. Values of van Genuchten fitting parameters for volume uncorrected SWCC's in terms of gravimetric water content (w), volumetric waster content (θ), and degree of saturation (S) for slurry specimens tested under net normal stress of 3kPa (token load)

Soil	Specimen Type	"a" Parameter			"n" Parameter			SWCC	Description
		w	θ	S	w	θ	S		
Anthem	Slurry	5	13	5	1.210	1.170	1.205	Uncorrected	Average of two replicates for each soil
Colorado	Slurry	5	18	5	1.250	1.170	1.250	Uncorrected	
San Antonio	Slurry	15	25	8	1.250	1.150	1.200	Uncorrected	

It can be seen from Table 3.5 that the "a" parameters found for the uncorrected SWCC's were extremely small. This is due to large amount of free water present within the slurry specimens at the beginning of the test. This free water drains out at a fast rate and causes the overall water content of the specimen to decrease drastically, and hence, very low amount of "a" parameter. The values of "a" and "n" parameter were determined for volume corrected SWCC's for slurry specimens and are shown in Table 3.6 along with air-entry values.

It can be seen from Table 3.6 that for any given soil, there are substantial differences between the "a" and "n" parameters and AEV between the volume corrected SWCC and volume uncorrected SWCC. The volume correction of SWCC takes into account the drastic decrease in the void ratio of slurries and hence leads to significant increase in the calculated values of degree of saturation at any suction throughout the test. This leads to larger amounts of "a" parameter. For example, the "a" parameter for the slurry specimen of Colorado soil increases from 5 for volume uncorrected SWCC to 850 for volume corrected SWCC. The AEV of Colorado soil increases from 5 for volume uncorrected SWCC to 700 for volume corrected SWCC.

It was found from Table 3.6 that the "n" parameter is also larger for the corrected SWCC's. As an example, for San Antonio soil, the "n" parameter for the uncorrected SWCC is 1.2 while this value is 1.29 for the corrected SWCC.

Table 3.6. Values of van Genuchten fitting parameters and air-entry value (AEV) for volume corrected and uncorrected SWCC's in terms of degree of saturation (S) for slurry specimens

Soil	Specimen Type	"a" Parameter	"n" Parameter	AEV	SWCC	Net Normal Stress
		S	S	S		
Anthem	Slurry	5	1.205	3	Uncorrected	3 kPa
Anthem	Slurry	350	1.270	200	Corrected	3 kPa
Colorado	Slurry	5	1.250	5	Uncorrected	3 kPa
Colorado	Slurry	850	1.320	700	Corrected	3 kPa
San Antonio	Slurry	8	1.200	5	Uncorrected	3 kPa
San Antonio	Slurry	700	1.290	500	Corrected	3 kPa

Table 3.7 shows "a" and "n" parameters along with the AEV's for volume corrected SWCC's in terms of degree of saturation. It can be seen in this table that for any given soil tested in this study, the value of "a" parameter and AEV are significantly larger for the volume corrected SWCC in terms of degree of saturation for slurry specimens compared to that of compacted specimens. As an example, the "a" parameter for the compacted specimen of Colorado soil is 150, while this value is 850 for the slurry specimen of the same soil. This is due to existence of clods in the compacted specimens. As previously mentioned, clods cause the behavior similar to that of coarse-grained materials. However, since there are no clods present in slurry specimens, the SWCC generated from these specimens seem to be more similar to SWCC's of clays with generally larger air-entry values. It can also be seen from the Table 3.7 that for a certain soil, the values of "n" parameter are generally larger for slurry specimens compared to the

compacted ones, which indicates that the slope of SWCC in the range of suction between air-entry and residual points is generally larger for the SWCC's of slurry specimens.

Table 3.7. Values of van Genuchten fitting parameters and air-entry value (AEV) for volume corrected SWCC's in terms of degree of saturation (S) for compacted and slurry specimens. The net normal stress used for slurry specimens is token load and for compacted specimens the net normal stress is seating load (7kPa)

Soil	Specimen Type	"a" Parameter	"n" Parameter	AEV	SWCC
		S	S	S	
Anthem	Compacted	60	1.170	50	Corrected
Anthem	Slurry	350	1.270	200	Corrected
Colorado	Compacted	150	1.220	90	Corrected
Colorado	Slurry	850	1.320	700	Corrected
San Antonio	Compacted	100	1.220	70	Corrected
San Antonio	Slurry	700	1.290	500	Corrected

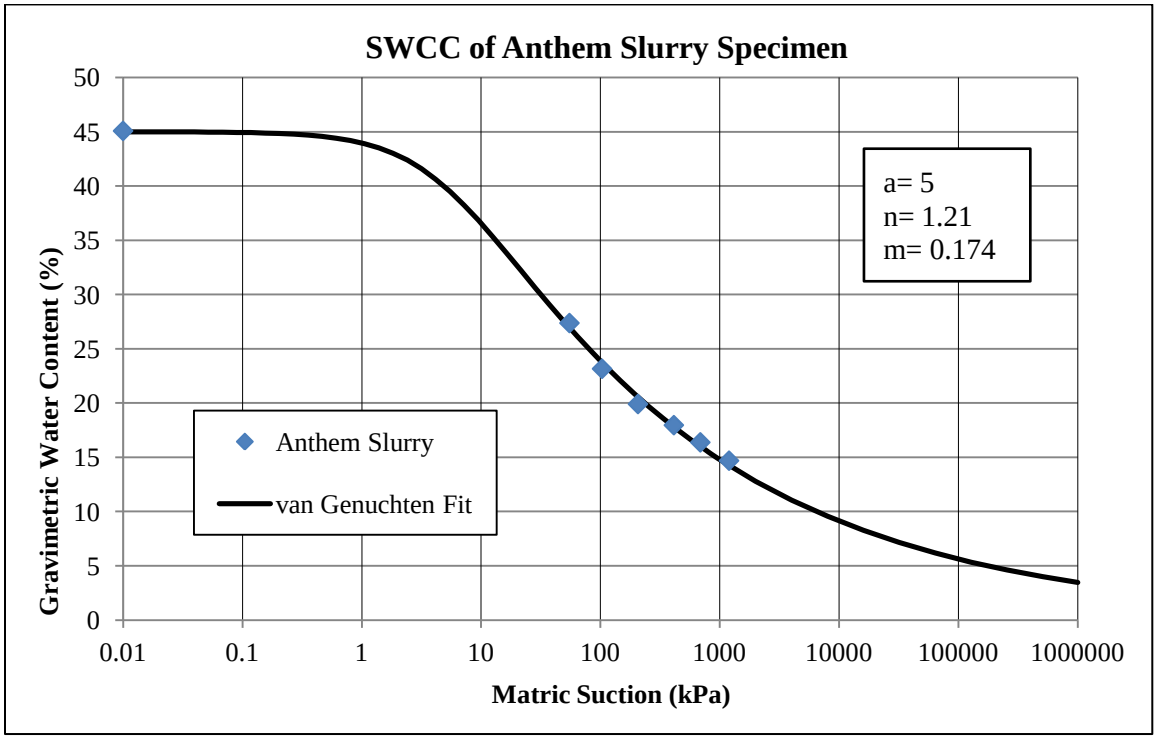

Figure 3.25. Gravimetric water content versus soil suction for slurry specimen of Anthem

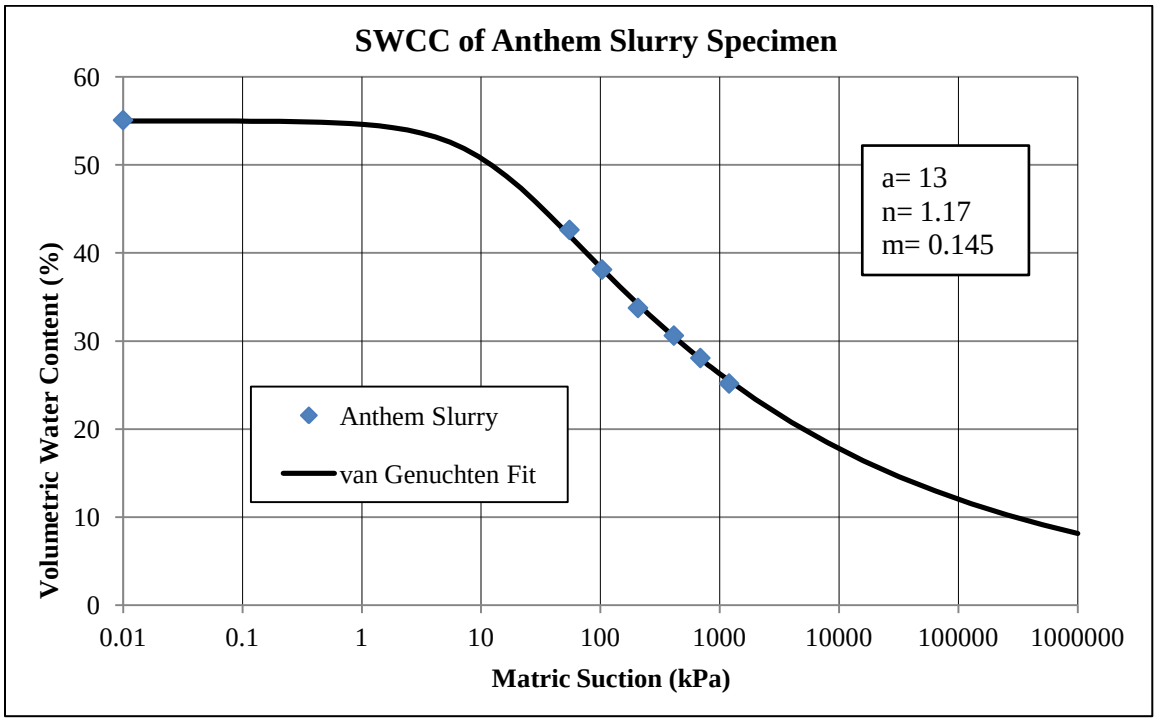

Figure 3.26. Volumetric water content versus soil suction for slurry specimen of Anthem

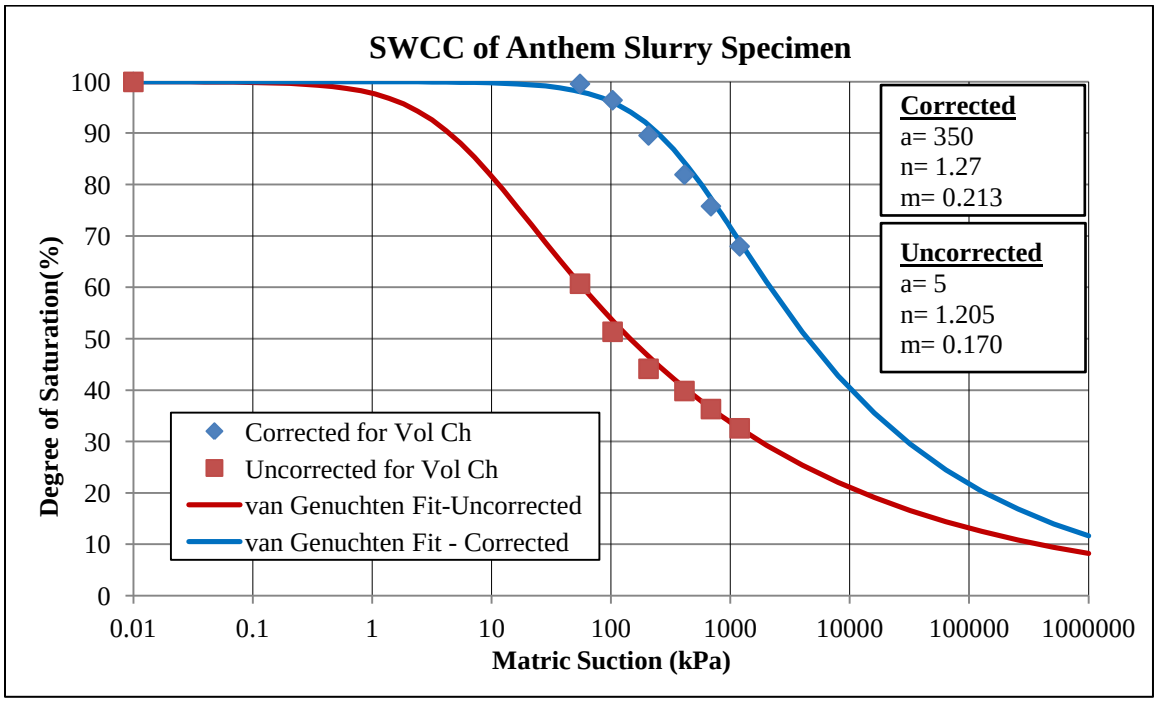

Figure 3.27. Volume corrected and uncorrected SWCC in terms of degree of saturation for slurry specimen of Anthem

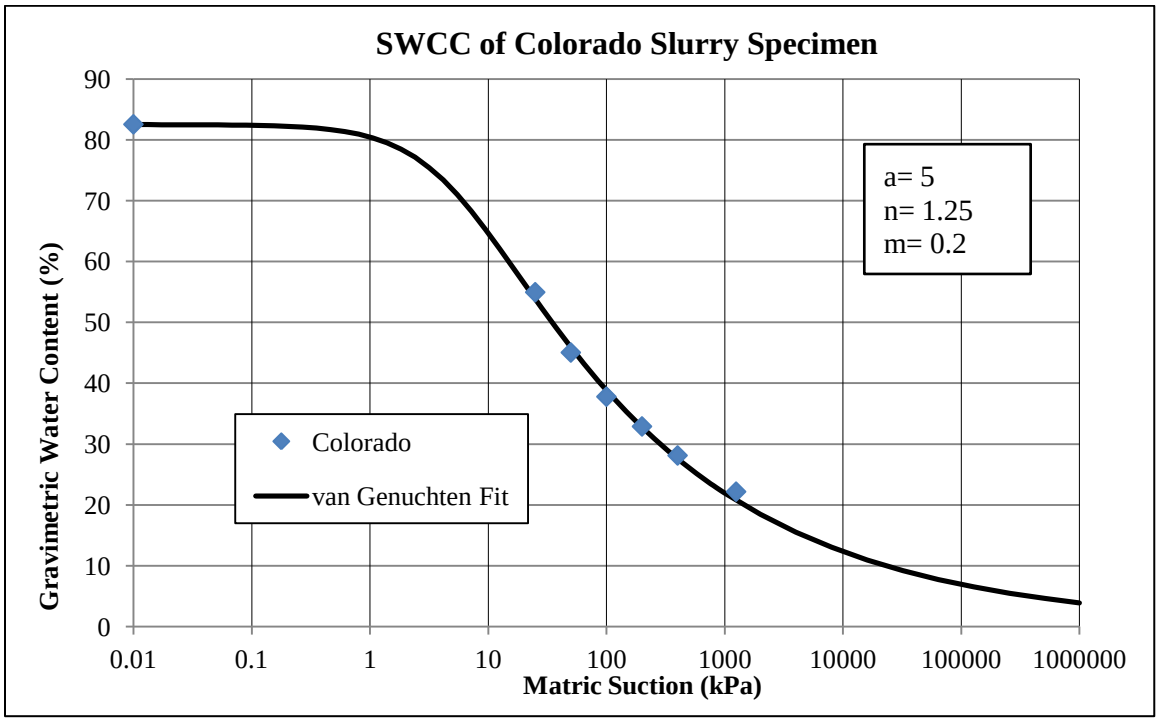

Figure 3.28. Gravimetric water content versus soil suction for slurry specimen of Colorado

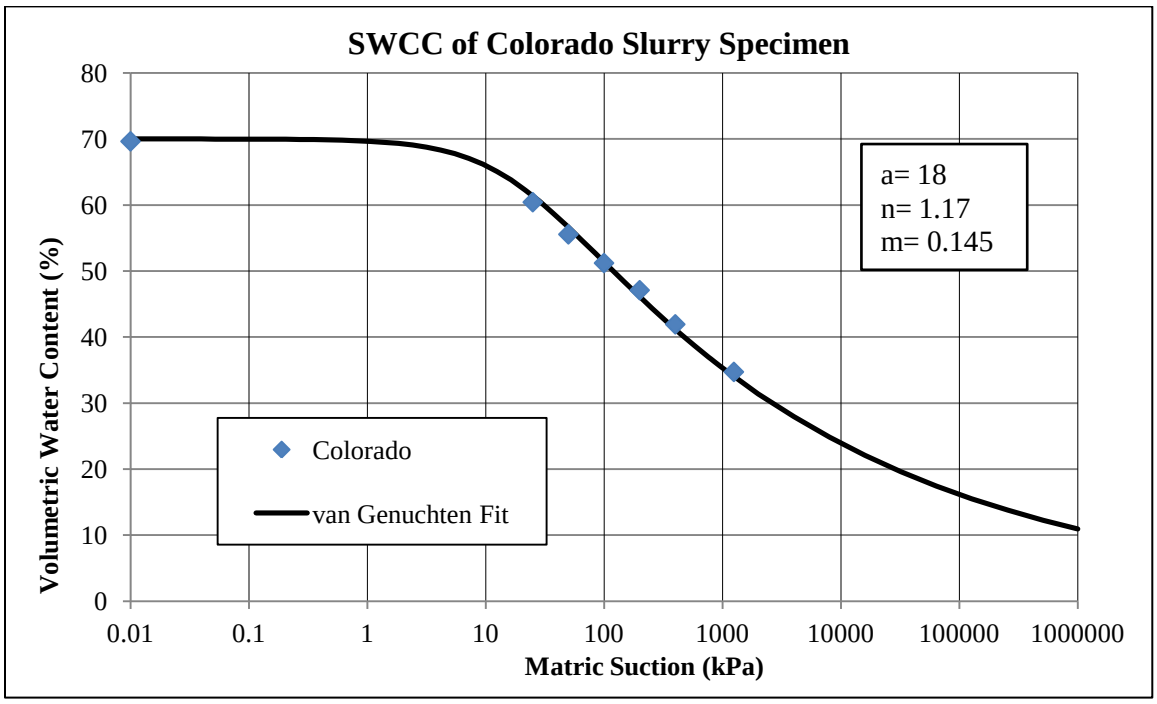

Figure 3.29. Volumetric water content versus soil suction for slurry specimen of Colorado

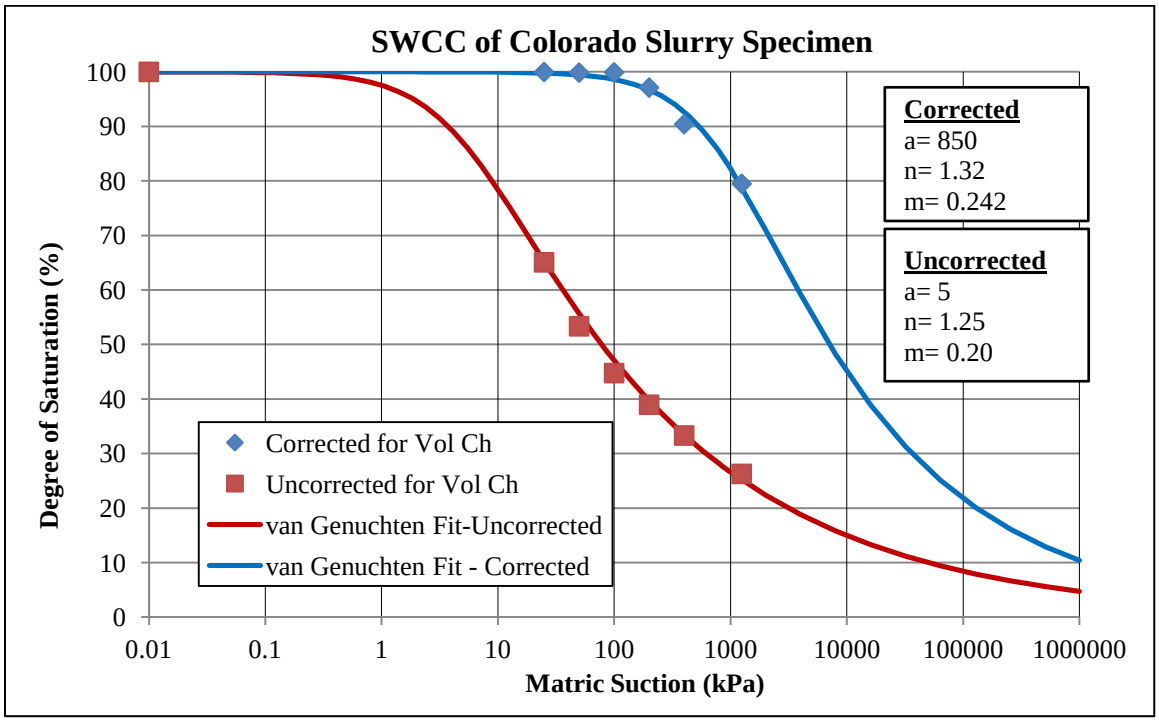

Figure 3.30. Volume corrected and uncorrected SWCC in terms of degree of saturation for slurry specimen of Colorado

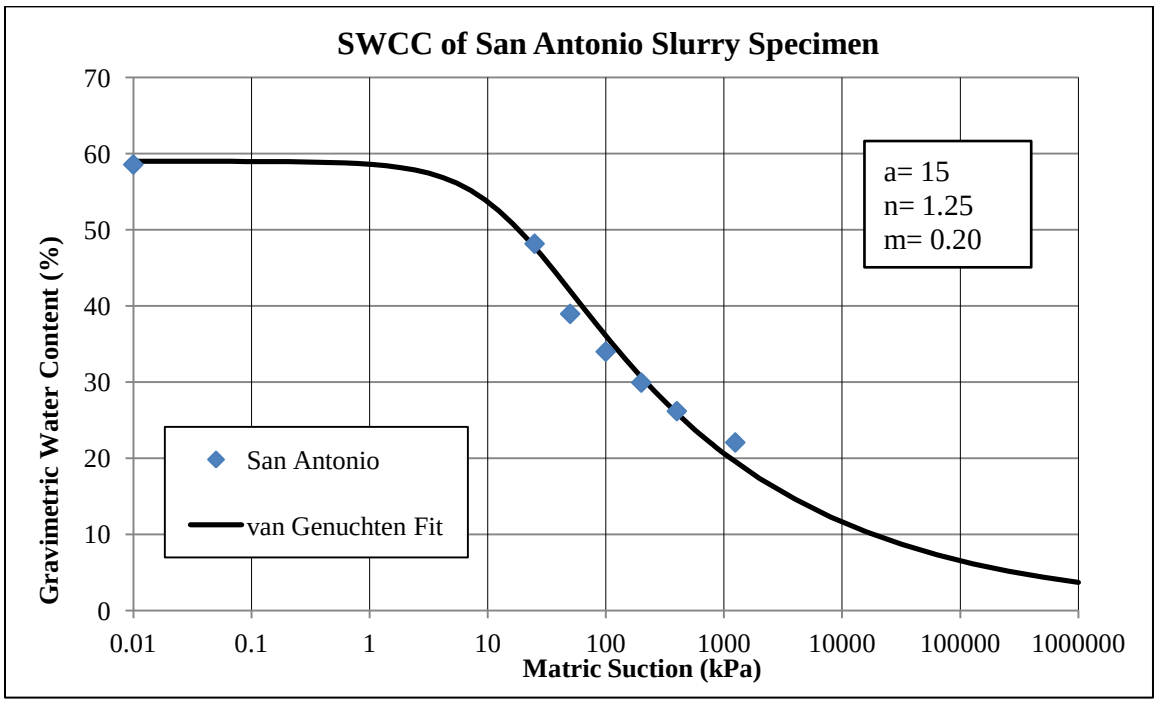

Figure 3.31. Gravimetric water content versus soil suction for slurry specimen of San Antonio

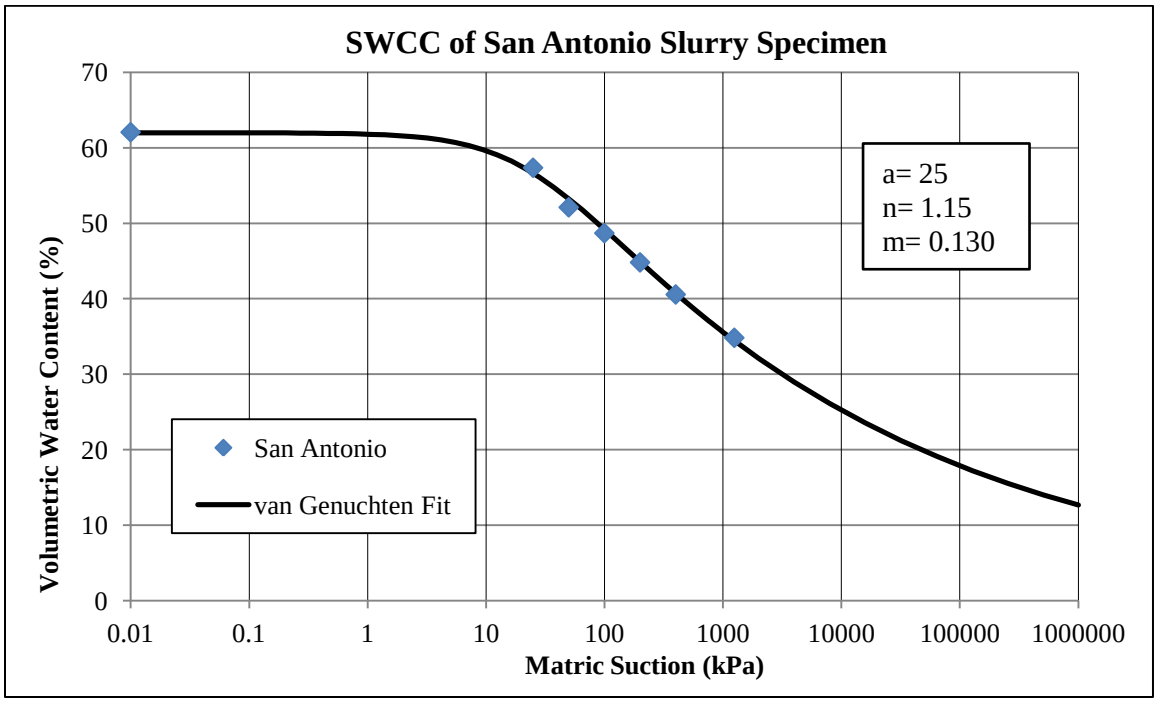

Figure 3.32. Volumetric water content versus soil suction for slurry specimens of San Antonio

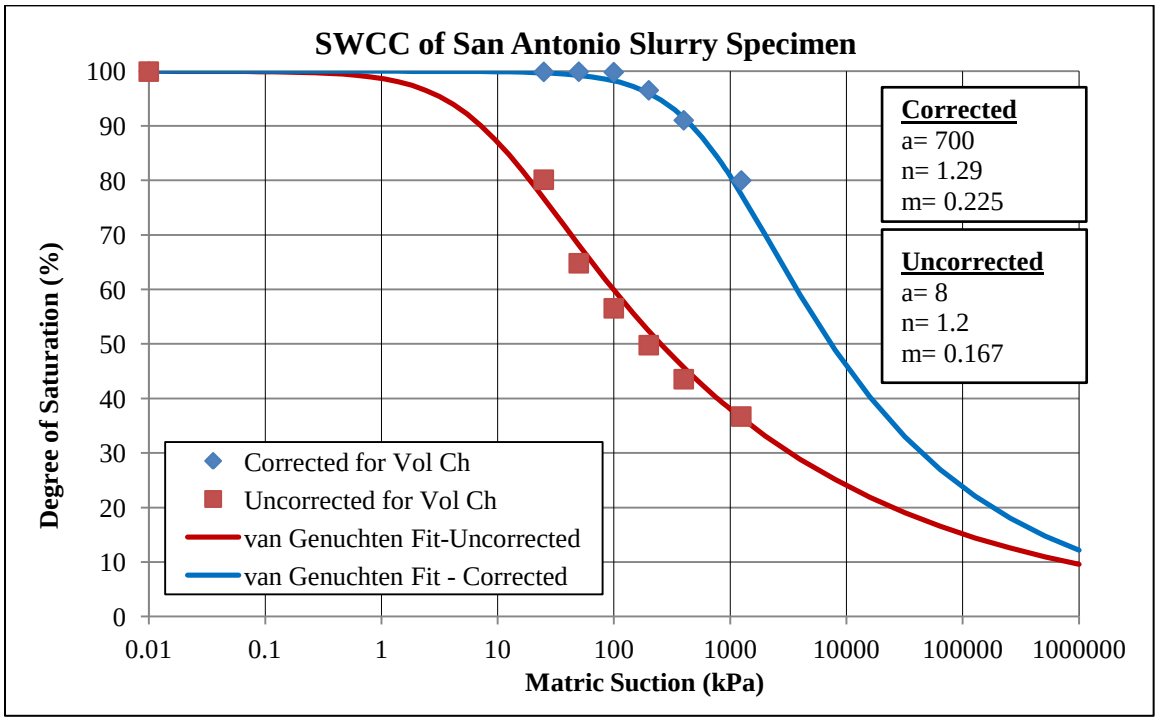

Figure 3.33. Volume corrected and uncorrected SWCC in terms of degree of saturation for slurry specimen of San Antonio

3.5.3. Drying and Wetting SWCC of Compacted Specimens with Various Net Normal Stresses

SWCC tests were conducted on compacted specimens of Anthem, Colorado, and San Antonio, this time with different net normal stresses. Table 3.8 below shows the features of the test experiments in which constant volume swell pressure data is also provided.

Table 3.8. SWCC tests carried out on compacted specimens to study the effect of net normal stress on soil volume change and its effect on SWCC

Test No.	Soil	Specimen Type	Swell Pressure (kPa)	Net Normal Pressure (kPa)	Net Normal Stress compared to Swell Pressure	SWCC Path
13	Anthem	Compacted	115	7	Seating Load	Drying and Wetting
14	Anthem	Compacted	115	26	23% Swell Pressure	Drying and Wetting
15	Anthem	Compacted	115	53	46% Swell Pressure	Drying and Wetting
16	Colorado	Compacted	250	7	Seating Load	Drying and Wetting
17	Colorado	Compacted	250	53	21% Swell Pressure	Drying and Wetting
18	Colorado	Compacted	250	105	42% Swell Pressure	Drying and Wetting
19	San Antonio	Compacted	180	7	Seating Load	Drying and Wetting
20	San Antonio	Compacted	180	49	27% Swell Pressure	Drying and Wetting
21	San Antonio	Compacted	180	98	54% Swell Pressure	Drying and Wetting

The purpose of this set of tests was to find the impact of net normal stress on volume change of the soil during SWCC test which in turn affects the shape of the SWCC. Figures 3.34 through 3.63 show results of SWCC test on the three soils with different net normal stress values. SWCC's are presented in terms of gravimetric moisture content, volumetric moisture content and degree of saturation versus suction. SWCC's in

terms of volumetric moisture content and degree of saturation were corrected for soil volume change.

Figures 3.64 through 3.70 show images of specimens at various suctions under various net normal stress values. It was found from this testing program that with an increase in net normal stress, radial shrinkage of the soil decreases and the vertical deformation increases. Also, the higher the net normal stress, the greater the overall volume decreases of the specimen for a given suction.

Table 3.9 presents values of "a" and "n" parameters for the experiments on compacted specimens with different net normal stresses. Similar to the results obtained from the SWCC tests on the compacted specimens conducted under seating load (i.e. 7kPa) that was described in previous section, the "a" parameter was found to be larger for SWCC's in terms of volumetric water content and degree of saturation for any given soil. This is due to increase in values of volumetric water content and degree of saturation upon correcting for volume change. "n" parameter also seems to be generally larger for the SWCC's in terms of volumetric water content and degree of saturation compared to the SWCC in terms of volumetric water content. This means SWCC's in terms of volumetric water content and degree of saturation have generally greater slopes compared to the SWCC in terms of volumetric water content.

Another result from the Table 3.9 is that in general, for any given soil, the value of "a" is smaller for the wetting cycle compared to the drying cycle. This can also be seen in Figure 3.34 through 3.63.

Table 3.9. Values of van Genuchten fitting parameters for volume corrected SWCC's in terms of gravimetric water content, volumetric water content, and degree of saturation for compacted specimens tested under different net normal stresses

Soil	Specimen Type	"a" Parameter			"n" Parameter			Net Normal Stress	Description
		w	θ	S	w	θ	S		
Anthem	Compacted	30	40	100	1.170	1.170	1.220	7 kPa	Drying Path
Anthem	Compacted	27	33	50	1.150	1.160	1.200	7 kPa	Wetting Path
Anthem	Compacted	30	40	100	1.170	1.170	1.210	23% SP	Drying Path
Anthem	Compacted	32	33	70	1.160	1.160	1.200	23% SP	Wetting Path
Anthem	Compacted	22	45	100	1.185	1.180	1.210	46% SP	Drying Path
Anthem	Compacted	18	30	90	1.170	1.170	1.205	46% SP	Wetting Path
Colorado	Compacted	85	100	160	1.185	1.190	1.220	7 kPa	Drying Path
Colorado	Compacted	45	45	130	1.148	1.160	1.208	7 kPa	Wetting Path
Colorado	Compacted	60	80	160	1.185	1.190	1.220	21% SP	Drying Path
Colorado	Compacted	60	55	115	1.155	1.170	1.208	21% SP	Wetting Path
Colorado	Compacted	45	80	160	1.185	1.190	1.220	42% SP	Drying Path
Colorado	Compacted	35	45	130	1.155	1.170	1.208	42% SP	Wetting Path
San Antonio	Compacted	55	80	90	1.185	1.190	1.190	7 kPa	Drying Path
San Antonio	Compacted	35	45	90	1.155	1.170	1.185	7 kPa	Wetting Path
San Antonio	Compacted	50	80	110	1.185	1.190	1.200	27% SP	Drying Path
San Antonio	Compacted	40	70	100	1.155	1.170	1.195	27% SP	Wetting Path
San Antonio	Compacted	45	90	160	1.210	1.200	1.220	54% SP	Drying Path
San Antonio	Compacted	35	55	100	1.185	1.180	1.205	54% SP	Wetting Path

In order to evaluate the impact of net normal stress on the shape and air-entry value of SWCC of compacted specimens, values of "a" and "n" for SWCC's in terms of degree of saturation for compacted specimens tested under different net normal stresses were compared against each other. These values of "a" and "n" are shown in Table 3.10. It can be seen that increase in net normal stress leads to increase in "a" parameter and

hence an increase in the air-entry value. This is, of course, due to the fact that greater net normal stress causes greater deformation of the soil and therefore greater volume reduction which in turn leads to larger degrees of saturation. The amount of increase in "a" parameter, however, is not significant. As an example, the "a" parameter for Colorado soil increases from 170 for net normal stress of 7kPa to 190 for the net normal stress of 53kPa (i.e. 21% of swell pressure). This value increases to 200 for net normal stress of 105kPa (i.e. 42% of swell pressure). This increase in net normal stress does not seem to be significant with respect to the shape of the SWCC for the amount of increase in the net normal stress considered in this study. This is also shown in Figures 3.43, 3.53, and 3.63 which present SWCC's in terms of degree of saturation for different net normal stresses.

These findings agree with the results reported by Vanapalli et al. (1999). As previously mentioned in Chapter 2, the authors found that in general, the applied normal stress does not seem to affect the shape of the SWCC significantly; however, the air-entry value seems to increase and the rate of degree of saturation change decreases with an increase in the net normal stress.

Increase in net normal stress does not seem to have a considerable impact on the "n" parameter. As seen in Table 3.10, a reasonable trend in values of "n" could not be found with increase in net normal stress.

Table 3.10. Values of van Genuchten fitting parameters for volume corrected SWCC's in terms of degree of saturation for compacted specimens tested under different net normal stresses

Soil	Specimen Type	"a" Parameter	"n" Parameter	SWCC	Net Normal Stress	Description
		S	S			
Anthem	Compacted	70	1.190	Corrected	7 kPa	Drying Path
Anthem	Compacted	90	1.200	Corrected	23% SP	Drying Path
Anthem	Compacted	100	1.190	Corrected	46% SP	Drying Path
Colorado	Compacted	170	1.250	Corrected	7 kPa	Drying Path
Colorado	Compacted	190	1.220	Corrected	21% SP	Drying Path
Colorado	Compacted	200	1.240	Corrected	42% SP	Drying Path
San Antonio	Compacted	100	1.200	Corrected	7 kPa	Drying Path
San Antonio	Compacted	120	1.200	Corrected	27% SP	Drying Path
San Antonio	Compacted	200	1.230	Corrected	54% SP	Drying Path

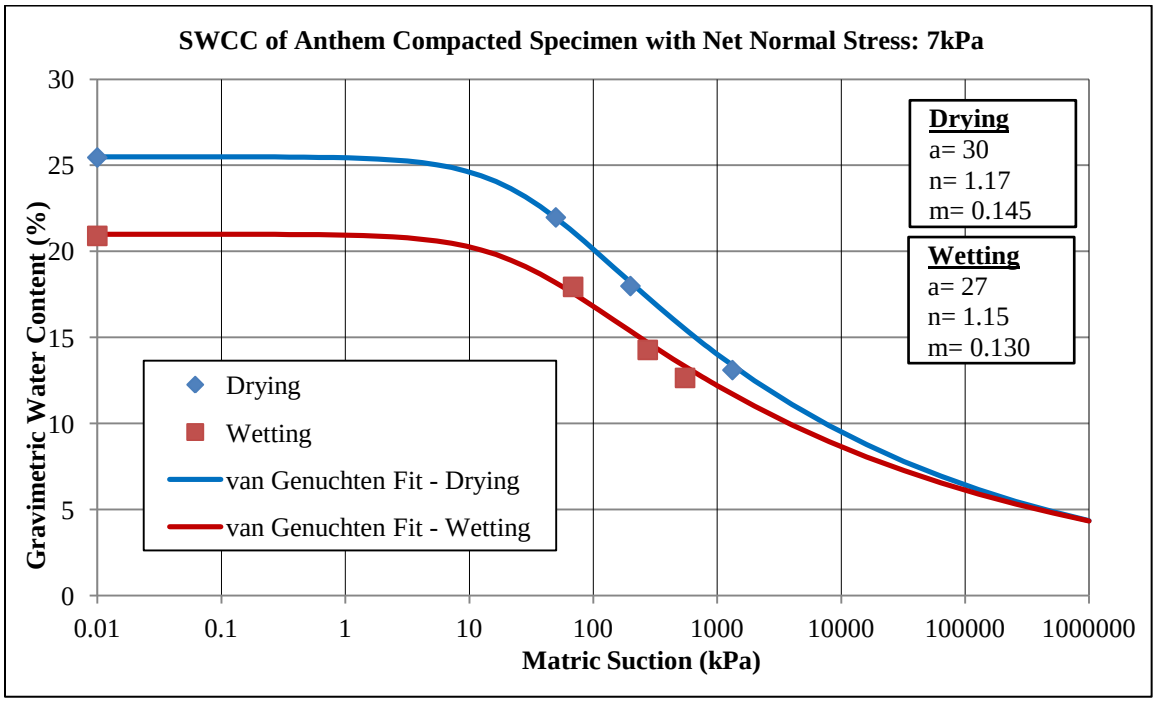

Figure 3.34. Drying and wetting SWCC in terms of gravimetric water content for Anthem soil (swell pressure: 115 kPa) under net normal stress of 7kPa

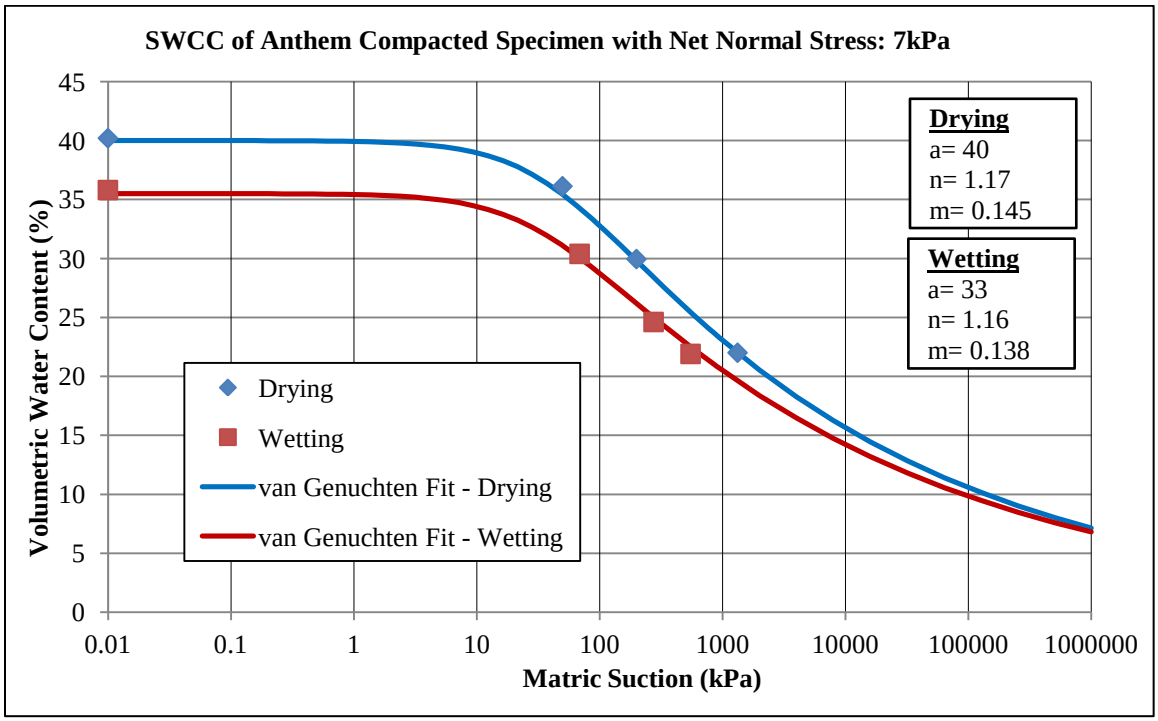

Figure 3.35. Drying and wetting SWCC in terms of volumetric water content for Anthem soil (swell pressure: 115 kPa) under net normal stress of 7kPa

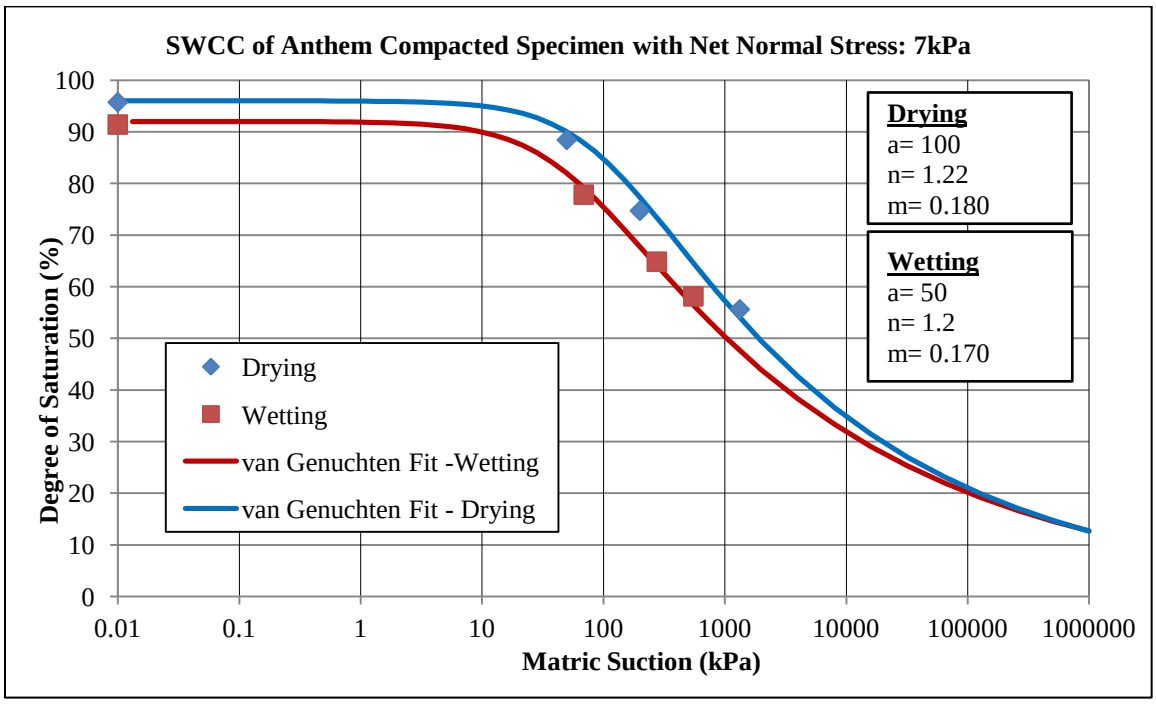

Figure 3.36. Drying and wetting SWCC in terms of degree of saturation for Anthem soil (swell pressure: 115 kPa) under net normal stress of 7kPa

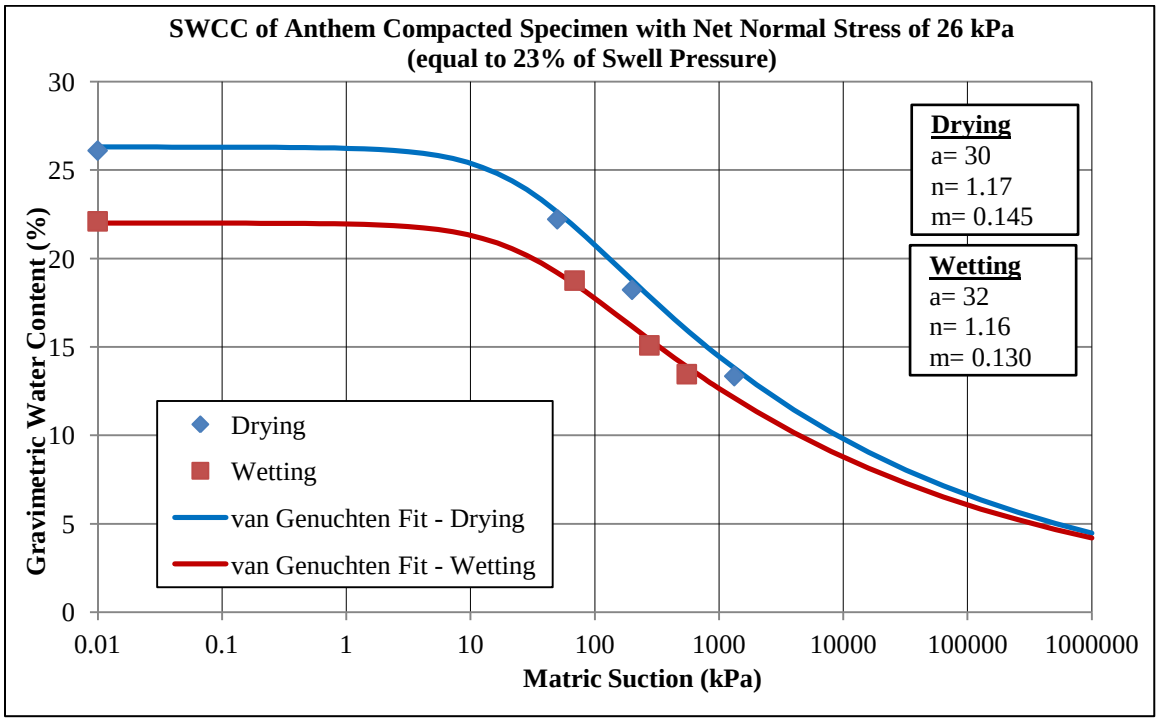

Figure 3.37. Drying and wetting SWCC in terms of gravimetric water content for Anthem soil (swell pressure: 115 kPa) under net normal stress equal to 23% swell pressure

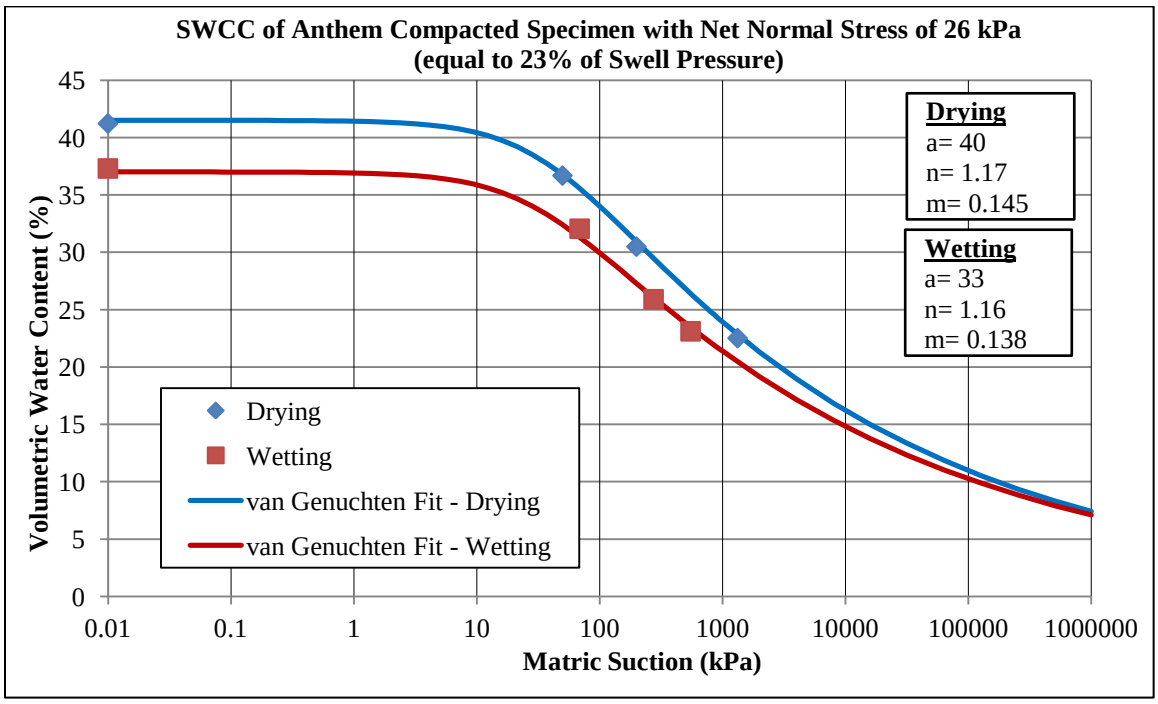

Figure 3.38. Drying and wetting SWCC in terms of volumetric water content for Anthem soil (swell pressure: 115 kPa) under net normal stress equal to 23% swell pressure

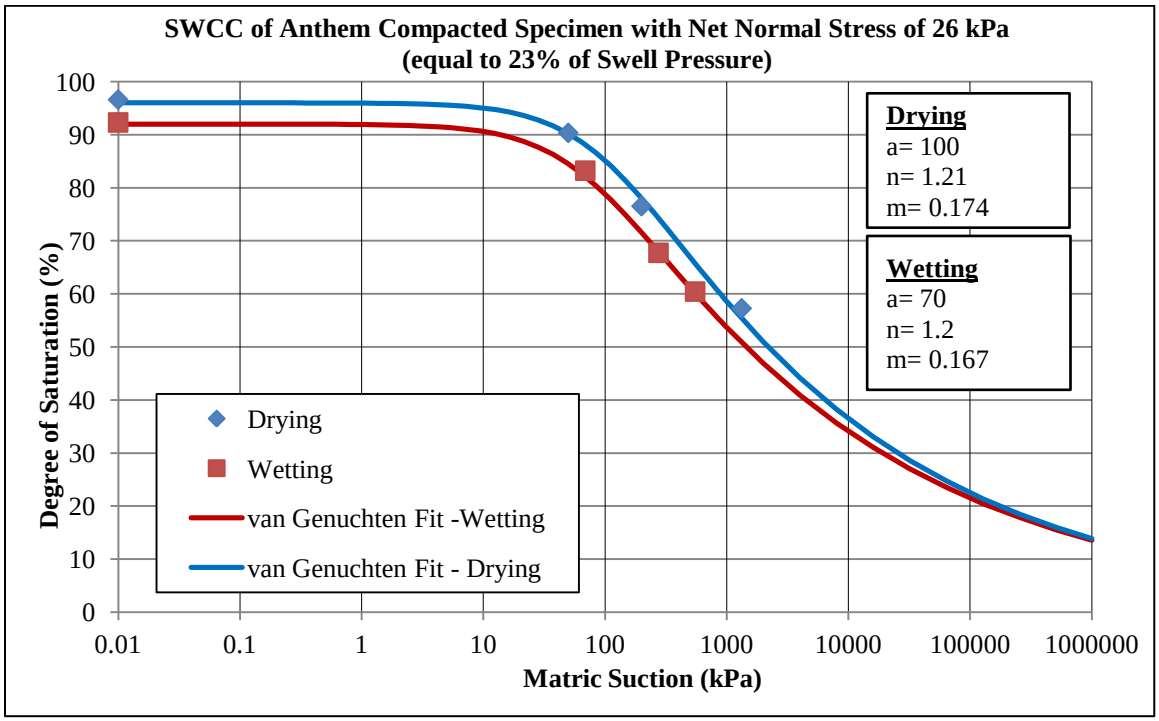

Figure 3.39. Drying and wetting SWCC in terms of degree of saturation for Anthem soil (swell pressure: 115 kPa) under net normal stress equal to 23% swell pressure

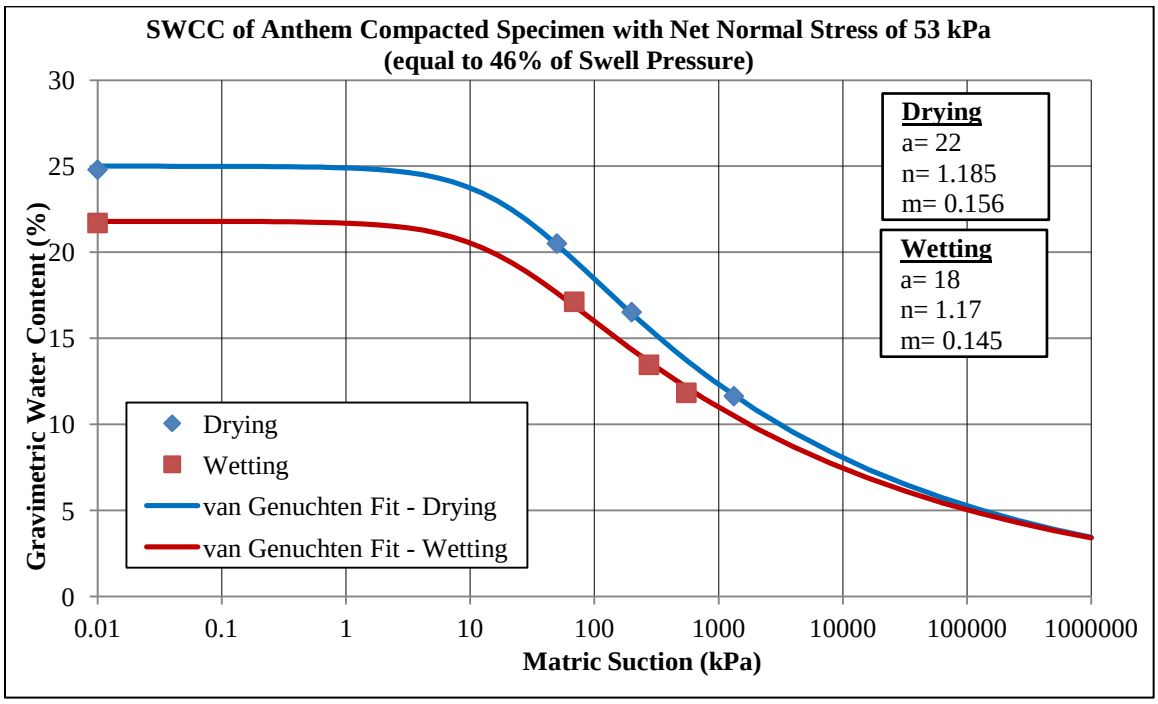

Figure 3.40. Drying and wetting SWCC in terms of gravimetric water content for Anthem soil (swell pressure: 115 kPa) under net normal stress equal to 46% swell pressure

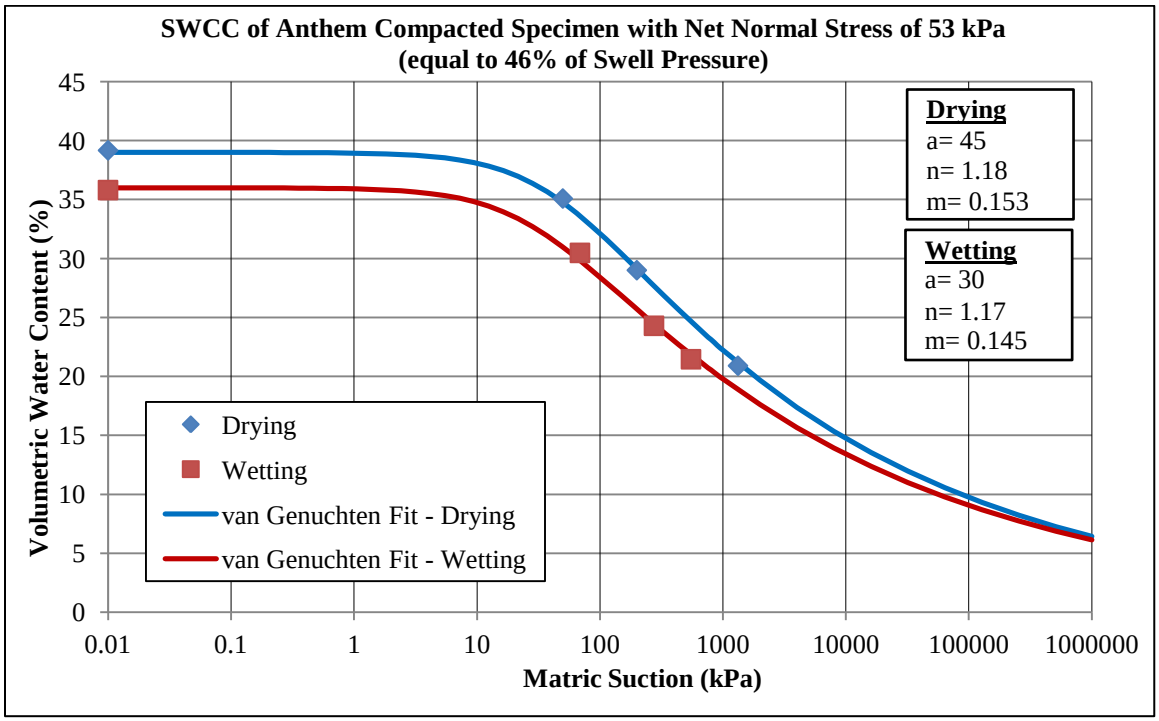

Figure 3.41. Drying and wetting SWCC in terms of volumetric water content for Anthem soil (swell pressure: 115 kPa) under net normal stress equal to 46% swell pressure

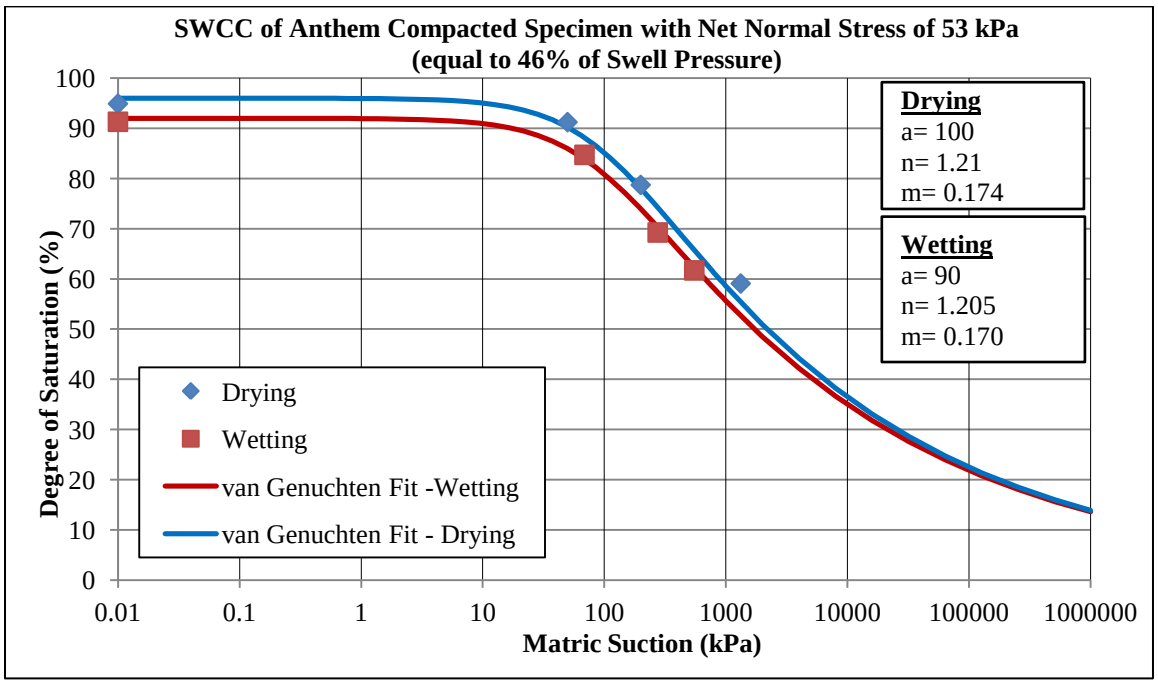

Figure 3.42. Drying and wetting SWCC in terms of degree of saturation for Anthem soil (swell pressure: 115 kPa) under net normal stress equal to 46% swell pressure

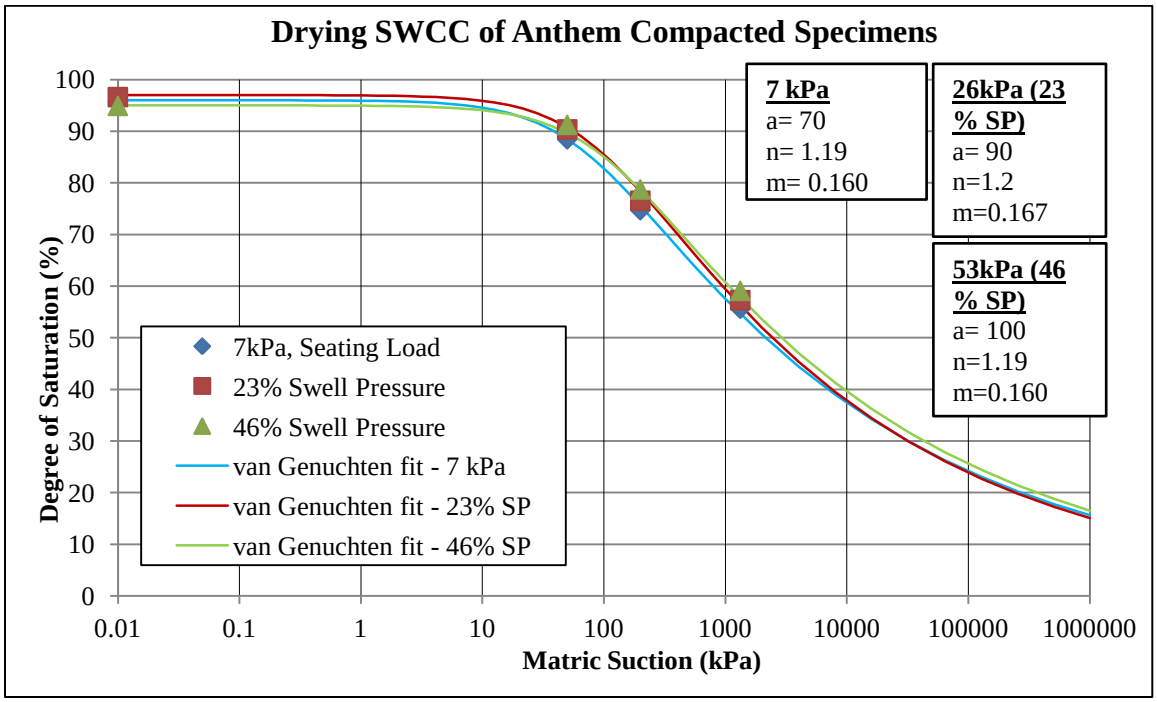

Figure 3.43. Drying SWCC in terms of degree of saturation for Anthem soil (swell pressure: 115 kPa) under various net normal stresses. Notice larger values of "a" parameter for tests under higher net normal stress

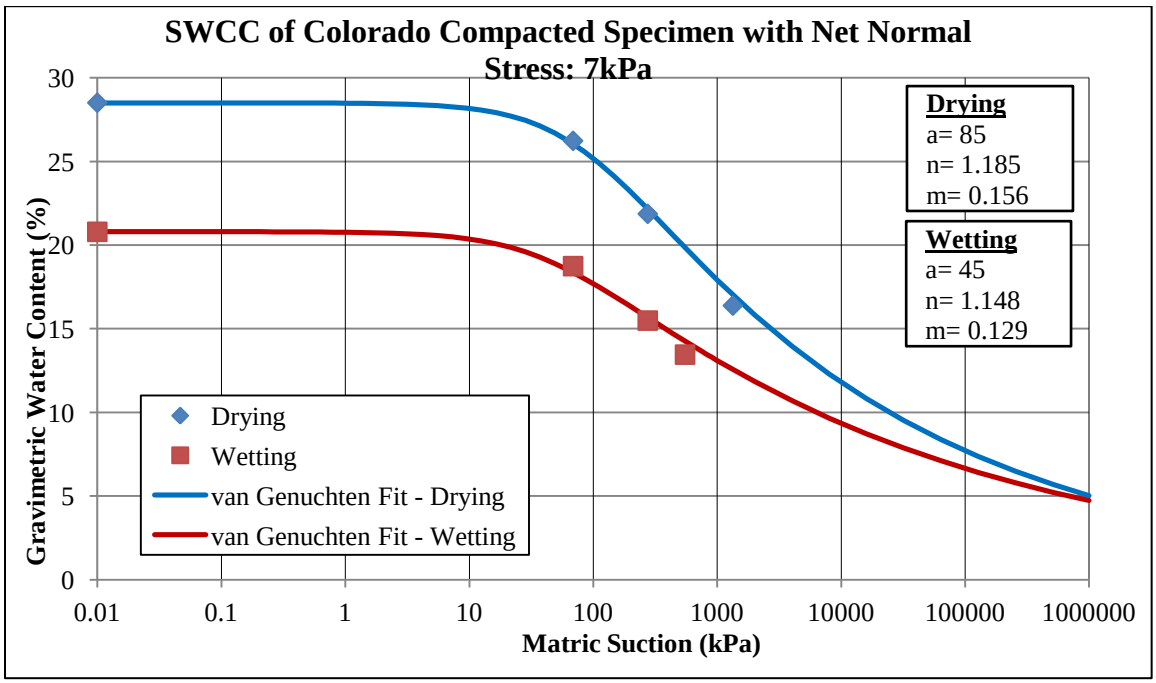

Figure 3.44. Drying and wetting SWCC in terms of gravimetric water content for Colorado soil (swell pressure: 250 kPa) under net normal stress of 7kPa

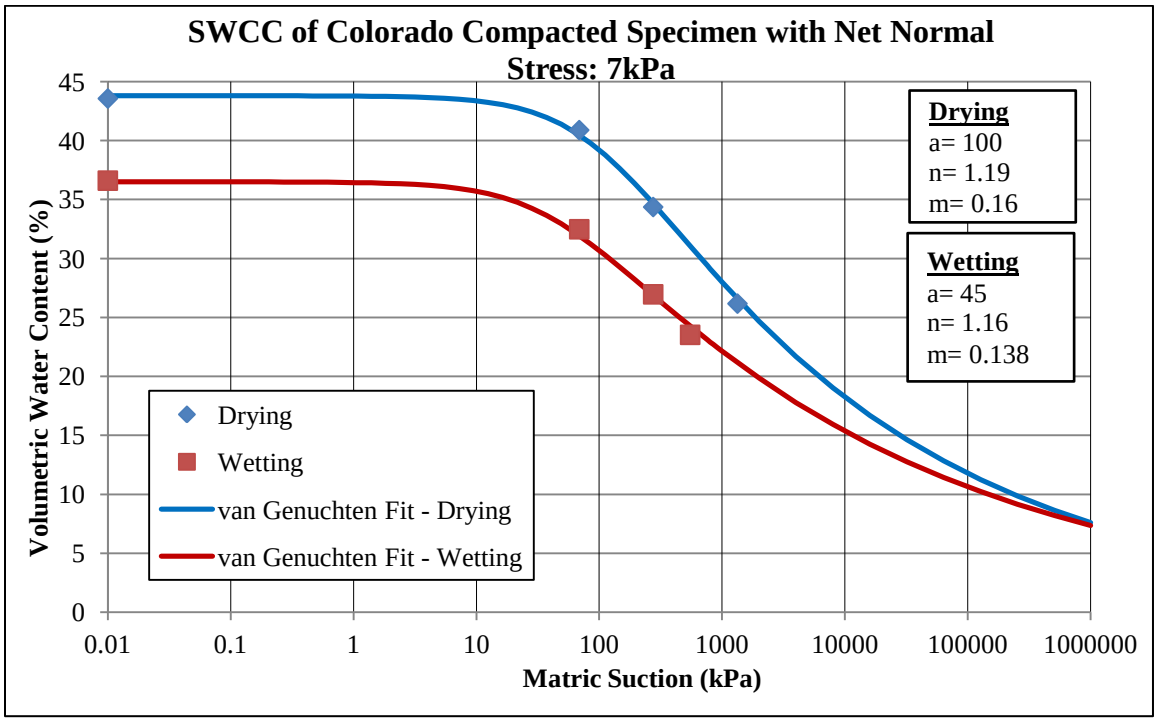

Figure 3.45. Drying and wetting SWCC in terms of volumetric water content for Colorado soil (swell pressure: 250 kPa) under net normal stress of 7kPa

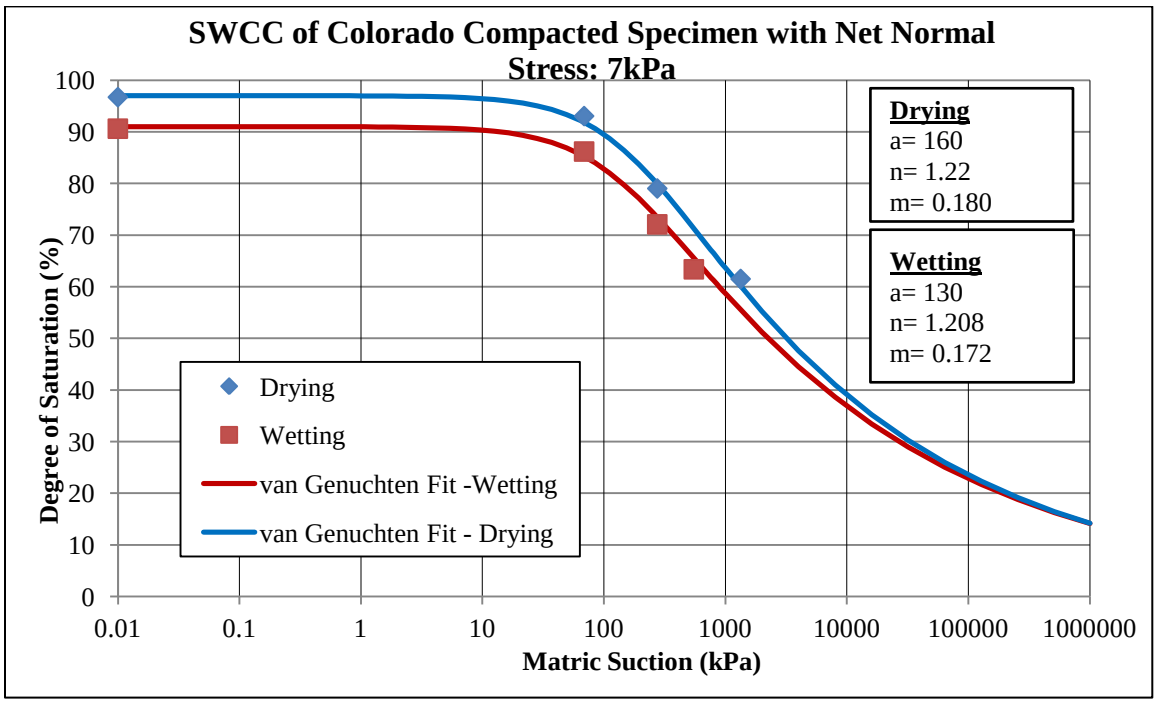

Figure 3.46. Drying and wetting SWCC in terms of degree of saturation for Colorado soil (swell pressure: 250 kPa) under net normal stress of 7kPa

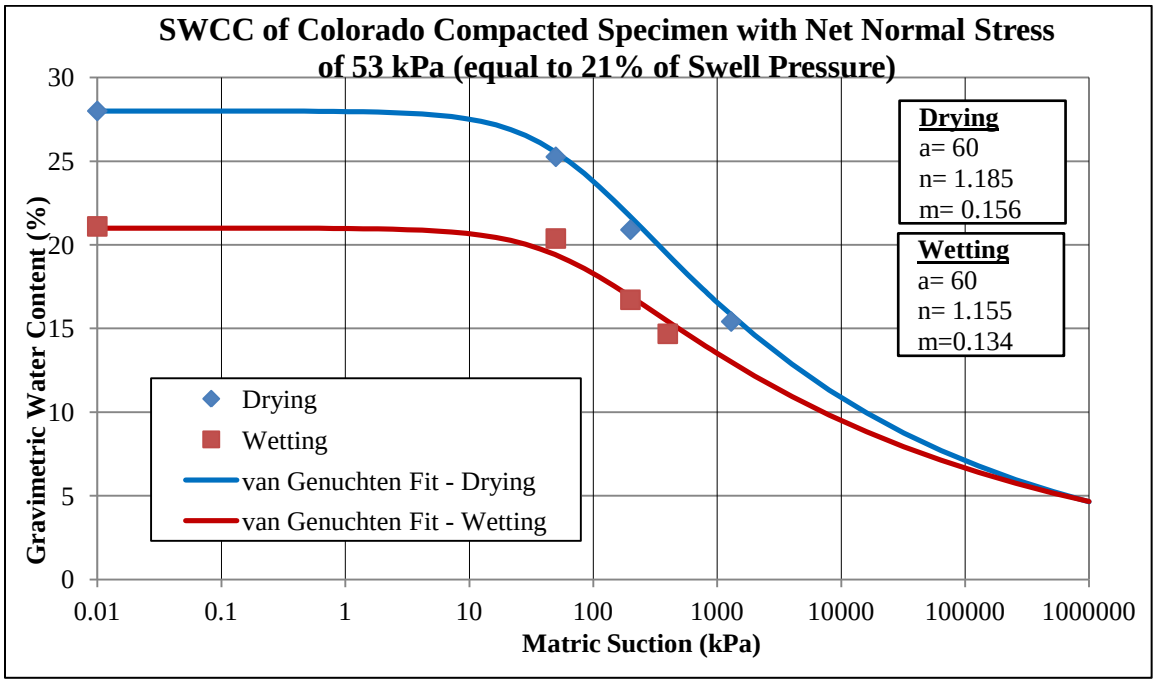

Figure 3.47. Drying and wetting SWCC in terms of gravimetric water content for Colorado soil (swell pressure: 250 kPa) under net normal stress equal to 21% swell pressure

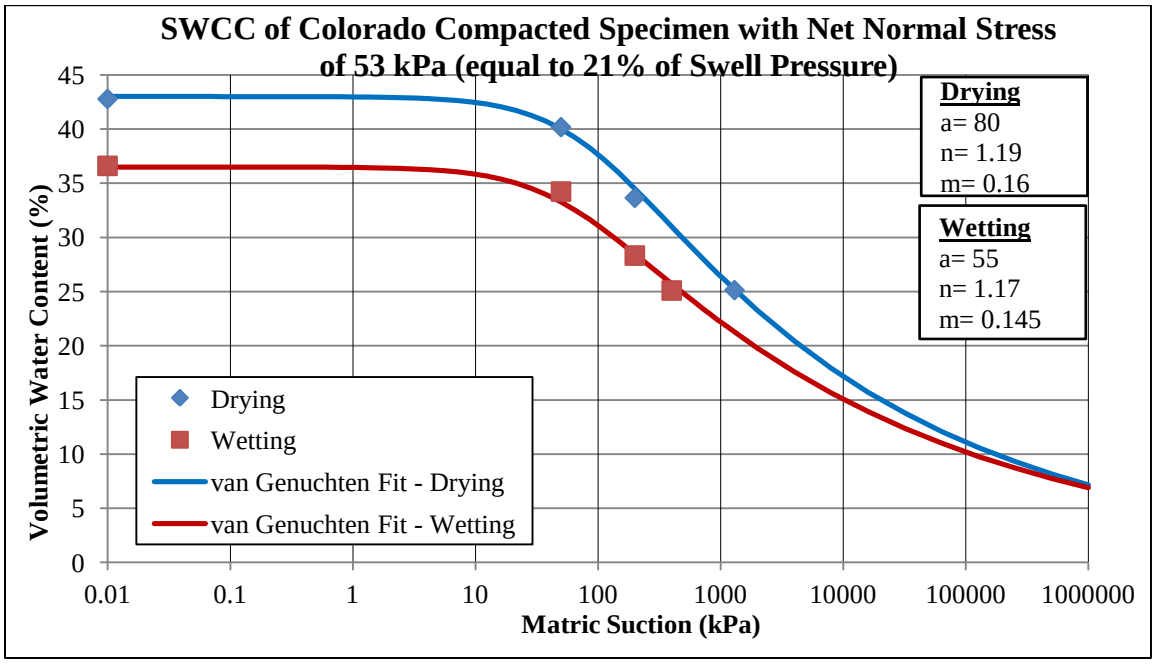

Figure 3.48. Drying and wetting SWCC in terms of volumetric water content for Colorado soil (swell pressure: 250 kPa) under net normal stress equal to 21% swell pressure

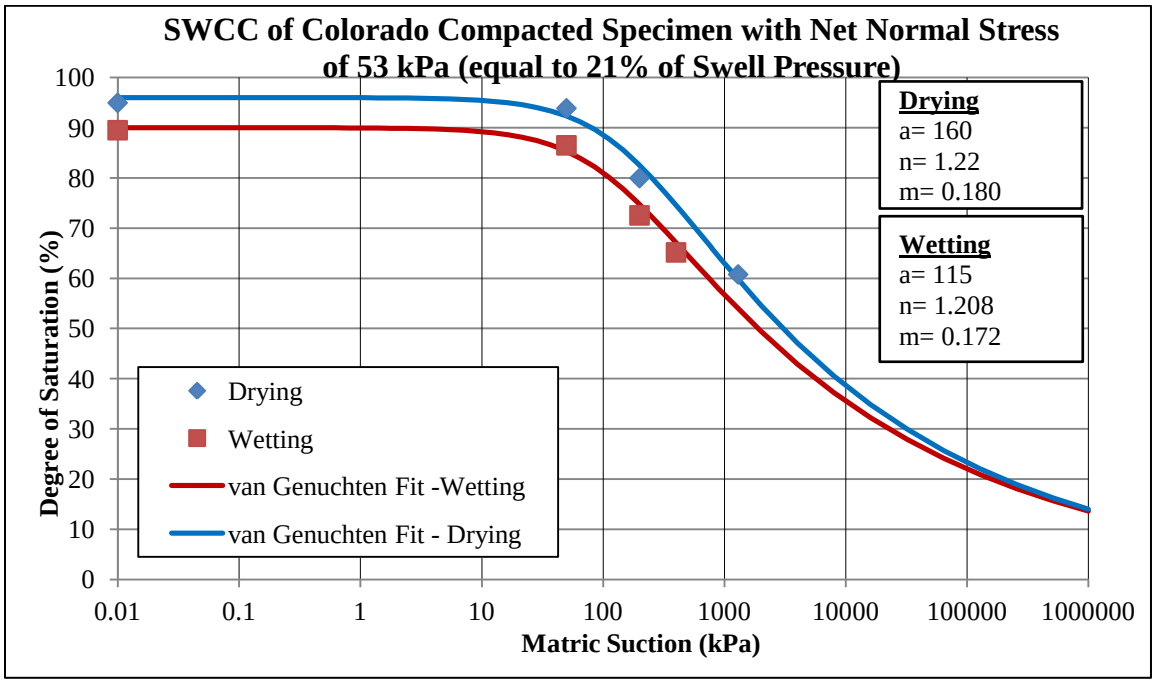

Figure 3.49. Drying and wetting SWCC in terms of degree of saturation for Colorado soil (swell pressure: 250 kPa) under net normal stress equal to 21% swell pressure

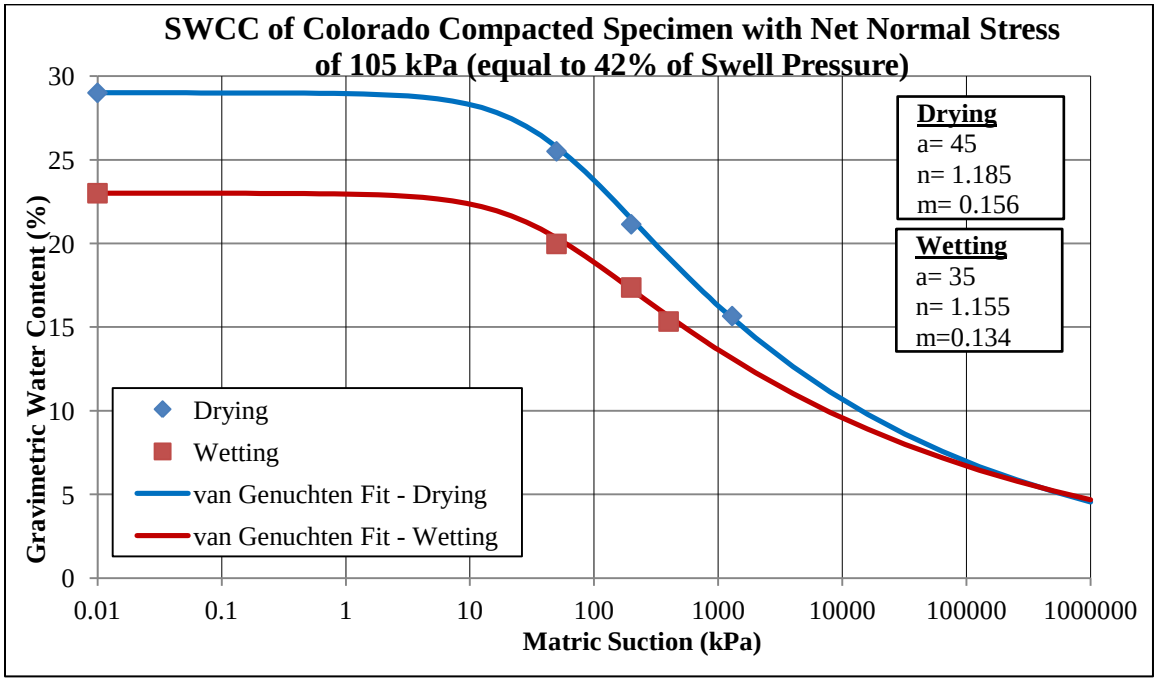

Figure 3.50. Drying and wetting SWCC in terms of gravimetric water content for Colorado soil (swell pressure: 250 kPa) under net normal stress equal to 42% swell pressure

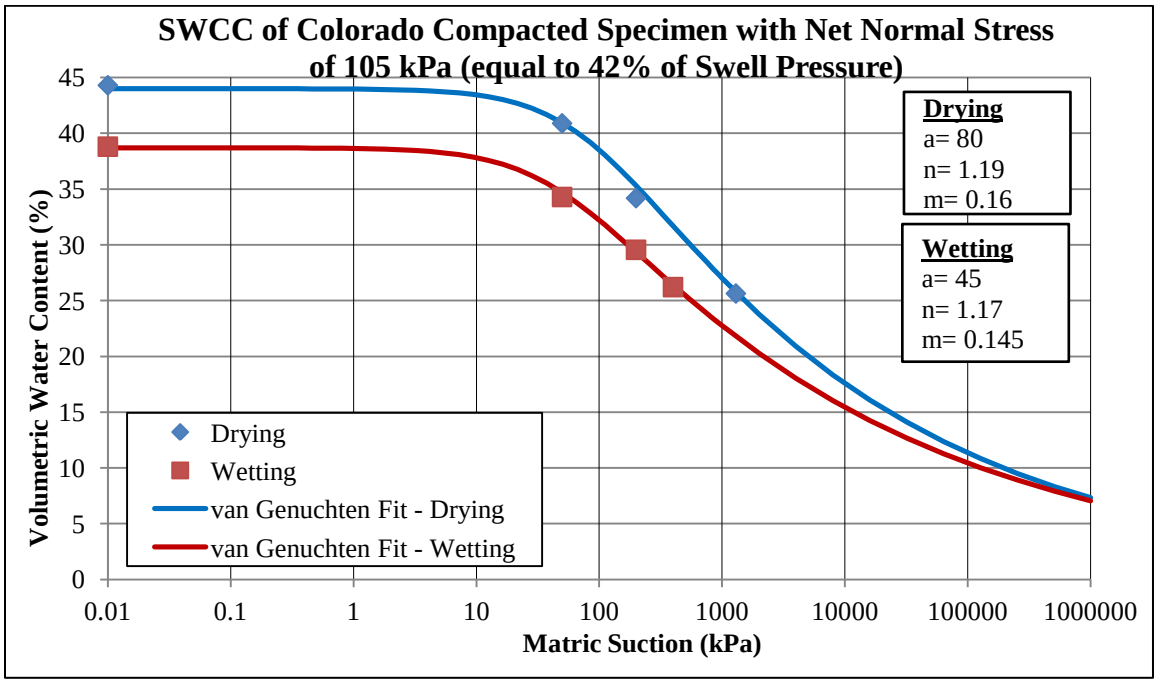

Figure 3.51. Drying and wetting SWCC in terms of volumetric water content for Colorado soil (swell pressure: 250 kPa) under net normal stress equal to 42% swell pressure

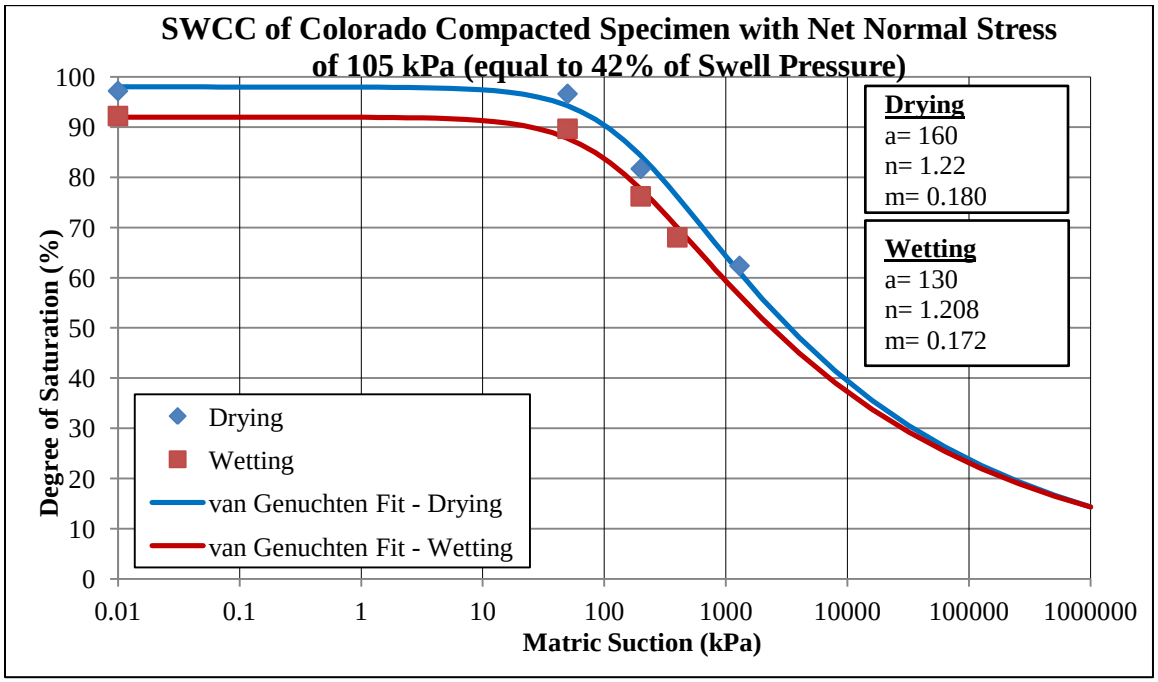

Figure 3.52. Drying and wetting SWCC in terms of degree of saturation for Colorado soil (swell pressure: 250 kPa) under net normal stress equal to 42% swell pressure

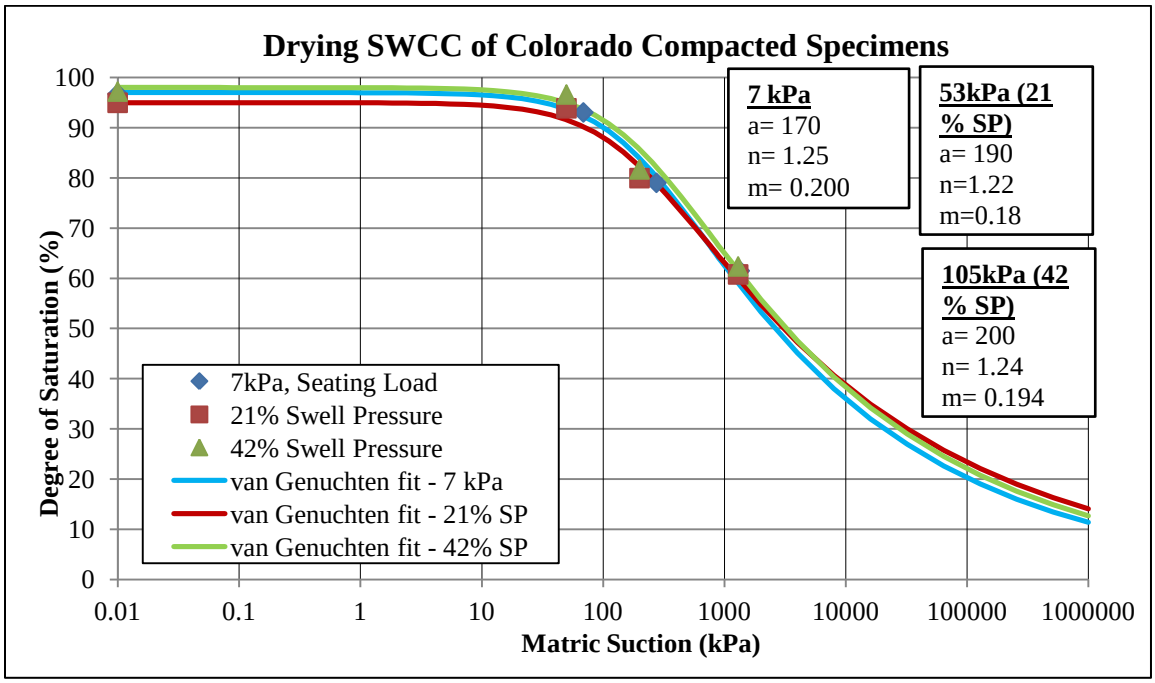

Figure 3.53. Drying SWCC in terms of degree of saturation for Colorado soil (swell pressure: 250 kPa) under various net normal stresses. Notice larger values of degree of "a" parameter for tests under higher net normal stress

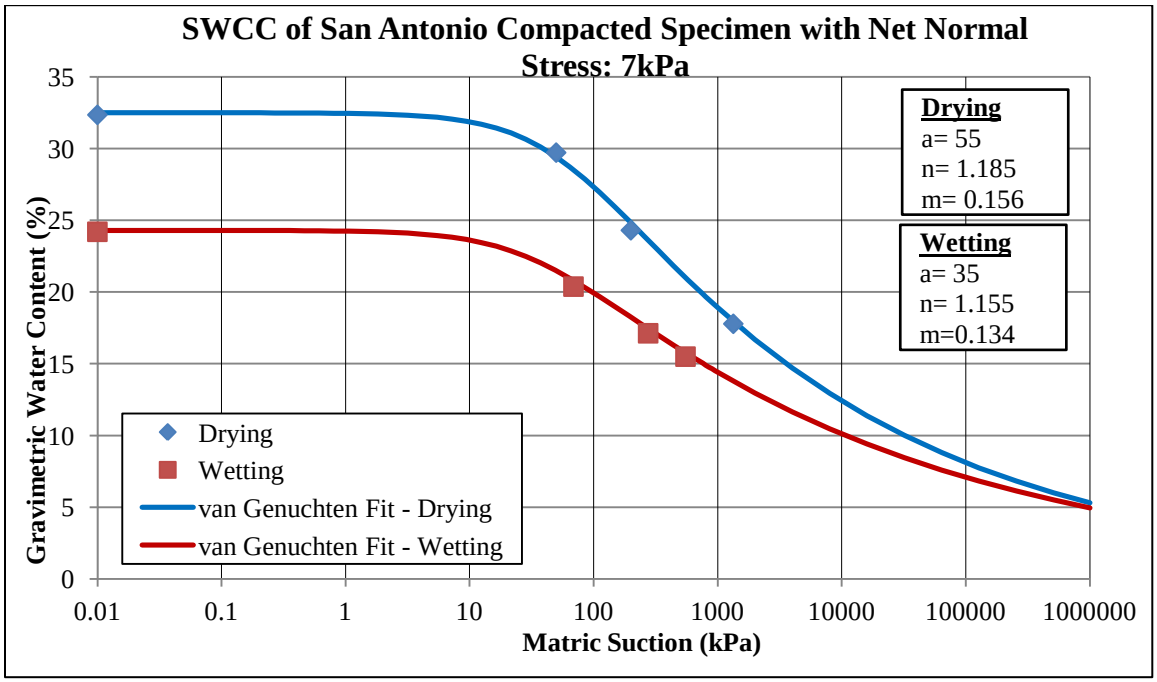

Figure 3.54. Drying and wetting SWCC in terms of gravimetric water content for San Antonio soil (swell pressure: 180 kPa) under net normal stress of 7kPa

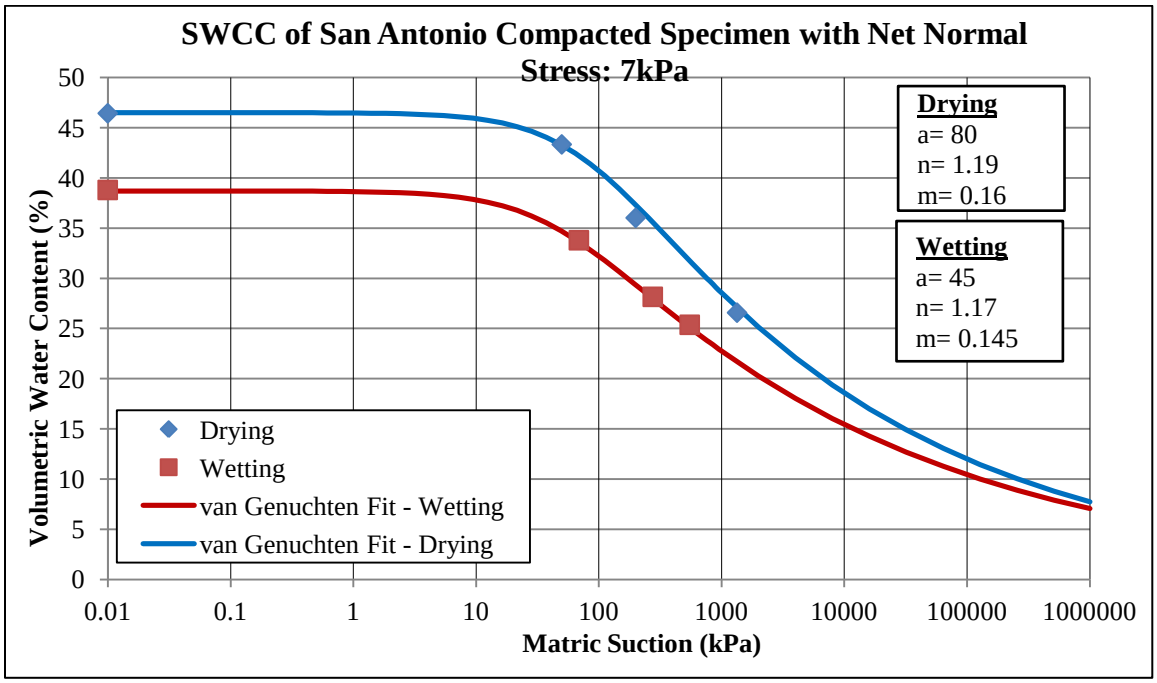

Figure 3.55. Drying and wetting SWCC in terms of volumetric water content for San Antonio soil (swell pressure: 180 kPa) under net normal stress of 7kPa

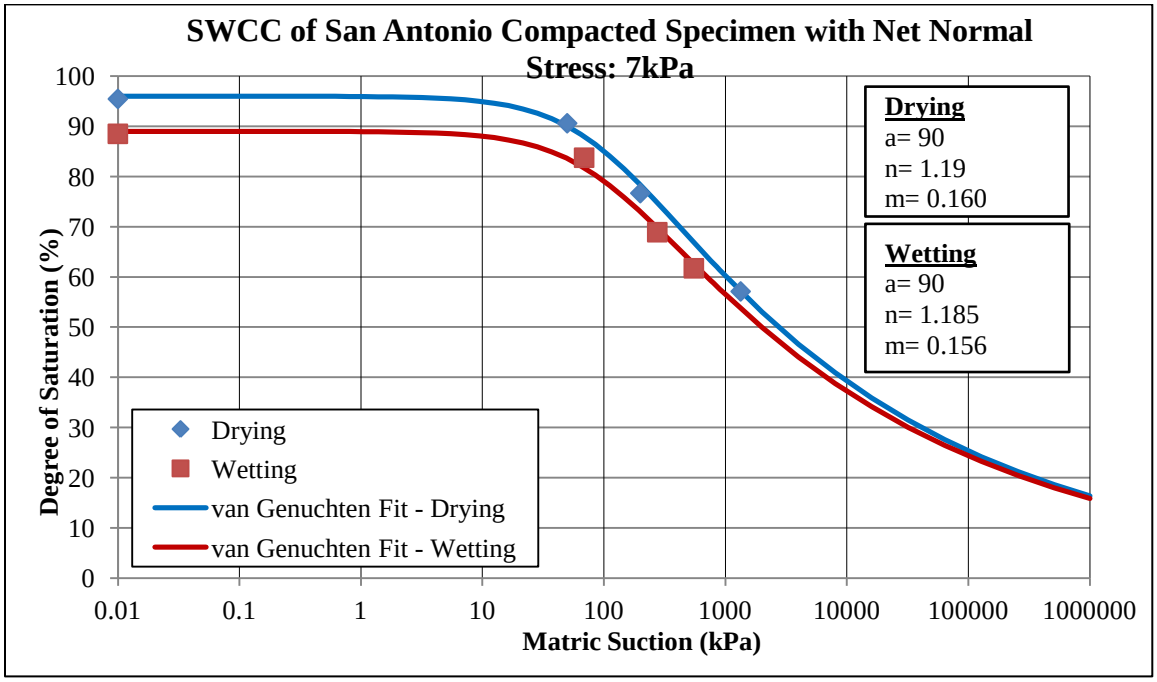

Figure 3.56. Drying and wetting SWCC in terms of degree of saturation for San Antonio soil (swell pressure: 180 kPa) under net normal stress of 7kPa

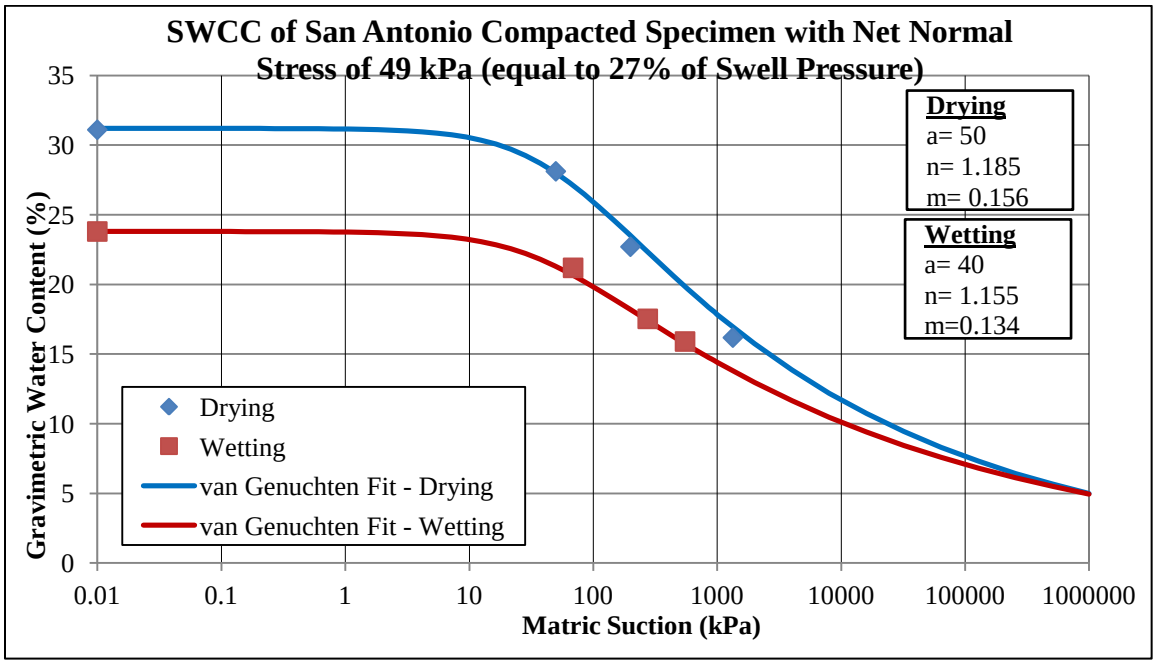

Figure 3.57. Drying and wetting SWCC in terms of gravimetric water content for San Antonio soil (swell pressure: 180 kPa) under net normal stress equal to 27% swell pressure

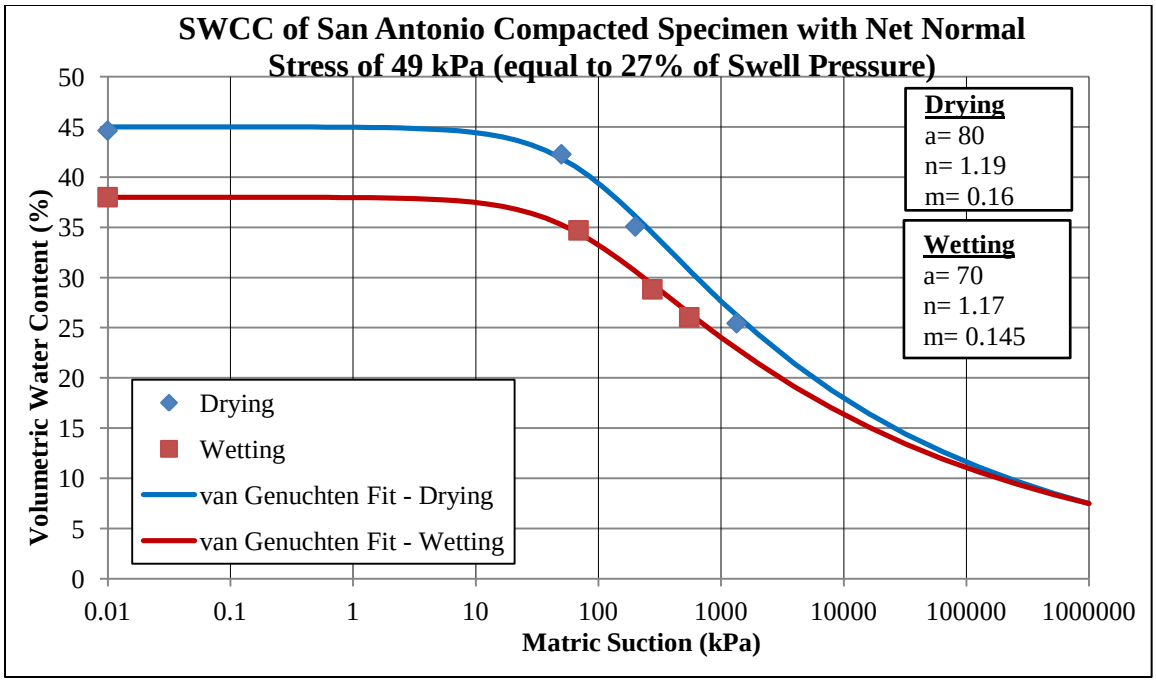

Figure 3.58. Drying and wetting SWCC in terms of volumetric water content for San Antonio soil (swell pressure: 180 kPa) under net normal stress equal to 27% swell pressure

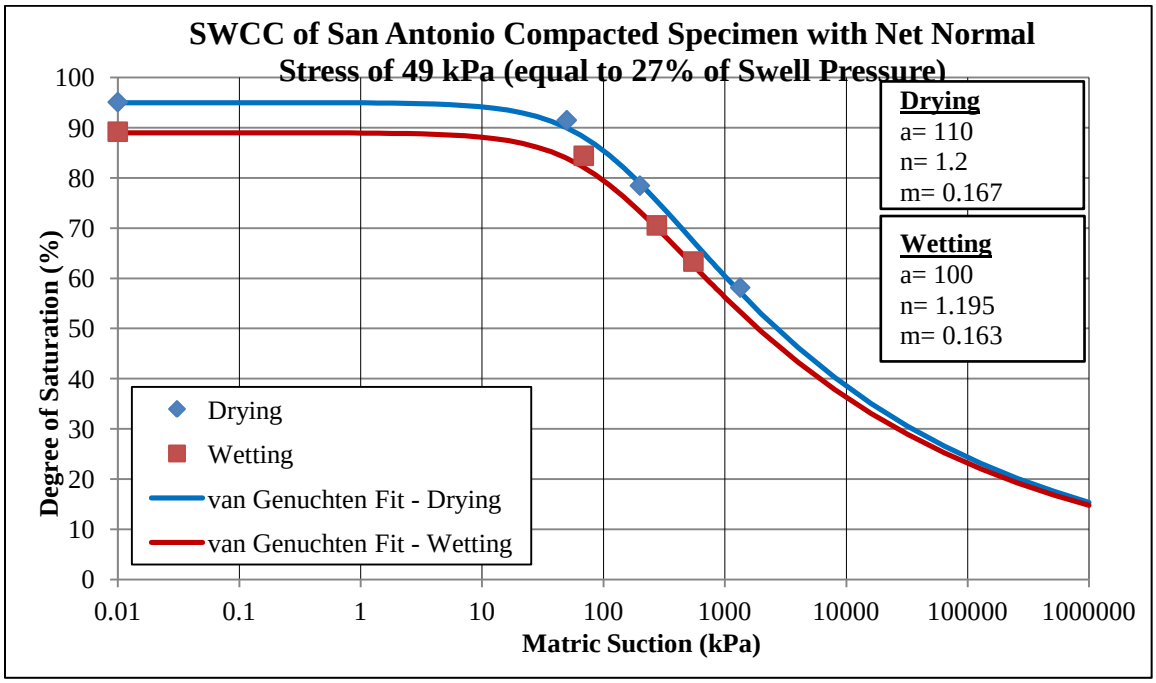

Figure 3.59. Drying and wetting SWCC in terms of degree of saturation for San Antonio soil (swell pressure: 180 kPa) under net normal stress equal to 27% swell pressure

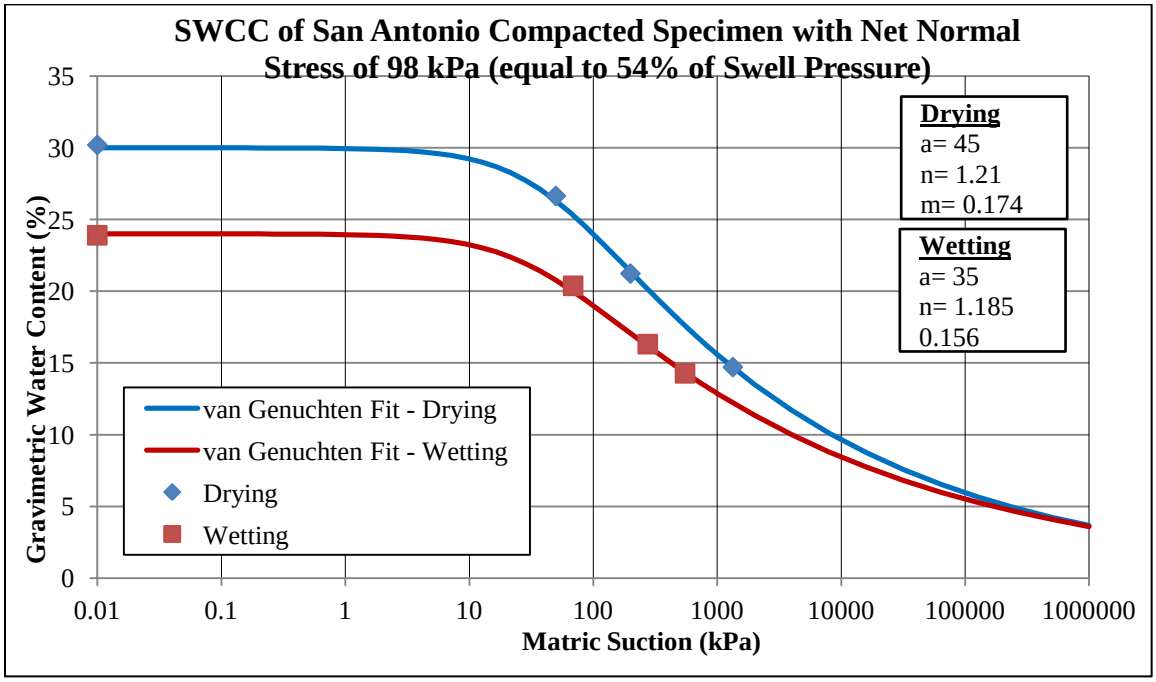

Figure 3.60. Drying and wetting SWCC in terms of gravimetric water content for San Antonio soil (swell pressure: 180 kPa) under net normal stress equal to 54% swell pressure

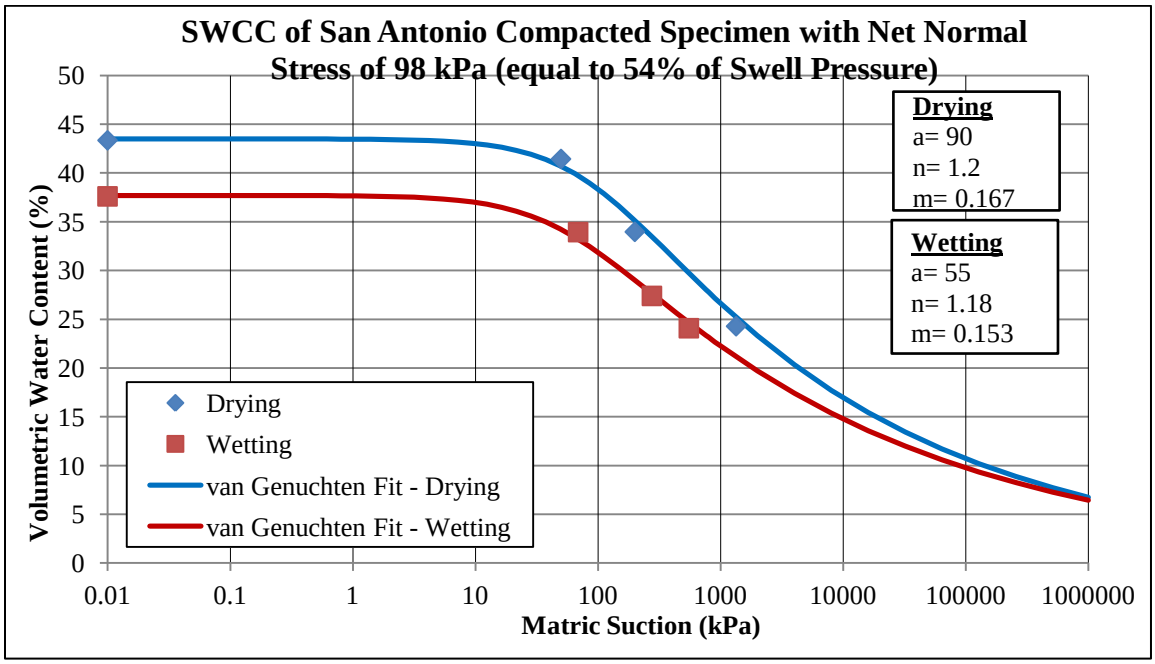

Figure 3.61. Drying and wetting SWCC in terms of volumetric water content for San Antonio soil (swell pressure: 180 kPa) under net normal stress equal to 54% swell pressure

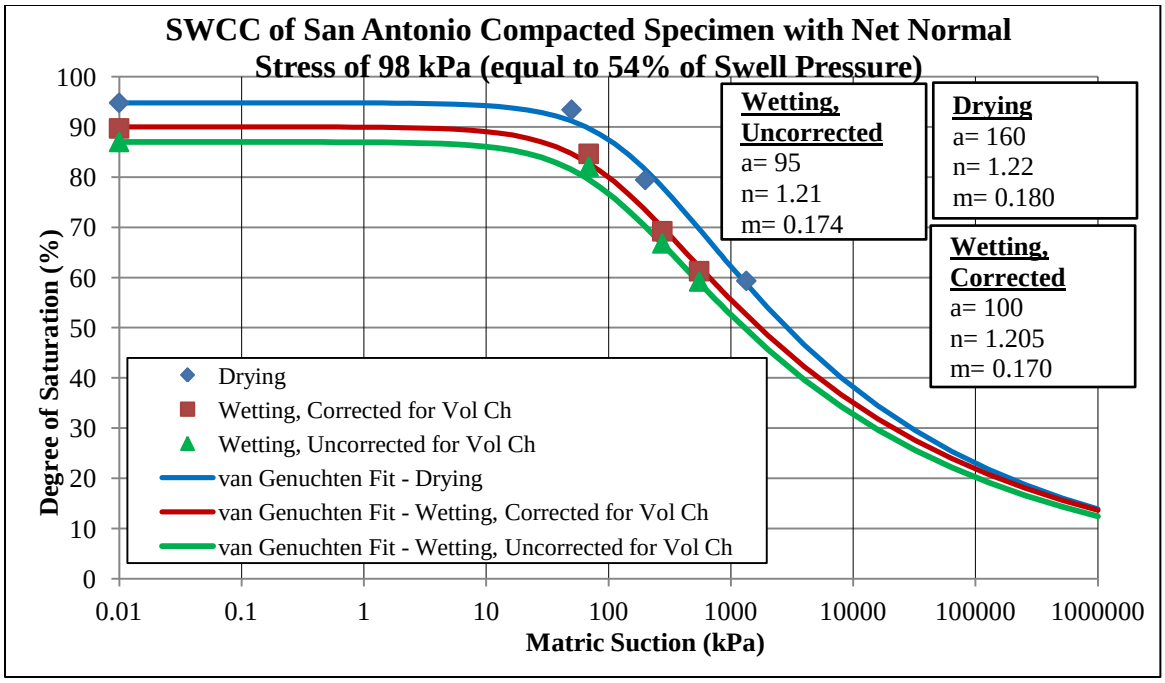

Figure 3.62. Drying and wetting (corrected and uncorrected) SWCC in terms of degree of saturation for San Antonio soil (swell pressure: 180 kPa) under net normal stress equal to 54% swell pressure

Figure 3.62 presents drying and wetting SWCC's for San Antonio compacted specimen tested under net normal stress of 98kPA (equal to 54% of swell pressure). This figure also shows the uncorrected wetting curve (green curve). It should be mentioned that for generating the uncorrected wetting curve, the initial volume of the specimen prior to starting the drying test was used. The volume of the specimen decreased during the test and therefore, the corrected wetting curve lies above the uncorrected wetting curve. In other words, the instantaneous volume of the specimen during the wetting test was smaller than the initial volume of the specimen (i.e. at the beginning of the drying test).

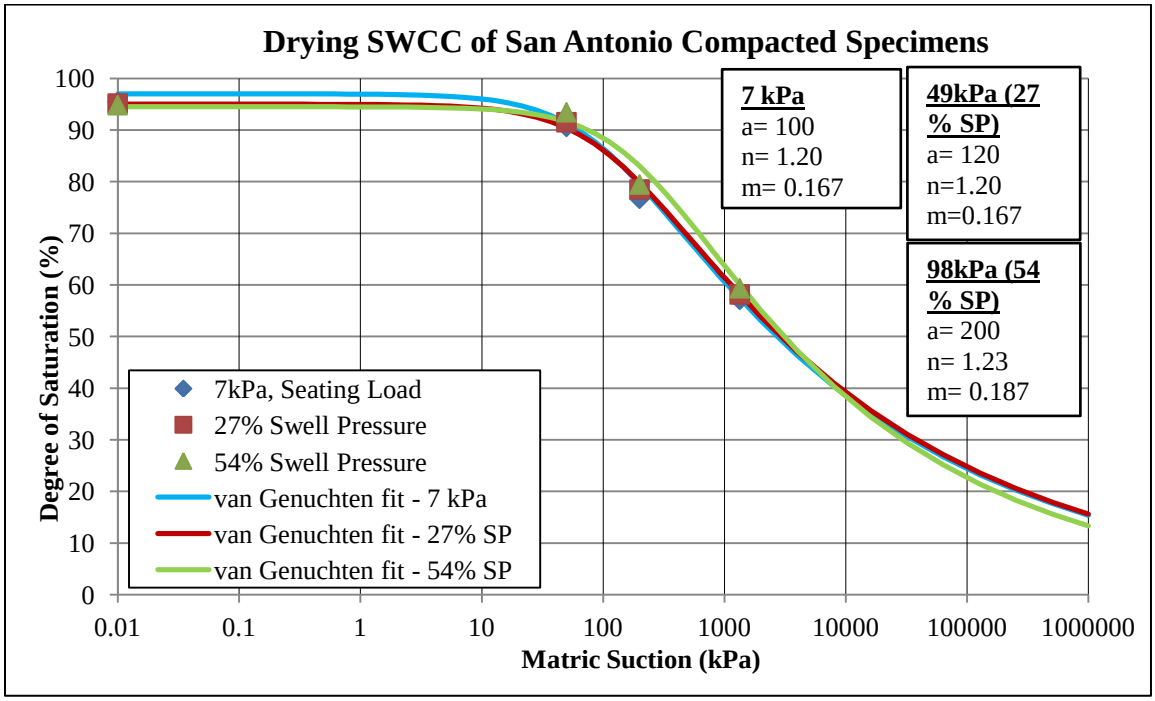

Figure 3.63. Drying SWCC in terms of degree of saturation for San Antonio soil (swell pressure: 180 kPa) under various net normal stresses. Notice larger values of "a" parameter for tests under higher net normal stress

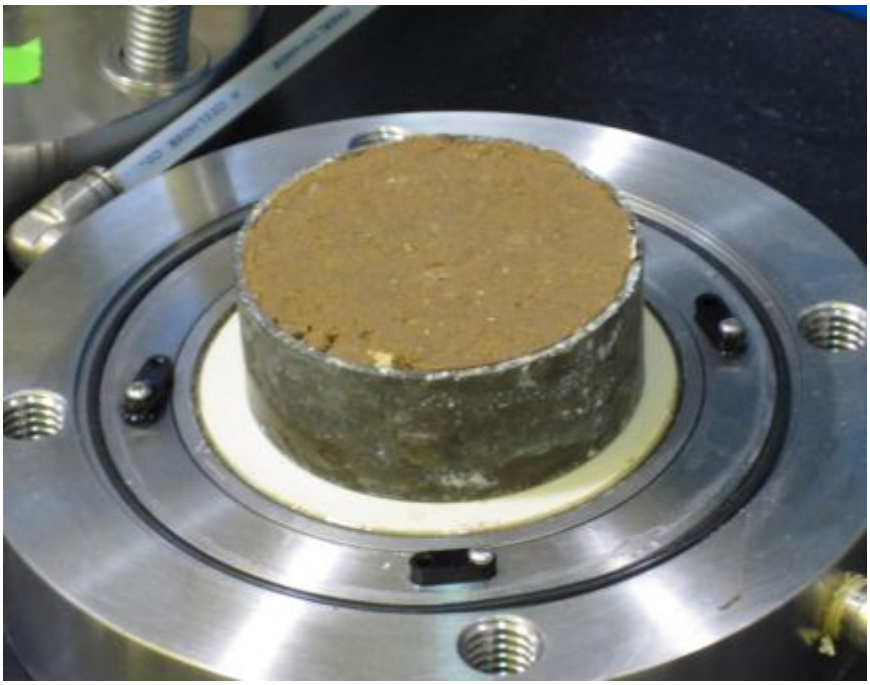

Figure 3.64. Drying SWCC, 200kPa suction, 7 kPa net normal stress (seating load), Anthem soil

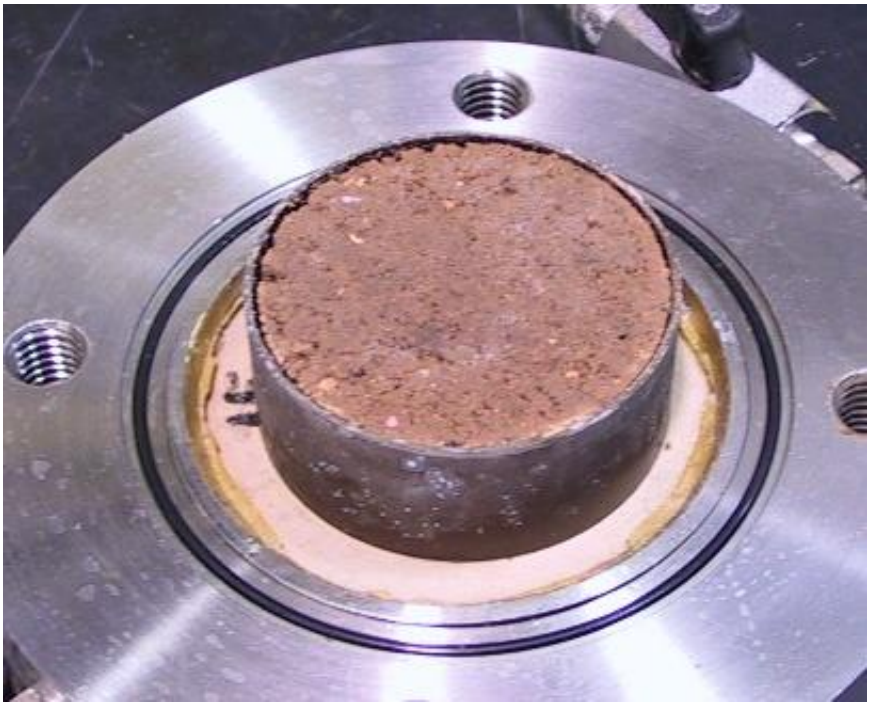

Figure 3.65. Drying SWCC, 1300kPa suction, 7 kPa net normal stress (seating load), Anthem soil

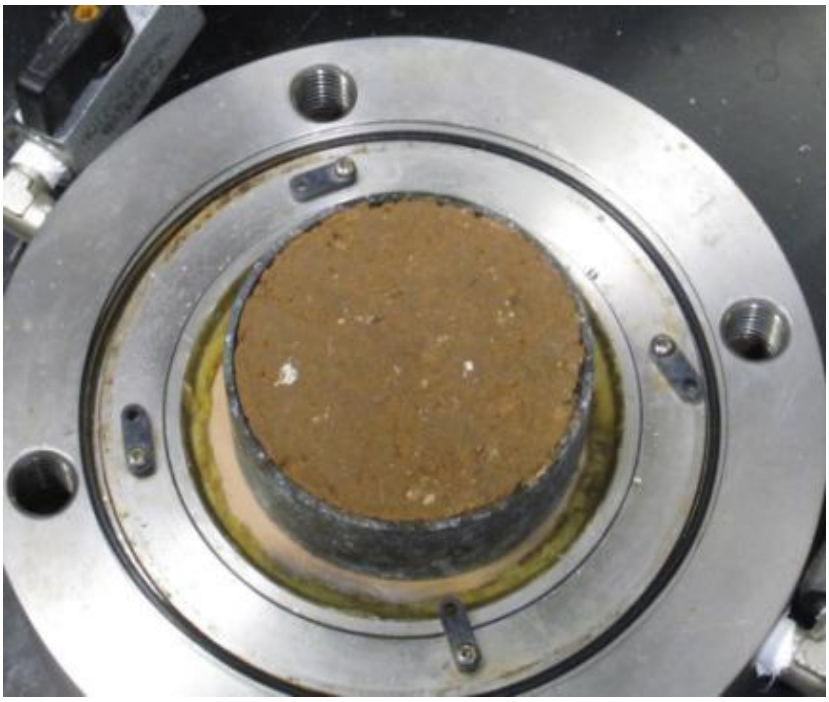

Figure 3.66. Drying SWCC, 400kPa suction, 26 kPa net normal stress (23% swell pressure), Anthem soil. Notice that almost no radial shrinkage has occurred, although there is some vertical displacement

Figure 3.67. Anthem specimen equilibrated at suction of 1330kPa under net normal stress of 53kPa (46% Swell Pressure). Note the minimal radial shrinkage in the specimen, although there is some vertical displacement

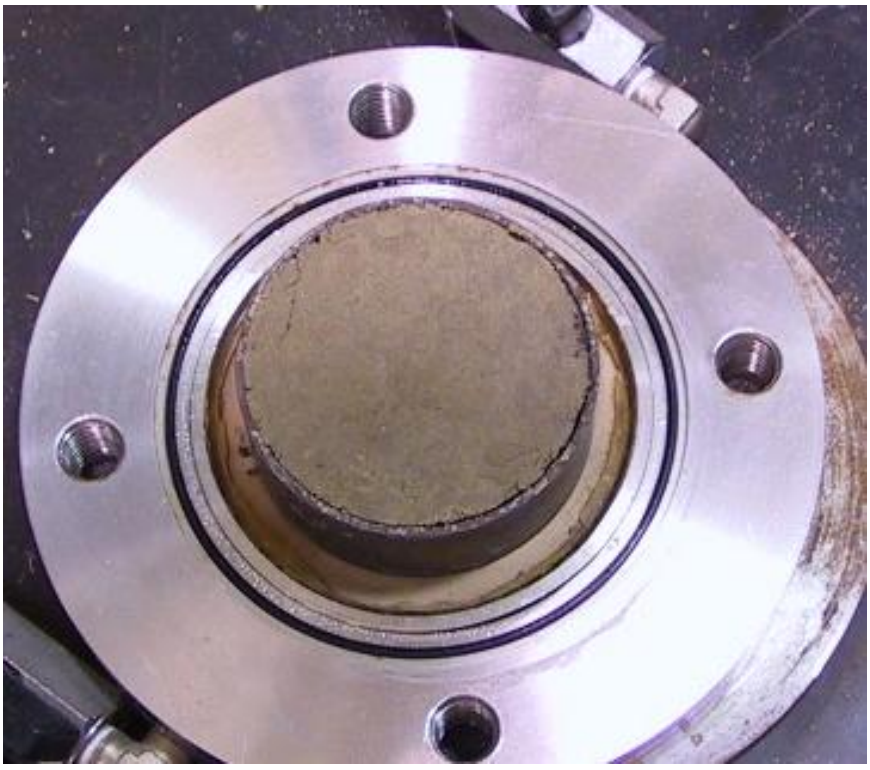

Figure 3.68. Drying SWCC, 400kPa suction, 7 kPa net normal stress (seating load), San Antonio soil

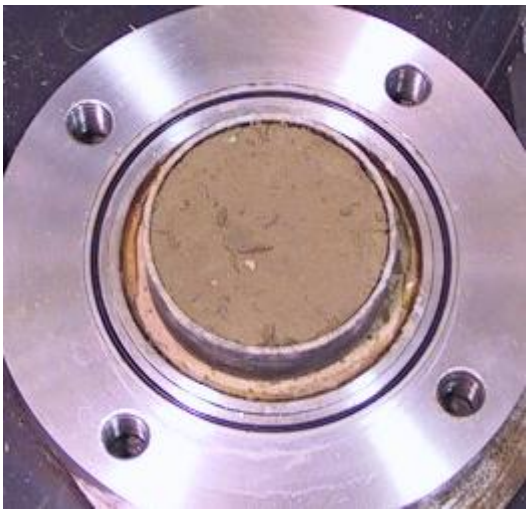

Figure 3.69. Drying SWCC, 1300kPa suction, 98 kPa net normal stress (54% swell pressure), San Antonio soil (Notice minimal radial shrinkage and some vertical deformation compared to net normal stress of 7kPa)

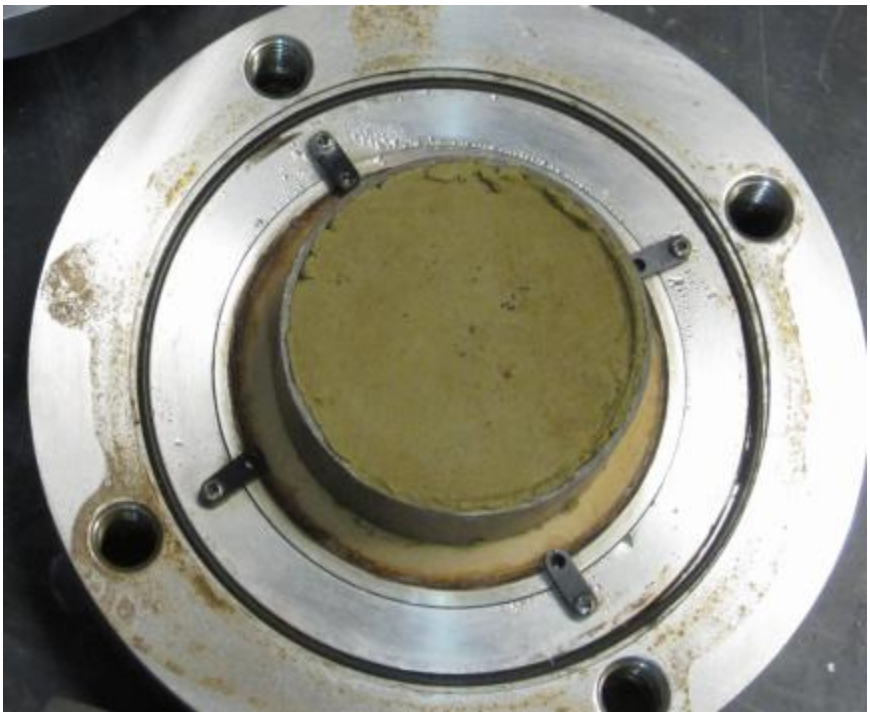

Figure 3.70. Drying SWCC, 400kPa suction, 105 kPa net normal stress (42% Swell Pressure), Colorado soil (Notice that almost no radial shrinkage has occurred, although there is some vertical displacement)

3.6. Summary and Conclusions

Soil Water Characteristic Curves (SWCC) of three expansive clays, Anthem, Colorado, and San Antonio, were determined through laboratory testing using a pressure plate oedometer device (SWC-150) for suctions up to 1500 kPa and using filter paper method for higher suctions. Volume change of the soils during suction change was measured and taken into account for establishing the SWCC's in terms of volumetric water content and degree of saturation. The measured data points along with van Genuchten fit parameters were presented for SWCC's corrected and uncorrected for volume change. The first set of tests was conducted on compacted specimens under net normal stress of 7kPa (seating load). The purpose of this set of test was to evaluate effect

of considering soil volume change on the shape of SWCC of expansive clays, with particular focus on the air-entry value.

Another set of tests were conducted in which slurry specimens of the soils were tested. The slurry specimens were prepared by mixing certain amount of soil and water to make sure that the specimen had reached 100% saturation. The effect of initial state of the specimen on its SWCC was studied by this set of experiments. It was found that slurry specimens undergo significant volume changes during SWCC test. Therefore, the difference between the volume corrected SWCC and uncorrected SWCC was more significant for slurry specimens compared to compacted.

The last set of laboratory experiments were intended to help evaluate the effect of net normal stress on the volume change of specimens and its impact on the shape of SWCC. For this set of experiments, different net normal stresses were used. The range of net normal stresses was from 7kPa to around 55% of the swell pressure of the tested soil.

Volume corrected SWCC's were developed by using the instantaneous volume of the specimen while in volume uncorrected SWCC's initial volume of the specimen was used and the soil volume change throughout the test was ignored.

It was found that volume change consideration plays a major role in shape of the SWCC particularly regarding the air-entry value (AEV) and slope in the transition zone. The air-entry value was shown to be larger for volume-corrected SWCC's compared to volume-uncorrected SWCC's. The slope of the curve in the transition zone also showed higher values for corrected SWCC's. These are shown in Figure 3.71 for Colorado soil.

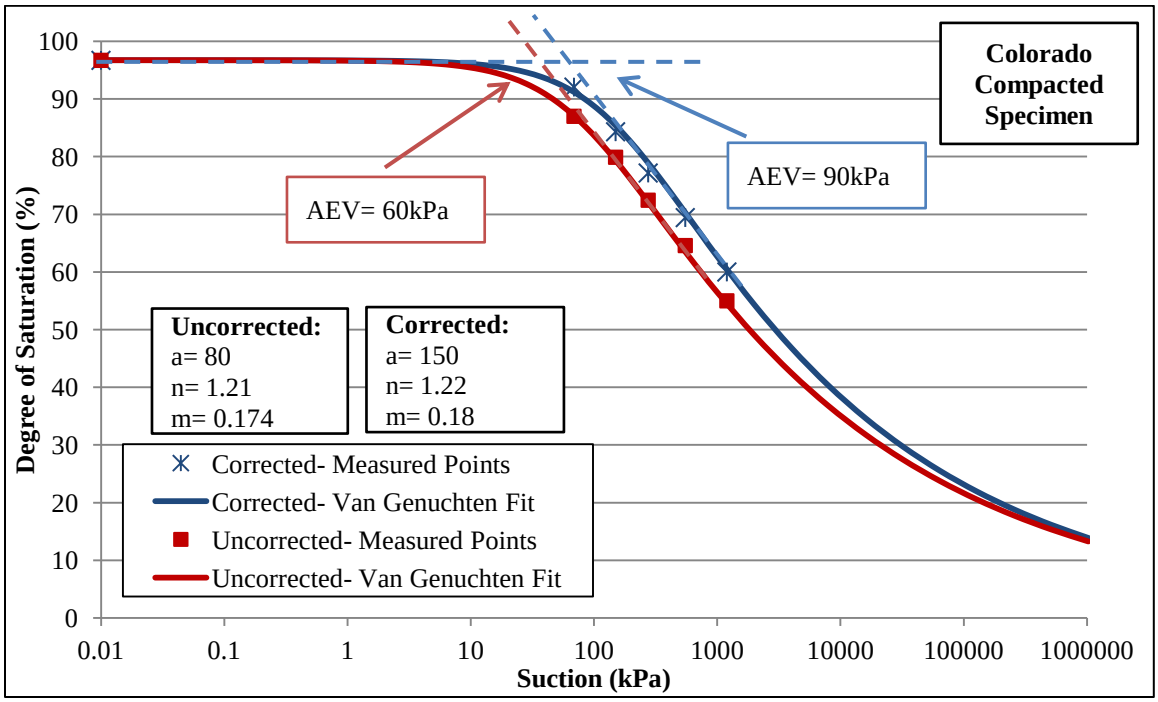

Figure 3.71. SWCC in terms of degree of saturation for compacted specimen of Colorado showing the method used for obtaining the AEV

It was found that the errors associated with the SWCC of expansive soils that are not volume-corrected are clear. AEV is wrong if volume change corrections are not made, and so is the slope of the SWCC in the transition zone. It was also found that in order to find the 'true' air-entry value and slope of the SWCC, the volume-corrected SWCC in terms of degree of saturation should be used.

Another major finding from this SWCC lab test was that due to existence of clods in soils with high plasticity during the compaction process, the air entry value of these soils turns out to be smaller than initially expected. The relatively low air entry values observed are believed to be the result of existence of clods creating air entry values more consistent with coarser-grained materials. In order to evaluate the effects of clods on SWCC of these clays, with particular focus on the air entry value, SWCC tests were

performed on slurry specimens. In slurry specimens, the pulverized soil was entirely saturated with water and therefore clods did not appear within the specimen.

Slurry specimens of Anthem, Colorado, and San Antonio soils were tested and the resulting SWCC's were compared against the SWCC's obtained from the compacted specimens of the same soils. It was found that initial state of the specimen has a significant effect on the shape of the SWCC, particularly due to high volume change of slurry specimens during the test. For any given soil tested, the air-entry value of volume-corrected SWCC's obtained from testing slurry specimens was found to be higher than that of compacted specimens. The slope in transition zone was also found to be higher for slurry specimens. It was found that Slurry specimens showed generally larger AEV compared to compacted due to a combination of volume change and structure effects. Figure 3.72 presents SWCC in terms of degree of saturation including both corrected and uncorrected curves for slurry specimen of San Antonio soil. The significant difference in AEV and slope in the transition zone between corrected and uncorrected curves are presented in this figure.

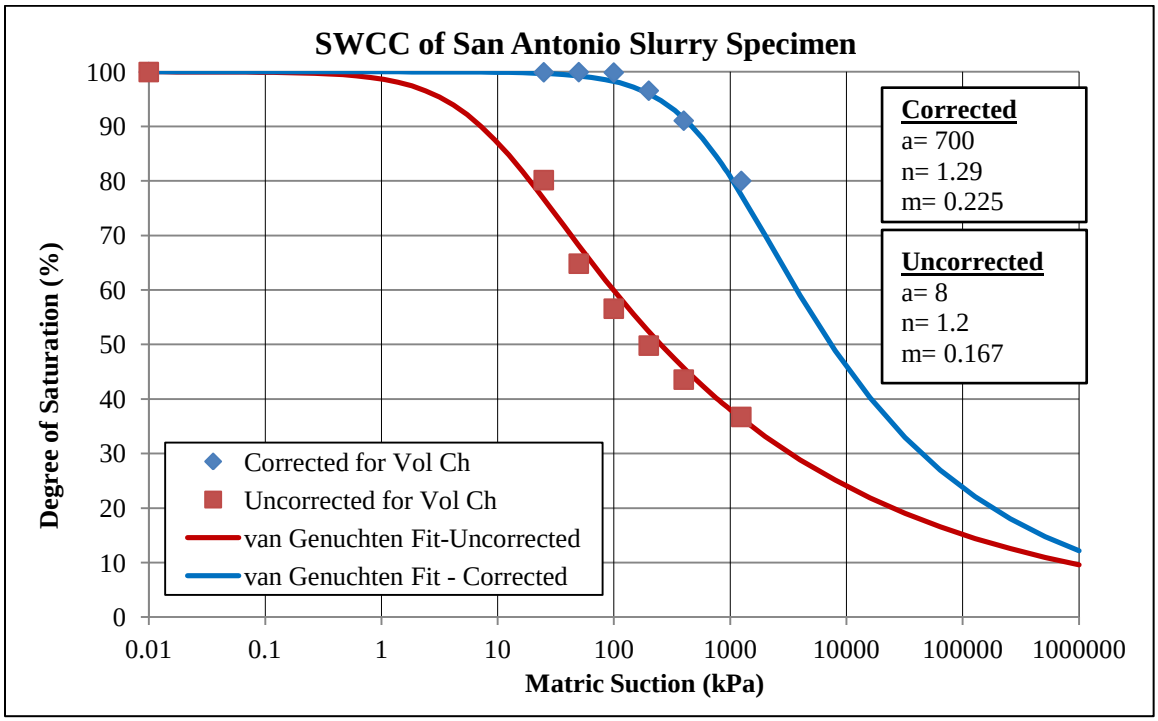

Figure 3.72. Volume corrected and uncorrected SWCC in terms of degree of saturation for slurry specimen of San Antonio

The SWCC's (drying and wetting paths) for three expansive soils of Anthem, Colorado, and San Antonio were. Determined. For this set of tests, the effects of net normal stress and hysteresis on the SWCC of expansive soils were studied. The net normal stress values applied to the soil specimens were varied form only a seating load (7 kPa) to around 54% of the swell pressure of the soil samples. Suction measurement and control methods used in the laboratory testing included axis translation and filter paper methods. Effect of net normal stress was found to be relatively insignificant with respect to volume change on compacted soils, although a slight increase in AEV of volume corrected SWCC was observed with larger net normal stresses. Radial shrinkage was observed to be minimized or eliminated in the cases of large net normal stress, particularly for compacted soils. Figure 3.73 shows drying SWCC's which were corrected

for soil volume change for Colorado soil for different net normal stresses tested. Slight increase in AEV with increase in net normal is found in this figure.

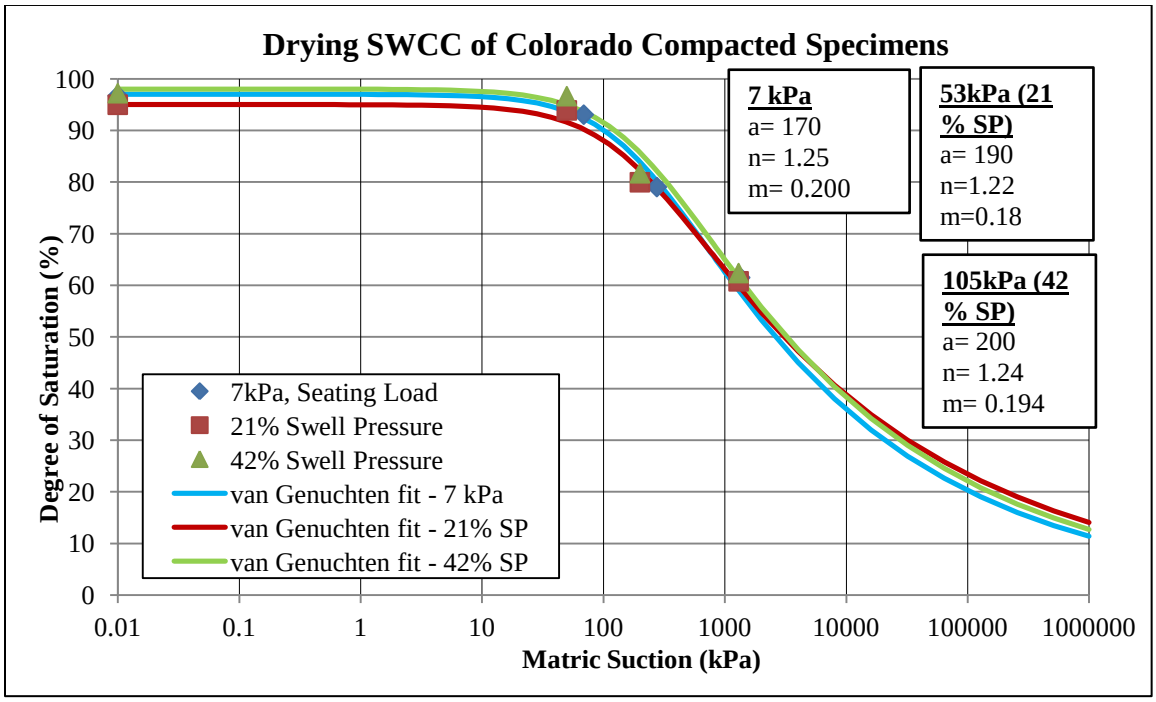

Figure 3.73. Drying SWCC in terms of degree of saturation for Colorado soil (swell pressure: 250 kPa) under various net normal stresses. Notice larger values of degree of "a" parameter for tests under higher net normal stress

As illustrated in the images of the specimens, generally larger radial shrinkage was observed at larger suction (e.g. around 1300kPa). It was found that with increase in suction, the radial shrinkage of the soil specimens also increase. This was true for the cases of both slurry and compacted specimens. It was also found form the results of the drying SWCC laboratory experiments of that for the tests that are conducted under seating or token load, the amount of shrinkage observed in the slurry specimens, were significantly larger compared to the shrinkage of the compacted specimens. When comparing the shrinkage of compacted specimens it was found that with increase in net normal stress, the amount of radial shrinkage of the soil decreases. It was found that for

the compacted specimens which were tested under large amounts of net normal stress (e.g. around 50% of the swell pressure of the soil) the radial shrinkage of the soil during the drying SWCC test was minimal such that the contact between the soil and the confining ring was maintained throughout the test even at relatively large suction values (i.e. around 1300 kPa). For such cases in which the contact between the soil and the confining ring is maintained throughout the test, it can be assumed the volume change of the soil is only in the vertical direction. This volume change can be measured much easier and with more accuracy. Of course, when the path is wetting rather than drying, there is no shrinkage issue to deal with in determining the SWCC.

Chapter 4

NUMERICAL MODELING OF EXPANSIVE CLAYS

4.1. Introduction

In the previous chapters it shown that correcting SWCC's for soil volume change can have a significant impact on the shape of the SWCC, particularly its air entry value (AEV) and slope in the transition zone (i.e. suction between AEV and residual). Since correcting for volume change alters the shape, slope and air entry value of the SWCC, considerable differences may appear between changes in suction in the soil with the SWCC corrected for volume change compared to that obtained with the uncorrected SWCC. Studies that capture the importance of correcting SWCC's for soil volume change through numerical modeling of water flow through soils, including its impact on the resulting soil deformations (e.g. expansion/shrinkage of expansive soils) could not be found through literature research, and thus this study represents a new contribution to the state of knowledge of moisture movement through expansive soils and associated deformations.

In a study conducted by GEO-SLOPE International Ltd. (2012), sensitivity of hydraulic simulation results to some material properties was evaluated, including a sensitivity study on air-entry value of soils found from SWCC. In order to find the sensitivity of unsaturated flow results to air-entry value (AEV), the authors changed AEV of a soil from 3kPa to 10kPa and kept the rest of the parameters constant. The authors found rather considerable difference in results of the analyses, as shown in Figures 4.1 and 4.2. The difference in capillary rise was evaluated for the two air entry values of

3kPa to 10kPa. The capillary rise is the height above the water table where negative pore-water pressures exist, but the soil remains essentially saturated due to capillary tension. It can be seen in the Figures 4.1 and 4.2 that for the case of higher AEV (i.e. 10 kPa) the capillary rise is greater than that of AEV of 3kPa for the numerical modeling results, suggesting that a higher AEV can result in wetter soil conditions at least for some boundary conditions. As explained in previous chapters of this study, one of the important considerations for finding the true AEV of expansive clays is to correct the SWCC's for soil volume change that happens during the change in suction under field-appropriate net normal stress conditions.

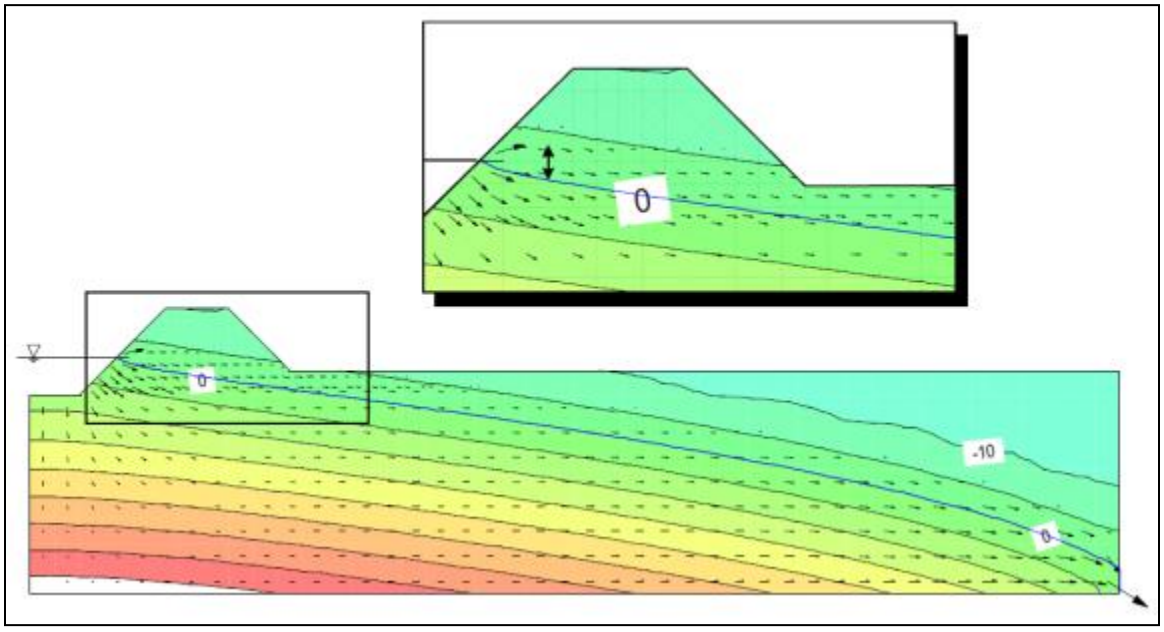

Figure 4.1. Pressure contours and flow vectors for a 3 kPa AEV material (GEO-SLOPE International Ltd., 2012)

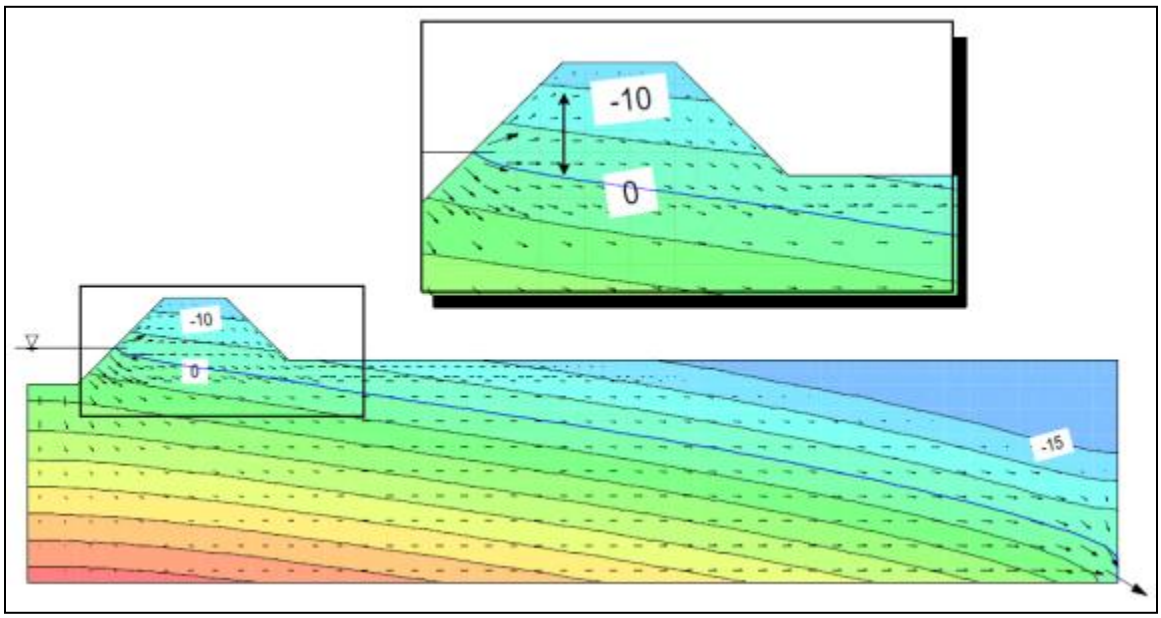

Figure 4.2. Pressure contours and flow vectors for a 10 kPa AEV material (GEO-SLOPE International Ltd., 2012)

Numerical modeling was performed as a part of this current study to find the impact of correcting SWCC for soil volume change (for soils with relatively high volume change potential, with emphasis on expansive clays in this study) and to evaluate the impact of SWCC volume change correction on fluid flow through the soil, and hence rate of progression of water movement and degree of wetting/drying in the soil. For example, for infiltrating water, rate of progression of wetted front and degree of wetting behind a wetting front can in turn have a significant effect on the amount of heave for expansive soils. In this study 1-D numerical unsaturated flow modeling was used to study the impact of volume change correction to the SWCC on fluid flow and associated suction changed induced deformation of expansive soils. Both uncoupled and coupled flow-deformation analyses were performed.

In the Uncoupled analyses, unsaturated flow is evaluated separately to obtain changes in water content and suction throughout the soil profile. These changes in soil

suction are subsequently used to compute soil deformations using a separate stress-deformation analysis. In the Coupled flow-deformation analyses, however, the governing partial differential equations for flow and deformation are combined such that flow of water through soil and also the amount of deformation caused by change in suction of the soil are solved for simultaneously. In other words, the flow-deformation analyses is performed such that the effect of suction change induced deformations on overall stress state is taken into account and the effect of stress change (e.g. net normal stress or suction) on deformation are taken into account as flow progresses.

Three computer programs of VADOSE/W, CODE-BRIGHT, and SVFLUX were used to evaluate the effect of correcting SWCC's on fluid flow through the unsaturated expansive clay soils. The resulting amount of expansion/shrinkage was subsequently determined, either in a decouple manner (using volume change computations done by hand) or by couple analyses (e.g. using CODE-BRIGHT). These unsaturated flow computer codes have the capability of simulating saturated and unsaturated flow of water through soils, although the emphasis in this study was on unsaturated flow, defined here as fluid flow through soils under negative pore water pressure (soil suction) conditions. The relatively simple CAD-based user interface of all three programs can be used to create the models effectively. During the modeling study, effect of considering volume change on hydraulic properties of the unsaturated soils with respect to fluid flow modeling and rate of advancement of wetted or drying front and suction change induced volume change in expansive soils within the profile were assessed. Although most of the analyses considered a wetting front, some cases of evaporation (drying) were

performed to obtain the results over a wider range of surface flux boundary conditions and associated suction profile cases. The laboratory results obtained from SWCC tests on three expansive soils of Anthem, Colorado, and San Antonio were used in the unsaturated flow modeling, and laboratory-measured suction compression indices on these soils were used for the stress-deformation computations (suction-changed induced volume change computations). One dimensional moisture movement through an expansive soil, using the same initial conditions and boundary conditions, was simulated once with the SWCC corrected and once with the SWCC uncorrected for volume change. To simulate the one-dimensional flow, geometry of 1m x 50m representing a column of soil was used. The next step in the modeling process was to define the material properties.

Regarding the material properties used, two separate models were created for: (1) SWCC corrected and (2) SWCC uncorrected for soil volume change. In the two models, all other material properties (e.g. saturated hydraulic conductivity), and all the boundary conditions were kept the same. As it was concluded from the previous chapters of this study (i.e. through literature search and laboratory testing), the SWCC in terms of degree of saturation (as opposed to SWCC in terms of gravimetric and volumetric water content) best illustrates the water retention characteristics of the soil (particularly its AEV), especially for soils with high volume change potential. However, VADOSE/W and SVFLUX only allow SWCC's to be entered in terms of volumetric water content. Therefore, the data points from the corrected and uncorrected SWCC in terms of volumetric water content were used in VADOSE/W and SVFLUX. On the other hand,

CODE-BRIGHT only allows SWCC's in terms of degree of saturation, and therefore, for modeling in CODE-BRIGHT, SWCC's in terms of degree of saturation were used.

Two types of analyses were done for the soils in this study: (1) Steady-State, and (2) Transient. In this study, the majority of simulations were carried out by steady-state analysis due to its simplicity and much shorter solution times compared to the transient flow analysis. A few transient analyses were also conducted in order to evaluate the progress of the model towards the steady-state condition and to study the impact of volume change corrections at intermediate stages of flow. The intermediate stages of flow are expected to exhibit at least some significant difference, perhaps even in trends (direction) of difference between corrected and uncorrected flow analyses results, due to the highly nonlinear nature of the unsaturated flow properties, particularly in the transition zone range of the SWCC.

Steady-State refers to a condition in which the flow through the soil has become steady and no change in the fluid potential condition occurs over time. In other words, in a steady-state analysis, the amount of flow into the system corresponds to the flow rate out of the system. A steady state analysis does not consider how long it takes to achieve a steady condition – the solution is to the homogenous form of the unsaturated flow partial differential equation. For steady state, it is implied that the boundary values have been in place forever and will be in place forever (Geo-Slope International, 2012).

For the case of transient flow, however, the condition of the domain is not constant and changes with time. The flow into the system may be different from the flow

out of the system because the system may store or release water, and this is accounted for in the transient flow analyses (GeoStudio 2012).

Flow of water in a saturated soil is governed by Darcy's law. In general, one-dimensional form Darcy's law (1856) may be written:

$$q = k\frac{\partial H}{\partial z} = ki \tag{4.1}$$

where:

q = flow rate of water

K = coefficient of hydraulic conductivity, assumed to be constant in saturated soil

H = hydraulic (total) head

z = length of the flow path

i = hydraulic gradient

In 1907, Buckingham proposed a modification of Darcy's law to describe water flow through unsaturated soil (Buckingham, 1907). In head units, the general one-dimensional form of Buckingham-Darcy flux law may be expressed as follows:

$$q = k(h)\frac{\partial H}{\partial z} = k(h)\frac{\partial(h+z)}{\partial z} = k(h)\left(\frac{\partial h}{\partial z}+1\right) \tag{4.2}$$

where H is the hydraulic head (equal to pressure head, h + elevation head, Z) and k(h) is the unsaturated hydraulic conductivity. The form of Equation 4.2 is similar to that of Equation 4.1 except that under conditions of unsaturated flow, the coefficient of unsaturated hydraulic conductivity does not remain constant, but varies with changes in water content and hence pore-water pressure.

The steady-state water flow is a special case of the fluid flow processes in soil. In general, water content and suction of the soil will change as water flows through the soil, and the matric suction and water content will be functions of time as well as of space. In general, fluid flow is transient, and flows are time-dependent and can be mathematically described by the water mass balance or continuity equation. The water mass balance is related to water flux, storage changes, and sources or sinks of water. This model is based on the mass conservation and correlates the change in mater storage of the domain to the water that enters the system and the water that exits (i.e. source and sink). The conservation of mass equation can be formulated by calculating the mass balance for the one-dimensional system during an arbitrarily small time period Δt between time t and t + Δt as follows (Jury, et al., 1991):

$$\frac{\partial q}{\partial z} + \frac{\partial \theta}{\partial t} + r_w = 0 \tag{4.3}$$

where:

θ = volumetric water content of soil

t = time

r_w = sources or sinks of water

Richards equation which is often used to predict the water content in unsaturated soils during transient flow was introduced by Richards (1931) who suggested that the Darcy's law originally proposed for saturated flow in porous media can also be applicable to unsaturated flow in porous media.

Richards equation can be presented in the following one-dimensional form:

$$\frac{\partial \theta}{\partial t} = \frac{\partial\left[k(h)\left(\frac{\partial h}{\partial z}+1\right)\right]}{\partial z} \tag{4.4}$$

Richards equation states that the rate of change of the volumetric water content (i.e. θ) with respect to time is equal to the rate of change of flow in a soil system (Chao, 2007). This equation can be written in terms of θ or h, or in a mixed form using both variables. The soil water characteristic curve is used to translate between θ and h.

The pressure head-based formulation of Richards equation is (Pachepsky et al., 2003):

$$\frac{\partial}{\partial x}(k(h)\frac{\partial h}{\partial x}) = \gamma_w m_{2w}\frac{\partial h}{\partial t} \tag{4.5}$$

Where k(h) or k_{unsat} is the unsaturated hydraulic conductivity as a function of h (m/s), x is the elevation (m), h is the total head (m), t is the time, γ_w is the specific weight of water (9.81 kN/m^3), m_{2w} is the storage capacity of soil that can be represented by the slope of the SWCC (m^2/kN), and t is the time (s).

There are many commercial and public domain software available to solve this equation. In this study, VADOSE/W (part of the GeoStudio software suite), SVFLUX (part of the SVOffice software suite), and CODE-BRIGHT were used to obtain a numerical solution to the unsaturated flow problems. The solution of Richards equation is sensitive to both SWCC and the k_{unsat} function of the soil. One of the most commonly used equations for estimating k_{unsat} function is van Genuchten equation (1980). The k_{unsat} function is often estimated based on soil properties such as the SWCC and saturated hydraulic conductivity due to the fact that the laboratory tests for measurement of k_{unsat}

are generally costly and time consuming. The SWCC and the k_{unsat} function are both sensitive to volume change of the soil that occurs in response suction change under a particular set of net normal stress conditions.

Finite element numerical methods (such as models embedded in computer programs VADOSE/W, SVFLUX, and CODE-BRIGHT) are based on the concept of subdividing a continuum into small pieces, describing the behavior or actions of the individual pieces and then reconnecting all the pieces to represent the behavior of the continuum as a whole (GeoStudio, 2012). This process of subdividing the continuum into smaller pieces is known as discretization or meshing. The pieces are known as finite elements or mesh. In order to make sure that the results are accurate, it is important to set the mesh equal to or smaller than the optimum size. Some programs (e.g. SVFLUX provide the user with the option of automatic mesh size optimization) while other program do not provide this feature (e.g. VADOSE/W). for the programs that do not do the automatic mesh size optimization, the user need to make sure to find the optimum mesh size for stability and convergence through trial and error. Discretization (mesh size selection) is a critical element of finite element modeling. In addition, defining material properties and boundary conditions are critical elements(GeoStudio, 2012)It is also important to investigate, through trial and error, the extent of the domain boundaries such that placement of the boundaries does not affect the solution in regions of primary interest for the problem.

The primary steps to create and analyze a model using VADOSE/W, SVFLUX, and CODE-BRIGHT are as follows:

Step 1: Define the type of analysis to be performed (i.e. steady state versus transient analysis). If transient analysis is selected, appropriate time steps including starting point, duration, and end point of each step should be defined

Step 2: Create model geometry using the CAD-based user interface. The softwares generally provide options of using regions, lines, points, and other tools to draw the desired geometry for the model

Step 3: Define and assign properties of the materials to be used in the analysis. This includes defining basic soil properties (e.g. specific gravity, and saturated moisture content), SWCC (i.e. in terms of volumetric water content or degree of saturation), k_{sat} (saturated hydraulic conductivity), and unsaturated hydraulic conductivity function.

Step 4: Define and assign boundary conditions to the created geometry. For transient analysis in addition to boundary conditions, initial condition of the model should also be defined. For the case of this study, the boundary conditions consists of no flow (for left and right sides of the soil column), constant negative pressure head at the bottom of the model and either constant flux or constant head for the top of the soil column.

Step 5: Adjust mesh size and refine mesh sizing if necessary. It was found important to refine mesh size for each run to make sure that the results are accurate. The mesh size that is too big, usually over-simplifies the solution and although convergence may be obtained easily, the results may be erroneous or inaccurate. The mesh size that is too small may lead to longer convergence

time which is not always necessary, with the numerical solutions the same as the ones in which the optimum mesh size has been used. SVFLUX is capable of automatically refining the mesh size based on the concurrent boundary conditions. However, VADOSE/W and CODE-BRIGHT do not provide this option.

Step 6: Analyze the model: If the problem has not been defined completely, the solver may not run and an error message may be displayed.

For each software, two base cases were studied; in the first case, the SWCC that was determined for the soil was corrected for soil volume change, while for the second case, the SWCC was not corrected for volume change. Other than the corrected and uncorrected SWCC's, the remaining factors including material properties and boundary conditions were kept the same for both cases. Effort was taken to be consistent among the three codes used in this study (CODE-BRIGHT, VADOSE/W and SVFLUX) regarding defining SWCC. VADOSE/W and SVFLUX allow SWCC data points or SWCC fitting equations. However, CODE-BRIGHT only allows use of the van Genuchten (1980) SWCC fit equation for SWCC. In order to be consistent, for all the simulations SWCC's were input by defining curve-fitting parameters of van Genuchten (1980) model for SWCC. The van Genuchten (1980) SWCC curve fitting equation was the only equation in common with the three codes of CODE-BRIGHT, VADOSE/W and SVFLUX. The computer codes use closed-form solutions to estimate SWCC based on user-specified curve-fitting parameters, and the same fitting parameters were used in each code.

4.2. Model Geometry

For modeling, a one dimensional flow through a soil was simulated in this study. The 1-D conditions were used due to extensive run-times often associated with transient unsaturated flow analyses for 2-D or 3-D conditions. To illustrate the one-dimensional flow, a geometry of 1m x 50m which is basically a column of soil was defined. The geometry of the model is presented in Figure 4.3.

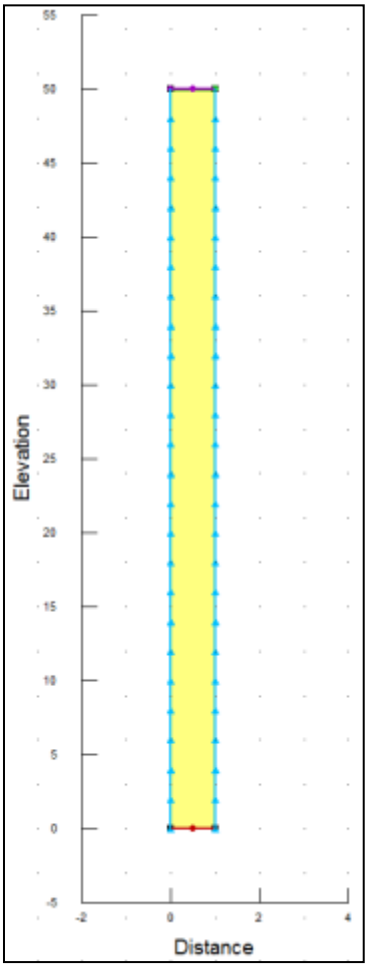

Figure 4.3. Geometry of the Model in VADOSE/W (Dimensions are in meters)

4.3. Soil Properties

Three soils of Anthem, Colorado, and San Antonio were used in numerical modeling. Numerical modeling of Anthem, Colorado, and San Antonio are described in this chapter. The properties of Anthem, Colorado, and San Antonio soils are presented in this section. Tables 4.1 and 4.2 present values of saturated hydraulic conductivities and other properties of these soils such as void ratios at the condition of full saturation.

Table 4.1. Saturated hydraulic conductivity of soils in this study

Soil	**Saturated Hydraulic Conductivity**		**Intrinsic Permeability**
	m/s	m/day	m^2
Anthem	1.00E-07	0.00864	9.286E-15
Colorado	1.00E-08	0.000864	9.286E-16
San Antonio	1.00E-08	0.000864	9.286E-16

Table 4.2. Void ratio and porosity (at 100% saturated condition) of soils in this study

Soil	**Degree of Sat**	**Gs**	**w at Saturation**	**$e=G_s*w/S$**	**n=e/(1+e)**
Anthem	1.00	2.723	0.25	0.68	0.405
Colorado	1.00	2.778	0.30	0.83	0.455
San Antonio	1.00	2.795	0.32	0.89	0.472

As previously mentioned, in order to be consistent among the three programs of VADOSE/W, SVFLUX, and CODE-BRIGHT, van Genuchten (1980) fit for SWCC was used for all of the analyses. One of the differences between the codes was that VADOSE/W and SVFLUX allow SWCC in terms of volumetric water content, whereas CODE-BRIGHT allows SWCC only in terms of degree of saturation.

Van Genuchten-Mualem (1980) equation for predicting k_{unsat} function embedded in CODE-BRIGHT, VADOSE/W and SVFLUX were used to estimate k_{unsat} function of the soils. The van Genuchten-Mualem equation used in VADOSE/W and SVFLUX

allows van Genuchten SWCC fitting parameters ('a', 'n', and 'm') in terms of volumetric water content. However, the van Genuchten-Mualem equation that is utilized in CODE-BRIGHT allows van Genuchten SWCC fitting parameters ('a', 'n', and 'm') in terms of degree of saturation only. It was established in Chapter 3, that for a given expansive soil, the SWCC in terms of degree of saturation may have different fitting parameters than the SWCC in terms of volumetric water content. The van Genuchten-Mualem equation used in VADOSE/W and SVFLUX uses SWCC in terms of volumetric water content and its saturated hydraulic conductivity and generates estimation for k_{unsat} function. In CODE-BRIGHT, however, the Van Genuchten-Mualem equation uses SWCC in terms of degree of saturation (as opposed to volumetric water content in VADOSE/W and SVFLUX). Therefore, the k_{unsat} functions generated by VADOSE/W and SVFLUX are the same but they are different from the k_{unsat} functions generated by CODE-BRIGHT.

It can be seen from all the figures showing k_{unsat} functions (such as Figure 4.6) for different soils that the values of k_{unsat} are larger for the cases in which SWCC is corrected for soil volume change (in which case AEV was found to be larger than uncorrected SWCC). This can be explained by the mechanism of water flow through the soil. In a saturated soil, all the pore spaces between the solid particles are filled with water. Once the air-entry value is exceeded (i.e. suctions greater than AEV), air enters the largest pores and the air-filled pores become non conductive conduits to flow and increase the tortuosity of the flow path. As a result, the ability of the soil to transport water (the hydraulic conductivity) decreases (GEO-SLOPE International Ltd., 2012). Since the SWCC that is corrected for soil volume change generally has a higher AEV

(shown in Figures such as 4.5), the desaturation of this soil starts at higher suctions which means that the decrease in soil hydraulic conductivity occurs at higher suctions. This leads to larger k_{unsat} values for volume corrected SWCC, on average, compared to the uncorrected SWCC case. This means that for expansive soils, if the SWCC is corrected for soil volume change the estimated unsaturated hydraulic conductivity will be larger compared to the case in which the SWCC is not corrected for soil volume change, and therefore, water moves faster through the soil with volume corrected SWCC.

SVFLUX and VADOSE/W use van Genuchten-Mualem (1980) equation for predicting k_{unsat} functions of soils. Van Genuchten (1980) proposed the following closed form equation to describe the hydraulic conductivity of a soil as a function of matric suction:

$$k = k_{sat} \frac{\left[1 - \left(a\psi^{(n-1)}\right)\left(1 + \left(a\psi^{n}\right)^{-m}\right)\right]^{2}}{\left(\left(1 + a\psi\right)^{n}\right)^{\frac{m}{2}}} \tag{4.6}$$

Where:

k_{sat} = saturated hydraulic conductivity,

a, n, and m = curve fitting parameters, where $n = 1/(1\text{-}m)$, or $m = (n-1)/n$ and

ψ = required suction range.

From the above equations, the hydraulic conductivity function of a soil can be estimated once the saturated conductivity and the two curve fitting parameters, ‘a’ and ‘m’ (or ‘n’) are known.

In CODE-BRIGHT by default, the consistent form of relative hydraulic conductivity with van Genuchten model-Mualem (1980) is used (Saaltink et al., 2005). The form of the equation is as below:

$$k = k_{sat}\left[\sqrt{S}\left(1-\left(1-S^{1/m}\right)^{m}\right)^{2}\right] \tag{4.7}$$

S (degree of saturation) is defined in such a way that ranges between 0 and 1, and 'm' is the van Genuchten parameter for SWCC fit which is the slope of the curve in the transition zone. The equation used by SVFLUX, VADOSE/W and CODE-BRIGHT for predicting k_{unsat} function are van Genuchten model-Mualem (1980) and are interchangeable.

Although all three computer codes use the same van Genuchten model-Mualem equation (1980) for predicting k_{unsat} function, the k_{unsat} function predicted by CODE-BRIGHT is different than the ones determined by SVFLUX and VADOSE/W. The reason for this difference is that the van Genuchten model-Mualem (1980) equation in SVFLUX and VADOSE/W uses van Genuchten parameter ('a', 'n', and 'm') that correspond to SWCC in terms of volumetric water content. However, the van Genuchten model-Mualem (1980) equation in CODE-BRIGHT uses S (degree of saturation) and 'm' parameter of SWCC in terms of degree of saturation. As it was established earlier, for a given soil that exhibits volume change, the van Genuchten parameters of SWCC in terms of volumetric water content may be different that the van Genuchten parameters of SWCC in terms of degree of saturation. This difference in van Genuchten parameters leads to differences in estimated k_{unsat} function.

4.3.1. Anthem Soil

Figures 4.4 and 4.5 show the SWCC of Anthem soil in terms of volumetric moisture content and degree of saturation. The data points shown in these figures were obtained from laboratory tests described in Chapter 3. Shown in these figures are also the van Genuchten (1980) fits to the SWCC data points. It can be seen that for both SWCC's (in terms of volumetric water content and degree of saturation) the "a" parameter (which corresponds to AEV) is higher for the corrected curve.

Figure 4.6 shows hydraulic conductivity versus suction, otherwise known as k_{unsat} function for Anthem soil found by van Genuchten-Mualem (1980) embedded in SVFLUX and CODE-BRIGHT. It can be seen that for any given suction, the k_{unsat} generated by either SVFLUX or CODE-BRIGHT is higher for corrected curve compared to the uncorrected curve.

It was also found that for Anthem soil the k_{unsat} values estimated by CODE-BRIGHT are generally smaller than the k_{unsat} values estimated by SVFLUX. This is due to the difference in the equation used for estimating the k_{unsat} function. Therefore, it generally takes longer for the model in CODE-BRIGHT to reach equilibrium compared to the same model in SVFLUX. In other words, the rate of changes in suction (e.g. progression of wetted front) is larger for corrected SWCC compared to uncorrected case.

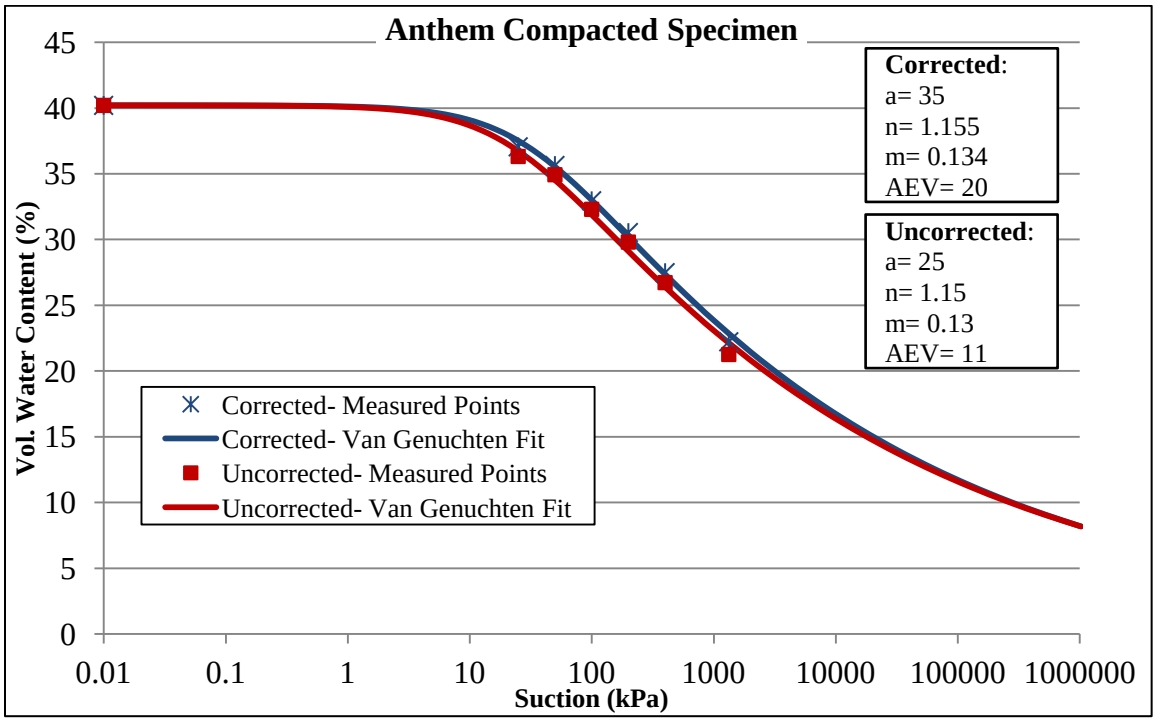

Figure 4.4. SWCC of Anthem soil in terms of volumetric water content, corrected and uncorrected for soil volume change used in VADOSE/W and SVFLUX

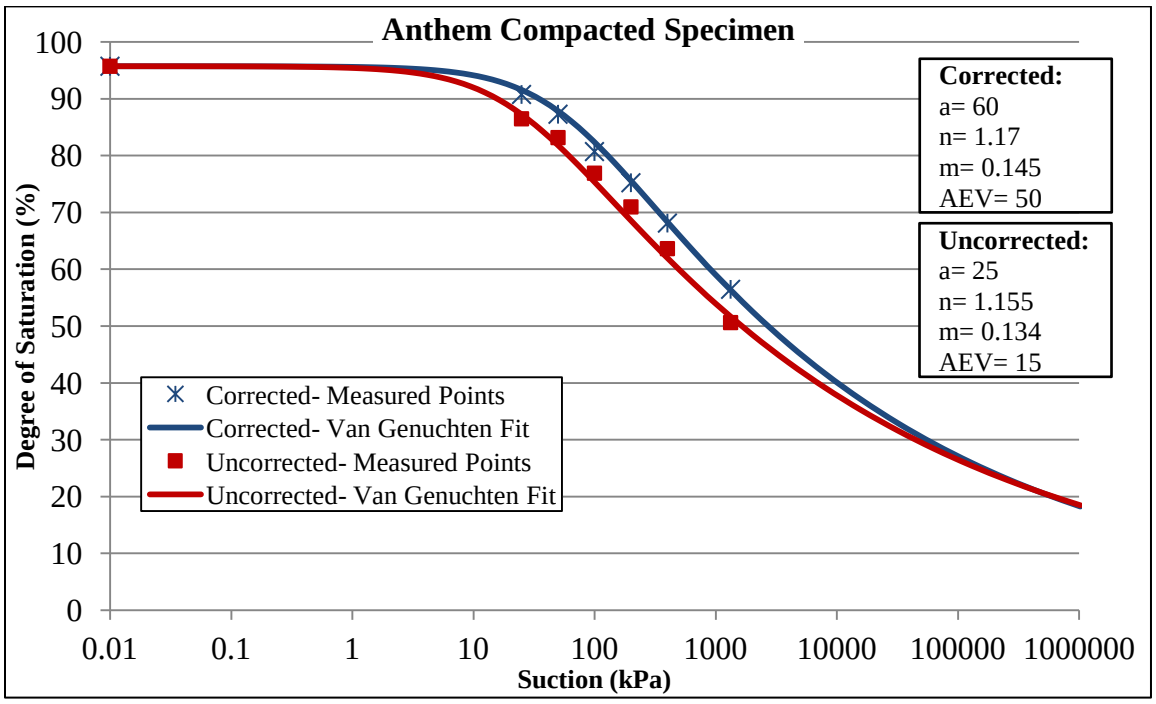

Figure 4.5. SWCC of Anthem soil in terms of degree of saturation, corrected and uncorrected for soil volume change used in CODE-BRIGHT

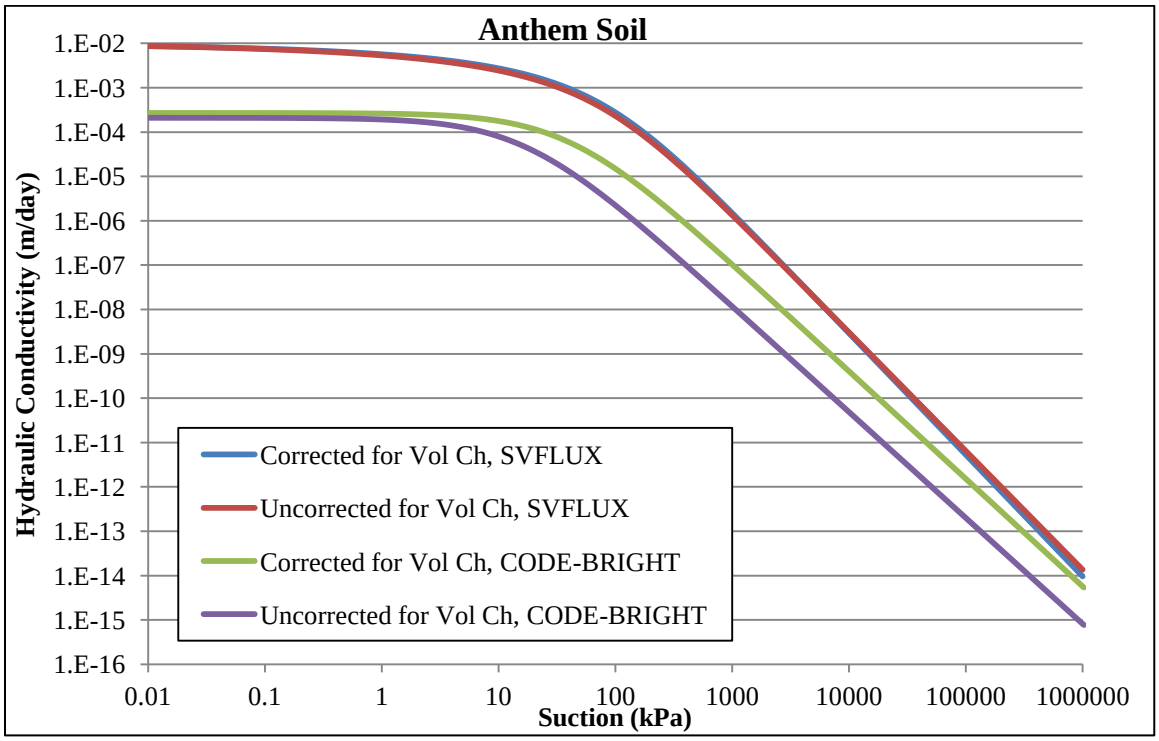

Figure 4.6. k_{unsat} function of Anthem soil estimated by SVFLUX and CODE-BRIGHT

4.3.2. Colorado Soil

Figures 4.7 and 4.8 show the SWCC of Colorado soil in terms of volumetric moisture content and degree of saturation. Shown in the figures are also the van Genuchten (1980) fits to the SWCC data points obtained from laboratory experiments. Figure 4.9 shows hydraulic conductivity versus suction, otherwise known as k_{unsat} function for Colorado soil. It can be seen that the difference in volume corrected and uncorrected SWCC's are more pronounced for Colorado soil compared to Anthem soil. This is due to the fact that during the SWCC test, Colorado soil exhibited larger volume change.

Figure 4.9 shows hydraulic conductivity versus suction, otherwise known as k_{unsat} function for Colorado soil found by van Genuchten-Mualem (1980) embedded in

SVFLUX and CODE-BRIGHT. It can be seen that for any given suction, the k_{unsat} generated by either SVFLUX or CODE-BRIGHT is higher for corrected curve compared to the uncorrected curve.

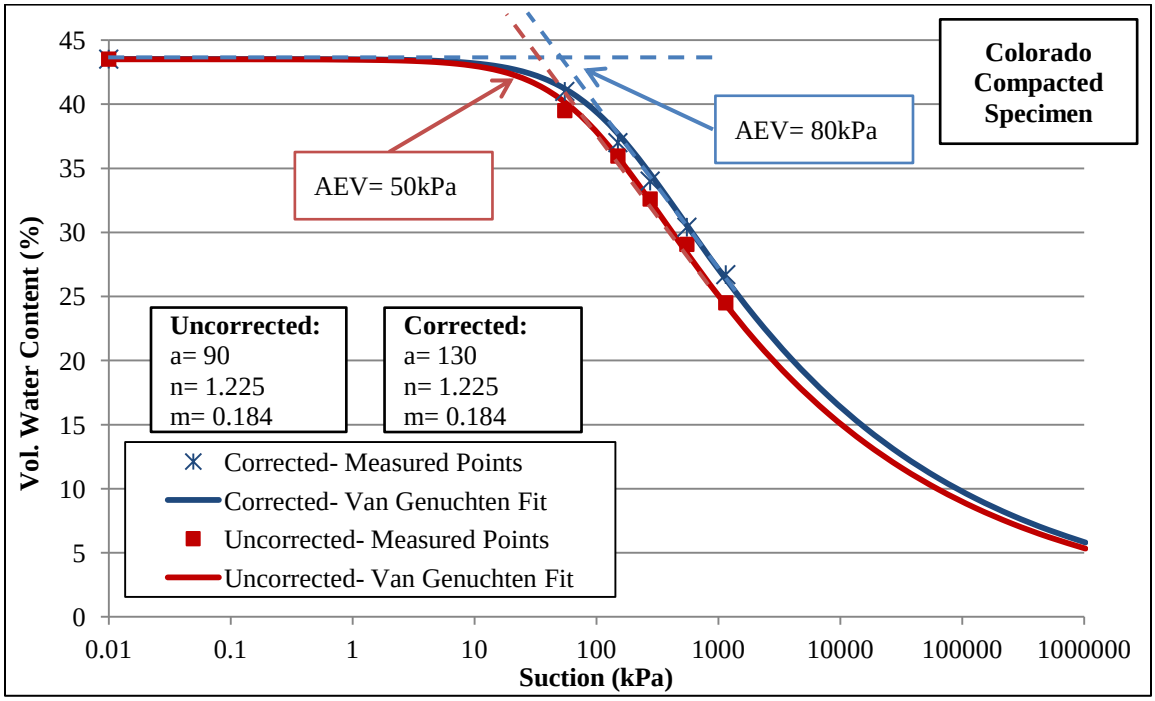

Figure 4.7. SWCC of Colorado soil in terms of volumetric water content, corrected and uncorrected for soil volume change used in VADOSE/W and SVFLUX showing the method used for obtaining the AEV

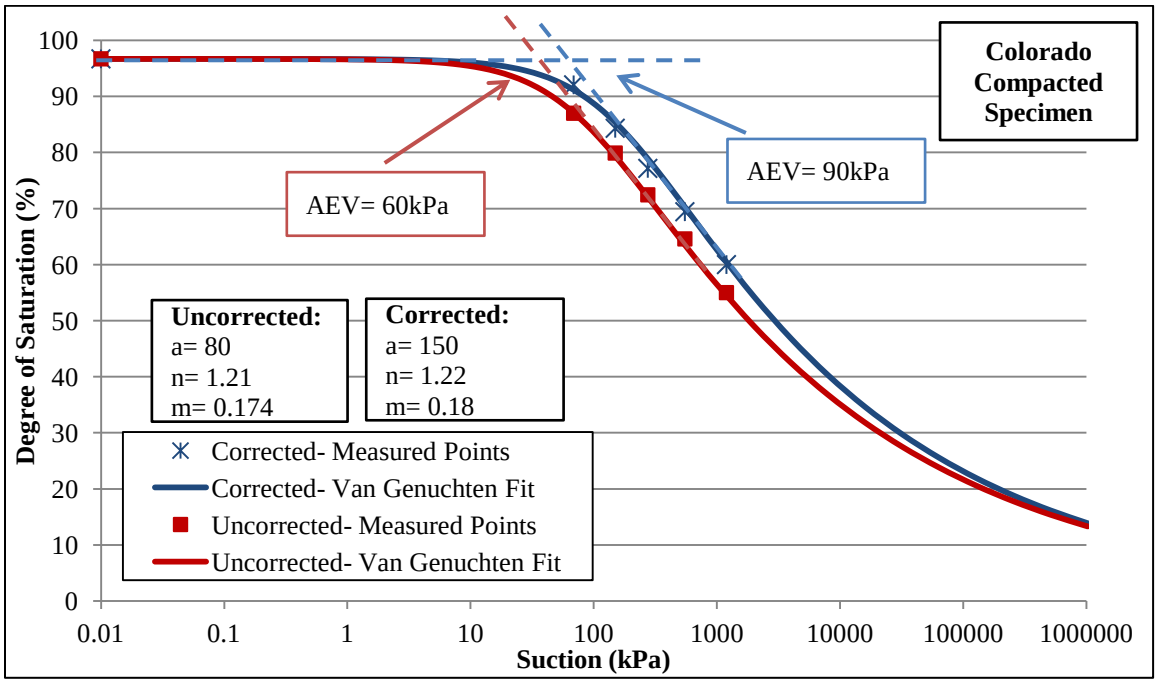

Figure 4.8. SWCC of Colorado soil in terms of degree of saturation, corrected and uncorrected for soil volume change used in CODE-BRIGHT showing the method used for obtaining the AEV

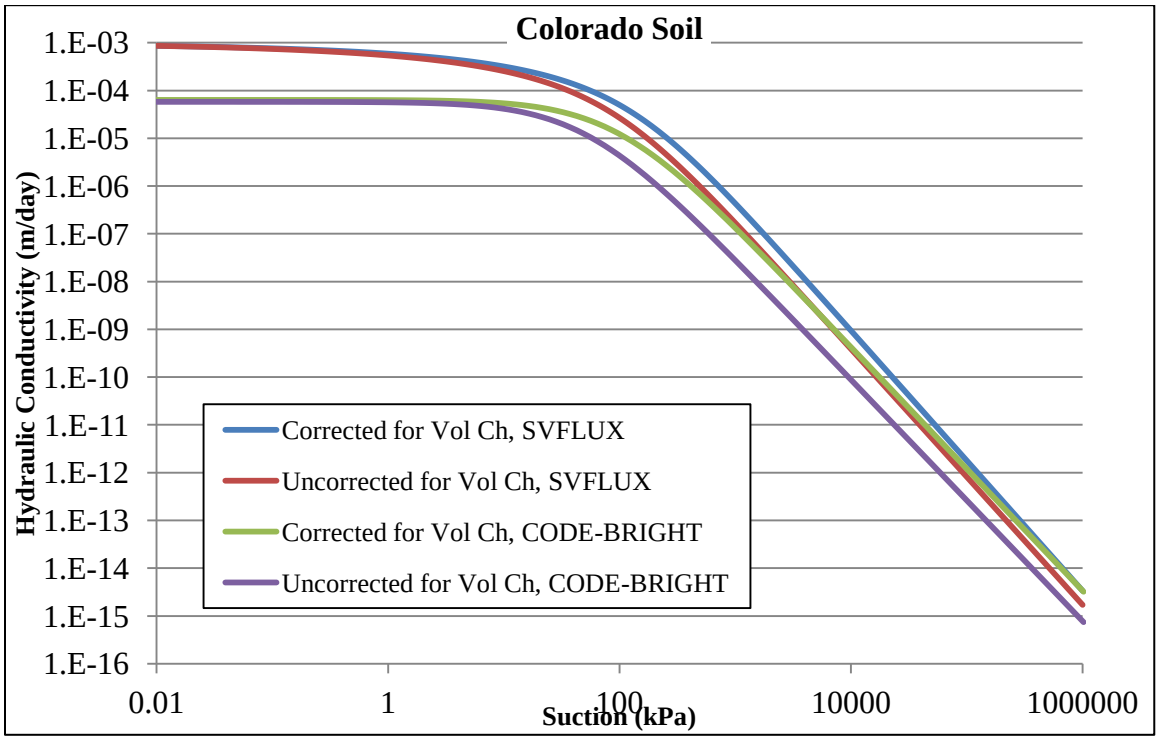

Figure 4.9. k_{unsat} function of Colorado soil estimated by SVFLUX and CODE-BRIGHT

4.3.3. San Antonio Soil

Figures 4.10 and 4.11 show the SWCC of San Antonio soil in terms of volumetric moisture content and degree of saturation. Shown in the figures are also the van Genuchten (1980) fits to the SWCC data points obtained from laboratory experiments. Figure 4.12 shows hydraulic conductivity versus suction, otherwise known as k_{unsat} function for San Antonio soil. It can be seen that for any given suction, the k_{unsat} generated by either SVFLUX or CODE-BRIGHT is higher for corrected curve compared to the uncorrected curve.

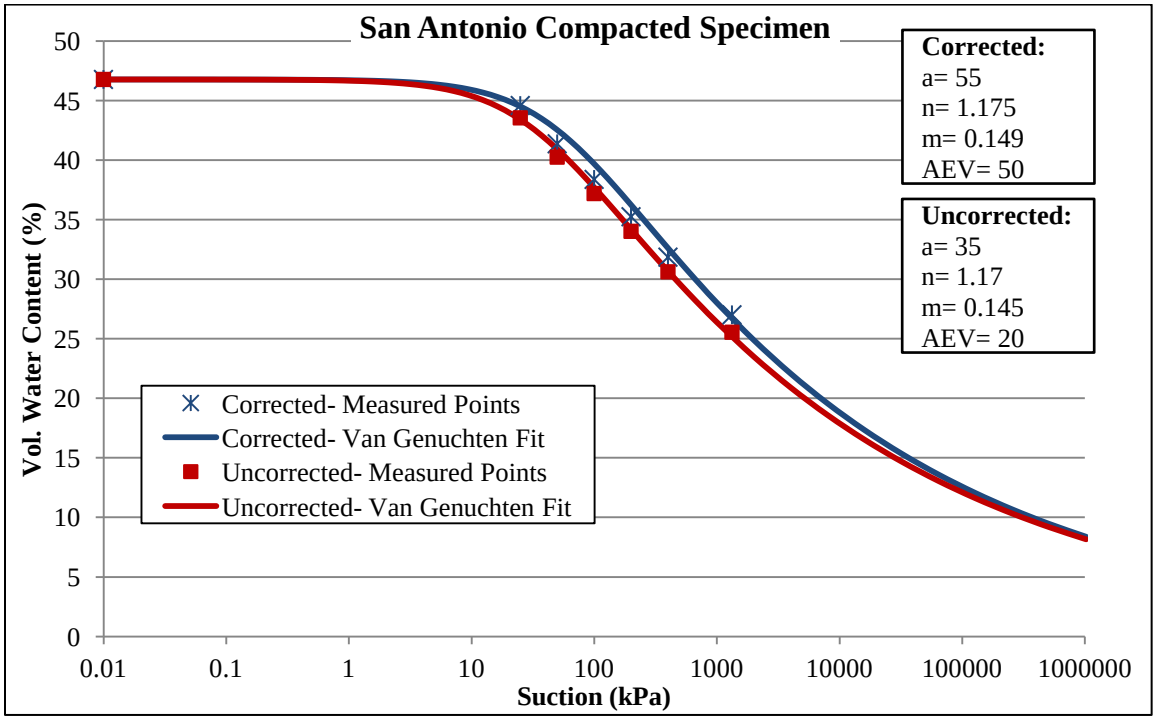

Figure 4.10. SWCC of San Antonio soil in terms of volumetric water content, corrected and uncorrected for soil volume change used in VADOSE/W and SVFLUX

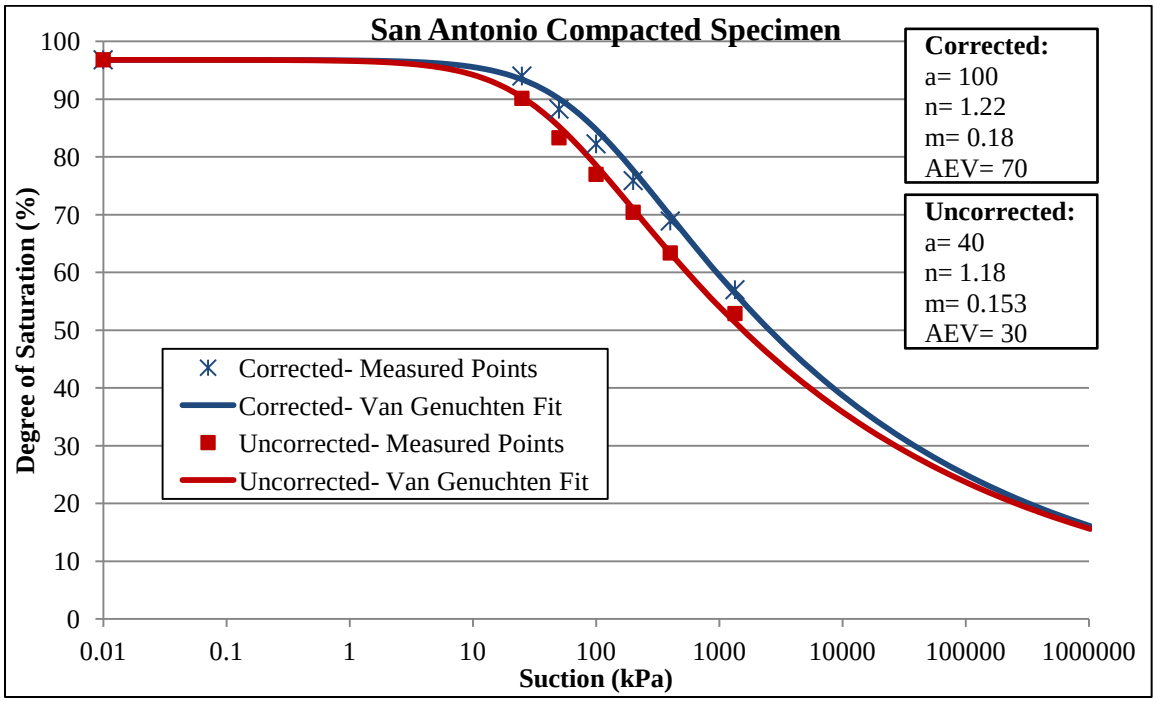

Figure 4.11. SWCC of San Antonio soil in terms of degree of saturation, corrected and uncorrected for soil volume change used in CODE-BRIGHT

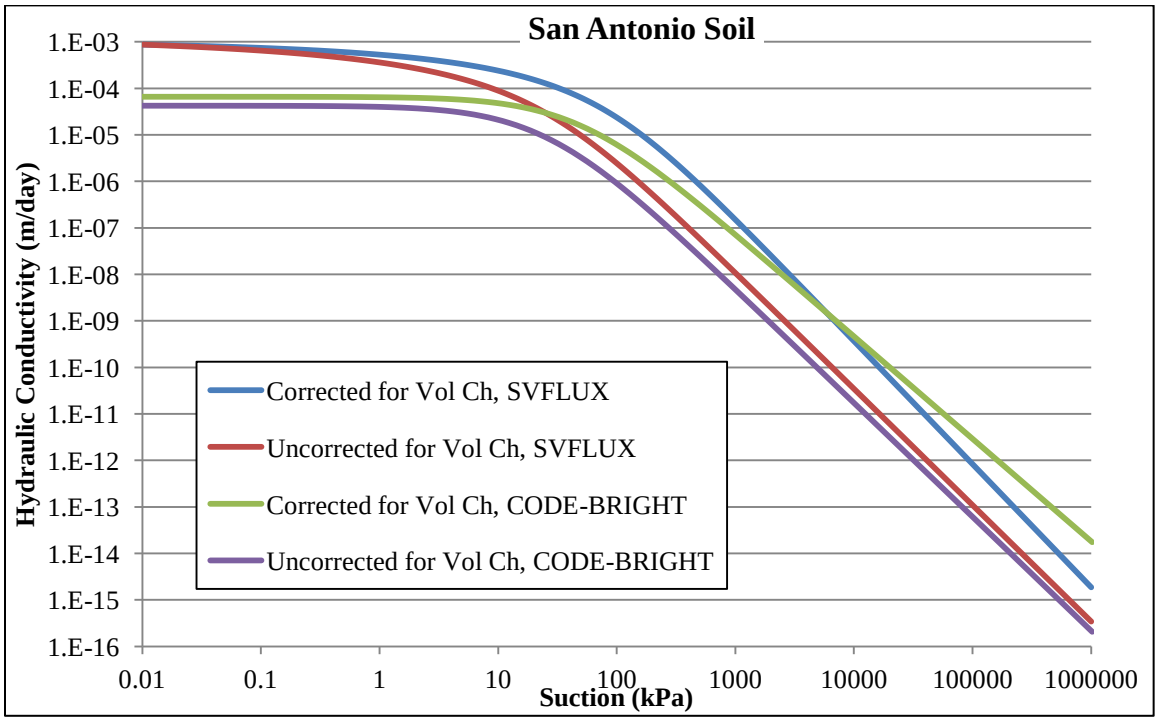

Figure 4.12. k_{unsat} function of San Antonio soil estimated by SVFLUX and CODE-BRIGHT

4.4. Boundary Conditions

Specifying conditions on the boundaries of a problem is one of the key components of a numerical analysis. The boundary condition of this soil column were set in the way that the left and right (vertical) sides have no flow (No-flux boundary condition), while the bottom has various pressure head values (with majority of cases analyzed with base boundary condition of -10m) and at the top the boundary condition is either fixed flux (with values varying form much less than saturated hydraulic conductivity ($k\text{-}_{sat}$) of the soil to values greater than $k\text{-}_{sat}$) or fixed head of 1m. The boundary conditions used for the model are shown in Table 4.3.

Table 4.3. Boundary Conditions used for the numerical modeling

Location	Condition	Amount
Top	Fixed Pressure Head (m)	1
Top	Fixed Unit Flux (m/days)	Varies
Left side	Total Flux (m^3/days)	0
Right side	Total Flux (m^3/days)	0
Bottom	Pressure Head (m)	Varies (e.g.-10)

Head Boundary Condition: Total head is made up of pressure head and elevation head, where the elevation head represents the gravitational component. In equation form the total head is defined as:

$$H = \frac{u}{\gamma_w} + y \tag{4.8}$$

where:

H = the total head (meters or feet, for example),

u = the pore-water pressure (kPa or psf),

γ_w = the unit weight of water (kN/m^3 or pcf), and

y = the elevation (meters or feet).

The term $\frac{u}{\gamma_w}$ is referred to as pressure head (represented in units of length). For the cases of the simulation with fixed pressure head at the top of the soil column in this study, the quantity of this pressure head is 1m. This can represent a ponding condition at the surface of the soil.

Flux Boundary Condition: The second type of boundary conditions used in this study was a fixed rate of flow across the edge of an element. An example may be the rate of infiltration or application of precipitation. This is often referred to as a flux boundary. Different values of fixed flux boundary conditions at the top of the soil column were used, some of the fixed flux values were smaller than k_{sat}, and some were greater. The results were then compared against one another. For the cases in which the top boundary condition was fixed flux with flux values smaller than k_{sat}, the soil column gets wet but since the flux is not big enough, the water pressure throughout the soil does not become positive. In other words, there is suction within the entire soil profile (at the steady-state condition). If the value of top fixed flux is equal to k_{sat} the soil gets wet and the suction for the majority of the soil profile ends up near zero. If the value of top fixed flux is larger than k_{sat}, the soil gets wet and the final (i.e. steady-state) condition shows positive water pressure within the profile. It should noticed that since the bottom boundary condition is set to negative water pressure values (e.g. -100kPa or pressure head of -10m), the bottom part of the soil column will have suction (negative water pressure) for all of the cases.

4.5. VADOSE/W

One of the computer codes used for the numerical modeling in this study was VADOSE/W. VADOSE/W is a commercial software that is being used by numerous practitioners to model fluid flow through soils. VADOSE/W is a finite element program that can be used to model movement and distribution of pore water within porous materials such as soil and bedrock. VADOSE/W can model both saturated and unsaturated flow.

In VADOSE/W for an unsaturated flow analysis the finite element equation prior to solving for the unknowns is (Geo-Slope International, 2012):

$$[K]\{H\} = \{Q\} \tag{4.9}$$

Where:

$[K]$ = a matrix of coefficients related to geometry and materials properties (global property matrix),

$\{H\}$ = a vector of the total hydraulic heads at the nodes, and

$\{Q\}$ = a vector of the flow quantities at the node.

The objective is to solve for the primary unknowns, which in an unsaturated flow analysis are the total hydraulic head at each node (Geo-Slope International, 2012). The specified H or Q values are the boundary conditions. It should be mentioned that specified head boundary conditions can be converted into nodal Q values. When H is specified, the solution to the finite element Equation 4.9 above will provide Q. Alternatively, when Q is specified, the solution will provide H. The equation always needs to be in balance. So when an H is specified at a node, the computed Q is the Q that

is required to maintain the specified H, therefore, the Q cannot be controlled by the user as it is computed. Similarly, when Q is specified, the computed H is the H that is required to maintain the specified flow Q (Geo-Slope International, 2012).

For the case of VADOSE/W and SVFLUX the van Genuchten (1980) equation used for estimating SWCC is as below:

$$\theta_w = \theta_r + \frac{\theta_s - \theta_r}{\left[1 + \left(\frac{\psi}{a}\right)^n\right]^m} \tag{4.10}$$

Where:

θ_w = Volumetric moisture content at any soil suction (%)

θ_r = Residual volumetric moisture content (%)

θ_s = volumetric moisture content at saturation (%)

ψ = soil suction (i.e. negative pore-water pressure) (kPa)

a, n, and m: Curve fitting parameters

Although the terminology of the 'a', 'n' and 'm' parameters are similar to those of Fredlund and Xing (1994) equation (which was described in previous chapters), the definitions are slightly different. The 'a' parameter in particular cannot be estimated by the air-entry value, but instead is a pivot point about which the n parameter changes the slope of the function. The parameter 'm' affects the sharpness of the sloping portion of the curve as it enters the lower plateau (GEO-SLOPE International Ltd., 2012).

As previously described, the ability of a soil to transport or conduct water under both saturated and unsaturated conditions is reflected by the hydraulic conductivity

function. In a saturated soil, all the pores are filled with water. Once the air-entry value is exceeded, desaturation of the soil occurs and the air-filled pores become non-conductive. As a result, the ability of the soil to transport water (the hydraulic conductivity) decreases. As pore-water pressures become increasingly more negative, more pores become air-filled and the hydraulic conductivity decreases further (GEO-SLOPE International Ltd., 2012). By this description, it is clear that the ability of water to flow through a soil profile depends on how much water is present in the soil, which is represented by the SWCC.

Measuring the hydraulic conductivity function is a time-consuming and expensive procedure; however, a few functions have been developed by researchers (e.g. Van Genuchten-Mualem, 1980 and Fredlund et al, 1994) which can be readily used for estimating the hydraulic conductivity function. Majority of available functions utilize a measured SWCC and the saturated hydraulic conductivity. VADOSE/W and SVFLUX have built-in predictive methods that can be used to estimate the hydraulic conductivity function once the SWCC and a k_{sat} value have been specified. The model developed by van Genuchten-Mualem (1980) which is built into VADOSE/W was used to estimate the $k\text{-}_{unsat}$ function necessary for this modeling study. Van Genuchten (1980) proposed the following closed form equation to describe the hydraulic conductivity of a soil as a function of matric suction:

$$k_w = k_s \frac{\left[1-\left(a\psi^{(n-1)}\right)\left(1+\left(a\psi^{n}\right)^{-m}\right)\right]^2}{\left(\left(1+a\psi\right)^{n}\right)^{\frac{m}{2}}} \tag{4.11}$$

where:

k_s = saturated hydraulic conductivity,

a, n, and m = curve fitting parameters, where $n = 1/(1-m)$, and

ψ = required suction range.

From the above equations, the hydraulic conductivity function of a soil can be estimated once the saturated conductivity and the two curve fitting parameters, a and m are known.

Van Genuchten (1980) showed that the curve fitting parameters can be estimated graphically based on the SWCC of the soil. According to van Genuchten, the best point to evaluate the curve fitting parameters is the halfway point between the residual and saturated water content of the SWCC. The slope of the function can be calculated as:

$$S_p = \frac{1}{(\theta_s - \theta_r)}\left|\frac{d\theta_p}{d(\log\psi_p)}\right| \tag{4.12}$$

where:

θ_s and θ_r = the saturated and residual volumetric water contents respectively,

θ_p = the volumetric water content at the halfway point of the SWCC, and

ψ_p = the matric suction at the same point

Van Genuchten (1980) proposed the following formula to estimate the parameters 'm' and 'a' when S_p is calculated:

$$m = 1 - \exp(-0.8S_p) \text{ ; for } 0 < S_p < 1 \tag{4.13}$$

$$m = 1 - \frac{0.5755}{S_p} + \frac{0.1}{S_p^2} + \frac{0.025}{S_p^3} \text{ ; for } S_p > 1 \tag{4.14}$$

$$a = \frac{1}{\psi}\left(2^{\frac{1}{m}} - 1\right)^{(1-m)} \tag{4.15}$$

As previously motioned, a transient analysis by definition means one that it changes with time. In order to move forward in time during a transient analysis, the soil conditions at the start of the time period should be input in the program. In other words, initial conditions as well as current or future boundary conditions should be provided. An incremental time sequence is required for all transient analyses (Geo-Slope International, 2012). The accuracy of the computed results depends to some extent on the size of the time steps. Over the period of one time increment, the process is considered to be linear (i.e. a mini steady-state analysis). For the same rate of change, large time steps lead to more of an approximation than small time steps. It follows that when the rate of change is high, the time steps should be small, and when the rate of change is low, the time steps should be large (Geo-Slope International, 2012).

The finite element solution for a transient analysis is a function of time as indicated by the $\{P_t\}$ term in the finite element equation below. Writing the finite element mass transfer equation (ignoring vapor flow) in terms of finite differences leads to the following equation (Segerlind, 1984):

$$\left(\omega\Delta t\left[\frac{K}{\rho g}\right] + \left[\frac{M}{\rho g}\right]\right)\{P_1\} = \Delta t\left((1-\omega)\{Q_0\} + \omega\{Q_1\}\right) + \left(\left[\frac{M}{\rho g}\right] - (1-\omega)\Delta t\left[\frac{K}{\rho g}\right]\right)$$
$$\{P_0\} - [K]\{Y\}\Delta t \tag{4.16}$$

where:

Δt = time increment,

ω = a ratio between 0 and 1,

$\{P_1\}$ = pressure at end of time increment,

$\{P_0\}$ = pressure at start of time increment,

$\{Q_1\}$ = nodal flux at end of time increment,

$\{Q_0\}$ = nodal flux at start of time increment, and

$[K]$ = element characteristic

$[M]$ = element mass matrix

VADOSE/W uses the Backward Difference Method, a method that sets to 1.0, the finite element equation is then simplified to:

$$\left(\Delta t\left[\frac{K}{\rho g}\right]+\left[\frac{M}{\rho g}\right]\right)\{P_1\}+\Delta t[D_2]\{T_1\}=\Delta tQ_1+\left[\frac{M}{\rho g}\right]\{P_0\}-[K]\{Y\}\Delta t \qquad (4.17)$$

It is evident from the equation that in order to solve for the new heads at the end of the time increment, it is necessary to know the pressure at the start of the increment, along with the average material properties calculated at the average of the new and old pressures.

The shape and size of an element (mesh) is tied into the assembly of the [K] and [M] matrices. Mesh sizes that are too large can result in poor material property averaging, while elements that are too small can lead to overshoot problems as well, hence, it is very important to find the optimize mesh size by trial and comparing the results with different mesh sizes (Geo-Slope International, 2012). SVFLUX provides an option in which the user can ask the program to do the mesh refinement automatically, meaning using the optimum mesh size. However, VADOSE/W does not provide this option. Therefore, for

the case of VADOSE/W, mesh refinement (i.e. determining optimum mesh size) has to be done manually by trial and error.

VADOSE/W is formulated on the basis that the flow of water through both saturated and unsaturated soil follows an appropriate form of a Darcy type flow law. Darcy's Law for water flow was originally derived for saturated soil, but later research showed that it can also be applied to flow through unsaturated soil (Richards, 1931 and Childs & Collins-George, 1950). The only difference is that under conditions of unsaturated flow the hydraulic conductivity is no longer a constant but varies with changes in water content and indirectly varies with changes in pore-water pressure. The general governing differential equation for two-dimensional unsaturated flow can be expressed as (Geo-Slope International, 2012):

$$\frac{1}{\rho}\frac{\partial}{\partial x}\left(D_v\frac{\partial P_v}{\partial x}\right)+\frac{1}{\rho}\frac{\partial}{\partial y}\left(D_v\frac{\partial P_v}{\partial y}\right)+\frac{\partial}{\partial x}\left(k_x\frac{\partial\left(\frac{P}{\rho g}+y\right)}{\partial x}\right)+\frac{\partial}{\partial y}\left(k_y\frac{\partial\left(\frac{P}{\rho g}+y\right)}{\partial y}\right)+Q=\lambda\frac{\partial P}{\partial t} \tag{4.18}$$

where:

P = pressure,

P_v = vapor pressure of soil moisture,

m_v = slope of the SWCC,

k_x = hydraulic conductivity in the x-direction,

k_y = hydraulic conductivity in the y-direction,

Q = applied boundary flux,

D_v = vapor diffusion coefficient as described by Wilson (1990),

y = elevation head,

ρ = density of water,

g = acceleration due to gravity, and

t = time.

The equation states that the difference between the flow entering and leaving an elemental volume at a point in time is equal to the change in the volumetric water content. More fundamentally, it states that the sum of the rates of change of flows in the x and y directions plus the external applied flux is equal to the rate of change of the volumetric water or heat contents with respect to time.

The mass transfer equation can be derived directly from the Richards equation for transient flow in unsaturated soils. By definition, under steady-state conditions, the flux entering and leaving an elemental volume is the same at all times. Therefore, the last term of the equation vanishes and the equation for mass transfer, neglecting vapor flow reduces to:

$$\frac{\partial}{\partial x}\left(k_x \frac{\partial\left(\frac{P}{\rho g}+y\right)}{\partial x}\right)+\frac{\partial}{\partial y}\left(k_y \frac{\partial\left(\frac{P}{\rho g}+y\right)}{\partial y}\right)+Q=0 \qquad (4.19)$$

This equation reduces to equation below for one dimensional analysis in y direction which is the case in this study:

$$\frac{\partial}{\partial y}\left(k_y \frac{\partial\left(\frac{P}{\rho g}+y\right)}{\partial y} \right) + Q = 0 \qquad (4.20)$$

4.6. SVFLUX

Modeling with SVFLUX is very much similar to modeling in VADOSE/W. SVFLUX utilizes FlexPDE as the engine to run the analysis. FlexPDE is a fully integrated partial differential equation (PDE) solver, combining several modules to provide a complete problem solving system. SVFLUX solution technique utilizes automatic mathematically designed mesh generation as well as automatic mesh refinement.

Similar to VADOSE/W, the following steps are required to set up the model in SVFLUX:

1. Create the model file including necessary analysis types
2. Generate geometry
3. Specify boundary conditions (i.e. define and assign to the geometry)
4. Apply material properties
5. Specify initial conditions (for transient analysis only)
6. Specify model output
7. Run model
8. Visualize results

Similar to VADOSE/W, the unsaturated flow theory utilized in SVFLUX is based on Darcian flow and conservation of mass. The unsaturated flow theory implemented in

SVFLUX is based on Darcian flow and an implementation of the Richards equation. The continuous relationship for the amount of water stored in the soil pores is given in terms of volume of water (Thode and Gitirana, 2008). The change in volume of water stored in the soil pores can be expressed as function of a coefficient of water storage, m_2^w as follows:

$$\frac{dV_w}{V_0} = m_2^w d\left(u_a - u_w\right) \tag{4.21}$$

Where:

$$m_2^w = \frac{d\left(V_w / V_0\right)}{d\left(u_a - u_w\right)} = \frac{e}{1+e}\frac{dS}{d\left(u_a - u_w\right)} \tag{4.22}$$

V_w / V_0 = volumetric water content

e= void ratio

S= degree of saturation, and

$u_a - u_w$ = matric suction

The flow rate of liquid water in saturated/unsaturated soils can be described by using a generalization of Darcy's law, where the driving mechanism is the total hydraulic head gradient. The hydraulic conductivity is considered to vary with matric suction. The generalized Darcy's law can be written as follows (Thode and Gitirana, 2008):

$$\upsilon_x^w = -k_x^w(\theta)\frac{\partial h}{\partial x}; \upsilon_y^w = -k_y^w(\theta)\frac{\partial h}{\partial y};\ \upsilon_z^w = -k_z^w(\theta)\frac{\partial h}{\partial z} \tag{4.23}$$

Where:

υ_i^w = liquid pore-water flow rate in the i-direction across a unit area of the soil due to hydraulic head gradients, m/s

$k_i^w(\theta)$ = hydraulic conductivity function in the i-direction,

h= hydraulic head, m, $h = \frac{u_w}{\gamma_w} + y$

u_w = pore-water pressure

γ_w = unit weight of water, and

y= elevation

In SVFLUX, the hydraulic conductivity function is described as $k^w(\theta)$ which provides the relationship between the hydraulic conductivity and the matric suction or volumetric water content. The use of a continuous $k^w(\theta)$ function provides a smooth transition between saturated and unsaturated soil conditions.

The hydraulic conductivity function may be obtained experimentally using laboratory of field tests, or estimated using the saturated hydraulic conductivity and the SWCC (Fredlund et al., 1994). SVFLUX provides several options for estimating the hydraulic conductivity function.

Considering the reference volume constant and the water incompressible, the following equation is obtained for one-dimensional transient saturated/unsaturated flow (Thode and Gitirana, 2008):

$$\frac{\partial}{\partial y}\left[\left(k_y^w + k^{vd}\right)\frac{\partial h}{\partial y} - k^{vd}\right] = -\gamma_w m_2^w \frac{\partial h}{\partial t} \qquad (4.24)$$

Where

y= the vertical direction, corresponding to elevation.

The PDE governing flow and storage of water within a saturated/unsaturated soil is posed using total head, h, as the primary variable. However, pore-water pressure, u_w, can also be used producing identical results.

For steady-state conditions, the PDE for flow reduces to the following equation:

$$\frac{\partial}{\partial y}\left[\left(k_y^w + k^{vd}\right)\frac{\partial h}{\partial y} - k^{vd}\right] = 0 \tag{4.25}$$

Similar to one-dimensional transient saturated/unsaturated flow equation, considering the reference volume, V_o, constant and the water incompressible, the following equation is obtained for two-dimensional transient saturated/unsaturated flow (Thode and Gitirana, 2008):

$$\frac{\partial}{\partial x}\left[\left(k_x^w + k^{vd}\right)\frac{\partial h}{\partial x}\right] + \frac{\partial}{\partial y}\left[\left(k_y^w + k^{vd}\right)\frac{\partial h}{\partial y} - k^{vd}\right] = -\gamma_w m_2^w \frac{\partial h}{\partial t} \tag{4.26}$$

Where

x= the horizontal direction, and

y= the vertical direction, corresponding to elevation.

For stead-state conditions, the PDE for flow reduces to the following equation:

$$\frac{\partial}{\partial x}\left[\left(k_x^w + k^{vd}\right)\frac{\partial h}{\partial x}\right] + \frac{\partial}{\partial y}\left[\left(k_y^w + k^{vd}\right)\frac{\partial h}{\partial y} - k^{vd}\right] = 0 \tag{4.27}$$

Neglecting vapor flow and considering the soil saturated, the PDE governing steady state flow reduces to:

$$\frac{\partial}{\partial x}\left[k_x^w \frac{\partial h}{\partial x}\right] + \frac{\partial}{\partial y}\left[k_y^w \frac{\partial h}{\partial y}\right] = 0 \tag{4.28}$$

Where:

h = total head,

k_x^w = hydraulic conductivity of the soil in the x direction,

k_y^w = hydraulic conductivity of the soil in the y direction.

For one dimensional (in y direction) saturated, steady-state flow gets reduced to:

$$\frac{\partial}{\partial y}\left(k_y \frac{\partial h}{\partial y}\right) = 0 \tag{4.29}$$

As mentioned previously, as a soil dries, there is less and less water present in the soil matrix. Since water will flow only where there is water present, the hydraulic conductivity decreases accordingly as the volumetric water content decreases (Thode et al 2005). For the case of a steady-state problem with hydraulic conductivity varying with suction change, the governing partial differential equation remains the same as the previous example and is shown below, in which $k_x(\psi)$ and $k_y(\psi)$ are hydraulic conductivity of the soil as a function of suction in x and y directions, respectively.

$$\frac{\partial}{\partial x}\left(k_x(\psi)\frac{\partial h}{\partial x}\right) + \frac{\partial}{\partial y}\left(k_y(\psi)\frac{\partial h}{\partial y}\right) = 0 \tag{4.30}$$

As previously mentioned, in the studies of flow in the unsaturated zone, the fluid motion is assumed to obey the classical Richards equation. This equation may be written in several forms. The three forms of the unsaturated flow equation are identified as the "h-based" form, the "q- based" form, and the "mixed form". SVFLUX implements both the "h-based" and "mixed" forms of the Richards equation (Thode et al 2005).

The "h-based" formulation for two dimensional transient flow is shown below:

$$\frac{\partial}{\partial x}\left[\left(k_x^w(\theta)+k^{vd}(\theta)\right)\frac{\partial h}{\partial x}\right]+\frac{\partial}{\partial y}\left[\left(k_y^w(\theta)+k^{vd}(\theta)\right)\frac{\partial h}{\partial y}-k^{vd}(\theta)\right]=-\gamma_w m_2^w\frac{\partial h}{\partial t} \qquad (4.31)$$

Where:

h = total head,

$k_x^w(\theta)$ = hydraulic conductivity of the soil in the x direction,

$k_y^w(\theta)$ = hydraulic conductivity of the soil in the y direction,

γ_w = the unit weight of water (9.81 kN/m^3),

m_w^2 = the slope of the soil-water characteristic curve

The formulation presented above states that the difference between the flow (flux) entering or leaving a unit volume is equal to the change in volumetric water content. Since under steady-state conditions, the flux entering and leaving a unit volume is the same, the storage term (right-hand side of the equation) becomes zero.

The mixed-form of the governing partial differential equation for two dimensional transient flow is shown below:

$$\frac{\partial}{\partial x}\left[\left(k_x^w(\theta)+k^{vd}(\theta)\right)\frac{\partial h}{\partial x}\right]+\frac{\partial}{\partial y}\left[\left(k_y^w(\theta)+k^{vd}(\theta)\right)\frac{\partial h}{\partial y}-k^{vd}(\theta)\right]=\frac{\partial \theta}{\partial t} \qquad (4.32)$$

Where:

θ = volumetric water content.

There are a number of options for inputting SWCC data into SVFLUX. The options are as follows (Thode and Gitirana, 2008):

- Fredlund and Xing equation (1994)
- Fredlund Bimodal equation (2000)

- Van Genuchten and Mualem equation (1975)
- Van Genuchten equation (1980)
- Gardner equation (1956)
- Brooks and Corey equation (1964)
- Inputting SWCC data points obtained from laboratory tests

These equations were described in the literature review chapter in this study. For the purpose of being consistent between the three codes used in this study (SVFLUX, VADOSE/W, and CODE-BRIGHT), van Genuchten (1980) SWCC fit equation was used, as van Genuchten equation (1980) is the only equation used in all three codes for inputting SWCC data.

Van Genuchten (1980) presented a three-parameter equation with the flexibility to fit a wide range of materials. The parameters of the equation were typically found using a least-squares algorithm.

$$\theta_w = \theta_{res} + (\theta_s - \theta_{res}) \left[\frac{1}{\left[1 + (a_{vg}\psi)^{n_{vg}}\right]^{m_{vg}}} \right] \tag{4.33}$$

Where:

θ_w = volumetric water content at any soil suction

θ_{res} = residual volumetric water content

θ_s = saturated volumetric water content

a_{vg} = a material parameter which is primarily a function of the air entry value of the soil

n_{vg} = a material parameter which is primarily a function of the rate of water extraction from the soil once the air entry value has been exceeded

m_{vg} = fitting parameter

ψ =soil suction

For estimation of the unsaturated hydraulic conductivity function, estimation methods (also known as pedo-transfer functions) are provided in the SVFLUX (Thode and Gitirana, 2008). Most estimation methods are based on a description of the SWCC and therefore require a specific fit to be present in the software. Commonly used estimation methods are provided and are as follows:

- Brooks and Corey estimation (1964)
- Modified Campbell estimation (1973)
- Fredlund et al. estimation (1994)
- Van Genuchten estimation (1980)

Several researchers such as Brooks and Corey (1964) and Mualem (1976) have proposed closed form equations for predicting the hydraulic conductivity of unsaturated soil based on Burdine's theory (1953). Brooks and Corey (1964) equation does not converge rapidly when used in numerical solutions of flow in saturated-unsaturated soils. Mualem (1976) equation is in integral form and enables to derive closed-form analytical equations provided only when suitable equations for the SWCC are available (Thode and Gitirana, 2008).

Similar to SWCC, there is only one k-$_{unsat}$ function estimation model that the three codes (SVFLUX, VADOSE/W, and CODE-BRIGHT) have in common and that is the van Genuchten-Mualem (1980) estimation.

The equation proposed for fitting the SWCC by van Genuchten-Mualem (1980) is flexible, continuous and has a continuous slope and it is as follows (Thode and Gitirana, 2008):

$$k(\psi) = k_s \left[\frac{\left\{1-(a\psi)^{nm}\left[1+(a\psi)^{n}\right]^{-m}\right\}^{2}}{\left[1+(a\psi)^{n}\right]^{m/2}} \right] \tag{4.34}$$

Where:

k = hydraulic conductivity of the water phase,

k_s = saturated hydraulic conductivity of the water phase

a, n, and m= Van Genuchten SWCC fitting parameters

ψ = soil suction

4.7. CODE-BRIGHT

CODE-BRIGHT (COupled DEformation of BRIne Gas and Heat Transport) is a tool designed to handle coupled problems in geological media. Basically, the code couples mechanical, hydraulic and thermal problems in geological media. CODE-BRIGHT uses GiD system for preprocessing and post-processing. GiD is an interactive graphical user interface that is used for the definition, preparation and visualization of all the data related to the numerical simulations conducted by CODE-BRIGHT. This data includes the definition of the geometry, materials, conditions, solution information and other parameters. The program can also generate the finite element mesh and write the

information for a numerical simulation program for CODE-BRIGHT. For geometry definition, the program works quite like a CAD (Computer Aided Design) system. All materials, conditions and solution parameters can also be defined on the geometry without the user having any knowledge of the mesh. The meshing is performed once the problem has been fully defined.

The steps taken to generate and run a simulation with CODE-BRIGHT are as follows:

1. Define geometry by using points, lines, and surfaces
2. Define attributes and conditions:
    a. Problem data (e.g. type of analysis)
    b. Materials
    c. Boundary conditions
    d. Interval data (i.e. time steps)
3. Generating mesh
4. Carrying out the simulation
5. View the results

The CODE-BRIGHT module calculates the flow properties (Darcy flux of liquid and/or gas, saturation, temperature, density, etc.). Constitutive laws have to be used to express the mass balance equations as function of the state variables.

The total mass balance of water in CODE-BRIGHT is expressed as:

$$\frac{\partial}{\partial t}\left(\omega_l^w \rho_l S_l \phi + \omega_g^w \rho_g S_g \phi\right) + \nabla .\left(j_l^w + j_g^w\right) = f^w \qquad (4.35)$$

where subscripts *l* and *g* refer to liquid and gas and superscript *w* to water, ω is the mass fraction (kg kg^{-1}) of a component in a phase, ρ is the density (kg m^{-3}) of a phase, *S* is the hydraulic saturation (m^3 m^{-3}), ϕ is the porosity (m^3 m^{-3}), j (kg m^{-2} s^{-1}) is the total flux (advective, dispersive and diffusive) and *f* is an external source/sink term (kg m^{-3} s^{-1}).

Note that the first term represents the change of mass of water in the liquid phase, the second term represents the change of mass of water in the gas phase (i.e., vapor) and the third and fourth terms represent the transport of water in liquid and the gas phase, respectively. Similar to the mass balance of water, the mass balance of air can be expressed as:

$$\frac{\partial}{\partial t}\left(\omega_l^a \rho_l S_l \phi + \omega_g^a \rho_g S_g \phi\right) + \nabla.\left(j_l^a + j_g^a\right) = f^a \tag{4.36}$$

Where superscript "*a"* refers to air.

Boundary conditions and expressions for the source/sink terms (f^w, and f^a) have to be written for the mass balance equation for water, air and heat. CODE-BRIGHT expresses nodal flow rates for every component (water, air and heat) and every phase (liquid, gas) as function of the state variables (P_l, P_g and *T*) and some prescribed values, specified by the user. For instance, the mass flow rate of water as a component of the gas phase (i.e., vapor) is (Saaltink et al. 2005):

$$j_g^w = \left(\omega_g^w\right)^0 \left(j_g^0 + \Delta j_g^0 \frac{dt}{\Delta t} \right) + \left(\omega_g^w\right)^0 \gamma_g \left(\left(P_g^0 + \Delta P_g^0 \frac{dt}{\Delta t} \right) - P_g \right) + \beta \left(\left(\rho_g \omega_g^w\right)^0 - \left(\rho_g \omega_g^w\right) \right) \tag{4.37}$$

Where the superscript $()^{o}$ stands for the prescribed values and the terms $\Delta(.)\ dt/\Delta t$ allow for executing a linear variation of the variable (.) during the time step. This general form of boundary condition includes three terms. The first one is the mass inflow or outflow that takes place when a flow rate of gas (j_g^0) is prescribed. Second term is the mass inflow or outflow that takes place when gas phase pressure (P_g^0) is prescribed at a node. The coefficient γ_g is a leakage coefficient, i.e., a parameter that allows a boundary condition of the Cauchy type (i.e. a force computed as the stiffness of a spring times the displacement increment). A Cauchy boundary condition imposed on an ordinary differential equation or a partial differential equation specifies both the values a solution of a differential equation is to take on the boundary of the domain and the normal derivative at the boundary. The third term is the mass inflow or outflow that takes place when vapor mass fraction is prescribed at the boundary.

For liquid phase a similar set of equations can be utilized which comes from the mass fraction definition, as described below, where positive values of mass flow rate indicate injection into the medium (CODE-BRIGHT, 2012):

$$j_l^a = \left(\omega_l^a\right)^0 j_l^0 + \left(\omega_l^a\right)^0 \gamma_l \left(P_l^0 - P_l\right) + \beta_l \left(\left(\rho_l \omega_l^a\right)^0 - \left(\rho_l \omega_l^a\right)\right) \tag{4.38}$$

$$j_l^w = \left(\omega_l^w\right)^0 j_l^0 + \left(\omega_l^w\right)^0 \gamma_l \left(P_l^0 - P_l\right) + \beta_l \left(\left(\rho_l \omega_l^w\right)^0 - \left(\rho_l \omega_l^w\right)\right) \tag{4.39}$$

$$\left(\omega_l^w\right)^0 = 1 - \left(\omega_l^a\right)^0 \tag{4.40}$$

Where ω_l^w = prescribed mass fraction of water (kg/kg), ω_l^a = prescribed mass fraction of air (kg/kg), j_l = prescribed liquid flow rate (kg/s), P_l = Prescribed liquid

pressure (MPa), γ_l = A leakage coefficient needed to be ≠ 0 when P_l is prescribed (kg/s/MPa). If γ_l is very large, pressure will tend to reach the prescribed value. However, an extremely large value can produce matrix ill conditioning and a lower one can produce inaccuracy in prescribing the pressure. β_l = Parameter needed only when mass transport problem is considered (kg/s/MPa), ρ_l = Prescribed liquid density (kg/m^3)

In CODE-BRIGHT, the SWCC (or water retention curve) is defined as degree of saturation versus suction. Unlike VADOSE/W and SVFLUX (which allow SWCC only in terms of volumetric water content), CODE-BRIGHT uses SWCC's in terms of degree of saturation. In CODE-BRIGHT, unlike SVFLUX and VADOSE/W, there is no option for inputting SWCC data points, meaning that SWCC has to be defined by inputting fitting parameters of an equation. SWCC fit equations that can be used are Van Genuchten (1980), Linear model, and Square law (Saaltink et al., 2005). These equations are described as follows.

Linear model is described as:

$$S_e = \frac{S_l - S_{rl}}{S_{ls} - S_{rl}} = 1 - \frac{P_g - P_l}{P_o} \tag{4.41}$$

Where S_e = effective degree of saturation, S_{rl} = Residual degree of saturation, S_{ls} = Maximum degree of saturation, and P_o = Measured *P* at certain temperature (MPa).

Square law is defined as:

$$S_e = \frac{S_l - S_{rl}}{S_{ls} - S_{rl}} = \frac{1}{\sqrt{1 + \frac{P_g - P_l}{P_o}}} \tag{4.42}$$

van Genuchten model (1980) can be written as:

$$S_e = \frac{S_l - S_{rl}}{S_{ls} - S_{rl}} = \left(1 + \left(\frac{P_g - P_l}{P_o}\right)^{\frac{1}{1-\lambda}}\right)^{-\lambda} \quad (4.43)$$

$$P = P_o \frac{\sigma}{\sigma_o} \quad (4.44)$$

$$\sigma = 0.03059 \exp\left(\frac{252.93}{273.15 + T}\right) + 0.04055\omega_l^h \quad \text{(N/m)} \quad (4.45)$$

Where: λ= Shape function for retention curve, σ = surface tension (N/m), σo=0.072 N/m at 20ºC,

Van Genuchten equation was used for modeling in CODE-BRIGHT, as it is the most popular model that this code provides. SVFLUX and VADOSE/W also provide the option to use Van Genuchten model. However, in SVFLUX and VADOSE/W SWCC is defined in terms of volumetric water content (unlike CODE-BRIGHT which utilizes degree of saturation).

By definition, intrinsic permeability is related to hydraulic conductivity of the soil with the following equation:

$$\kappa = k \frac{\mu}{\rho g} \quad (4.46)$$

Where:

κ : Intrinsic permeability, m^2

k: hydraulic conductivity, m/s

μ : Dynamic viscosity, kg/(m·s) = 0.000911 for water at 24 ^{0}C (Thermexcel, 2003)

ρ : Density of the fluid, kg/m^3 (water in this case)

g: acceleration due to gravity, m/s^2= 9.81 m/s^2

The equation used for intrinsic permeability in CODE-BRIGHT is the Kozeny's model (Saaltink et al., 2005):

$$k = k_o \frac{\phi^3}{(1-\phi)^2} \frac{(1-\phi_o)^2}{\phi_o{}^3} \tag{4.47}$$

Where

ϕ_o = reference porosity, and k_o = intrinsic permeability for matrix ϕ_o. For the case of this study, it was assumed that the intrinsic permeability in all three principal directions is the same (i.e. 1.857E-16 m^2).

In CODE-BRIGHT by default, the consistent form of relative hydraulic conductivity with van Genuchten model is used (Saaltink et al., 2005). The form of the equation is as below:

$$k_{rl} = \sqrt{S}\left(1-\left(1-S^{1/m}\right)^m\right)^2 \tag{4.48}$$

S_{rl} and S_{ls} are lower and upper bounds of saturation. Effective saturation S (degree of saturation) is defined in such a way that ranges between 0 and 1, and 'm' is the van Genuchten parameter for SWCC fit which is the slope of the curve in the transition zone. In principle, the same values S_{rl} and S_{ls} should be defined for liquid and gas relative conductivity and for retention curve.

4.8. Uncoupled Analysis

Uncoupled (flow only) analyses were conducted for the models in SVFLUX, VADOSE/W, and CODE-BRIGHT in order to evaluate impact of volume change-

corrected SWCC on computed hydraulic properties of soils and on soil suction profiles (e.g. progression of wetted front, degree of wetting), and hence soil volume change due to wetting for expansive clays. The rate of change of suction, including for infiltration cases, the progression of the wetted front was studied and the amount of suction-induced volume change was determined based on the generated suction profile of the soil column. For this purpose, suction compression curves (void ratio versus suction) of specimens obtained from SWCC laboratory experiments were utilized.

For the steady-state uncoupled analyses, boundary conditions only needed to be defined for the model. These boundary conditions included the flow/head conditions explained in earlier sections of this chapter. The boundary conditions were set in the way that the left and right (vertical) sides have no flow (No-flux boundary condition), while the bottom has a constant pressure head (e.g. -10m) and at the top the boundary condition is either fixed flux (with values varying from evaporation to positive flux of magnitude much less than saturated hydraulic conductivity ($k\text{-}_{sat}$) of the soil to values greater than $k\text{-}_{sat}$) or fixed head of 1m.

For transient uncoupled analysis, however, in addition to the mentioned boundary conditions, initial conditions of the model must also be defined. For the majority of cases, as the initial suction profile of the model, it was assumed that the soil is unsaturated with groundwater located 10 meters below the bottom of the soil column. This initial suction profile is shown in Figure 4.13. It can be seen that the initial suction at the bottom of the soil column is -100kPa and the initial suction at the top of the soil column is -600kPa. The suction variation between these two points changes linearly. After the initial

flow/head has been set, the fixed head/fixed flux is added at the top of the soil column. By doing this, the initially unsaturated soil starts to become wet from the top. By setting appropriate time steps, progression of wetted front can be estimated through transient uncoupled analysis.

The computer codes used for unsaturated flow modeling generate the suction profile for the various models. Based on the generated suction profile and by using the suction compression curves which is available for soils Anthem, Colorado, and San Antonio through the SWCC tests, initial and final void ratio profiles can be estimated. By having initial and final values of void ratio, amount of suction-change induced deformation can be calculated.

It should be mentioned that for the case of Anthem, Colorado, and San Antonio soils, the k_{sat} value was assumed to be constant. In other words, k_{sat} was not updated for changes in void ratio. Given the amount of volume change experienced by the compacted specimens of expansive clays studied here, this would not be expected to result in big differences in k_{sat} due to change in void ratio. However, this is not true for slurry specimens or any other soils having extremely high volume change. Issues related to k_{sat} changes and volume changes for soil suction change below the AEV are the next chapter which focuses on extremely high volume change slurry materials.

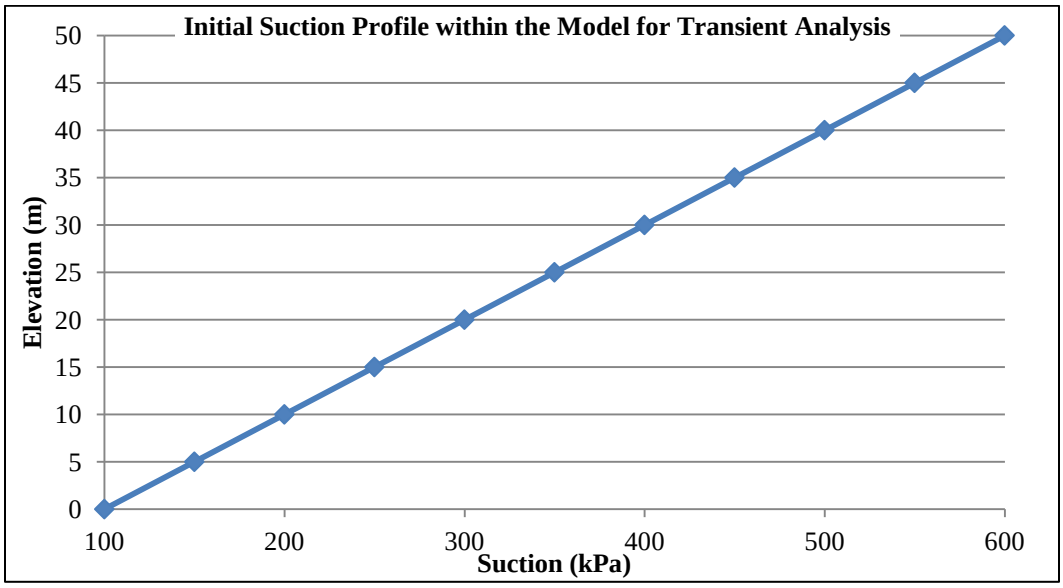

Figure 4.13. An example of initial suction versus elevation profile used for majority of coupled and uncoupled transient modeling

4.9. Coupled Flow-Deformation Analysis

Coupled flow-deformation analysis was conducted using CODE-BRIGHT to find the amount of deformation as the soil becomes wet by introducing fixed flux at the top of the soil column. This analysis was done for Colorado soil and the results were compared with results of uncoupled analysis. In coupled flow-deformation analysis, the program takes initial void ratio (or porosity) of the soil profile and calculates the final void ratio due to wetting of the soil. By having initial and final values of void ratio as well as thickness of the soil layer (i.e. 50 meters for the case of this study) the amount of deformation can be determined.

The coupled flow-deformation analysis was done by CODE-BRIGHT. CODE-BRIGHT requires input of time steps for conducting the analysis. In other words, CODE-BRIGHT is a transient coupled/uncoupled model. If the user is interested in the steady-state results generated by CODE-BRIGHT, this can be achieved by inputting large

enough time durations appropriate for the model. This can be done through trial and error. The results generated for different times throughout the process can be evaluated. Once the results do not change over time, it can be assumed that the steady-state condition has been achieved. It should be mentioned that for all the transient modeling conducted in this study (both uncoupled and coupled) the results were evaluated to make sure that the system has reached the steady state condition.

Similar to transient uncoupled, initial conditions were defined for transient coupled analyses. The initial conditions required for this analyses includes flow/head and stress/deformation conditions. The flow/head initial conditions are similar to the ones used defined in transient uncoupled (i.e. initial suction profile within the soil column and initial flow conditions for bottom, top, and sides of the soil model). In addition to these conditions, initial void ratio (or porosity) profile should be defined within the soil column. Table 4.4 shows the initial void ratio profile used for the transient coupled analysis conducted for Colorado soil.

Table 4.4. Example of initial conditions for transient coupled analysis including initial void ratio and a_1 and a_2 parameters for Colorado Soil

Elevation (m)	Sub-layer No.	Thickness of layer (m)	Suction (kPa)	Suction (kPa) in the mid-point	Initial "e"	Initial porosity "n"	a_1	a_2
50			600					
45	1	5	550	575	0.75985	0.4318	-0.02046	-0.00842
40	2	5	500	525	0.76135	0.4323	-0.02044	-0.00842
35	3	5	450	475	0.76285	0.4327	-0.02042	-0.00842
30	4	5	400	425	0.76435	0.4332	-0.02040	-0.00841
25	5	5	350	375	0.76585	0.4337	-0.02039	-0.00841
20	6	5	300	325	0.76735	0.4342	-0.02037	-0.00841
15	7	5	250	275	0.76885	0.4347	-0.02035	-0.00841
10	8	5	200	225	0.77035	0.4351	-0.02033	-0.00840
5	9	5	150	175	0.77185	0.4356	-0.02032	-0.00840
0	10	5	100	125	0.77335	0.4361	-0.02030	-0.00840

In addition to initial void ratio profile, initial stress distribution within the soil profile should also be defined. For this purpose, first density (or unit weight) profile of the model was determined (using laboratory data obtained from SWCC tests). The initial unit weight profile of the soil column is shown in Figure 4.14.

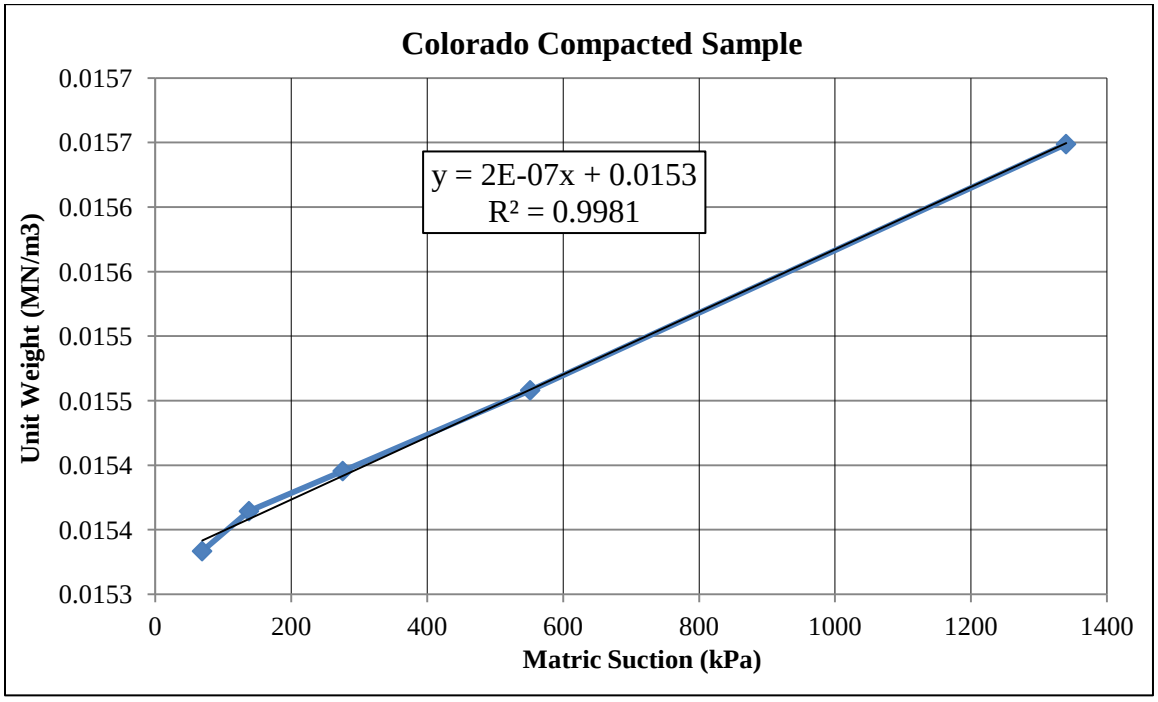

Figure 4.14. Unit Weight versus suction for Colorado soil compacted specimens obtained from SWCC laboratory test

By having values of unit weight throughout the soil profile, the overburden pressure (caused by soil weight) can be determined for different points within the soil profile. These values should be assigned to the model as the initial stress conditions. Table 4.5 shows the values of initial stress condition within the soil profile.

Table 4.5. Example of initial conditions for transient coupled analysis including unit weight and overburden stress profile for Colorado Soil

Elevation (m)	Sub-layer No.	Thickness of layer (m)	unit weight (MN/m^3)	Overburden Stress (MPa)
50				
45	1	5	0.01542	0.07708
40	2	5	0.01541	0.15410
35	3	5	0.01540	0.23108
30	4	5	0.01539	0.30800
25	5	5	0.01538	0.38488
20	6	5	0.01537	0.46170
15	7	5	0.01536	0.53848
10	8	5	0.01535	0.61520
5	9	5	0.01534	0.69188
0	10	5	0.01533	0.76850

Displacement boundary conditions should also be defined for the bottom and sides of the model such that only vertical deformation is allowed.

For coupled flow-deformation analysis elastic properties and loading condition of the soil column should be defined. In CODE-BRIGHT strain is calculated according to the following equation:

$$\frac{\Delta e}{1+e} = a_1 \Delta \ln(-p') + a_2 \Delta \ln\left(\frac{s+0.1}{0.1}\right) + a_3 \Delta\left[\ln(-p')\ln\left(\frac{s+0.1}{0.1}\right)\right] \qquad (4.49)$$

where p' is mean effective stress (mean stress plus maximum of liquid and gas pressure) and s is suction (gas pressure minus liquid pressure). Shear strain is linearly elastic with modulus G or, alternatively, a constant value of the Poisson's ratio can be used.

The required inputs for solving the equations by CODE-BRIGHT are:

1. $a_1 = \frac{-\kappa}{1+e}$ where κ is the slope of the unload/reload curve in the (e - lnp') diagram
2. $a_2 = \frac{-\kappa_s}{1+e}$ where κ_s is the slope of the unload/reload curve in the (e - $\ln\left(\frac{s+0.1}{0.1}\right)$) diagram
3. a_3 can be set as zero, which assumes that suction does not have a direct impact on the mean stress
4. υ = Poisson's ratio.

Determining a_1:

For finding value of a_1, κ should be determined. By definition, κ is the slope of unloading-reloading line (url) in void ration versus ln p' space (e - lnp'), where $p' = \left(\sigma_1^{'} + \sigma_2^{'} + \sigma_3^{'}\right)/3$. This is shown in Figure 4.15 (Muir Wood, 1991). In this figure υ stands for void ratio (usually called 'e' in the literature). Another method to illustrate load-compression curve is to the curve showing void ratio versus $\log \sigma_v^{'}$. This is usually obtained from one-dimensional compression test in oedometer device (shown in Figure 4.16). Slopes of loading and reloading curves in Figure 4.16 are often measured and are called compression index (C_c) and swelling index (C_s). Swelling index (C_s) is also referred to as recompression index (C_r) (Holtz et al. 2010).

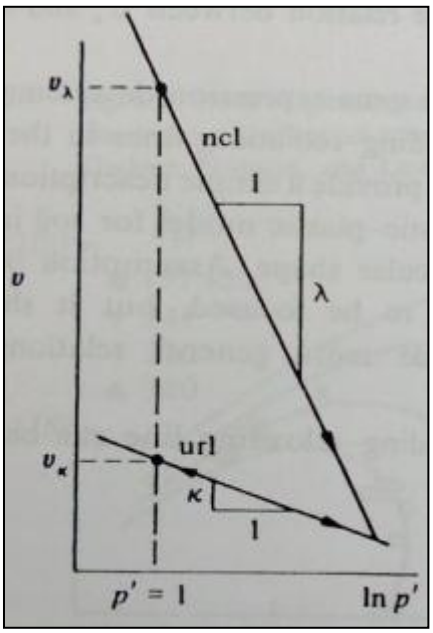

Figure 4.15. Normal compression line (ncl) and unloading-reloading line (url) in void ratio: ln(p')) compression plane (Muir Wood, 1991)

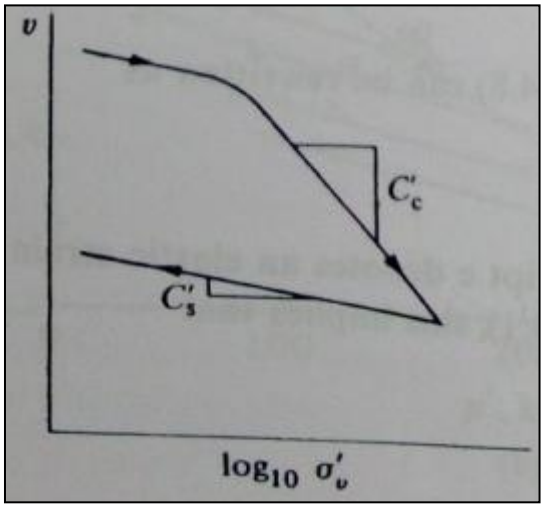

Figure 4.16. Results of one-dimensional compression test in oedometer interpreted in terms of compression index C_c and swelling index C_s (Muir Wood, 1991)

C_r and κ are related by the following equation (Muir Wood, 1991):

$$C_r \approx \kappa \ln 10 \approx 2.3\kappa \tag{4.50}$$

There are equations developed by researchers in the literature to estimate C_r for different soil types. For the case of Colorado soil, equation below which was developed by Nagaraj and Murthy (1985) was used to estimate value of C_r:

$$C_r = 0.000463 \times w_{LL} \times G_s \tag{4.51}$$

Where w_{LL} is the liquid limit of the soil and G_s is the specific gravity. For Colorado soil C_r is determined to be around 0.083 as follows:

$$C_r = 0.000463 \times w_{LL} \times G_s = 0.000463 \times 65 \times 2.778 = 0.084$$

By having value of C_r, κ can be calculated by equation:

$$\kappa \approx \frac{C_r}{2.3} = \frac{0.084}{2.3} = 0.036 \tag{4.52}$$

As mentioned previously, void ratio of Colorado soil can be calculated by knowing the values of G_s (specific gravity) and volumetric water content at saturation (0.3 for Colorado soil).

$$S \times e = G_s \times w \tag{4.53}$$

Where S is the degree of saturation, e is the void ratio, and w is the water content. At saturation, e can be calculated as: $e = \frac{G_s \times w}{S} = \frac{2.778 \times 0.3}{1} = 0.83$

By having values of and void ratio, a_1 can be calculated as:

$$a_1 = \frac{-\kappa}{1+e} = \frac{-(0.036)}{1+0.83} = -0.0197$$

Determining a_2:

As previously mentioned, $a_2 = \frac{-\kappa_s}{1+e}$ where κ_s is the slope of the unload/reload curve in the (e - $\ln\left(\frac{s+0.1}{0.1}\right)$) diagram. In other words κ_s is the suction compression index when suction is plotted on a semi-natural log scale. The Suction Compression Index, Cs, is the change in soil volume for a 1- log cycle change in suction. The magnitude of the suction compression index indicates if the soil is expansive or not. Small slope characterizes a swelling soil while a large slope indicates a non-expansive soil (Dye 2008).

Determination of the suction compression index is necessary for predicting the suction-change induced deformation of expansive soils (Perko et al. 2000). The suction compression index, κ_s or as sometimes referred to as Cs when determined on void ratio versus log suction plot, can be measured using 1-D laboratory tests .

κ_s is the slope of suction compression curve in the semi-logarithmic space (e - $\ln\left(\frac{s+0.1}{0.1}\right)$).

For the soil in this study (Anthem, Colorado, and San Antonio), suction compression curve was measured. Table 4.6 shows part of the void ratio versus matric suction measured during SWCC test of Colorado soil.

Table 4.6. Void ratio versus matric suction for Colorado soil with net normal stress of 7kPa

Suction (kPa)	ln(Suction)	Void Ratio
69	4.23	0.7762
138	4.93	0.7726
276	5.62	0.7691
552	6.31	0.7619
1340	7.20	0.7404

The slope of (e - $\ln\left(\frac{s+0.1}{0.1}\right)$), otherwise called κ_s, for the suction range of 69kPa to 1340kPa can be calculated as follows:

$$\kappa_s = \frac{0.7404 - 0.7762}{7.2 - 4.23} = -0.01206 \tag{4.54}$$

By having the value of κ_s, the value of a_2 can be calculated by using equation

$$a_2 = \frac{-\kappa_s}{1+e}$$

The values of a_1 and a_2 for the soil profile are shown in Table 4.15.

Determining Poisson's ratio (υ):

Poisson's ratio for clay soil is in the range of 0.3-0.5. For this study, the Poisson's ratio for Colorado soil was assumed to be 0.4.

4.10. Results of Numerical Modeling

Several coupled and uncoupled analyses were conducted by using the three programs SVFLUX, VADOSE/W, and CODE-BRIGHT, with CODE-BRIGHT being the only code used for transient coupled analyses. The results of the analyses showed the differences in changes in suction within the profile, degree of wetting of the soil and

amount of deformation for both volume-corrected and volume-uncorrected SWCC's. The details of the results of the analyses are presented in the following section.

4.10.1. Results of Uncoupled Analyses

Transient and steady-state analyses were conducted by SVFLUX, VADOSE/W, and CODE-BRIGHT in which a soil column becomes wet (positive flux) or dry (negative flux) from top with either fixed flux or fixed head. The results of the flow-only (uncoupled) analyses are presented in this section.

4.10.1.1. Anthem Soil

Table 4.7 provides a list of numerical modeling conducted on the models based on the properties of Anthem soil. Simulations were run using Anthem soil properties. Figure 4.17 through 4.20 show results of transient uncoupled analyses using CODE-BRIGHT for Anthem soil. The top boundary condition for this set of runs was fixed flux of 1.0E-3 m/day. Results of the analyses showed that at stead-state condition (i.e. at the time that the model has become saturated due to the positive flux at the top) in the case modeled with uncorrected SWCC the suction throughout the soil column is smaller compared to the one with corrected SWCC (suction of 10kPa for uncorrected SWCC versus 26kPa for corrected SWCC for the majority of the soil profile). However, for a time before the model reaches the steady-state (e.g. 4000 days shown in Figure 4.19) the uncorrected case shows higher suction values at some of the points within the soil profile. This is due to the fact that the progression of wetted front has a higher rate for corrected SWCC compared to uncorrected SWCC. As shown in Figure 4.19 at the elevations between 7m and 15m (from the datum which is located at the bottom of the soil layer), the values of

suction is higher for uncorrected SWCC compared to corrected SWCC. This makes it difficult to determine in advance if corrected or uncorrected curves will lead to higher suction values.

Table 4.7. List of numerical modeling conducted for Anthem soil

Model No.	Soil	k-sat (m/day)	Top BC: Fixed Flux (m/day)	Top BC: Fixed Head (m)	SWCC	Software	Analysis Type	Coupled/ Uncoupled
1	Anthem	8.64E-03	1.00E-03		Corrected	CODE-BRIGHT	Transient	Uncoupled
2	Anthem	8.64E-03	1.00E-03		Uncorrected	CODE-BRIGHT	Transient	Uncoupled
3	Anthem	8.64E-03	5.00E-04		Corrected	SVFLUX	Steady-State	Uncoupled
4	Anthem	8.64E-03	5.00E-04		Uncorrected	SVFLUX	Steady-State	Uncoupled
5	Anthem	8.64E-03	1.00E-03		Corrected	SVFLUX	Steady-State	Uncoupled
6	Anthem	8.64E-03	1.00E-03		Uncorrected	SVFLUX	Steady-State	Uncoupled
7	Anthem	8.64E-03	3.00E-03		Corrected	SVFLUX	Steady-State	Uncoupled
8	Anthem	8.64E-03	3.00E-03		Uncorrected	SVFLUX	Steady-State	Uncoupled
9	Anthem	8.64E-03	7.00E-03		Corrected	SVFLUX	Steady-State	Uncoupled
10	Anthem	8.64E-03	7.00E-03		Uncorrected	SVFLUX	Steady-State	Uncoupled
11	Anthem	8.64E-03	8.64E-03		Corrected	SVFLUX	Steady-State	Uncoupled
12	Anthem	8.64E-03	8.64E-03		Uncorrected	SVFLUX	Steady-State	Uncoupled
13	Anthem	8.64E-03	1.00E-02		Corrected	SVFLUX	Steady-State	Uncoupled
14	Anthem	8.64E-03	1.00E-02		Uncorrected	SVFLUX	Steady-State	Uncoupled
15	Anthem	8.64E-03		1	Corrected	SVFLUX	Steady-State	Uncoupled
16	Anthem	8.64E-03		1	Uncorrected	SVFLUX	Steady-State	Uncoupled
17	Anthem	8.64E-03	5.00E-04		Corrected	VADOSE/W	Steady-State	Uncoupled
18	Anthem	8.64E-03	5.00E-04		Uncorrected	VADOSE/W	Steady-State	Uncoupled
19	Anthem	8.64E-03	3.00E-03		Corrected	VADOSE/W	Steady-State	Uncoupled
20	Anthem	8.64E-03	3.00E-03		Uncorrected	VADOSE/W	Steady-State	Uncoupled
21	Anthem	8.64E-03	1.00E-02		Corrected	VADOSE/W	Steady-State	Uncoupled
22	Anthem	8.64E-03	1.00E-02		Uncorrected	VADOSE/W	Steady-State	Uncoupled

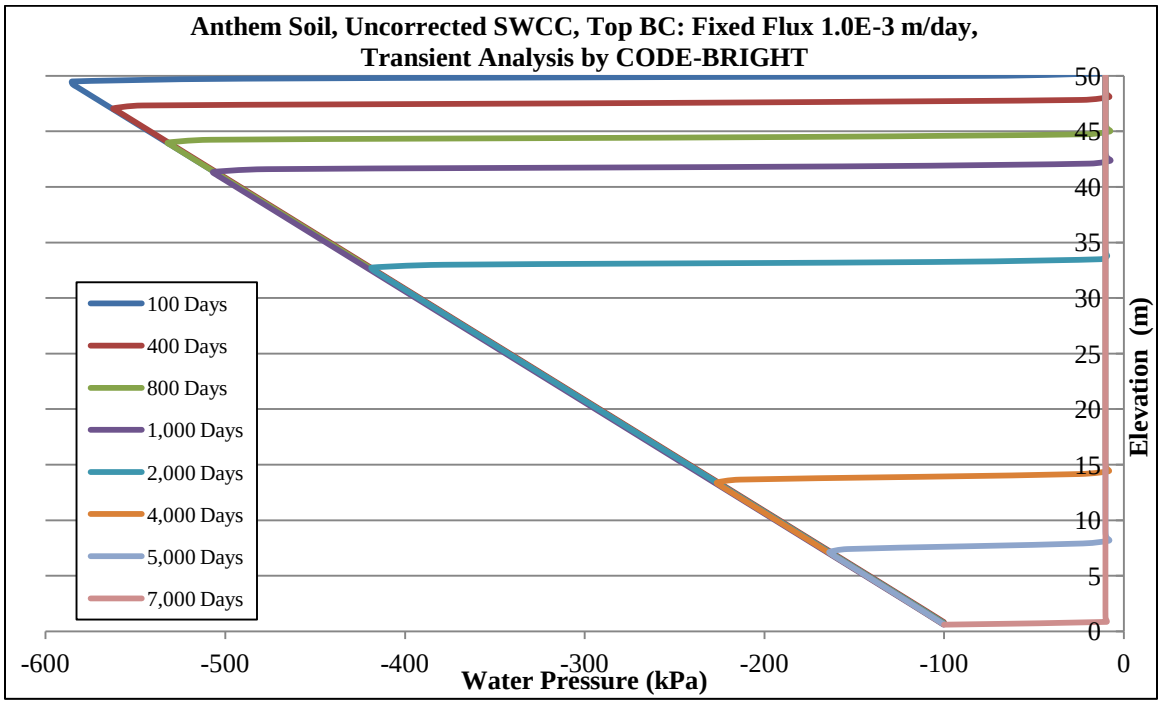

Figure 4.17. Transient analysis on Anthem soil with SWCC uncorrected for volume change (AEV= 15kPa) and top fixed flux of 1.0e-3 m/day using CODE-BRIGHT

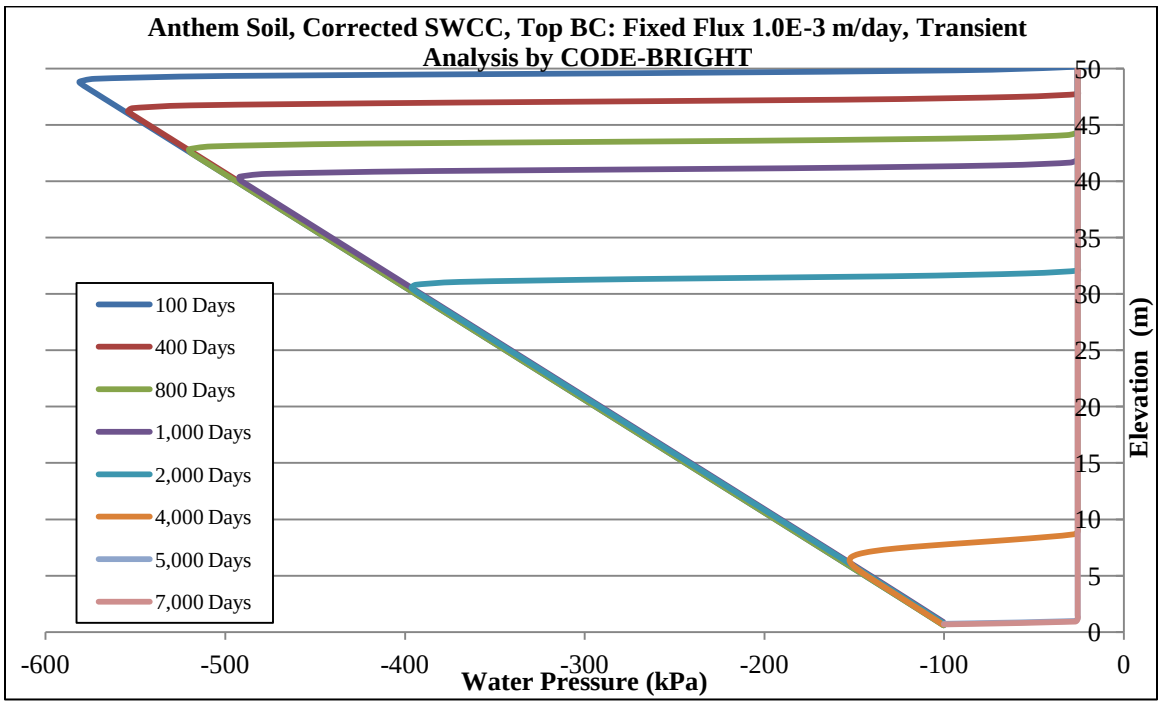

Figure 4.18. Transient analysis on Anthem soil with SWCC corrected for volume change (AEV= 50kPa) and top fixed flux of 1.0e-3 m/day using CODE-BRIGHT

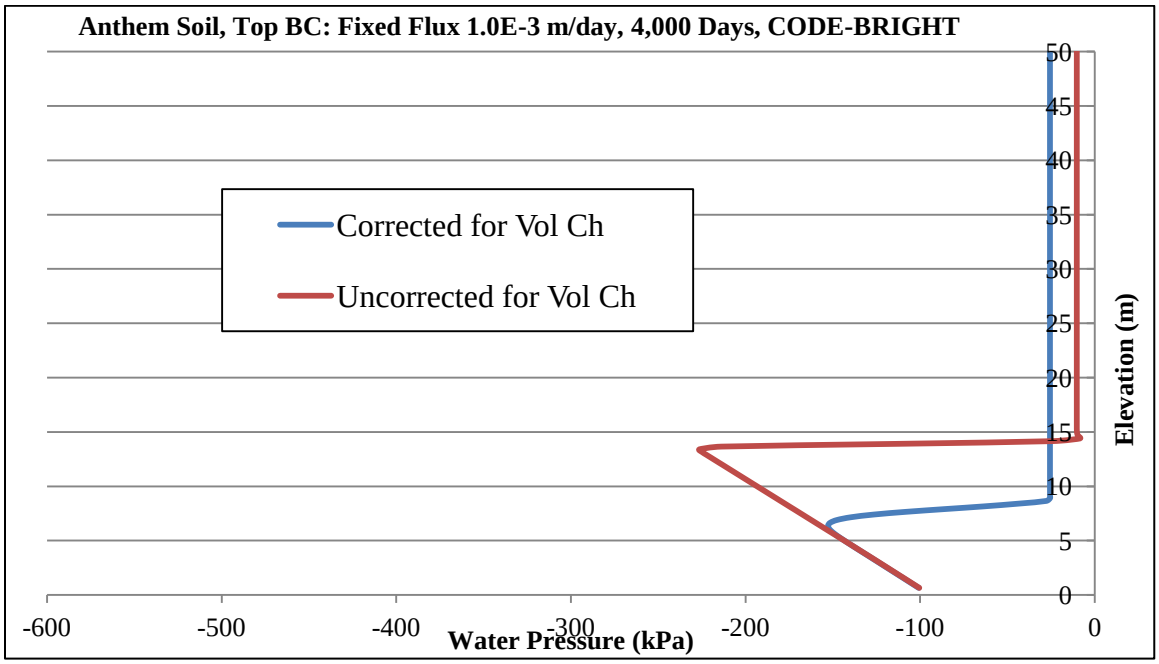

Figure 4.19. Water pressure versus elevation at time 4,000days (11 years) for Anthem soil with SWCC corrected (AEV= 50kPa) and uncorrected (AEV= 15kPa) for volume change and top fixed flux of 1.0E-3 m/day using CODE-BRIGHT

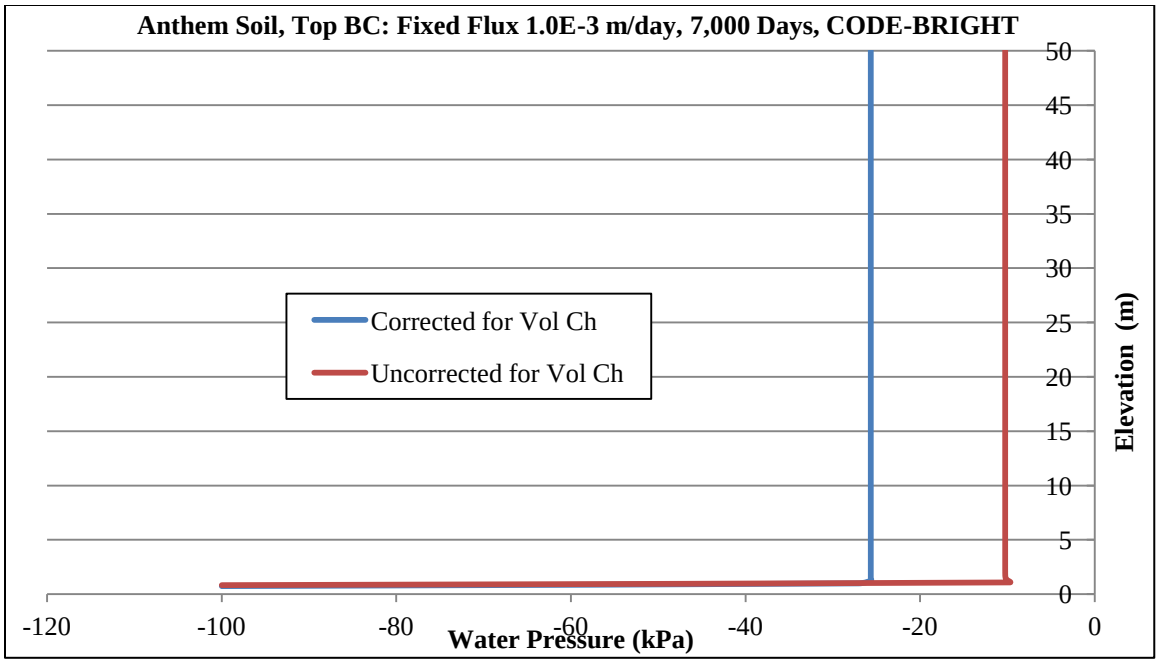

Figure 4.20. Water pressure versus elevation at steady-state condition (time: 7,000 days) for Anthem soil with SWCC corrected (AEV= 50kPa) and uncorrected (AEV= 15kPa) for volume change and top fixed flux of 1.0E-3 m/day using CODE-BRIGHT

4.10.1.2. Colorado Soil

Table 4.8 provides a list of numerical modeling conducted based on Colorado soil properties. Figures 4.21 through 4.31 show results of modeling using Colorado soil. Similar result trends to Anthem soil were found for Colorado soil. At the times long-enough for the model to reach the steady-state (i.e. saturated in this case), the model based on uncorrected SWCC shows smaller final suction throughout the soil column compared to the model based on corrected SWCC (suction of 15kPa for uncorrected SWCC versus 28kPa for corrected SWCC for the majority of the soil profile). In addition, the rate of progression of wetted front is larger for the case of SWCC corrected for volume change due to larger unsaturated hydraulic conductivity values. This leads to higher suctions at some points within the soil profile (for the times prior to steady-state) for uncorrected SWCC. This is shown in Figure 4.23 which illustrates the suction profile of both corrected and uncorrected SWCC models at time 7,000 days. It can be seen that at this time, at the elevations between 10m and 25m (from the bottom of the soil column), the values of suction is higher for uncorrected SWCC. Similar to observed results from the runs on Anthem soil, this makes it difficult to determine in advance if corrected or uncorrected curves will lead to higher suction values.

Table 4.8. List of numerical modeling conducted for Colorado soil

Model No.	Soil	k-sat (m/day)	Top BC: Fixed Flux (m/day)	Top BC: Fixed Head (m)	SWCC	Software	Analysis Type	Coupled/ Uncoupled
1	Colorado	8.64E-04	1.00E-03		Corrected	SVFLUX	Transient	Uncoupled
2	Colorado	8.64E-04	1.00E-03		Uncorrected	SVFLUX	Transient	Uncoupled
3	Colorado	8.64E-04	5.00E-04		Corrected	CODE-BRIGHT	Transient	Uncoupled
4	Colorado	8.64E-04	5.00E-04		Uncorrected	CODE-BRIGHT	Transient	Uncoupled
5	Colorado	8.64E-04	5.00E-04		Corrected	CODE-BRIGHT	Transient	Coupled
6	Colorado	8.64E-04	5.00E-04		Uncorrected	CODE-BRIGHT	Transient	Coupled
7	Colorado	8.64E-04	5.00E-05		Corrected	SVFLUX	Steady-State	Uncoupled
8	Colorado	8.64E-04	5.00E-05		Uncorrected	SVFLUX	Steady-State	Uncoupled
9	Colorado	8.64E-04	1.00E-04		Corrected	SVFLUX	Steady-State	Uncoupled
10	Colorado	8.64E-04	1.00E-04		Uncorrected	SVFLUX	Steady-State	Uncoupled
11	Colorado	8.64E-04	3.00E-04		Corrected	SVFLUX	Steady-State	Uncoupled
12	Colorado	8.64E-04	3.00E-04		Uncorrected	SVFLUX	Steady-State	Uncoupled
13	Colorado	8.64E-04	5.00E-04		Corrected	SVFLUX	Steady-State	Uncoupled
14	Colorado	8.64E-04	5.00E-04		Uncorrected	SVFLUX	Steady-State	Uncoupled
15	Colorado	8.64E-04	7.00E-04		Corrected	SVFLUX	Steady-State	Uncoupled
16	Colorado	8.64E-04	7.00E-04		Uncorrected	SVFLUX	Steady-State	Uncoupled
17	Colorado	8.64E-04	8.64E-04		Corrected	SVFLUX	Steady-State	Uncoupled
18	Colorado	8.64E-04	8.64E-04		Uncorrected	SVFLUX	Steady-State	Uncoupled
19	Colorado	8.64E-04	1.00E-03		Corrected	SVFLUX	Steady-State	Uncoupled
20	Colorado	8.64E-04	1.00E-03		Uncorrected	SVFLUX	Steady-State	Uncoupled
21	Colorado	8.64E-04		1	Corrected	SVFLUX	Steady-State	Uncoupled
22	Colorado	8.64E-04		1	Uncorrected	SVFLUX	Steady-State	Uncoupled
23	Colorado	8.64E-04	1.00E-04		Corrected	VADOSE/W	Steady-State	Uncoupled
24	Colorado	8.64E-04	1.00E-04		Uncorrected	VADOSE/W	Steady-State	Uncoupled
25	Colorado	8.64E-04	7.00E-04		Corrected	VADOSE/W	Steady-State	Uncoupled
26	Colorado	8.64E-04	7.00E-04		Uncorrected	VADOSE/W	Steady-State	Uncoupled
27	Colorado	8.64E-04	1.00E-03		Corrected	VADOSE/W	Steady-State	Uncoupled
28	Colorado	8.64E-04	1.00E-03		Uncorrected	VADOSE/W	Steady-State	Uncoupled

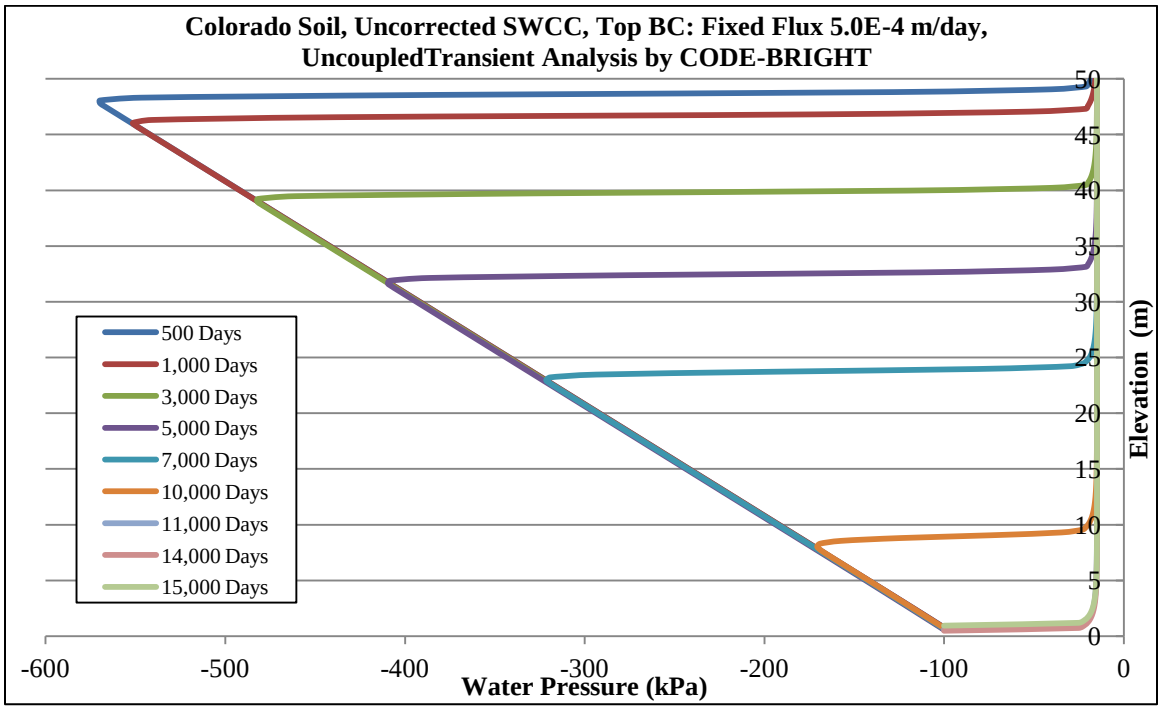

Figure 4.21. Transient analysis on Colorado soil with SWCC uncorrected for volume change (AEV= 60kPa) and top fixed flux of 5.0e-4 m/day using CODE-BRIGHT

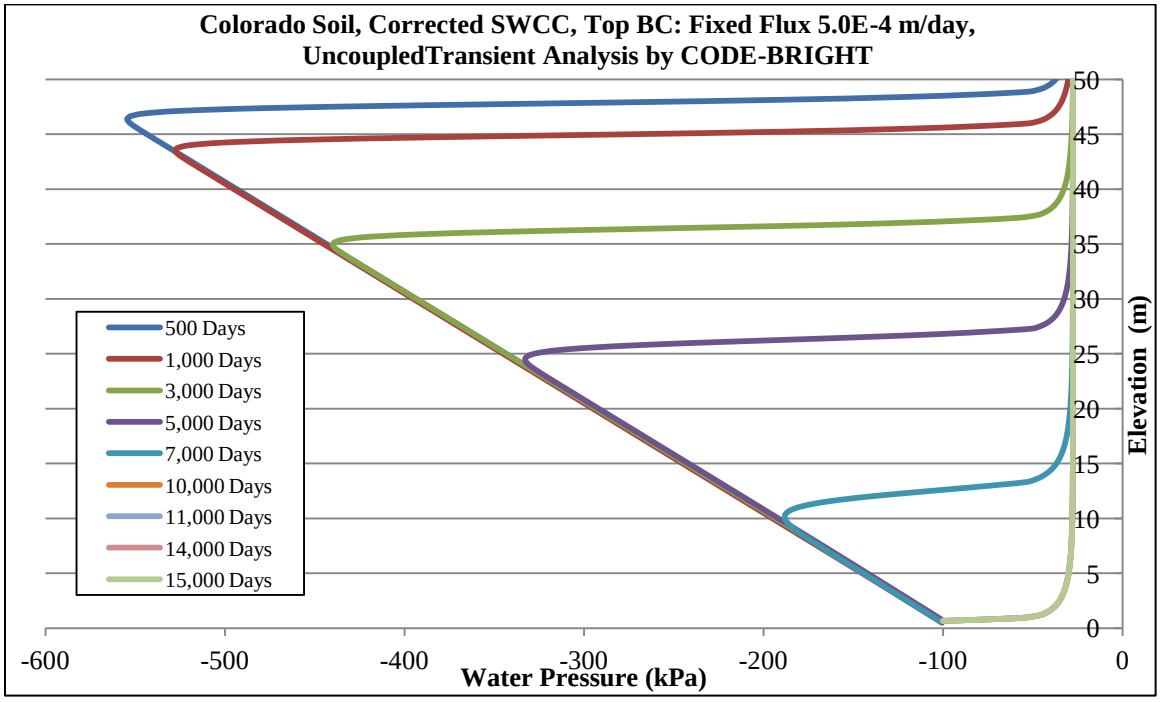

Figure 4.22. Transient analysis on Colorado soil with SWCC corrected for volume change (AEV= 90kPa) and top fixed flux of 5.0e-4 m/day using CODE-BRIGHT

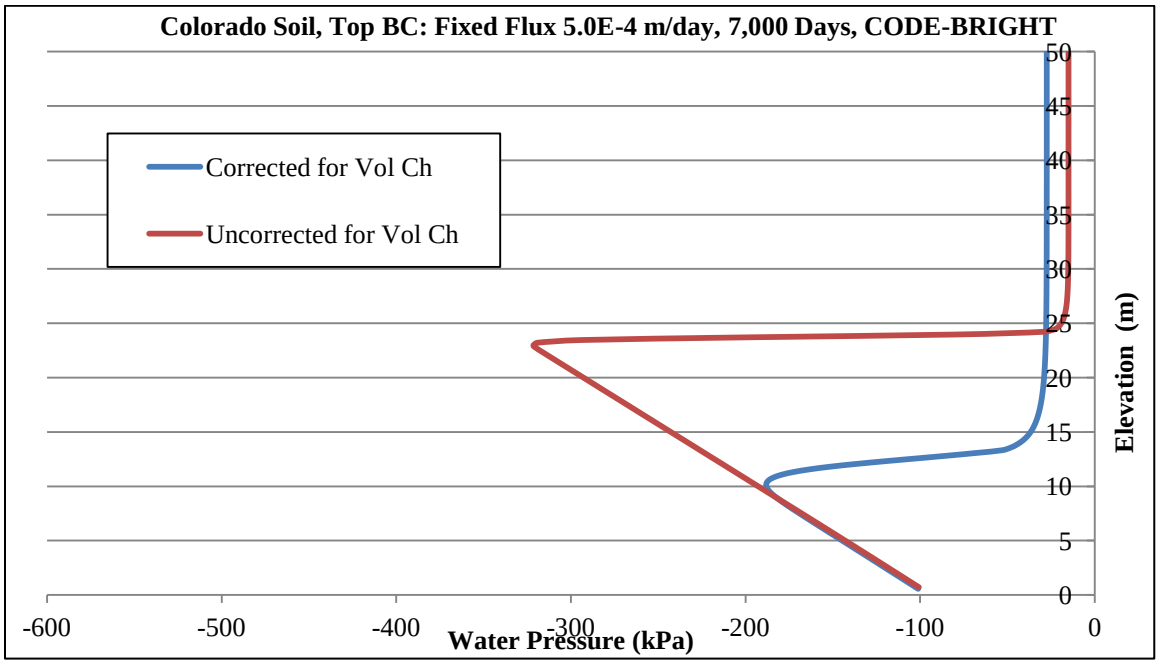

Figure 4.23. Water pressure versus elevation at time 7,000days (19 years) for Colorado soil with SWCC corrected (AEV= 90kPa) and uncorrected (AEV= 60kPa) for volume change and top fixed flux of 5.0e-4 m/day using CODE-BRIGHT

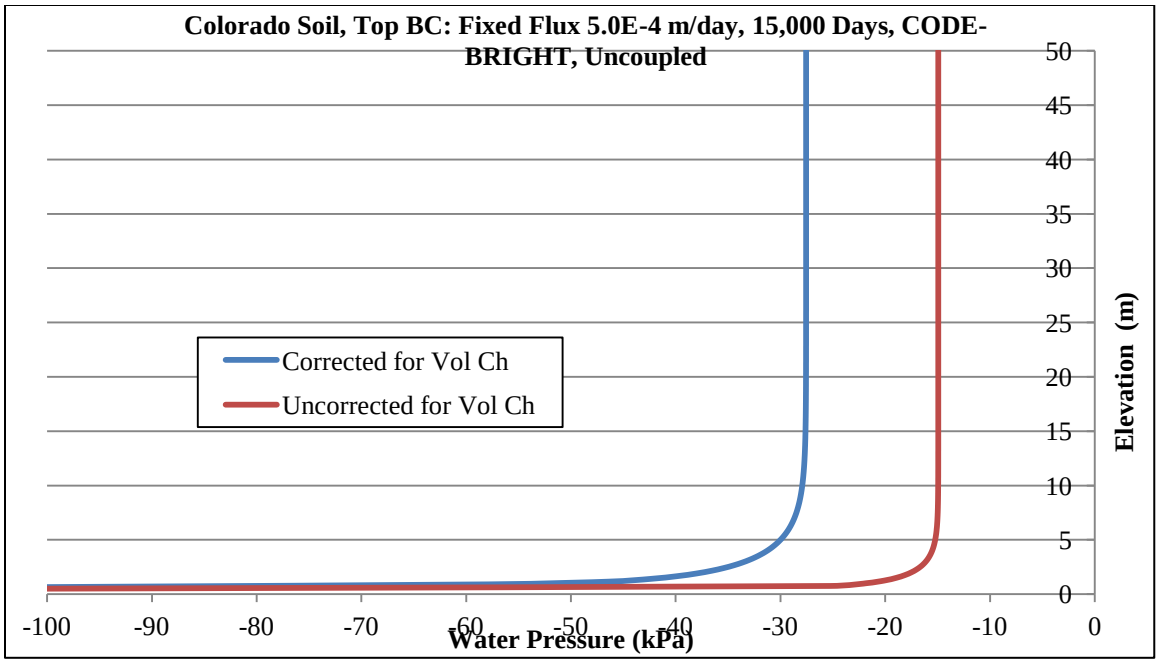

Figure 4.24. Water pressure versus elevation at steady-state condition (time: 15,000 days) for Colorado soil with SWCC corrected (AEV= 90kPa) and uncorrected (AEV= 60kPa) for volume change and top fixed flux of 5.0e-4 m/day using CODE-BRIGHT

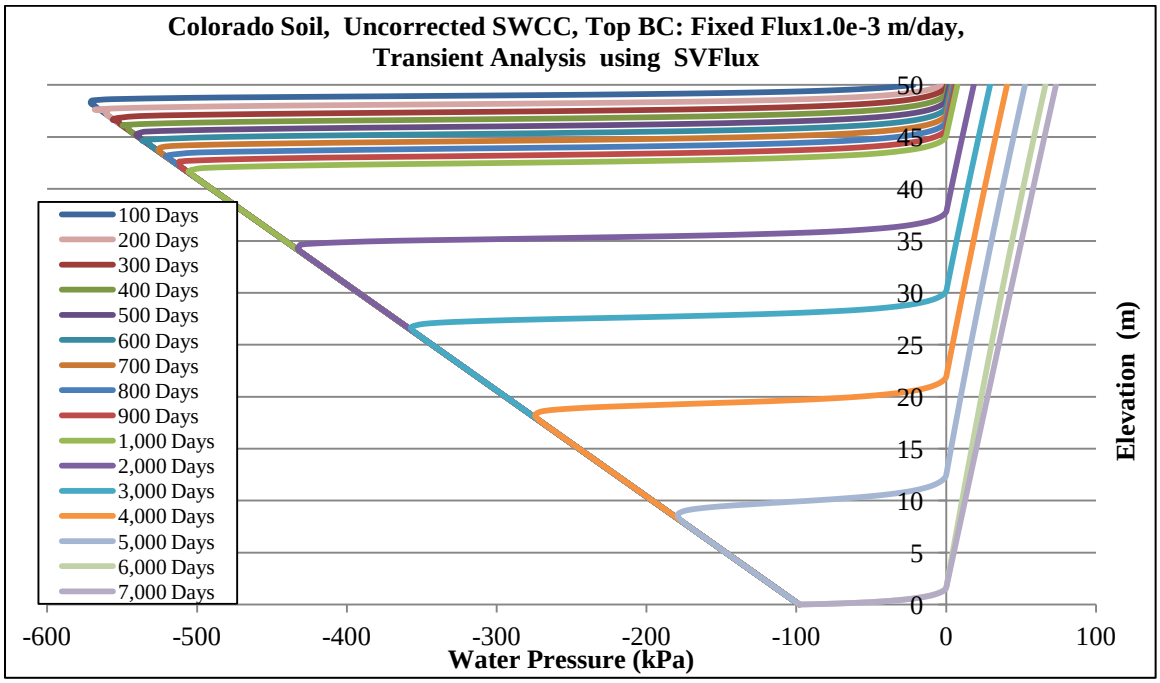

Figure 4.25. Transient analysis on Colorado soil with SWCC uncorrected for volume change (AEV= 50kPa) and top fixed flux of 1.0e-3 m/day using SVFLUX

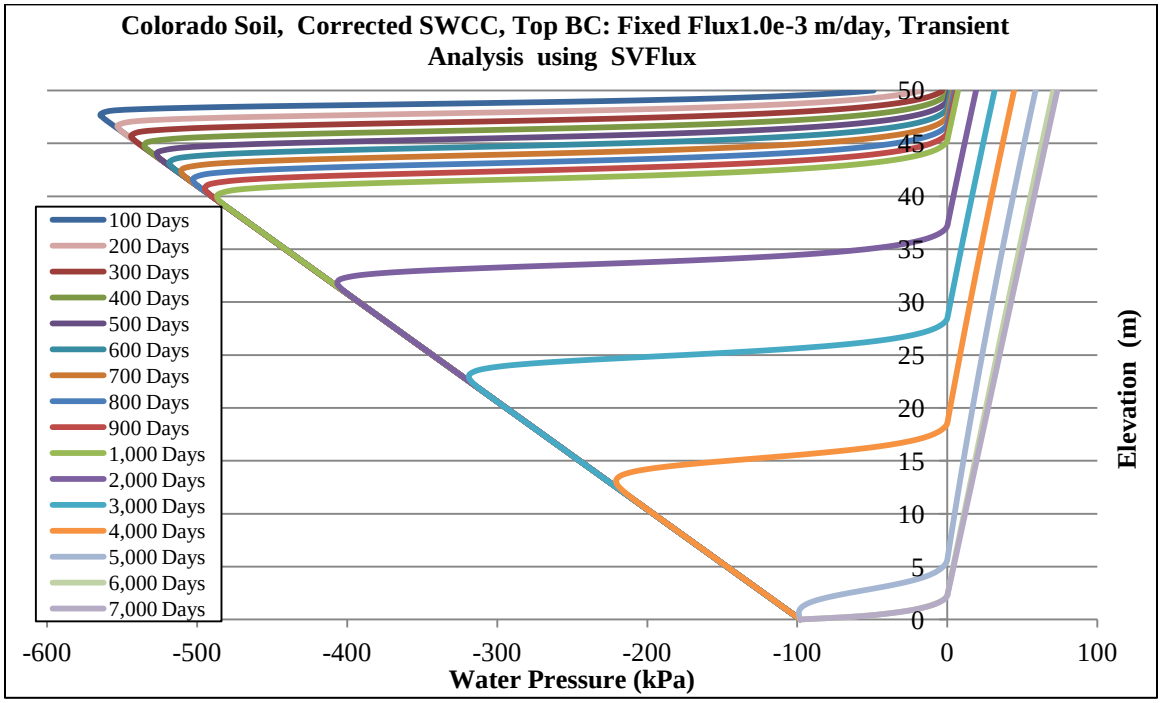

Figure 4.26. Transient analysis on Colorado soil with SWCC corrected for volume change (AEV= 80kPa) and top fixed flux of 1.0e-3 m/day using SVFLUX

Figure 4.27 shows a case of top boundary condition of negative fixed flux (i.e. evaporation) for Colorado soil analyzed by transient uncoupled run using CODE-BRIGHT. This figure shows that for some portions of the soil profile, the suction is higher for uncorrected case and for some other portions of the soil depth; the suction is smaller for the case of uncorrected case. This suggests the fact that it is difficult to determine in advance if corrected or uncorrected curves will lead to higher suction values. This is believed to be a result of the high nonlinearity of the SWCC and k_{unsat} function.

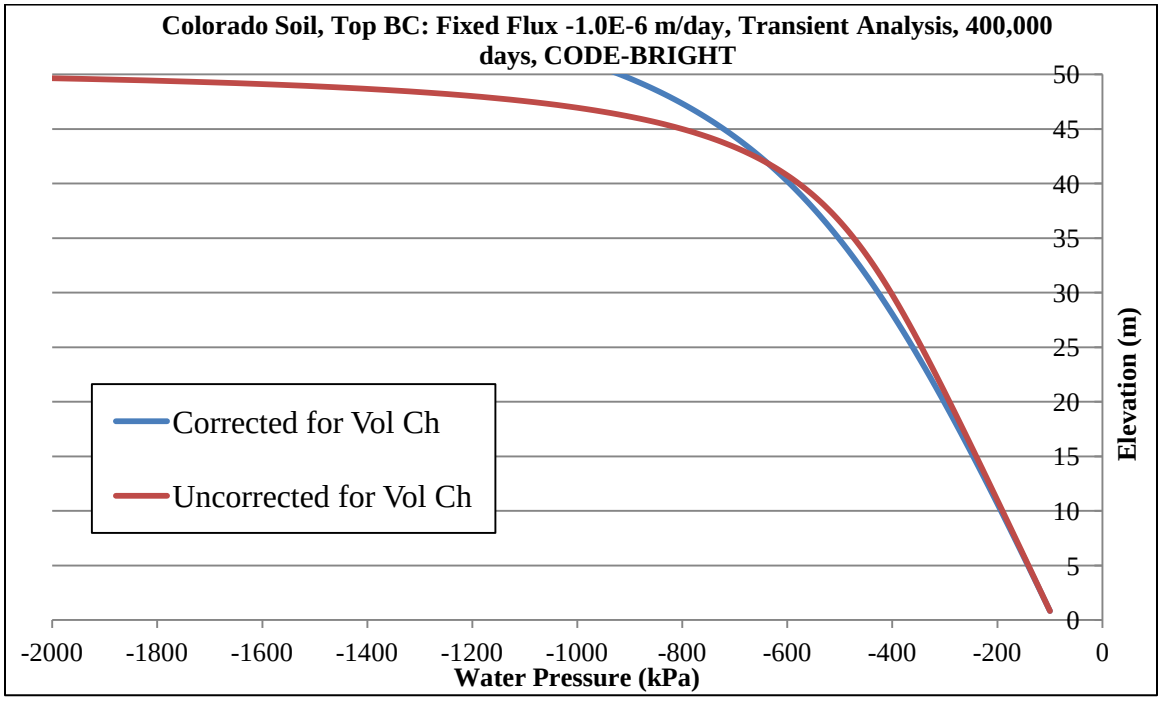

Figure 4.27. Water pressure versus elevation at time 400,000days (1095 years) for Colorado soil with SWCC corrected (AEV= 90kPa) and uncorrected (AEV= 60kPa) for volume change and top fixed flux of -1.0E-6 m/day (evaporation) using CODE-BRIGHT

Another set of simulations were analyzed for Colorado soil. The initial condition for this set of runs included higher amounts of suction. Figure 4.28 shows the initial suction condition for this set of runs.

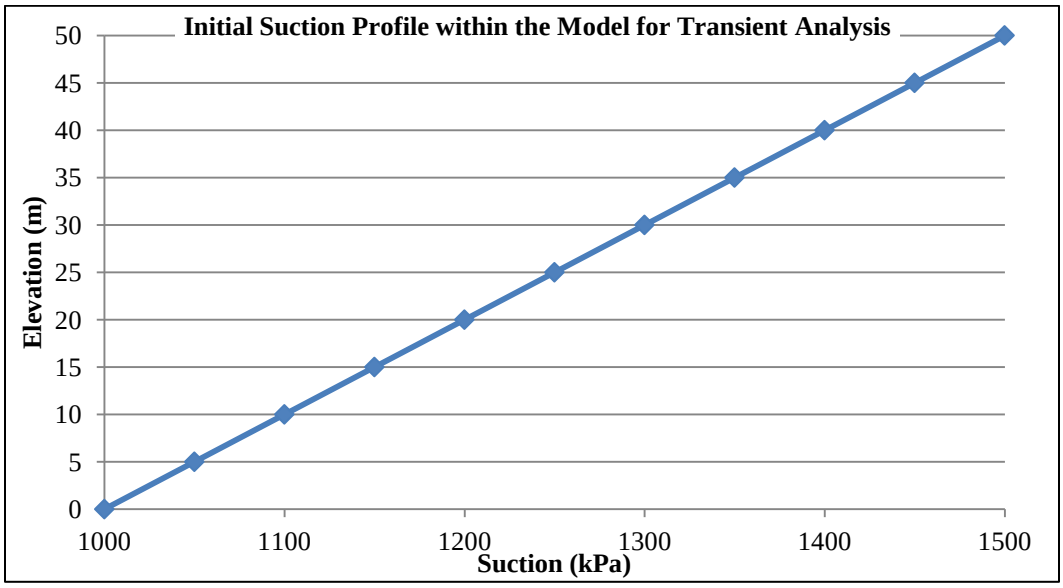

Figure 4.28. An example of initial suction versus elevation profile showing higher suction values used for uncoupled transient modeling of Colorado soil

The top boundary condition for this case of runs was fixed flux of 1.0E-4m/day. Upon introduction of top BC, the initially unsaturated soil column starts to become wet from the top, and therefore, the suction within the soil profile decreases. Figures 4.29 through 4.31 show the plots of water pressure versus elevation within the soil column at different times for both corrected and uncorrected SWCC. Similar to previous case, it was found that the rate of progression of wetted front is higher for corrected SWCC compared to uncorrected SWCC. It can be seen that although the initial suction profile is larger than previous cases (in which the suction was in the range of 100kPa and 600kPa), with the fixed flux as the top boundary condition, the soil eventually becomes wet for both cases of corrected and uncorrected SWCC. Figure 4.31 shows that the generated suction profile at time 90,000 days (which corresponds to steady-state) is smaller for uncorrected SWCC compared to the corrected SWCC. This is due to difference in air-entry values of SWCC corrected and uncorrected for volume change. As previously

explained, the uncorrected SWCC has generally smaller AEV, which leads to smaller final suction profile within the soil compared to the corrected SWCC.

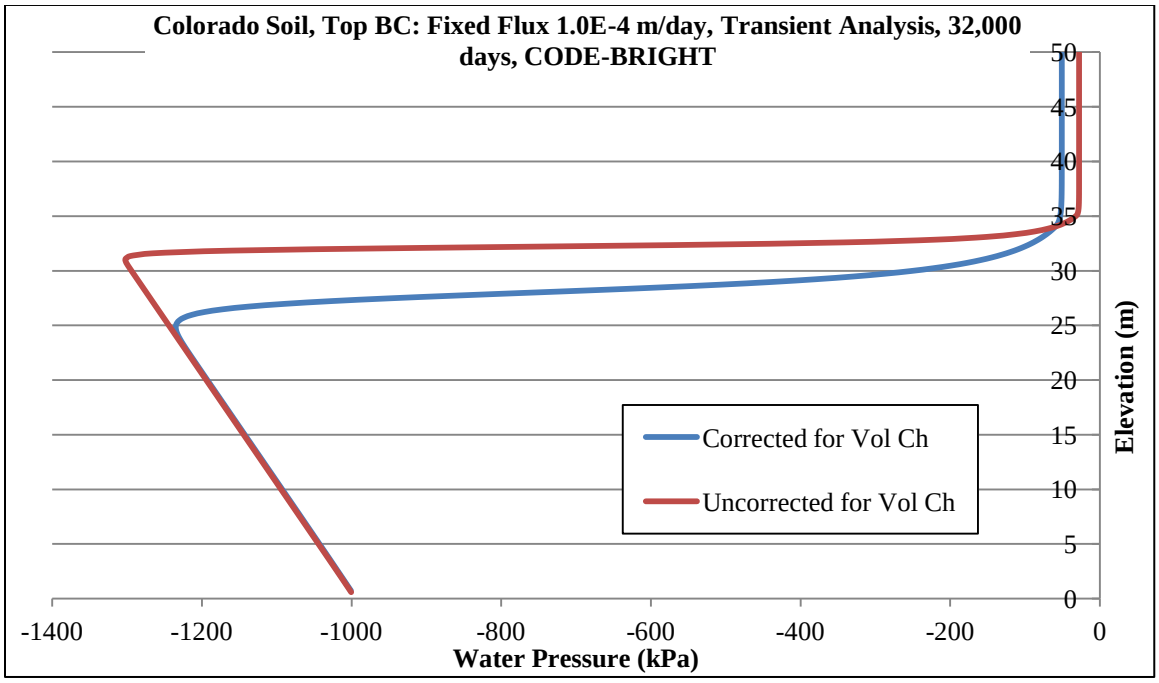

Figure 4.29. Water pressure versus elevation at time 32,000days for Colorado soil with SWCC corrected (AEV= 90kPa) and uncorrected (AEV= 60kPa) for volume change and top fixed flux of 1.0E-4 m/day using CODE-BRIGHT

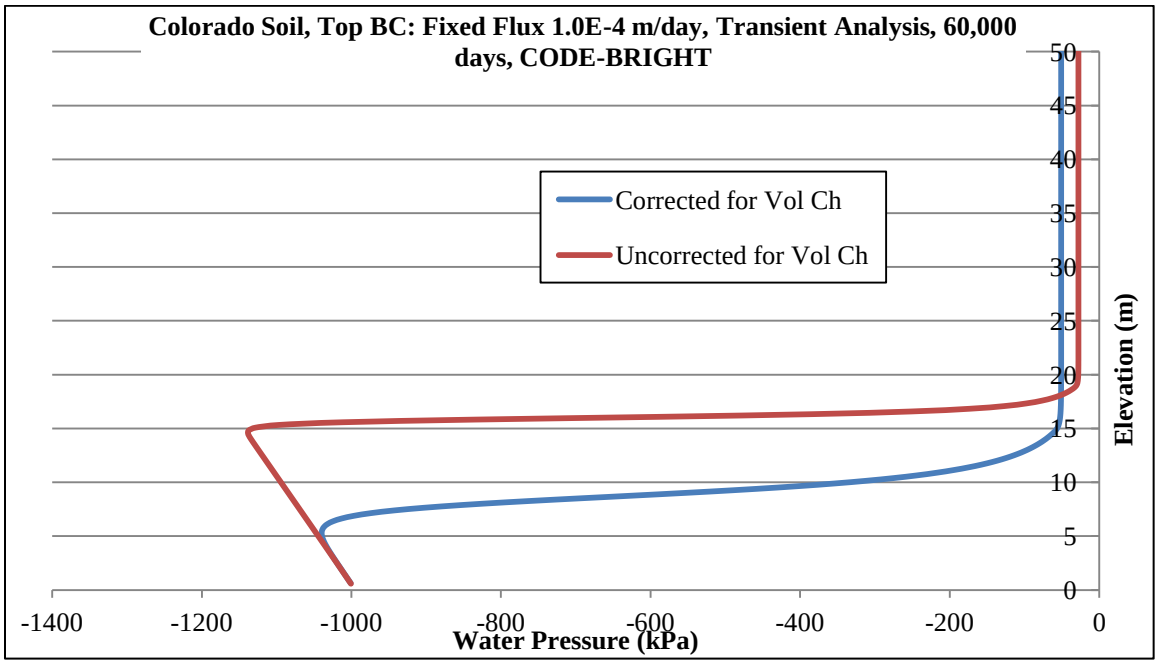

Figure 4.30. Water pressure versus elevation at time 60,000days for Colorado soil with SWCC corrected (AEV= 90kPa) and uncorrected (AEV= 60kPa) for volume change and top fixed flux of 1.0E-4 m/day using CODE-BRIGHT

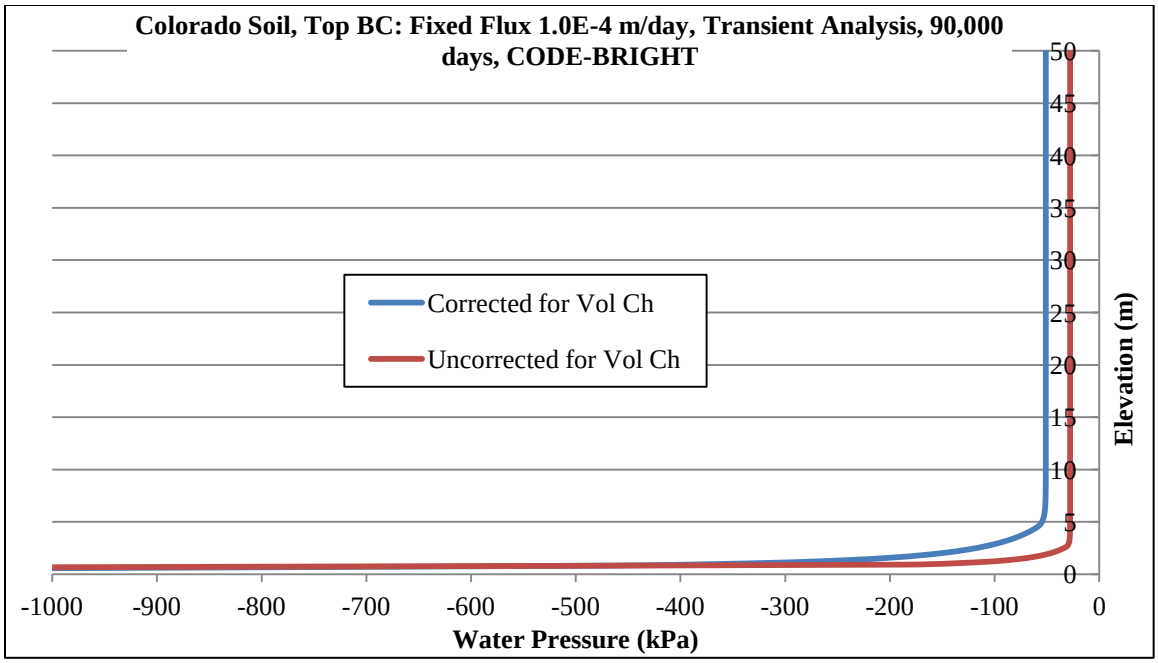

Figure 4.31. Water pressure versus elevation at time 90,000days (steady-state) for Colorado soil with SWCC corrected (AEV= 90kPa) and uncorrected (AEV= 60kPa) for volume change and top fixed flux of 1.0E-4 m/day using CODE-BRIGHT

4.10.1.3. San Antonio Soil

Table 4.9 provides a list of numerical modeling conducted based on properties of San Antonio soil. Figures 4.32 through 4.36 show results of modeling using San Antonio soil. Similar result trends to Anthem, and Colorado soils were found for San Antonio soil. At time 15,000 days which is a long-enough time for the model to reach the steady-state (i.e. the soil profile has become wetted), in the model based on uncorrected SWCC the final suction throughout the soil column is smaller than the final suction of the model based on corrected SWCC (suction of 8kPa for uncorrected SWCC versus 18kPa for corrected SWCC for the majority of the soil profile). In addition, the rate of progression of wetted front is larger for the case of SWCC corrected for volume change due to higher unsaturated hydraulic conductivity. This leads to higher suctions for uncorrected SWCC at some points within the soil profile at times prior to 15,000 days. This is shown in Figures 4.34 and 4.35 in which at times 6,000 days and 10,000 days, in some portions of the soil depth the uncorrected SWCC shows higher suction values compared to suctions of corrected SWCC. This is due to the fact that at times 6,000 days and 10,000 days the depth of wetting is larger for volume-corrected SWCC.

Table 4.9. List of numerical modeling conducted for San Antonio soil

Model No.	Soil	k-sat (m/day)	Top BC: Fixed Flux (m/day)	Top BC: Fixed Head (m)	SWCC	Software	Analysis Type	Coupled/ Uncoupled
1	San Antonio	8.64E-04	5.00E-04		Corrected	CODE-BRIGHT	Transient	Uncoupled
2	San Antonio	8.64E-04	5.00E-04		Uncorrected	CODE-BRIGHT	Transient	Uncoupled
3	San Antonio	8.64E-04	5.00E-05		Corrected	SVFLUX	Steady-State	Uncoupled
4	San Antonio	8.64E-04	5.00E-05		Uncorrected	SVFLUX	Steady-State	Uncoupled
5	San Antonio	8.64E-04	1.00E-04		Corrected	SVFLUX	Steady-State	Uncoupled
6	San Antonio	8.64E-04	1.00E-04		Uncorrected	SVFLUX	Steady-State	Uncoupled
7	San Antonio	8.64E-04	3.00E-04		Corrected	SVFLUX	Steady-State	Uncoupled
8	San Antonio	8.64E-04	3.00E-04		Uncorrected	SVFLUX	Steady-State	Uncoupled
9	San Antonio	8.64E-04	7.00E-04		Corrected	SVFLUX	Steady-State	Uncoupled
10	San Antonio	8.64E-04	7.00E-04		Uncorrected	SVFLUX	Steady-State	Uncoupled
11	San Antonio	8.64E-04	8.64E-04		Corrected	SVFLUX	Steady-State	Uncoupled
12	San Antonio	8.64E-04	8.64E-04		Uncorrected	SVFLUX	Steady-State	Uncoupled
13	San Antonio	8.64E-04	1.00E-03		Corrected	SVFLUX	Steady-State	Uncoupled
14	San Antonio	8.64E-04	1.00E-03		Uncorrected	SVFLUX	Steady-State	Uncoupled
15	San Antonio	8.64E-04		1	Corrected	SVFLUX	Steady-State	Uncoupled
16	San Antonio	8.64E-04		1	Uncorrected	SVFLUX	Steady-State	Uncoupled
17	San Antonio	8.64E-04	1.00E-04		Corrected	VADOSE/W	Steady-State	Uncoupled
18	San Antonio	8.64E-04	1.00E-04		Uncorrected	VADOSE/W	Steady-State	Uncoupled
19	San Antonio	8.64E-04	7.00E-04		Corrected	VADOSE/W	Steady-State	Uncoupled
20	San Antonio	8.64E-04	7.00E-04		Uncorrected	VADOSE/W	Steady-State	Uncoupled
21	San Antonio	8.64E-04	1.00E-03		Corrected	VADOSE/W	Steady-State	Uncoupled
22	San Antonio	8.64E-04	1.00E-03		Uncorrected	VADOSE/W	Steady-State	Uncoupled

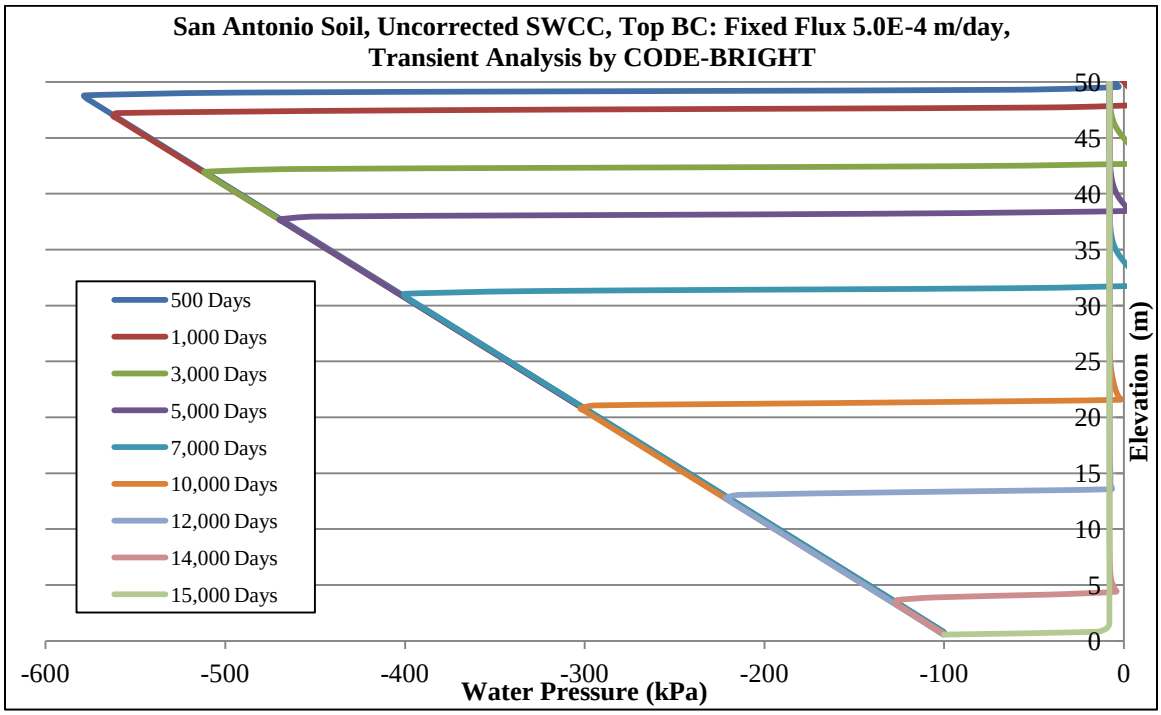

Figure 4.32. Transient analysis on San Antonio soil with SWCC uncorrected for volume change (AEV= 30kPa) and top fixed flux of 5.0e-4 m/day using CODE-BRIGHT

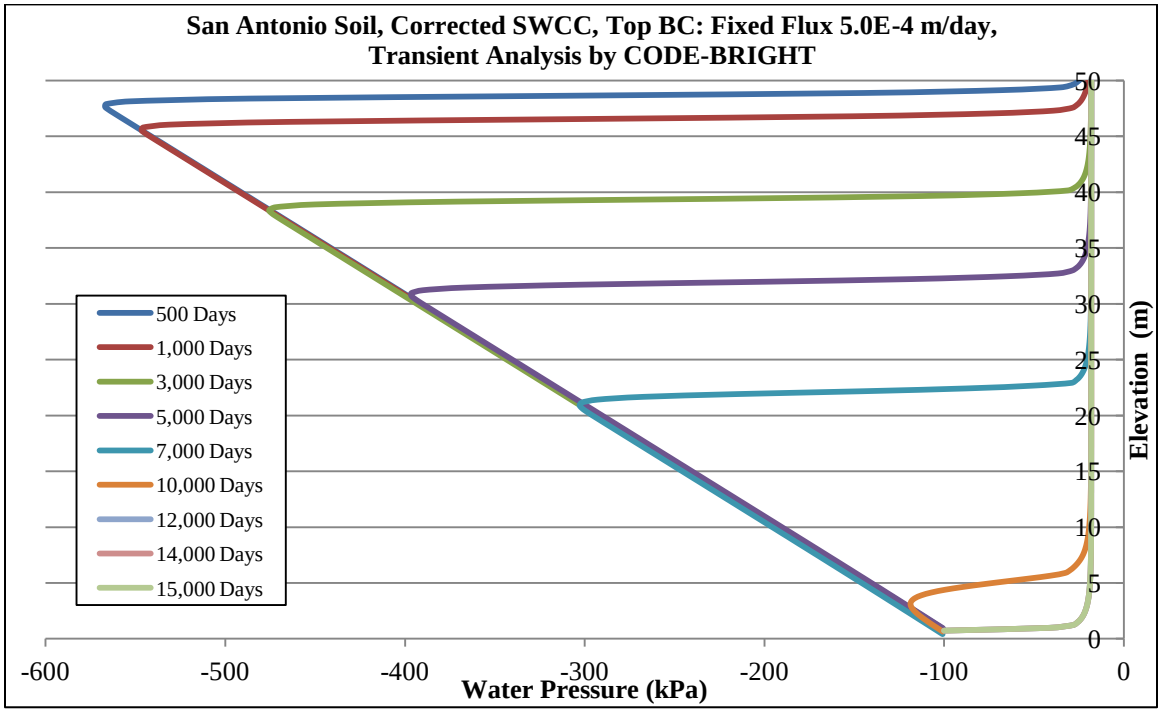

Figure 4.33. Transient analysis on San Antonio soil with SWCC corrected for volume change (AEV= 70kPa) and top fixed flux of 5.0e-4 m/day using CODE-BRIGHT

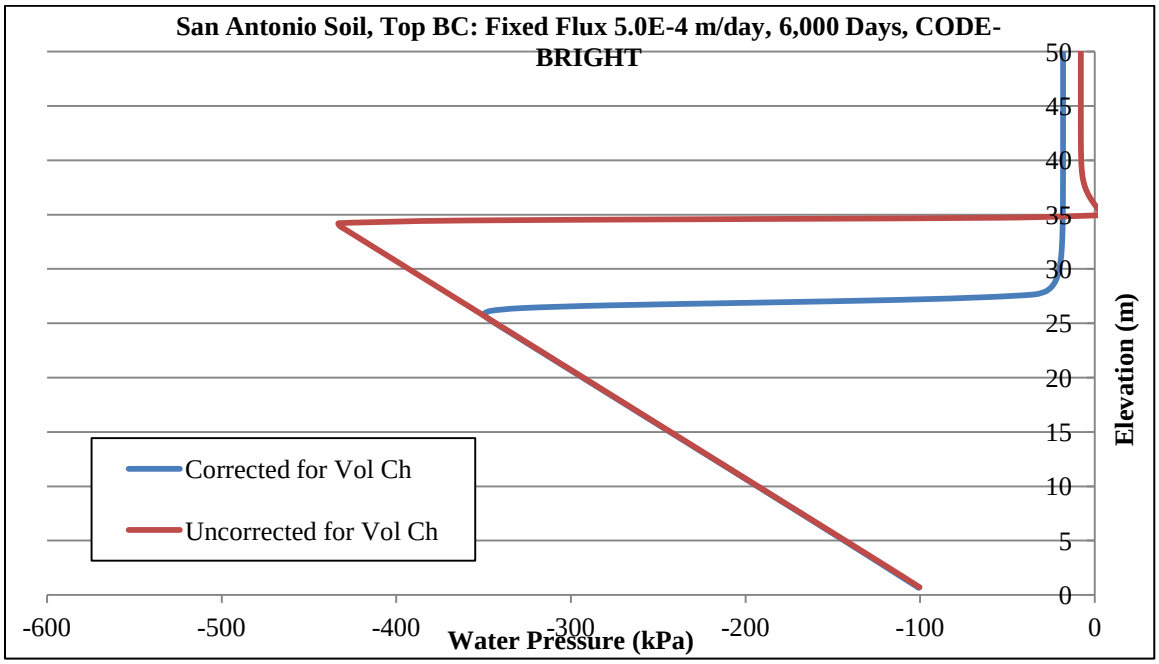

Figure 4.34. Water pressure versus elevation at time 6,000 days (16 years) for San Antonio soil with SWCC corrected (AEV= 70kPa) and uncorrected (AEV= 30kPa) for volume change and top fixed flux of 5.0e-4 m/day using CODE-BRIGHT

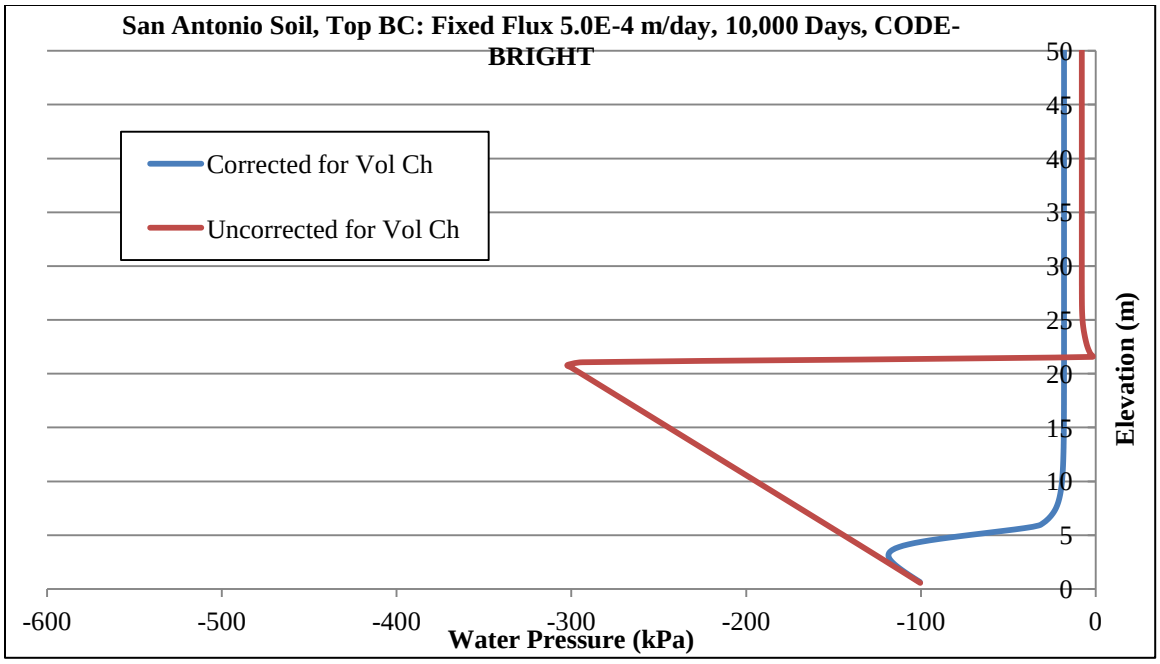

Figure 4.35. Water pressure versus elevation at time 10,000 days (27 years) for San Antonio soil with SWCC corrected (AEV= 70kPa) and uncorrected (AEV= 30kPa) for volume change and top fixed flux of 5.0e-4 m/day using CODE-BRIGHT

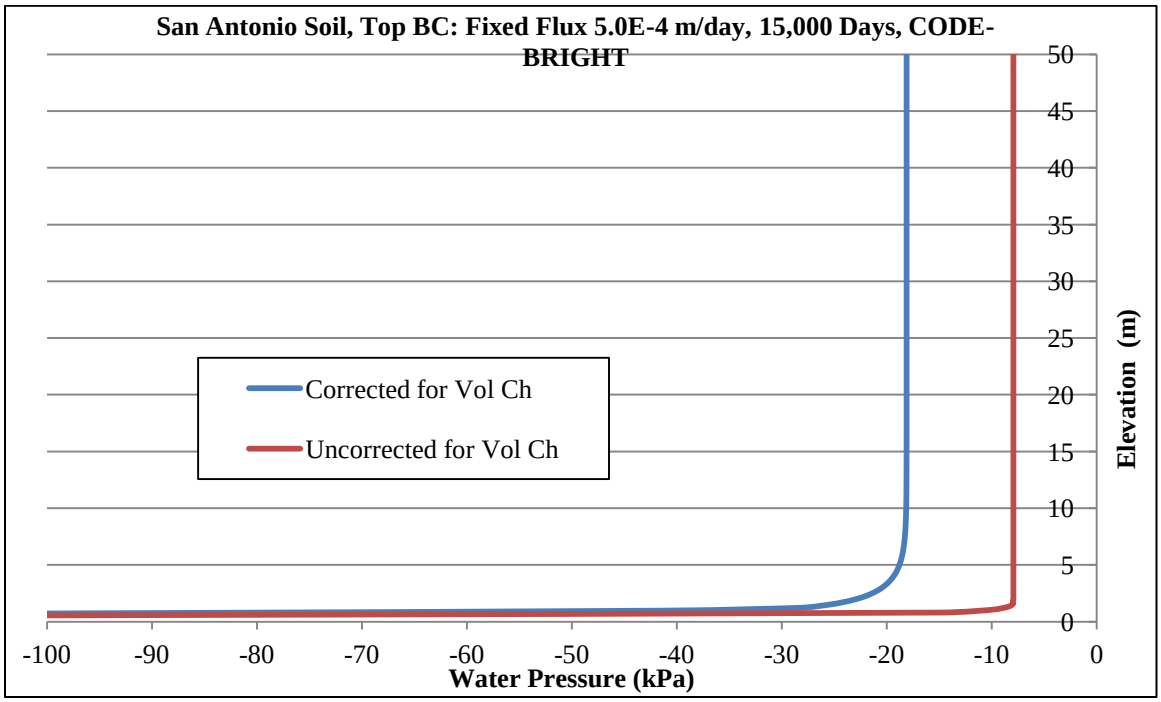

Figure 4.36. Water pressure versus elevation at steady-state condition for San Antonio soil with SWCC corrected (AEV= 70kPa) and uncorrected (AEV= 30kPa) for volume change and top fixed flux of 5.0e-4 m/day using CODE-BRIGHT

4.10.1.4. Comparing Results Produced by VADOSE/W, SVFLUX, and CODE-BRIGHT

Comparison was made between results generated from the three codes used in this study (i.e. SVFLUX, VADOSE/W, and CODE-BRIGHT). Figures 4.37 and 4.38 show comparison between the codes for Colorado and San Antonio soils. It was found that the results obtained from SVFLUX and VADOSE/W were identical. The reason for this is that these two codes utilize the exact same flow equation, SWCC fit equation (van Genuchten fit for SWCC in terms of volumetric water content), and saturated hydraulic conductivity estimation model (van Genuchten-Mualem equation based on SWCC in terms of volumetric water content). The results obtained from CODE-BRIGHT were close to the ones generated by SVFLUX and VADOSE/W but there were differences in

results. These differences can be found in Figures 4.37 and 4.38. Table 4.10 presents the values of final suction found by different computer codes.

Table 4.10. Range of final water pressure generated for different soil and various top BC fixed flux values using three codes VADOSE/W, SVFLUX, and CODE-BRIGHT

			Final Water Pressure Range (kPa)		
Soil	**Top BC Fixed Flux (m/day)**	**SWCC**	**SVFLUX**	**VADOSE/W**	**CODE-BRIGHT**
Colorado	5.00E-04	Corrected	-100 to -6	-100 to -6	-100 to -28
Colorado	5.00E-04	Uncorrected	-100 to -4	-100 to -4	-100 to -15
San Antonio	5.00E-04	Corrected	-100 to -3	-100 to -3	-100 to -18
San Antonio	5.00E-04	Uncorrected	-100 to -1	-100 to -1	-100 to -8

Some differences between codes was of course expected, as unlike SVFLUX and VADOSE/W which allows SWCC only in terms of volumetric water content, CODE-BRIGHT allows SWCC only in terms of degree of saturation. As previously described in Chapter 3, there may be considerable differences between SWCC's in terms of volumetric water content and SWCC's in terms of degree of saturation (particularly with regard to AEV) for soils that undergo significant volume change during SWCC test. The difference in SWCC (particularly AEV) can lead to different suction profiles generated by the computer programs. Furthermore, the model used for estimating unsaturated hydraulic conductivity function that is utilized in CODE-BRIGHT is different than the model used for estimating unsaturated hydraulic conductivity function used in SVFLUX and VADOSE/W. Therefore, the estimated unsaturated hydraulic conductivity function for a certain soil is different for CODE-BRIGHT compared to SVFLUX and VADOSE/W. This was explained earlier in this chapter where plots of different estimated unsaturated hydraulic conductivity function were presented. All these factors affect the suction profile

generated by three programs and explain the difference in results generated by CODE-BRIGHT.

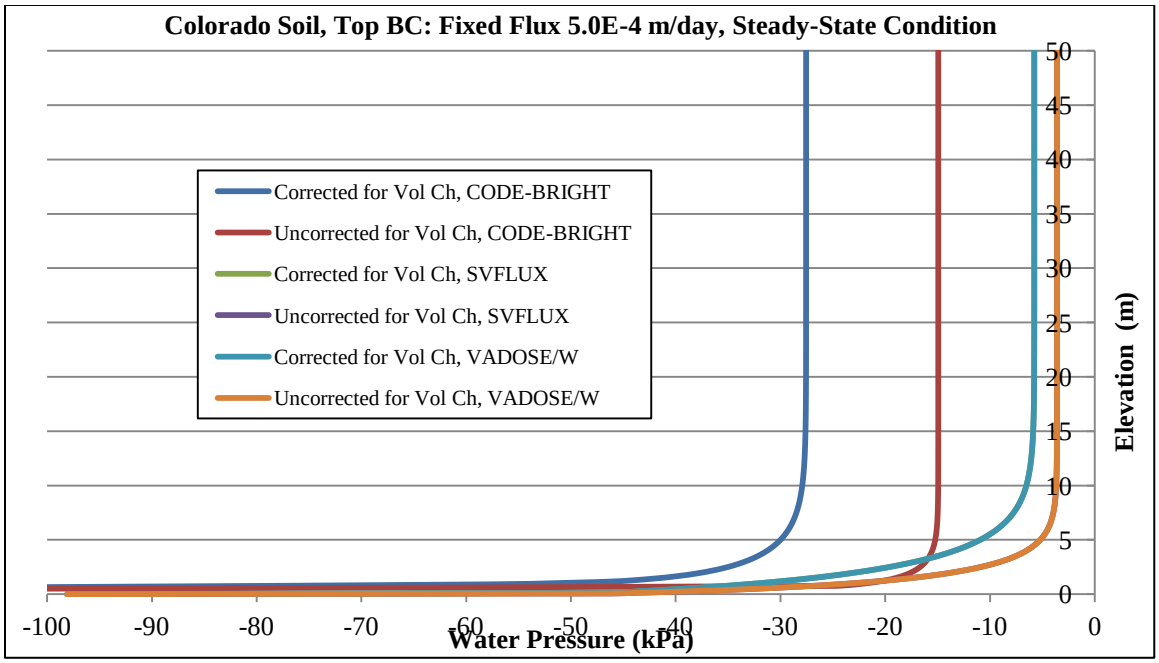

Figure 4.37. Water pressure versus elevation at steady-state condition for Colorado soil with SWCC corrected and uncorrected for volume change and top fixed flux of 5.0e-4 m/day using SVFLUX, VADOSE/W, and CODE-BRIGHT

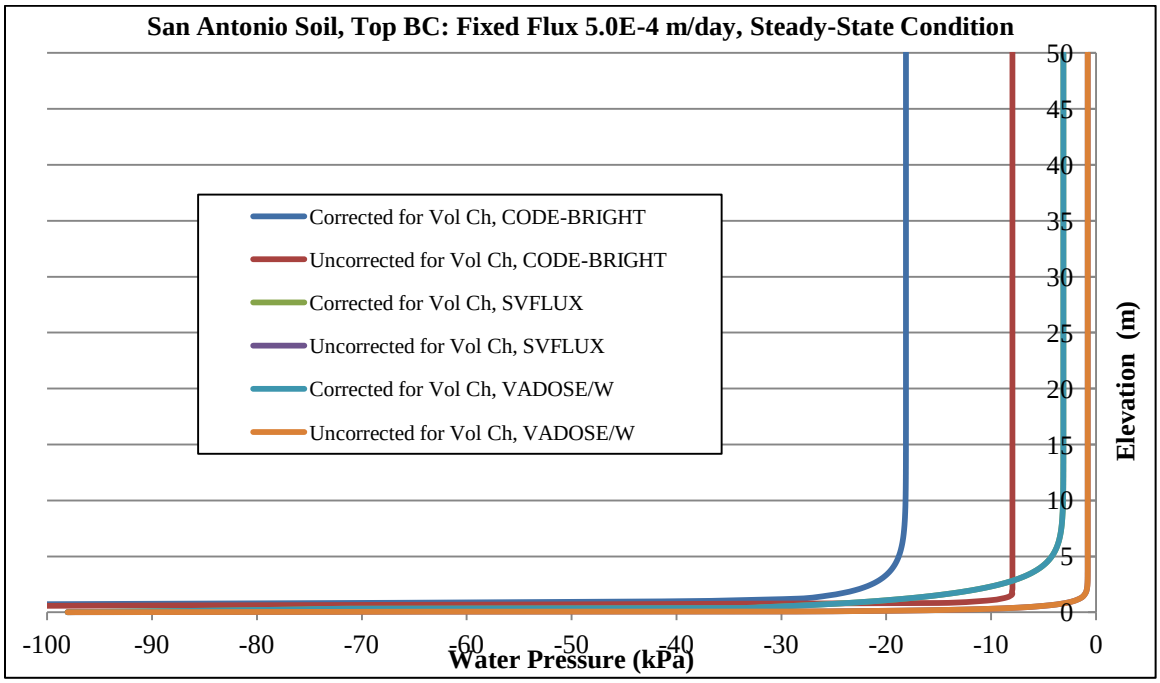

Figure 4.38. Water pressure versus elevation at steady-state condition for San Antonio soil with SWCC corrected and uncorrected for volume change and top fixed flux of 5.0e-4 m/day using SVFLUX, VADOSE/W, and CODE-BRIGHT

4.10.1.5. Deformations (Heave) from Uncoupled Analyses

Deformation of Colorado Soil:

Figure 4.39 illustrates the suction compression curve Colorado soil. It can be seen from the suction compression curve of Colorado soil that a decrease in suction from 1400kPa to 60kPa leads to increase in void ratio from 0.740 to 0.776 (i.e. increase of 0.036 in void ratio).

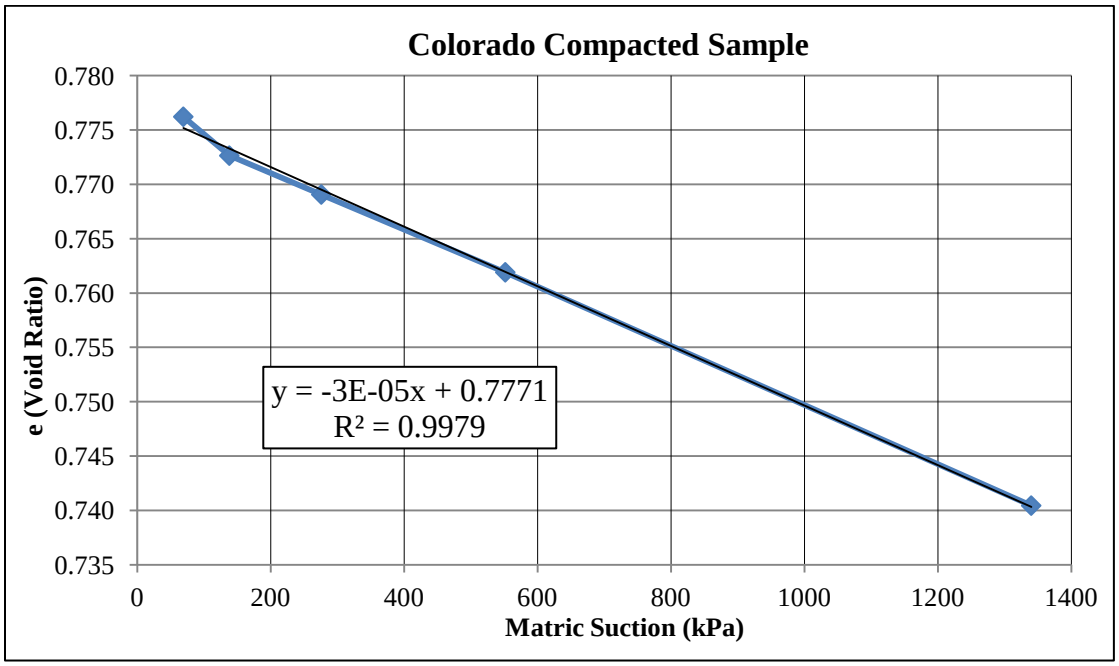

Figure 4.39. Suction compression curve for Colorado soil compacted specimens obtained from SWCC laboratory test

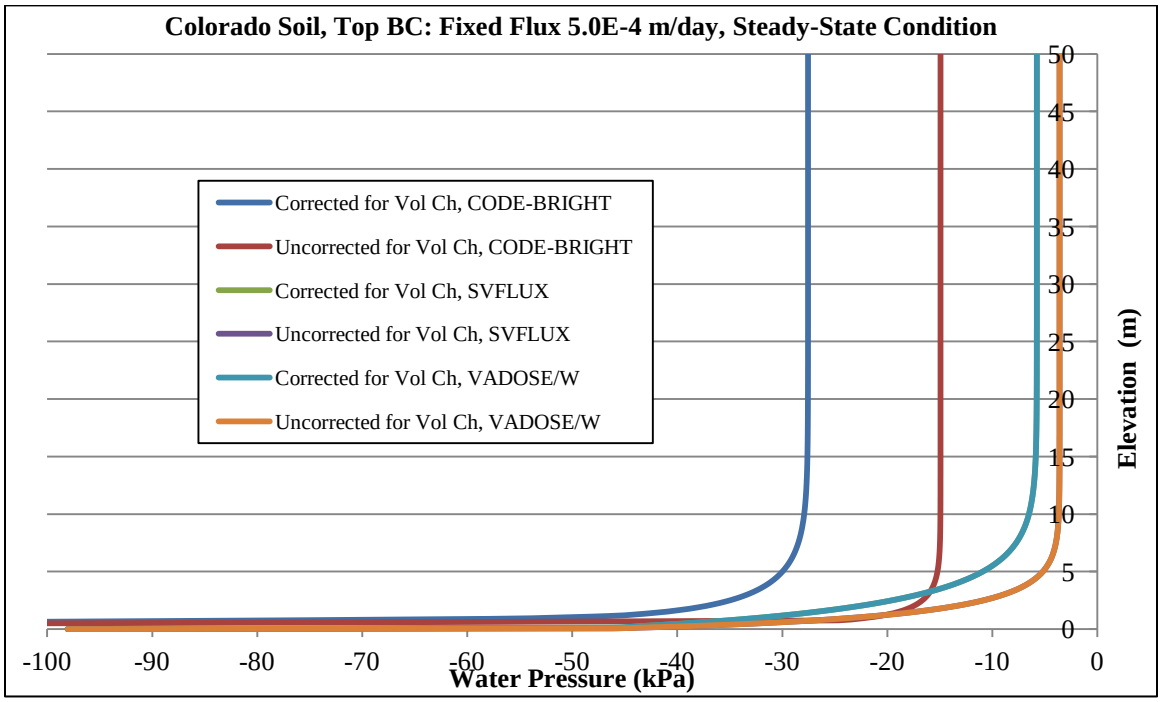

Figure 4.40. Water pressure versus elevation at steady-state condition for Colorado soil with SWCC corrected and uncorrected for volume change and top fixed flux of 5.0e-4

m/day using SVFLUX, VADOSE/W, and CODE-BRIGHT. The soil profile has become fully saturated in this case

Initial void ratio profile for Colorado soil was calculated by having the suction profile and using the suction compression curve (data shown in Table 4.11). CODE-BRIGHT, SVFLUX, and VADOSE/W codes were used to model the flow through the soil column modeled with Colorado soil properties (once with SWCC corrected and once with SWCC uncorrected for soil volume change). For these models, top BC was fixed flux of 5.0E-4 m/day. The resulting suction versus elevation profiles at the time that both cases (i.e. corrected and uncorrected SWCC) has become fully saturated using the three computer codes are presented in Figure 4.40.

Table 4.11. Initial suction and void ratio profile for Colorado soil model

Elevation (m)	Sub-layer No.	Thickness of layer (m)	Suction (kPa)	Suction (kPa) in the mid-point	Initial "e"
50			600		
45	1	5	550	575	0.75985
40	2	5	500	525	0.76135
35	3	5	450	475	0.76285
30	4	5	400	425	0.76435
25	5	5	350	375	0.76585
20	6	5	300	325	0.76735
15	7	5	250	275	0.76885
10	8	5	200	225	0.77035
5	9	5	150	175	0.77185
0	10	5	100	125	0.77335

The suction versus elevation results generated by CODE-BRIGHT and SVFLUX were used to calculate the final void ratio profile of the soil and the results were compared against each other. When the soil profile becomes wet by introducing the top fixed flux, the suction of the soil decreases. A decrease in suction of the Colorado soil

(which is an expansive soil) leads to increase in void ratio (as shown in the suction compression curve of Colorado soil that was obtained from SWCC test). CODE-BRIGHT and SVFLUX estimated the amounts of suction within the soil profile at times large enough that the soil has becomes saturated. By having the values of suction and using the suction compression curve of Colorado soil, the final void ratio profile of the soil was determined. By having the values of initial and final void ratio, the deformation was calculated. By having initial and final values of void ratio, strain and deformation of soil can be found using following equations:

$$\varepsilon = \frac{\Delta e}{1 + e_o} \tag{4.55}$$

$$\Delta H = \varepsilon * H_o \tag{4.56}$$

The final void ratio profile and deformation based on the results generated by CODE-BRIGHT and SVFLUX are presented in Tables 4.12 and 4.13. It was found from the results that the values of wetting induced heave for the model based on Colorado soil for both cases of SWCC corrected and uncorrected for soil volume change are relatively close. The amount of heave for the analyses done by CODE-BRIGHT was found to be 0.2729 meters and 0.2842 meters for volume corrected SWCC and volume uncorrected SWCC, respectively. The amount of heave for the analyses done by SVFLUX was found to be 0.2908 meters and 0.2931 meters for volume corrected SWCC and volume uncorrected SWCC, respectively. This is due to the proximity of results found for the cases with SWCC corrected and uncorrected. It can be seen that the final suction for the majority of the depth of soil column found by SVFLUX is around 3.5kPa for uncorrected SWCC and 5.5kPa for corrected SWCC. This is a relatively small difference in suction

which leads to small differences in void ratios calculated based on suction (i.e. from the suction compression curve). However, this difference in the results obtained from the analyses done by CODE-BRIGHT is more pronounced compared to the difference in deformation values found from the results of runs by SVFLUX. It can be seen from Figure 4.40 that the suction generated by CODE-BRIGHT for the majority of soil depth for uncorrected SWCC is around 15kPa while this value is around 28kPa for corrected SWCC. This difference in final suction values between corrected and uncorrected SWCC is more pronounced than this difference in results of SVFLUX. This leads to more pronounced differences in calculated void ratio and deformation for corrected and uncorrected SWCC analyzed by CODE-BRIGHT.

It was also found that the deformation determined form SVFLUX results were slightly larger than the ones calculated from CODE-BRIGHT results. This is due to the fact that the final suction profile (for both SWCC corrected and uncorrected) generated by SVFLUX are smaller than the values generated by CODE-BRIGHT. This leads to relatively larger void ratios calculated by using the suction compression curve.

Table 4.12. Final void ratio profile and deformation for the uncoupled Colorado soil model with top BC fixed flux of 5.0E-4 m/day analyzed by CODE-BRIGHT

	Final "e"		ε=Δe/(1+eo)		ΔH=Ho*ε (m)	
Sub-layer No.	Corrected	Uncorrected	Corrected	Uncorrected	Corrected	Uncorrected
1	0.776273	0.776652	0.0093	0.0095	0.0467	0.0477
2	0.776273	0.776652	0.0085	0.0087	0.0424	0.0434
3	0.776273	0.776652	0.0076	0.0078	0.0381	0.0391
4	0.776273	0.776652	0.0068	0.0070	0.0338	0.0349
5	0.776273	0.776652	0.0059	0.0061	0.0295	0.0306
6	0.776273	0.776652	0.0050	0.0053	0.0252	0.0263
7	0.776272	0.776652	0.0042	0.0044	0.0210	0.0221
8	0.776268	0.776652	0.0033	0.0036	0.0167	0.0178
9	0.776241	0.776650	0.0025	0.0027	0.0124	0.0135
10	0.775907	0.7764450	0.0014	0.0017	0.0072	0.0087
Total Deformation					**0.2729**	**0.2842**

Table 4.13. Final void ratio profile and deformation for the uncoupled Colorado soil model with top BC fixed flux of 5.0E-4 m/day analyzed by SVFLUX

	Final "e"		ε=Δe/(1+eo)		ΔH=Ho*ε (m)	
Sub-layer No.	Corrected	Uncorrected	Corrected	Uncorrected	Corrected	Uncorrected
1	0.776927	0.776992	0.0097	0.0097	0.0485	0.0487
2	0.776927	0.776992	0.0088	0.0089	0.0442	0.0444
3	0.776927	0.776992	0.0080	0.0080	0.0399	0.0401
4	0.776927	0.776992	0.0071	0.0072	0.0356	0.0358
5	0.776927	0.776992	0.0063	0.0063	0.0314	0.0315
6	0.776927	0.776992	0.0054	0.0055	0.0271	0.0273
7	0.776926	0.776992	0.0046	0.0046	0.0228	0.0230
8	0.776917	0.776992	0.0037	0.0038	0.0185	0.0188
9	0.776861	0.776978	0.0028	0.0029	0.0141	0.0145
10	0.776378	0.776541	0.0017	0.0018	0.0085	0.0090
Total Deformation					**0.2908**	**0.2931**

Another estimation of deformation (heave) was performed for the time 7,000 days (~19 years) since the start of the wetting of the soil from the top using fixed flux of 5.0E-4 m/day. This analysis was done by using the runs from CODE-BRIGHT. At the time

7,000 days, the soil profile has not become completely saturated yet. Figure 4.41 shows the suction profile of both corrected and uncorrected cases at time 7,000 days. It can be seen that the suction for the uncorrected SWCC is higher at some portions of the soil profile.

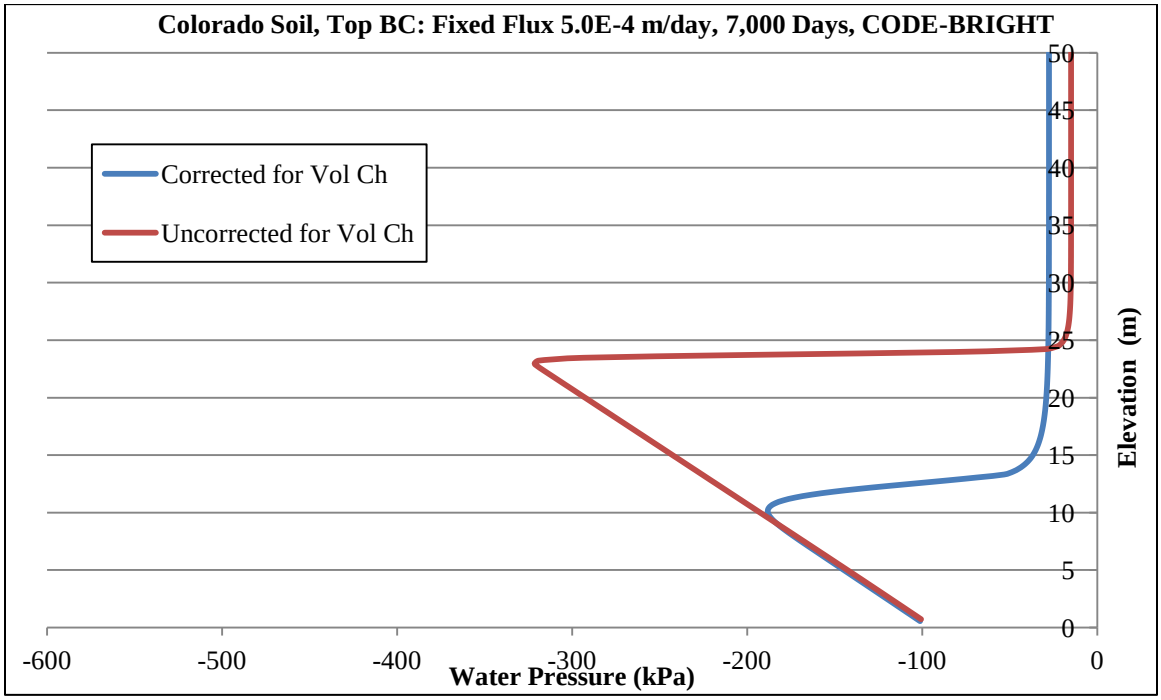

Figure 4.41. Water pressure versus elevation at 7,000 days for Colorado soil with SWCC corrected (AEV= 90kPa) and uncorrected (AEV= 60kPa) for volume change and top fixed flux of 5.0e-4 m/day using CODE-BRIGHT. The soil profile has not become fully saturated at the time of 7,000 days

The initial conditions of the model were the same as the ones showed previously in Table 4.11. By having the values of suction within the soil profile which was generated by CODE-BRIGHT and using the suction compression curve (shown in Figure 4.43) the values of void ratio at time 7,000 days was found (shown in Table 4.14). The calculated heave for uncorrected case at 7,000 days was found to be around 0.19 meters, while for corrected case the heave is larger at 7,000 days (0.245 meters). It is important to notice

that for the steady-state (which occurs at very long term and both corrected and uncorrected cases have become fully saturated) the heave for uncorrected case was found to be larger than for the corrected case. The opposite is true when comparing the heave of corrected and uncorrected cases at time 7,000 days. In other words, in 7,000 days the heave of corrected case is larger than the heave of the uncorrected case. This is due to the fact that the rate of progression of wetted front is higher for corrected case due to higher k_{unsat} values and larger portion of the soil profile has become wet at 7,000 days for the corrected case. It should also be noticed that the difference between deformation of volume-corrected and volume-uncorrected cases is higher for 7,000 days compared to the steady-state (i.e. 15,000 days where both cases have become saturated).

Table 4.14. Void ratio profile and deformation at 7,000 days for the uncoupled Colorado soil model with top BC fixed flux of 5.0E-4 m/day analyzed by CODE-BRIGHT

	Final "e"		**ε=Δe/(1+eo)**		**ΔH=Ho*ε (m)**	
Sub-layer No.	Corrected	Uncorrected	Corrected	Uncorrected	Corrected	Uncorrected
1	0.776273	0.776652	0.0093	0.0095	0.0467	0.0477
2	0.776273	0.776652	0.0085	0.0087	0.0424	0.0434
3	0.776273	0.776652	0.0076	0.0078	0.0381	0.0391
4	0.776272	0.776654	0.0068	0.0070	0.0338	0.0349
5	0.776268	0.773728	0.0059	0.0045	0.0295	0.0223
6	0.776249	0.767795	0.0050	0.0003	0.0252	0.0013
7	0.776140	0.769241	0.0041	0.0002	0.0206	0.0011
8	0.772607	0.770707	0.0013	0.0002	0.0064	0.0010
9	0.772387	0.772185	0.0003	0.0002	0.0015	0.0009
10	0.773617	0.773530	0.0002	0.0001	0.0008	0.0005
Total Deformation					**0.2448**	**0.1923**

4.10.2. Results of Coupled Analyses

Coupled flow-deformation analyses were conducted on Colorado soil using CODE-BRIGHT with top boundary condition of 5.0e-4 m/day. The purpose of transient

coupled analyses was to analyze the flow through the soil column and also determine the wetting induced deformation for SWCC's corrected and uncorrected for volume change and compare the results.

As previously mentioned, for the transient coupled analyses, initial condition of the model including initial void ratio profile has to be defined based on the initial suction conditions along the column depth (shown in Figure 4.42).

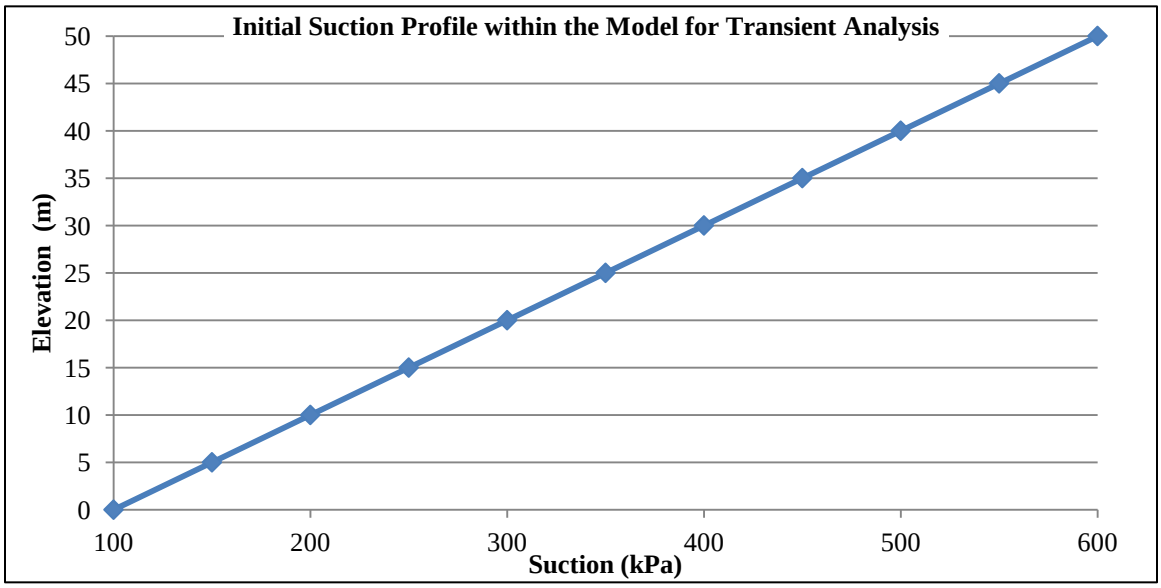

Figure 4.42. Initial suction versus elevation profile used for coupled and uncoupled transient modeling

In order to define initial void ratio profile for Colorado soil, the suction compression curve obtained from laboratory SWCC test on compacted specimens of Colorado soil were used (shown in Figure 4.43). Changes in void ratio during SWCC test also affects unit weight of the specimen (shown in Figure 4.44). The unit weight profile was used to determine initial stress (i.e. overburden stress) profile within the soil column. In order to generate more accurate results, the soil column was divided into 10 sub-layers

each with thickness of 5 meters and initial conditions of each layer was defined separately.

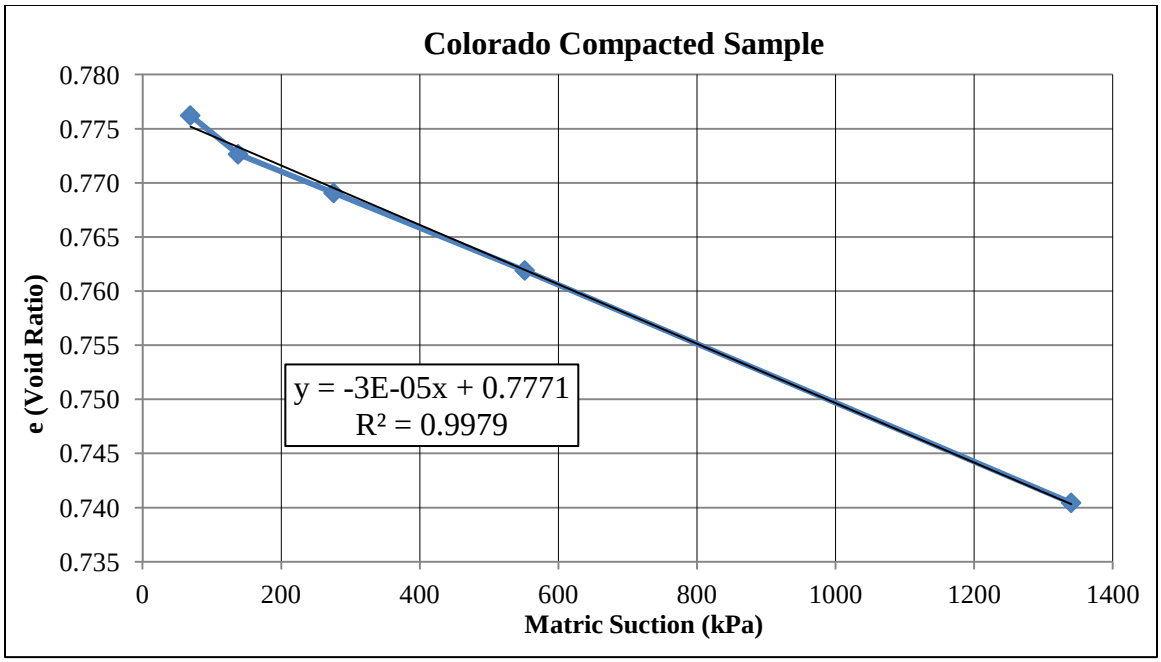

Figure 4.43. Suction compression curve for Colorado soil compacted specimens obtained from SWCC laboratory test

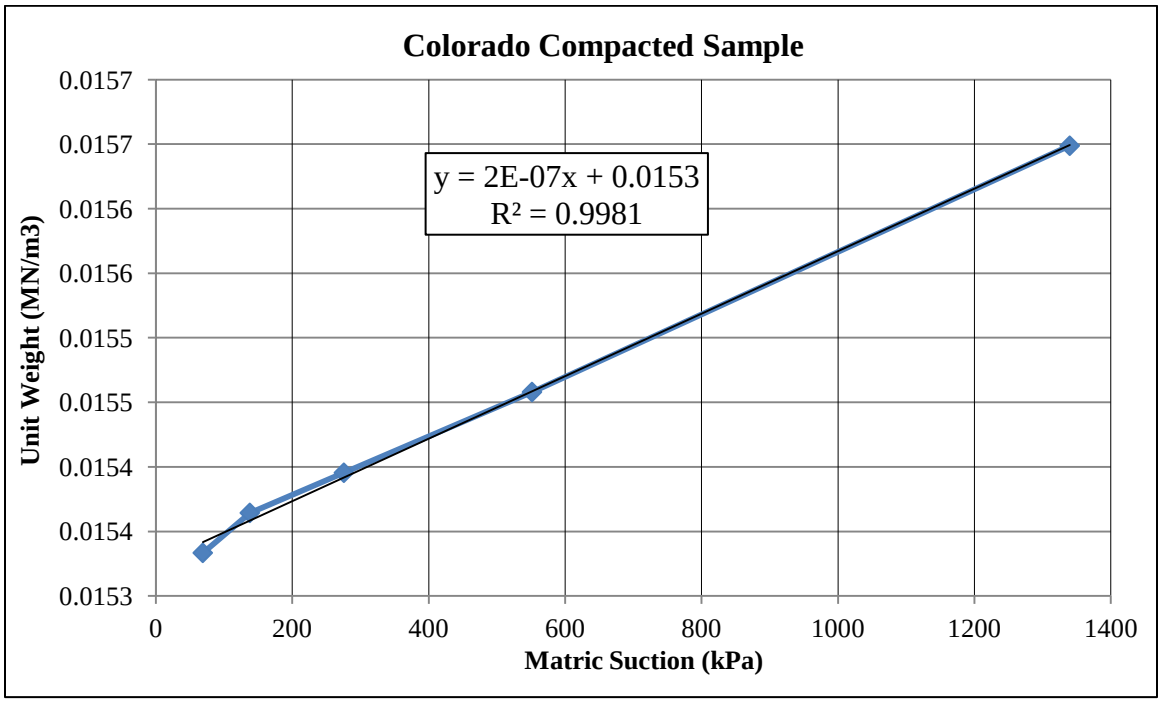

Figure 4.44. Unit Weight versus suction for Colorado soil compacted specimens obtained from SWCC laboratory test

Figure 4.45 shows sub-layering of soil column in order to assign initial void ratios and other initial conditions to each sub-layer. Table 4.15 illustrates values of initial suction and void ratio used for coupled transient analyses for Colorado soil.

Coupled flow-deformation analyses elastic properties and loading condition of the soil column should also be defined. In CODE-BRIGHT strain is calculated according to the following equation:

$$\frac{\Delta e}{1+e} = a_1 \Delta \ln(-p') + a_2 \Delta \ln\left(\frac{s+0.1}{0.1}\right) + a_3 \Delta\left[\ln(-p')\ln\left(\frac{s+0.1}{0.1}\right)\right] \qquad (4.57)$$

The required inputs for solving the equations by CODE-BRIGHT are:

1. $a_1 = \dfrac{-\kappa}{1+e}$ where κ is the slope of the unload/reload curve in the (e - lnp') diagram

2. $a_2 = \frac{-\kappa_s}{1+e}$ where κ_s is the slope of the unload/reload curve in the (e - $\ln\left(\frac{s+0.1}{0.1}\right)$) diagram
3. a_3 can be set as zero, which assumes that suction does not have a direct impact on the mean stress
4. υ = Poisson's ratio.

Values of a_1 and a_2 parameters were also determined for each sub-layer by having initial void ratio and are listed in Table 4.15. Results of coupled analysis on Colorado soil using CODE-BRIGHT including progression of change in water pressure and void ratio versus elevation are shown in Figures 4.46 through 4.53. It can be seen from Figure 4.51 that although the initial void ratio profile is the same for both cases of corrected and uncorrected SWCC's, the final void ratio of the case with uncorrected void ratio shows larger values.

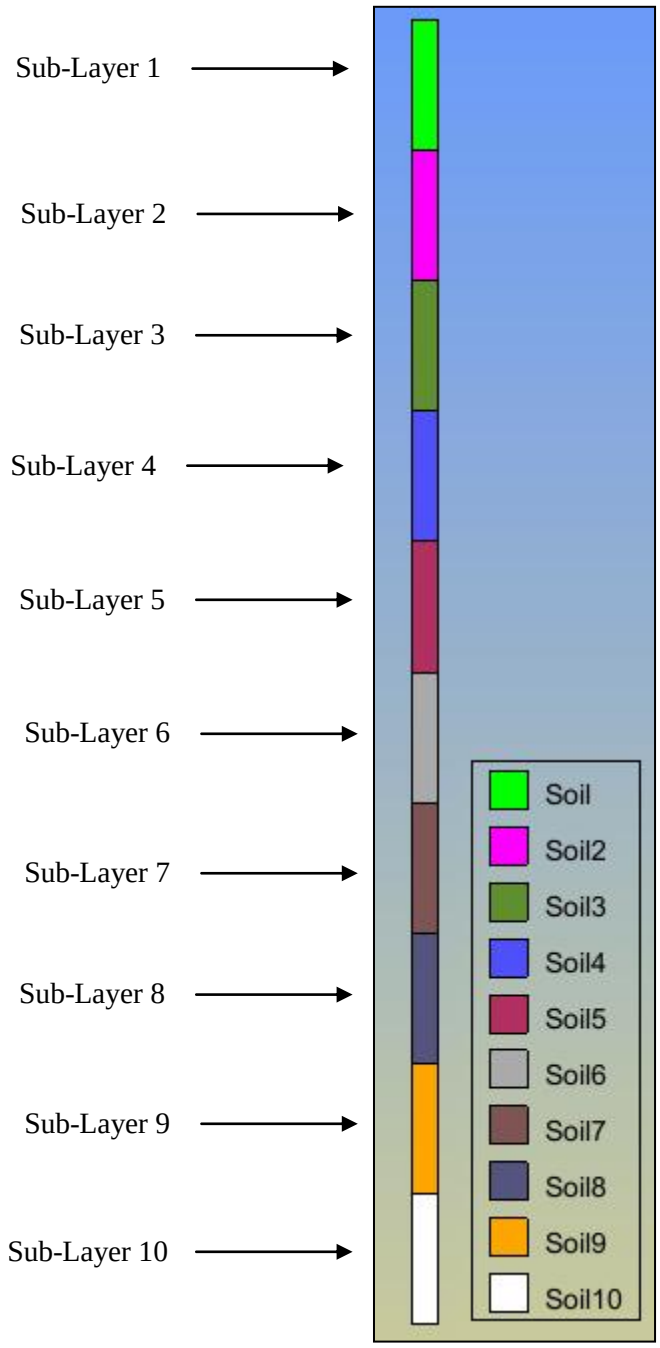

Figure 4.45. Sub-layering the soil column for defining initial void ratio more accurately to each sub-layer

Table 4.15. Initial conditions for transient coupled analysis including initial void ratio and a1 and a2 parameters for Colorado Soil

Elevation (m)	Sub-layer No.	Thickness of layer (m)	Suction (kPa)	Suction (kPa) in the mid-point	Initial "e"	Initial porosity "n"	a_1	a_2
50			600					
45	1	5	550	575	0.75985	0.4318	-0.02046	-0.00842
40	2	5	500	525	0.76135	0.4323	-0.02044	-0.00842
35	3	5	450	475	0.76285	0.4327	-0.02042	-0.00842
30	4	5	400	425	0.76435	0.4332	-0.02040	-0.00841
25	5	5	350	375	0.76585	0.4337	-0.02039	-0.00841
20	6	5	300	325	0.76735	0.4342	-0.02037	-0.00841
15	7	5	250	275	0.76885	0.4347	-0.02035	-0.00841
10	8	5	200	225	0.77035	0.4351	-0.02033	-0.00840
5	9	5	150	175	0.77185	0.4356	-0.02032	-0.00840
0	10	5	100	125	0.77335	0.4361	-0.02030	-0.00840

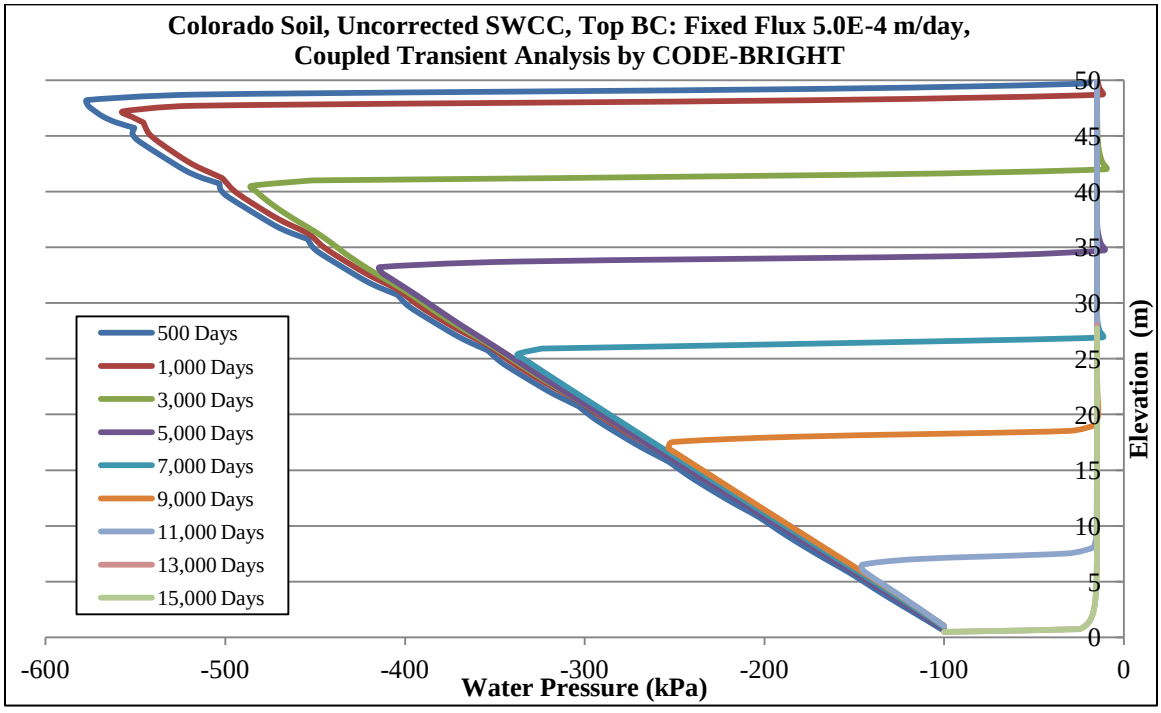

Figure 4.46. Transient coupled flow-deformation analysis on Colorado soil with SWCC uncorrected for volume change (AEV= 60kPa) and top fixed flux of 5.0e-4 m/day using CODE-BRIGHT

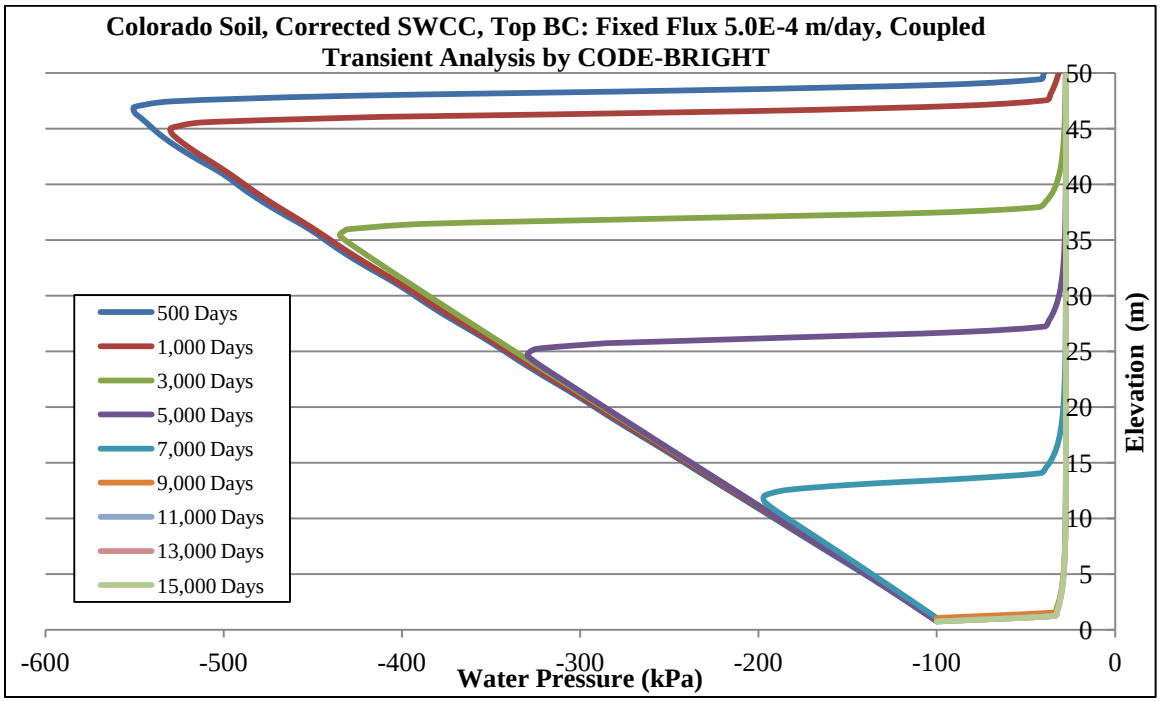

Figure 4.47. Transient coupled flow-deformation analysis on Colorado soil with SWCC corrected for volume change (AEV= 90kPa) and top fixed flux of 5.0e-4 m/day using CODE-BRIGHT

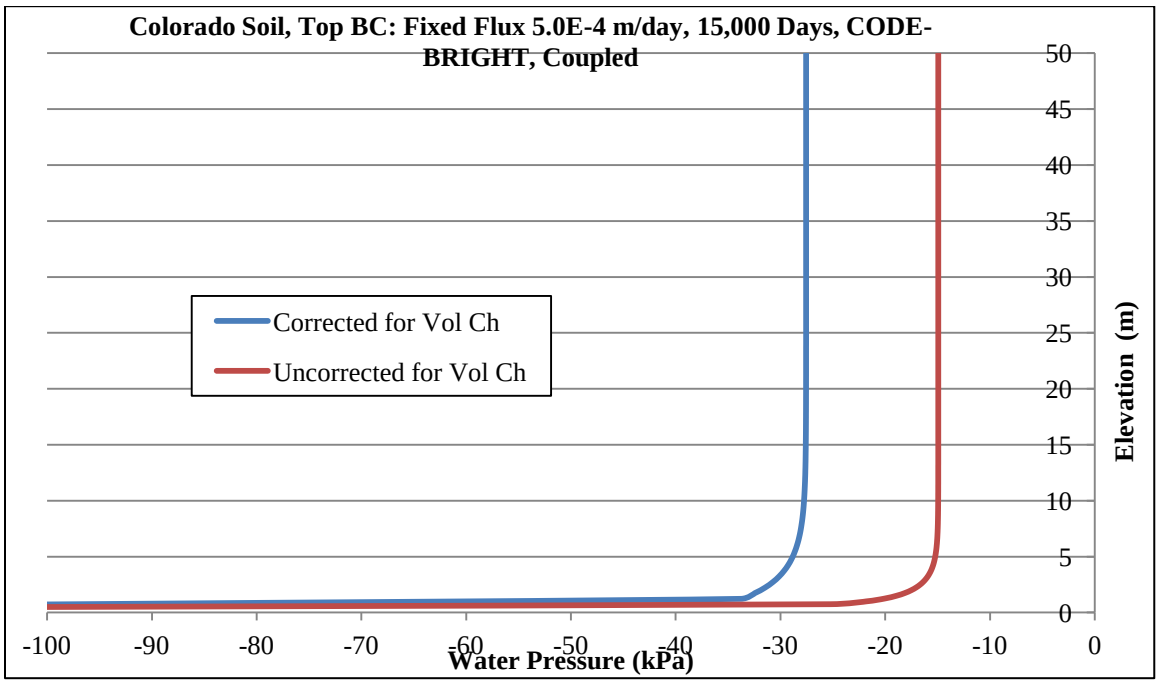

Figure 4.48. Water pressure versus elevation at steady-state condition for coupled flow-deformation analysis on Colorado soil with SWCC corrected (AEV= 90kPa) and

uncorrected (AEV= 60kPa) for volume change and top fixed flux of 5.0e-4 m/day using CODE-BRIGHT

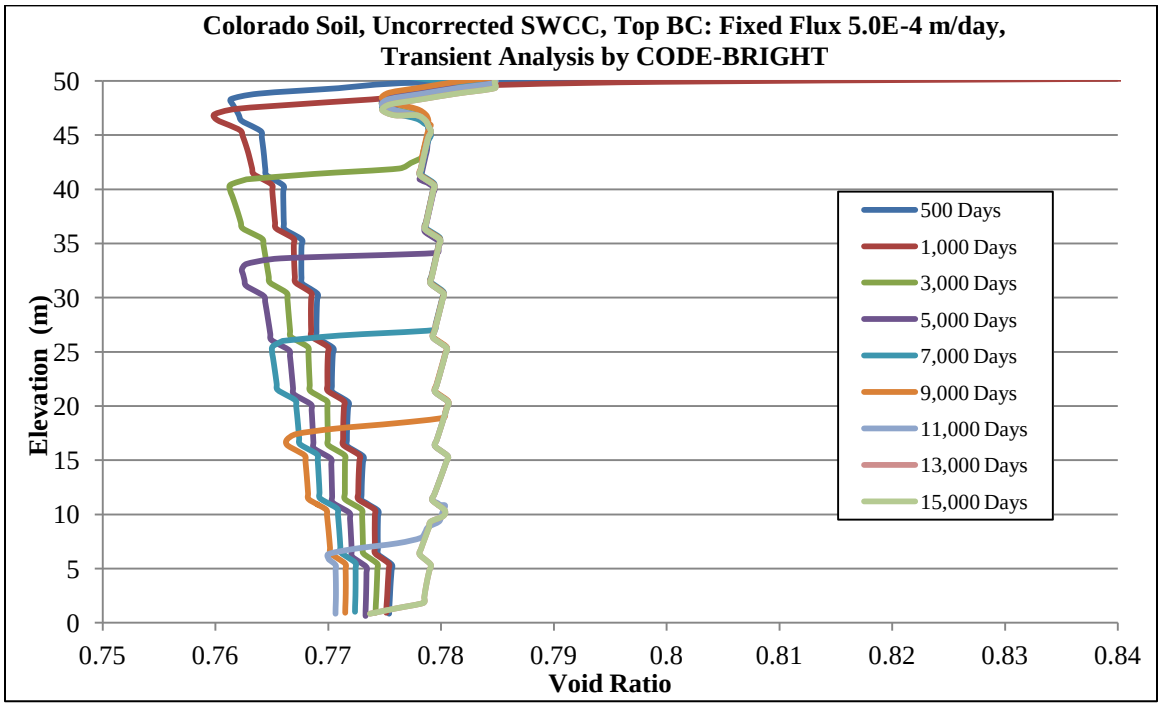

Figure 4.49. Transient coupled flow-deformation analysis on Colorado soil with SWCC uncorrected for volume change (AEV= 60kPa) and top fixed flux of 5.0e-4 m/day using CODE-BRIGHT

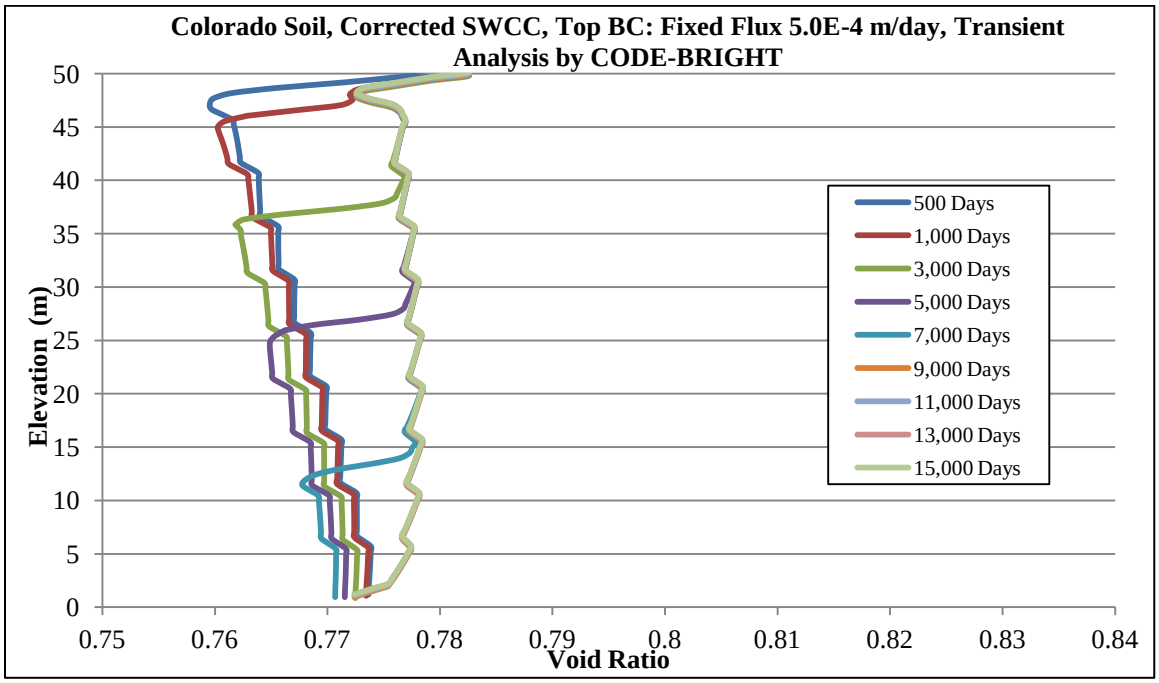

Figure 4.50. Transient coupled flow-deformation analysis on Colorado soil with SWCC corrected for volume change (AEV= 90kPa) and top fixed flux of 5.0e-4 m/day using CODE-BRIGHT

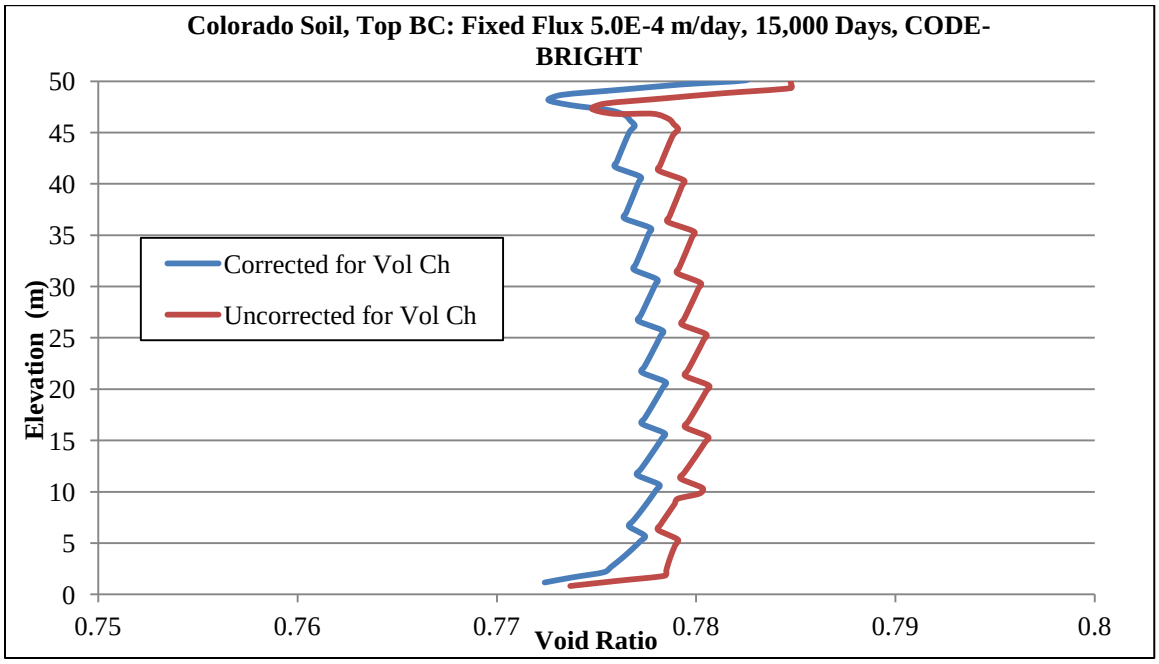

Figure 4.51. Void ratio versus elevation at steady-state condition for coupled flow-deformation analysis on Colorado soil with SWCC corrected (AEV= 90kPa) and

uncorrected (AEV= 60kPa) for volume change and top fixed flux of 5.0e-4 m/day using CODE-BRIGHT

Table 4.16 shows final values of void ratio (at time 15,000 days when the model has reached the steady-state and fully wetted) found by transient coupled analysis on Colorado soil using CODE-BRIGHT. By having initial and final values of void ratio, strain and deformation of soil can be found using following equations:

$$\varepsilon = \frac{\Delta e}{1 + e_o} \tag{4.58}$$

$$\Delta H = \varepsilon * H_o \tag{4.59}$$

Calculated values of strain and deformation for each sub-layer and the ultimate deformation of the soil column which is found by summation of deformations of each sub-layer are also shown in Table 4.16 for both cases of SWCC corrected and uncorrected for volume change.

Table 4.16. Final conditions (time 15,000 days) found from transient coupled analysis including final void ratio and deformation

	Final "e"		**ε=Δe/(1+eo)**		**ΔH=Ho*ε (m)**	
Sub-layer No.	Corrected	Uncorrected	Corrected	Uncorrected	Corrected	Uncorrected
1	0.77597	0.78002	0.0092	0.0115	0.0458	0.0573
2	0.77643	0.77867	0.0086	0.0098	0.0428	0.0492
3	0.77690	0.77908	0.0080	0.0092	0.0399	0.0460
4	0.77737	0.77954	0.0074	0.0086	0.0369	0.0431
5	0.77764	0.77981	0.0067	0.0079	0.0334	0.0395
6	0.77784	0.78001	0.0059	0.0072	0.0297	0.0358
7	0.77788	0.78005	0.0051	0.0063	0.0255	0.0317
8	0.77770	0.77988	0.0042	0.0054	0.0208	0.0269
9	0.77729	0.77877	0.0031	0.0039	0.0154	0.0195
10	0.77561	0.77783	0.0013	0.0025	0.0064	0.0126
Total Deformation					**0.2964**	**0.3616**

It can be seem from the Table 4.16 that the deformation for the case of SWCC that is uncorrected for soil volume change is larger than the case in which SWCC is corrected for soil volume change. This is expected as for the case that SWCC is uncorrected for soil volume change; the final soil suction is smaller within the soil profile compared to the case in which SWCC is corrected for soil volume change.

The values of deformation found from coupled and uncoupled analyses were also compared against each other, as shown in Table 4.17.

Table 4.17. Deformation values found by transient uncoupled and coupled analyses using CODE-BRIGHT for Colorado soil with top BC fixed flux of 5.0E-4 at steady-state condition (15,000 days)

				Deformation (m)	
Soil	**Top BC Fixed Flux (m/day)**	**SWCC**	**Program Used**	**Uncoupled Analyses**	**Coupled Analyses**
Colorado	5.00E-04	Corrected	CODE-BRIGHT	0.2729	0.2964
Colorado	5.00E-04	Uncorrected	CODE-BRIGHT	0.2842	0.3616

Table 4.17 shows that the deformations found from the uncoupled analyses are larger than the ones found from the coupled analyses. This is due to the fact that in the coupled analyses another factor is added to the analysis and that is the term $a_1 \Delta \ln(-p')$ in the equation presented for coupled analysis by CODE-BRIGHT. This term is ignored in the uncoupled (i.e. flow only) analysis and that is the reason why the deformations found by the uncoupled analysis are smaller.

It should also be mentioned that for Colorado soil which unlike Oil Sands tailings does not exhibit extreme values of volume change upon wetting and drying, the difference in the estimated amounts of deformation for volume corrected and uncorrected SWCC's is not very large (30cm versus 36cm for the case of the coupled analysis, as

shown in Table 4.16). However, this difference is expected to be a lot more pronounced for soils with extreme volume change potential such as Oil Sands tailings. Therefore, it is recommended that the volume corrected SWCC's to be used for the soils with extreme expansion potential (e.g. Oil Sands tailings).

Another estimation of deformation (heave) was performed for the time 7,000 days (~19 years) since the start of the wetting of the soil from the top using fixed flux of 5.0E-4 m/day. These results were obtained from coupled flow-deformation analyses done by CODE-BRIGHT. Figure 4.52 shows the suction profile for both corrected and uncorrected case at 7,000 days. It can be seen that the wetted front has progressed more for the case of corrected SWCC due to its higher k_{unsat} values.

Figure 4.53 shows the void ratio profile at 7,000 days for both corrected and uncorrected cases obtained from coupled flow-deformation analyses done by CODE-BRIGHT.

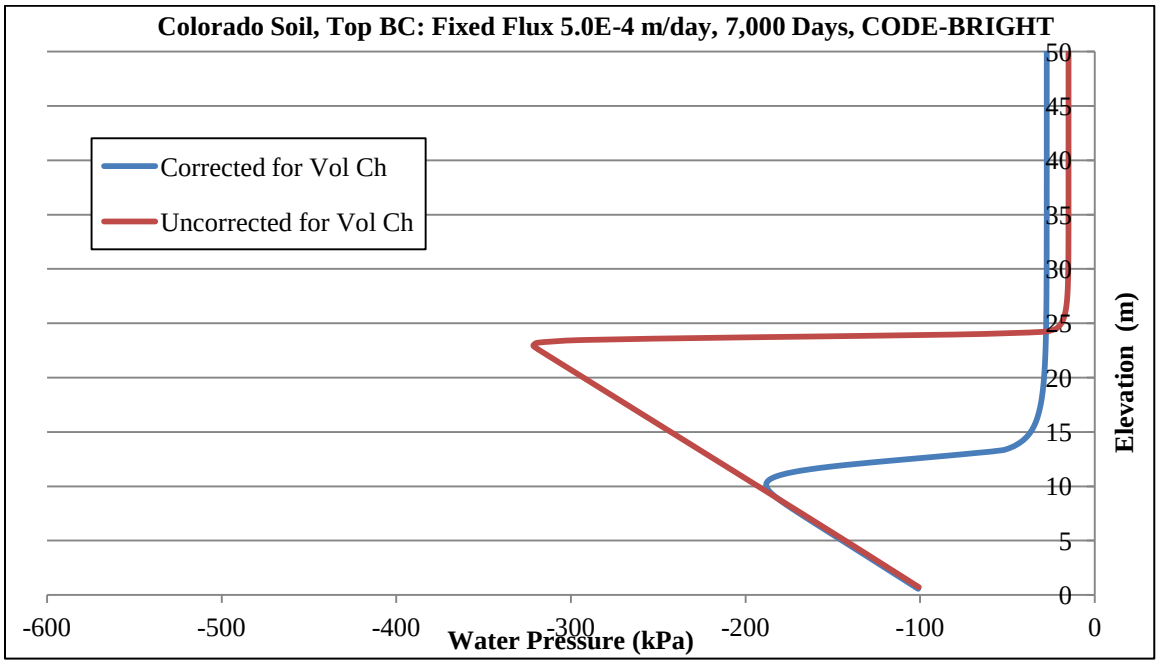

Figure 4.52. Water pressure versus elevation at 7,000 days for Colorado soil with SWCC corrected (AEV= 90kPa) and uncorrected (AEV= 60kPa) for volume change and top fixed flux of 5.0e-4 m/day using CODE-BRIGHT. The soil profile has not become fully saturated at the time of 7,000 days

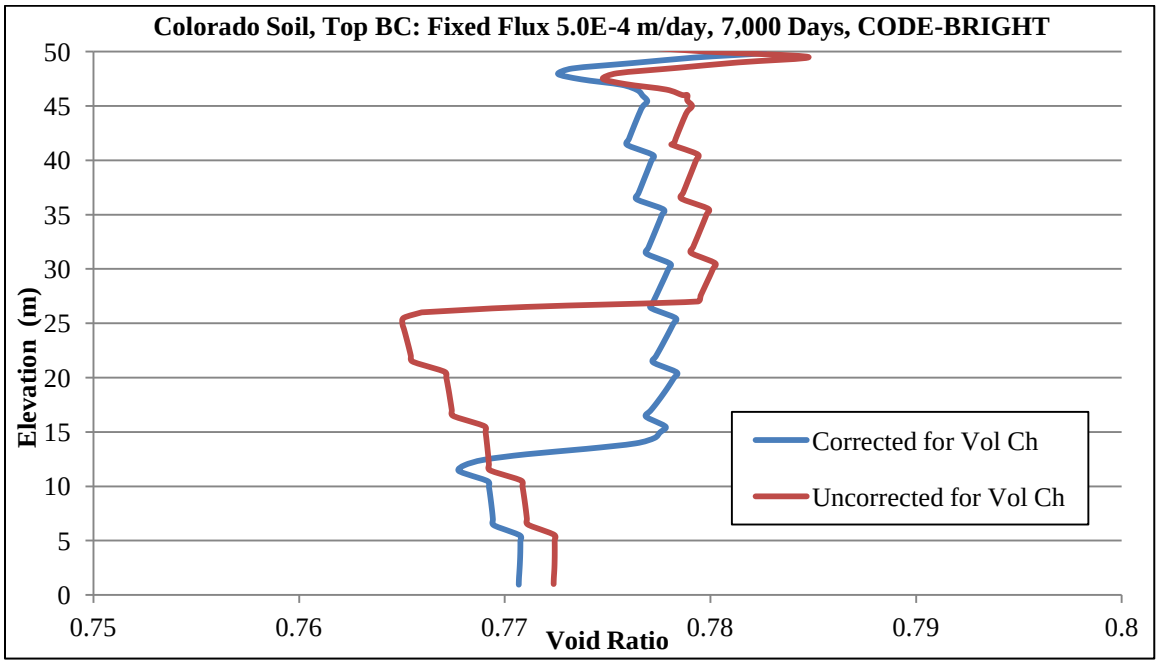

Figure 4.53. Void ratio versus elevation at 7,000 days for Colorado soil with SWCC corrected (AEV= 90kPa) and uncorrected (AEV= 60kPa) for volume change and top

fixed flux of 5.0e-4 m/day using CODE-BRIGHT. The soil profile has not become fully saturated at the time of 7,000 days

Table 4.18 shows the void ratio profile at 7,000 days for both corrected and uncorrected cases obtained from the couple flow-deformation analyses by CODE-BRIGHT. This table also shows the amounts of deformation (heave) for uncorrected and corrected SWCC at time 7,000 days. It can be seen that the corrected SWCC shows more deformation. It should be mentioned that for the case of long-term wetting of the soil (where the whole soil profile becomes saturated) the deformation of the uncorrected case is larger than the deformation of the corrected case. Therefore, it is difficult to determine in advance if corrected or uncorrected curves will lead to higher suction values and deformation within the profile.

Table 4.19 compares amounts of heave found from transient coupled and uncoupled analyses at time 7,000 days performed by CODE-BRIGHT. It can be seen that there is a very good agreement between the results found from coupled and uncoupled analyses for both corrected and uncorrected SWCC's.

Table 4.18. Void ratio profile versus elevation and total deformation (heave) for time 7,000 days obtained from transient coupled analysis using CODE-BRIGHT

	Final "e"		ε=Δe/(1+eo)		ΔH=Ho*ε (m)	
Sub-layer No.	Corrected	Uncorrected	Corrected	Uncorrected	Corrected	Uncorrected
1	0.77636	0.77854	0.0094	0.0106	0.0469	0.0531
2	0.77643	0.77867	0.0086	0.0098	0.0428	0.0492
3	0.77690	0.77912	0.0080	0.0092	0.0398	0.0462
4	0.77736	0.77957	0.0074	0.0086	0.0369	0.0431
5	0.77762	0.77375	0.0067	0.0045	0.0333	0.0224
6	0.77778	0.76581	0.0059	0.0009	0.0295	0.0044
7	0.77755	0.76781	0.0049	0.0006	0.0246	0.0029
8	0.77155	0.76963	0.0007	0.0004	0.0034	0.0020
9	0.76961	0.77140	0.0013	0.0003	0.0063	0.0013
10	0.77072	0.77241	0.0015	0.0015	0.0074	0.0074
Total Deformation					**0.2435**	**0.1959**

Table 4.19. Deformation (heave) values found by transient uncoupled and coupled analyses at time 7,000 days using CODE-BRIGHT for Colorado soil with top BC fixed flux of 5.0E-4

				Deformation (m)	
Soil	**Top BC Fixed Flux (m/day)**	**SWCC**	**Program Used**	**Uncoupled Analyses**	**Coupled Analyses**
Colorado	5.00E-04	Corrected	CODE-BRIGHT	0.2448	0.2435
Colorado	5.00E-04	Uncorrected	CODE-BRIGHT	0.1923	0.1959

4.11. Summary and Conclusions

Numerical modeling was performed to find the impact of correcting the SWCC for soil volume change (for soils with high volume change potential) on unsaturated flow through the soil, and hence on the rate and degree of change of soil suction in response to various imposed surface flux boundary conditions on a soil column. The rate of change in soil suction (e.g. progression of wetted front) can, in turn, have a significant effect on the amount of suction-change induced volume change of expansive soils. These effects

were assessed as a part of this study using uncoupled and coupled flow-deformation analyses.

For uncoupled analyses, the unsaturated flow only is evaluated and then the results from the flow analysis (i.e., initial and final soil suction profiles) are used as input to a separate deformation analysis. For a coupled flow-deformation analysis, however, unsaturated flow and suction-change induced deformations are solved for at the same time, considering any effect of suction change on deformation and any effect of deformation on soil suction, by solving the governing partial differential equations for flow and stress-deformation simultaneously. Three computer programs of VADOSE/W, CODE-BRIGHT, and SVFLUX were used to evaluate the effect of volume-corrected SWCC's on fluid flow through the soils and the resulting suction-change induced deformation. These computer codes have the capability of simulating saturated and unsaturated flow of water through soils and are commonly used in industry and/or academia (research projects).

The laboratory results obtained from SWCC tests on the three expansive soils of Anthem, Colorado, and San Antonio were used in the numerical modeling. One dimensional flow through a soil was simulated to study the flow through a column of soil once with the SWCC corrected and once with the SWCC uncorrected for volume change.

Uncoupled (flow only) analyses were conducted for the models in SVFLUX, VADOSE/W, and CODE-BRIGHT in order to evaluate impact of correcting SWCC on hydraulic properties of soils and the rate of change and change of soil suction in the profile, and hence soil volume change due to wetting or drying. For positive flux surface

boundary conditions, rate of progression of wetted front was studied and amount of soil expansion (heave at the surface) was determined based on the initial and final suction profiles of the soil column. For this purpose, the suction compression curves (void ratio versus log of suction) of specimens obtained from SWCC laboratory experiments on the expansive clays were utilized.

In this study, the initial condition of the modeled soil was set as unsaturated. For the cases in which the soil becomes wetted from the top by adding a positive fixed flux to the surface boundary, the suction of the soil decreases. In other words, the wetting path on the SWCC is followed as the soil becomes wetted. It was previously established that the volume corrected SWCC generally has larger AEV compared to the uncorrected SWCC. This means that in the soil with volume corrected SWCC, desaturation starts at a larger suction compared to the soil with uncorrected SWCC. That is to say, the soil with corrected SWCC stays saturated at larger suction ranges compared to the soil with uncorrected SWCC. Therefore, once the soil becomes wet and the suction decreases (i.e. wetting path on the SWCC), for the soil with corrected SWCC, the soil becomes saturated (i.e. close to AEV on SWCC) at a larger suction. Whereas, the suction within the soil with uncorrected SWCC must decrease further (compared to the soil with corrected SWCC) in order for the suction to reach AEV (i.e. saturation or close-to-saturation state). This mechanism illustrates the reason for the difference in final suction values for the cases of volume corrected SWCC and volume uncorrected SWCC when the soil becomes wetted. It should be mentioned that for a certain expansive soil and given initial head (suction) boundary conditions, the smaller final suction within the soil

profile leads to larger values of deformation. An example of generated suction profile for Colorado soil with base boundary condition set as suction of 100kPa is shown in Figure 4.54. It can be seen that if the model is allowed to run for long-enough time so that the soil gets fully wetted (i.e. steady-state); the generated suction is smaller for the uncorrected SWCC case compared to the corrected SWCC case. This is due to the fact that for any given expansive soil, the volume-corrected SWCC has a larger air-entry value compared to volume-uncorrected SWCC. Therefore, when the soil becomes wet (i.e. wetting path on SWCC) the volume-corrected SWCC reaches the saturated condition at a higher suction.

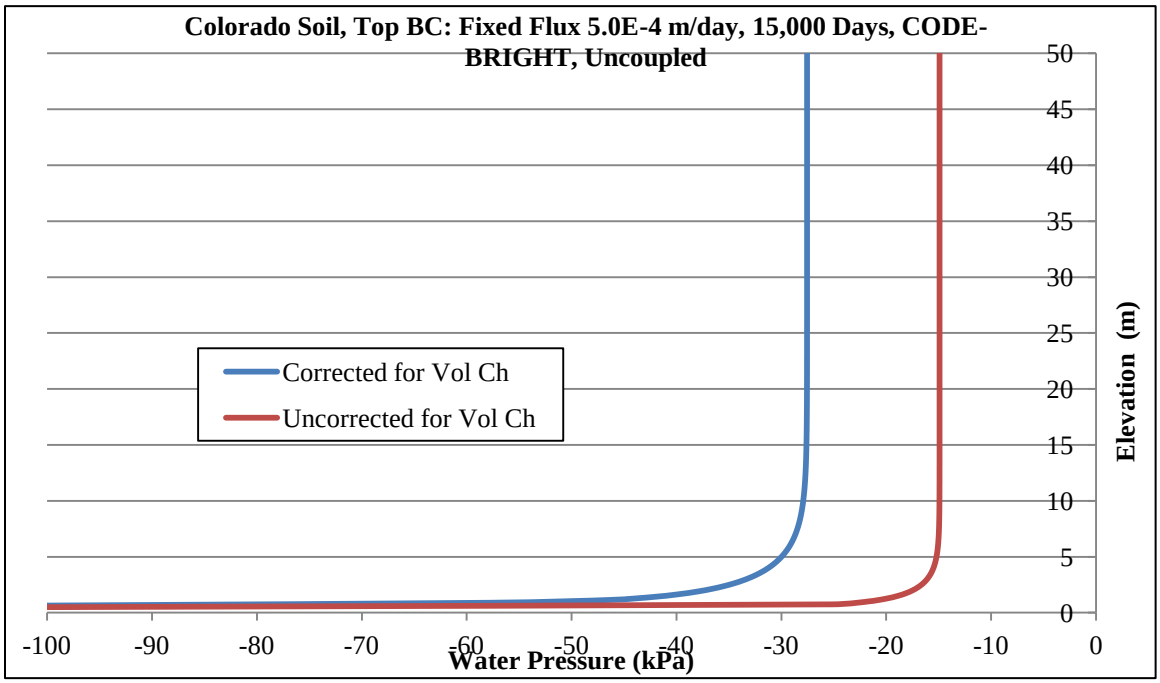

Figure 4.54. Water pressure versus elevation at steady-state condition (time: 15,000 days) for Colorado soil with SWCC corrected (AEV= 90kPa) and uncorrected (AEV= 60kPa) for volume change and top fixed flux of 5.0e-4 m/day using CODE-BRIGHT

It was found that in the models with volume-corrected SWCC that the soil gets wet quicker (faster rate of progression of wetted front and changes in soil suction)

because the unsaturated hydraulic conductivity of the soil with corrected SWCC is higher than the unsaturated hydraulic conductivity of the same soil with volume uncorrected SWCC. Larger values of k_{unsat} result in faster water penetration through the soil.

For the times prior to the steady-state, in some portions of the soil profile, the suction of uncorrected SWCC is higher than the suction of the corrected SWCC. This is due to the fact that k_{unsat} is generally higher for corrected SWCC and hence, at a given time, the depth of wetting is generally larger for the corrected SWCC compared to uncorrected SWCC. This may lead to overall larger heave for the corrected SWCC compared to uncorrected SWCC at certain times during the analysis. Figure 4.55 shows an example which compares the depth of wetting of volume-corrected and volume-uncorrected SWCC at the time of 7,000 days for top boundary condition of fixed flux of 5.0E-4 m/day for Colorado soil. It can be seen that the depth of wetting is larger for corrected SWCC (due to higher k_{unsat} values).

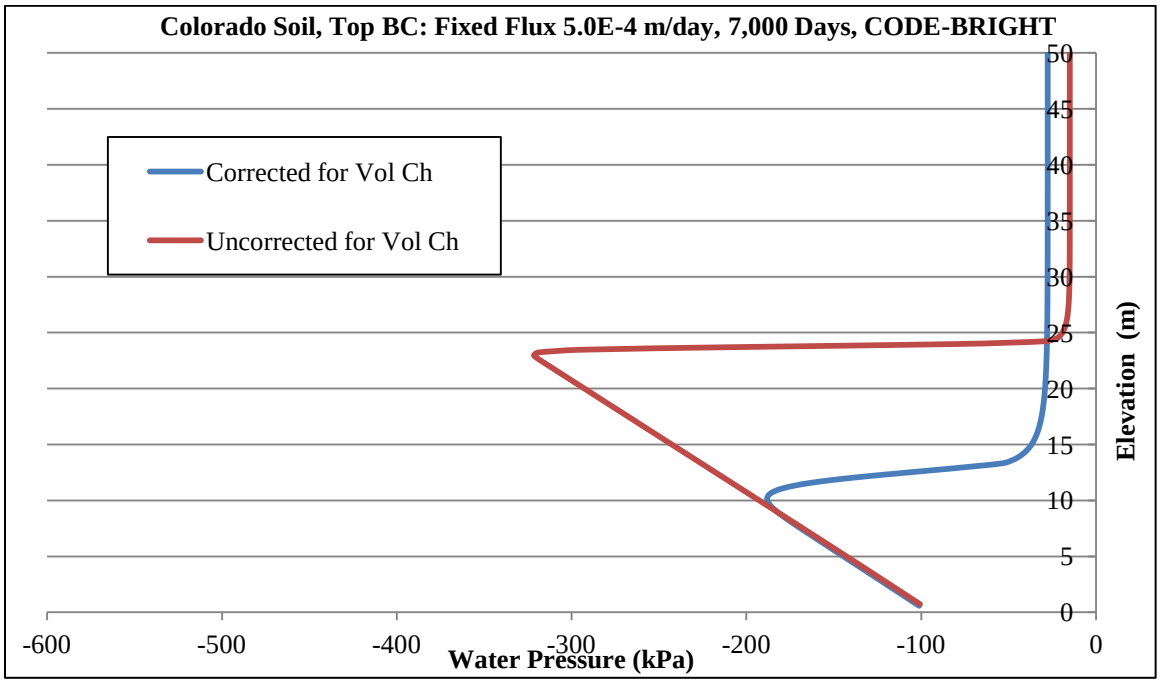

Figure 4.55. Water pressure versus elevation at time 7,000days (19 years) for Colorado soil with SWCC corrected (AEV= 90kPa) and uncorrected (AEV= 60kPa) for volume change and top fixed flux of 5.0e-4 m/day using CODE-BRIGHT

It was found that for top boundary conditions of negative flux (evaporation) that at some segments of the soil column the generated suction was larger for volume-corrected SWCC, while for some other segments of the soil column, the generated suction was larger for volume-uncorrected SWCC. This demonstrates that it is not always possible to determine in advance if corrected or uncorrected curves will lead to higher suction values, particularly for evaporation cases and for more complex surface flux boundary conditions associated with real world problems. This is believed to be a result of the high nonlinearity of the SWCC and k_{unsat} function. Figure 4.56 shows an example for top boundary condition of evaporation for Colorado soil. It can be seen that for some parts within the soil profile, the suction curve for uncorrected SWCC shows higher values compared to corrected SWCC, while at some other parts the opposite trend is noticed.

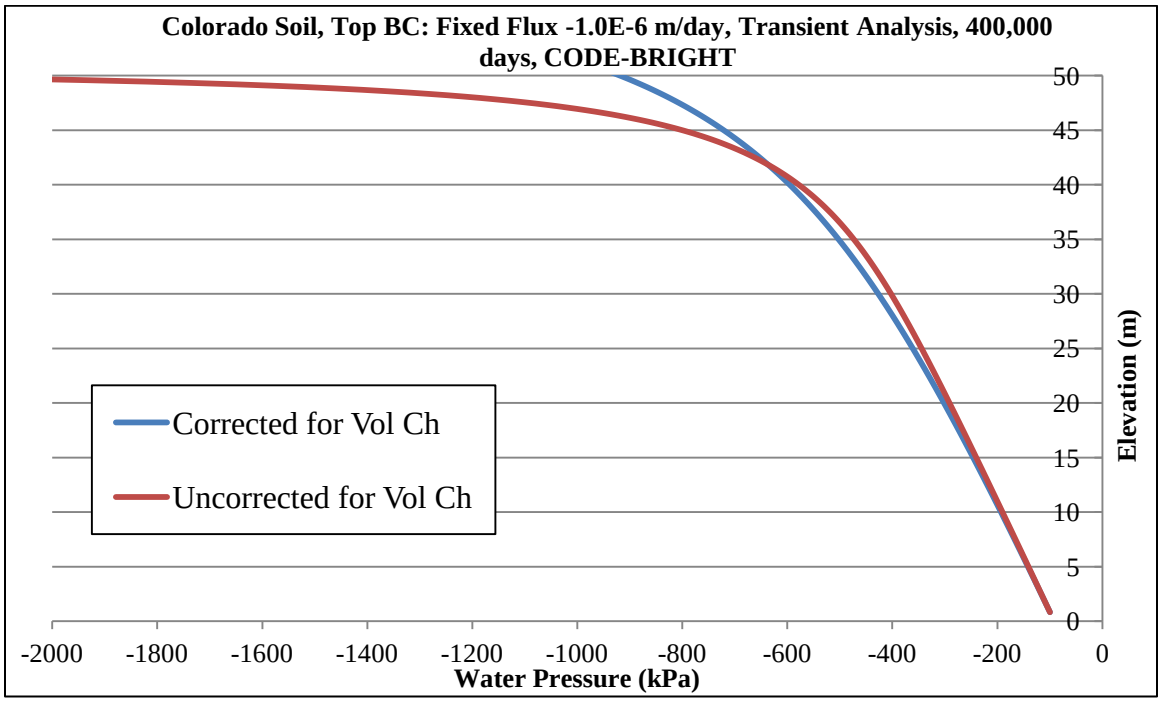

Figure 4.56. Water pressure versus elevation at time 400,000days (1095 years) for Colorado soil with SWCC corrected (AEV= 90kPa) and uncorrected (AEV= 60kPa) for volume change and top fixed flux of -1.0E-6 m/day (evaporation) using CODE-BRIGHT

A number of simulations were analyzed in which the initial conditions of the model consisted of higher suction values (i.e. suction of 1000kPa at the base and suction of 1500kPa at the top of the model). The top boundary condition of positive fixed flux was then introduced to cause soil wetting. The trends of this set of runs was found to be the same as the trends that were previously found for the models with lower suction initial condition (i.e. suction of 100kPa at the base and suction of 600kPa at the top of the model). It was found that similar to previous results, the rate of progression of wetted front is higher for corrected SWCC compared to uncorrected SWCC. A typical result for a positive fix flux surface condition is shown in Figure 4.57.

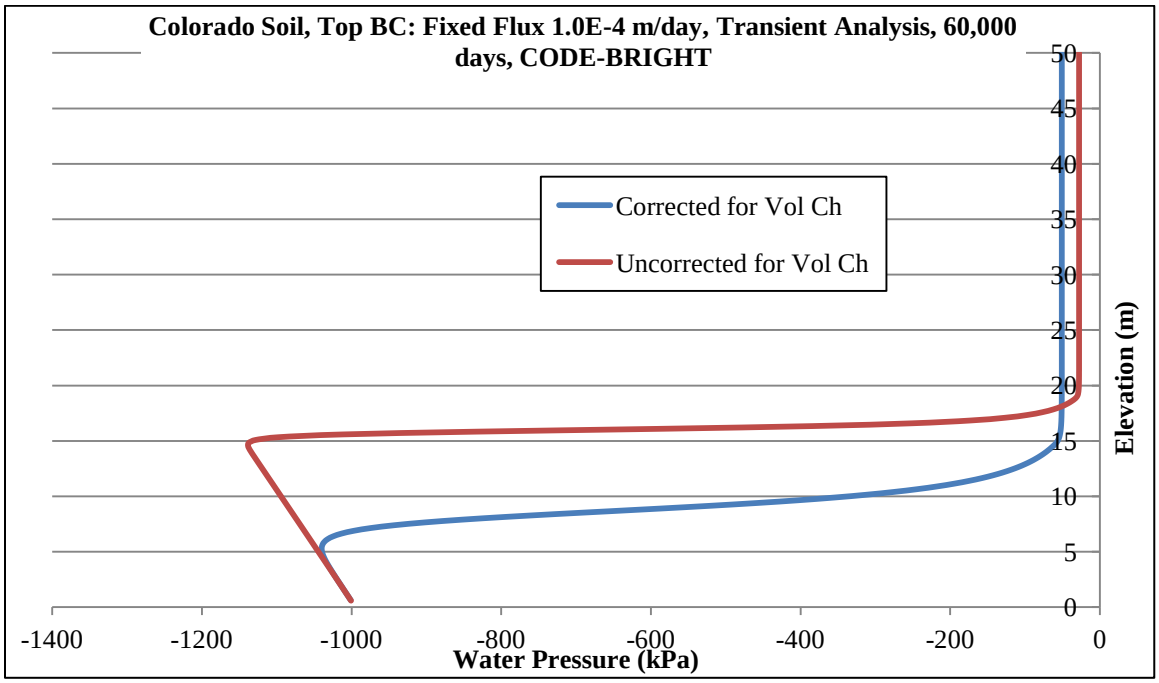

Figure 4.57. Water pressure versus elevation at time 60,000days for Colorado soil with SWCC corrected (AEV= 90kPa) and uncorrected (AEV= 60kPa) for volume change and top fixed flux of 1.0E-4 m/day using CODE-BRIGHT

Figure 4.58 shows that similar to models which were analyzed with low initial suction, for the models with higher initial suction, the final suction profile shows smaller values for uncorrected SWCC compared to corrected SWCC. This is, of course, due to the fact that the air-entry value of corrected SWCC is higher than air-entry value of uncorrected SWCC.

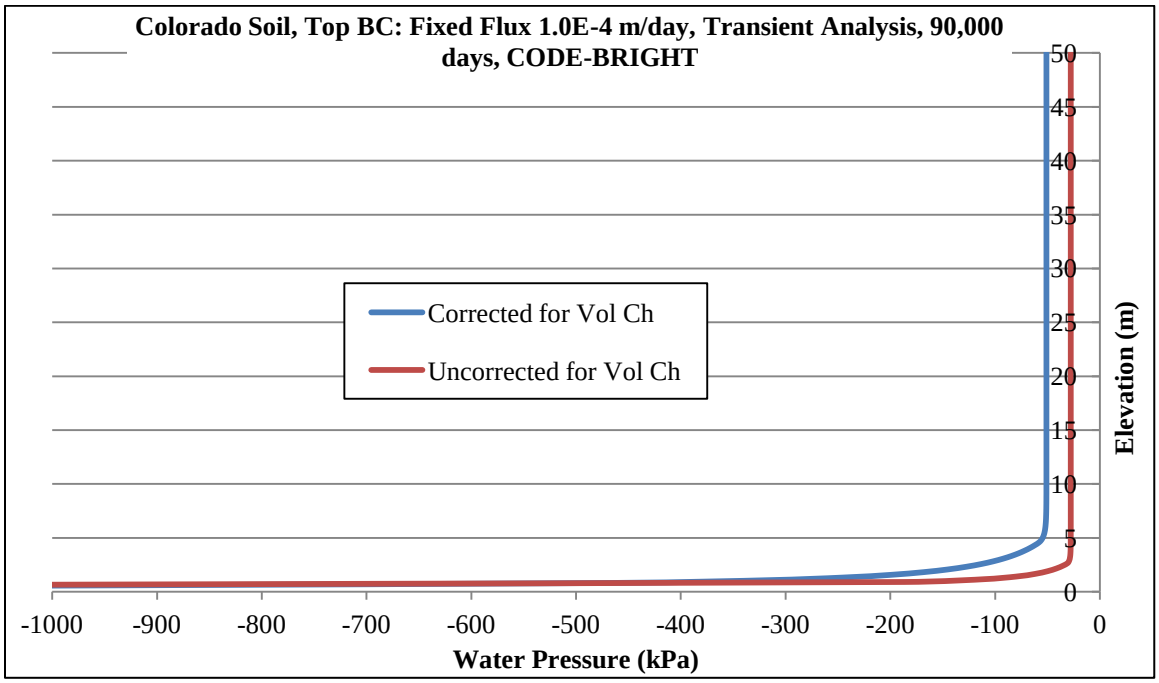

Figure 4.58. Water pressure versus elevation at time 90,000days (steady-state) for Colorado soil with SWCC corrected (AEV= 90kPa) and uncorrected (AEV= 60kPa) for volume change and top fixed flux of 1.0E-4 m/day using CODE-BRIGHT

When comparing the results generated for a certain soil by the three codes used in this study (i.e. SVFLUX, VADOSE/W, and CODE-BRIGHT), it was found that the results generated by SVFLUX and VADOSE/W were the same. However, the results generated by CODE-BRIGHT were different from the ones from SVFLUX and VADOSE/W. This is due to the fact that unlike SVFLUX and VADOSE/W which allow SWCC only in terms of volumetric water content, CODE-BRIGHT allows SWCC only in terms of degree of saturation. It was previously established that for any given expansive soil tested in this study, the key parameters (e.g. AEV and van Genuchten fitting parameters) of SWCC in terms of degree of saturation are different from those of SWCC in terms of volumetric water content. This leads to completely different SWCC's used in SVFLUX and VADOSE/W (i.e. in terms of volumetric water content) compared to the

SWCC's used in CODE-BRIGHT (i.e. in terms of degree of saturation) which results in different results generated by the programs. Figure 4.59 shows a comparison of results obtained from SVFLUX, VADOSE/W, and CODE-BRIGHT for Colorado soil with top boundary condition of 5.0E-4 m/day. The figure shows reasonable agreement among the results obtained from the three computer codes.

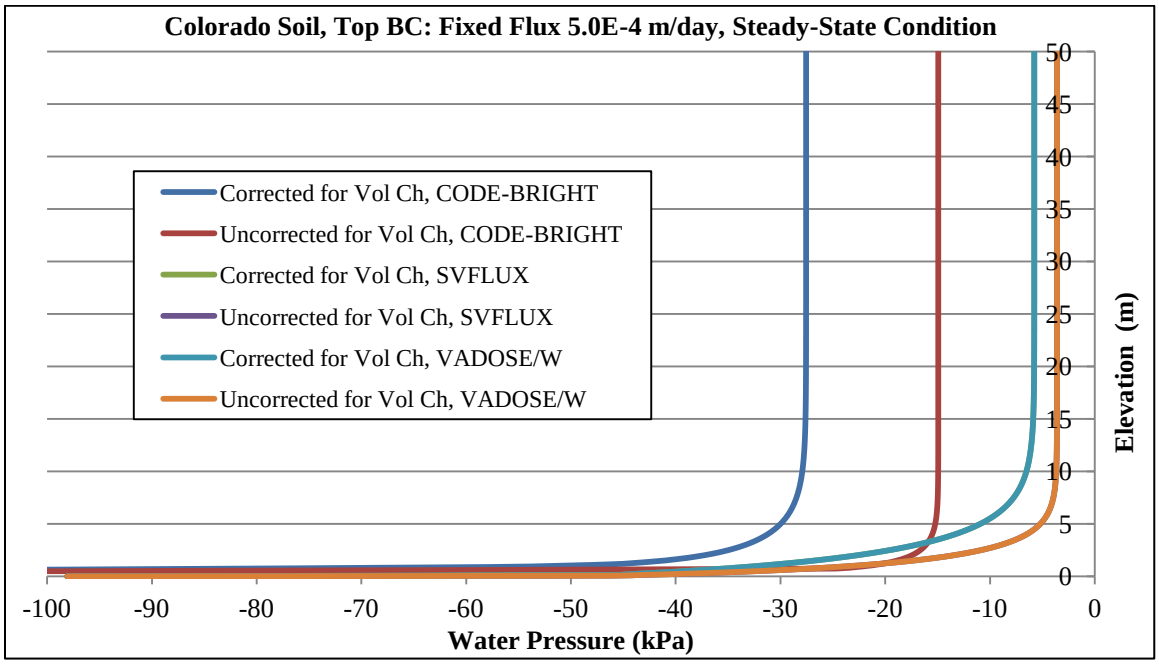

Figure 4.59. Water pressure versus elevation at steady-state condition for Colorado soil with SWCC corrected and uncorrected for volume change and top fixed flux of 5.0e-4 m/day using SVFLUX, VADOSE/W, and CODE-BRIGHT

It was found from the results that the values of wetting induced heave for the Colorado soil at time 15,000 days when the model has reached the steady-state (saturated soil profile) for both cases of SWCC corrected and uncorrected are relatively close. The amount of heave found by CODE-BRIGHT was 0.2729 meters and 0.2842 meters for volume corrected SWCC and volume uncorrected SWCC, respectively. The amount of heave found by SVFLUX was found to be 0.2908 meters and 0.2931 meters for volume

corrected SWCC and volume uncorrected SWCC, respectively. The reason that the final heave values are so similar is that the profiles were wetted to essentially full saturation in both cases (15,000 days of constant positive flux surface boundary condition leads to full wetting in both corrected and uncorrected cases).

The amounts of deformation found for uncoupled and coupled flow-deformation analyses for the Colorado soil showed close agreement for both steady-state condition (where the soil has become fully wetted) and substantially unsaturated soil cases. Tables 4.20 and 4.21 present comparison between amounts of deformation for corrected and uncorrected SWCC found by uncoupled and coupled flow-deformation analyses. It can be seen that there is close agreement between the results.

Table 4.20. Deformation values found by transient uncoupled and coupled analyses using CODE-BRIGHT for Colorado soil with top BC fixed flux of 5.0E-4 at steady-state condition (15,000 days)

				Deformation (m)	
Soil	**Top BC Fixed Flux (m/day)**	**SWCC**	**Program Used**	**Uncoupled Analyses**	**Coupled Analyses**
Colorado	5.00E-04	Corrected	CODE-BRIGHT	0.2729	0.2964
Colorado	5.00E-04	Uncorrected	CODE-BRIGHT	0.2842	0.3616

Table 4.21. Deformation (heave) values found by transient uncoupled and coupled analyses at time 7,000 days using CODE-BRIGHT for Colorado soil with top BC fixed flux of 5.0E-4

				Deformation (m)	
Soil	**Top BC Fixed Flux (m/day)**	**SWCC**	**Program Used**	**Uncoupled Analyses**	**Coupled Analyses**
Colorado	5.00E-04	Corrected	CODE-BRIGHT	0.2448	0.2435
Colorado	5.00E-04	Uncorrected	CODE-BRIGHT	0.1923	0.1959

It was found from the uncoupled and coupled flow-deformation analyses on Colorado soil with top boundary condition of fixed flux of 5.0e-4 m/day that at time 7,000 days when the models has not reached the steady-state (not fully wetted), the deformation is larger for corrected SWCC compared to uncorrected SWCC (0.245m and 0.19m for corrected and uncorrected cases, respectively). This is due to higher rate of progression of wetted front for the case of corrected SWCC compared to uncorrected SWCC. The difference in deformation of volume-corrected and volume-uncorrected cases were found to be smaller at steady-state (full saturation) condition, compared to the earlier times in the process (i.e. when the soils have not become saturated), as expected. It was also found that for the conditions of fully wetted soils, the deformation is slightly larger for volume-uncorrected SWCC (due to smaller suction values within the profile) compared to volume-corrected SWCC. However, at times prior to steady-state (when the soil is not saturated) the deformation was found to be larger for volume-corrected SWCC because the water progresses more rapidly through the volume-corrected soil profile case.

It should also be mentioned that for the expansive soils in this study, which do not exhibit extreme volume change upon wetting and drying, the difference in the estimated amounts of deformation for volume corrected and uncorrected SWCC's is not very large. However, this difference is expected to be significantly more pronounced for more highly expansive soils (e.g. higher PI soils), for conditions resulting in larger changes in soil suction, and also for any extremely high volume change soils, such as slurry materials.

The effect of volume change on the shape of the SWCC, including AEV and slope in the transition zone, is clearly demonstrated, and when volume change corrections

are not made, it results in an error in the AEV and slope of the SWCC. However, it is less clear whether volume change corrections to the SWCC in estimating $k_{unsa}t$ functions leads to improved unsaturated flow results. The uncertainty results from the fact that the k_{unsat} function models have been developed using data that was not volume corrected. This may lead to existence of compensating errors in the analyses. On the other hand, most of the data used for developing and validating k_{unsat} function models was not on clays, but rather on silts and sands and materials with no significant volume change. Therefore, correcting the SWCC's for volume change may be a reasonable practice for soils with high volume change potential (such as expansive soils and slurry specimens). More studies are definitely needed in this area to evaluate the effect of change on SWCC key parameters, particularly AEV and slope in transition zone, on the unsaturated flow properties (k_{unsat} versus suction) of high volume change soils. The study here on effects of volume change on SWCC's, k_{unsat} functions, and unsaturated flow/deformation analyses represents only a start on understanding the complex issues at play for unsaturated flow/deformation modeling of high volume change soils.

Chapter 5

NUMERICAL MODELING OF OIL SANDS TAILINGS

5.1. Introduction

Computer codes VADOSE/W, SVFLUX, and CODE-BRIGHT were used to model one-dimensional flow through a soil column of oil sands tailings. The geometry and initial and boundary conditions for oil sands tailings modeling were the same as the models for expansive soils analyses described in Chapter 4.

The properties of Oil Sands tailings were obtained from the studies that were previously conducted by Fredlund and Houston (2013), and Fredlund et al. (2011). Fredlund et al. (2011) presented some of the properties of oil sands tailings. The authors measured and established SWCC's of Oil Sands tailings that were mixed with 10% sand and 45% sand. The material with 10% sand was found to have plastic and liquid limits of 30 and 55, respectively (PI= 25). The material with 45% sand was found to have plastic and liquid limits of 15 and 38 (PI= 23) (Fredlund et al., 2011). The authors mentioned that approximately 60% of the material classifies as clay size particles.

The SWCC's of oil sands tailings were established by drying SWCC testing of the slurry specimens. The initially saturated slurry specimens of oil sands tailings exhibit extreme volume change upon increase in suction. Slurry specimens of oil sands tailings exhibit shrinkage as suction is increased, including at suction values smaller than air-entry value when the specimen is still saturated. Volume changes that occur at suctions smaller than the air-entry value can be quite significant for the oil sands, and therefore affect the k_{sat} value of these specimens. It is recommended that the value of k_{sat} be

corrected for changes in void ratio (e) that occurs at small suctions where the specimen is still saturated. The Kozeny-Carman equation can be used for correcting the k_{sat} at suctions smaller than air-entry value. The Kozeny-Carman equation relates the hydraulic conductivity to void ratio of the soil. This equation was proposed by Kozeny (1927) and later modified by Carman (1937, 1956). One of the most commonly used forms of this equation is as follows:

$$k = C \frac{g}{\mu_w \rho_w} \frac{e^3}{S^2 G_s^2 (1+e)} \tag{5.1}$$

where k is the hydraulic conductivity, C is a constant, g is the gravitational constant, μ_w is the dynamic viscosity of water, ρ_w is the density of water, G_s is the specific gravity of solids, S is the specific surface, and e is the void ratio. This equation proposes that for a given soil, there should be a linear relationship between k and $\frac{e^3}{(1+e)}$. Another correlation that can be used for this correction is one that correlates the hydraulic conductivity to e^2.A study by Tse (1985) describes that hydraulic conductivity of clayey soils is correlated to the squared void ratio (i.e. e^2). Tse (1985) plotted measured amounts of k versus e for a number of clays and found that hydraulic conductivity is correlated to e^2.

Although it is recommended to correct the k_{sat} for changes in void ratio, none of the computer codes used in this study (i.e. VADOSE/W, SVFLUX, and CODE-BRIGHT) has the capability to do corrections for k_{sat} as the volume of slurry oil sands tailings changes at suctions smaller than the air-entry value. Therefore, as important as

this correction may be, it was not accounted for in this study because only unaltered commercial codes were used. Therefore, the results obtained on the oil sands should not be taken as indicative of actual field behavior. Rather, these are simply numerical studies on high volume change slurry material to investigate the effect of volume change corrections to the SWCC on unsaturated flow suction profiles, under the assumption that the saturated hydraulic conductivity remains unchanged throughout the process.

Tables 5.1 and 5.2 present values of saturated hydraulic conductivity and other properties of Oil Sands tailings such as void ratios at the condition of full saturation.

Table 5.1. Saturated hydraulic conductivity of Oil Sands tailings (Fredlund et al, 2011)

Soil	**Saturated Hydraulic Conductivity**		**Intrinsic Permeability**
	m/s	m/day	m^2
Oil Sands tailings	2.00E-09	0.0001728	1.857E-16

Table 5.2. Void ratio and porosity (at 100% saturated condition) of Oil Sands tailings (Fredlund et al, 2011)

Soil	**Degree of Sat**	**Gs**	**w at Saturation**	**$e=G_s*w/S$**	**n=e/(1+e)**
Oil Sands tailings	1.00	2.4	0.39	0.94	0.483

As previously mentioned, in order to be consistent among the three programs of VADOSE/W, SVFLUX, and CODE-BRIGHT, the van Genuchten (1980) fit for SWCC was used for all of the analyses. One of the differences between the codes was that VADOSE/W and SVFLUX allow input of SWCC in terms of volumetric water content, but not degree of saturation, whereas CODE-BRIGHT allows input of SWCC only in terms of degree of saturation.

Van Genuchten-Mualem (1980) equation for predicting k_{unsat} function embedded in CODE-BRIGHT, VADOSE/W and SVFLUX were used to estimate k_{unsat} function of

the soils. The van Genuchten-Mualem equation used in VADOSE/W and SVFLUX allows van Genuchten SWCC fitting parameters ('a', 'n', and 'm') in terms of volumetric water content. However, the van Genuchten-Mualem equation that is utilized in CODE-BRIGHT allows van Genuchten SWCC fitting parameters ('a', 'n', and 'm') in terms of degree of saturation only. It was established in Chapter 3, that for a given expansive soil, the SWCC in terms of degree of saturation may have different fitting parameters than the SWCC in terms of volumetric water content. The van Genuchten-Mualem equation used in VADOSE/W and SVFLUX uses SWCC in terms of volumetric water content and its saturated hydraulic conductivity and generates estimation for k_{unsat} function. In CODE-BRIGHT, however, the Van Genuchten-Mualem equation uses SWCC in terms of degree of saturation (as opposed to volumetric water content in VADOSE/W and SVFLUX). Therefore, the k_{unsat} functions generated by VADOSE/W and SVFLUX are the same but they are different than the k_{unsat} functions generated by CODE-BRIGHT.

It can be seen from the figure showing k_{unsat} functions (such as Figure 5.3) that the values of k_{unsat} are larger for the cases in which SWCC is corrected for soil volume change (in which case AEV was found to be larger than uncorrected SWCC). Since the SWCC that is corrected for soil volume change generally has a higher air-entry value (shown in Figures such as 5.1 and 5.2), the desaturation of this soil starts at higher suctions which means that the decrease in soil hydraulic conductivity related to desaturation occurs at higher suctions. This leads to larger k_{unsat} values for volume corrected SWCC, on average, compared to the uncorrected SWCC case. This means that for oil sands tailings, if the SWCC is corrected for soil volume change the estimated

unsaturated hydraulic conductivity will be larger compared to the case in which the SWCC is not corrected for soil volume change, and therefore, water moves faster through the soil with volume corrected SWCC. Based on these results, it is expected for infiltration problems that the rate of progression of wetted front would be greater for the case in which the volume corrected SWCC is used.

The k_{unsat} functions used in the numerical analyses for the oil sands tailings are presented in the following sections. SVFLUX and VADOSE/W use van Genuchten-Mualem (1980) equation for predicting k_{unsat} functions of soils. Van Genuchten (1980) proposed the following closed form equation to describe the hydraulic conductivity of a soil as a function of matric suction:

$$k = k_{sat} \frac{\left[1-\left(a\psi^{(n-1)}\right)\left(1+\left(a\psi^{n}\right)^{-m}\right)\right]^{2}}{\left(\left(1+a\psi\right)^{n}\right)^{\frac{m}{2}}} \tag{5.2}$$

Where:

k_{sat} = saturated hydraulic conductivity,

a, n, and m = curve fitting parameters, where $n = 1/(1-m)$, or $m = (n-1)/n$ and

ψ = required suction range.

From the above equations, the hydraulic conductivity function of a soil can be estimated once the saturated conductivity and the two curve fitting parameters, ‘a’ and ‘m’ (or ‘n’) are known.

In CODE-BRIGHT by default, the consistent form of relative hydraulic conductivity with van Genuchten model-Mualem (1980) is used (Saaltink et al., 2005). The form of the equation is as below:

$$k = k_{sat}\left[\sqrt{S}\left(1-\left(1-S^{1/m}\right)^{m}\right)^{2}\right] \quad (5.3)$$

S (degree of saturation) is defined in such a way that ranges between 0 and 1, and 'm' is the van Genuchten parameter for SWCC fit which is the slope of the curve in the transition zone. The equation used by SVFLUX, VADOSE/W and CODE-BRIGHT for predicting k_{unsat} function are van Genuchten model-Mualem (1980) and are interchangeable.

Although all three computer codes use the same van Genuchten model-Mualem equation (1980) for predicting k_{unsat} function, the k_{unsat} function predicted by CODE-BRIGHT is different than the ones determined by SVFLUX and VADOSE/W. The reason for this difference is that the van Genuchten model-Mualem (1980) equation in SVFLUX and VADOSE/W uses van Genuchten parameter ('a', 'n', and 'm') that correspond to SWCC in terms of volumetric water content. However, the van Genuchten model-Mualem (1980) equation in CODE-BRIGHT uses S (degree of saturation) and 'm' parameter of SWCC in terms of degree of saturation. As it was established earlier, for a given soil that exhibits volume change, the van Genuchten parameters of SWCC in terms of volumetric water content may be different that the van Genuchten parameters of SWCC in terms of degree of saturation. This difference in van Genuchten parameters leads to differences in estimated k_{unsat} function.

The geometry of the models for oil sands tailings was the same as the geometry that was used for the expansive soils, as presented in Chapter 4 (i.e. 1mx50m).

5.2. Properties of Oil Sands Tailings

One of the soils modeled in this study was the Oil Sands tailings studied by Fredlund and presented in Fredlund and Houston (2013), and Fredlund et al. (2011). The 2011 article, "Interpretation of Soil-Water Characteristic Curves when Volume Change Occurs as Soil Suction is Changed," presents properties of Oil Sands tailings which exhibit extensive volume change upon wetting and drying.

Specific gravity of Oil Sands tailings was reported to be 2.4 and water content at saturated condition was reported to be 39% (Fredlund and Houston, 2013, and Fredlund et al., 2011). Therefore, at a condition of full saturation, the void ratio is calculated to be 0.936 (by using the equation of $S*e=G_s*w$; 100% *e= 2.4*0.39; e= 0.936).

Figures 5.1 and 5.2 show the SWCC of Oil Sands tailings in terms of volumetric water content and degree of saturation along with van Genuchten (1980) fit. These figures illustrate the large difference between the SWCC corrected for volume change and SWCC uncorrected for volume change. It can be seen that for both SWCC in terms of volumetric water content and degree of saturation, van Genuchten 'a' parameter is larger for corrected case compared to the uncorrected. This means that the air-entry value is higher for corrected SWCC.

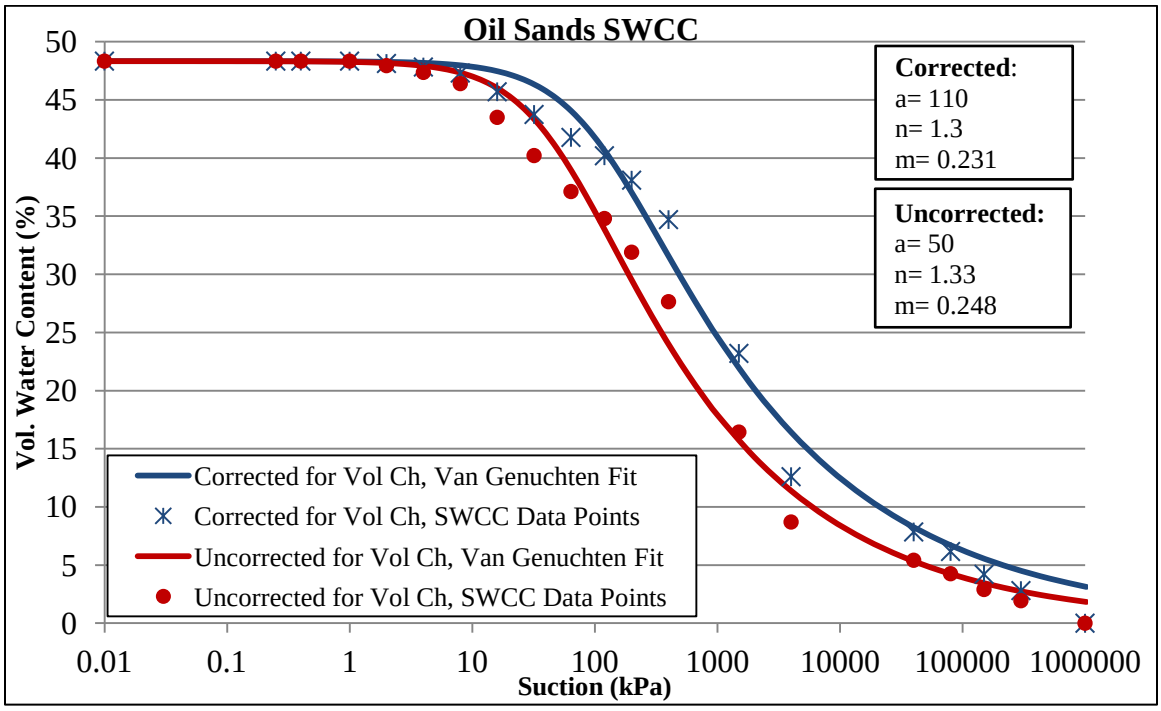

Figure 5.1. SWCC of Oil Sands tailings in terms of volumetric water content used in VADOSE/W and SVFLUX

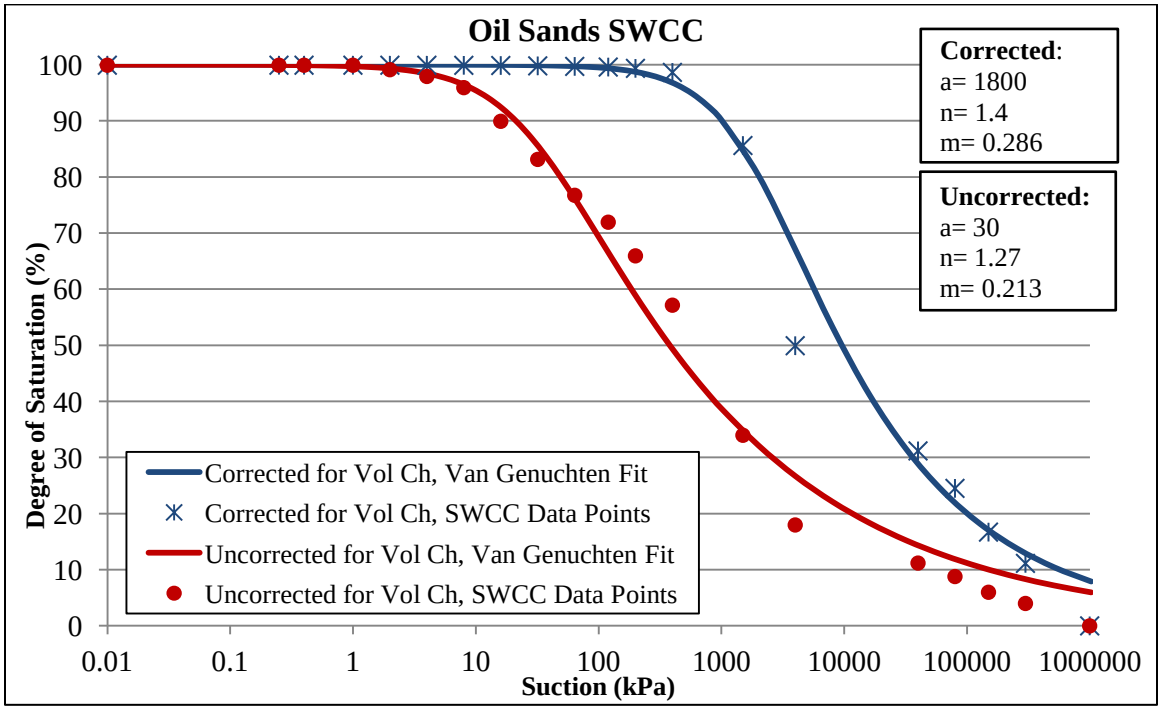

Figure 5.2. SWCC of Oil Sands tailings in terms of degree of saturation used in CODE-BRIGHT

Figure 5.3 shows hydraulic conductivity versus suction, otherwise known as k_{unsat} function for Oil Sands tailings found by van Genuchten-Mualem (1980) equations embedded in SVFLUX and CODE-BRIGHT. It can be seen that at any given suction, k_{unsat} is higher for corrected SWCC.

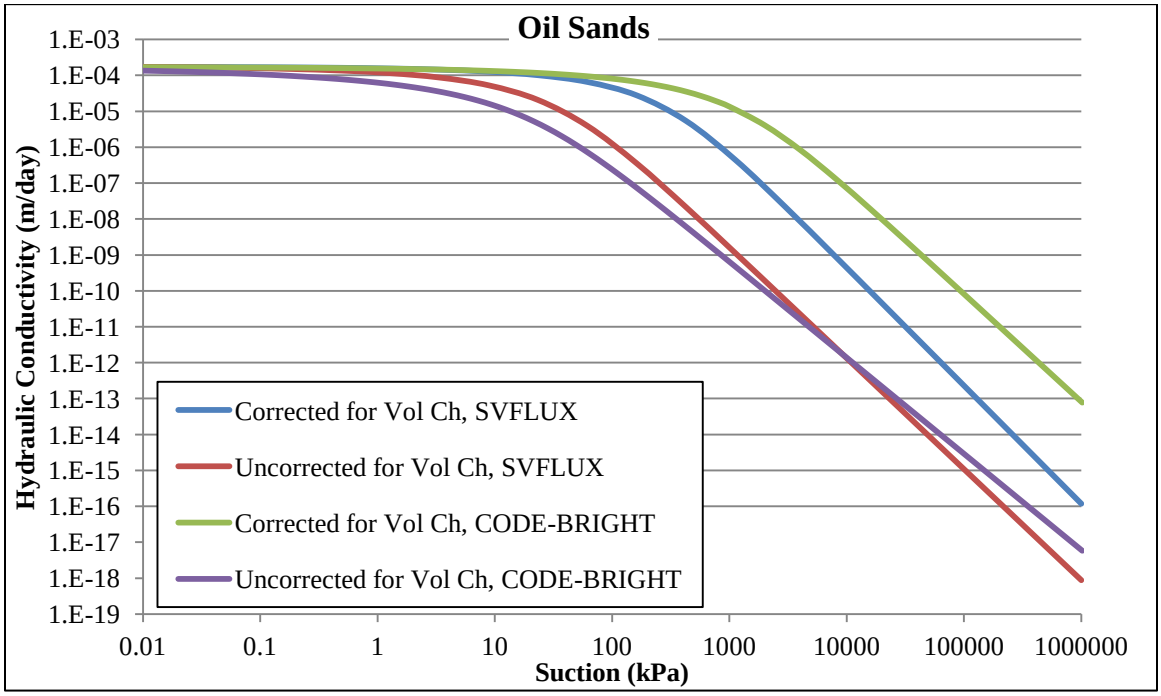

Figure 5.3. k_{unsat} function of Oil Sands tailings estimated by SVFLUX and CODE-BRIGHT

5.3. Boundary Conditions

Specifying conditions on the boundaries of a problem is one of the key components of a numerical analysis. The boundary condition of this soil column were set in the way that the left and right (vertical) sides have no flow (No-flux boundary condition), while the bottom has various pressure head values (with majority of cases analyzed with base boundary condition of -10m) and at the top the boundary condition is either fixed flux (with values varying form much less than saturated hydraulic

conductivity ($k\text{-}_{sat}$) of the soil to values greater than $k\text{-}_{sat}$) or fixed head of 1m. The boundary conditions used for the modeling Oil Sands tailings are shown in Table 5.3.

Table 5.3. Boundary Conditions used for the modeling

Location	Condition	Amount
Top	Fixed Pressure Head (m)	1
Top	Fixed Unit Flux (m/days)	Varies
Left side	Total Flux (m^3/days)	0
Right side	Total Flux (m^3/days)	0
Bottom	Pressure Head (m)	Varies (e.g.-10)

5.4. Uncoupled Analyses of Oil Sands Tailings

Uncoupled (flow only) analyses were conducted for the models based on Oil Sands tailings in SVFLUX, VADOSE/W, and CODE-BRIGHT in order to evaluate the impact of volume change-corrected SWCC on hydraulic properties of soils and the rate of changes in soil suction, degree of wetting, and hence soil volume change due to wetting for expansive clays. The rate of changes in soil suction was studied and the amount of suction-change induced deformation was determined based on the generated suction profile. For this purpose, suction compression curves (void ratio versus suction) of Oil Sands tailings obtained from the research previously done by Fredlund and Houston (2013), and Fredlund et al. (2011) was used.

For the steady-state uncoupled analyses, boundary conditions were defined for the model. These boundary conditions included the flow/head conditions explained in earlier sections of this chapter. The boundary conditions were set in the way that the left and right (vertical) sides have no flow (No-flux boundary condition), while the bottom has a constant pressure head (e.g. -10m) and at the top the boundary condition is either fixed

flux (with values varying form much less than saturated hydraulic conductivity ($k\text{-}_{sat}$) of the soil to values greater than $k\text{-}_{sat}$) or fixed head of 1m.

For transient uncoupled analyses, however, in addition to the mentioned boundary conditions, initial conditions of the model must also be defined. As the initial suction profile of the model, it was assumed that the soil is relatively dry with groundwater located 10 meters below the bottom of the soil column. Only one initial condition was considered in the numerical analyses using oil sands properties. This initial suction profile is shown in Figure 5.4. It can be seen that the initial water pressure at the bottom of the soil column is -100kPa and the initial water pressure at the top of the soil column is -600kPa. It was assumed that the suction variation between these two points changes linearly. After the initial flow/head has been set, the fixed head/fixed flux is added at the top of the soil column. By doing this, the initially unsaturated soil starts to become wet from the top. By setting appropriate time steps, progression of wetted front can be estimated through transient uncoupled analyses.

The computer codes used for modeling generate the suction profile for the various models. Based on the generated suction profile and by using the suction compression curves which is available through the research previously done by Fredlund and Houston (2013), and Fredlund et al. (2011), initial and final void ratio profiles can be estimated. By having initial and final values of void ratio, amount of wetting induced deformation was calculated.

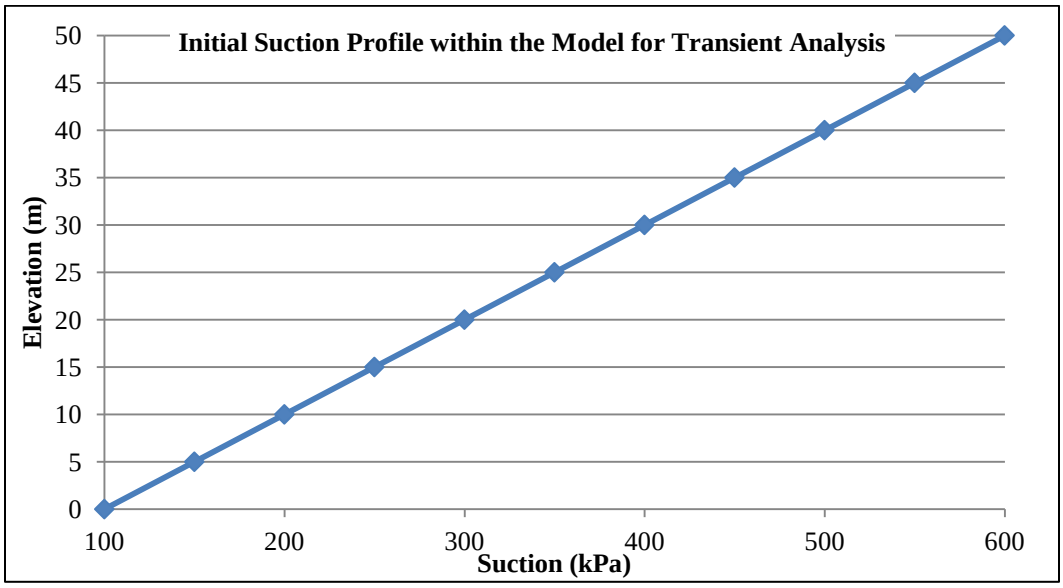

Figure 5.4. Initial suction versus elevation profile used for coupled and uncoupled transient modeling

5.5. Results of Uncoupled Analyses of Oil Sands Tailings

Transient and steady-state analyses were conducted by SVFLUX, VADOSE/W, and CODE-BRIGHT in which a soil column becomes wet (positive flux) or dry (negative flux) from top with either fixed flux or fixed head. The results of the flow-only (uncoupled) analyses are presented in this section.

Table 5.4 provides a list of numerical modeling conducted on oil sands tailings. Results of transient analyses performed using SVFLUX for the oil sands tailings (SWCC's corrected and uncorrected for volume change) are shown in Figures 5.5 and 5.6. Some slight instability of the solution in the vicinity of the wetted front can be seen in Figure 5.5, which suggests that a finer mesh refinement should have been used for those analyses. Nonetheless, the results of Figure 5.6 appear to give reasonable global trends in progression of the wetted front. These plots show the progression of wetted front and how the suction of the soil profile decreases upon wetting for top boundary

condition of fixed flux of 2e-4 m/day (slightly larger than k_{sat}). It can be seen that in the case with corrected SWCC, the soil gets wet quicker (faster rate of progression of wetted front). This is due to the fact that the unsaturated hydraulic conductivity of the soil with corrected SWCC is higher than that of uncorrected SWCC. The k_{unsat} functions of oil sands tailings were presented earlier in this chapter and it was found that the k_{unsat} values are generally greater for volume corrected SWCC's compared to uncorrected SWCC's. Higher values of k_{unsat} result in water penetrating through the soil faster than for the case in which values of k_{unsat} are lower. Figure 5.7 can be used to compare the final (steady-state condition) of the suction within the soil profile for the two cases of SWCC corrected and uncorrected for soil volume change. This condition corresponds to the long-enough time since the start of the top fixed flux, so that the soil profile has become saturated. It can be seen that although for both cases, the soil has become fully wetted; the overall suction of the soil is smaller (i.e. larger water pressure values) for the case in which SWCC is uncorrected for soil volume change.

Table 5.4. List of numerical modeling conducted for oil sands tailings

Model No.	Soil	k-sat (m/day)	Top BC: Fixed Flux (m/day)	Top BC: Fixed Head (m)	SWCC	Software	Analysis Type	Coupled/ Uncoupled
1	Oil Sands Tailings	1.73E-04	2.00E-04		Corrected	SVFLUX	Transient	Uncoupled
2	Oil Sands Tailings	1.73E-04	2.00E-04		Uncorrected	SVFLUX	Transient	Uncoupled
3	Oil Sands Tailings	1.73E-04	2.00E-04		Corrected	VADOSE/W	Transient	Uncoupled
4	Oil Sands Tailings	1.73E-04	2.00E-04		Uncorrected	VADOSE/W	Transient	Uncoupled
5	Oil Sands Tailings	1.73E-04	1.00E-04		Corrected	CODE-BRIGHT	Transient	Uncoupled
6	Oil Sands Tailings	1.73E-04	1.00E-04		Uncorrected	CODE-BRIGHT	Transient	Uncoupled
7	Oil Sands Tailings	1.73E-04	1.00E-05		Corrected	SVFLUX	Steady-State	Uncoupled
8	Oil Sands Tailings	1.73E-04	1.00E-05		Uncorrected	SVFLUX	Steady-State	Uncoupled
9	Oil Sands Tailings	1.73E-04	2.00E-05		Corrected	SVFLUX	Steady-State	Uncoupled
10	Oil Sands Tailings	1.73E-04	2.00E-05		Uncorrected	SVFLUX	Steady-State	Uncoupled
11	Oil Sands Tailings	1.73E-04	9.00E-05		Corrected	SVFLUX	Steady-State	Uncoupled
12	Oil Sands Tailings	1.73E-04	9.00E-05		Uncorrected	SVFLUX	Steady-State	Uncoupled
13	Oil Sands Tailings	1.73E-04	1.00E-04		Corrected	SVFLUX	Steady-State	Uncoupled
14	Oil Sands Tailings	1.73E-04	1.00E-04		Uncorrected	SVFLUX	Steady-State	Uncoupled
15	Oil Sands Tailings	1.73E-04	1.73E-04		Corrected	SVFLUX	Steady-State	Uncoupled
16	Oil Sands Tailings	1.73E-04	1.73E-04		Uncorrected	SVFLUX	Steady-State	Uncoupled
17	Oil Sands Tailings	1.73E-04	2.00E-04		Corrected	SVFLUX	Steady-State	Uncoupled
18	Oil Sands Tailings	1.73E-04	2.00E-04		Uncorrected	SVFLUX	Steady-State	Uncoupled
19	Oil Sands Tailings	1.73E-04	3.00E-04		Corrected	SVFLUX	Steady-State	Uncoupled
20	Oil Sands Tailings	1.73E-04	3.00E-04		Uncorrected	SVFLUX	Steady-State	Uncoupled
21	Oil Sands Tailings	1.73E-04	4.00E-04		Corrected	SVFLUX	Steady-State	Uncoupled
22	Oil Sands Tailings	1.73E-04	4.00E-04		Uncorrected	SVFLUX	Steady-State	Uncoupled
23	Oil Sands Tailings	1.73E-04		1	Corrected	SVFLUX	Steady-State	Uncoupled
24	Oil Sands Tailings	1.73E-04		1	Uncorrected	SVFLUX	Steady-State	Uncoupled

Table 5.4. (Continue) List of numerical modeling conducted for Oil Sands Tailings

Model No.	Soil	k-sat (m/day)	Top BC: Fixed Flux (m/day)	Top BC: Fixed Head (m)	SWCC	Software	Analysis Type	Coupled/ Uncoupled
25	Oil Sands Tailings	1.73E-04	1.00E-05		Corrected	VADOSE/W	Steady-State	Uncoupled
26	Oil Sands Tailings	1.73E-04	1.00E-05		Uncorrected	VADOSE/W	Steady-State	Uncoupled
27	Oil Sands Tailings	1.73E-04	2.00E-05		Corrected	VADOSE/W	Steady-State	Uncoupled
28	Oil Sands Tailings	1.73E-04	2.00E-05		Uncorrected	VADOSE/W	Steady-State	Uncoupled
29	Oil Sands Tailings	1.73E-04	9.00E-05		Corrected	VADOSE/W	Steady-State	Uncoupled
30	Oil Sands Tailings	1.73E-04	9.00E-05		Uncorrected	VADOSE/W	Steady-State	Uncoupled
31	Oil Sands Tailings	1.73E-04	1.00E-04		Corrected	VADOSE/W	Steady-State	Uncoupled
32	Oil Sands Tailings	1.73E-04	1.00E-04		Uncorrected	VADOSE/W	Steady-State	Uncoupled
33	Oil Sands Tailings	1.73E-04	1.73E-04		Corrected	VADOSE/W	Steady-State	Uncoupled
34	Oil Sands Tailings	1.73E-04	1.73E-04		Uncorrected	VADOSE/W	Steady-State	Uncoupled
35	Oil Sands Tailings	1.73E-04	2.00E-04		Corrected	VADOSE/W	Steady-State	Uncoupled
36	Oil Sands Tailings	1.73E-04	2.00E-04		Uncorrected	VADOSE/W	Steady-State	Uncoupled
37	Oil Sands Tailings	1.73E-04	3.00E-04		Corrected	VADOSE/W	Steady-State	Uncoupled
38	Oil Sands Tailings	1.73E-04	3.00E-04		Uncorrected	VADOSE/W	Steady-State	Uncoupled
39	Oil Sands Tailings	1.73E-04	4.00E-04		Corrected	VADOSE/W	Steady-State	Uncoupled
40	Oil Sands Tailings	1.73E-04	4.00E-04		Uncorrected	VADOSE/W	Steady-State	Uncoupled
41	Oil Sands Tailings	1.73E-04	-1.00E-05		Corrected	VADOSE/W	Steady-State	Uncoupled
42	Oil Sands Tailings	1.73E-04	-1.00E-05		Uncorrected	VADOSE/W	Steady-State	Uncoupled
43	Oil Sands Tailings	1.73E-04	-1.00E-06		Corrected	VADOSE/W	Steady-State	Uncoupled
44	Oil Sands Tailings	1.73E-04	-1.00E-06		Uncorrected	VADOSE/W	Steady-State	Uncoupled
45	Oil Sands Tailings	1.73E-04	-1.00E-07		Corrected	VADOSE/W	Steady-State	Uncoupled
46	Oil Sands Tailings	1.73E-04	-1.00E-07		Uncorrected	VADOSE/W	Steady-State	Uncoupled
47	Oil Sands Tailings	1.73E-04		1	Corrected	VADOSE/W	Steady-State	Uncoupled
48	Oil Sands Tailings	1.73E-04		1	Uncorrected	VADOSE/W	Steady-State	Uncoupled

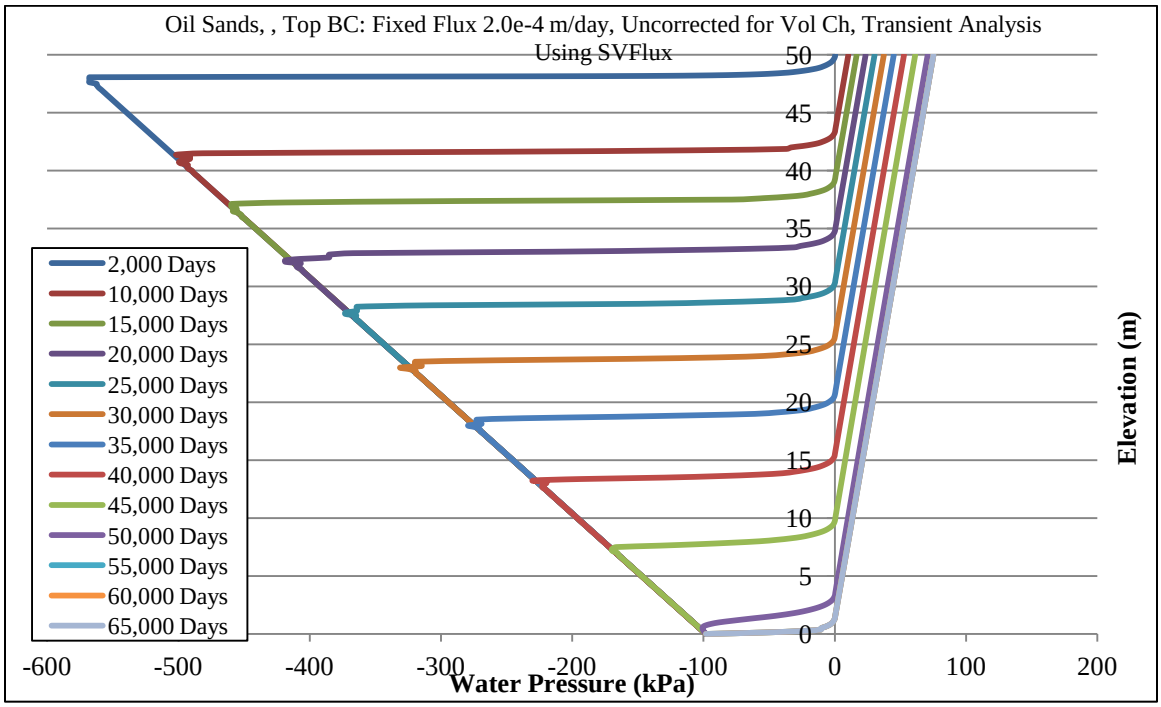

Figure 5.5. Transient analyses on Oil Sands tailings with SWCC uncorrected for volume change and top fixed flux of 2.0e-4 m/day using SVFLUX

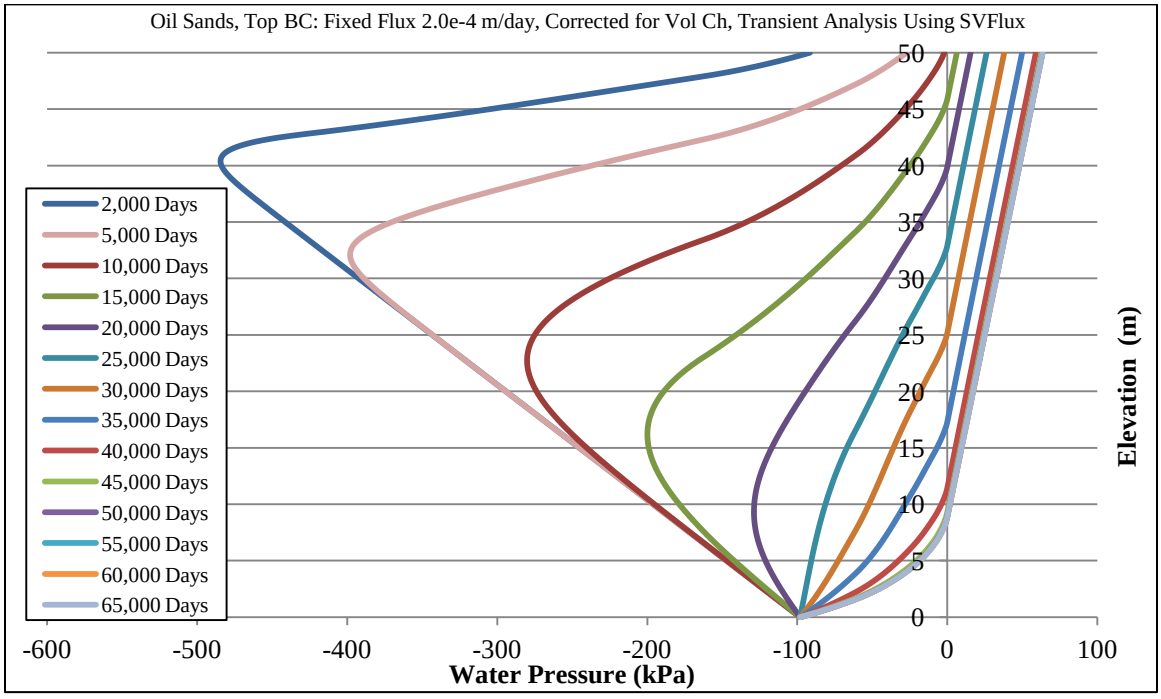

Figure 5.6. Transient analyses on Oil Sands tailings with SWCC corrected for volume change and top fixed flux of 2.0e-4 m/day using SVFLUX

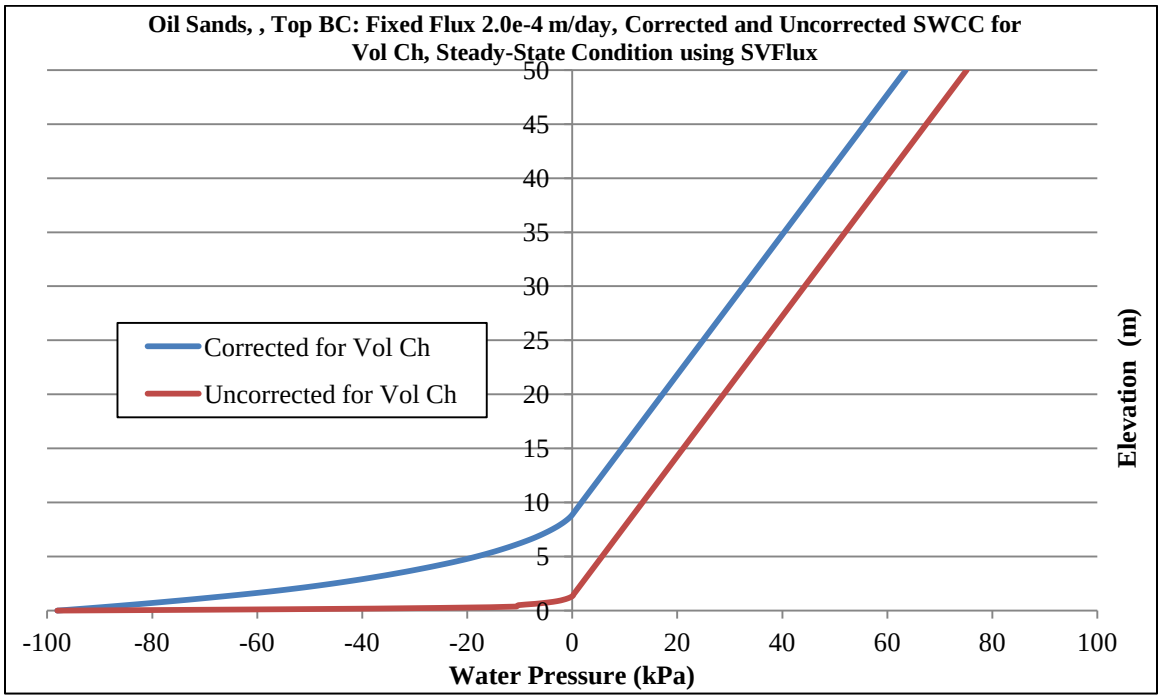

Figure 5.7. Water pressure versus elevation at steady-state condition for Oil Sands tailings with SWCC corrected and uncorrected for volume change and top fixed flux of 2.0e-4 m/day using SVFLUX

Figures 5.8 through 5.11 illustrate results of transient analyses on Oil Sands tailings using CODE-BRIGHT. In this set of runs, depth and rate of progression of wetted front were compared for SWCC's corrected and uncorrected for volume change. The top boundary condition for this set of runs was 1.0E-4 m/day which is less than saturated hydraulic conductivity of Oil Sands tailings (k_{sat}= 1.73E-4 m/day). Therefore, the final water pressure throughout the soil profile is negative, although it gets wet compared to its initial condition which has larger amounts of suction throughout the soil. It was found that rate of progression of wetted front is larger for the case in which SWCC is corrected for volume change (shown in Figures 5.8 and 5.9). It was also found that the final suction throughout the soil profile is smaller for the case in which SWCC is uncorrected for volume change.

Initial condition of the soil is unsaturated with suction of 100kPa at the bottom and suction of 600kPa at the top of the model. When the soil becomes wet from the top by adding the fixed flux, the suction of soil starts to decrease. In other words, the wetting path on the SWCC will be followed when the soil becomes wet. It was previously established that the volume corrected SWCC generally has larger air-entry value compared to the uncorrected SWCC. This means that in the soil with volume corrected SWCC, desaturation starts at a larger suction compared to the soil with uncorrected SWCC. That is to say, the soil with corrected SWCC stays saturated at larger suction ranges compared to the soil with uncorrected SWCC. Therefore, once the soil becomes wet and the suction decreases (i.e. wetting path on the SWCC), for the soil with corrected SWCC, the soil becomes saturated at a larger suction (close to air-entry value). Whereas, the suction within the soil with uncorrected SWCC should further decrease (compared to the soil with corrected SWCC) in order for the soil to reach the air-entry value (saturated condition). This mechanism illustrates the reason for the difference in generated suction values for the cases of volume corrected SWCC and volume uncorrected SWCC. It should be mentioned that for a certain expansive soil, the smaller final suction within the soil profile indicates larger deformation. This is due to the general shape of suction compression curves, in which the void ratio of the expansive soils is larger at smaller suction values. The soil deformations calculated using the final suction profile of the soil and its suction compression curve are described later in this chapter.

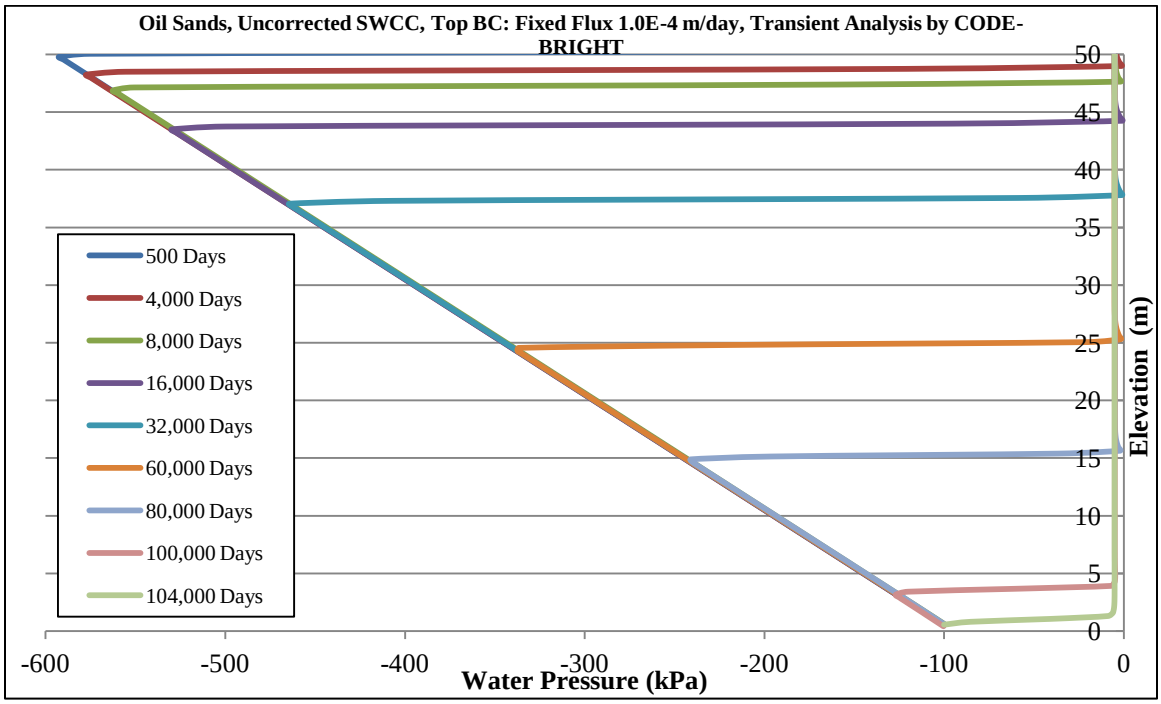

Figure 5.8. Transient analyses on Oil Sands tailings with SWCC uncorrected for volume change and top fixed flux of 1.0e-4 m/day using CODE-BRIGHT

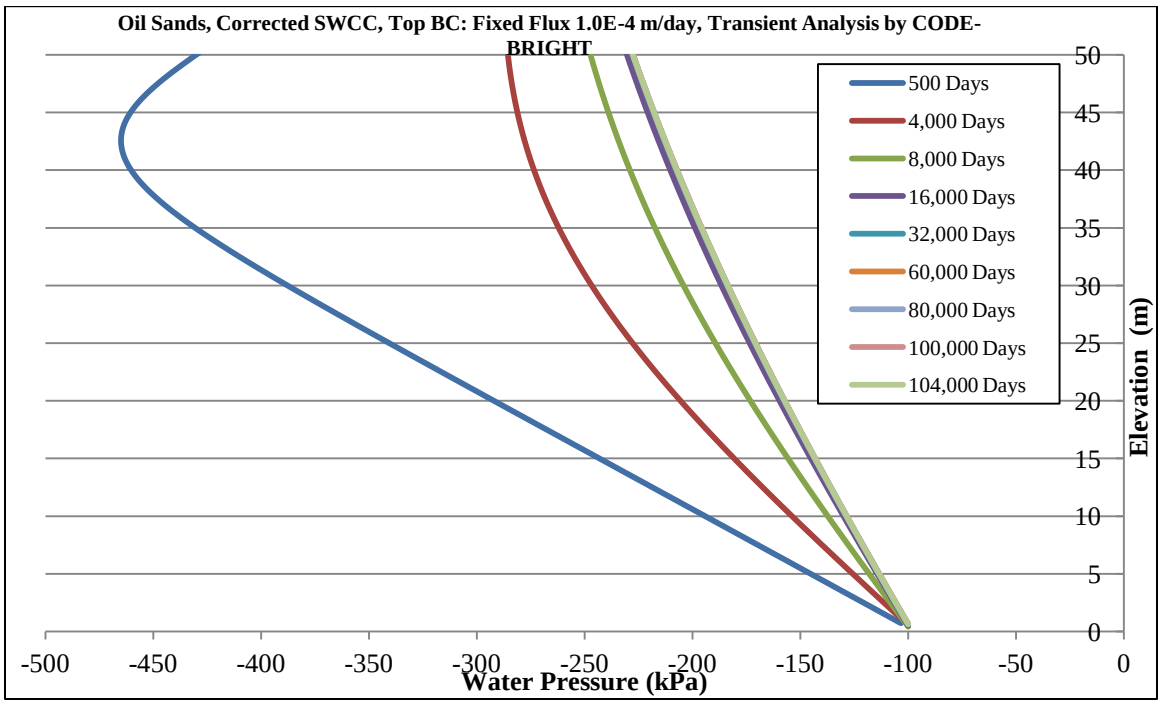

Figure 5.9. Transient analyses on Oil Sands tailings with SWCC corrected for volume change and top fixed flux of 1.0e-4 m/day using CODE-BRIGHT

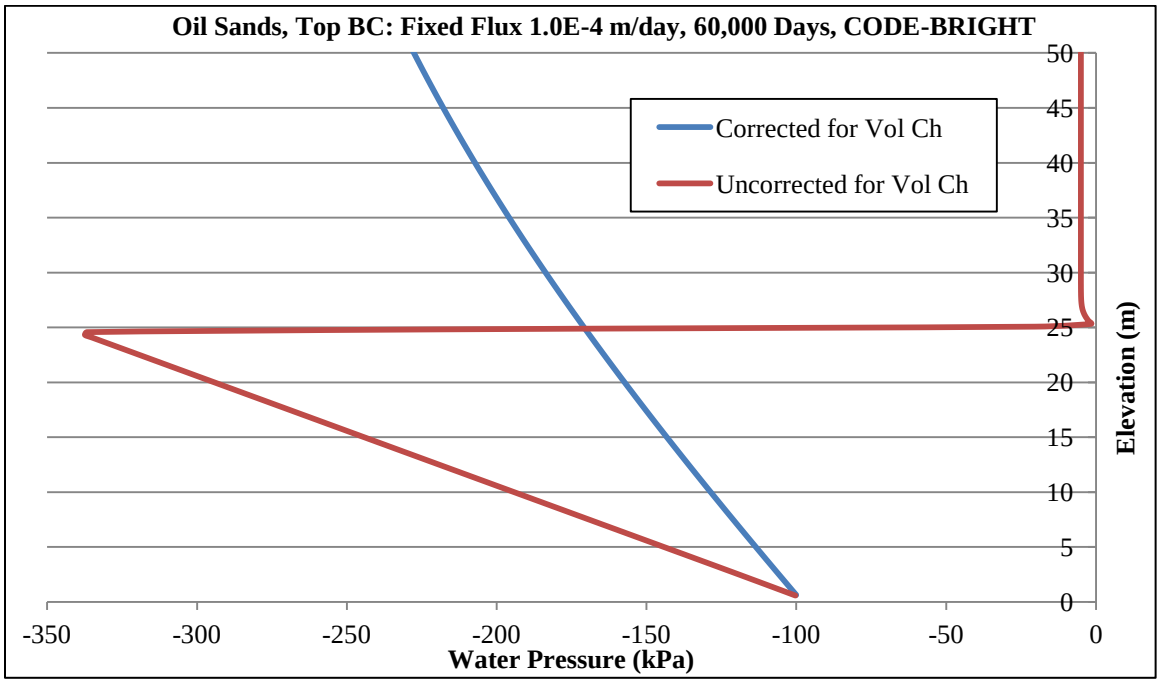

Figure 5.10. Water pressure versus elevation at time 60,000 days (164 years) for Oil Sands tailings with SWCC corrected and uncorrected for volume change and top fixed flux of 1.0e-4 m/day using CODE-BRIGHT

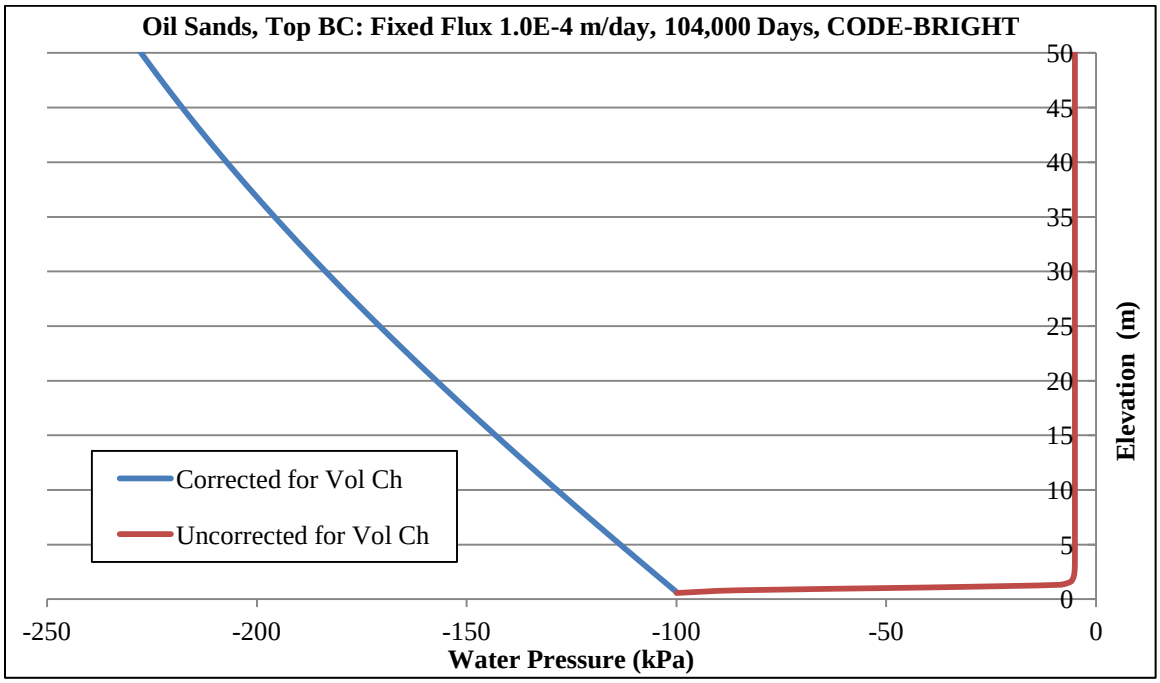

Figure 5.11. Water pressure versus elevation at steady-state condition (104,000 days) for Oil Sands tailings with SWCC corrected and uncorrected for volume change and top fixed flux of 1.0e-4 m/day using CODE-BRIGHT

It can be seen from Figure 5.10 (corresponding to 60,000 days) that the progression of wetted front is faster for corrected SWCC. The blue curve which shows the corrected case is already showing the saturated case, while for the uncorrected case (red curve) the wetted front has progressed for only about half of the soil column. It can also be seen that for some segments of the profile (e.g. between elevations 0 and 25), the suction for uncorrected SWCC is higher than corrected case. This shows that depending upon the progression of wetted front; the uncorrected curve may have higher or lower suction compared to the corrected SWCC. This makes it difficult to determine in advance if corrected or uncorrected curves will lead to higher suction values.

Figure 5.12 shows wetting of the soil column in case of Oil Sands tailings when the top boundary condition is fixed head of 1 meter. It can be seen that similar to previous

figure, for the case in which SWCC is uncorrected for soil volume change, the suction throughout the soil profile is smaller than the case in which SWCC is corrected for volume change. Other plots of water pressure versus elevation for various surface fluxes for Oil Sands tailings are presented in Appendix B of this report.

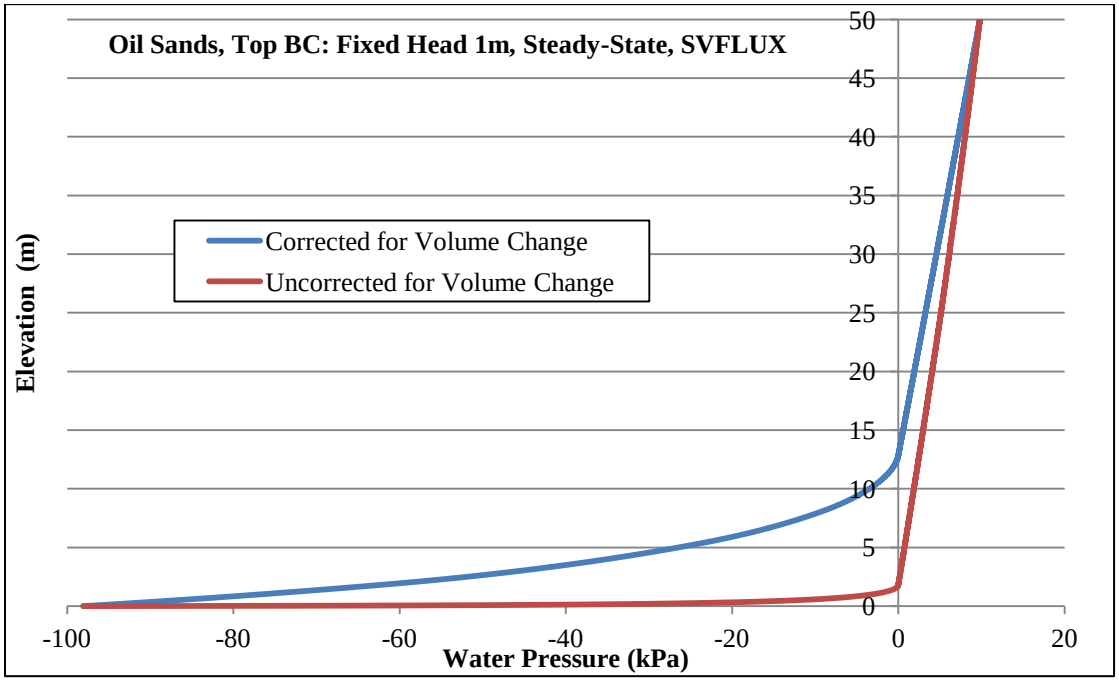

Figure 5.12. Water pressure versus elevation at steady-state condition for Oil Sands tailings with SWCC corrected and uncorrected for volume change and top fixed head of 1m using SVFLUX

Figures 5.13 and 5.14 show the results of runs with top boundary condition of -1.0E-6 m/day and -1.0E-7 m/day (i.e. evaporation) analyzed with VADOSE/W. In both of the figures, the suction is larger for uncorrected SWCC compared to corrected SWCC.

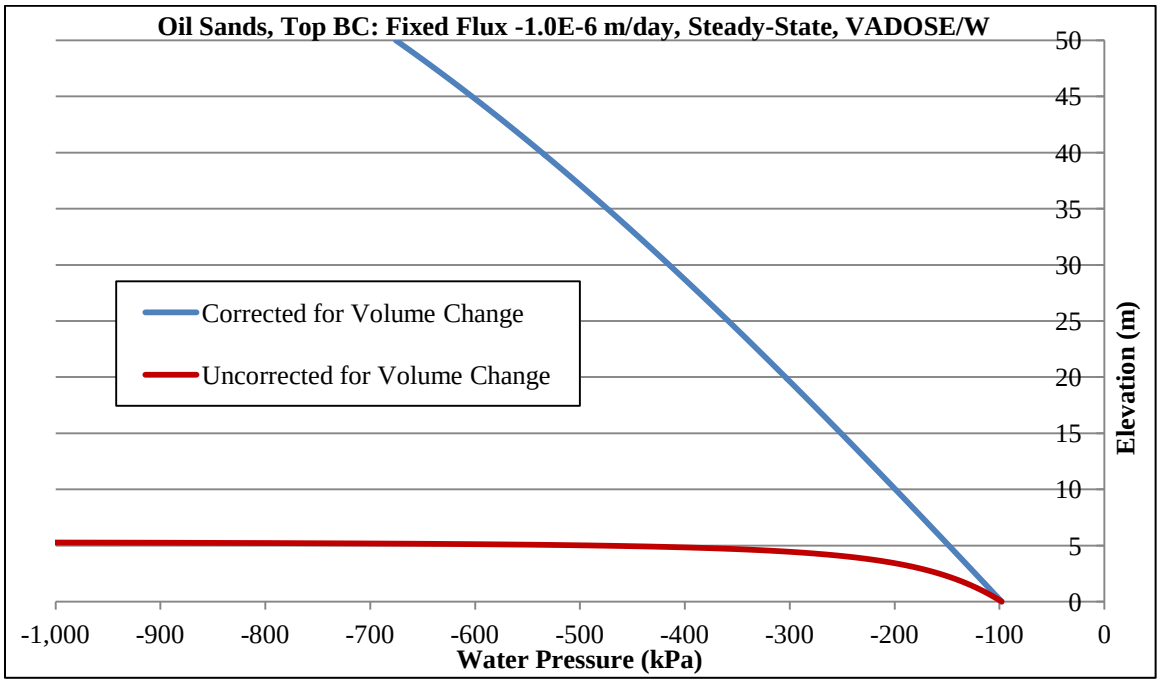

Figure 5.13. Water pressure versus depth at steady-state condition for oil sands tailings with SWCC corrected and uncorrected for volume change and top fixed flux of -1.0E-6 m/day (evaporation) using VADOSE/W

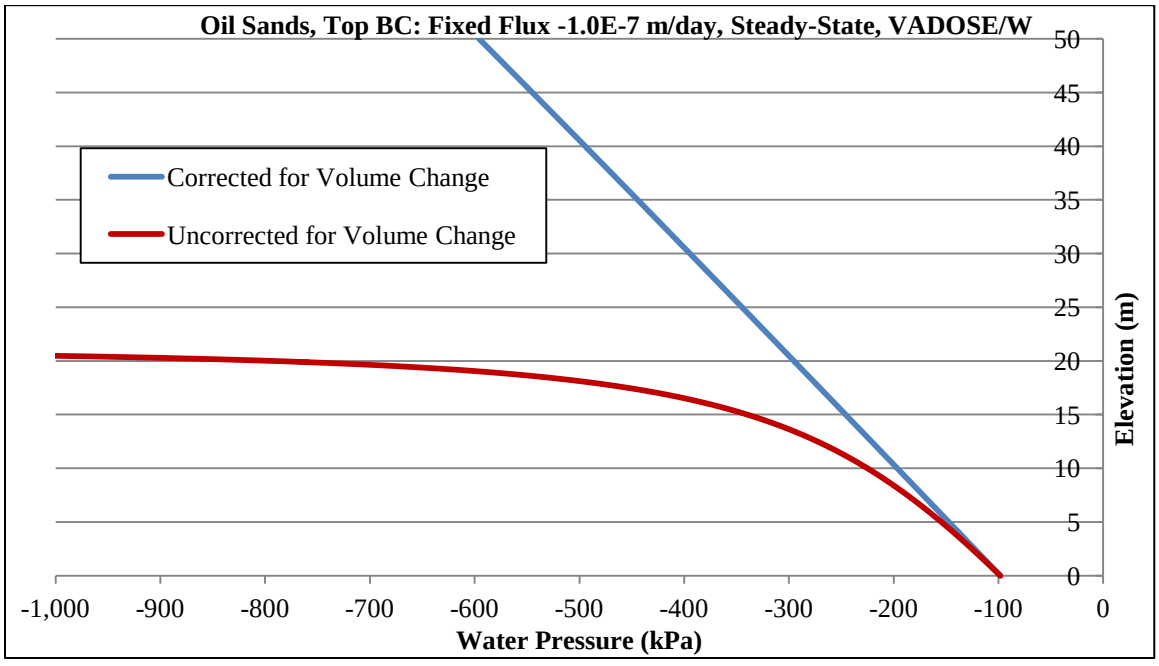

Figure 5.14. Water pressure versus depth at steady-state condition for oil sands tailings with SWCC corrected and uncorrected for volume change and top fixed flux of -1.0E-7 m/day (evaporation) using VADOSE/W

5.5.1. Deformations from Uncoupled Analyses

Results of water pressure versus elevation found from uncoupled analyses on Oil Sands tailings were used to determine the wetted induced heave. For this purpose suction compression curves that were extracted from the article by Fredlund and Houston (2013), and Fredlund et al. (2011) was used. The suction compression curves of Oil Sands tailings is shown in Figure 5.15. Although only the wetting path (resulting in expansion of the soil with decreased suction) was studied here, the more interesting path for field applications for oil sands deposits is the drying path. It must also be noted that the suction compression curve on the oil sands was determined for the drying path. Although the wetting and drying paths were assumed to be the same for the analyses presented herein, it is not evident that there would be no path dependency (i.e. it is not clear that the wetting path void ratio versus suction plot would be the same as the drying void ratio versus suction plot). Nonetheless, the oil sands properties are merely used as an example of very high volume change soils and effect of volume change corrections to SWCC – just to study trends.

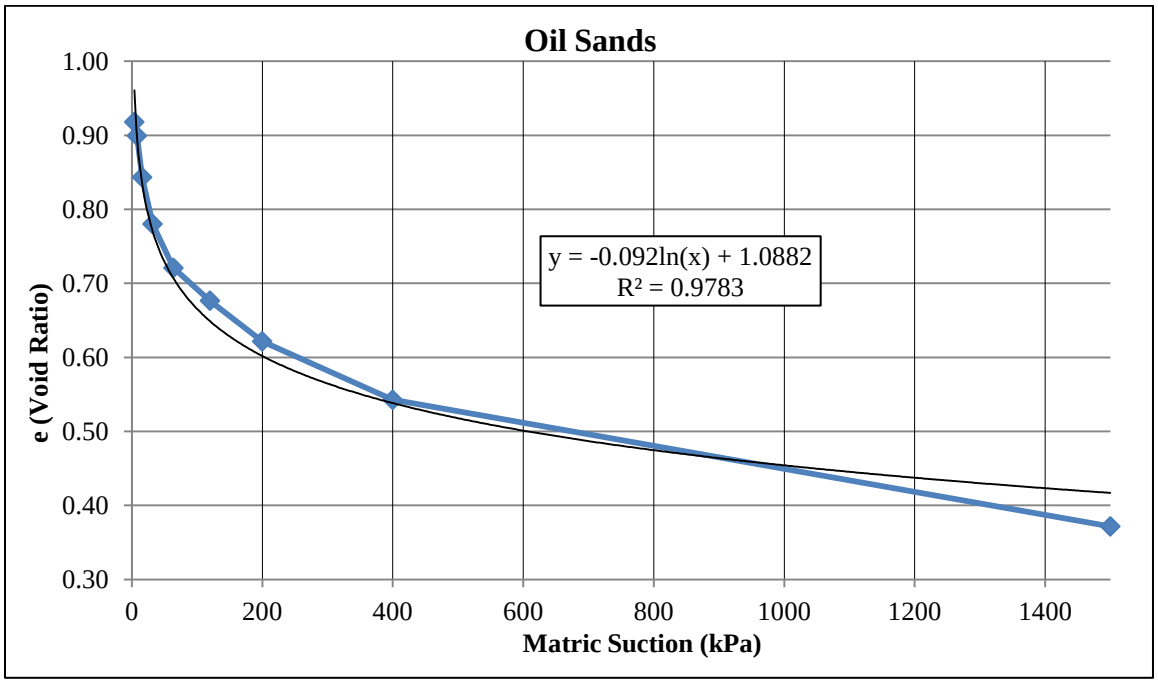

Figure 5.15. Suction compression curve for Oil Sands tailings (Fredlund and Houston, 2013, and Fredlund et al., 2011)

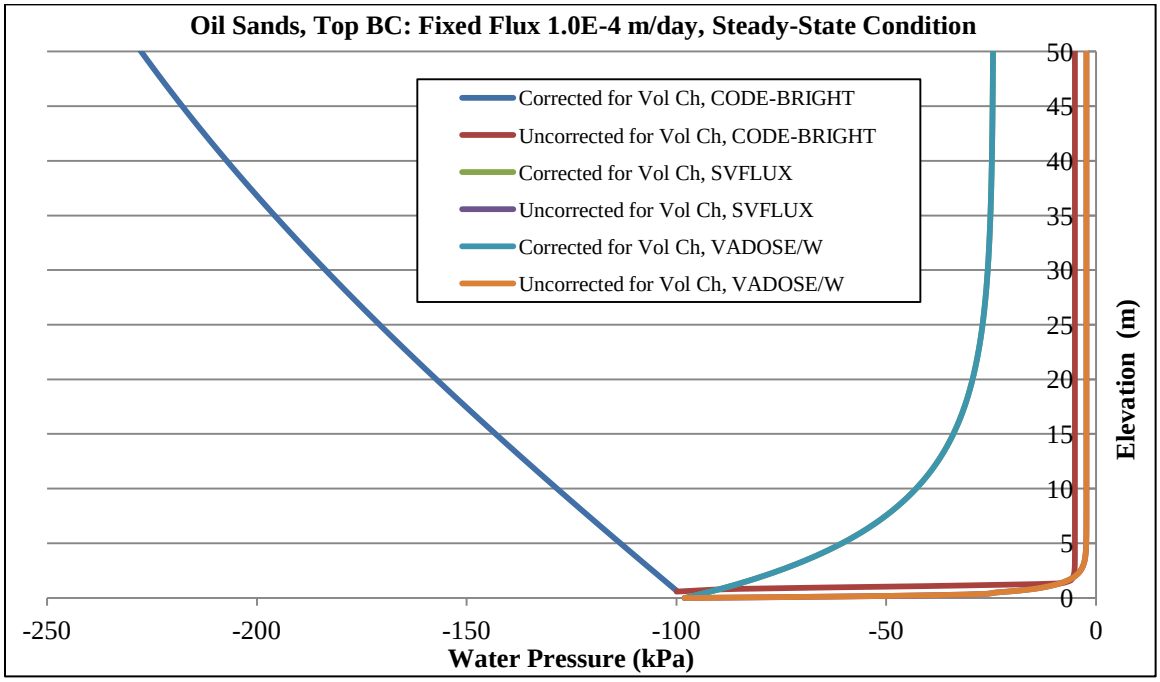

Figure 5.16. Water pressure versus elevation at steady-state condition for Oil Sands tailings with SWCC corrected and uncorrected for volume change and top fixed flux of 1.0e-4 m/day using SVFLUX, VADOSE/W, and CODE-BRIGHT

For finding the deformation caused by wetting of the soil column modeled by Oil Sands tailings properties by adding fixed flux at the top of the column, initial and final profiles of void ratio were determined using suction compression curve. By having initial and final values of void ratio, strain and deformation of soil was found by using the following equations:

$$\varepsilon = \frac{\Delta e}{1 + e_o} \tag{5.4}$$

$$\Delta H = \varepsilon * H_o \tag{5.5}$$

When using the suction compression curve, by knowing the value of suction, void ratio can be estimated. Table 5.5 shows the initial void ratio profile for Oil Sands tailings, which was calculated from the suction compression curve shown in Figure 5.15.

Table 5.5. Initial suction and void ratio profile for the Oil Sands tailings model

Elevation (m)	Sub-layer No.	Thickness of layer (m)	Suction (kPa)	Suction (kPa) in the middle of the layer	Initial "e"
50			600		
45	1	5	550	575	0.48986
40	2	5	500	525	0.50014
35	3	5	450	475	0.51145
30	4	5	400	425	0.52401
25	5	5	350	375	0.53816
20	6	5	300	325	0.55433
15	7	5	250	275	0.57320
10	8	5	200	225	0.59588
5	9	5	150	175	0.62428
0	10	5	100	125	0.66230

The initial condition of the soil column is suction of 100kPa at the bottom and 600kPa at the top. The soil column becomes wet with setting the top boundary condition as the fixed flux of 1.0E-4 m/day. The results of this analysis using CODE-BRIGHT,

SVFLUX, and VADOSE/W was presented in the previous sections (Figure 5.16). It can be seen that the soil gets wet and the suction throughout the soil decreases. By having final values of suction versus elevation, one can estimate final value of void ratio within the soil profile by using suction compression curve of Oil Sands tailings. The values of final void ratio versus elevation and the resulting deformation for the analyses conducted on Oil Sands tailings with top boundary condition of 1.0E-4 m/day using CODE-BRIGHT are presented in Table 5.6.

Table 5.6. Final void ratio profile and deformation for the uncoupled Oil Sands tailings model with top BC fixed flux of 1.0E-4 m/day analyzed by CODE-BRIGHT

	Final "e"		**ε=Δe/(1+eo)**		**ΔH=Ho*ε (m)**	
Sub-layer No.	Corrected	Uncorrected	Corrected	Uncorrected	Corrected	Uncorrected
1	0.61140	0.92588	0.0816	0.2927	0.4079	1.4633
2	0.61555	0.92588	0.0769	0.2838	0.3847	1.4190
3	0.61996	0.92588	0.0718	0.2742	0.3590	1.3710
4	0.62496	0.92588	0.0662	0.2637	0.3312	1.3185
5	0.63075	0.92588	0.0602	0.2521	0.3010	1.2604
6	0.63689	0.92588	0.0531	0.2390	0.2656	1.1952
7	0.64436	0.92588	0.0452	0.2242	0.2261	1.1209
8	0.65272	0.92588	0.0356	0.2068	0.1781	1.0339
9	0.66235	0.92589	0.0234	0.1857	0.1172	0.9284
10	0.67294	0.88495	0.0064	0.1339	0.0320	0.6697
Total Deformation					**2.6027**	**11.7804**

It can be seen in Table 5.6 that: (1) large amounts of wetted induced heave happens when the Oil Sands tailings get wet. (2) There is a large difference between the two cases of SWCC corrected and uncorrected for soil volume change. The large amounts of heave of Oil Sands tailings is expected as Oil Sands tailings exhibit large volume change upon wetting and drying. This fact is shown in the suction compression curve of Oil Sands tailings in which the decrease in suction from 1400kPa to 60kPa leads

to increase in void ratio from around 0.35 to 0.72 (i.e. increase of 0.37 in void ratio). This large amount of increase in void ratio leads to large amounts of strain and thus heaves.

As shown in Figure 5.16, the final suction profile of the case in which SWCC is uncorrected is much smaller than the suction within the Oil Sands tailings in case of corrected SWCC. By using the same suction compression curve, much larger final void ratio profile for the case with uncorrected SWCC is found compared to the case in which SWCC is corrected. Larger final void ratio throughout the soil column leads to more deformation of the model with uncorrected SWCC.

The same model was analyzed using SVFLUX, and VADOSE/W. as previously mentioned, the results of modeling with SVFLUX, and VADOSE/W were identical due to the same flow equation and SWCC and k_{unsat} function models. As shown in Figure 5.16 the final suction profile estimated by SVFLUX, and VADOSE/W is different from the suction profile estimated by CODE-BRIGHT. Therefore, wetted induced heave based on SVFLUX results was also calculated (by using the same suction compression curve of Oil Sands tailings) and the results are presented in Table 5.7.

Table 5.7. Final void ratio profile and deformation for the uncoupled Oil Sands tailings model with top BC fixed flux of 1.0E-4 m/day analyzed by SVFLUX

	Final "e"		**ε=Δe/(1+eo)**		**ΔHi=Ho*ε**	
Sub-layer No.	Corrected	Uncorrected	Corrected	Uncorrected	Corrected	Uncorrected
1	0.79453	0.99228	0.2045	0.3372	1.0225	1.6861
2	0.79409	0.99228	0.1959	0.3281	0.9797	1.6403
3	0.79325	0.99228	0.1864	0.3181	0.9322	1.5906
4	0.79171	0.99228	0.1756	0.3073	0.8782	1.5363
5	0.78884	0.99228	0.1630	0.2952	0.8149	1.4762
6	0.78357	0.99228	0.1475	0.2818	0.7374	1.4088
7	0.77431	0.99228	0.1278	0.2664	0.6391	1.3319
8	0.75896	0.99228	0.1022	0.2484	0.5109	1.2419
9	0.73530	0.99198	0.0684	0.2264	0.3418	1.1319
10	0.70082	0.91746	0.0232	0.1535	0.1159	0.7675
Total Deformation					**6.9727**	**13.8116**

It can be seen that the deformation calculated from the results of SVFLUX is larger than the deformation calculated from the results of CODE-BRIGHT. This is due to the fact that the final suction profile generated by SVFLUX is smaller than the one generated by CODE-BRIGHT. Smaller final suctions lead to larger final void ratio values (calculated form suction compression curve), which in turn leads to larger deformation values. Similar to the results from CODE-BRIGHT, the deformation for the model with uncorrected SWCC analyzed by SVFLUX is much larger than the deformation for the model with corrected SWCC. This is due to the fact that the final suction profile of the model with uncorrected SWCC is smaller than the final suction profile for the model with corrected SWCC.

5.5.2. Comparing Results Produced by VADOSE/W, SVFLUX, and CODE-BRIGHT

Comparison was made between results generated from the three codes used in this study (i.e. SVFLUX, VADOSE/W, and CODE-BRIGHT). Figure 5.17 shows

comparison between the codes for Oil Sands tailings. It was found that the results obtained from SVFLUX and VADOSE/W were identical. The reason for this is that these two codes utilize the exact same flow equation, SWCC fit equation (van Genuchten fit for SWCC in terms of volumetric water content), and saturated hydraulic conductivity estimation model (van Genuchten-Mualem equation based on SWCC in terms of volumetric water content). The results obtained from CODE-BRIGHT were close to the ones generated by SVFLUX and VADOSE/W but there were differences in results. Table 5.8 presents the values of final suction found by different computer codes for Oil Sands tailings.

Table 5.8. Range of final water pressure generated for Oil Sands tailings with various top BC fixed flux values using three codes VADOSE/W, SVFLUX, and CODE-BRIGHT

			Final Water Pressure Range (kPa)		
Soil	**Top BC Fixed Flux (m/day)**	**SWCC**	**SVFLUX**	**VADOSE/W**	**CODE-BRIGHT**
Oil Sands tailings	1.00E-04	Corrected	-100 to -25	-100 to -25	-100 to -225
Oil Sands tailings	1.00E-04	Uncorrected	-100 to -2	-100 to -2	-100 to -5

These differences were of course expected, as unlike SVFLUX and VADOSE/W which allows SWCC only in terms of volumetric water content, CODE-BRIGHT allows SWCC only in terms of degree of saturation. As previously described in Chapter 3, there may be considerable differences between SWCC's in terms of volumetric water content and SWCC's in terms of degree of saturation (particularly with regard to AEV) for soils that undergo significant volume change during SWCC test. The difference in SWCC (particularly AEV) can lead to different final suction profiles.

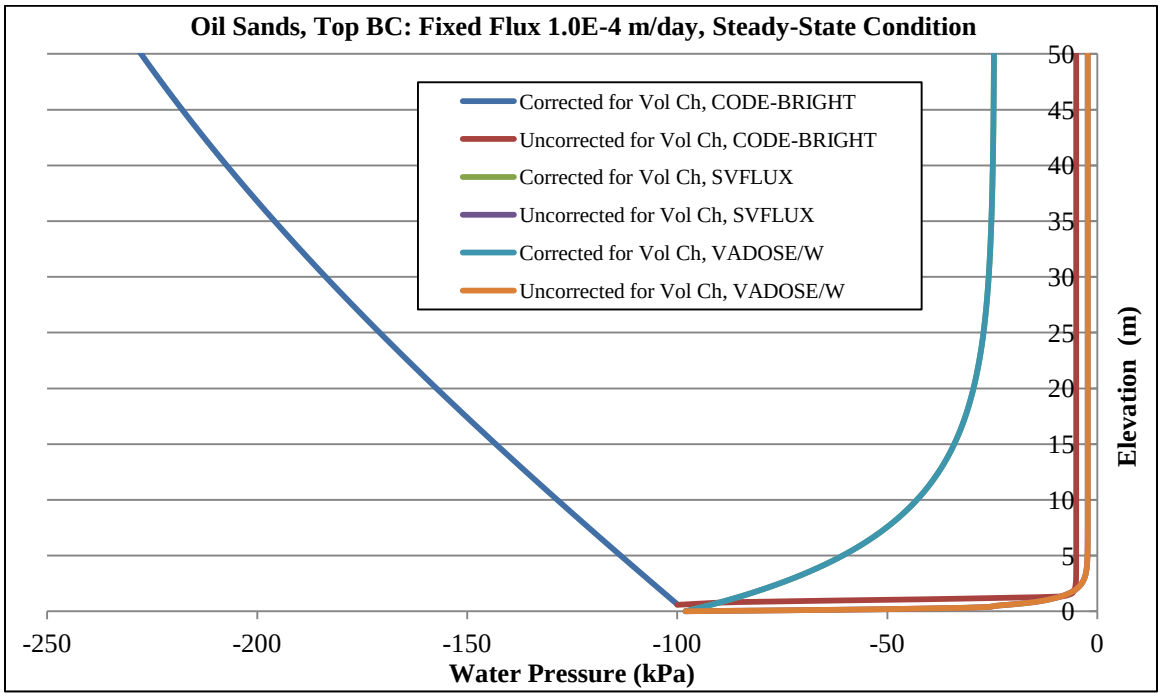

Figure 5.17. Water pressure versus elevation at steady-state condition for Oil Sands tailings with SWCC corrected and uncorrected for volume change and top fixed flux of 1.0e-4 m/day using SVFLUX, VADOSE/W, and CODE-BRIGHT

5.6. Summary and Conclusions

Numerical modeling was performed to evaluate the impact of correcting SWCC for soil volume change for oil sands tailings which exhibit extreme volume change potential, and to evaluate the impact of SWCC volume-correction on fluid flow through the soil, and hence rate of changes in soil suction (e.g. progression of wetted front). Rate of changes in soil suction can, in turn, have a significant effect on the amount of suction-change induced deformation of expansive soils. These effects were assessed as a part of this study during which uncoupled and coupled flow-deformation analyses were performed. It must be emphasized that the results presented are not intended to represent actual behavior of the soils sands, and in particular the results are not expected to represent field behavior where large volume change and associated changes in k_{sat}, not

accounted for here, would occur. Further, the results presented herein do not consider wetting/drying path dependency on the suction compression index.

The SWCC's of oil sands tailings were previously established by Fredlund and Houston (2013) and Fredlund et.al. (2011), by drying SWCC testing of the slurry specimens. The initially saturated slurry specimens of oil sands tailings exhibit extreme volume change upon increase in suction. Slurry specimens of oil sands tailings exhibit shrinkage at suctions even smaller than air-entry value when the specimen is still saturated. Volume changes at suctions smaller than air-entry value is believed to affect the k_{sat} value of these specimens. The Kozeny-Carman can be used for correcting the k_{sat} at suctions smaller than air-entry value (Kozeny, 1927, and Carman, 1937, 1956). However, none of the computer codes used in this study (i.e. VADOSE/W, SVFLUX, and CODE-BRIGHT) has the capability to do corrections for k_{sat} as the volume of the soil changes at suctions smaller than the air-entry value. Therefore, as important as this correction may be for slurry soils, it could not be accounted for in this study. The effect of this k_{sat} correction for compacted or native soil expansive clays is not expected to be significant; whereas the effect of the ksat correction for suctions below the AEV would be very substantial for slurry soils such as oil sands. In addition to the points made above, there are several reasons why the results on the oil sands should not be taken to be representative of any actual field condition. The most interesting field path for oil sands is drying from a slurry. In the field the oil sands start at saturated conditions and then dry. For the simulations of this study, the oil sands were started at an initial condition of an unsaturated state and then either wetted or dried. Further, the suction compression curve

(void ratio versus suction) of oil sands tailings obtained from previous research by Fredlund et al. (2011) was utilized, and in those studies a drying path was followed. For the cases in which a wetting path was simulated in the numerical analyses for the oil sands tailings, no modification to the void ratio versus suction relationship to account for difference in wetting and drying path were made in this study.

Uncoupled (flow only) analyses were conducted for the models based on properties of oil sands tailings in SVFLUX, VADOSE/W, and CODE-BRIGHT in order to evaluate effect of volume-correcting SWCC on hydraulic properties of soils and changes in soil suction (e.g. progression of wetted front) and hence soil volume change due to wetting. The rate of changes in soil suction was studied and amount of suction-change induced deformation was determined based on the generated suction profile of the soil column. For this purpose, the suction compression curve (void ratio versus suction) of oil sands tailings obtained from previous research by Fredlund and Houston (2013), and Fredlund et al. (2011) was utilized.

Initial condition of the soil unsaturated (suction of 100kPa at the bottom and suction of 600kPa at the top of the model). For the simulations in which the soil becomes wet from the top by adding the positive fixed flux, the suction of soil starts to decrease. In other words, the wetting path on the SWCC is followed. It was previously established that the volume corrected SWCC generally has larger AEV compared to the uncorrected SWCC. This means that in the soil with volume corrected SWCC, desaturation starts at a larger suction compared to the soil with uncorrected SWCC. That is to say, the soil with corrected SWCC stays saturated at larger suction ranges compared to the soil with

uncorrected SWCC. Therefore, once the soil becomes wet and the suction decreases (i.e. wetting path on the SWCC), for the soil with corrected SWCC, the soil becomes saturated (i.e. close to AEV on SWCC) at a larger suction. Whereas, the suction within the soil with uncorrected SWCC should further decrease (compared to the soil with corrected SWCC) in order for the suction to reach AEV (i.e. saturation or close-to-saturation state). This mechanism illustrates the reason for the difference in final suction profile for the cases of volume corrected SWCC and volume uncorrected SWCC. It should be mentioned that for a certain expansive soil, the smaller final suction within the soil profile indicates larger values of deformation. This is due to the general shape of suction compression curves, in which the void ratio of the expansive soils is larger at smaller suction values (i.e. when the soil is wetter).

An example of generated suction profile for oil sands tailings with base BC set as suction of 100kPa is shown in Figure 5.18. It can be seen that if the model is allowed to run for long-enough time so that the soil gets fully wetted (i.e. steady-state); the generated suction is smaller for uncorrected SWCC compared to corrected SWCC. This is due to the fact that the volume-corrected SWCC has a larger air-entry value compared to volume-uncorrected SWCC. Therefore, when the soil becomes wet (i.e. wetting path on SWCC) the volume-corrected SWCC reaches the saturated condition at a higher suction.

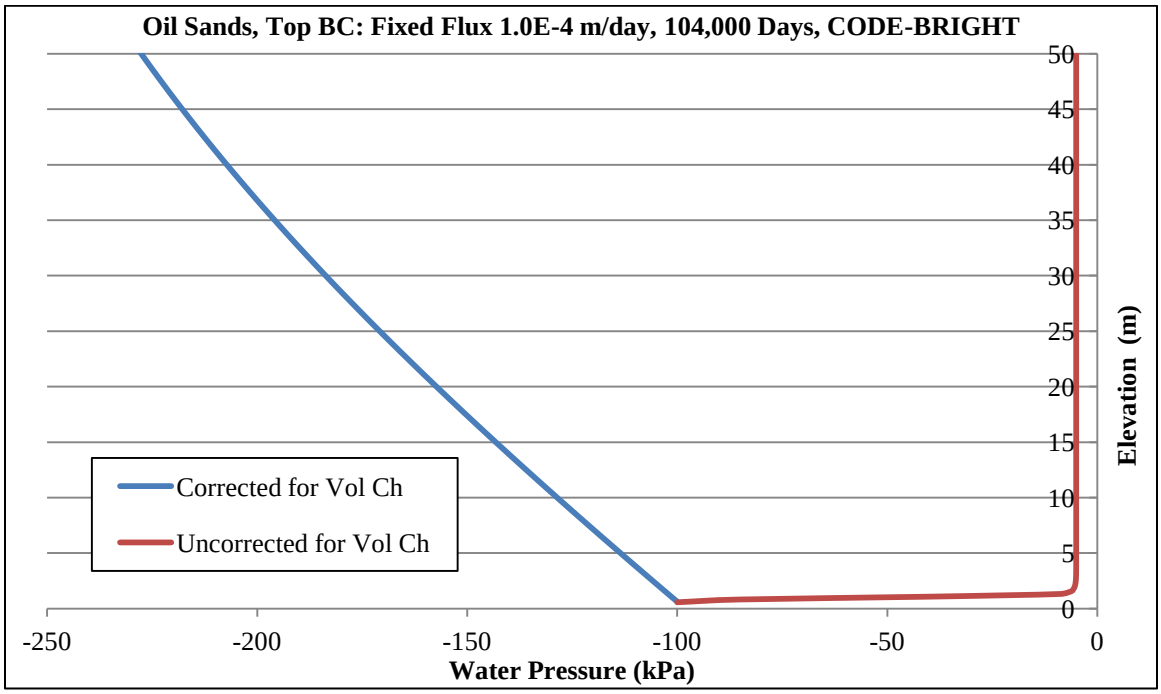

Figure 5.18. Water pressure versus elevation at steady-state condition (104,000 days) for Oil Sands tailings with SWCC corrected and uncorrected for volume change and top fixed flux of 1.0e-4 m/day using CODE-BRIGHT

It was found that in the models with volume corrected SWCC, the soil gets wet quicker (faster rate of progression of wetted front), as the unsaturated hydraulic conductivity of the soil with corrected SWCC is higher than the unsaturated hydraulic conductivity of the same soil with volume uncorrected SWCC. Larger values of k_{unsat} indicates that water penetrates through the soil faster.

For the times prior to the steady-state, in some portions of the soil profile, the suction of uncorrected SWCC is higher than the suction of the corrected SWCC. This is due to the fact that k_{unsat} is generally higher for corrected SWCC and hence, at a given time, the depth of wetting is generally larger for corrected SWCC compared to uncorrected SWCC. Figure 5.19 shows an example which compares the depth of wetting of volume-corrected and volume-uncorrected SWCC at the time 60,000 days for top

boundary condition of fixed flux of 1.0E-4 m/day for oil sands tailings. It can be seen that the depth of wetting is larger for corrected SWCC (due to higher k_{unsat} values). Figure 5.19shows that at time 60,000 days the model with the volume-corrected SWCC has reached the steady-state (fully wetted condition) while the model with the volume-corrected SWCC is only wetted half-way through the depth of column.

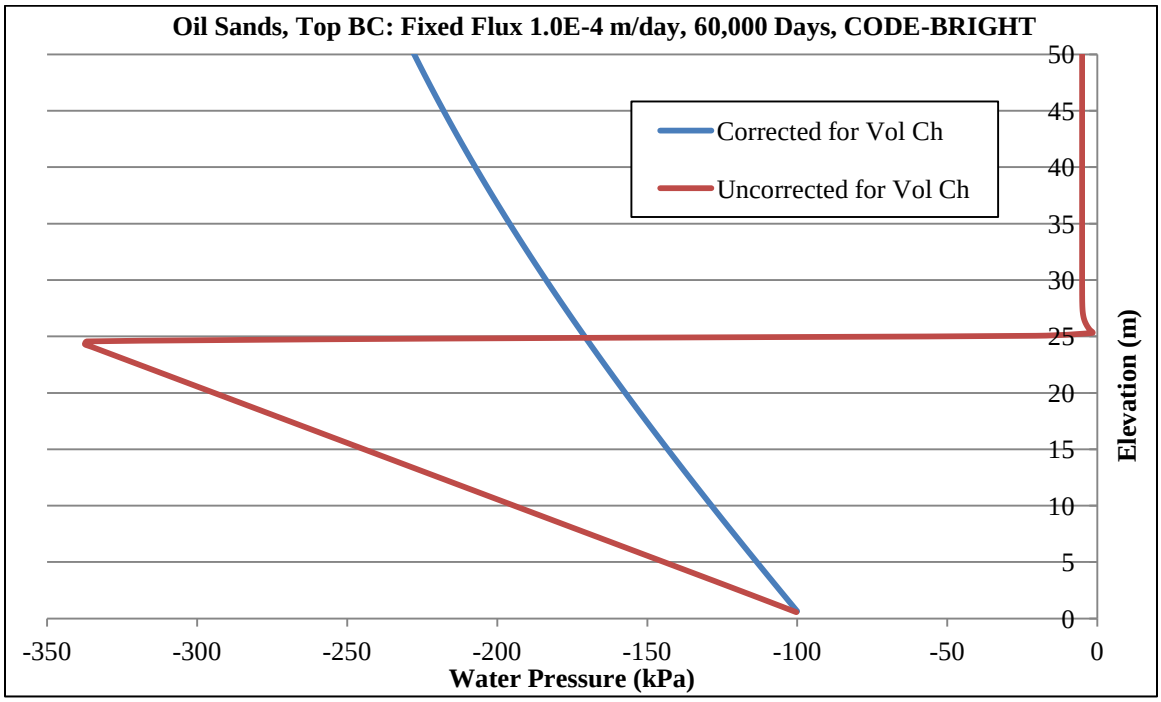

Figure 5.19. Water pressure versus elevation at time 60,000 days (164 years) for Oil Sands tailings with SWCC corrected and uncorrected for volume change and top fixed flux of 1.0e-4 m/day using CODE-BRIGHT

Figure 5.20 shows an example for top boundary condition of evaporation for oil sands tailings. It was found that for top boundary conditions of negative flux (evaporation) the generated suction was larger for volume-uncorrected SWCC compared to volume-corrected SWCC. This makes it difficult to determine in advance if corrected or uncorrected curves will lead to higher suction values, particularly for evaporation

cases. This is believed to be a result of the high nonlinearity of the SWCC and K_{unsat} function.

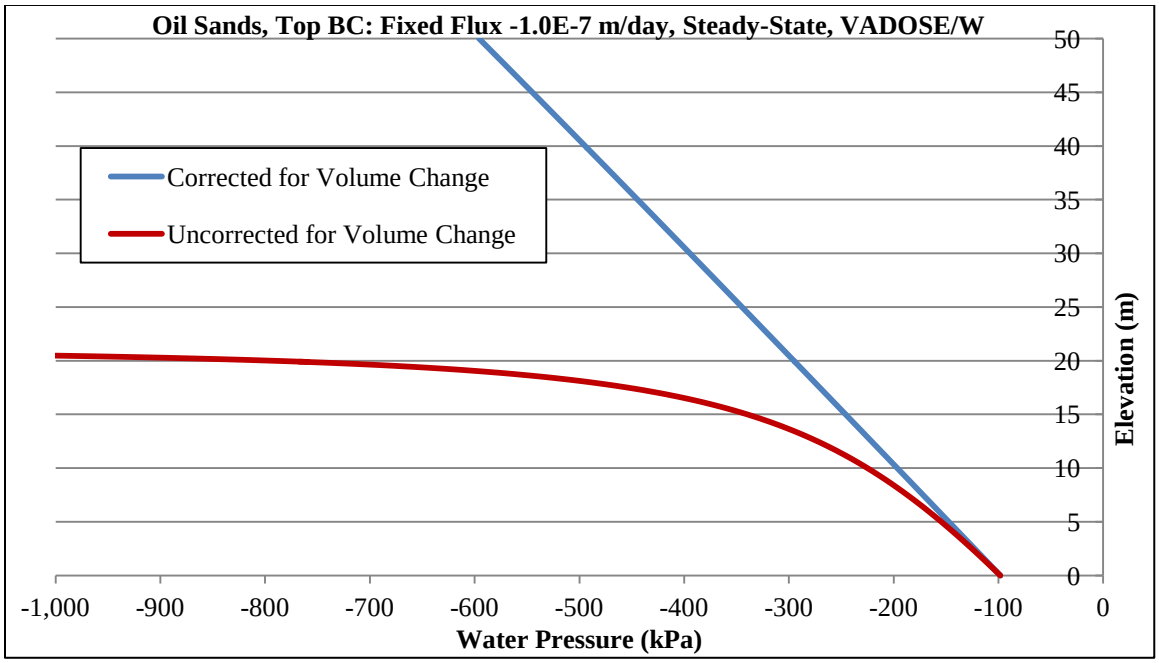

Figure 5.20. Water pressure versus depth at steady-state condition for oil sands tailings with SWCC corrected and uncorrected for volume change and top fixed flux of -1.0E-7 m/day (evaporation) using VADOSE/W

It was found from the calculation of deformation based on results of uncoupled analyses using Oil Sands tailings data that at steady-state condition (i.e. the time that the soil has become completely wet) that: (1) large amounts of wetted induced heave happens when the Oil Sands tailings get wet, neglecting path dependency on the measured void ratio versus suction plot for the oil sands. (2) There is a large difference between the two cases of SWCC corrected and uncorrected for soil volume change. The large amounts of deformation of Oil Sands tailings is expected as Oil Sands tailings were assumed to exhibit large volume change upon change in suction. This fact is shown in the suction compression curve of Oil Sands tailings in which the decrease in suction from 1400kPa to

60kPa leads to increase in void ratio from around 0.35 to 0.72 (i.e. increase of 0.37 in void ratio) when it is assumed that the wetting and drying path void ratio versus suction curves are the same. This large amount of increase in void ratio leads to large amounts of strain and thus heave. The final suction profile of the case in which SWCC is uncorrected is much smaller than the suction within the Oil Sands tailings in case of corrected SWCC. By using the same suction compression curve, much larger final void ratio profile for the case with uncorrected SWCC is found compared to the case in which SWCC is corrected. Larger final void ratio throughout the soil column leads to more deformation of the model with uncorrected SWCC (2.6m and 11.8m for corrected and uncorrected SWCC, respectively found by uncoupled analyses using CODE-BRIGHT).

It was also found that depending upon the time and amount of progression of wetted front within the profile, uncorrected SWCC may exhibit higher or lower suction compared to the corrected SWCC. This makes it difficult to determine in advance if corrected or uncorrected curves will lead to higher suction values, and further research is needed to study this phenomenon from a fundamental unsaturated soil mechanics perspective.

Chapter 6

SUMMARY, CONCLUSIONS AND RECOMMENDATIONS FOR FUTURE RESEARCH

6.1. Summary

The SWCC can be used to estimate unsaturated soil properties such as unsaturated hydraulic conductivity. Therefore, the accuracy of the unsaturated soil property depends on the accuracy of the SWCC. Several factors such as soil structure, initial water content, void ratio, and compaction method can have significant effects on the SWCC, suggesting that matching the laboratory conditions for SWCC determination to field conditions may be most appropriate. Even though the soil water characteristic curve has been measured and used by numerous researchers throughout the years, the effect of volume change for high volume change soils (e.g. expansive soils) has rarely been considered when determining the SWCC's. Failure to consider volume change leads to inaccurate SWCC's including errors in the air-entry value and the slope in the transition zone, and the errors are most pronounced for soils that exhibit high volume change in response to changes in soil suction. Furthermore, it has been the common practice to estimate some of the major unsaturated soil property functions (e.g., unsaturated hydraulic conductivity function and unsaturated soil shear strength) by using the saturated soil properties together with the SWCC, which gives further support for recognizing the importance of establishing accurate SWCC for high volume change soils. In recent years, the importance of considering the volume change of soils during suction change has been recognized by a number of researchers, including Salager et al. (2010), Pe´ron et al. (2007), Nuth and

Laloui (2011), Stange and Horn (2005), Mbonimpa et al. (2006), Fredlund et al. (2011), and Fredlund and Houston, (2013).

Through literature study it was found that the effect of net normal stress which is applied to the soil specimen during the SWCC testing has also been under-studied, particularly the effect of net normal stress on suction-changed induced soil volume change. Only very few researchers have conducted studies for evaluating the impact of net normal stress on volume change of expansive soils and its impact on shape of the SWCC. Furthermore, the effect of the initial state of the soil specimen, including initial moisture content and structure, on the SWCC has not been studied extensively. It is known that the initial condition of the soil (slurry versus compacted) can have a significant effect on the SWCC of the soil, particularly with regard to soil volume change (Fredlund, 2002), yet SWCC's used in practice are often determined for conditions of the soils that do not match those anticipated in the field prototype.

Correction of SWCC's for soil volume change has been shown to have a considerable impact on air-entry value and shape of the SWCC (including the slope in the transition zone). This, in turn, has a significant impact on unsaturated soil properties derived from the SWCC's (e.g. unsaturated hydraulic conductivity function). No studies could be found in that literature using numerical modeling to demonstrate the effect of correction of SWCC for soil volume change on hydraulic properties of the soils (e.g. advancement of wetted front) and its impact on the amount of suction-change induced deformation of expansive soils.

An extensive literature review was conducted on the methods of SWCC determination and the models available to best-fit the SWCC data obtained from laboratory experiments. It was found that, although not always mentioned, the underlying assumption of SWCC fitting equations is that the soil is sufficiently stiff so that there is no change in pore size distribution during the test (Mbonimpa et al., 2006, Chiu and Ng, 2012.

It was found through literature search that researchers have measured soil volume change for determination of SWCC(Stange and Horn (2005), Cui et al. (2006) , Chao et al. (2008), Perez-Garcia, et al. (2008), Salager et al. (2010), Vazquez and Durand (2011), Qi and Michel (2011), Chiu and Ng (2012), Ng et al. (2012), Liu et al. (2012, 2011)). It was also found that some researchers who studied the effect of volume change on SWCC's have recommended using degree of saturation SWCC as opposed to gravimetric or volumetric moisture content SWCC's (Li et al., 2007, Parent et al., 2007, Nuth and Laloui, 2008, Chiu and Ng, 2012, Fredlund and Houston, 2013).

Use of soil water characteristic curves in constitutive relations for unsaturated soils, in particular unsaturated hydraulic conductivity functions, was also studied through a literature search. Commonly used equations to estimate unsaturated hydraulic conductivity functions of soils based on the SWCC were studied. This part of the literature search included studying the methodologies and database used for developing the equations for estimating unsaturated hydraulic conductivity functions as well as the applications of the proposed equations. It was found that the most common equations used for estimating unsaturated hydraulic conductivity functions of soils were developed

for silts and sands, that is using a database developed primarily on silts and sands. Undisturbed and compacted specimens of silts and sands were typically used for developing or validating these equations. Volume change of soils was not considered when developing these equations for estimation of unsaturated hydraulic conductivity, and the equations were found to work best for silts and sands. There appears to be a need for improvement to estimation of unsaturated hydraulic conductivity functions for high volume change soils, including expansive clays, and a larger database for development of improved unsaturated hydraulic conductivity estimation methods is needed, particularly for fine-grained soils.

The importance of correcting SWCC's (including SWCC's in terms of volumetric water content and degree of saturation) for soil volume change was studied through literature search. Additional literature search was carried out to assess the effect of net normal stress on the shape of SWCC with regard to the soil volume change throughout the test. Moreover, the importance of the initial condition of the specimen (slurry versus compacted specimen) was evaluated through literature search. The literature review showed that slurry specimens undergo significant volume change during SWCC test. Therefore, for a certain clay soils the SWCC of the slurry specimen may be significantly different from that of the compacted specimen.

The hysteresis loop present between the wetting and drying paths of a SWCC was also studied through literature search. Numerous researchers have measured SWCC's including drying and wetting paths and presented the hysteresis associated with the curves. It is well known that at a given soil suction, the water content of the drying curve

is higher than that of the wetting curve (i.e. the drying curve lies above the wetting curve). Furthermore, the end point of the wetting curve differs from the starting point of the drying curve because of air entrapment in the soil that occurs upon drying. Furthermore, the slope of the drying curve is approximately parallel to that of the wetting curve.

The impact of net normal stress applied to the specimen during the SWCC test was studied through literature search. Very limited data was found regarding the effect of net normal stress on the shape of the SWCC's. It was found that in general, the applied normal stress does not seem to affect the shape of the SWCC significantly; however, the AEV increases and the rate of degree of saturation change decreases with increasing the net normal stress (Ng and Pang 2000 and Vanapalli et al. 1999).

As the next part of study, soil water characteristic curves (SWCC) of three expansive clays, Anthem, Colorado, and San Antonio, were determined through laboratory tests. The first set of tests was conducted on compacted specimens under net normal stress of 7kPa (seating load). The purpose of this set of test was to evaluate effect of considering soil volume change on the shape of SWCC of expansive clays, with particular focus on the air-entry value. Another set of tests were conducted in which slurry specimens of the soils were tested. The slurry specimens were prepared by mixing certain amount of soil and water to make sure that the specimen had reached 100% saturation. The effect of initial state of the specimen on its SWCC was studied by this set of experiments. It was found that slurry specimens undergo significant volume changes during SWCC testing as soil suction is changed. Therefore, the difference between the

volume corrected SWCC and uncorrected SWCC was more significant for slurry specimens compared to compacted specimens.

The last set of laboratory experiments were intended to help evaluate the effect of net normal stress on the volume change of specimens and its impact on the shape of SWCC. For this set of experiments, different net normal stresses were used. The range of net normal stresses was from 7kPa to around 55% of the swell pressure of the tested soil. Volume corrected SWCC's were developed by using the instantaneous volume of the specimen while in volume uncorrected SWCC's the initial volume of the specimen was used as the reference and the soil volume change throughout the test was ignored.

The next part of the study included numerical modeling that was performed to find the impact of correcting SWCC for soil volume change (for soils with high volume change potential) and to evaluate the impact of SWCC correction on fluid flow through the soil, and hence rate and degree of change of suction within the soil profile. Rate of changes in soil suction can, in turn, have a significant effect on the amount of deformation of expansive soils. The effects of volume change correction on the SWCC and the associated estimation of the k_{unsat} function on suction-change induced deformations were assessed as a part of this study using uncoupled and coupled flow-deformation analyses. For uncoupled analyses, the unsaturated flow only is evaluated and then the results from the flow analysis (i.e., initial and final soil suction profiles) are used as input to a separate deformation analysis. For a coupled flow-deformation analysis, however, unsaturated flow and suction-change induced deformation are solved for at the same time, considering any effect of suction change on deformation and any effect of

deformation on soil suction, by solving the governing partial differential equations for flow and stress-deformation simultaneously.

Three computer programs of VADOSE/W, CODE-BRIGHT, and SVFLUX were used to evaluate the effect of volume-correcting SWCC's on fluid flow through the soils and the resulting suction-change induced deformation. These computer codes have the capability of simulating saturated and unsaturated flow of water through soils and are commonly used in industry and/or academia (research projects).

The laboratory results obtained from SWCC tests on the three expansive soils of Anthem, Colorado, and San Antonio as well as data obtained from previous research conducted on oil sands tailings by Fredlund and Houston (2013) and Fredlund et.al. (2011) were used in the numerical modeling. One-dimensional flow through a soil was simulated to study the flow through a column of soil once with the SWCC corrected and once with the SWCC uncorrected for volume change.

Uncoupled (flow only) analyses were conducted for the models in SVFLUX, VADOSE/W, and CODE-BRIGHT in order to evaluate impact of correcting the SWCC for volume change on hydraulic properties of soils and the rate of change of soil suction in the profile, and hence soil volume change due to wetting or drying. For positive flux surface boundary conditions, the rate of progression of wetted front was studied and the amount of soil expansion (heave) was determined based on the initial and final suction profile of the soil column. For this purpose, the suction compression curves (void ratio versus log of suction) of specimens obtained from SWCC laboratory experiments on the

expansive clays were utilized as well as the suction compression curves obtained from previous research conducted on oil sands tailings by Fredlund et.al. (2011).

6.2. Conclusions

During the literature review, particular focus was placed upon studying whether in common practice SWCC's are corrected for soil volume change. This was studied particularly for the soils with high volume change potential. Soil water characteristic curve fitting equations have been generated by a number of researchers (e.g., Gardner 1956; Brooks and Corey 1964; van Genuchten 1980; Fredlund and Xing 1994). Although not always mentioned, the underlying assumption of most SWCC fitting equations is that the soil is sufficiently stiff so that there is no change in void ratio of the soil (i.e. no soil volume change) during the test (Mbonimpa et al., 2006, Chiu and Ng, 2012). It was found that in recent years a number of researchers have recognized the importance of considering soil volume change when establishing SWCC's. Some researchers have conducted SWCC tests during which the volume and mass of the specimen has been recorded and the volume change of the specimen has been incorporated when generating the SWCC's (Stange and Horn 2005, Cui et al. 2006, Chao et al. 2008, Salager et al. 2010, Vazquez and Durand 2011, Qi and Michel 2011, Chiu and Ng 2012, Ng et al. 2012, Liu et al. 2012, 2011, Perez-Garcia, et al. 2008). At the same time, the measured data comparing volume change corrected and uncorrected SWCC's was very limited and the researchers reported either the SWCC that is corrected for volume change or the SWCC uncorrected for volume change. It was found through literature study that only very few researchers have compared SWCC's with and without volume change consideration to assess the impact on key SWCC parameters such as AEV and slope in transition zone.

A number of researchers recommended using degree of saturation SWCC as opposed to gravimetric moisture content. The authors reported that when the soil undergoes volume change during a suction increase, only the degree of saturation variable clearly defines the air-entry value for the soil (as opposed to gravimetric and volumetric water content).

No researchers were found to have evaluated the effect of initial state of expansive soils specimens (i.e. slurry versus compacted specimens) on SWCC with focus on volume change. Very few studies on effect of net normal stress on soil volume change and its impact on SWCC of expansive clays was found in the literature.

Three of the most commonly used equations for estimating the unsaturated hydraulic conductivity function of soils were studied through literature search. The purpose of this part of the literature review was to study the basis upon which these unsaturated hydraulic conductivity fitting equations have been developed and validated, and also to find the database and applications for each model (i.e. is the model applied best for coarse or fine-grained materials). The description of three common unsaturated hydraulic conductivity estimation models includes the methods which the researchers utilized for developing the models as well as the validation of the models by comparing the estimated values against measured values of unsaturated hydraulic conductivity. The three models that are described are the model by Green and Corey (1971), Fredlund et al. (2004), and van Genuchten (1980). It was found that the underlying assumption for generating these equations, in all cases, is that the volume change of the soil structure is negligible. It was found that the most common equations used for estimating unsaturated

hydraulic conductivity functions of soils were developed using data on silts and sands. Undisturbed and compacted specimens of silts and sands were used for developing or validating these equations. Volume change of soils was not considered when developing these equations for estimating unsaturated hydraulic conductivity and these equations are expected to work best for silts and sands but may not accurately estimate unsaturated hydraulic conductivity functions of clays or for any soils that exhibit significant volume change as soil suction changes under a given net normal stress condition.

No studies were found on the effect of volume change consideration on the hydraulic properties of the soils together with associated unsaturated flow modeling (e.g. advancement of wetted front). No researchers were found to have focused on the effect of volume change on the SWCC as related to unsaturated flow/deformation analyses for expansive clays.

As a main scope of this research, the SWCC's of three expansive soils were measured through laboratory testing using an oedometer pressure plate device for suction up to 1500 kPa) and the filter paper method for higher suctions. Volume change of the soils during suction change was measured and taken into account for establishing the SWCC's in terms of volumetric water content and degree of saturation. The measured data points along with the van Genuchten (1980) SWCC fitting parameters were presented.

Volume corrected SWCC's were developed by using the instantaneous volume of the specimen while volume uncorrected SWCC's were developed using initial volume of the specimen (i.e. volume changes throughout the test was ignored).

It was found that volume change correction have a significant effect on the shape of the SWCC, particularly regarding the air-entry value (AEV) and slope in the transition zone. The air-entry value was shown to be larger for volume-corrected SWCC's compared to volume-uncorrected SWCC's. The slope of the curve in the transition zone was also found to be steeper for corrected SWCC's. These typical trends were shown in Figure 3.71 for the Colorado soil, and are repeated below in Figure 6.1.

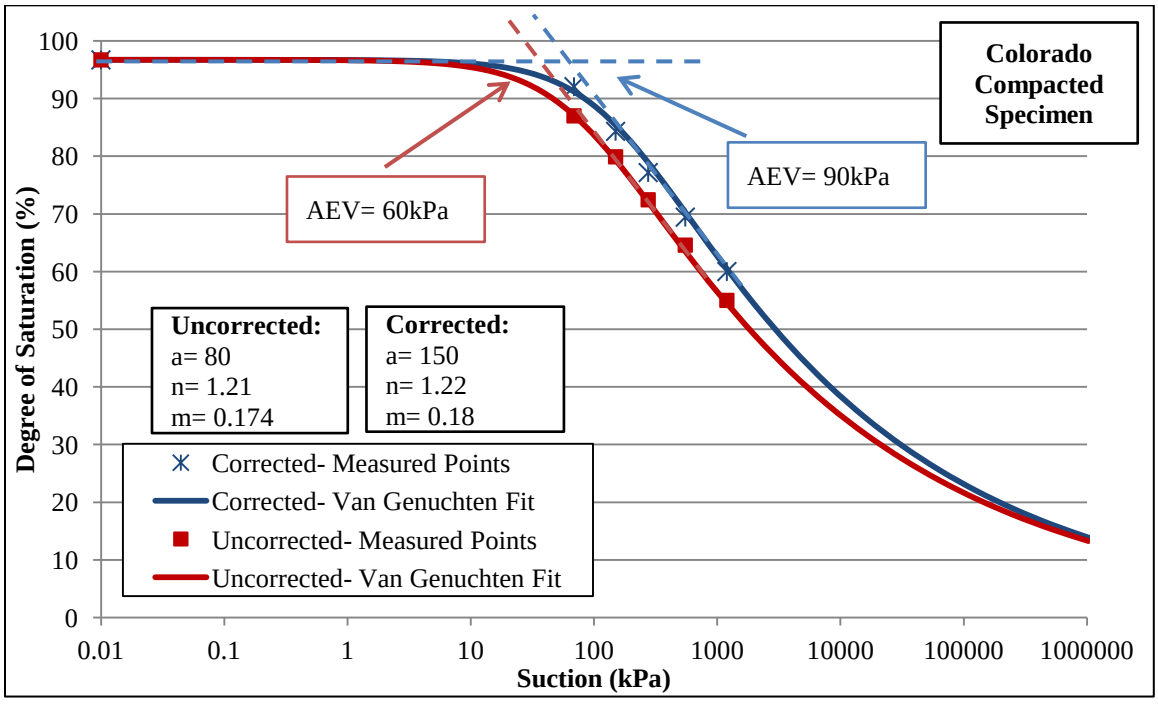

Figure 6.1. Typical impact of volume change correction on shape of the SWCC - example here is for compacted specimen of Colorado

Errors in the AEV and slope of the transition zone for volume-uncorrected SWCC of expansive soils are clear. The AEV is underestimated if volume change corrections are not made, and so is the slope of the SWCC in the transition zone. It was also found that in order to find the 'true' air-entry value and slope of the SWCC, the volume-

corrected SWCC in terms of degree of saturation, which givens the highest AEV, should be used, as previously discussed by Fredlund and Houston (2013).

Another major finding from the SWCC lab testing program is that due to the existence of clods in soils with high plasticity during the compaction process, the air-entry value of these soils turns out to be lower than what is normally expected for high plasticity soils. The relatively low air-entry values observed are believed to be the result of existence of clods creating air-entry values more consistent with coarser-grained materials. In order to evaluate the effects of clods on the SWCC of the three clays of this study, with particular focus on the air-entry value, SWCC tests were performed on slurry specimens. In slurry specimens, the pulverized soil was entirely saturated with water and therefore clods did not appear within the specimen. Slurry specimens of Anthem, Colorado, and San Antonio soils were tested and the resulting SWCC's were compared against the SWCC's obtained from the compacted specimens of the same soils. It was found that the initial state of the specimen has a significant effect on the shape of the SWCC, as a result of both structure and volume change. In particular, the shape of the SWCC including volume corrections was dramatically affected on the slurry specimens due to high volume change experienced by the slurry specimens as suction changes were imposed. For any given soil tested, the air-entry value of volume-corrected SWCC's obtained from testing slurry specimens was found to be higher than that of compacted specimens. The slope in transition zone was also found to be higher for slurry specimens. It was found that slurry specimens showed generally larger AEV compared to compacted specimens due to a combination of volume change and structure effects. Figure 6.2,

shows the SWCC in terms of degree of saturation including both corrected and uncorrected curves for slurry specimen of San Antonio soil. Also shown is the volume-corrected SWCC for compacted specimen of San Antonio soil. The figure shows the significant difference in AEV and slope in the transition zone between corrected and uncorrected curves for the slurry specimen. Furthermore, the differences discussed above between slurried and compacted soil specimen SWCC's are obvious in Figure 6.2. It should be mentioned that the net normal stress in both cases (slurry and compacted specimens tested) was a token load, but some differences could be due to slurry specimens having 3kPa token load while the compacted specimen had 7kPa token load.

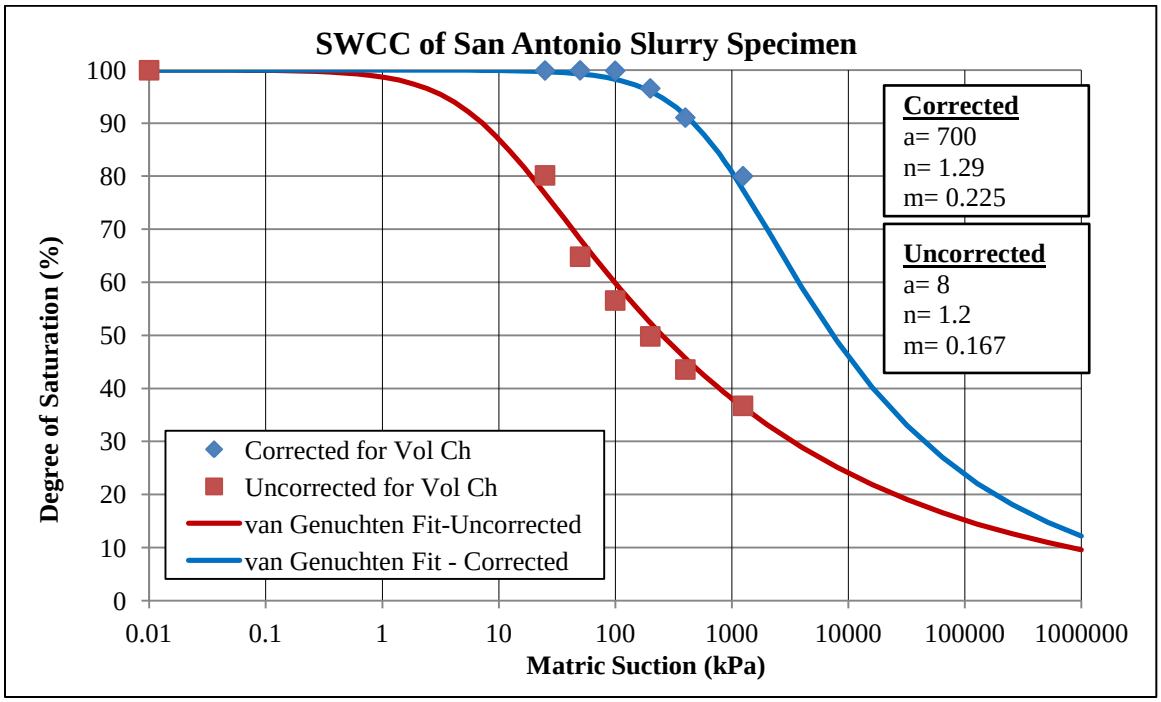

(a)

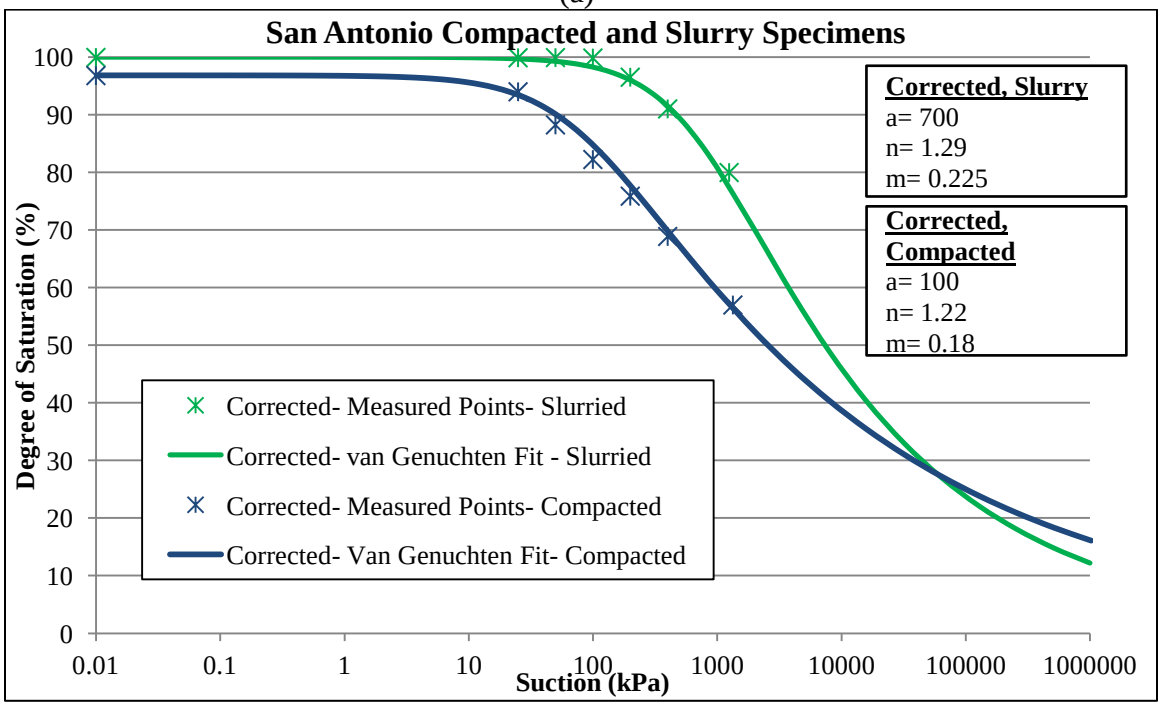

(b)

Figure 6.2. (a) Example of volume corrected and uncorrected SWCC's in terms of degree of saturation for slurry specimen and the corresponding van Genuchten parameters (for San Antonio soil), and (b) Example of volume corrected SWCC's in terms of degree of

saturation for compacted and slurry specimens and the corresponding van Genuchten parameters (for San Antonio soil)

The SWCC's (drying and wetting paths) for three expansive soils of Anthem, Colorado, and San Antonio were determined. For this set of tests, the effects of net normal stress and hysteresis on the SWCC of expansive soils were studied. The net normal stress values applied to the soil specimens were varied from a light seating load (7 kPa) to around 54% of the swell pressure of the soil samples. The effect of net normal stress was found to be relatively insignificant with respect to volume change on compacted soils, although a slight increase in AEV of volume corrected SWCC was observed with larger net normal stresses. Radial shrinkage was observed to be minimized or eliminated in the cases of large net normal stress, particularly for compacted soils. Figure 6.3 shows typical drying SWCC's which were corrected for soil volume change, with the example shown being for Colorado soil for different net normal stresses tested. Slight increase in AEV with increase in net normal is shown in this figure.

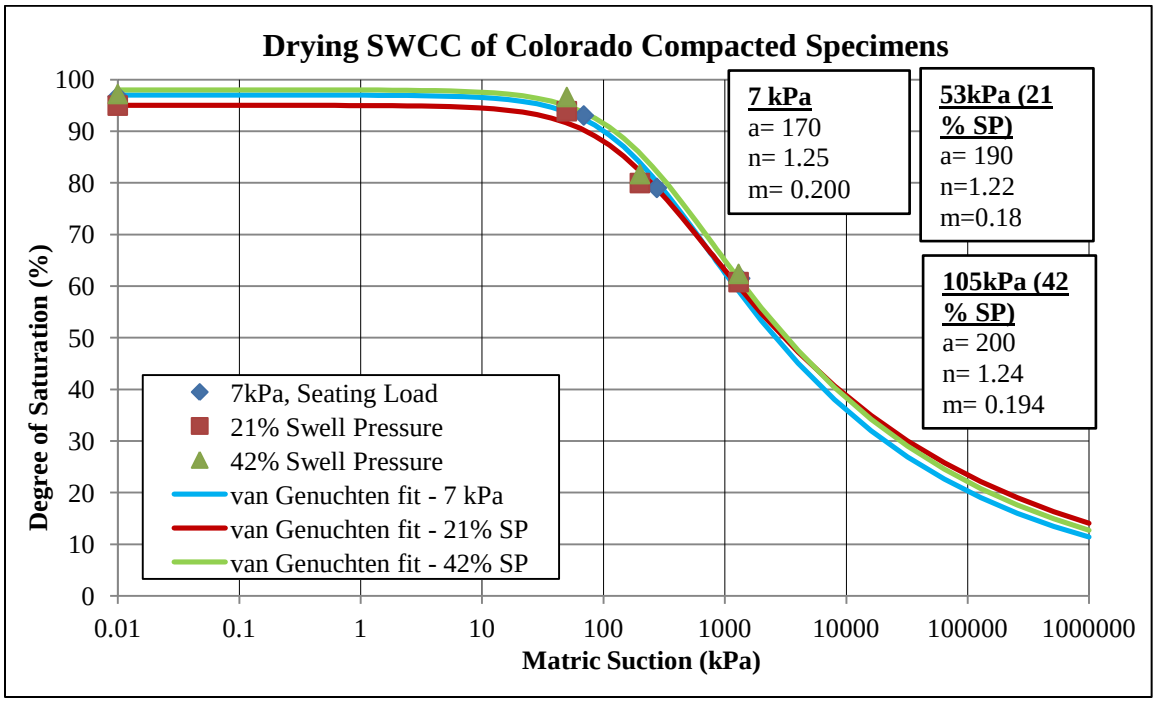

Figure 6.3. Typical effect of net normal stress on compacted expansive soils SWCC's – shown here are Drying SWCC's for Colorado soil (swell pressure: 250 kPa) under various net normal stresses. Notice larger values of "a" parameter for tests under higher net normal stress

As illustrated in the images of the specimens shown in Chapter 3, generally larger radial shrinkage was observed at larger suctions (e.g. around 1300 kPa) compared to at lower suctions (e.g. 200 kPa). It was found that with increase in suction, the radial shrinkage of the soil specimens also increase, as expected. This was true for the cases of both slurry and compacted specimens, although the compacted specimens generally exhibit relatively small radial shrinkage during drying curve SWCC determination, even under low confining stress. When comparing the shrinkage of compacted specimens it was found that with increase in net normal stress, the amount of radial shrinkage of the soil decreases. It was found that for the compacted specimens which were tested under large amounts of net normal stress (e.g. around 50% of the swell pressure of the soil) the

radial shrinkage of the soil during the drying SWCC test was minimal such that the contact between the soil and the confining ring was maintained throughout the test even at relatively large suction values (i.e. around 1300 kPa). For such cases in which the contact between the soil and the confining ring is maintained throughout the test, the volume change of the soil is only in the vertical direction. This volume change can be measured much easier and with more accuracy compared to cases where the specimen shrinks away from the specimen ring. Of course, when the path is wetting rather than drying, there is no shrinkage issue to deal with in determining the SWCC. Given that the wetting path is commonly the path of interest in the field, it could be argued that further study on the impact/improvement for using the wetting path in determining the SWCC is needed.

The laboratory results obtained from the SWCC tests on the three soils of Anthem, Colorado, and San Antonio were used in the unsaturated flow/deformation numerical modeling studies. One-dimensional unsaturated flow through a soil was simulated to study the flow through a column of soil once with the SWCC corrected and once with the SWCC uncorrected for volume change.

Uncoupled (flow only) analyses were conducted for the models in SVFLUX, VADOSE/W, and CODE-BRIGHT in order to evaluate impact of correcting SWCC for volume change on hydraulic properties of soils and the rate of change and magnitude of change of soil suction in the profile, and hence soil volume change due to wetting or drying. For positive flux surface boundary conditions, rate of progression of wetted front was studied and amount of soil expansion (heave) was determined based on the initial

and final suction profile of the soil column. For this purpose, the suction compression curves (void ratio versus log of suction) of specimens obtained from SWCC laboratory experiments on the expansive clays were utilized.

In this study, the initial condition of the modeled soil was set as unsaturated. For the cases in which the soil becomes wetted from the top by adding a positive fixed flux to the top of the soil column, the suction of soil starts to decrease. In other words, the wetting path on the SWCC is followed when the soil becomes wetted. It was previously established that the volume corrected SWCC generally has larger AEV compared to the uncorrected SWCC. This means that in the soil with volume corrected SWCC, desaturation starts at a larger suction compared to the soil with uncorrected SWCC. That is to say, the soil with corrected SWCC stays saturated at larger suction ranges compared to the soil with uncorrected SWCC. Therefore, once the soil becomes wet and the suction decreases (i.e. wetting path on the SWCC), for the soil with corrected SWCC, the soil becomes saturated (i.e. close to AEV on SWCC) at a larger suction; whereas, the suction within the soil with uncorrected SWCC must decrease further (compared to the soil with corrected SWCC) in order for the suction to reach the AEV (i.e. saturation or close-to-saturation state). This mechanism illustrates the reason for the difference in final suction values for the cases of volume corrected SWCC and volume uncorrected SWCC when the soil becomes wetted. It should be mentioned that for a certain expansive soil and given initial head (suction) boundary conditions, the smaller final suction within the soil profile leads to larger values of deformation. An example of generated suction profile for Colorado soil with base boundary condition set as suction of 100kPa is shown in Figure

6.4. It can be seen that if the model is allowed to run for long-enough time so that the soil gets fully wetted (i.e. steady-state); the generated suction is smaller for uncorrected SWCC compared to corrected SWCC. This is because for any given expansive soil, the volume-corrected SWCC has a larger air-entry value compared to volume-uncorrected SWCC. Therefore, when the soil becomes wet the volume-corrected SWCC reaches the saturated condition at a higher suction.

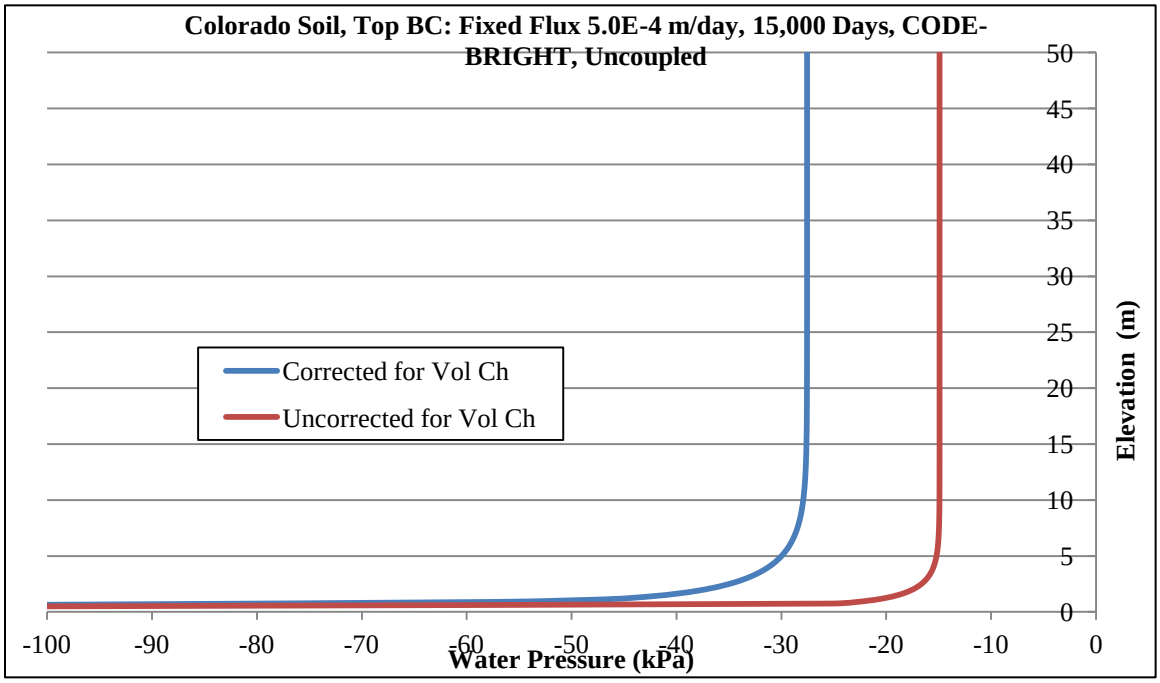

Figure 6.4. Example profile of soils suction for corrected and uncorrected SWCC. Water pressure versus elevation at steady-state condition (time: 15,000 days) for Colorado soil with SWCC corrected (AEV= 90kPa) and uncorrected (AEV= 60kPa) for volume change and top fixed flux of 5.0e-4 m/day using CODE-BRIGHT

For positive flux surface boundary conditions it was found that in the models with volume corrected SWCC, the soil gets wet quicker (faster rate of progression of wetted front) because the unsaturated hydraulic conductivity of the soil with corrected SWCC is higher than the unsaturated hydraulic conductivity of the same soil with volume

uncorrected SWCC. Larger values of k_{unsat} result in water penetrating through the soil faster.

For times prior to the steady-state in some portions of the soil profile the suction for the uncorrected SWCC is higher than the suction for the corrected SWCC. This is because k_{unsat} is generally higher for corrected SWCC and hence, at a given time, the depth of wetting is generally greater for corrected SWCC compared to uncorrected SWCC. This generally leads to overall larger amounts of soil expansion (heave) for the corrected SWCC compared to uncorrected SWCC at certain times during the analyses. Figure 6.5 shows an example which compares the depth of wetting of volume-corrected and volume-uncorrected SWCC at the time of 7,000 days for top boundary condition of fixed flux of 5.0E-4 m/day for Colorado soil. It can be seen that the depth of wetting is larger for corrected SWCC (due to higher k_{unsat} values).

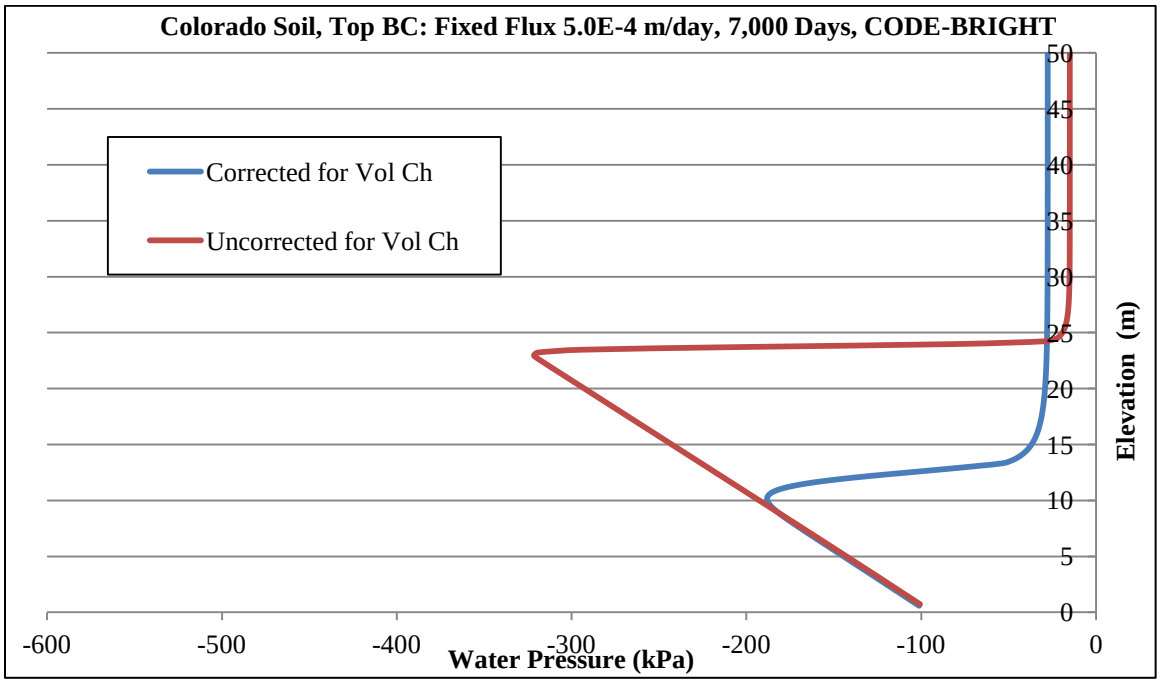

Figure 6.5. Example profile of soils suction for corrected and uncorrected SWCC. Water pressure versus elevation profile at time 7,000days (19 years) for Colorado soil with SWCC corrected (AEV= 90kPa) and uncorrected (AEV= 60kPa) for volume change and top fixed flux of 5.0e-4 m/day using CODE-BRIGHT

It was found that for top boundary conditions of negative flux (evaporation), at some segments of the soil column the generated suction was larger for the volume-corrected SWCC compared to the uncorrected case, while in some other segments of the soil column, the generated suction was larger for the volume-uncorrected SWCC case. This demonstrates that it is not always possible to determine in advance if corrected or uncorrected curves will lead to higher suction values, particularly for evaporation cases and for more complex surface flux boundary conditions associated with real world problems. This is believed to be a result of the high nonlinearity of the SWCC and k_{unsat} function. Figure 6.6 shows an example for top boundary condition of evaporation for Colorado soil. It can be seen that for some parts within the soil profile, the suction curve

for uncorrected SWCC shows higher values compared to corrected SWCC, while at some other parts the opposite trend is noticed.

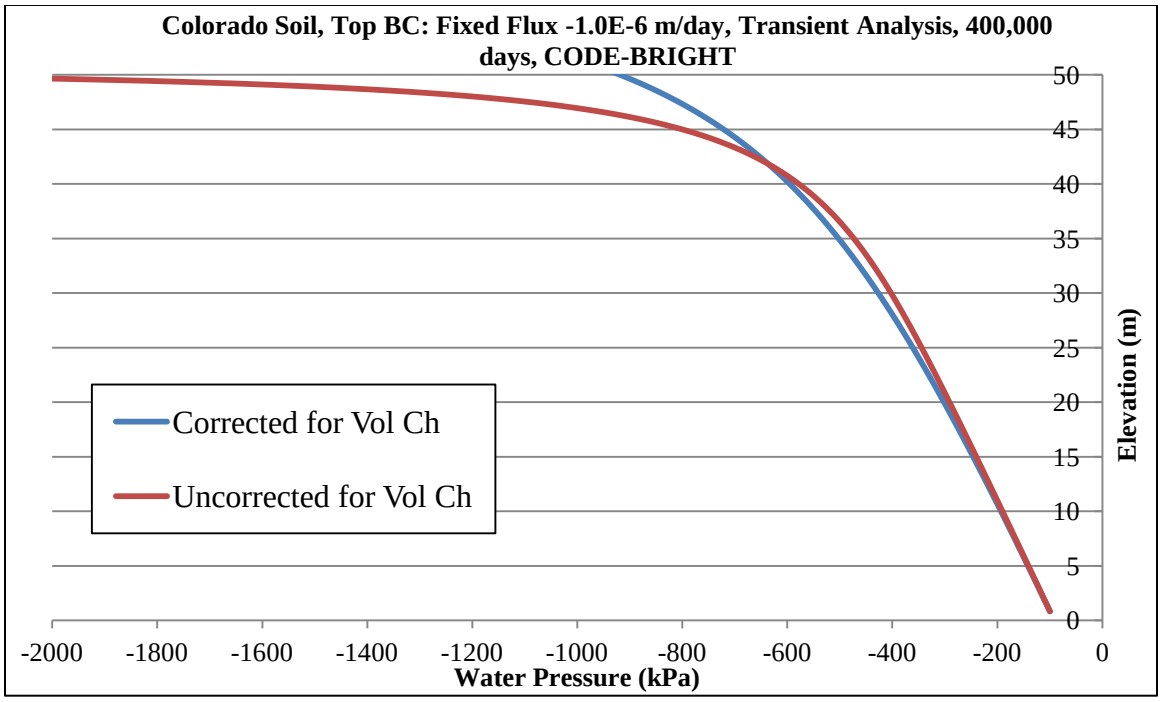

Figure 6.6. Example profile of soils suction for corrected and uncorrected SWCC. Water pressure versus elevation profile at time 400,000days (1095 years) for Colorado soil with SWCC corrected (AEV= 90kPa) and uncorrected (AEV= 60kPa) for volume change and top fixed flux of -1.0E-6 m/day (evaporation) using CODE-BRIGHT

A number of simulations were analyzed in which the initial conditions of the model consisted of higher suction values, above the AEV of the soils (i.e. suction of 1000kPa at the base and suction of 1500kPa at the top of the model). The top boundary condition of positive fixed flux was then introduced to induce soil wetting. The trends for this set of runs was found to be the same as the trends that were previously found for the models with lower suction initial condition (i.e. suction of 100kPa at the base and suction of 600kPa at the top of the model). It was found that similar to previous results, the rate

of progression of wetted front is higher for corrected SWCC compared to uncorrected SWCC. A typical result for a positive fixed flux surface condition is shown in Figure 6.7.

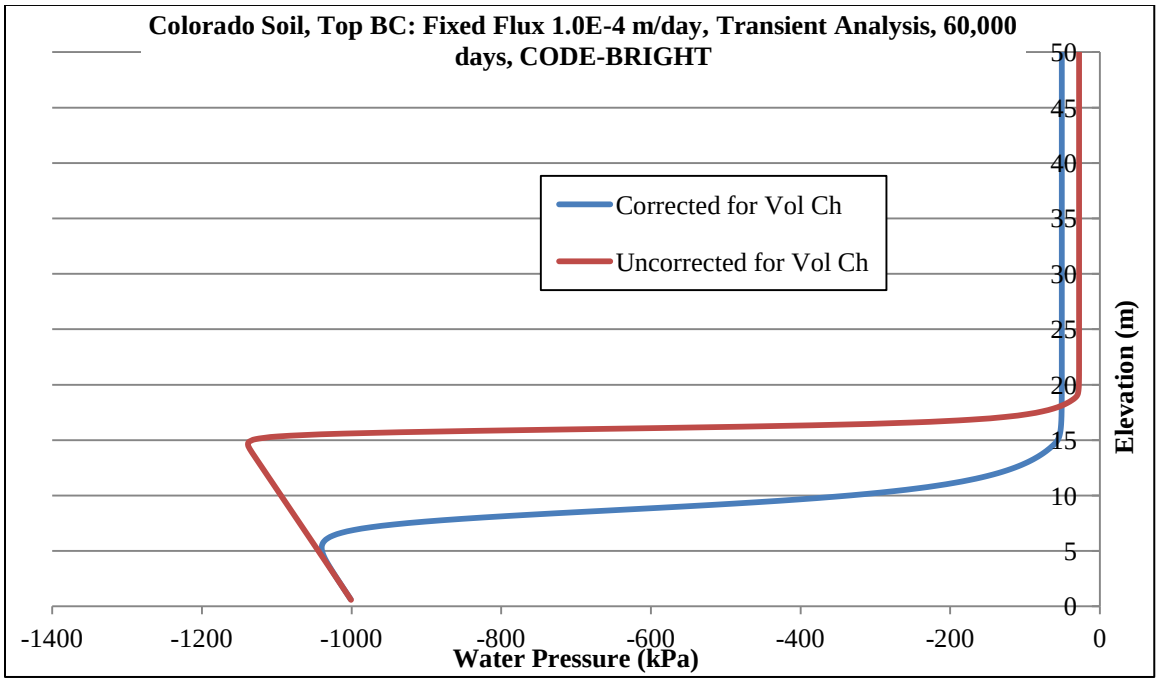

Figure 6.7. Example profile of soils suction for corrected and uncorrected SWCC. Water pressure versus elevation profile at time 60,000days for Colorado soil with SWCC corrected (AEV= 90kPa) and uncorrected (AEV= 60kPa) for volume change and top fixed flux of 1.0E-4 m/day using CODE-BRIGHT

Figure 6.8 shows that similar to models which were analyzed with low initial suction, for the models with higher initial suction, the final suction profile shows smaller values for uncorrected SWCC compared to corrected SWCC. This is, of course, is due to the fact that the air-entry value of corrected SWCC is higher than air-entry value of uncorrected SWCC.

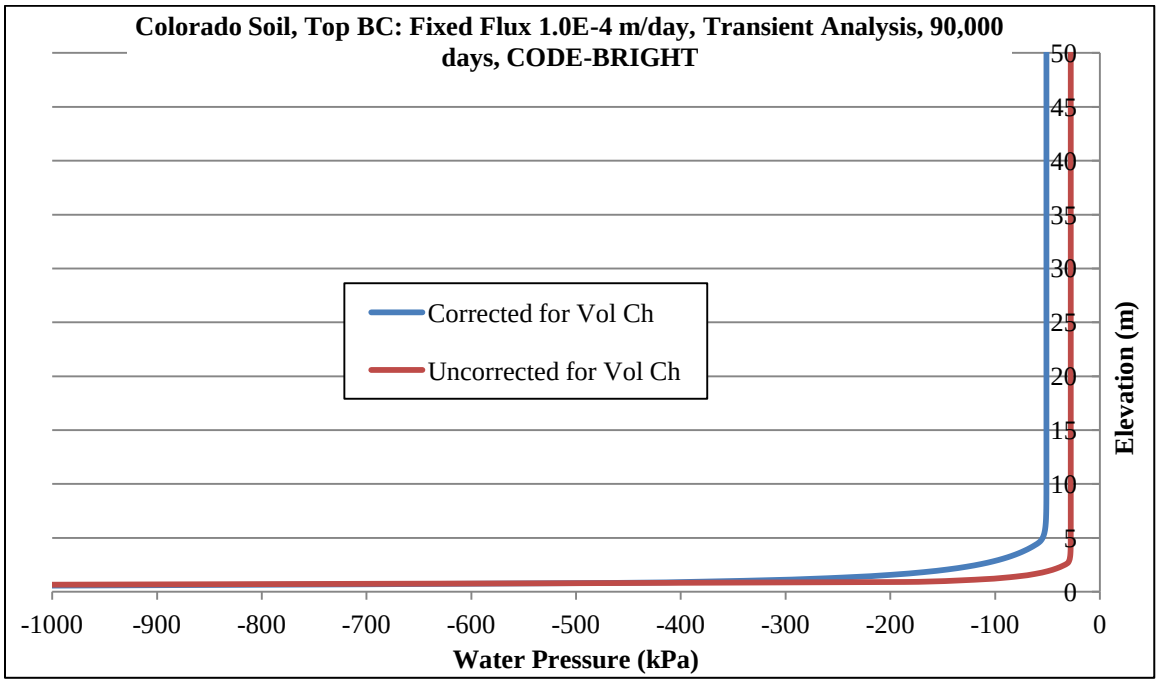

Figure 6.8. Example profile of soils suction for corrected and uncorrected SWCC. Water pressure versus elevation profile at time 90,000days (steady-state) for Colorado soil with SWCC corrected (AEV= 90kPa) and uncorrected (AEV= 60kPa) for volume change and top fixed flux of 1.0E-4 m/day using CODE-BRIGHT

When comparing the results generated for a certain soil by the three codes used in this study (i.e. SVFLUX, VADOSE/W, and CODE-BRIGHT), it was found that the results generated by SVFLUX and VADOSE/W were the same. However, the results generated by CODE-BRIGHT were different from the ones from SVFLUX and VADOSE/W. This is due to the fact that unlike SVFLUX and VADOSE/W which allow SWCC only in terms of volumetric water content, CODE-BRIGHT allows SWCC only in terms of degree of saturation. The van Genuchten-Mualem equation used in VADOSE/W and SVFLUX allows van Genuchten SWCC fitting parameters ('a', 'n', and 'm') in terms of volumetric water content. However, the van Genuchten-Mualem equation that is utilized in CODE-BRIGHT allows van Genuchten SWCC fitting parameters ('a', 'n', and

'm') in terms of degree of saturation only. It was established in Chapter 3, that for a given expansive soil, the SWCC in terms of degree of saturation may have different fitting parameters than the SWCC in terms of volumetric water content. The van Genuchten-Mualem equation used in VADOSE/W and SVFLUX uses SWCC in terms of volumetric water content and its saturated hydraulic conductivity and generates estimation for k_{unsat} function. In CODE-BRIGHT, however, the Van Genuchten-Mualem equation uses SWCC in terms of degree of saturation (as opposed to volumetric water content in VADOSE/W and SVFLUX). Therefore, the k_{unsat} functions generated by VADOSE/W and SVFLUX are the same but they are different from the k_{unsat} functions generated by CODE-BRIGHT. Figure 6.9 shows a comparison of results obtained from SVFLUX, VADOSE/W, and CODE-BRIGHT for Colorado soil with top boundary condition of 5.0E-4 m/day. The figure shows reasonable agreement among the results obtained from the three computer codes.

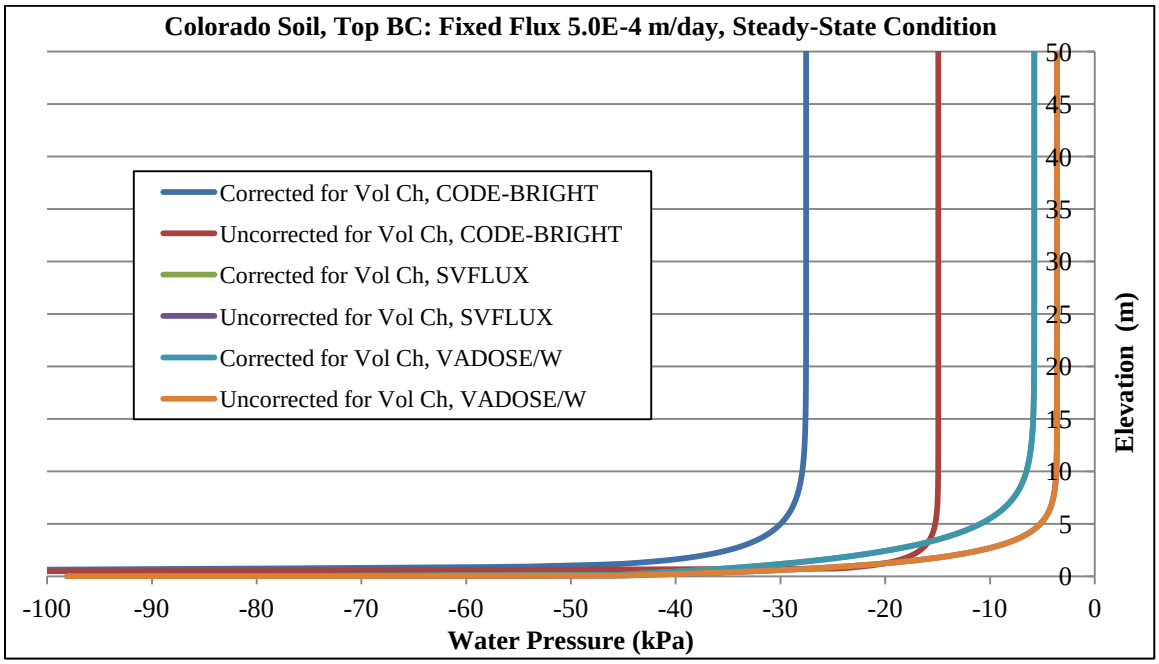

Figure 6.9. Example profile of soils suction for corrected and uncorrected SWCC. Water pressure versus elevation profile at steady-state condition for Colorado soil with SWCC corrected and uncorrected for volume change and top fixed flux of 5.0e-4 m/day using SVFLUX, VADOSE/W, and CODE-BRIGHT

It was found from the results that the values of wetting induced soil expansion for the Colorado soil at time 15,000 days, when the model has reached the steady-state (essentially saturated soil profile), for both cases of SWCC corrected and uncorrected are relatively close. This is because steady-state conditions for positive surface flux result in essentially full wetting of the soils in the column. For uncoupled analyses, the amount of soil expansion (heave) computed by CODE-BRIGHT was 0.2729 meters and 0.2842 meters for volume corrected SWCC and volume uncorrected SWCC, respectively. The amount of heave computed using unsaturated flow results from SVFLUX was found to be 0.2908 meters and 0.2931 meters for volume corrected SWCC and volume uncorrected SWCC, respectively. The reason that the final heave values are so similar is that the profiles were wetted to essentially full saturation in both cases (15,000 days of

constant positive flux surface boundary condition leads to full wetting in both corrected and uncorrected cases).

The amounts of deformation found for Colorado soil from uncoupled and coupled flow-deformation analyses showed close agreement for both steady-state condition (where the soil has become fully wetted) and for transient flow where substantially unsaturated soil conditions (relatively high soil suction conditions) in the profile existed. Tables 6.1 and 6.2 below (and previously presented in Chapter 4), present comparisons between amounts of deformation for corrected and uncorrected SWCC found by uncoupled and coupled flow-deformation analyses. It can be seen that there is close agreement between the results. Also shown are comparisons between volume-corrected and uncorrected SWCC results.

Table 6.1. Deformation values found by transient uncoupled and coupled analyses using CODE-BRIGHT for Colorado soil with top BC fixed flux of 5.0E-4 at steady-state condition (15,000 days)

				Deformation (m)	
Soil	**Top BC Fixed Flux (m/day)**	**SWCC**	**Program Used**	**Uncoupled Analyses**	**Coupled Analyses**
Colorado	5.00E-04	Corrected	CODE-BRIGHT	0.2729	0.2964
Colorado	5.00E-04	Uncorrected	CODE-BRIGHT	0.2842	0.3616

Table 6.2. Deformation (heave) values found by transient uncoupled and coupled analyses at time 7,000 days using CODE-BRIGHT for Colorado soil with top BC fixed flux of 5.0E-4

				Deformation (m)	
Soil	**Top BC Fixed Flux (m/day)**	**SWCC**	**Program Used**	**Uncoupled Analyses**	**Coupled Analyses**
Colorado	5.00E-04	Corrected	CODE-BRIGHT	0.2448	0.2435
Colorado	5.00E-04	Uncorrected	CODE-BRIGHT	0.1923	0.1959

It was found from the uncoupled and coupled flow-deformation analyses on Colorado soil with top boundary condition of fixed flux of 5.0e-4 m/day that at time 7,000 days when the models has not reached the steady-state (not fully wetted), the deformation (soil expansion) is significantly larger for corrected SWCC compared to uncorrected SWCC (0.245m and 0.19m for corrected and uncorrected cases, respectively). This is due to higher rate of progression of wetted front for the case of corrected SWCC compared to uncorrected SWCC. The difference in deformation of volume-corrected and volume-uncorrected cases were found to be insignificant at steady-state condition where positive surface flux boundary conditions were applied, compared to the earlier times in the process (i.e. when the soils have not become saturated), as expected due to steady state conditions leading to essentially fully wetted conditions (nearly zero suction). It was also found that for the conditions of fully wetted soils, the deformation is slightly larger for volume-uncorrected SWCC (due to smaller suction values within the profile) compared to volume-corrected SWCC resulting from difference in the corrected and uncorrected curve AEV's. However, at times prior to steady-state (when the soil is not saturated) the deformation was found to be larger for volume-corrected SWCC because the water progresses more rapidly through the volume-corrected soil profile case.

It should also be mentioned that for the expansive soils in this study, which do not exhibit extreme volume change upon wetting and drying, the difference in the estimated amounts of deformation for volume corrected and uncorrected SWCC's is not very large. However, the difference observed here are expected to be substantially more pronounced

for more highly expansive soils (e.g. higher PI soils), for conditions resulting in larger changes in soil suction, and also for any extremely high volume change soils, such as slurry materials.

The effect of volume change on the shape of the SWCC, including AEV and slope in the transition zone, is clearly demonstrated, and when volume change corrections are not made, errors in the AEV and slope of the SWCC result. However, it is less clear whether volume change corrections to the SWCC in estimating k_{unsat} functions leads to improved unsaturated flow results. The uncertainty results from the fact that the k_{unsat} function models have been developed using data that was not volume corrected. This may lead to existence of compensating errors in the analyses. On the other hand, most of the data used for developing and validating k_{unsat} function models was not on clays, but rather on silts, sands, and materials with no significant volume change. Therefore, correcting the SWCC's for volume change may be a reasonable practice for soils with high volume change potential (such as expansive soils and slurry specimens). More studies are needed to evaluate the effect of volume change on SWCC key parameters, particularly AEV and slope in transition zone, on the unsaturated flow properties (k_{unsat} versus suction) of high volume change soils. The study here on effects of volume change on SWCC's, k_{unsat} functions, and unsaturated flow/deformation analyses represents only a start on understanding the complex issues at play for unsaturated flow/deformation modeling of high volume change soils.

The SWCC's of oil sands tailings were previously established by Fredlund and Houston (2013) and Fredlund et.al. (2011), by drying SWCC testing of the slurry

specimens. The initially saturated slurry specimens of oil sands tailings exhibit extreme volume change upon increase in suction. Slurry specimens of oil sands tailings exhibit shrinkage at suctions even smaller than air-entry value when the specimen is still saturated. Volume changes at suction smaller than air-entry value affects the k_{sat} value of these specimens. The Kozeny-Carman is one method that can be used for correcting the k_{sat} at suctions smaller than air-entry value (Kozeny, 1927, and Carman, 1937, 1956). However, none of the computer codes used in this study (i.e. VADOSE/W, SVFLUX, and CODE-BRIGHT) has the capability to do corrections for k_{sat} as the volume of the soil changes at suctions smaller than the air-entry value. Therefore, as important as this correction may be for slurry soils, it could not be accounted for in this study. The effect of this k_{sat} correction for compacted or native soil expansive clays is not expected to be significant, whereas the effect of the k_{sat} correction for suctions below the AEV would be very substantial for slurry soils such as oil sands tailings. In addition to the points made above, there are several reasons why the results on the oil sands tailings should not be taken to be representative of any actual field condition. The most interesting field path for oil sands tailings is drying from a slurry. In the field, the oil sands tailings start at saturated conditions and then dry. For the simulations of this study, the oil sands tailings were started at an initial condition of an unsaturated state and then either wetted or dried. Further, the suction compression curve (void ratio versus suction) of oil sands tailings obtained from previous research by Fredlund et al. (2011) was utilized, and in those studies, a drying path was followed. For the cases in which a wetting path was simulated in the numerical analyses for the oil sands tailings, no modification to the void ratio

versus suction relationship to account for difference in wetting and drying path were made in this study.

Uncoupled (flow only) analyses on oil sands tailings were conducted for the models based on properties of oil sands tailings in SVFLUX, VADOSE/W, and CODE-BRIGHT in order to evaluate effect of volume-correcting SWCC on hydraulic properties of soils and rate of changes in soil suction and the resulting suction-change induced deformation. The rate of changes in soil suction was studied and amount of suction-change induced deformation was determined based on the generated suction profile of the soil column. The initial condition of the oil sand tailings was set to be unsaturated (suction of 100kPa at the bottom and suction of 600kPa at the top of the model). For the simulations in which the soil becomes wetted from the top by adding the positive fixed flux, the suction of soil starts to decrease. It was previously established that the volume corrected SWCC generally has larger AEV compared to the uncorrected SWCC. This means that in the soil with volume corrected SWCC, desaturation starts at a larger suction compared to the soil with uncorrected SWCC. That is to say, the soil with corrected SWCC stays saturated at larger suction ranges compared to the soil with uncorrected SWCC. Therefore, once the soil becomes wet and the suction decreases (i.e. wetting path on the SWCC), for the soil with corrected SWCC, the soil becomes saturated (i.e. close to AEV on SWCC) at a larger suction; whereas, the suction within the soil with uncorrected SWCC should further decrease (compared to the soil with corrected SWCC) in order for the suction to reach AEV (i.e. saturation or close-to-saturation state). This mechanism illustrates the reason for the difference in final suction profile for the cases of volume

corrected SWCC and volume uncorrected SWCC. An example of generated suction profile for oil sands tailings with base boundary condition set as suction of 100kPa is shown in Figure 6.10. It can be seen that if the model is allowed to run for long-enough time so that the soil gets fully wetted (i.e. steady-state); the generated suction is smaller for uncorrected SWCC compared to corrected SWCC. This is due to the fact that the volume-corrected SWCC has a larger air-entry value compared to volume-uncorrected SWCC. Therefore, when the soil becomes wet (i.e. wetting path on SWCC) the volume-corrected SWCC reaches the saturated condition at a higher suction.

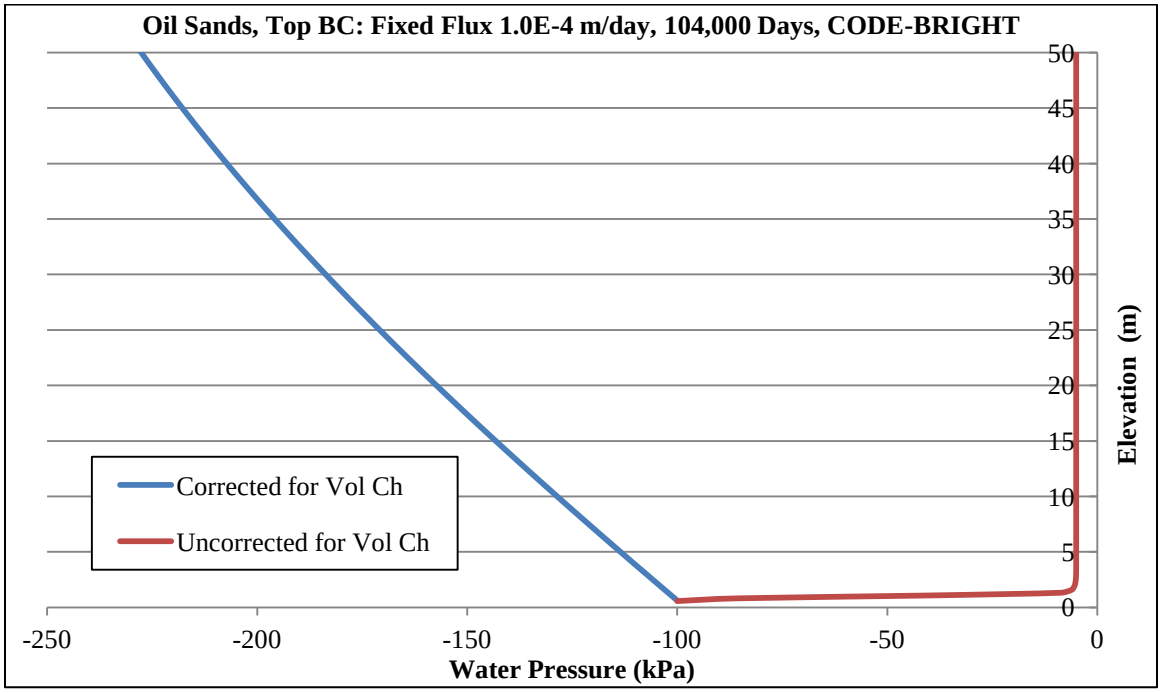

Figure 6.10. Example profile of soils suction for corrected and uncorrected SWCC. Water pressure versus elevation profile at steady-state condition (104,000 days) for Oil Sands tailings with SWCC corrected and uncorrected for volume change and top fixed flux of 1.0e-4 m/day using CODE-BRIGHT

For the wetting simulations (positive flux boundary condition) it was found that in the models with volume corrected SWCC, the soil gets wet quicker (faster rate of

progression of wetted front), as the unsaturated hydraulic conductivity of the soil with corrected SWCC is higher than the unsaturated hydraulic conductivity of the same soil with volume uncorrected SWCC. Larger values of k_{unsat} results in water penetrating through the soil faster.

For the times prior to the steady-state, in some portions of the soil profile, the suction of uncorrected SWCC is higher than the suction of the corrected SWCC. This is due to the fact that k_{unsat} is generally higher for corrected SWCC and hence, at a given time, the depth of wetting is generally larger for corrected SWCC compared to uncorrected SWCC. Figure 6.11 shows an example which compares the depth of wetting of volume-corrected and volume-uncorrected SWCC at the time 60,000 days for top boundary condition of fixed flux of 1.0E-4 m/day for oil sands tailings. It can be seen that the depth of wetting is larger for corrected SWCC (due to higher k_{unsat} values). Figure 6.11 shows that at time 60,000 days the model with the volume-corrected SWCC has reached the steady-state (fully wetted condition) while the model with the volume corrected SWCC is only wetted half-way through the depth of column.

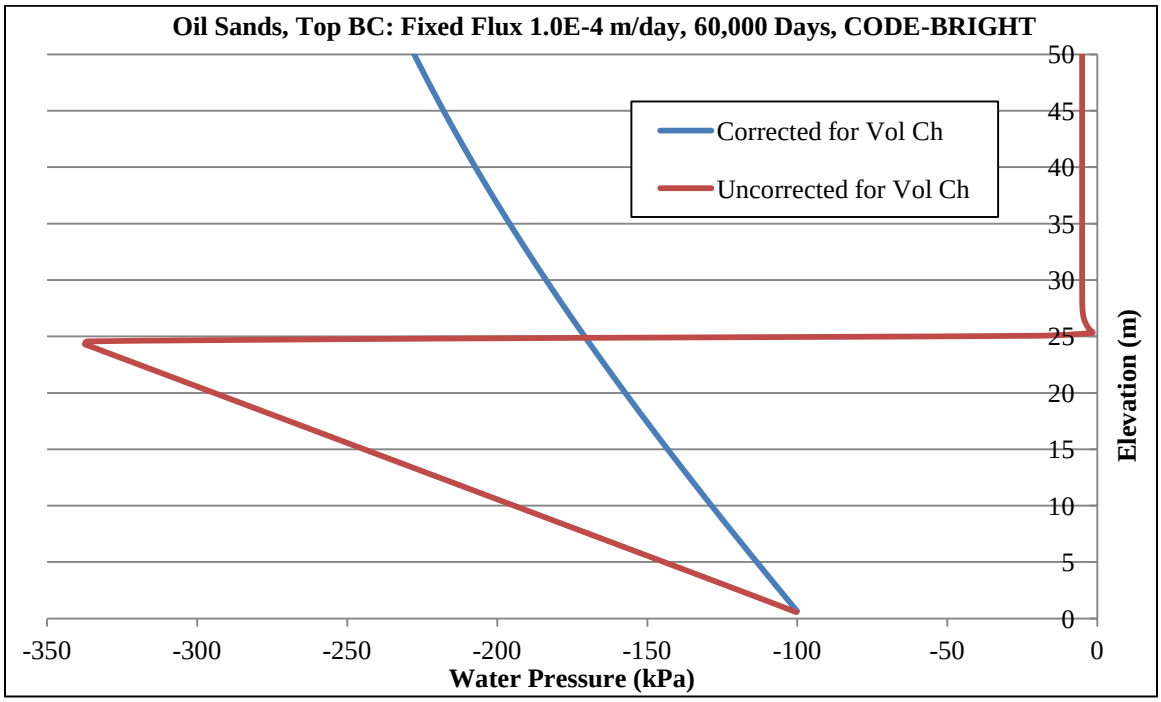

Figure 6.11. Example profile of soils suction for corrected and uncorrected SWCC. Water pressure versus elevation profile at time 60,000 days (164 years) for Oil Sands tailings with SWCC corrected and uncorrected for volume change and top fixed flux of 1.0e-4 m/day using CODE-BRIGHT

Figure 6.12 shows an example for top boundary condition of evaporation for oil sands tailings. It was found that for top boundary conditions of negative flux (evaporation) the generated suction was larger for volume-uncorrected SWCC compared to volume-corrected SWCC. This makes it difficult to determine in advance if corrected or uncorrected curves will lead to higher suction values, particularly for evaporation cases. This is believed to be a result of the high nonlinearity of the SWCC and k_{unsat} function.

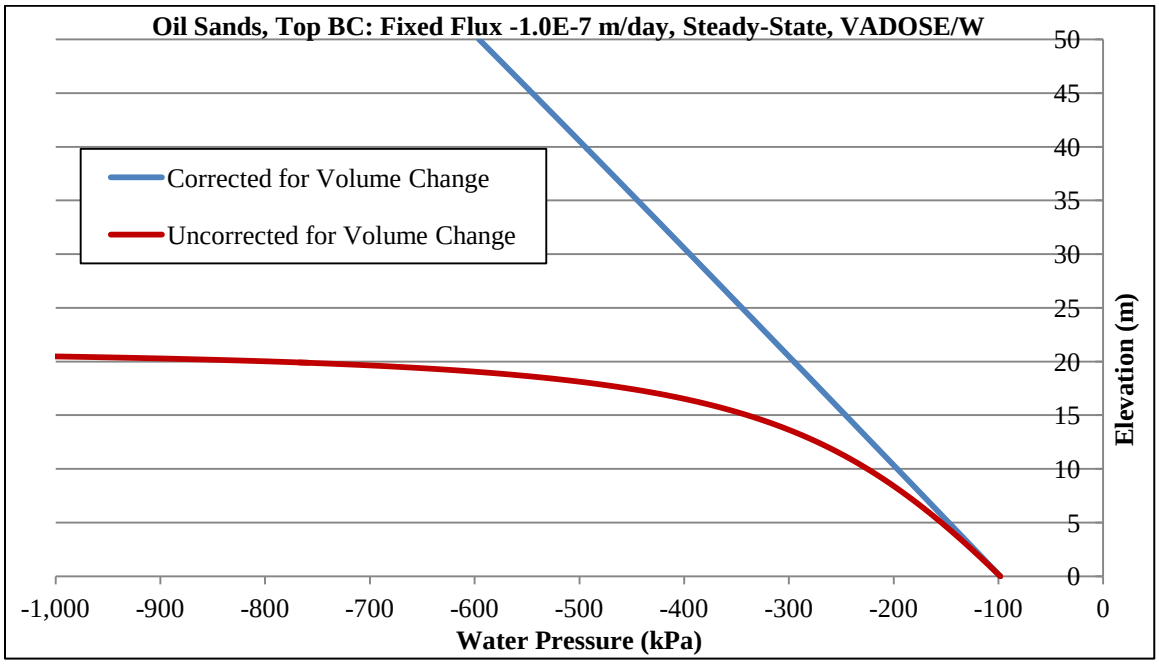

Figure 6.12. Example profile of soils suction for corrected and uncorrected SWCC. Water pressure profile versus depth at steady-state condition for oil sands tailings with SWCC corrected and uncorrected for volume change and top fixed flux of -1.0E-7 m/day (evaporation) using VADOSE/W

It was found from the calculation of deformation based on results of uncoupled analyses using Oil Sands tailings data that at steady-state condition (i.e. the time that the soil has become completely wet) that: (1) large amounts of wetted induced heave happens when the Oil Sands tailings get wet, neglecting path dependency on the measured void ratio versus suction plot for the oil sands tailings. (2) There is a large difference between the two cases of SWCC corrected and uncorrected for soil volume change. The large amounts of deformation of Oil Sands tailings is expected as Oil Sands tailings were assumed to exhibit large volume change upon change in suction. This fact is shown in the suction compression curve of Oil Sands tailings in which the decrease in suction from 1400kPa to 60kPa leads to increase in void ratio from around 0.35 to 0.72 (i.e. increase of 0.37 in void ratio) when it is assumed that the wetting and drying path void ratio versus

suction curves are the same. This large amount of increase in void ratio leads to a large amount of strain and thus heave. The final suction profile of the case in which SWCC is uncorrected is much smaller than the suction within the Oil Sands tailings in the case of the corrected SWCC. By using the same suction compression curve, much larger final void ratio profile for the case with uncorrected SWCC is found compared to the case in which SWCC is corrected. Larger final void ratio throughout the soil column leads to more deformation at the column surface for the model with volume-uncorrected SWCC (2.6m and 11.8m for corrected and uncorrected SWCC, respectively, were found by uncoupled analyses using CODE-BRIGHT).

It was also found, as with the results on expansive soils, that depending upon the time and amount of changes in soil suction (e.g. progression of wetted front) within the profile, uncorrected SWCC may exhibit higher or lower suction compared to the corrected SWCC. This makes it difficult to determine in advance if corrected or uncorrected curves will lead to higher suction values, and further research is needed to study this phenomenon from a fundamental unsaturated soil mechanics perspective.

6.3. Recommendations for Future Research

Based on the results of this study, the following recommendations for future research are offered:

- It is recommended that SWCC measurement devices which are capable of accurate volume change measurement be developed. This type of device can aid in more accurate measurement of dimensions of tested specimens which leads to more accurate SWCC's. Existing oedometer-type pressure plate

devices as such a device, but present some challenges for drying path when only light net normal stress is applied and for extremely high volume change soils (e.g. slurry) when high suctions are applied.

- It was found in this research, through literature review and laboratory testing, that the SWCC in terms of degree of saturation best describes the unsaturated properties of expansive soils. It is recommended that degree of saturation representations for SWCC's be used for unsaturated flow analyses. It is recommended that equations for predicting k_{unsat} functions for clays (particularly expansive clays) be developed which account for soil volume change. Development of new formulations for k_{unsat} functions for other high volume change soils such as slurry soils and collapsible soils are also needed.
- It was established that when volume change of slurry specimens may present errors in predicting the k_{sat} of this material, particularly for suctions smaller than the air-entry value due to volume change that occurs under saturated negative pore water pressure conditions. It is recommended that unsaturated flow codes be enhanced to be able to do the necessary corrections to k_{sat} when simulating flows for slurry It is recommended to conduct numerical modeling using a wider range of top boundary conditions fixed flux (both positive flux and evaporation and more field-representative surface flux conditions), a wider range of base boundary conditions head values, and a wider range of material properties, including air-entry value and slope in transition zone.

- Further research and studies on a wider range of high volume change soils is needed. Flow and deformation analyses through uncoupled and coupled flow/deformation numerical modeling for collapsible soils and other high volume change soils should be done.
- It is recommended that further study of the effect of net normal stress on volume change of slurry specimens and other high volume change soil be conducted with respect to SWCC be performed through laboratory testing.

REFERENCES

Abbaszadeh, M. (2011). The Effect of Cracks on Unsaturated Flow and Volume Change Properties of Expansive Clays and Impacts on Foundation Performance. Dissertation for Doctor of Philosophy. Arizona State University.

Abou-Bekr, N., Derdouf, F. M., and Bekkouche, A., (2005). "Behaviour Upon Drying-wetting Paths of Maghnia Bentonite (West of Algeria). Proceedings of the International Symposium Advanced Experimental Unsaturated Soil Mechanics, Experus 05, Tarantino et al., Eds., Balkema, pp. 145–169.

Aitchison, G.D., 1973. A quantitative description of the stress deformation behavior of expansive soils, Proceedings, 3rd International Conference on Expansive Soils, Haifa, vol. 2, pp. 79– 82.

Al-Mhaidib, A. I., 2008, Mathematical Model to Predict Swelling of Expansive Soil, the 12th International Conference of International Association for Computer Methods and Advances in Geomechanics (IACMAG)

Al-Shamrani, M. A. and Dhowian A. W., 2003, Experimental study of lateral restraint effects on the potential heave of expansive soils, Engineering Geology 69, pp 63–81

Al-Zoubi, M. Sh., 2008, Swell Characteristics of Natural and Treated Compacted Clays, EJGE

American Society for Testing and Materials (ASTM) (2007) "Standard Test Method for Particle-Size Analysis of Soils", ASTM D422 - 63(2007)

American Society for Testing and Materials (ASTM) (2010) "Standard Test Methods for Specific Gravity of Soil Solids by Water Pycnometer", ASTM D854 - 10

American Society for Testing and Materials (ASTM) (2010) "Standard Test Methods for Liquid Limit, Plastic Limit, and Plasticity Index of Soils", ASTM D4318 - 10

American Society for Testing and Materials (ASTM) (2010) "Standard Test Method for Measurement of Soil Potential (Suction) Using Filter Paper" ASTM D5298 - 10

American Society for Testing and Materials (ASTM) (2012) "Standard Test Methods for Laboratory Compaction Characteristics of Soil Using Standard Effort", ASTM D698 - 12

Barbour S. L. (1998). The soil-water characteristic curve: a historical perspective. *Canadian Geotechnical Journal* 35, 873-894.

Baumgartl, T., Rostek, J., Horn, R., (2000). Internal and external stresses affecting the water retention curve. Advances in GeoEcology 32: 13-21

Biarez, J., Fleureau, J. M., Zerhouni, M. I., and Soepandji, B. S. (1987). "Variations de volumes des sols argileux lors de cycles de drainage humidification." Rev. Fr. Géotech., 41: 63–71.

Bilsel, h., (2004), Hydraulic properties of soils derived from marine sediments of Cyprus, Journal of Arid Environments 56 (2004) 27–41

Brooks, R. H., and Corey, A. T. (1964). "Hydraulic properties of porous media." *Hydrology Paper No. 3*, Colorado State Univ., Fort Collins, Colo.

Brutsaert, W. (1967). "Some methods of calculating unsaturated permeability." *Trans. ASAE*, 10, 400–404.

Buckingham, E. (1907). "Studies of the Movement of Soil Moisture." *U.S.D.A. Bur. Of Soils, Bulletin No. 38.*

Bulut, R. and Wray, W. K. (2005). "Free Energy of Water-Suction-in Filter Papers." *Geotechnical Testing Journal*, 28(4), 1 – 10.

Bulut, R., Lytton, R. L., and Wray, W. K. (2001). "Soil Suction Measurements by Filter Paper." *Proceedings of Geo-Institutes Shallow Foundation and Soil Properties Committee Sessions at the ASCE 2001 Civil Engineering Conference*, Houston, Texas. October 10-31, 243 – 261.

Burdine, N. (1953). Relative permeability calculations from pore-size distribution data, Pet. Trans. Am. Inst. of Mining and Met. Eng. 198, 71-77

Cabral, A.R., Planchet, L., Marinho, F.A., and Lefebvre, G. 2004. Determination of the soil water characteristic curve of highly compressible materials: Case study of pulp and paper by-product. Geotechnical Testing Journal, 27: 154–162.

Campbell, G. S. (1974). "A simple method for determining unsaturated conductivity from moisture retention data." *Soil Sci.*, 117(6), 311–314.

Campbell, J.D. (1973). Pore pressures and volume changes in unsaturated soils. Ph.D. thesis, University of Illinois at Urbana- Champaign, Urbana-Champaign, Ill.

Celia, M.A., and Bouloutas, E.T., (1990) A general mass-conservative numerical solution for the unsaturated flow equation. Water Resources Research, Vol. 26, No 7, pp. 1483-1496, July.

Chandler R.J. and Gutierrez C.I. (1986). The filter paper method of suction measurement. Geotechnique, 36, pp- 265 -268.

Chao, K. C. (1995). "Hydraulic Properties and Heave Prediction for Expansive Soil." *Maters Thesis, Colorado State University*, Fort Collins, Colorado.

Chao, K. C. (2007), Design Principles For Foundations On Expansive Soils, PhD Dissertation, Colorado State University, Fort Collins, Colorado

Chao, K. C., Durkee, D. B., Miller, D. J., and Nelson, J. D. (1998). "Soil Water Characteristic Curve for Expansive Soil." *Thirteenth Southeast Asian Geotechnical Conference*, Taipei, Taiwan.

Chao, K.C., Nelson, J.D., Overton, D.D., and Cumbers, J.M. (2008), Soil water retention curves for remolded expansive soils, Unsaturated Soils: Advances in Geo-Engineering- Toll et al. (eds): 243-248

Chertkov, V.Y. (2004). A physically based model for the water retention curve of clay pastes. Journal of Hydrology, 286: 203– 226. doi:10.1016/j.jhydrol.2003.09.019.

Childs, E., and Collis-George. N. (1950). The permeability of porous materials. Proc. Roy. Soc. London. A: 201, 392-405.

Ching, R. K. H. and Fredlund, D. G. (1984). "A Small Saskatchewan Town Copes with Swelling Clay Problems." *Proc. 5th Int. Conf. Expansive Soils*, 306 – 310.

Chiu, C. F., Ng, C. W. W., (2012), Coupled water retention and shrinkage properties of a compacted silt under isotropic and deviatoric stress paths, Can. Geotech. J. 49: 928–938, doi:10.1139/T2012-055

Code_Bright Pre-Process, Problem Data (2012). CODE-BRIGHT Manual

Cokca, E,. 2000, Comparison of suction and oedometer methods for the measurement of swell pressure, Quarterly Journal of Engineering Geology and Hydrology, 33, pp 141-147

Çokca, E. 2002, Relationship between methylene blue value, initial soil suction, and swell percent of expansive soil. Turkish J. Eng. Env. Sci. 26 , 521–529.

Croney D. 1952. The movement and distribution of water in soil. Géotechnique. 3 (1), 1-16.

Croney, D., and Coleman, J.D., (1961). Pore pressure and suction in soils. Proceedings, Conference on Pore Pressures and Suction in Soils. Butterworths, London. Pp. 31-37

Cui, Y., Mantho, A., Cui, K., Audiguier, M., (2006), Water retention properties and volume change behavior of natural Romainville clay. Unsaturated Soils, pp: 873- 882

Darcy, H. (1856). “Les fontaines publiques de la ville de Dijon.” *V. Dalmont*, Paris, 647

Delage, P., Suraj De Silva G.P.R., De Laure, E., (1987). Un nouvel appareil triaxial pour les sols non satures. Comptes-rendus de la lome Conf. europeene de Mecanique des Sols et des Travaux de Fooundation, Dublin, vol. 1: 26-28

Dye, H. B., (2008). Moisture movement through expansive soil and impact on performance of residential structures, PhD Dissertation, Arizona State University

Ebrahimi-B, N., Gitirana, G. F. N., Jr., Fredlund, D. G., Fredlund, M. D., and Samarasekera, L. (2004). “A lower limit for the water permeability coefficient.” *Proc., 57th Canadian Geotechnical Conf.*, Vol. 1, Quebec City, Que., Canada, 12–19.

Eching, S. and Hopmans, J. (1993). Optimization of hydraulic functions from transient outflow and soil water pressure data. SSSAJ. 57, 1167-1175.

Edgar, T. V., Nelson, J. D., and McWhorter, D. B. (1989).“Nonisothermal Consolidation in Unsaturated Soil.” *The Journal of Geotechnical Engineering*, 115(10), 1351 – 1372.

Elrick, E. C., and Bowman, D. H., (1964). Note on an improved apparatus for soil flow moisture measurements. Soil Sci. Soc. Amer. Proc. 28: 450-453

Erzin Y., and Erol O., 2007, Swell pressure prediction by suction methods, Engineering Geology 92, pp133–145

Farrel, D. A., and Larson, W. E. (1972). “Modeling the pore structure of porous media.” *Water Resour. Res.*, 8(3), 699–706.

Feng, M., and Fredlund, D. G. (1999). “Hysteretic influence associated with thermal conductivity sensor measurements.” *Proc., 52nd Canadian Geotechnical Conf.*, Regina, Sask., Canada, 651–657.

Fernandez-Galvez, J., Barahona, E. (2006). Changes in water retention due to soil kneading. Journal of Agricultural water management, Elsevier B. V. No. 76. P. 53-61.

Fleureau, J. M., Kheirbek-Saoud, S., Soemitro, R., and Taibi, S. (1993). “Behavior of clayey soils on drying-wetting paths.” *Can. Geotech. J.*, 30: 287–296.

Fleureau, J. M., Verbrugge, J. C., Huergo, P. J., Correia, A. G., and Kheirbek-Saoud, S. (2002). “Aspects of the behaviour of compacted clayey soils on drying and wetting paths.” *Can. Geotech. J.*, 39: 1341–1356.

Fleureau, J.M., Hadiwarrdoyo, S., and Kheirbek-Saoud, S. (2004). Simplified approach to the behavior of compacted soils on drying and wetting paths. *In* Proceedings

of the Third International Conference on Unsaturated Soils, Recife, Brazil, 10–13 March 2002. *Edited by* J.F.T. Juca, T.M.P. de Campos, and F.A.M. Marinho. A.A. Balkema, Lisse, the Netherlands.

Fleureau, J.M., Kheirbek-Saoud, S., and Taibi, S. (1995). Experimental aspects and modeling of the behaviour of soils with a negative pressure. *In* Proceedings of the 1st International Conference on Unsaturated Soils, Paris, France, 6–8 September 1995, *Edited by* X. Alonso and X. Delage. A.A. Balkema, Rotterdam, the Netherlands. Vol. 1. pp. 57–62.

Fredlund, D. G. (2000). "The 1999 R.M. Hardy Lecture: The Implementation of Unsaturated Soil Mechanics into Geotechnical Engineering." *Canadian Geotechnical Journal*, 37, 963 – 986.

Fredlund, D. G. (2002). "Use of Soil-Water Characteristic Curves in the Implementation of Unsaturated Soil Mechanics." *Third International Conference on Unsaturated Soils*. Recife, Brazil.

Fredlund, D. G. and Rahardjo, H. (1993). Soil mechanics for unsaturated soils. New York: Wiley.

Fredlund, D. G., and Morgenstern, N. R. (1977). "Stress state variables for unsaturated soils." J. Geotech. Eng. Div., Am. Soc. Civ. Eng., 103(5), 447–466.

Fredlund, D. G., and Rahardjo, H. (1993). "The role of unsaturated soil behavior in geotechnical practice." Proc., 11th Southeast Asian Geotechnical Conference, Invited Keynote Address, Singapore, 37–49.

Fredlund, D. G., and Xing, A. (1994). "Equations for the soil-water characteristic curve." *Can. Geotech. J.*, 31(4), 521–532.

Fredlund, D. G., Houston, S. L. (2009). Protocol for the assessment of unsaturated soil properties in geotechnical engineering practice, Can. Geotech. J. 46: 694–707. doi:10.1139/T09-010

Fredlund, D. G., Houston, S. L., (2013). Interpretation of Soil-Water Characteristic Curves when Volume Change Occurs as Soil Suction is Changed, Pan-American Conference on Unsaturated Soils, Cartagena de Indias, Colombia

Fredlund, D. G., Sheng, D., Zhao, J. (2011). Estimation of soil suction from the soil-water characteristic curve. Can. Geotech. J. 48: 186–198. doi:10.1139/T10-060

Fredlund, D. G., Shuai, F., and Feng, M. (2000). "Increased accuracy in suction measurement using an improved thermal conductivity sensor." Proc., 7th Int. Conf. on Tailings and Mine Waste, Fort Collins, Colo., 443–450.

Fredlund, D. G., Xing, A., and Huang, S. (1994). Predicting the permeability function for unsaturated soils using the soil-water characteristic curve. *Canadian Geotechnical Journal*, 31(4), pp 533–546

Fredlund, D.G. (1964). Comparison of soil suction and one-dimensional consolidation characteristics of highly plastic clay. M.Sc. thesis, University of Alberta, Edmonton, Alta.

Fredlund, D.G., Stone, J., Stianson, J., (2011), Determination of Water Storage and Permeability Functions for Oil Sands Tailings, Proceedings Tailings and Mine Waste 2011, Vancouver, BC, November 6 to 9, 2011

Fredlund. D.G. (2006). Unsaturated Soil Mechanics in Engineering Practice, Journal of Geotechnical and Geoenvironmental Engineering, Vol. 132, No. 3, 286- 321

Fredlund, M. D., Fredlund, D. G., Houston, S. L., Houston, W. (2003). Assessment of unsaturated soil properties for seepage modeling through tailings and mine wastes. Tailings and Mine Waste '03, Swets and Zeitlinger, Lisses

Frost, J. D. and Park, J. Y. (2003). "A Critical Assessment of the Moist Tamping Technique." *ASTM Geotechnical Testing Journal*, 26(1), 57 – 70.

Gallipoli, D., Gens, A., Sharma, R., and Vaunat, J. (2003). "An elastoplastic model for unsaturated soil incorporating the effects of suction and degree of saturation on mechanical behaviour." Geotechnique, 53(1), 123–135.

Gallipoli, D., Gens, A., Vaunat, J., and Romero, E. (2002). Role of degree of saturation on the normally consolidated behavior of unsaturated soils. Experimental evidence and theoretical approaches in unsaturated soils, A. Tarantino and C. Mancuso, eds, Balkema, Rotterdam, The Netherlands: 115–120.

Gallipoli, D., Wheeler, S. J., and Karstunen, M. (2003). Modeling the variation of degree of saturation in a deformable unsaturated soil. Geotechnique, 53(1): 105–112.

Gardner W. (1958). Some steady-state solutions of the unsaturated moisture flow equation with applications to evaporation from a water table. Soil Sci. 85, 228-232.

Gardner, W. (1958). "Mathematics of isothermal water conduction in unsaturated soils." *Highway Research Board Special Rep. No. 40*, Int. Symp. on Physico-Chemical Phenomenon in Soils, Washington, D.C. pp. 78–87.

Gardner, W. R. (1956). "Calculation of capillary conductivity from pressure plate outflow data." *Soil Sci. Soc. Am. Proc.*, 20: 317–320.

GEO-SLOPE International Ltd. (2012). Vadose Zone Modeling with VADOSE/W, an Engineering Methodology

Geotechnical Consulting and Testing Systems, Inc. (GCTS). (2004). "Fredlund SWCC Device Operating Instructions." Tempe, Arizona.

Gillham, R. W., Klute, A., and Heerman, D. F., (1976) Hydraulic properties of a porous medium: measurement and empirical representation. Soil Sci. Soc. Am. J. 40, No. 2, 203-207

Green , R. E., Hanks, R. J., Larson, W. E. (1964). Estimates of field infiltration by numerical solution of the moisture flow equation, Soil. Sci. Soc. Amer. Proc. 28: 15-19

Green, R.E. and Corey, J.C., (1971) Calculation of Hydraulic Conductivity: A Further Evaluation of Some Predictive Methods. Soil Science Society of America Proceedings, Vol. 35, pp. 3-8.

Head, K.H. (1980). Manual of soil laboratory testing: soil classification and compaction tests. Pentech Press, London.

Hilf, J. W. (1956). "An investigation of pore-water pressure in compacted cohesive soils." Technical Memorandum No. 654,PhD thesis, Design and Construction Division, Bureau of Reclamation, United States Department of the Interior, Denver.

Hillel, D., 1980. Fundamentals of Soil Physics, Academic, San Diego, Calif.

Holtz, R. D., Kovacs, W. D., Sheahan, T. C. (2010). An Introduction to Geotechnical Engineering (2nd Edition). Prentice Hall;

Houston, S. L., Houston, W. R., and Wagner, A. M. (1994). "Laboratory Filter Paper Measurements." *Geotechnical Testing Journal*, 17(2), 185 – 194.

Huang, S.Y., Barbour, S.L., and Fredlund, D.G. 1998. Development and verification of a coefficient of permeability function for a deformable unsaturated soil. Canadian Geotechnical Journal, 35: 411–425. doi:10.1139/cgj-35-3-411.

Ito, M., Azam, S., (2010), Determination of Swelling and Shrinkage Properties of Undisturbed Expansive Soils, Geotech Geol Eng (2010) 28:413–422

Jacquemin, S., 2011. Laboratory determination of hydraulic conductivity functions for unsaturated cracked fine grained soil. Thesis for Master of Science. Arizona State University.

James M., Tinjum, Craig, H., Benson, Lisa, R., and Blotz (1997) "Soil-water characteristic curves for compacted clays." Journal of Geotechnical and Geo-environmental engineering

Jian Z., Jian-lin Y. (2005). Influences affecting the soil-water characteristic curve. Journal of Zhejan Iniversity Science. 6A(8): 797-804.

Johnson, L.D., Snethen, D.R., 1978. Prediction of potential heave of swelling soils, Geotechnical Testing Journal, ASTM 1 (3), 117– 124

Jury, W. A., Gardner, W. R., and Gardner, W. H. (1991). "Soil Physics, Fifth Edition." John Wiley & Sons, Inc., New York, NY.

Kassiff, G., and Benshalom, A. (1971), Experimental relationship between swell pressure and suction. Geotechnique 21: 245-255

Komornik, A. and David, D. (1969) Prediction of swelling pressure of clays: J. ASCE, Soil Mechanics and Foundation Division, SM No. 1, pp. 209-225.

Kunze, R.J., Vehara, G., and Graham, K., (1968). Factors Important in the Calculation of Hydraulic Conductivity. Soil Science of America Proceedings, Soil Physics, Vol. 32

Ladd, R. S. (1978). "Preparing Test Specimens Using Undercompaction." *ASTM Geotechnical Testing Journal*, 1(1), 16 – 23.

Laliberte, G. E. (1969). "A mathematical function for describing capillary pressure-desaturation data." *Bull. Int. Assoc. Sci. Hydrol.*, 14(2), 131–149.

Leong E., C., and Rahardjo, H. Permeability Functions for Unsaturated Soils. 1997 *Journal of Geotechnical and Geoenvironmental Engineering*, 123, (12): 1118-1126.

Leong, E. C. and Rahardjo, H. (1997). "Review of Soil-Water Characteristic Curve Equations." *Journal of Geotechnical and Geoenvironmental Engineering*, 123(12), 1106 – 1117.

Leong, E. C., He, L., and Rahardjo, H. (2002). "Factors Affecting the Filter Paper Method for Total and Matric Suction Measurements." *Geotechnical Testing Journal*, 25(3), 322 – 333.

Li, J., Sun, D.A., Sheng, D.C., Sloan, S. and Fredlund, D. (2007) Preliminary Study on Soil-Water Characteristics of Maryland Clay, Proc. 3rd Asian Conf. on Unsaturated Soils, Nanjing, China (ed. Z.Z. Yin, J.P. Yuan & A.C.F. Chiu), Beijing: Science Press, pp. 569-574.

Li, J.Y., Yang, Q., Li, P. Y., Yang, Q. L., (2009), Experimental Research on Soil-Water Characteristic Curve of Remolded Residual Soils, EJGE, Vol. 14 [2009], Bund. L

Lins, Y., and Schanz, T. (2004). "Determination of hydro-mechanical properties of sand." *Int. Conf. on Experimental Evidence towards Numerical Modeling of Unsaturated Soils*, T. Schanz, ed., Lecture Notes in Applied Mechanics, Springer, New York, 11–29.

Liu, Q., Yasufuku, N., Omine, K., Hazarike, H., (2012), Automatic soil water retention test system with volume change measurement for sandy and silty soils, Soils and Foundations 52 (2): 368-380

Liu, Q., Yasufuku, N., Omine, K., Kobayashi, T., (2011), Automatic soil water retention testing system with volume change measurement, Deformation Characteristics of Geomaterials

Lytton, R.L., (1977). The characterization of expansive soils in engineering, Presentation at the Symposium on Water Movement and Equilibrium in Swelling Soils, American Geophysical Union, San Francisco, CA

Lytton, R.L., 1994. Prediction of movement in expansive clays, In Proceedings of Vertical and Horizontal Deformations of Foundations and Embankments, Geotechnical Special Publication No. 40, ASCE, New York, pp. 1827–1845

Marshall, T.J. (1958). A relation between permeability and size distribution of pores. Journal of Soil Science, 9: 1 8.

Mbonimpa, M., Aubertin, M., Maqsoud, A., Bussière, B., (2006), Predictive Model for the Water Retention Curve of Deformable Clayey Soils, Journal of Geotechnical and Geoenvironmental Engineering, Vol. 132, No. 9: 1121- 1132

McCartney, J.S., Villar, L. F. S., Zornberg, J.G. (2007). Estimation of the Hydraulic Conductivity Function of Unsaturated Clays Using Infiltration Column Tests. NSAT- Volume 1- Parte 2.

McKee, C., and Bumb, A. (1987). "Flow-testing coalbed methane production wells in the presence of water and gas." *Proc., 1985 SPE Formation Evaluation Paper SPE 14447*, Society of Petroleum Engineers, Richardson, Tex., 599–608.

McKee, C.R., and Bumb, A.C. 1984. The importance of unsaturated flow parameters in designing a monitoring system for hazardous wastes and environmental emergencies. *In* Proceedings of the Hazardous Materials Control Research Institute National Conference, Houston, Tex., March 1984. pp. 50–58.

McKeen, R. G. (2001) "Investigating Field Behavior of Expansive Clay Soils", *Expansive Clay Soils and Vegetative Influence on Shallow Foundations*, Proceedings of Geo-Institute Shallow Foundation and Soil Properties Committee Sessions at the ASCE 2001 Civil Engineering Conference, Houston, Texas, Geotechnical Special Publication No. 115, 82-94.

McQueen, I. S. and Miller, R. F. (1968). "Calibration and Evaluation of Wide Range Gravimetric Method for Measuring Soil Moisture Stress." *Soil Science*, 10, 521 – 527.

Millington, R. J., and Quirk, J. P. (1959). Transport in porous media. Int. Cong. Soil Sci., Trans. 7th (Madison, Wis.) 1.3: 97-106

Millington, R.J., and Quirk, J.P., (1961). Permeability of Porous Solids. Transaction of the Faraday Society, Vol. 57, pp. 1200-1207

Moore, R.E. (1939). Water conduction from shallow water tables. Hilgardia, 12: 383-426.

Mualem, Y. (1976) .A new model for predicting the hydraulic conductivity of unsaturated porous media, WRR 12,513-522

Mualem, Y. (1976). Hysteretical models for prediction of the hydraulic conductivity of unsaturated porous media. Water Resources Research, 12: 1248-1 254.

Muir Wood, D. (1991). Soil Behaviour and Critical State Soil Mechanics, Cambridge [England] ; New York : Cambridge University Press

Mulilis, J. P., Chan, C. K., and Seed, H. B. (1975). "The Effects of Method of Sample Preparation on the Cyclic Stress Strain Behavior of Sands." EERC Report, 75 – 78.

Nagaraj, T. S. and Murthy, B. R. (1985) "Prediction of the Pre-consolidation Pressure and Recompression Index of Soils", Geotechnical Testing Journal, ASTM, 8(4), pp. 199–202.

Nayak, N.V., and Christensen, R.W. 1971, Swell characteristics of compacted expansive soils, Clays and clay minerals 19, 251-261

Nelson, J. D. (1985). "Constitutive Relationships and Testing of Unsaturated Soils." *Proceedings of the Eleventh International Conference on Soil Mechanics and Foundation Engineering*, San Francisco.

Nelson, J. D. and Miller, D. J. (1992). "Expansive Soils: Problems and Practice in Foundation and Pavement Engineering." John Wiley & Sons, Inc., New York, NY.

Nelson, J. D., Overton, D. D., and Durkee, D. B. (2001). "Depth of Wetting and the Active Zone." *Expansive Clay Soils and Vegetative Influence on Shallow Foundations, ASCE*, Houston, Texas. 95 – 109.

Ng, C.W.W., and Pang, Y.W. (2000). Influence of stress state on soil-water characteristics and slope stability. Journal of Geotechnical and Geoenvironmental Engineering, 126(2): 157–166. doi:10. 1061/(ASCE)1090-0241(2000)126:2(157)

Ng, C.W.W., Lai, C.H., and Chiu, C.F. (2012). A modified triaxial apparatus for measuring the stress path-dependent water retention curve. Geotechnical Testing Journal, 35(3): 490–495. doi:10.1520/ GTJ104203.

Nielsen D. R., Davidson, J. M., Biggar, J. W., and Miller R.J., (1964). Water movement through Panoche clay loam soil. Hilgardia 35: 491-506

Noorany, I. (1992). Discussion of "Stress Ratio on Collapse of Compacted Clayey Sand." by Lawton, E. C., Fragaszy, R. J., and Hardcastle, J. H., 1991, *Journal of Geotechnical Engineering*, 117(5), 714 – 730.

Noorany, I. (2005). E-Mail Letter to Kuo-Chieh Chao Regarding "Moist Tamping Equipment." January 10th.

Nuth, M., Laloui, L. (2008). Advances in modelling hysteretic water retention curve in deformable soils. Computers and Geotechnics 35 (2008) 835–844. doi:10.1016/j.compgeo.2008.08.001

Nuth, M., Laloui, L., (2011), A model for the water retention behavior of deformable soils including capillary hysteresis, Geo-Frontiers, ASCE, pp 3896-3905

Oliveira, O. M. and Fernando, F. A. M. (2006). "Evaluation of Filter Paper Calibration." *Proceedings of the Fourth International Conference on Unsaturated Soils*. Carefree, Arizona. 1845 – 1851.

Olivella, S., A. Gens, J. Carrera, E. E. Alonso, (1996), Numerical Formulation for a Simulator (CODE_BRIGHT) for the Coupled Analysis of Saline Media, Engineering Computations, Vol. 13, No 7, , pp: 87-112.

Olivella, S., J. Carrera, A. Gens, E. E. Alonso, (1994). Non-isothermal Multiphase Flow of Brine and Gas through Saline media. Transport in Porous Media, 15, 271:293

Olivella, S., J. Carrera, A. Gens, E. E. Alonso. (1996) Porosity Variations in Saline Media Caused by Temperature Gradients Coupled to Multiphase Flow and Dissolution/Precipitation. Transport in Porous Media, 25:1-25.

Olson, R. and Daniel, D. (1981). Measurement of the Hydraulic Conductivity of Fine Grained Soils, ASTM STP 746, 18-64.

O'Neil, M.W., and Gazzaly, O.I. 1977, Swell potential related to building performance, Journal of the Geotechnical Engineering Division, ASCE 103 (12), 1363 – 1379

Pachepsky, Y., Timlin, D., Rawls, W. (2003). Generalized Richards' equation to simulate water transport in unsaturated soils, Journal of Hydrology 272, pp. 3–13

Parent, S. E., Cabral, A., Zornberg, J. G., (2007). Water retention curve and hydraulic conductivity function of highly compressible materials. Canadian Geotech. Journal 44: 1200–1214, doi:10.1139/T07-091

Parker, J., Kool, J., and van Genuchten, M. (1985). Determining soil hydraulic properties from one- step outflow experiments by parameter estimation: II Experimental studies. SSSAJ. 49,1354-1359.

Pe´ron, H., Hueckel, T., and Laloui, L. (2007). An improved volume measurement for determining soil water retention curves. Geotechnical Testing Journal, Vol. 30, No. 1: 1–8.

Pereira, J.H.F., and Fredlund, D.G. 2000. Volume change behaviour of a residual soil of gneiss compacted at metastable structured conditions. Journal of Geotechnical and Geoenvironmental Engineering, **126**(10): 907–916. doi:10.1061/(ASCE) 1090-0241(2000)126:10(907).

Perera, Y. Y., Padilla, J. M., and Fredlund, D. G. (2004). "Determination of Soil-water Characteristic Curves Using the Fredlund SWCC Device." *Tailings and Mine Waste Management Short Course*, Vail, Colorado. October.

Perez-Garcia, N., Houston, S. L., Houston, W. N., and Padilla, J. M. (2008). An Oedometer-Type Pressure Plate SWCC Apparatus, Geotechnical Testing Journal (GTJ) / Citation Page, Volume 31, Issue 2 (March 2008),ISSN: pp 1945-7545

Perko, H. A., Thompson, R. W., Nelson, J. D., (2000). Suction Compression Index Based on CLOD Test Results. GeoDenver 2000 Advances in Unsaturated Geotechnics, 10.1061/40510(287)27

Pham, H. Q., Fredlund, D. G. (2008). Equations for the entire soil-water characteristic curve of a volume change soil. Can. Geotech. J. 45: 443–453. doi:10.1139/T07-117

Pham, H. Q., Fredlund, D. G., Barbour, A. L. (2003). Estimation of the hysteretic soil-water characteristic curves from the boundary drying curve. 56TH Canadian Geotechnical Conference, 4TH Joint Iah-Cnc/Cgs Conference

Pham, H. Q., Fredlund, D. G., Barbour, S. L. (2003). A practical hysteresis model for the soil-water characteristic curve for soils with negligible volume change. Geotechnique 53, No. 2, 293-298

Pham, H.Q. (2001). An engineering model of hysteresis for soil water characteristic curves. M.Sc. thesis, University of Saskatchewan, Saskatoon, Sask.

Pham, Q.H. 2005. A volume-mass constitutive model for unsaturated soils. Ph.D. dissertation, University of Saskatchewan, Saskatoon, Sask.

Powers, K. C., Vanapalli, S. K. and Garga, V. K. (2007). New and improved null pressure plate apparatus for the measurement of matric suction of unsaturated soils. Canadian Geotechnical Conference, Ottawa, Ontario, Canada.

Price, J.S., and Schlotzhauer, S.M. 1999. Importance of shrinkage and compression in determining water storage changes in peat: the case of a mined peat land. Hydrological Processes, 13: 2591– 2601. doi:10.1002/(SICI)1099

Qi, G., Michel J. C., (2011) A laboratory device for continual measurement of water retention and shrink/swell properties during drying/wetting cycles. HortScience 46 (9): 1298-1302

Rahardjo, H. and Leong, E.C., 2006. Suction Measurements, In Proceedings of Fourth International Conference of Unsaturated Soils, Carefree, Arizona, pp. 81-104.

Ranganatham, B. V. and Satyanarayan, B. (1965), A rational method of predicting swelling potential for compacted expansive clays: Proc. 6th Inter. Conf. Soil Mechanics Foundation Engng. Vol. 1, pp. 92-96

Rao A.S., Phanikumar B.R. and Sharma R.S., 2004, Prediction of swelling characteristics of remoulded and compacted expansive soils using free swell index, Quarterly Journal of Engineering Geology and Hydrogeology, 37, 217–226

Reginato, R. J., and van Bavel, C. H. M. (1962). "Pressure cell for soil cores." Soil Sci. Soc. Am. Proc., 26, 1–3.

Richard, R. M., and B. J. Abbott 1975, Versatile elastic-plastic stress-strain formula, Journal of Engineering Mechanics, ASCE, 10(4,) 511-515

Richards, B.G. (1965). Measurement of the free energy of soil moisture by the psychrometric technique using thermistors. *In* Moisture equilibria and moisture changes in soils beneath covered areas. *Edited* by G.D. Aitchison. Butterworths, Australia. pp. 39-46.

Richards, L.A., 1931. Capillary conduction of liquids in porous mediums, Physics 1, 318–333

Rogowski, A. S. (1971). Watershed physics: Model of the soil moisture characteristic. Water Resources Research 7(6): 1575-1582.

Romero, E., Gens, A., Lloret, A. (1999). Water permeability, water retention and microstructure of unsaturated compacted Boom clay. Engineering Geology 54 (1999) 117–127

Saaltink, M. W., Ayora, C., Olivella S., (2005). User's guide for RetrasoCodeBright (RCB)

Salager, S., El Youssoufi, M.S. , and Saix, C. (2010), Definition and experimental determination of a soil-water retention surface, Canadian Geotechnical Journal 47: 609–622, NRC Research Press

Seed, H. B., Woodward, R. J., Jr. and Lundgren, R. 1962, Prediction of swelling potential for compacted clays: J. ASCE, Soil Mechanics and Foundation Division, Vol. 88, No. SM-3, Part I, pp. 53-87.

Segerlind, L.J., 1984. Applied Finite Element Analysis. John Wiley and Sons.

Singhal, S. (2010), Expansive Soil Behavior: Property Measurement Techniques and Heave Prediction Methods, PhD Dissertation, Arizona State University

Stange, C. F., Horn, R. (2005), Modeling the Soil Water Retention Curve for Conditions of Variable Porosity, Soil Science Society of America, Vadose Zone Journal 4:602–613 (2005)

Tani, M. 1982. The properties of a water-table rise produced by a one-dimensional, vertical, unsaturated flow. Journal of Japan Forestry Society, **64**: 409–418. [In Japanese.]

Terzaghi, K. (1943). Theoretical soil mechanics, Wiley, New York.

Thode, R., Gitirana, G. (2008). SVFLUX theory manual. SoilVision Systems Ltd. Saskatoon, Saskatchewan, Canada

Thode, R., Stianson, J, Fredlund, M. (2005). SVFLUX theory manual, SoilVision Systems Ltd., Saskatoon, Saskatchewan, Canada

Tinjum, J. M., Benson, C. H., Blotz, L. R. (1997). Soil-water characteristic curves for compacted clays. Journal of Geotechnical and Geoenvironmental Engineering. ASCE. Vol. 123, No. 11. P. 1060 – 1069.

Topp, G. C., (1969). Soil-water hysteresis measured in a sandy loam and compared with a hysteretic domain model. Soil. Sci. Soc. Amer. Proc. 33: 645-651

Topp, G. C., and Miller, E. E. (1966). Hysteretic moisture characteristics and hydraulic conductivities for glass bead media. Soil Sci. Soc. Amer. Proc. 30: 156-162.

Tse, E. C. (1985). Influence of structure change on pore pressure and deformation behavior of soft clays under surface loading. PhD Dissertation. University of California, Berkley

van Genuchten, M. (1980). A closed-form equation for predicting the hydraulic conductivity of unsaturated soils, SSSAJ. 44, 892-898.

Vanapalli, S. K., Fredlund, D. G., & Pufahl, D. E. (1999). The influence of soil structure and stress history on the soil-water characteristics of a compacted till. Geotechnique. 49, No. 2, 143-159.

Vanapalli, S. K., Pufahl, D. E., and Fredlund, D. G. (1998). "The Effect of Stress State on the Soil-Water Characteristic Behavior of a Compacted Sandy-Clay Till." *Proc., 51st Can. Geotech. Conf.*, 81 – 86.

Vanapalli, S.K., Sillers, W.S., and Fredlund, M.D. (1998). The meaning and relevance of residual water content to unsaturated soils. *In* Proceedings of the 51st Canadian Geotechnical Conference, Edmonton, Alta., 4–7 October 1998. BiTech Publishers Ltd., Richmond, B.C. pp. 101–108.

Vazquez, M., Durand, P., (2011), Soil-Water Characteristic Curve (SWCC) and volumetric deformation law for a plastic clay under high suction, Unsaturated Soils-Alonso and Gens: 509-512

Vijayvergiya V. N., and Ghazzaly O.I., (1973) Prediction of swelling potential for natural clays. In: Proceedings of the 3rd International Conference on Expansive Soils, Haifa, Israel, 1, 227–236.

Walcaz, R. T., Moreno, F., Slawinski, C., Fernadez, E. Arrue, J. L. (2006). Modeling of soil water retention curve using soil solid phase parameters, Journal of hydrology, Elsevier B. V. No. 329, P. 527 – 533

Watson, K. K., Reginato, R. J., and Jackson, R. D. (1975). Soil water hysteresis in a field soil. Soil Sci. Soc. Am. Proc. 39, No. 2, 242-246

Wildenschild, D., Jensen, K., Hollenbeck, K., Illangasekare, T., Znidarcic, D., Sonnenborg, T., and Butts, M. (1997). A two stage procedure for determining unsaturated hydraulic characteristics using a syringe pump and outflow observations

Wray, W.K., 1989a. Mitigation of damage to structure supported on expansive soils, National Science Foundation Report

Yang, H., Rahardjo, H., Leong, E. C., and Fredlund, D. G. (2004). "A study of infiltration on three sand capillary barriers." *Can. Geotech. J.*, 41(4), 629–643.

Zapata, C.E., Houston, W.N., Houston, S.L., and Walsh, K.D. (2000). Soil-water characteristic curve variability. *In* Advances in Unsaturated Geotechnics (GSP 99), Proceedings of the GeoDenver Conference, Denver, Colo., 5–8 August 2000. *Edited by* C.D. Shackelford, S.L. Houston, and N.-Y. Chang. American Society of Civil Engineers, Reston, Va. pp. 84–124.

Zerhouni, M. I., (1991). Rôle de la pression interstitielle négative dans le comportement des sols Application au calcul des routes, Ph.D. Thesis, Ecole Nationale des Ponts et Chaussées, Paris.

Zhou, J. & Yu, J. (2005). Influences affecting the soil-water characteristic curve", Journal of Zhejiang University SCIENCE, 6A(8): 797-804.

APPENDIX A

IMAGES OF SOIL SPECIMENS TESTED BY SWC-150 DEVICE

Figure A.1. Slurry Specimen of Anthem on High Air Entry Ceramic Stone of SWCC Cell Equilibrated at 25kPa Suction under Token Load

Figure A.2. Slurry Specimen of Anthem on High Air Entry Ceramic Stone of SWCC Cell Equilibrated at 50kPa Suction under Token Load

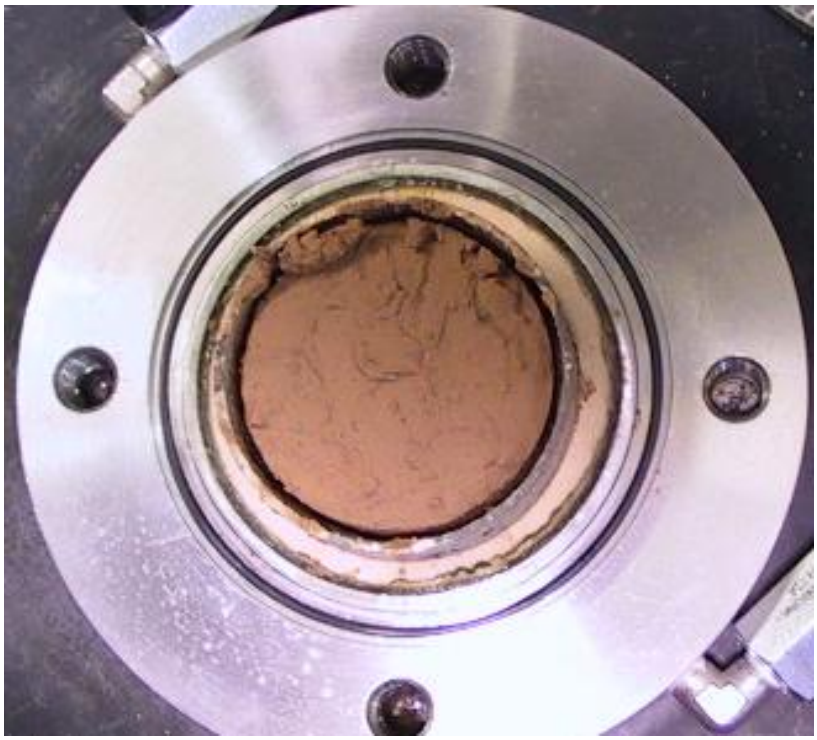

Figure A.3. Slurry Specimen of Anthem on High Air Entry Ceramic Stone of SWCC Cell Equilibrated at 100kPa Suction under Token Load

Figure A.4. Slurry Specimen of Anthem on High Air Entry Ceramic Stone of SWCC Cell Equilibrated at 200kPa Suction under Token Load

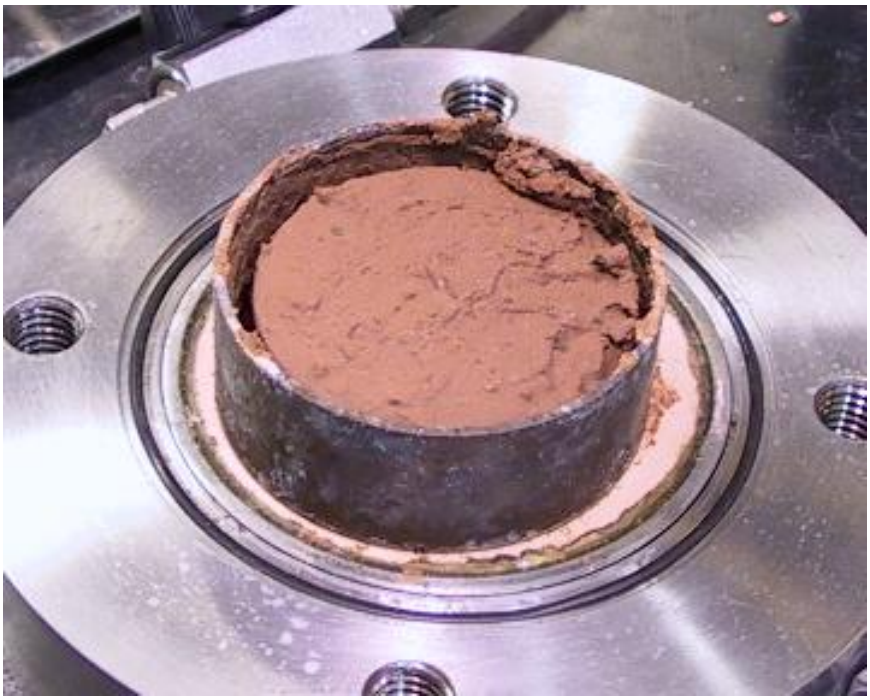

Figure A.5. Slurry Specimen of Anthem on High Air Entry Ceramic Stone of SWCC Cell Equilibrated at 400kPa Suction under Token Load

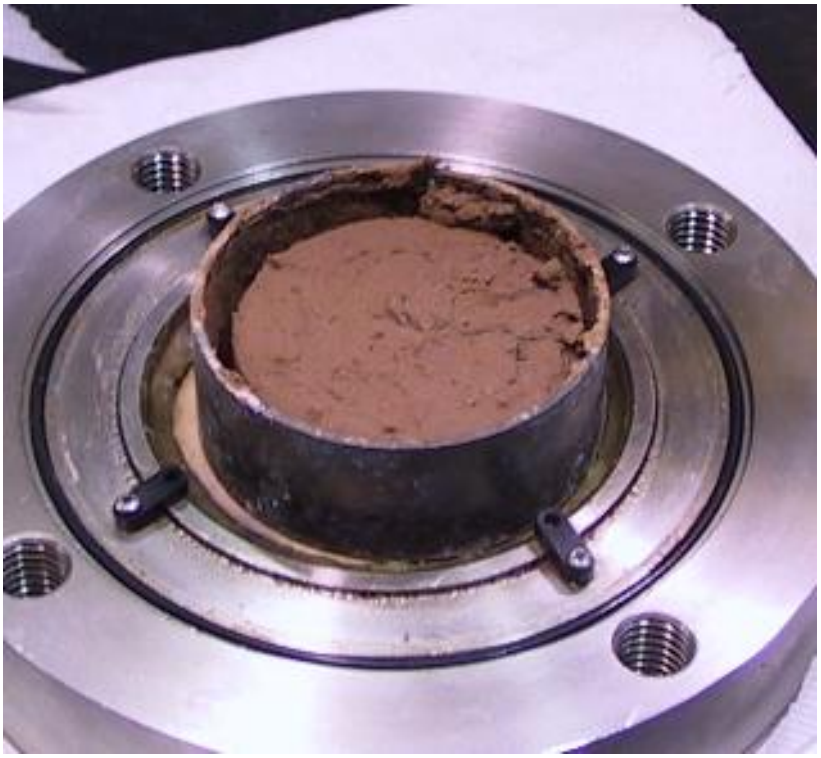

Figure A.6. Slurry Specimen of Anthem on High Air Entry Ceramic Stone of SWCC Cell Equilibrated at 1,250kPa Suction under Token Load

Figure A.7. Slurry Specimen of Colorado on High Air Entry Ceramic Stone of SWCC Cell Equilibrated at 25kPa Suction under Token Load

Figure A.8. Slurry Specimen of Colorado on High Air Entry Ceramic Stone of SWCC Cell Equilibrated at 50kPa Suction under Token Load

Figure A.9. Slurry Specimen of Colorado on High Air Entry Ceramic Stone of SWCC Cell Equilibrated at 100kPa Suction under Token Load

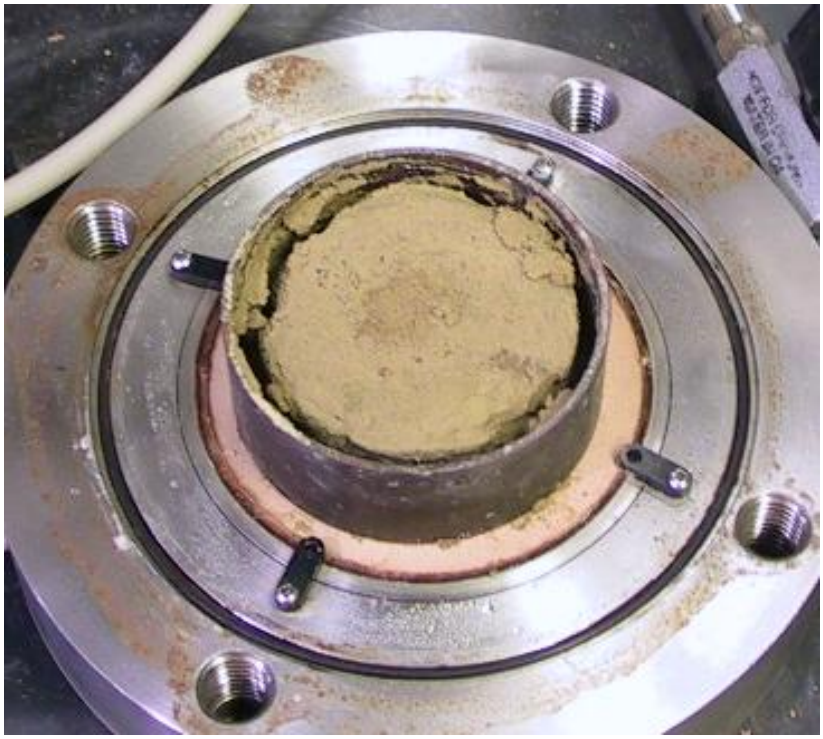

Figure A.10. Slurry Specimen of Colorado on High Air Entry Ceramic Stone of SWCC Cell Equilibrated at 200kPa Suction under Token Load

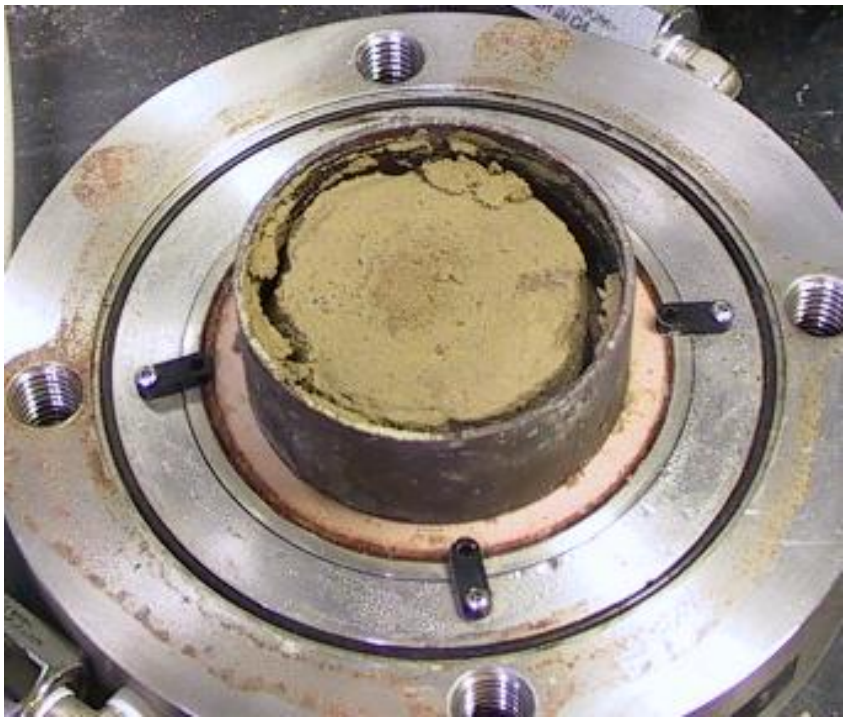

Figure A.11. Slurry Specimen of Colorado on High Air Entry Ceramic Stone of SWCC Cell Equilibrated at 400kPa Suction under Token Load

Figure A.12. Slurry Specimen of San Antonio on High Air Entry Ceramic Stone of SWCC Cell Equilibrated at 25kPa Suction under Token Load

Figure A.13. Slurry Specimen of San Antonio on High Air Entry Ceramic Stone of SWCC Cell Equilibrated at 50kPa Suction under Token Load

Figure A.14. Slurry Specimen of San Antonio on High Air Entry Ceramic Stone of SWCC Cell Equilibrated at 100kPa Suction under Token Load

Figure A.15. Slurry Specimen of San Antonio on High Air Entry Ceramic Stone of SWCC Cell Equilibrated at 200kPa Suction under Token Load

Figure A.16. Slurry Specimen of San Antonio on High Air Entry Ceramic Stone of SWCC Cell Equilibrated at 400kPa Suction under Token Load

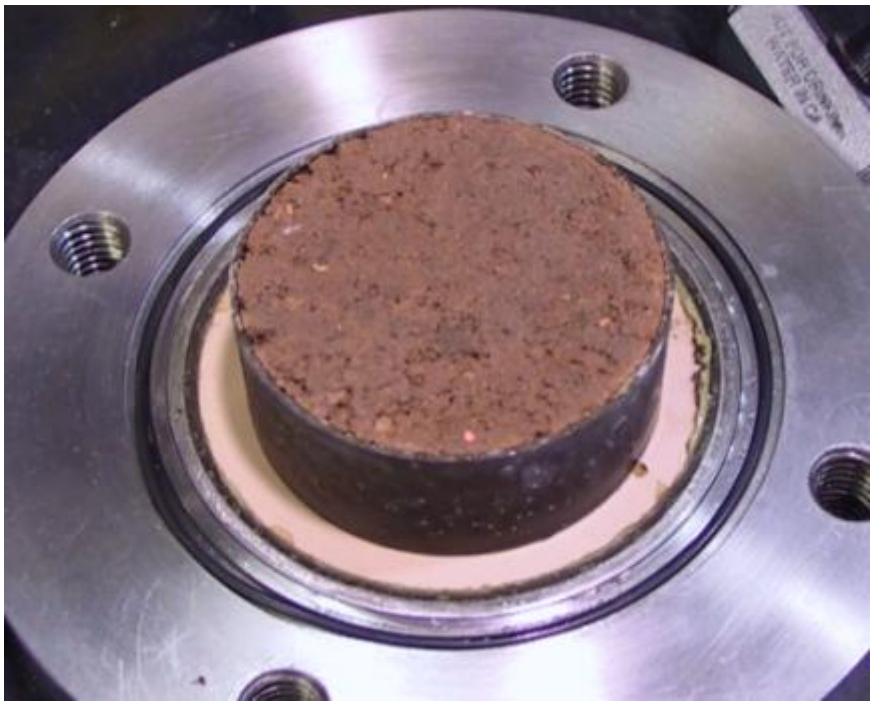

Figure A.17. Compacted Specimen of Anthem on High Air Entry Ceramic Stone of SWCC Cell Equilibrated at 100kPa Suction under Seating Load

Figure A.18. Compacted Specimen of Anthem on High Air Entry Ceramic Stone of SWCC Cell Equilibrated at 400kPa Suction under Seating Load

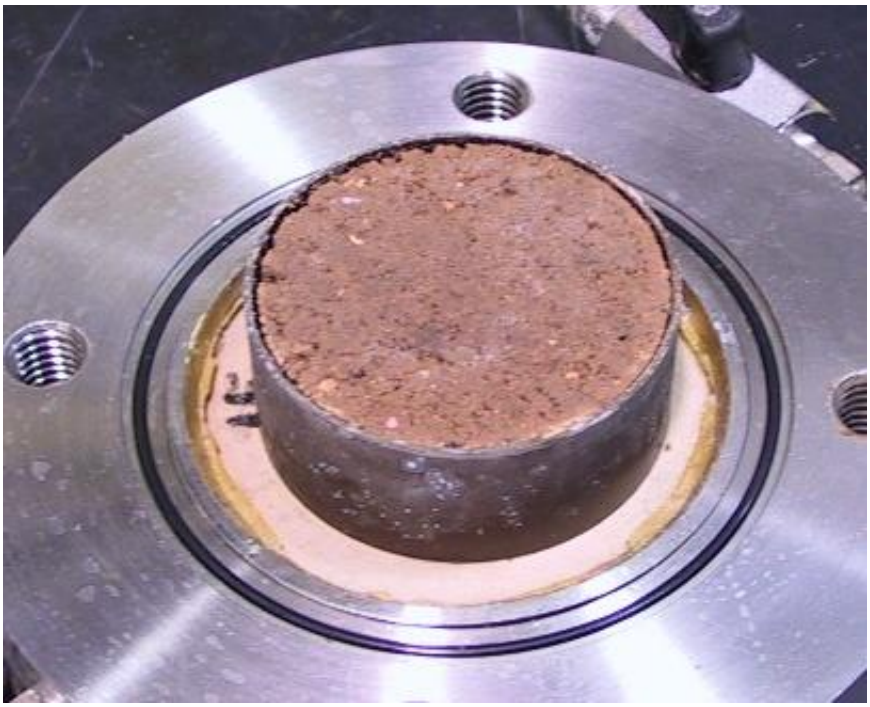

Figure A.19. Compacted Specimen of Anthem on High Air Entry Ceramic Stone of SWCC Cell Equilibrated at 1,300kPa Suction under Seating Load

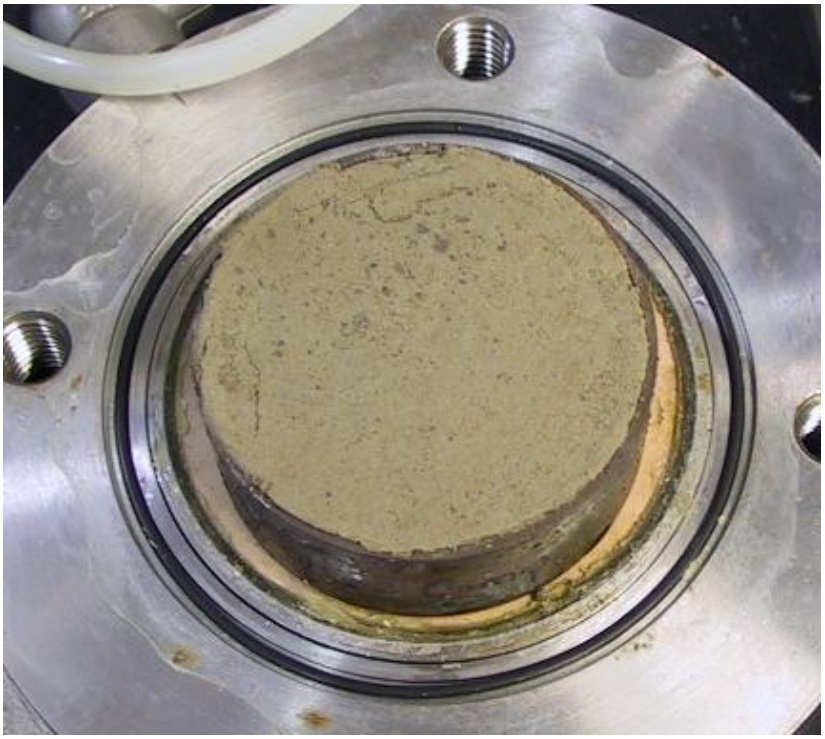

Figure A.20. Compacted Specimen of Colorado on High Air Entry Ceramic Stone of SWCC Cell Equilibrated at 100kPa Suction under Seating Load

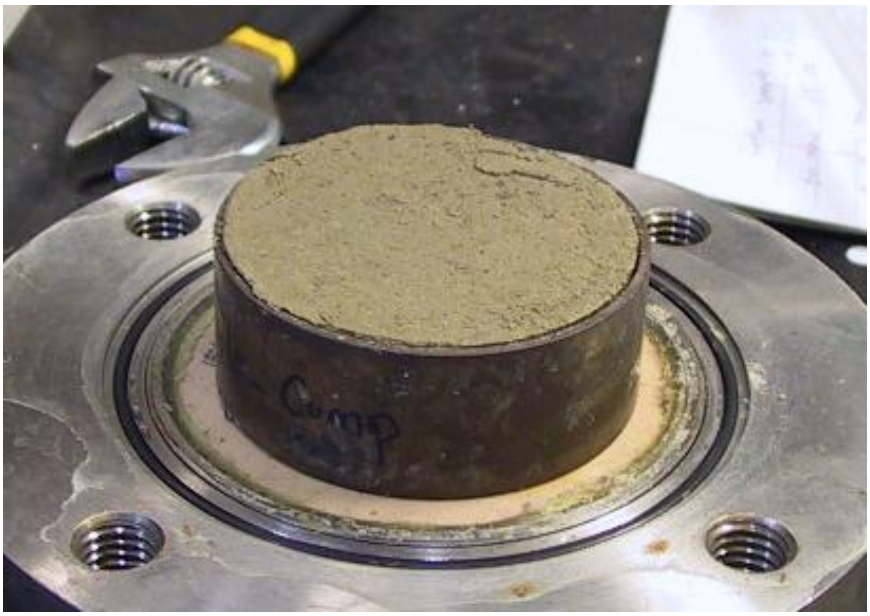

Figure A.21. Compacted Specimen of Colorado on High Air Entry Ceramic Stone of SWCC Cell Equilibrated at 200kPa Suction under Seating Load

Figure A.22. Compacted Specimen of Colorado Equilibrated at 400kPa Suction under Seating Load

Figure A.23. Compacted Specimen of San Antonio on High Air Entry Ceramic Stone of SWCC Cell Equilibrated at 400kPa Suction under Seating Load

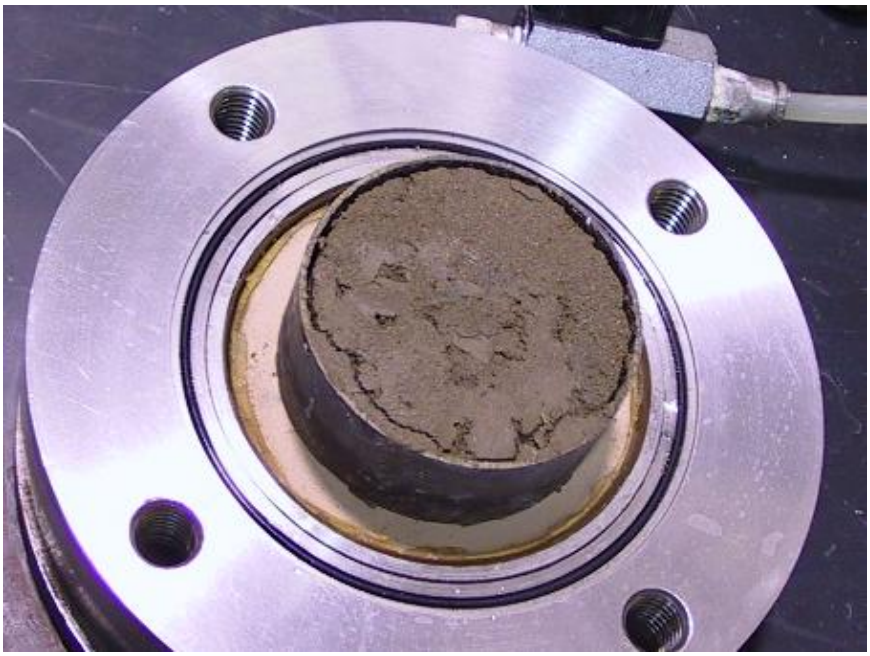

Figure A.24. Compacted Specimen of San Antonio on High Air Entry Ceramic Stone of SWCC Cell Equilibrated at 1,200kPa Suction under Seating Load

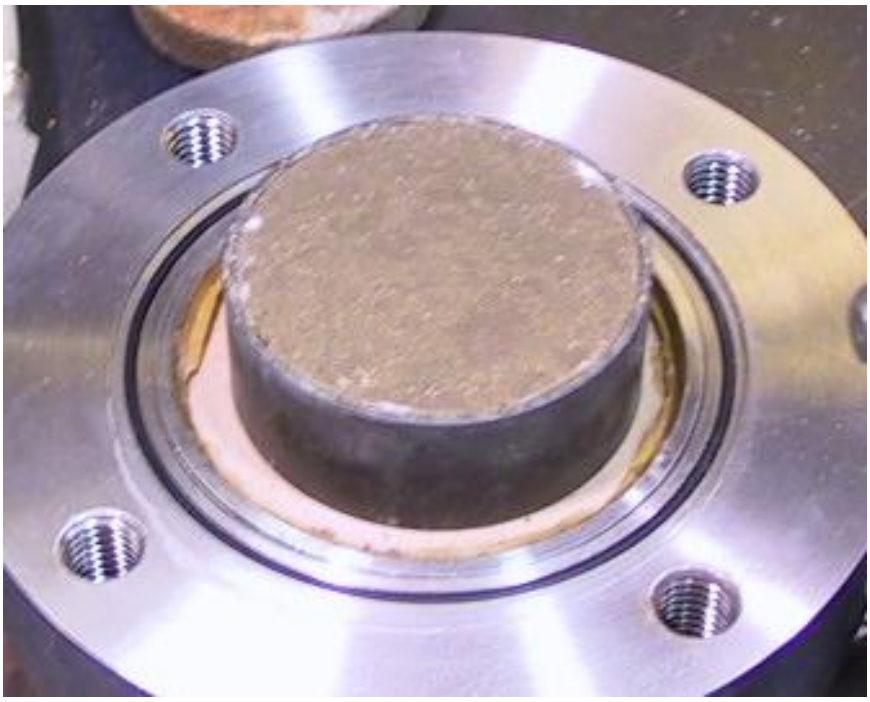

Figure A.25. Compacted Specimen of San Antonio on High Air Entry Ceramic Stone of SWCC Cell Equilibrated at 200kPa Suction under Seating Load

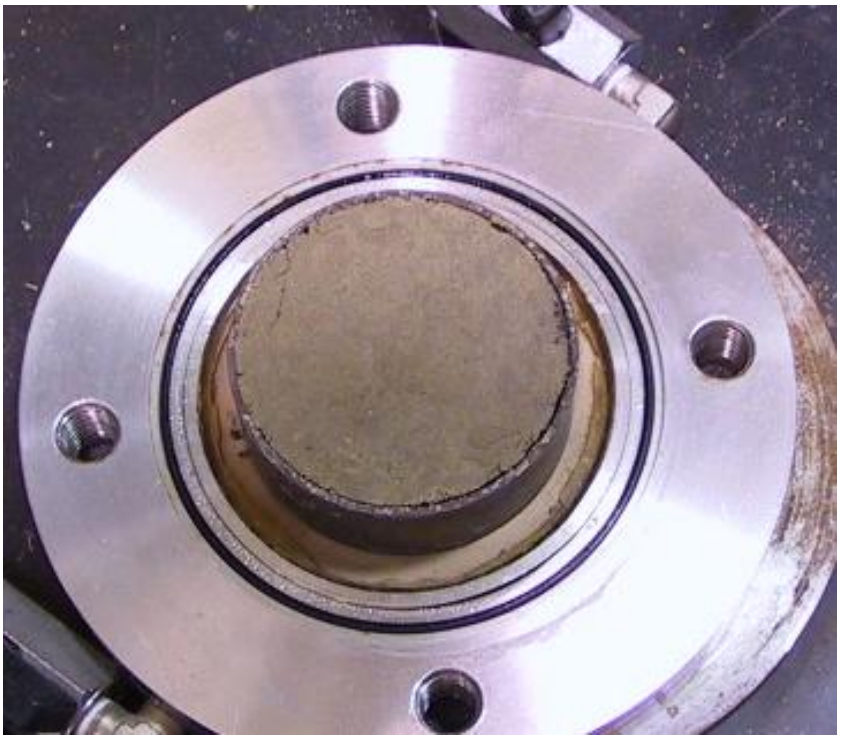

Figure A.26. Compacted Specimen of San Antonio on High Air Entry Ceramic Stone of SWCC Cell Equilibrated at 400kPa Suction under Seating Load

Figure A.27. Application of Net Normal Pressure to Specimens and Monitoring Vertical displacement Using Dial Gauges

Figure A.28. Application of Net Normal Pressure to Specimens and Monitoring Vertical displacement Using Dial Gauges

APPENDIX B

RESULTS OF NUMERICAL MODELING: PROFILES OF SOILS SUCTION FOR CORRECTED AND UNCORRECTED SWCC'S

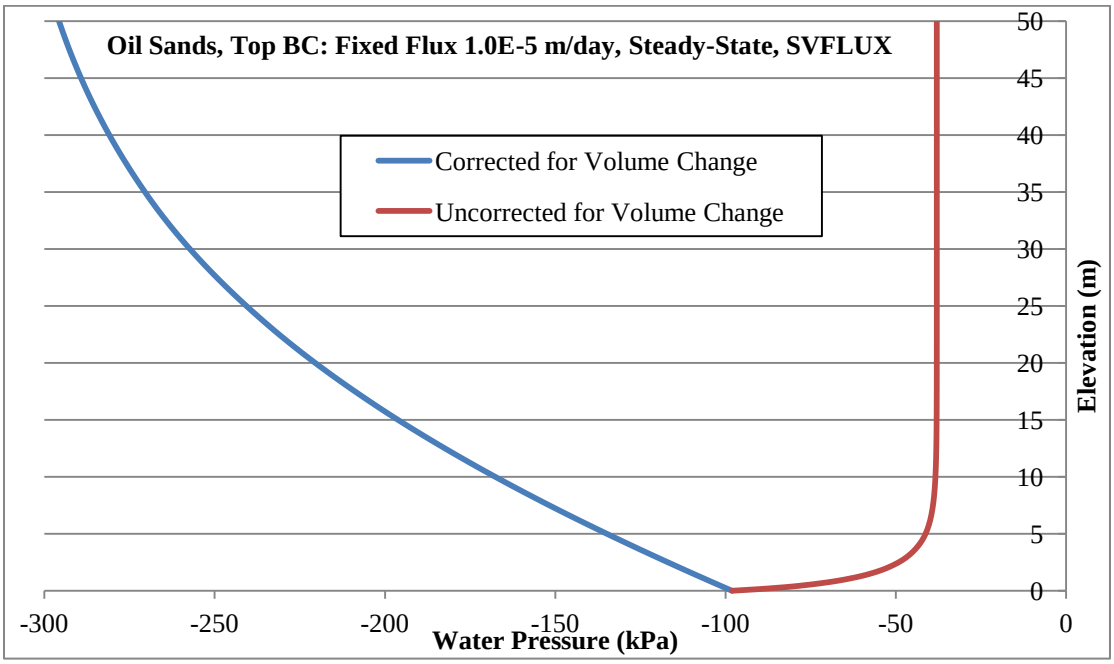

Figure B.1. Water pressure versus depth at steady-state condition for oil sands tailings with SWCC corrected and uncorrected for volume change and top fixed flux of 1.0E-5 m/day using SVFLUX

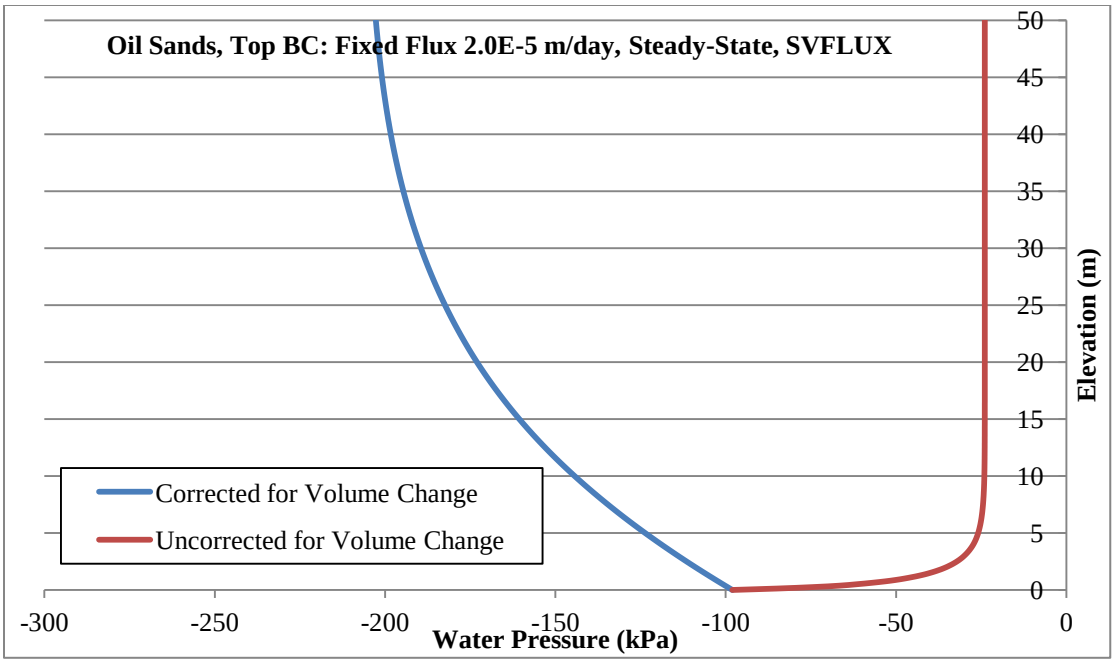

Figure B.2. Water pressure versus depth at steady-state condition for oil sands tailings with SWCC corrected and uncorrected for volume change and top fixed flux of 2.0E-5 m/day using SVFLUX

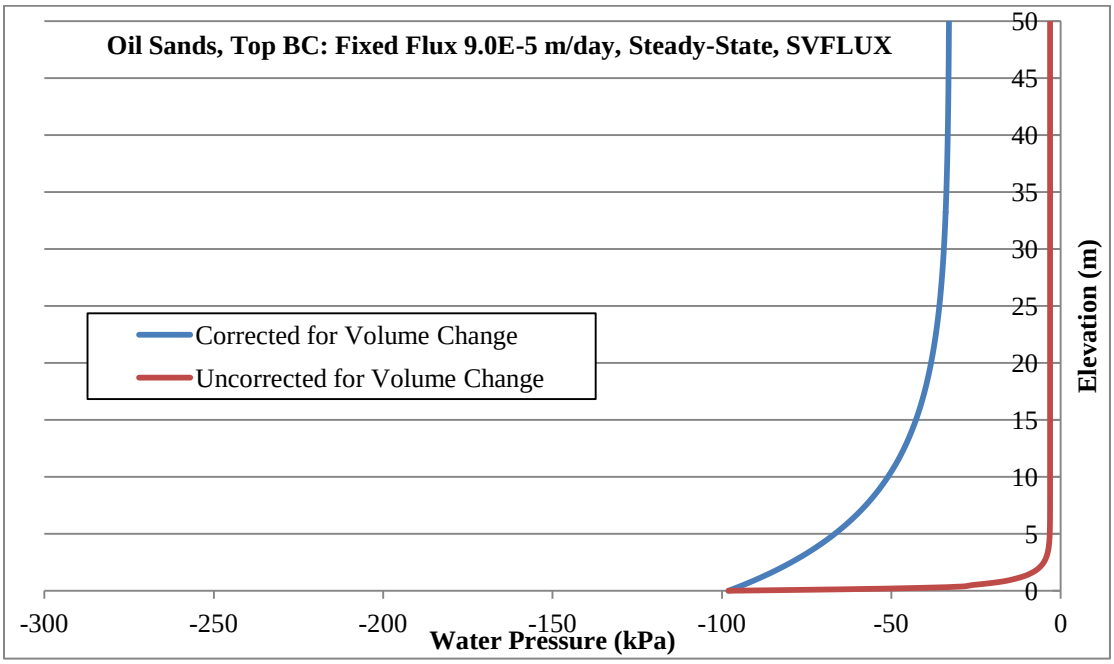

Figure B.3. Water pressure versus depth at steady-state condition for oil sands tailings with SWCC corrected and uncorrected for volume change and top fixed flux of 9.0E-5 m/day using SVFLUX

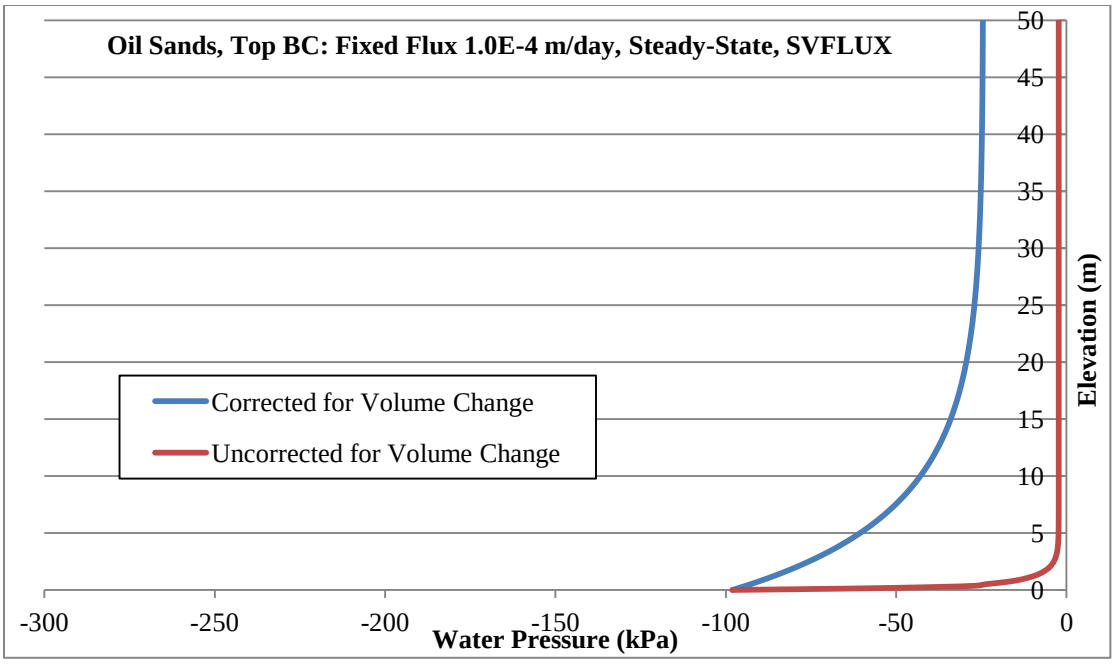

Figure B.4. Water pressure versus depth at steady-state condition for oil sands tailings with SWCC corrected and uncorrected for volume change and top fixed flux of 1.0E-4 m/day using SVFLUX

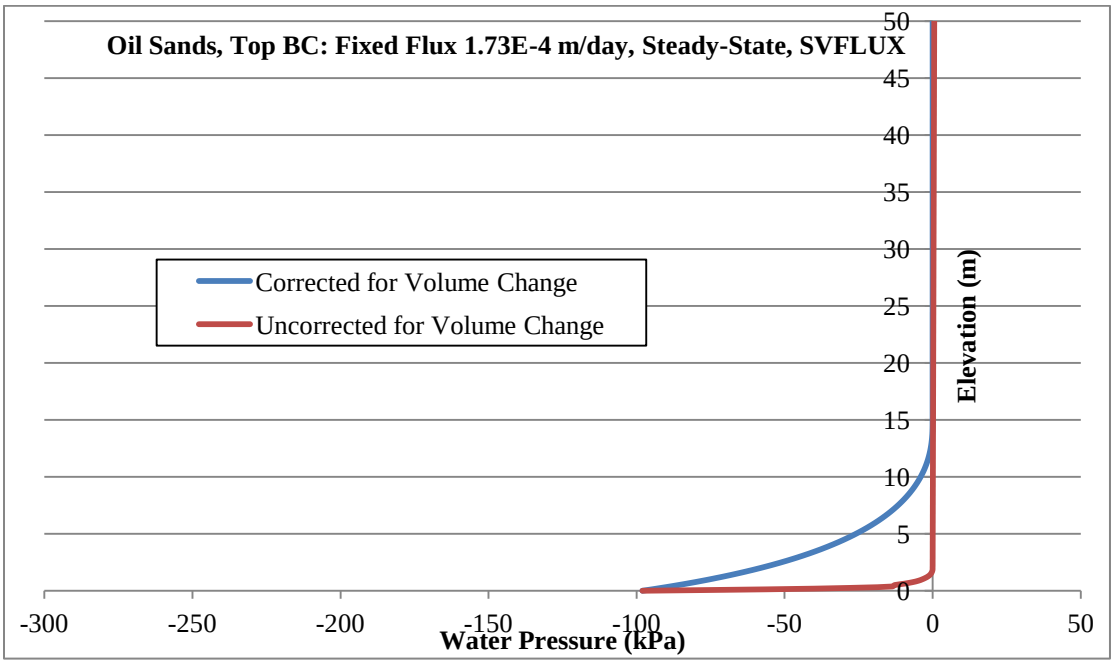

Figure B.5. Water pressure versus depth at steady-state condition for oil sands tailings with SWCC corrected and uncorrected for volume change and top fixed flux of 1.73E-4 m/day using SVFLUX

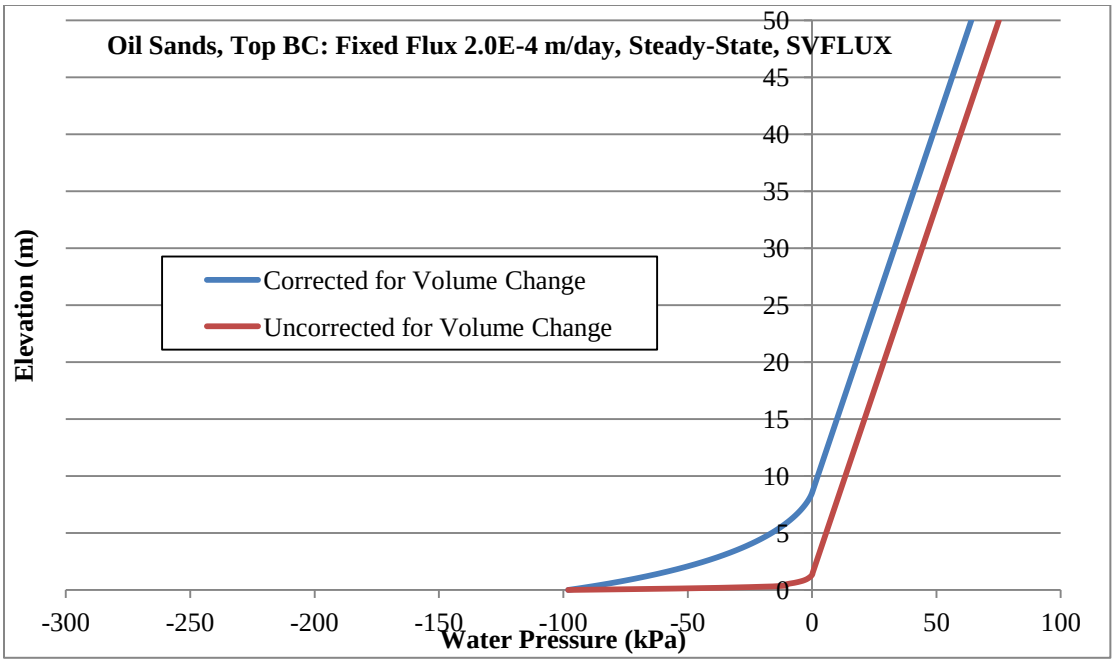

Figure B.6. Water pressure versus depth at steady-state condition for oil sands tailings with SWCC corrected and uncorrected for volume change and top fixed flux of 2.0E-4 m/day using SVFLUX

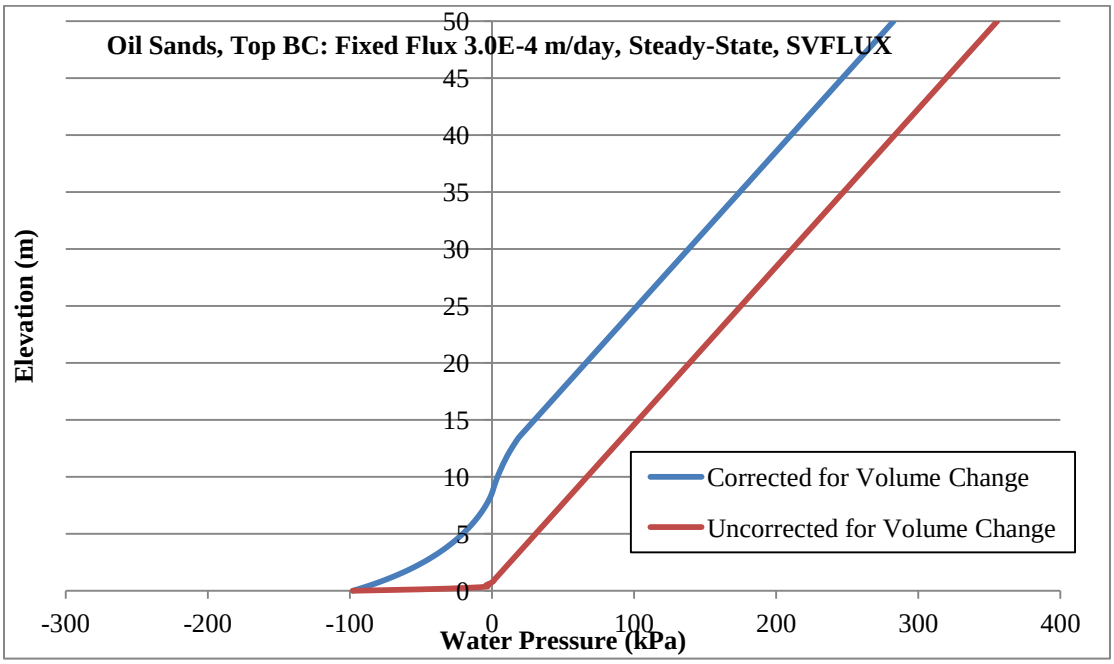

Figure B.7. Water pressure versus depth at steady-state condition for oil sands tailings with SWCC corrected and uncorrected for volume change and top fixed flux of 3.0E-4 m/day using SVFLUX

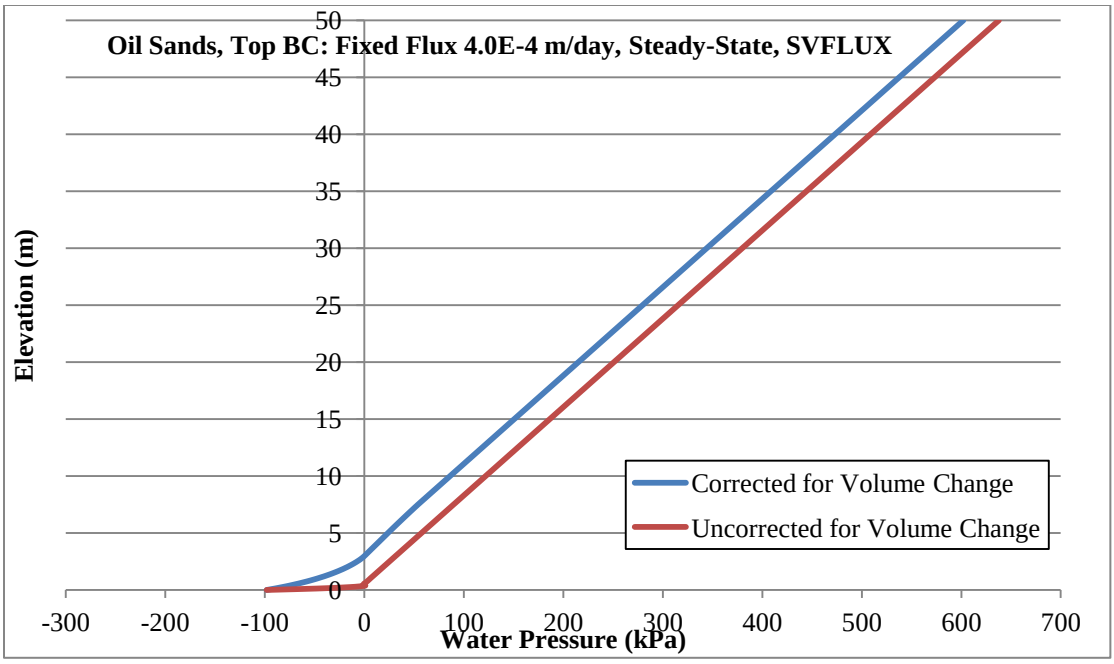

Figure B.8. Water pressure versus depth at steady-state condition for oil sands tailings with SWCC corrected and uncorrected for volume change and top fixed flux of 4.0E-4 m/day using SVFLUX

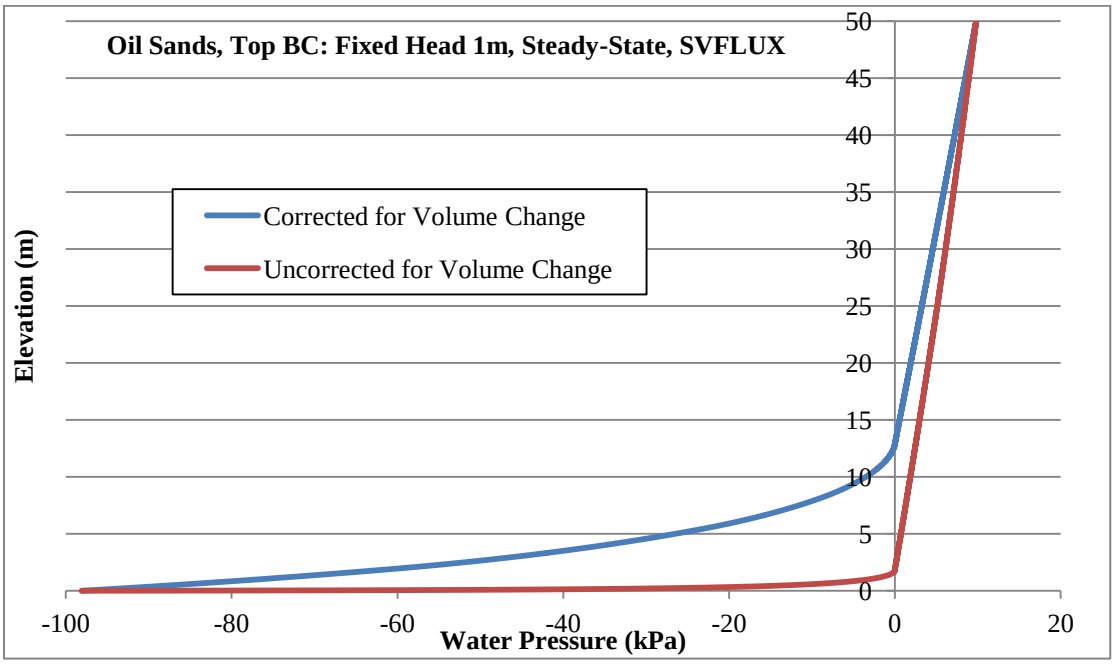

Figure B.9. Water pressure versus depth at steady-state condition for oil sands tailings with SWCC corrected and uncorrected for volume change and top fixed head of 1m using SVFLUX

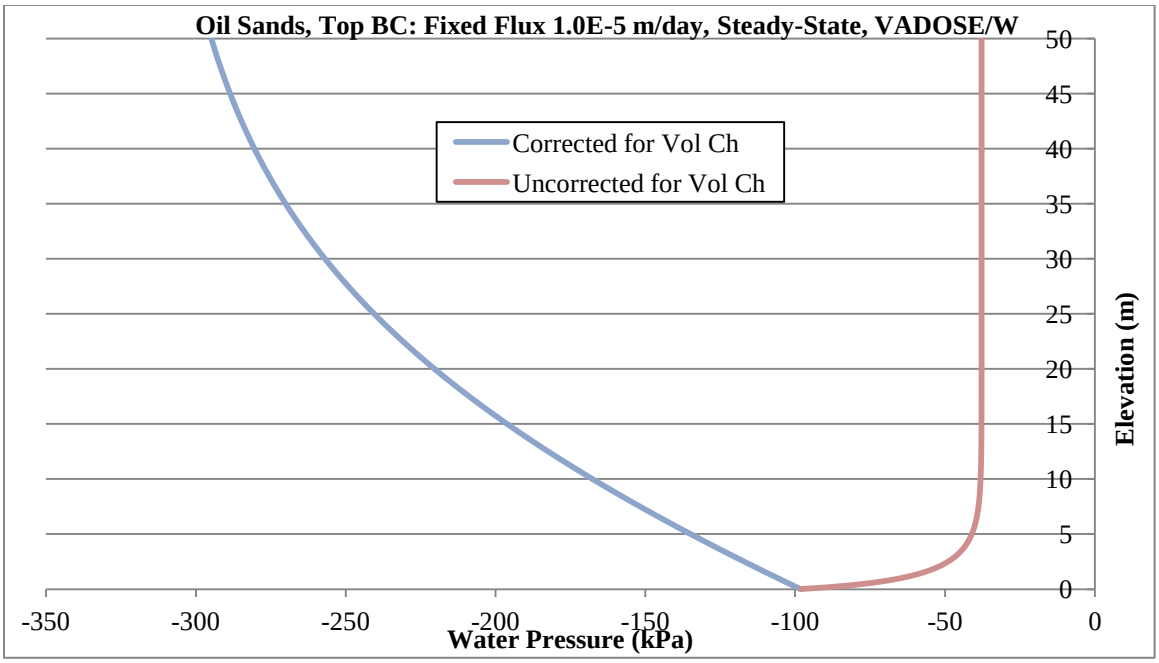

Figure B.10. Water pressure versus depth at steady-state condition for oil sands tailings with SWCC corrected and uncorrected for volume change and top fixed flux of 1.0E-5 m/day using VADOSE/W

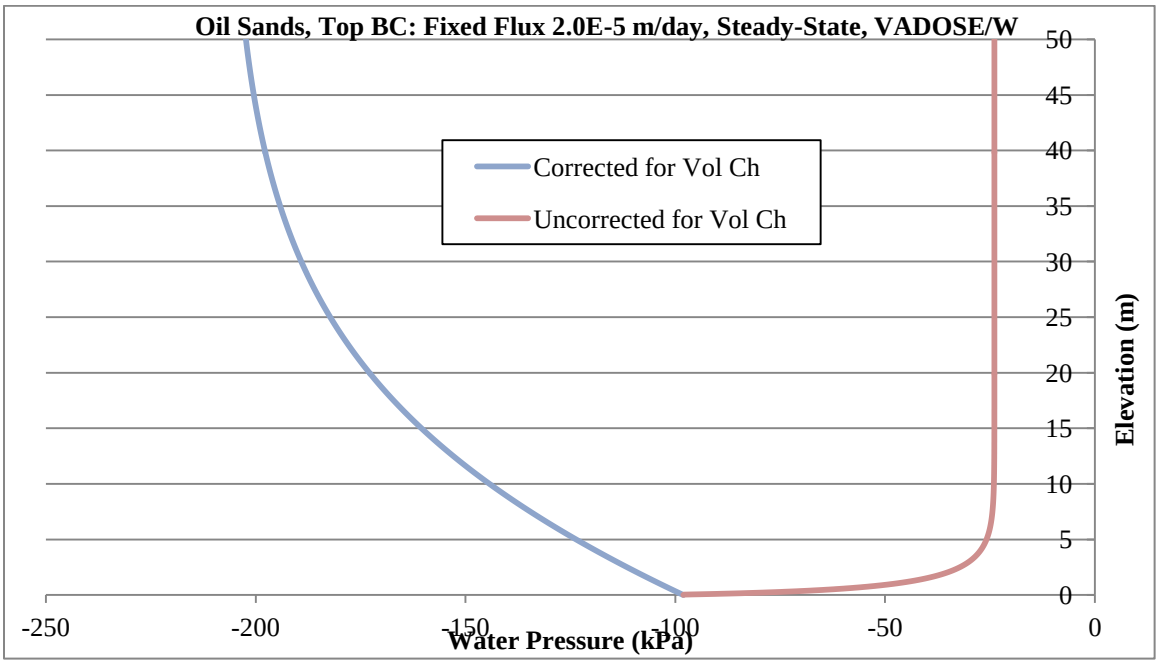

Figure B.11. Water pressure versus depth at steady-state condition for oil sands tailings with SWCC corrected and uncorrected for volume change and top fixed flux of 2.0E-5 m/day using VADOSE/W

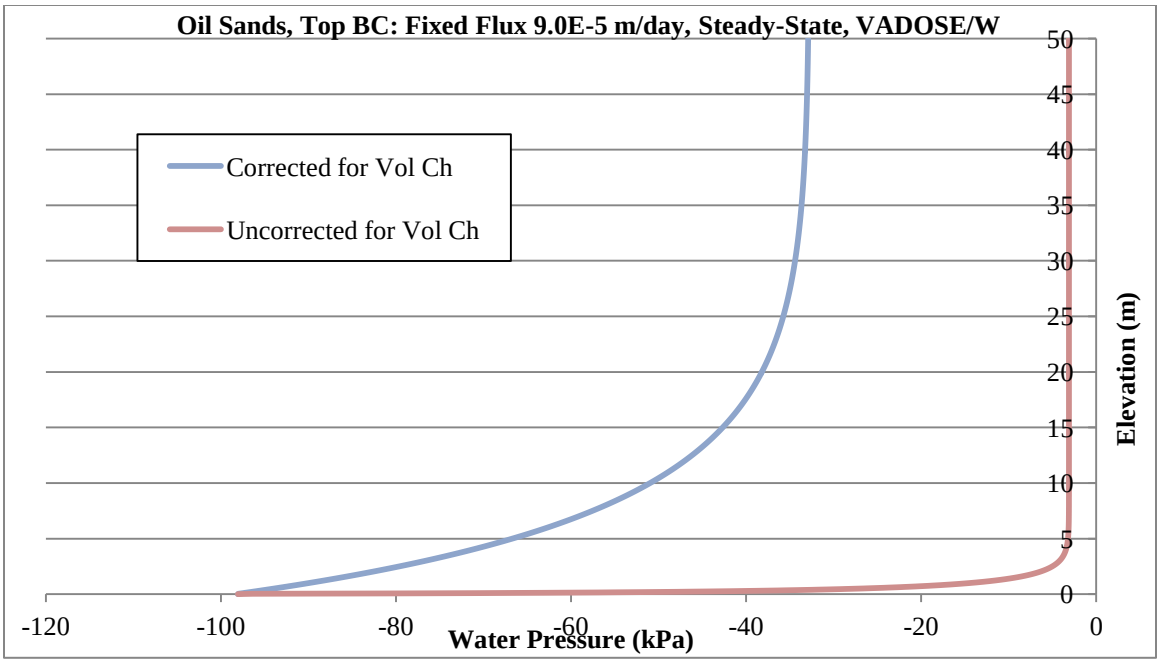

Figure B.12. Water pressure versus depth at steady-state condition for oil sands tailings with SWCC corrected and uncorrected for volume change and top fixed flux of 9.0E-5 m/day using VADOSE/W

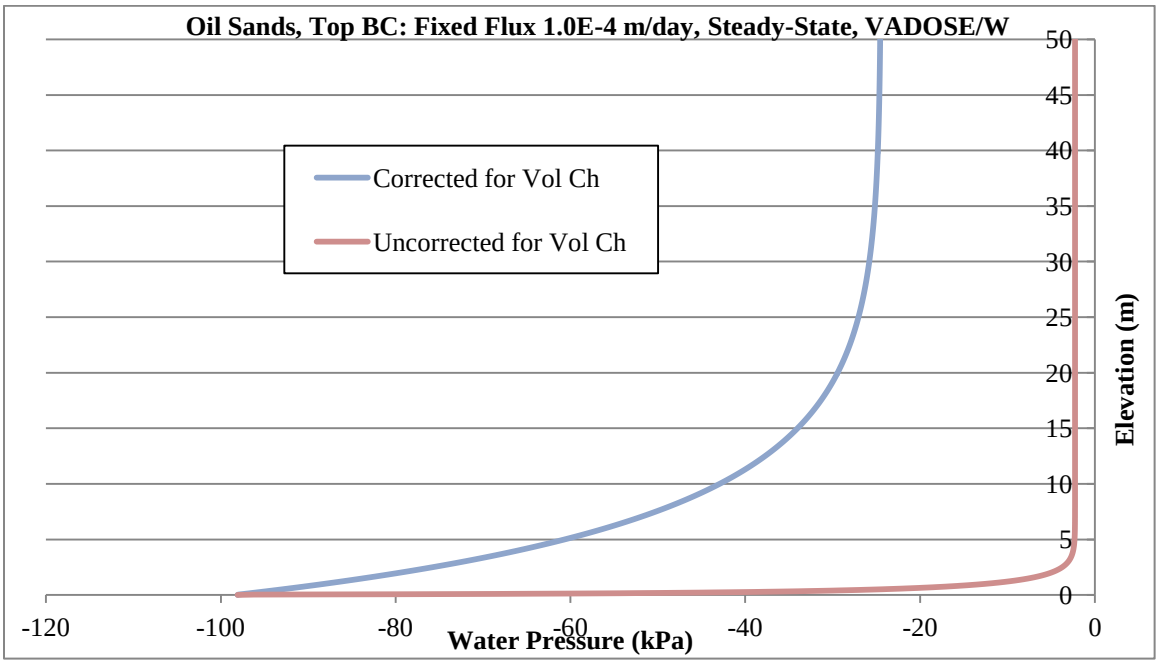

Figure B.13. Water pressure versus depth at steady-state condition for oil sands tailings with SWCC corrected and uncorrected for volume change and top fixed flux of 1.0E-4 m/day using VADOSE/W

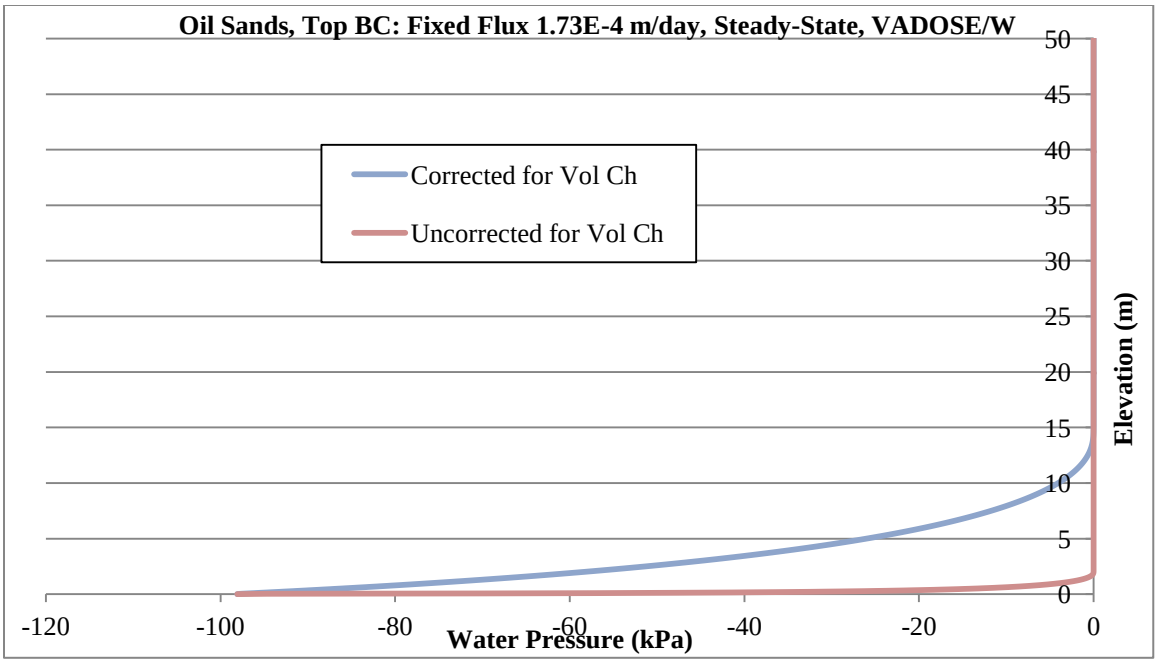

Figure B.14. Water pressure versus depth at steady-state condition for oil sands tailings with SWCC corrected and uncorrected for volume change and top fixed flux of 1.73E-4 m/day using VADOSE/W

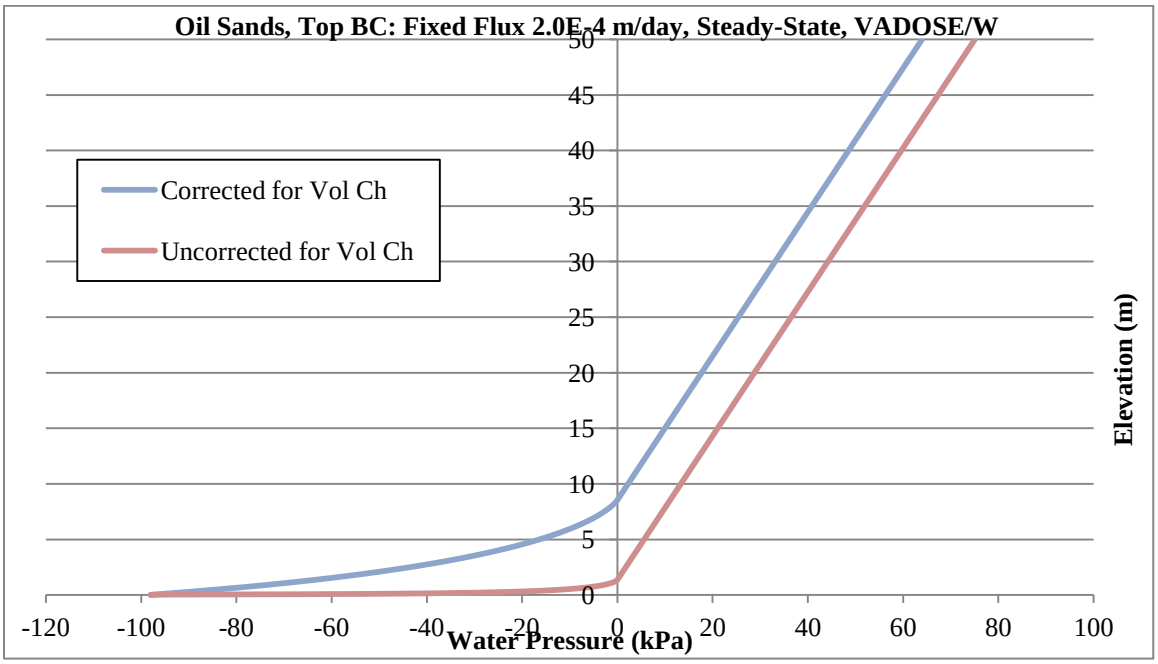

Figure B.15. Water pressure versus depth at steady-state condition for oil sands tailings with SWCC corrected and uncorrected for volume change and top fixed flux of 2.0E-4 m/day using VADOSE/W

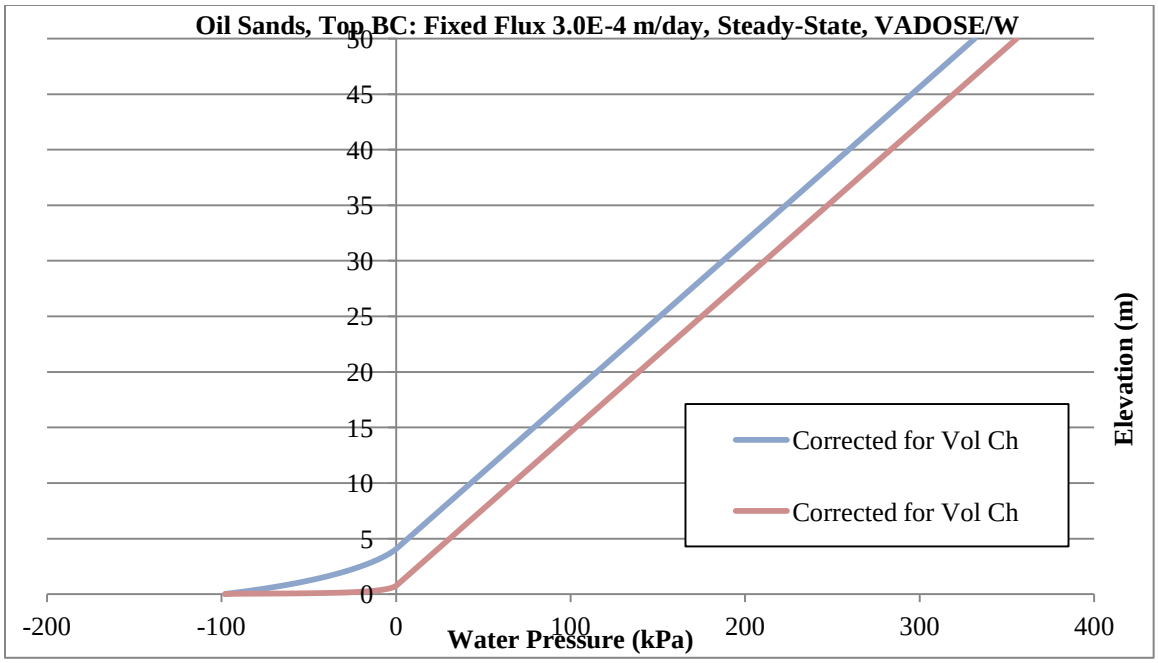

Figure B.16. Water pressure versus depth at steady-state condition for oil sands tailings with SWCC corrected and uncorrected for volume change and top fixed flux of 3.0E-4 m/day using VADOSE/W

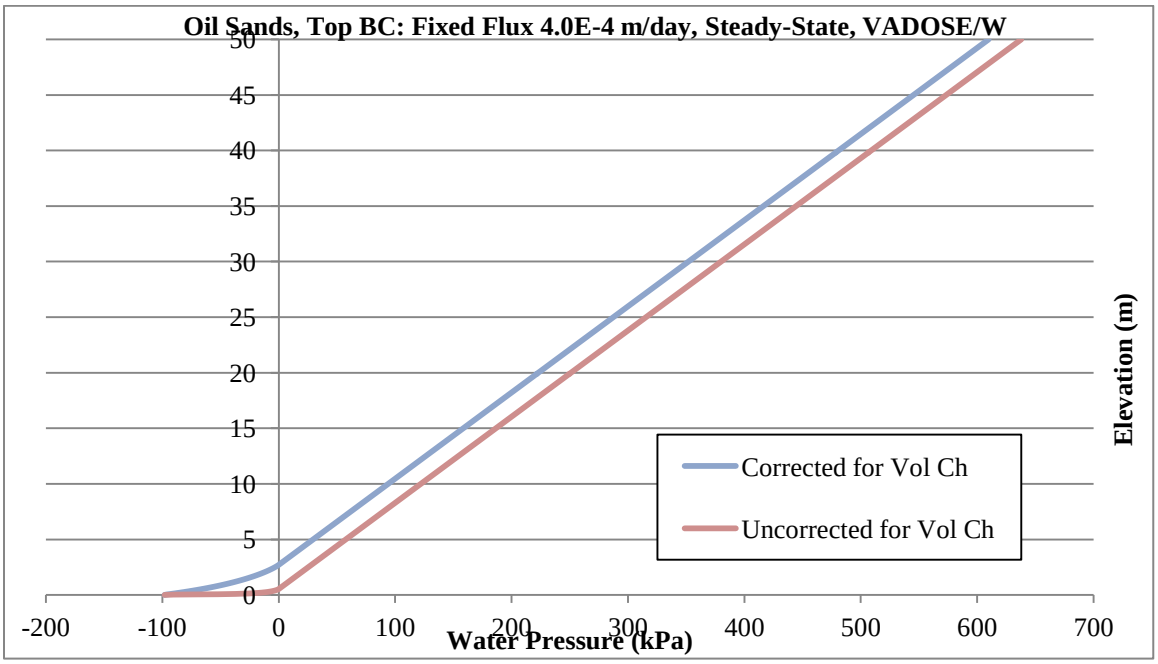

Figure B.17. Water pressure versus depth at steady-state condition for oil sands tailings with SWCC corrected and uncorrected for volume change and top fixed flux of 4.0E-4 m/day using VADOSE/W

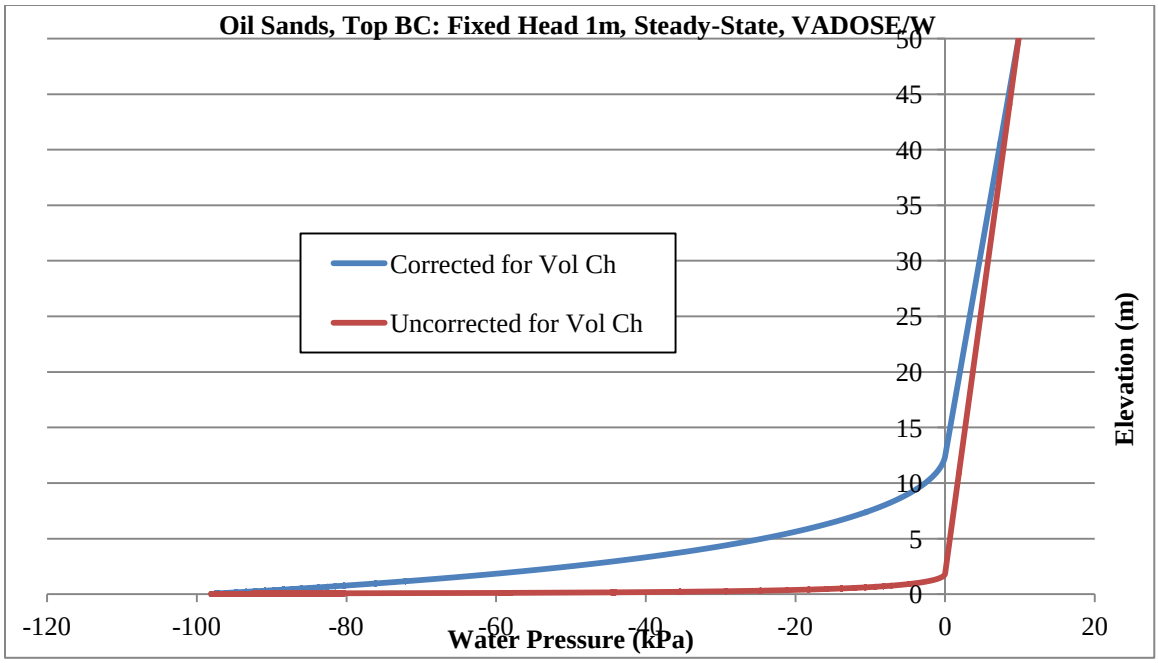

Figure B.18. Water pressure versus depth at steady-state condition for oil sands tailings with SWCC corrected and uncorrected for volume change and top fixed head of 1m using VADOSE/W

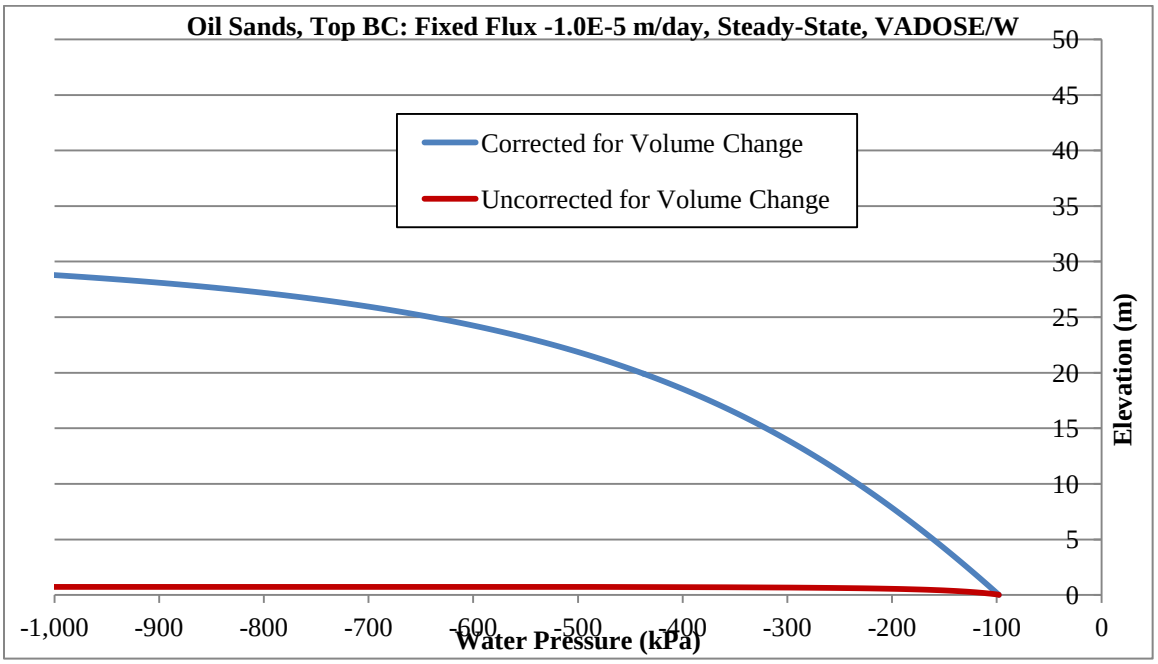

Figure B.19. Water pressure versus depth at steady-state condition for oil sands tailings with SWCC corrected and uncorrected for volume change and top fixed flux of -1.0E-5 m/day (evaporation) using VADOSE/W

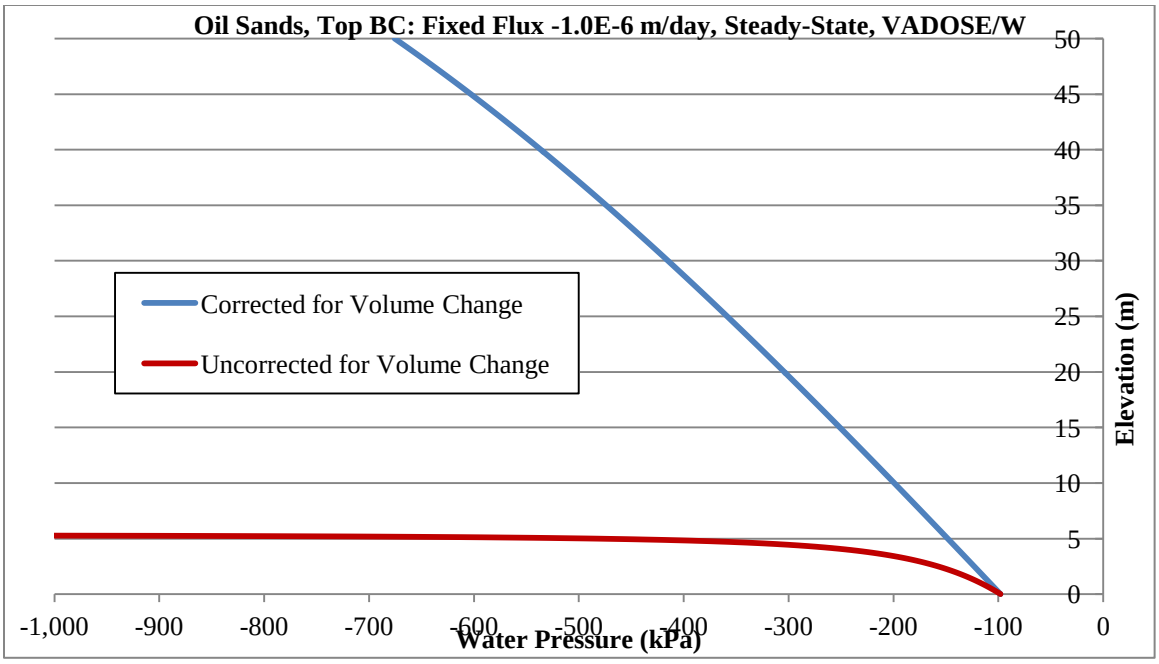

Figure B.20. Water pressure versus depth at steady-state condition for oil sands tailings with SWCC corrected and uncorrected for volume change and top fixed flux of -1.0E-6 m/day (evaporation) using VADOSE/W

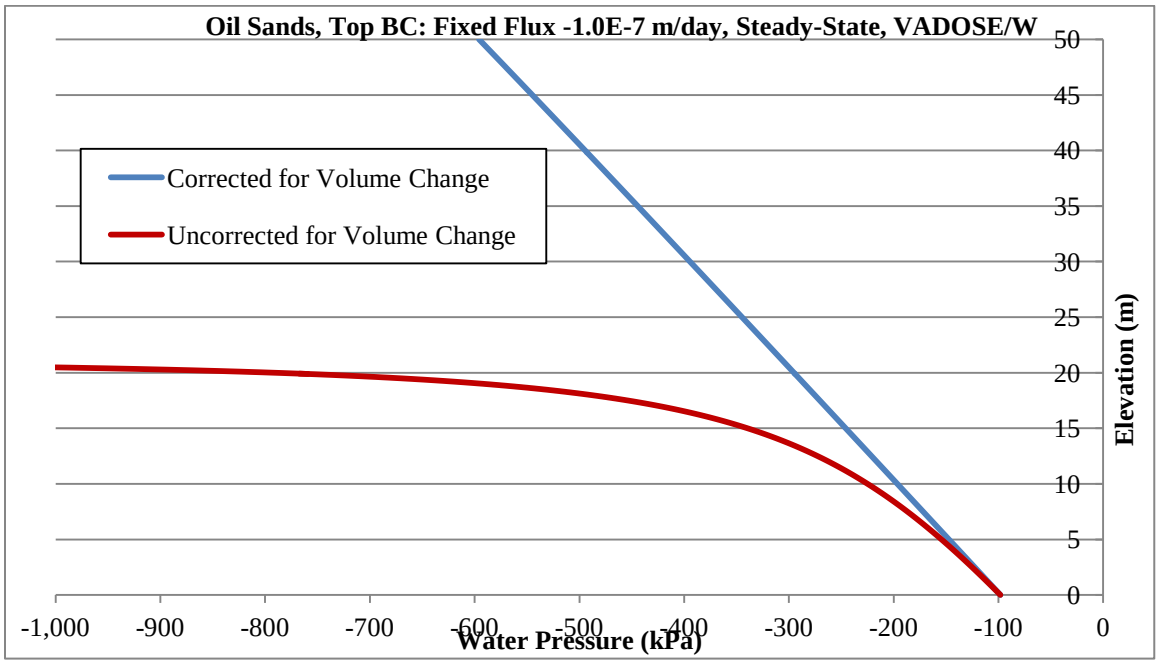

Figure B.21. Water pressure versus depth at steady-state condition for oil sands tailings with SWCC corrected and uncorrected for volume change and top fixed flux of -1.0E-7 m/day (evaporation) using VADOSE/W

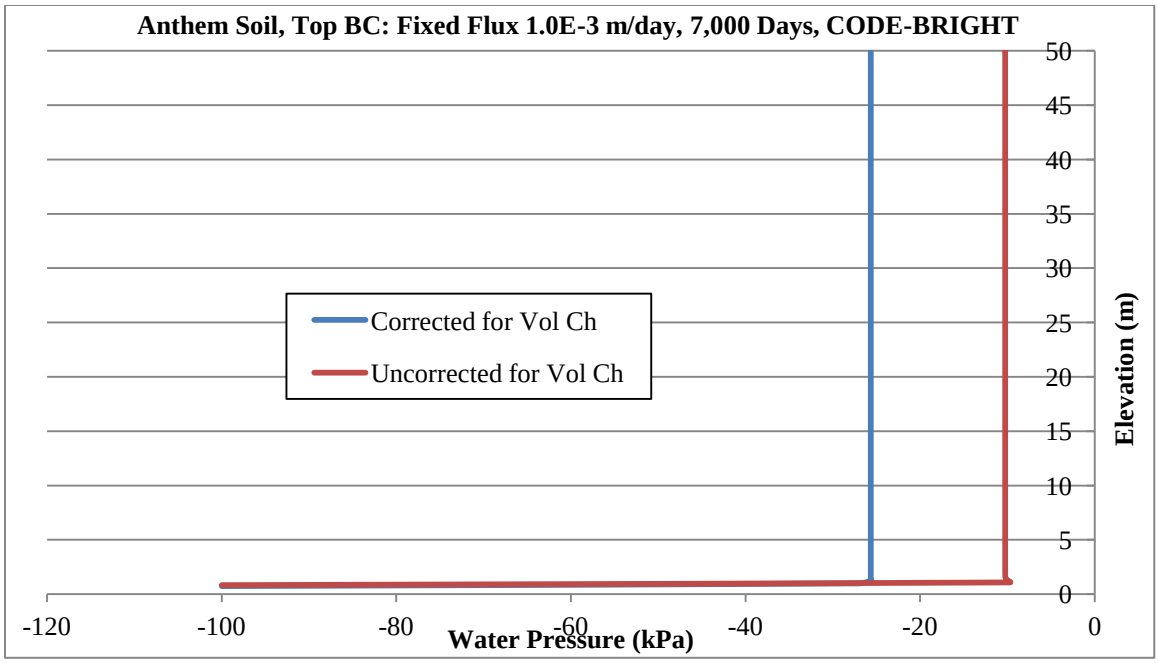

Figure B.22. Water pressure versus depth at steady-state condition for Anthem soil with SWCC corrected and uncorrected for volume change and top fixed flux of 1.0E-3 m/day using CODE-BRIGHT

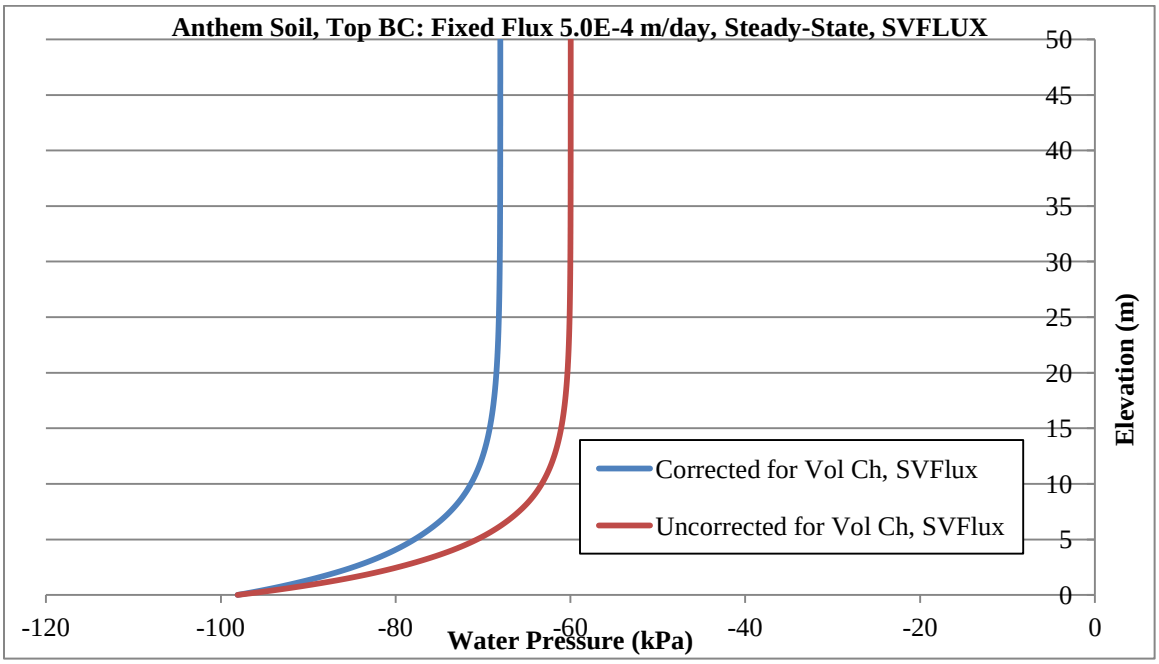

Figure B.23. Water pressure versus depth at steady-state condition for Anthem soil with SWCC corrected and uncorrected for volume change and top fixed flux of 5.0E-4 m/day using SVFLUX

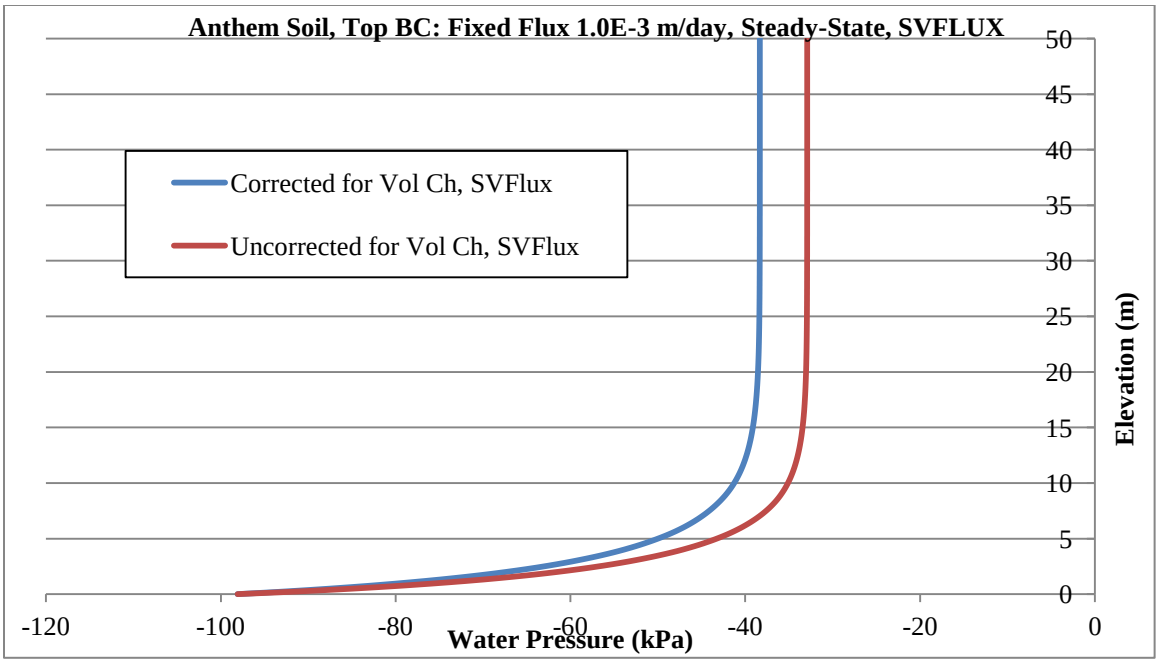

Figure B.24. Water pressure versus depth at steady-state condition for Anthem soil with SWCC corrected and uncorrected for volume change and top fixed flux of 1.0E-3 m/day using SVFLUX

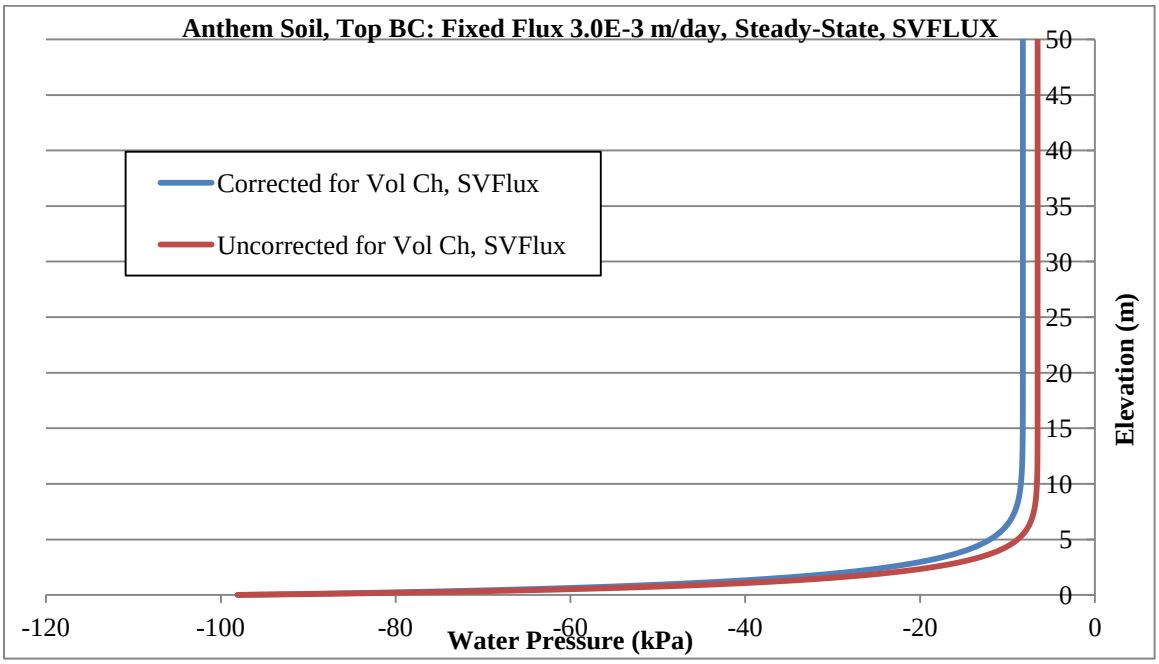

Figure B.25. Water pressure versus depth at steady-state condition for Anthem soil with SWCC corrected and uncorrected for volume change and top fixed flux of 3.0E-3 m/day using SVFLUX

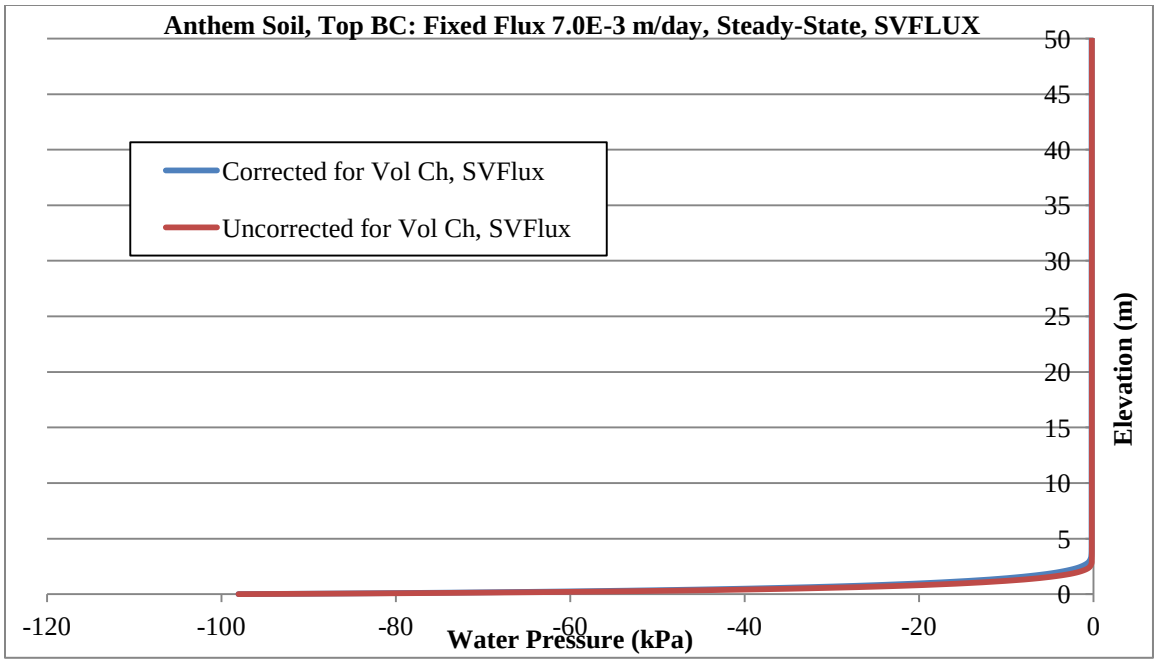

Figure B.26. Water pressure versus depth at steady-state condition for Anthem soil with SWCC corrected and uncorrected for volume change and top fixed flux of 7.0E-3 m/day using SVFLUX

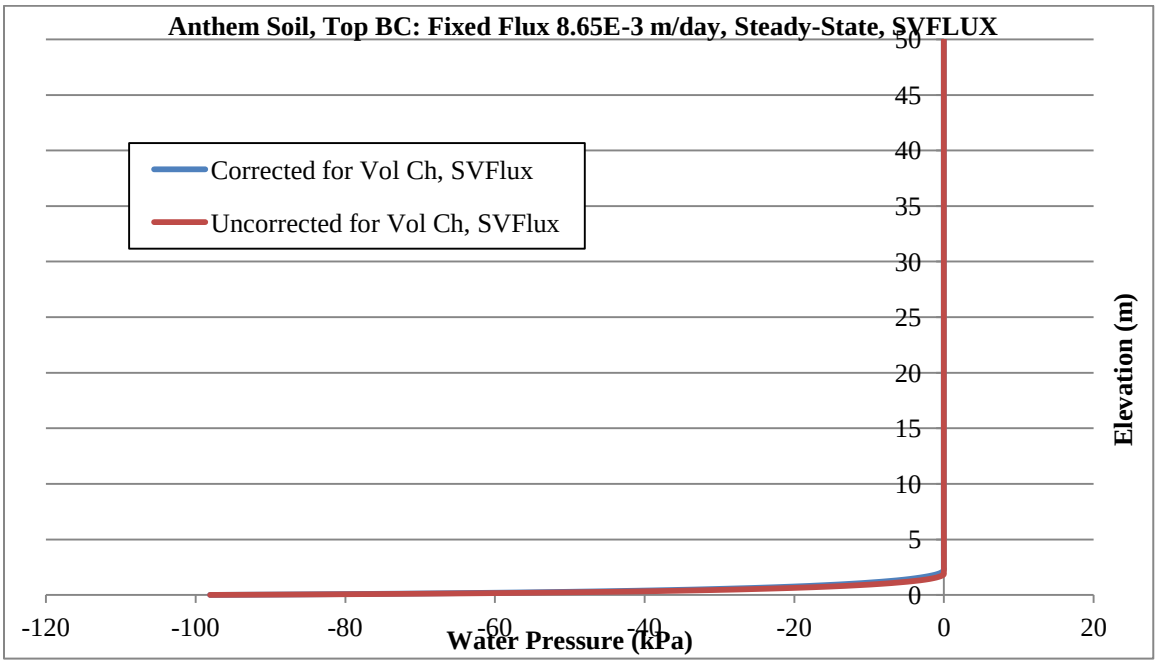

Figure B.27. Water pressure versus depth at steady-state condition for Anthem soil with SWCC corrected and uncorrected for volume change and top fixed flux of 8.65E-3 m/day using SVFLUX

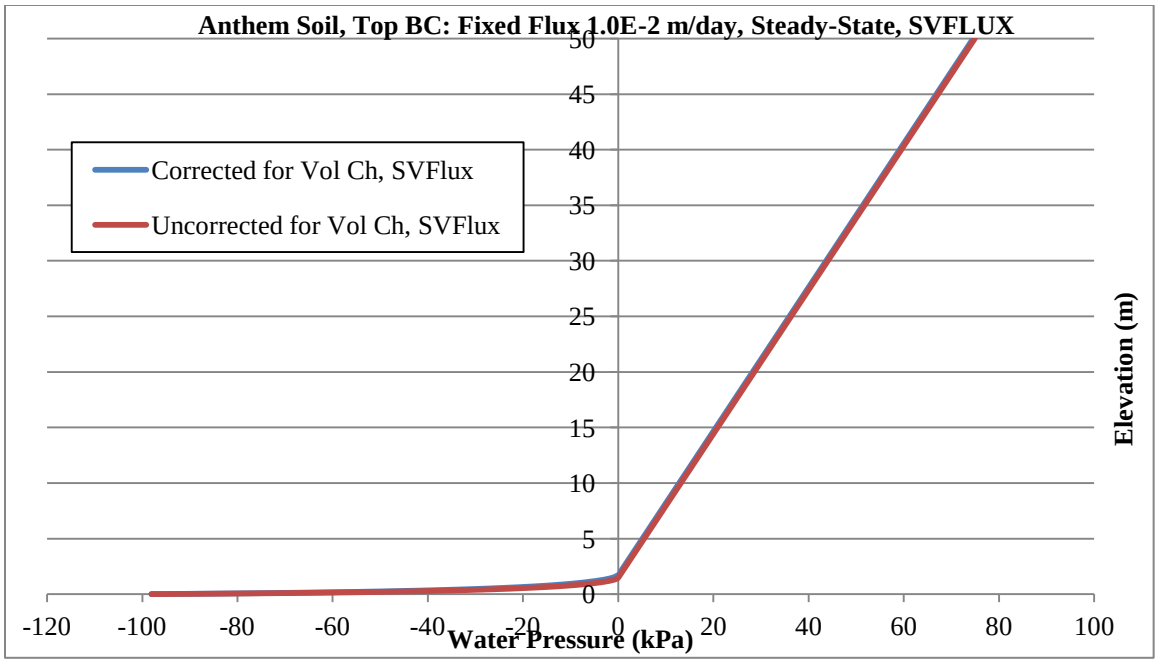

Figure B.28. Water pressure versus depth at steady-state condition for Anthem soil with SWCC corrected and uncorrected for volume change and top fixed flux of 1.0E-2 m/day using SVFLUX

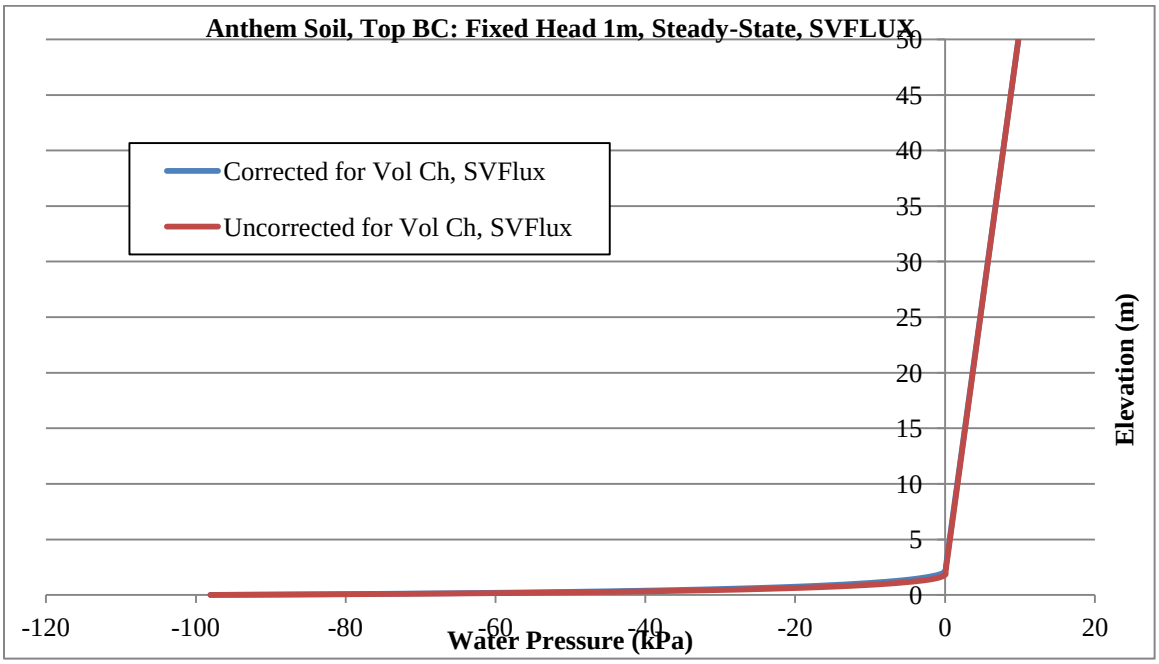

Figure B.29. Water pressure versus depth at steady-state condition for Anthem soil with SWCC corrected and uncorrected for volume change and top fixed head of 1m using SVFLUX

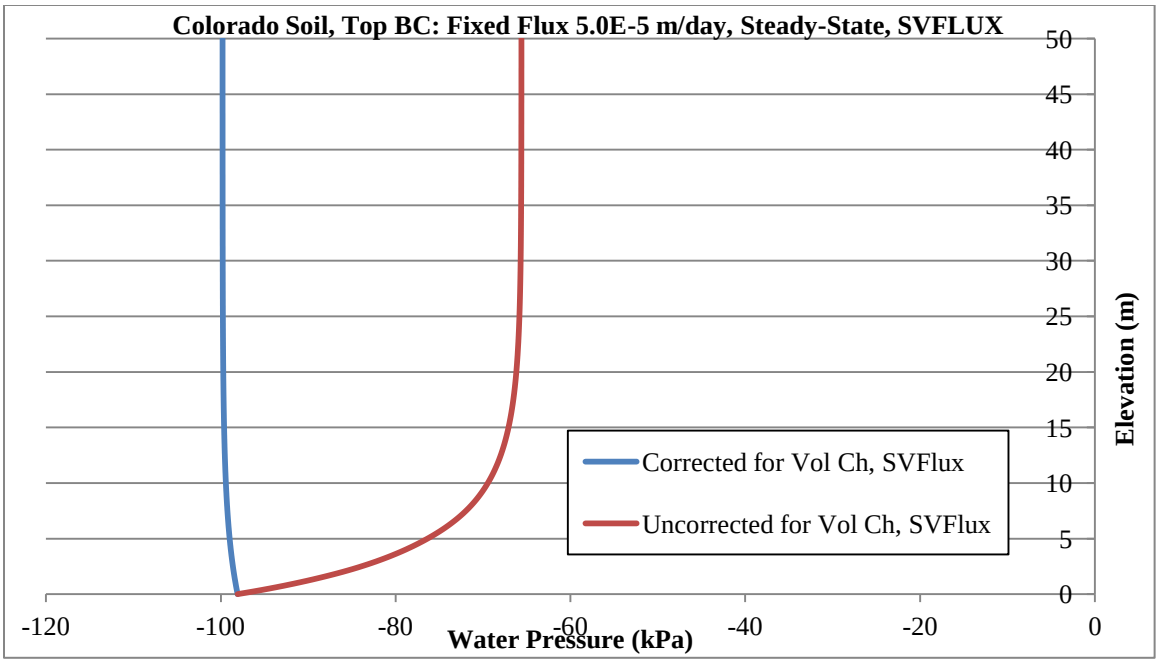

Figure B.30. Water pressure versus depth at steady-state condition for Colorado soil with SWCC corrected and uncorrected for volume change and top fixed flux of 5.0E-5 m/day using SVFLUX

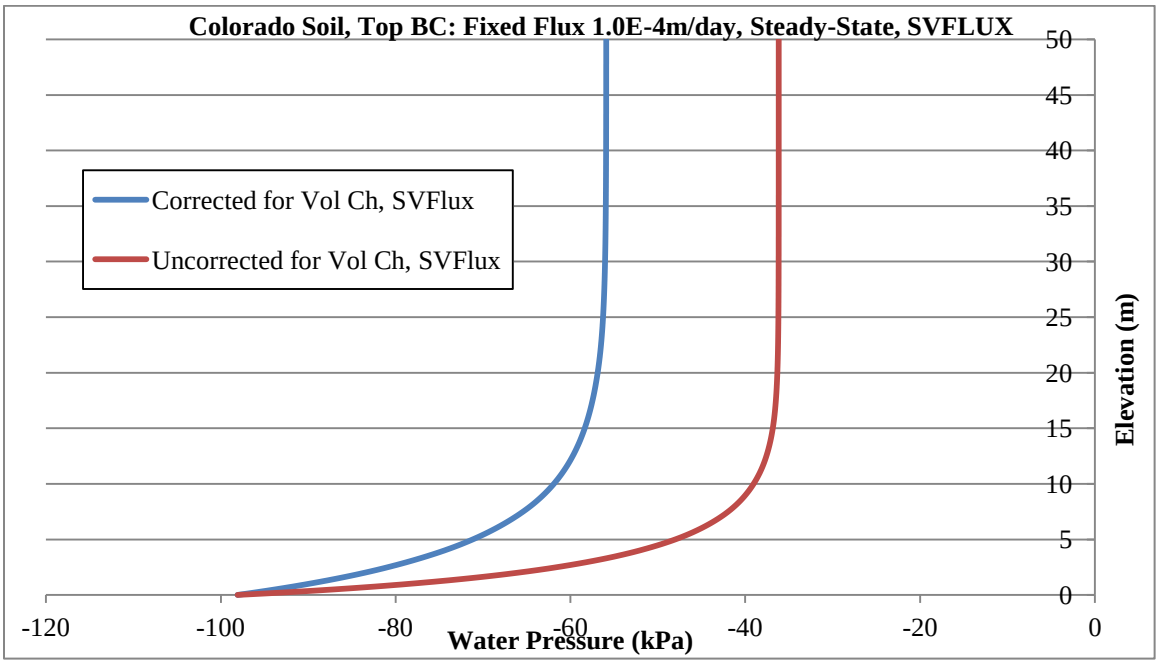

Figure B.31. Water pressure versus depth at steady-state condition for Colorado soil with SWCC corrected and uncorrected for volume change and top fixed flux of 1.0E-4 m/day using SVFLUX

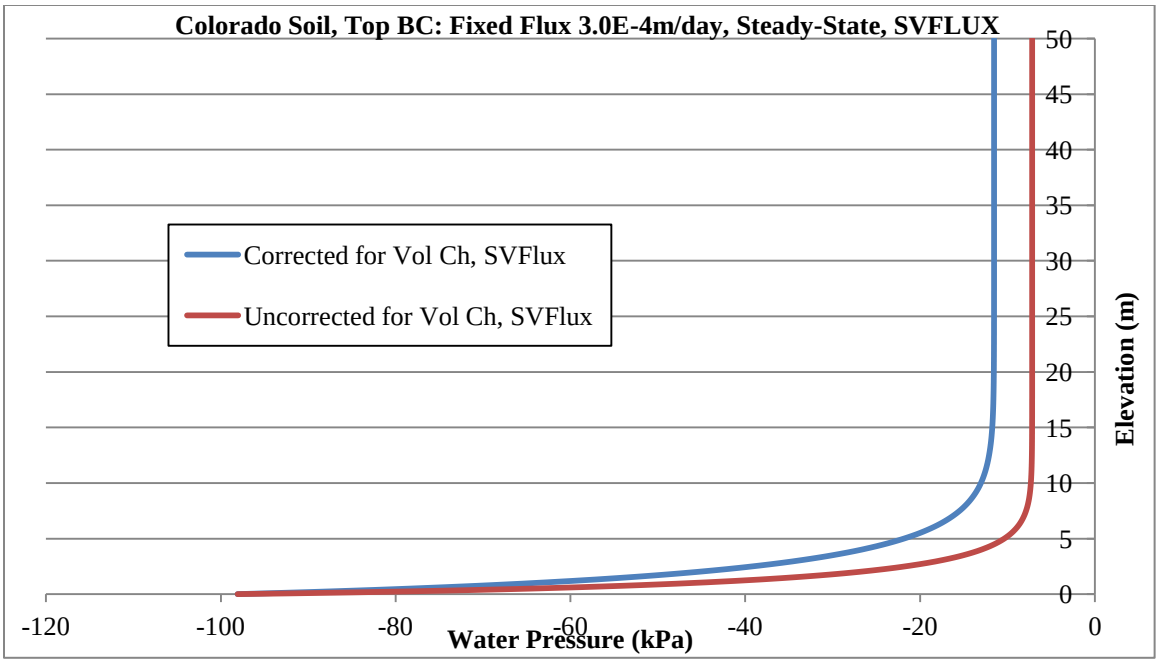

Figure B.32. Water pressure versus depth at steady-state condition for Colorado soil with SWCC corrected and uncorrected for volume change and top fixed flux of 3.0E-4 m/day using SVFLUX

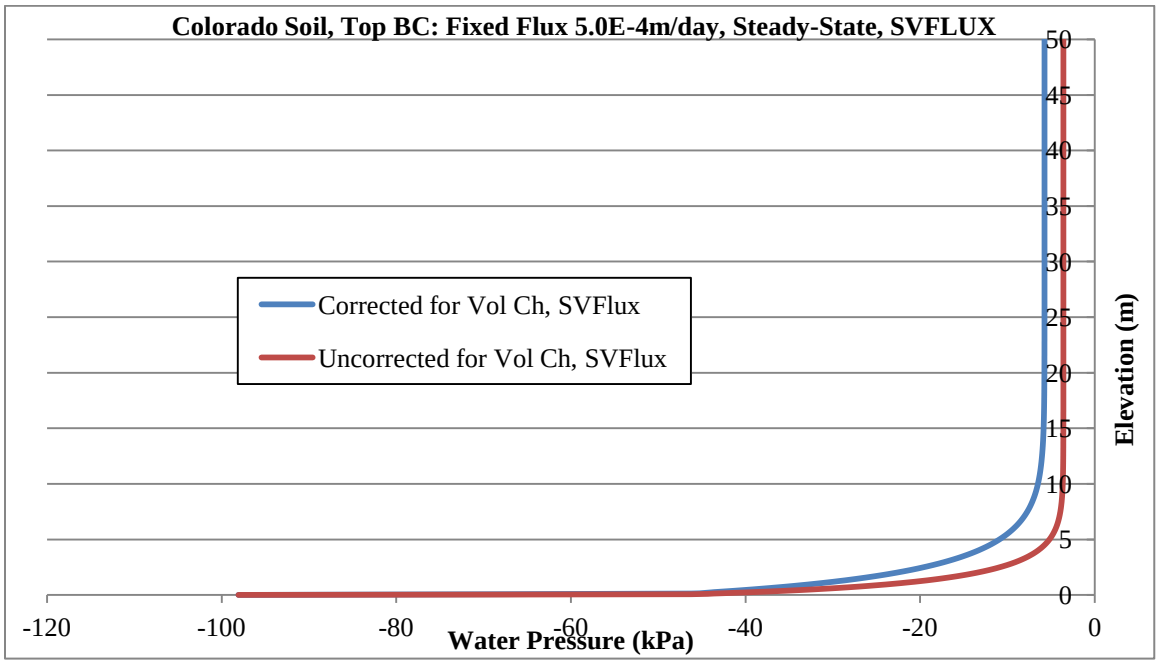

Figure B.33. Water pressure versus depth at steady-state condition for Colorado soil with SWCC corrected and uncorrected for volume change and top fixed flux of 5.0E-4 m/day using SVFLUX

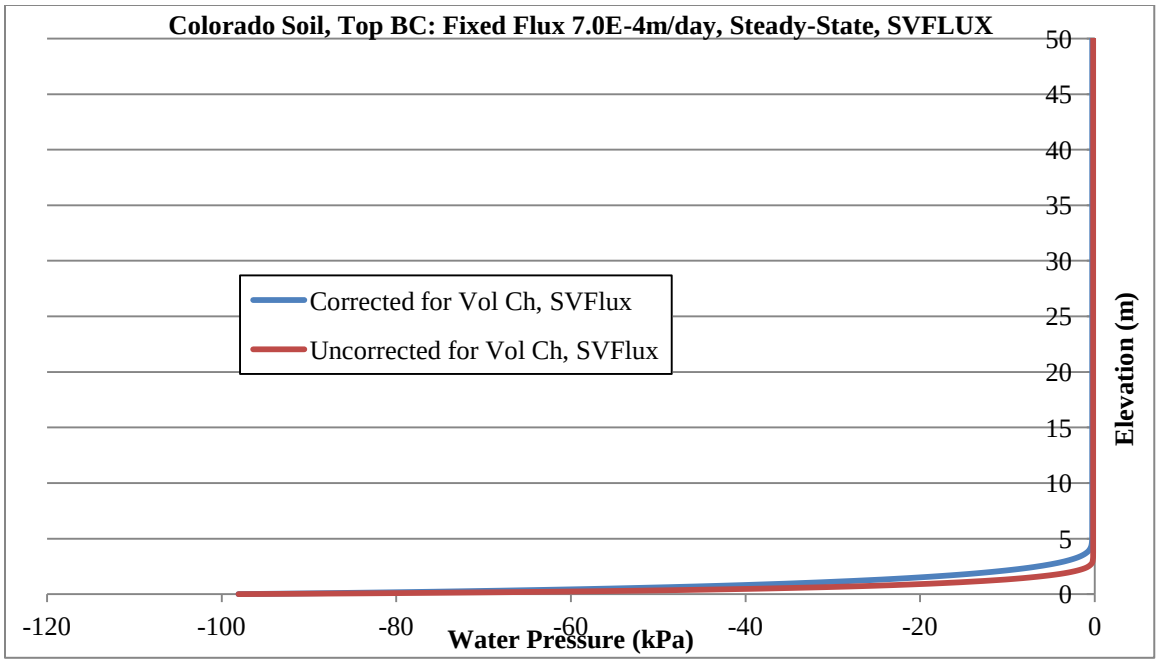

Figure B.34. Water pressure versus depth at steady-state condition for Colorado soil with SWCC corrected and uncorrected for volume change and top fixed flux of 7.0E-4 m/day using SVFLUX

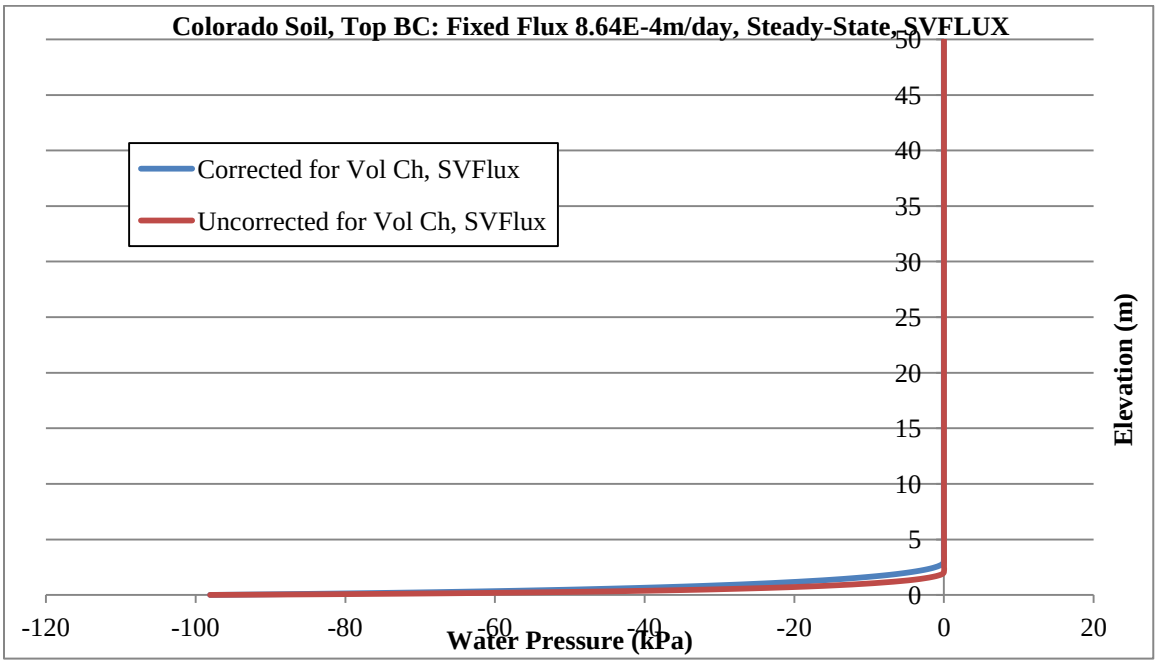

Figure B.35. Water pressure versus depth at steady-state condition for Colorado soil with SWCC corrected and uncorrected for volume change and top fixed flux of 8.64E-4 m/day using SVFLUX

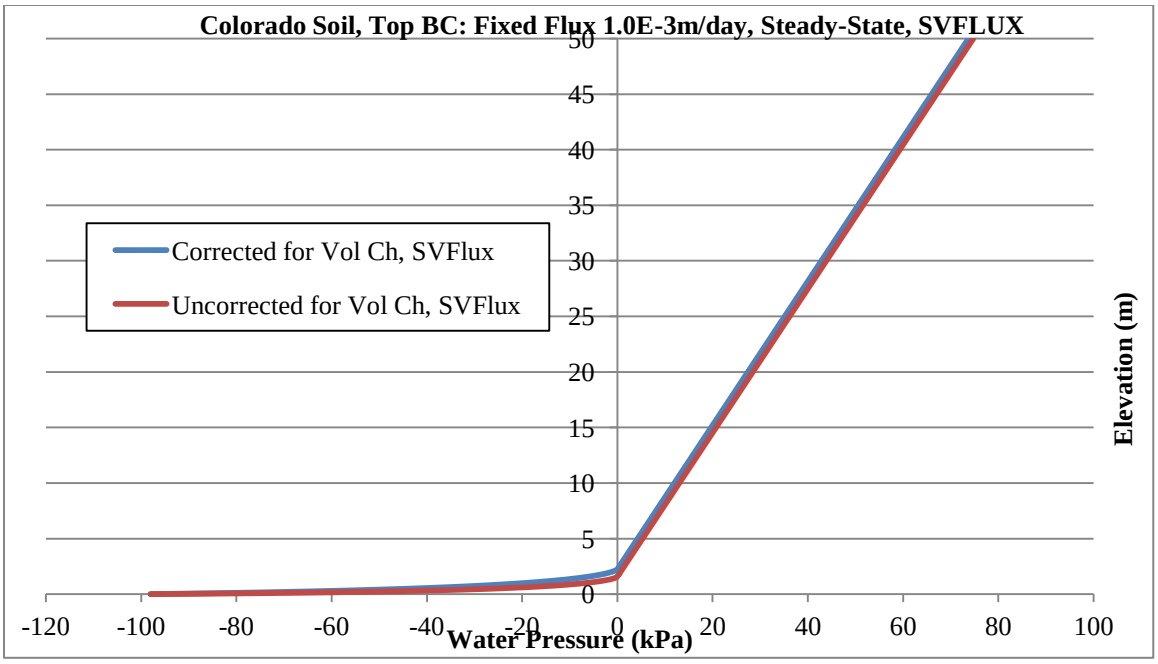

Figure B.36. Water pressure versus depth at steady-state condition for Colorado soil with SWCC corrected and uncorrected for volume change and top fixed flux of 1.0E-3 m/day using SVFLUX

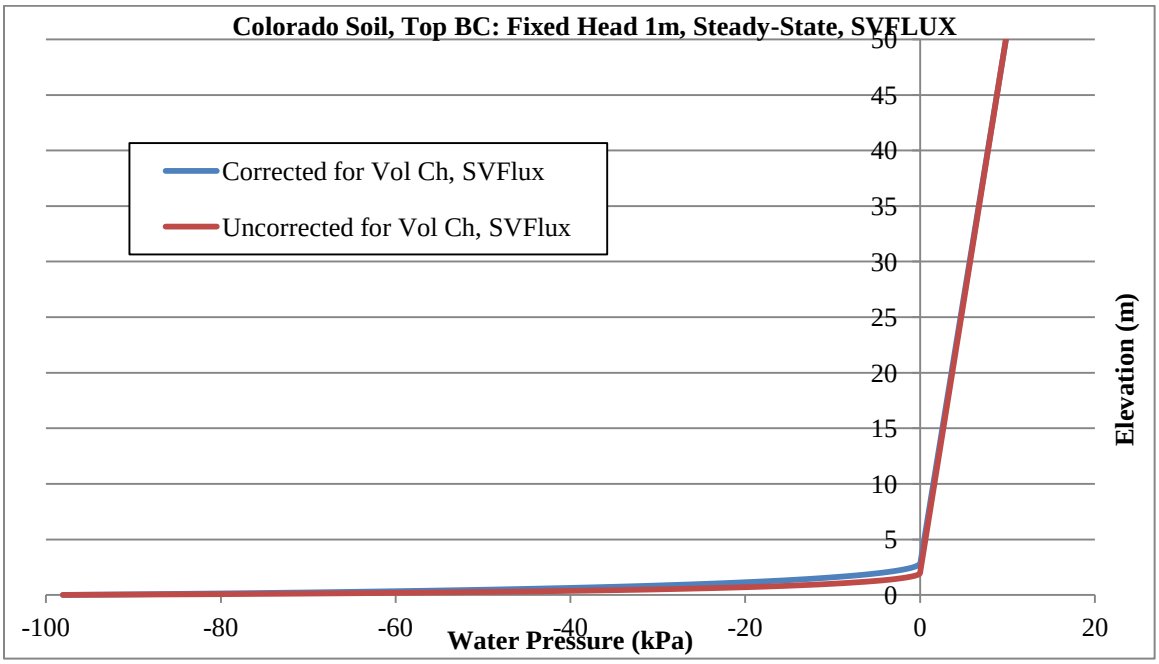

Figure B.37. Water pressure versus depth at steady-state condition for Colorado soil with SWCC corrected and uncorrected for volume change and top fixed head of 1m using SVFLUX

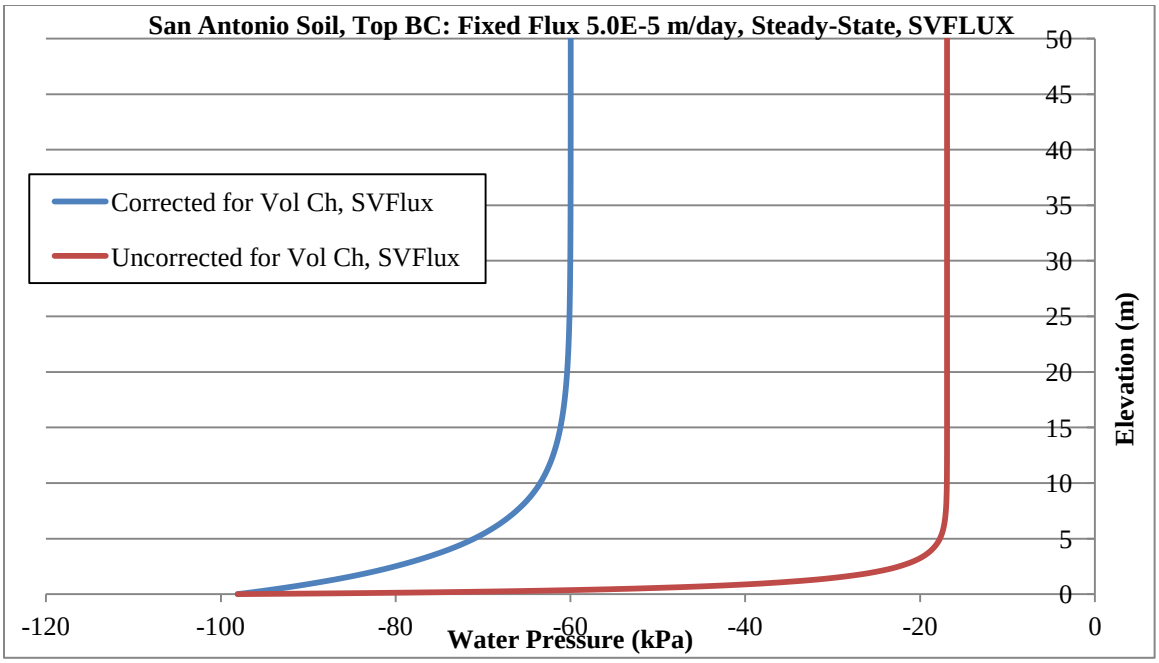

Figure B.38. Water pressure versus depth at steady-state condition for San Antonio soil with SWCC corrected and uncorrected for volume change and top fixed flux of 5.0E-5 m/day using SVFLUX

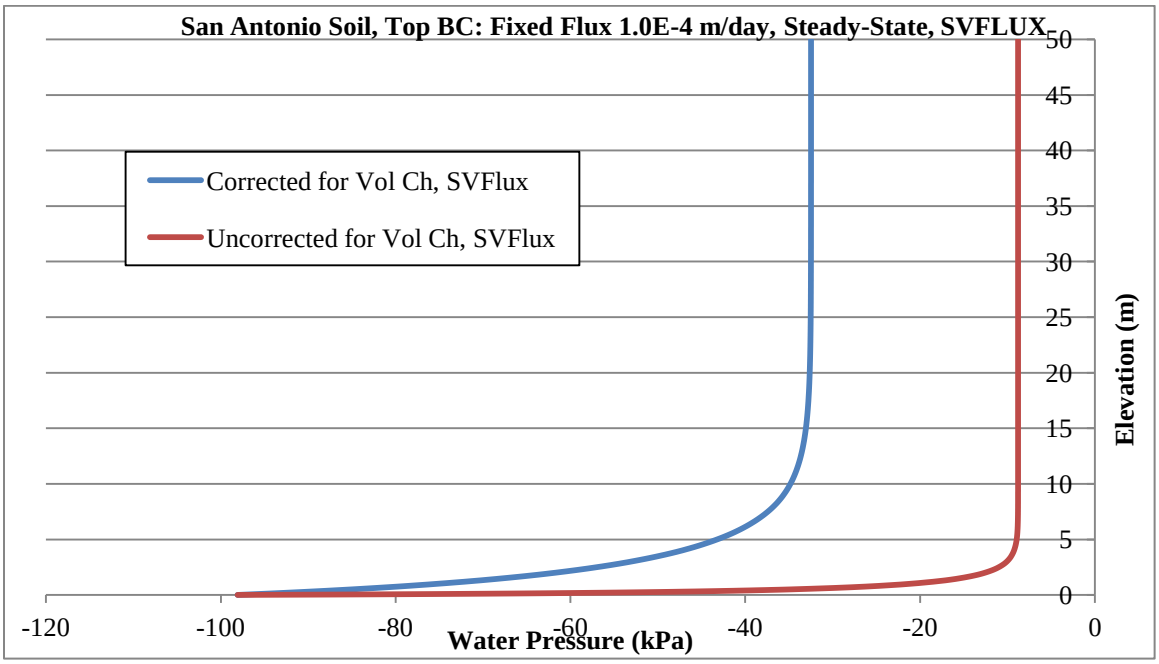

Figure B.39. Water pressure versus depth at steady-state condition for San Antonio soil with SWCC corrected and uncorrected for volume change and top fixed flux of 1.0E-4 m/day using SVFLUX

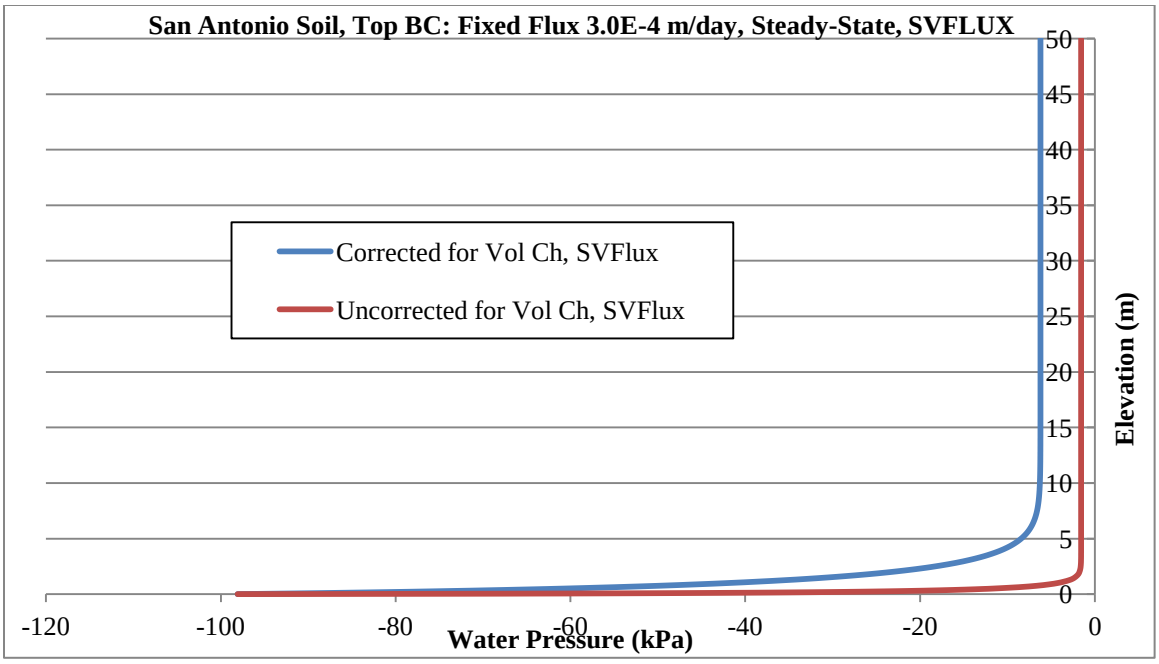

Figure B.40. Water pressure versus depth at steady-state condition for San Antonio soil with SWCC corrected and uncorrected for volume change and top fixed flux of 3.0E-4 m/day using SVFLUX

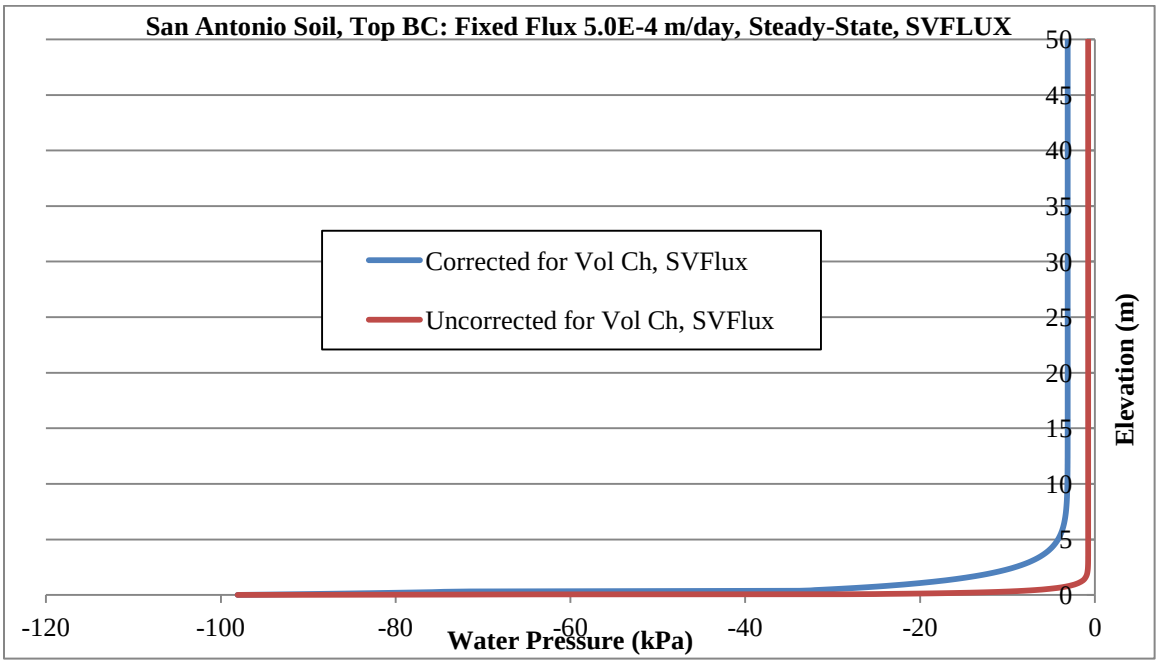

Figure B.41. Water pressure versus depth at steady-state condition for San Antonio soil with SWCC corrected and uncorrected for volume change and top fixed flux of 5.0E-4 m/day using SVFLUX

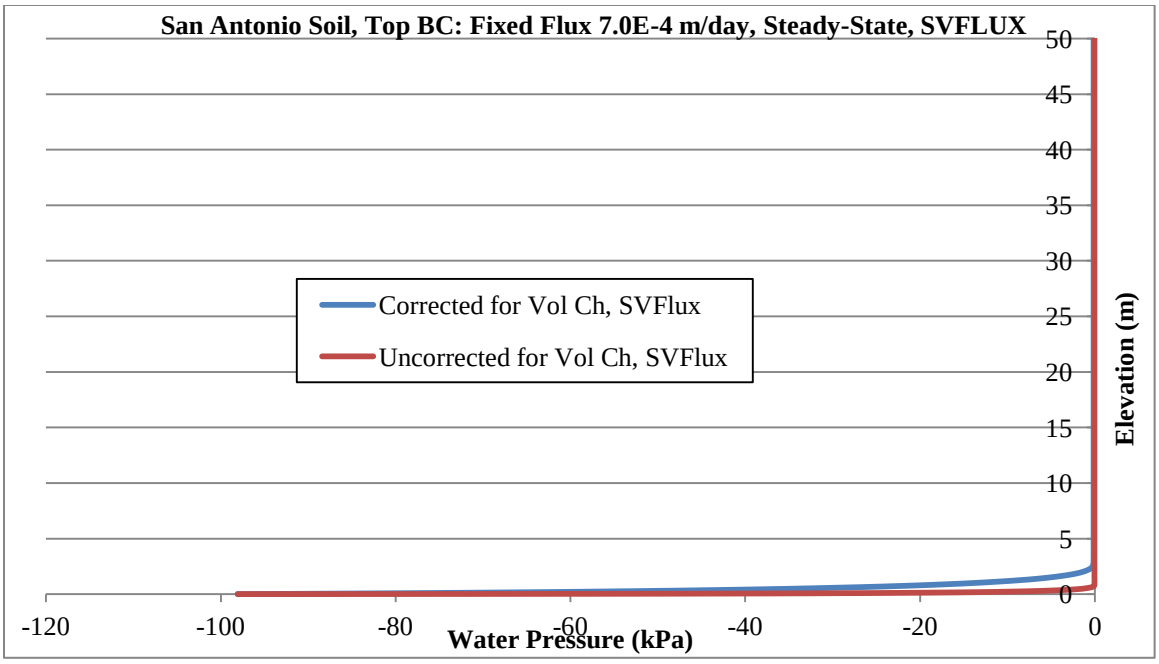

Figure B.42. Water pressure versus depth at steady-state condition for San Antonio soil with SWCC corrected and uncorrected for volume change and top fixed flux of 7.0E-4 m/day using SVFLUX

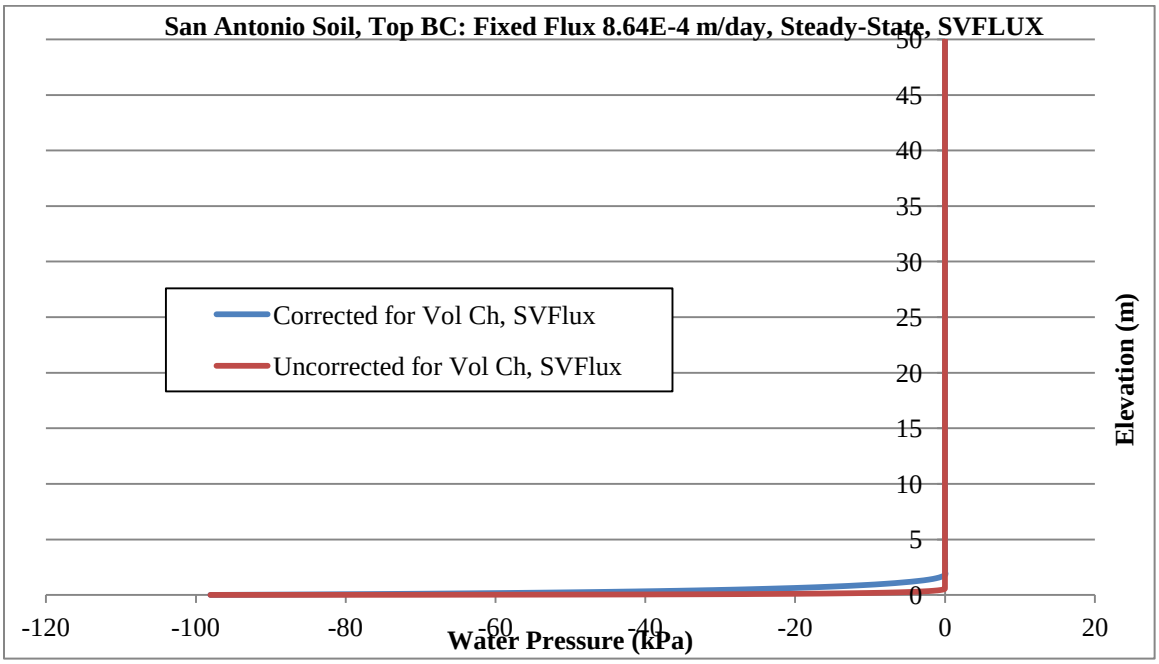

Figure B.43. Water pressure versus depth at steady-state condition for San Antonio soil with SWCC corrected and uncorrected for volume change and top fixed flux of 8.64E-4 m/day using SVFLUX

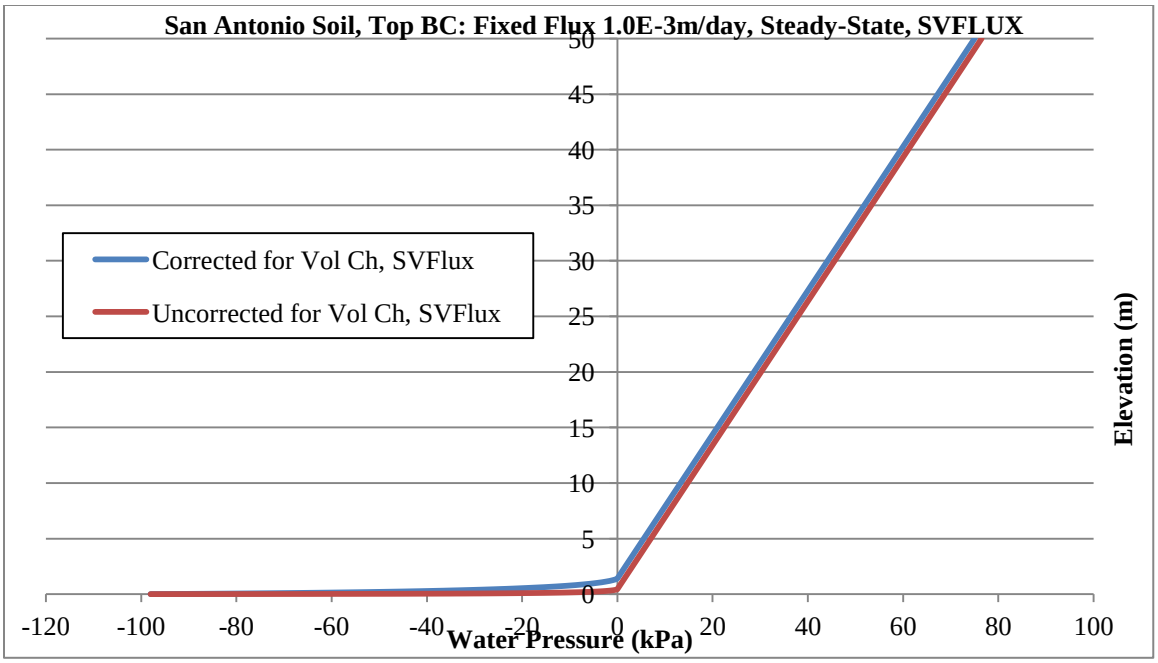

Figure B.44. Water pressure versus depth at steady-state condition for San Antonio soil with SWCC corrected and uncorrected for volume change and top fixed flux of 1.0E-3 m/day using SVFLUX

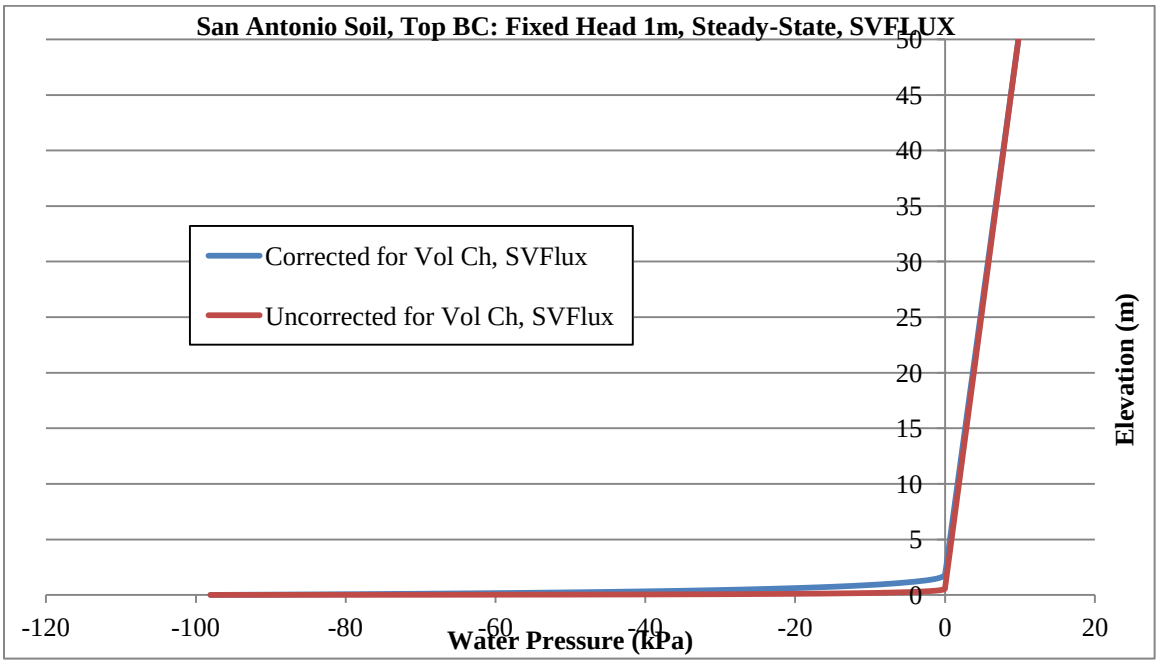

Figure B.45. Water pressure versus depth at steady-state condition for San Antonio soil with SWCC corrected and uncorrected for volume change and top fixed head of 1m using SVFLUX